Future Spacecraft Propulsion Systems

Enabling Technologies for Space Exploration

Paul A. Czysz and Claudio Bruno

Future Spacecraft Propulsion Systems

Enabling Technologies for Space Exploration

Springer

Published in association with
Praxis Publishing
Chichester, UK

PRAXIS

Professor Paul A. Czysz
Oliver L. Parks Endowed Chair in Aerospace Engineering
Parks College of Engineering and Aviation
St Louis University
St Louis
Missouri
USA

Professor Claudio Bruno
Dipartimento di Meccanica e Aeronautica
Università degli Studi di Roma
La Sapienza
Rome
Italy

SPRINGER–PRAXIS BOOKS IN ASTRONAUTICAL ENGINEERING
SUBJECT *ADVISORY EDITOR*: John Mason, M.Sc., B.Sc., Ph.D.

ISBN 10: 3-540-23161-7 Springer-Verlag Berlin Heidelberg New York

Springer is part of Springer-Science + Business Media (springeronline.com)

Bibliographic information published by Die Deutsche Bibliothek

Die Deutsche Bibliothek lists this publication in the Deutsche Nationalbibliografie; detailed bibliographic data are available from the Internet at http://dnb.ddb.de

Library of Congress Control Number: 2005934712

Printed in Germany

Cover design: Jim Wilkie
Project management: Originator Publishing Services, Gt Yarmouth, Norfolk, UK

Printed on acid-free paper

Contents

Preface

Humankind has been dreaming of traveling to space for a long time. Jules Verne thought we could reach the moon with a giant cannon in the 1800s. In the early 1960s there was a dedicated push to develop the vehicle configurations that would permit us to travel to space, and back through the atmosphere, as readily and conveniently as flying on an airliner to another continent and back. That idea, or intuition, was necessarily coupled with advanced propulsion system concepts, that relied on capturing the oxygen within our atmosphere instead of carrying it onboard from the ground up, as rockets developed in Germany in the 1940s did, and as satellite launchers still do. During the 1960s the concept of space travel extended beyond our planet, to our Solar System and the Galaxy beyond (see Chapter 1), using power sources other than chemical, such as fission and fusion. Not much is left nowadays of those dreams, except our present capability to build those advanced propulsion systems.

Traveling to space in the foreseeable future is a multi-step process. The first step is to achieve a two-way transport to and from orbit around our Earth, that is, a Low Earth Orbit (LEO), see Chapters 2, 4 and 5. This is a critical first step as it is the key to moving away from our Earth environment. For any future development in space, travel that transits to and from LEO must be frequent and affordable. From a vision of spacecraft parked in LEOs there are then several options. One is a Geo-Synchronous Orbit or Geo-Stationary Orbit (GSO) that is at an altitude of 35,853 km (22,278 statute miles) and has an equatorial orbital period of 24 hours, so it is stationary over any fixed point on Earth. Another option for the next step is an elliptical transfer orbit to the Moon. The orbital speed to reach the Moon is *less* than the speed to reach Earth's orbit, so the transfer orbit is elliptical, and (contrary to current popular belief), requires less energy to accomplish (but more logistics) than reaching GSO. Depending on the specific speed (orbit) selected, the time to reach the Moon is between 100 to 56 hours. In fact, the Apollo program selected a speed corresponding to a 72-hour travel time from LEO to the vicinity of the Moon (see Chapter 6): in terms of the time needed to reach it, the Moon is truly close to us. All circular and elliptical orbits are, mathematically speaking, closed conics.

Another and far more eventful option is to achieve *escape* speed, that is a factor square root of two faster than orbital speed. At escape speed and faster the spacecraft trajectory is an open conic (i.e., a parabola or hyperbola), and there is no longer a closed path returning the spacecraft to Earth. So now we can move away from the gravitational control of Earth (not from gravity!) and proceed to explore our Solar System and beyond. However, after taking such a step, there is a challenge of time, distance and propulsion as we proceed farther and farther to explore our Solar System, then nearby Galactic space and finally our Galaxy. Exploring beyond our Galaxy is technically beyond our current or projected capabilities. In order to achieve travel beyond our Galaxy our current understanding of thrust, mass, inertia and time will have to be different (see Chapters 8 and 9). Mass/inertia may be the most challenging. An article by Gordon Kane in the July 2005 *Scientific American* entitled "The Mysteries of Mass" explains our current understanding of what we call mass. From another paper presented by Theodore Davis at the 40th Joint Propulsion Conference [Davis, 2004] we have the following statement:

> $E = mc^2$ is the expression of mass–energy equivalence and applies to all forms of energy. That includes the energy of motion or kinetic energy. The faster an object is going relative to another object, the greater the kinetic energy. According to Einstein mass and energy are equivalent, therefore the extra energy associated with the object's inertia manifests itself in the same way mass manifests itself ... As a result, the kinetic energy adds to the object's inertial component and adds resistance to any change in the objects motion. In other words, both energy and mass have inertia.

Inertia is a resistance to change in speed or direction. As we approach light speed, the inertia/mass approaches infinity. As the mass approaches infinity the thrust required to maintain constant acceleration also approaches infinity. Thus, at this point we do not know how to exceed the speed of light. If that remains the case, we are trapped within the environs of our Solar System.

There is a second major issue. Human tolerance to a continuous acceleration for long periods has yet to be quantified. Nominally that is considered about three times the surface acceleration of gravity. At that rate of acceleration the time to reach a distant destination is numerically on the same order as the distance in light years. So if a crewed spacecraft is to return to Earth within the lifetime of its occupants, we are again limited to 20 light years of so. That is within the distance to the seven or eight closest stars to our star, the Sun.

As much as the authors would hope to travel in Galactic space, it will require a breakthrough in our understanding of mass, acceleration and propulsion. Until that time we have much to explore and discover within the environs of our Solar System.

Coming down from Galactic space to intelligent life on Earth, the authors would like to acknowledge the contributions of Elena and David Bruno, Catherine Czysz, Dr Babusci at the INFN (Italian Nuclear Physics Institute), Dr Romanelli at the

ENEA Fusion Laboratories, Mr Simone, GS, H. David Froning, Gordon Hamilton, Dr Christopher P. Rahaim and Dr John Mason, Praxis Subject Advisory Editor. Special thanks go to Clive Horwood of Praxis, for his patience, constant encouragement, and prodding, without which writing this book would have taken much longer.

Paul A. Czysz and Claudio Bruno

Figures

Tables

Introduction

We begin with the fundamental element, or you may say, the first step of traveling to space: orbiting around Earth or another celestial body. Consider an object orbiting the Earth; unless there are factors such interaction with the upper atmosphere, solar winds, and inertial energy losses, the object will orbit indefinitely. The reason is that *all* objects in orbit are essentially falling around the body they are orbiting. This is relatively simple to illustrate. The acceleration of gravity at the surface of the Earth is 32.1741 ft/sec^2 (9.8067 m/sec^2) and that means, from Newton's Laws, in one second an object will fall 16.087 feet or 4.9033 meters from rest.

The radius of the Earth at the equator is 3,963.19 statute miles (6,378.14 km). If the Earth were a smooth sphere with the radius of the Earth's equator, then the distance traversed along the surface from a point A to a point B 16.087 feet lower than point A is 25,947 feet (7,908.7 meters). So if an object were one foot above the surface of this perfect sphere, and traveling at a speed of 25,947 ft/sec (7,908.7 m/sec) parallel to the surface, then it would fall the same distance as the surface of the Earth curves and falls away from the starting point. That is, it would continuously fall 'around the sphere' at an altitude of one foot, without ever striking the surface. It would in fact be in orbit around the sphere. So an object in orbit around a body is falling around that body at sufficient speed that it does not move closer to the surface. Occupants in that orbiting body are not experiencing zero gravity, they are experiencing zero net force.

To show that, consider the acceleration of a body moving along a curved path that is at constant speed V, but with a constantly varying flight path angle. The acceleration perpendicular to the flight path that is necessary to maintain the curved path is:

$$a_{\text{normal}} = \frac{V^2}{\text{radius}}$$

Using the equatorial radius of the Earth, with the magnitude of the speed $V = 25,947$ ft/sec (7,908.7 m/sec), the normal (perpendicular) acceleration is equal to the acceleration to gravity in magnitude but acting in the opposite direction. So an object in orbit around a body is free falling around that object and there are no net forces on the object or on anything on that object. That is often described mistakenly but colorfully by the popular press as a condition of 'zero-gravity'; instead it is the difference between two essentially equal and opposite forces. Microgravity would instead be a more appropriate term, for there is always a minute residual difference between gravity and normal acceleration. The balance is so delicate that on an orbital station an occupant that sneezes can ruin a microgravity experiment. Technically, such disturbances go by the name of microgravity 'jitters'.

So in order to go to space, we first need a transportation system from the surface to Earth orbit and return. To go to the Moon and beyond, for instance to Mars, we need a propulsion system that can leave Earth's orbit and then establish an orbit around its destination object. We are able to do this to the Moon relatively easily with the currently operational propulsion systems. That is because to reach the Moon an elliptical orbit containing the Earth and Moon at its foci is sufficient. To reach Mars instead we must reach and exceed escape speed. Mars requires a round trip of two years with current propulsion systems. So for Mars a propulsion system that ensures minimum radiation damage to human travelers is still in the laboratory. In order to go Pluto and beyond, we need propulsion systems not yet built, but envisioned by people that seek to travel beyond our solar system. However, to travel much farther beyond Pluto remains for the time being only an expectation.

If you were to ask the question, 'What is Space Propulsion ?' probably the most common answer would be *rockets*. Beginning in 1957 with Sputnik, chemical rockets have propelled payloads and satellites into Earth orbit, to Mercury, Venus, Mars and Titan, one of Saturn's satellites, and have propelled two Pioneer spacecraft (Pioneer 10 and 11) to the boundary between our solar system and interstellar space. Pioneer 10's last telemetry transmission to the NASA Deep Space Network (DSN) was 22 April 2002, having been launched on 2 March 1972. On 22 January 2003 the DSN recorded Pioneer 10's last weak radio signal at a distance of 7.6 billion miles (7.6×10^9 miles) from Earth. That signal took 11 hours and 20 minutes to reach DSN [AW&ST, 3/2003]. Pioneer 11's last telemetry transmission was in 1995. Its journey has taken nearly 31 years, and it still did not reach the boundary between our solar system and interstellar space (the so-called Heliopause). This is *the* problem we face with chemical rocket propulsion, the extremely long times to cover large distances, because the speed possible with chemical rockets is severely limited by how long they can function, and so it is low. Had an operational Pioneer spacecraft reached a distance from Earth that is 100 times the distance the Earth is from the Sun (i.e., of the order of the Heliopause) it would take light 14 hours to traverse the one-way distance, so a two-way communication requires 28 hours, four hours longer than one day! That is to say that, at light speed, Pioneer 10 would have the reached the Heliopause some 32 years ago! Pioneer 10 is on its way to the red star Aldebaran, but it will not arrive there for more than another 2 million years [AW&ST, 3/2003]. The Pioneer spacecraft team that was present when the Pioneer spacecraft passed by Jupiter, Saturn, Neptune or Uranus is no longer the group listening for the sporadic-distant signals being received from the Pioneer spacecraft. In reality the Pioneer spacecraft moves so slowly that following its progress is beyond the practical ground-based tracking team's functional duration. To move faster requires high accelerations, but those are limited by the rocket propulsion systems available and by human physiological and spacecraft hardware tolerance to acceleration ('g' tolerance). To approach light speed or faster than light (FTL) speed what is needed is not anti-gravity but anti-mass/inertia. A question is, Is FTL possible? A conclusion [Goff and Siegel, 2004] is:

> Current warp drive investigations [Goldin and Svetlichny, 1994] apply general relativity to try to produce spacetime curvature that propagates at superlight speeds. Special relativity is preserved inside the warp field, but the contents are perceived to move at FTL speeds from the external frames. Such a classical warp drive cannot avoid the temporal paradox (i.e., time travel). If quantum systems are the only system that permits backward-in-time causality without temporal paradox, then any rational warp drive will need to be based on quantum principles. This means that until we have a workable theory of quantum gravity, research into warp drives based on General Relativity is probably doomed to failure.

A second example of our chemical rocket speed limitations is a Pluto mission. The planet Pluto has a distance from the Sun varying from 2.78×10^9 to 4.57×10^9 statute miles, for an average of 3.67 x 109 statute miles. Depending on its distance, a one-way radio signal takes between 4 hours, 10 minutes and 6 hours, 48 minutes to reach Pluto from Earth. So the two-way transmission from Earth and return takes from about 8 hours to 13 hours. That is a considerable time to consider communicating with and controlling a spacecraft. If a correction to its flight path, or a correction to its software programming, or remedying a problem is necessary, it will be between 16 and 26 hours before a return signal can confirm whether or not the action was successful. In that period of time a great deal can happen to harm, injure or destroy the spacecraft. So these spacecraft that are operating at the fringe of practical control because of the propulsion system's performance must essentially be robots, capable of diagnosing and correcting problems without human intervention.

The question is: 'What propulsion performance is necessary to significantly change this chemical rocket paradigm?' The performance of a rocket is measured by its ability to change the magnitude of its speed in a given direction (velocity) by the ejection of mass at a characteristic velocity. That change in the magnitude of the speed, ΔV, can be expressed in the simplest way as: (1) where:

$$\Delta V = g\, I_{\mathrm{sp}} \ln(WR) = c^* \ln(WR) \tag{1}$$

where:

$$c^* = g\, I_{\mathrm{sp}} = \text{Characteristic velocity}$$

$$WR = \exp \frac{\Delta V}{g\, I_{\mathrm{sp}}} = \frac{\Delta V}{c^*} = \frac{\text{Initial mass}}{\text{Final mass}}$$

$$WR - 1 = \frac{\text{Propellant mass}}{\text{Final mass}}$$

$$I_{\mathrm{sp}} = \frac{T}{\dot{w}_{\mathrm{ppl}}} = \text{Thrust produced per unit mass flow rate of propellant}$$

So we have just two key parameters: the **weight** ratio, or mass ratio, is just a measure of how much propellant is carried. The **characteristic velocity**, or the **specific impulse**, I_{sp}, defines the performance of the propulsion system. The best cryogenic chemical rockets today have an I_{sp} of 460 sec (4,462 m/sec). That means that a mass flow of one kilogram per second generates 460 kilograms (4,462 newtons) of thrust. If our benchmark change of speed ΔV is the speed of light (299,790,000 m/sec) then the specific impulse required for a mass ratio of 6 is 17,062,060 sec. That is, one kilogram per second of propellant flow generates 17,062,060 kilograms of thrust. Or more pointedly, one microgram per second of propellant produces 17.06 kilograms of thrust! That is approaching a so-called 'massless' thrust-producing system, and is well beyond our current concept of generating thrust. Even if at some future time an Isp of 100,000 sec is achieved, the speed of light (299,790,000 m/sec) is 170 times faster the incremental velocity provided by a mass ratio of six.

If our benchmark **distance** is one light-year, or 5,880 billion ($5{,}880 \times 10^9$) statute miles, or 1,602 times more distant than Pluto, to reach that distance in a 15-year one-way time the specific impulse of the propulsion system would have to be 1,602 times greater than that of current rockets. If that was so, we could travel 1,602 times farther in the same 15-year time period. That is, the propulsion system I_{sp} must be 1,602 times 300 sec (the best I_{sp} feasible with storable propellants), or 480,600 sec, or a characteristic velocity of 4,713,000 m/sec, about 1.6% of the light speed. The most advanced nuclear electric propulsion we have today is capable of about 4,000 sec, just 13.3 times greater than current storable propellant rocket specific impulse, so that we can travel 13.3 times farther in the same 15-year time period, or 48.8 billion statute miles. This enables us to reach the so-called 'Oort Cloud', the origin of long-period comets, and a region of space very distant from any major astronomical object outside of our Solar System. So we are confined to our Solar System if our travel time is going to be the duration of a human project team and our current propulsion systems. At the distance of one light-year and with current *storable* propellants, the travel time to one light-year distance from Earth is about 24,032 years. That is about the length of human recorded history. With our best nuclear electric propulsion the distance to one light-year is 1,807 years.

Within our Galaxy, to reach α-Centauri (or: Alpha Centauri), one of the seven stars within 10 light-years of Earth and 6,580 times more distant than Pluto in 15 years' one-way travel, the specific impulse would have to be over 1.970×10^7 sec, or the characteristic velocity 64% of light speed. If we could develop a propulsion system with an exhaust velocity equal to the speed of light, the specific impulse would be 30,569,962 sec. Our Galaxy is a spiral about 100,000 light-years in diameter with a central 'bulge' about 20,000 light-years deep. Our Solar System is about 33,000 light-years from the galactic center. To reach past our Galaxy to our nearest galaxy, Andromeda, that is 3,158,000 times more distant than Pluto, the I_{sp} would have to be on the order of 950×10^9 sec and the characteristic velocity would have to be an impossible 6.47×10^{12} or 21,600 times the light speed. That velocity is not conceivable within our current understanding of physics. Figure 1 shows the spiral galaxy Andromeda in ultraviolet wavelength by the GALEX Satellite and in visible light (see the GALEX/JPL website). The Andromeda Galaxy is the most

Figure 1. Andromeda Galaxy from the GALEX/JPL website [*irastro.jpl.nasa.gov/GalCen*, 2005].

massive of the local group of galaxies, which includes our Milky Way, and is the nearest large galaxy similar to our own. The GALEX ultraviolet image shows regions of young hot, high-mass stars tracing out the spiral arms where star formation is occurring. The central white 'bulge' is populated by old and cooler stars formed long ago, and where a central supermassive black hole is very likely located. The GALEX image is compared to a visible light image. The stars in the foreground are stars in our Galaxy, the Milky Way. The composite image from the JPL website in Figure 2 reveals a star-forming region at the center of the Milky Way as recorded by several infrared wavelengths invisible to the eye [*irastro.jpl.nasa.gov/GalCen*, 2005]. A black hole three million times heavier than our Sun has a gravitational pull so powerful that not even light can escape from its surface. The dusty material (called the Northern Arm) in the picture is spiraling into the black hole, and may trigger the formation of new stars. The black hole continues to grow larger as this material falls into it. The small bright star just above the black hole and to the left of the larger star is a red super giant nearing the last stages of its life. It is 100,000 times brighter than our Sun. The scale of the MIRLIN (Mid-Infrared Large Well Imager) is indicated by the one light year bar

Related to this aspect of travel is the chance of discovering life, perhaps intelligent life, that has been the underlying purpose of all human exploration since *Homo erectus* started wandering and eventually moved out of Africa. As we know it, life *as we know it at least*, may exist only under a narrow band of planetary conditions: for instance, a life-hosting planet must orbit a star or stars not too hot or too cold, must be of the right density, and so on [Gonzalez et al., 2001]. Figure 3, from *Scientific American*, shows the Galactic habitable zone and the Solar habitable zone. To the

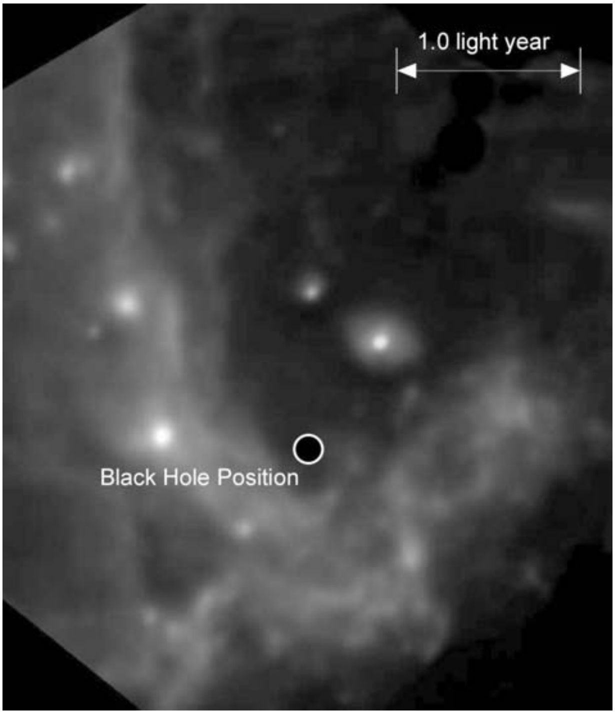

Figure 2. MIRLIN (Mid-Infrared Large Well Imager) image of the black hole at the center of the Milky Way [*irastro.jpl.nasa.gov/GalCen*, 2005].

center of our Galaxy radiation would not permit biological life to exist. Outside the Galactic habitable zone the planets forming around the stars would be gas giants as there are insufficient heavy molecular weight materials to produce rocky planets. The same it true for the Solar habitable zone. Venus is too hot and beyond Mars are only gas planets. Mars might have been habitable if it were larger and able to retain an atmosphere. To reach other galaxies or even stars within our Galaxy seems definitely impossible, as physics tells us, so we must reach other galaxies by means other than conventional ejected mass propulsion. Distances and times involved are currently beyond comprehension unless travel in Einstein's space-time coordinate can be accomplished. This is discussed in a speculative way in Chapter 9, as it is the only way we can leave the shackles of our own Solar System.

All travel within our own Solar System (and perhaps, some time in the future, to distant places in our Galaxy) depends on a regular schedule to reach Earth orbit. In other words establishing a transportation system to Earth orbit is analogous to establishing the transcontinental railroad from Council Bluffs, Iowa, to Sacramento, California, in the late 1800s. That includes the space equivalent to the rail switching yard and marshalling yards that store and organize the materials to be shipped and that are returned. The key identifying characteristic of a transportation is that the flow of goods and materials is *two-way transport*.

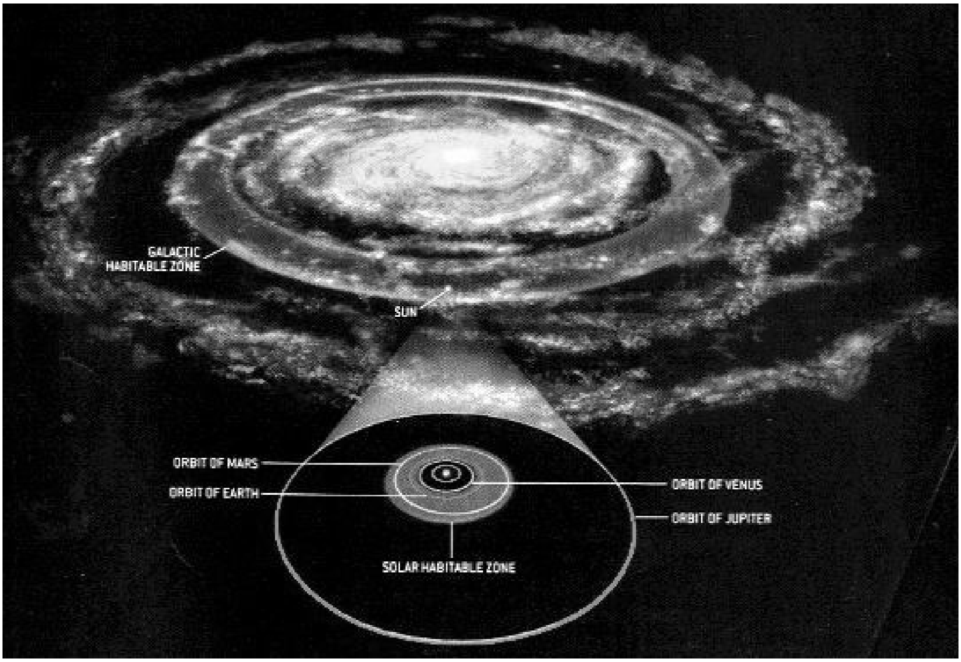

Figure 3. Habitable zones of life and Earth-like solar systems. Reproduced from Gonzales et al. [2001]

One last observation. In the space organizations today the primary word is 'Technology' with the implication that without technology progress cannot be made, or that the next generation launcher or satellite cannot be created without 'new' technology. Now, technology has played an important role in electronics, sensors and communications systems. Technology has played a role in improving the materials available for launchers by making them lighter and with better characteristics. But in the latter case, the new materials *are not* an enabling technology, but only an improvement technology. New classes of orbital vehicle and space launchers and associated propulsion systems were envisioned and were capable of being constructed for well over 40 years. The newly developed industrial capability is simply less difficult to handle than it would have been 40 years ago, and it is certainly possible with it to fabricate these launcher configurations and propulsion systems today. Figure 4 shows an airbreathing configuration that originated in the 1960s and spans from then to the 1990s keeping a remarkable similarity. What has not changed is the composition of the air, the behavior of the air, and the characteristics of the air flowing over a body at high speed or low speed. Our ability to analyze the details of the flow field have increased instead enormously. Our ability to use aerodynamic and thermodynamic analyses to create an efficient configuration, based on air behavior, established viable configurations decades ago. Comparing older and today's configurations it is obvious they are remarkably similar, even when considering different design teams in different countries over a span of 25 years.

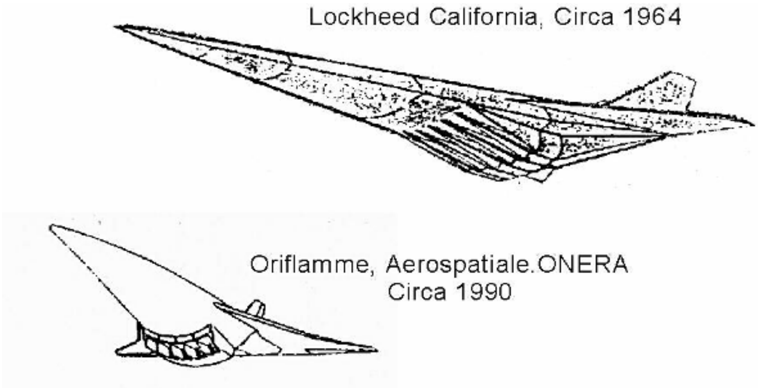

Figure 4. Two scramjet-powered space launchers for approximately Mach 12 airbreather operation.

Remember the Saturn I launcher was assembled from essentially scrap launcher tanks and engines, to demonstrate the feasibility of Saturn V. If we have lost anything, it is the ability *to make the decisions* that turn ideas and analyses into hardware. That is fraught with risk and uncertainty under the best of circumstances. To these authors, the difference between now and the past is the absence of extensive testing, and of the ability, or willingness, to alter designs when test results indicate an altered path is better. All the scientific and technological progress and improved understanding we have acquired during the past forty years has produced a paradoxical result: the ability to make decisions turning studies and ideas into *further* paper studies and numerical analyses, with the ultimate goal of eliminating *all risk* and unanswered questions. This circular thinking shies away from materially *testing* ideas and analyses; it prefers waiting for *further* proofs and *further* analyses. Test hardware failures are *not* failures, but milestones along the *paths* to success, by identifying analytical limitations and the need to correct the hardware. A truly real failure is a test that fails and is therefore canceled, without learning the cause and its remedy. A path that is void of material hardware is a path of undefined limits and undefined requirements. The path to *successful* hardware, is 'success framed by your failures', that enables you to know where the limits are, and why.

The remainder of this book strives to describe advanced propulsion embodying this philosophy. It starts by looking at what was accomplished in propulsion after the Sputnik days of the 1950s in order to improve the performance of the impressive but inefficient rocket launchers of that time. It then draws from the experience and attempts of the past to picture and suggest the future of propulsion. The logical framework for any new progress in propulsion is that of the missions that such progress can enable; thus, in what follows it will be marked by major yardsticks, from the first indispensable step, reaching Earth orbit more economically and routinely, to the building of a space infrastructure that is both technologically and economically viable; and, ultimately, in a far future, to human beings boldly exploring what lies beyond our Solar System.

BIBLIOGRAPHY

AW&ST: Aviation Week and Space Technology (2003) Vol. 158, No. 9, p. 19. McGraw-Hill, New York.

Davis, T. E. (2004), 'The Cosmic Matrix Displacement Model (An Explanation for Gravity and Inertia)', paper AIAA 2004-3759, 40th Joint Propulsion Conference, Fort Lauderdale, Florida, July 2004.

Goff, A., and Siegel, J. (2004) 'Can Conventional Warp Drive Avoid Temporal Paradox', AIAA 2004-3699, 40th Joint Propulsion Conference, Fort Lauderdale, Florida, July 2004.

Goldin, G., and Svetlichny, G. (1994) 'Nonlinear Schroedinger Equation and Separation Property', *Journal of Mathematical Physics*, **35**(7), 3322–3332.

Gonzalez, G., Brownlee, D., and Ward, P. D. (2001) 'Refuges for Life in a Hostile Universe', *Scientific American*, Vol. 284, No. 10, pp. 52–59.

1

Overview

1.1 THE CHALLENGE

Space travel represents a daunting challenge for human beings. Space is devoid of any life-support elements for Earth-born humans. Remember that one of those life-support elements is gravity. So human space travelers must carry all of their life-support systems along with them and find a way to create a sustained artificial gravity vector of yet-to-be determined minimum or maximum value. For short Earth orbit missions, carried consumables and repair parts that can be re-supplied from Earth provide a near-term, acceptable solution. For future long missions the supply of consumables (oxygen, water, food, and power) must be self-sustainable onboard the spacecraft. Spare parts must be in sufficient supply to assure operation of critical hardware. However, as humans attempt to explore further and further from Earth, the system that enables increasingly distance travels is still **propulsion**. In fact, food and other life-sustaining matter increase linearly with travel time and crew size, while Tsiolkowski's law shows that accelerating a spacecraft by expelling mass (i.e., using Newton's third principle) needs a propellant mass that increases exponentially with increasing speed and initial mass. Thus long travel times are a balance between the mass controlled by propulsion performance and the mass contributed by human support systems. No matter what support systems are available for humans, without appropriate propulsion the necessary time and distance cannot be traversed. So whether human travelers or an automatic robotic system occupies the spacecraft, the **propulsion system** is the single key element. Remember, in space whatever velocity is imparted remains essentially unchanged. In order to orbit a distant object, the spacecraft must slow down to the initial speed of launch, and equal propellant mass ratio must be expended to decelerate the vehicle as was spent accelerating the vehicle. As we shall see, this propellant mass is not trivial.

1.1.1 Historical developments

The former USSR orbited the first artificial satellite, Sputnik, in 1957. Eleven years later six Apollo missions to the moon enabled 12 astronauts to stand on the moon, explore its surface, and return samples [Stafford, 1970]. With one short-lived attempt at building an orbital station using an empty Saturn V upper stage tank, an empty Saturn V, S-IV upper stage tank was outfitted to be inhabitable as the Skylab [Skylab, *Aviation Week* 1985]. After Skylab was permitted to enter the atmosphere and be destroyed, all United States human exploration ended. Not until the next century would the United States, using Russian hardware, place an inhabitable orbital station into orbit. In that almost 30-year gap, the nations of the former Soviet Union (USSR) launched a series of Salyut orbital stations, culminating with MIR, the seventh Russian orbital station. MIR had served successfully for 15 years, which was about three times its design life. Then in 2001, after suffering the ravages of solar radiation and the space environment, it was deorbited into the Pacific Ocean [*Aviation Week*, MIR Deorbit, 2001]. This ended a long Russian history of humans living in space on an orbital station. In fact Salyut 6 had to be shut down because of a leak in the hypergolic propellant lines for the station-keeping rocket engines. A former student at Moscow Aviation Institute that had the Salyut orbital propulsion system as a design project was now a cosmonaut. After being launched to Salyut 6 on a Soyuz rocket, he repaired the leak with equipment he helped design and re-established the orbital station operation [Cosmonaut, Private Communication, Los Angeles, 1984]. In 2000 the International Space Station (ISS) was established in the Russian orbital plane of 55° and was constructed with a large fraction of Russian hardware. Its re-supply is primarily a responsibility of Russia with its Progress/Soyuz launch system, and many of the more massive components can be lifted with the Russian Proton launcher if the Space Shuttle is not available for the mission. As with MIR, the key to successful utilization of an orbital station is the frequent and reliable transportation system that can regularly maintain supplies and rotate crewmembers. In effect what is required is a 'train' to and from space that operates with the scheduled frequency and reliability of a real train. The principal difference between a rocket-to-space and a train-to-space is that trains are two-way transportation for people and materials. When one of the authors visited Baikonur in 1990, the Soyuz launch complex had launched 92 Soyuz rockets in the previous 12 months, which is a very good record, but other than allowing the return of astronauts, Soyuz it is a one-way transportation system.

The Russian experience is the only database about humans and long-term exposure to the near-Earth space and the microgravity-magnetic environment. In fact, discussions colleagues have had with Russian researchers indicate the human physiology might become irreversibly adapted to microgravity after periods in orbit that exceed one year [Hansson, 1987, 1991]. With other experiments that compared animal physiology response in low Earth orbit (LEO) to geostationary Earth orbit (GEO) using Rhesus monkeys [Hansson, 1987, 1991, 1993] there were differences in adrenal cortex manufactured hormone effectiveness that were initially attributed to the absence of the Earth's magnetic field in configuring hormone receptor sites. This experience showed how much remains to be learned about the adaptability of the human physiology and chemistry to space. In fact one conclusion that might be drawn from the Russian data is that the human physiology is too adaptable. That is, the human physiology attempts to convert a gravity physiology into a micro-gravity physiology. There is a debate as to whether the gravity of the Moon is sufficient to induce a gravity physiology. Former astronaut Thomas Stafford thinks that it might be, but only time spent on the Moon will tell [Stafford, 1990]. If the Russian data on the essential presence of a low-level magnetic field is confirmed, then that will be an additional environmental requirement for long-term human space travel. Now the Unites States is just beginning to gather data on long-term orbital exposure with the International Space Station (ISS) in the Russian orbital plane of 55°.

As distances of missions from Earth increase, the propulsion challenge increases because the mission time increases. Missions need to be made within the possible lifetime of the project team, that is approximately 20 earth years. Earth years are specified because as the fraction of light speed increases, the time dilatation for the crew increases. That is a 20-Earth-year mission for the Earth-bound project team will be less than 20 years for the crew.

There are two classes of mission possible. The first is a one-way mission that explores a distant object and electronically communicates the information to Earth. Remember that if that is to a celestial object one light-year away, then communication will take a two-Earth-year round trip! The second is a two-way mission in which something is returned to Earth after exploring a distant object. This can deliver a greater trove of information than the one-way mission. However, a return mission is far more challenging. If the returning spacecraft travels at the speed of light, then the returning spacecraft will appear at Earth at the same time the light traveling from their destination shows them leaving!

1.2 THE CHALLENGE OF FLYING TO SPACE

A predisposition to use rockets derived from military ballistic missiles, forced by the military competition between the United States and the former USSR, curtailed efforts to develop alternatives to chemical rockets together with practical commercial developments. With the orbiting of Sputnik, the aircraft path to space, represented in the US by the series of X planes [Miller, 2001] and with the X-15 [Jenkins and Landis, 2003] came to an end. With the X-15 demise, all efforts *to fly* to space ended and was replaced by the more familiar (but less practical) strategy based on blasting to space with expendable rockets derived from not-so-well-tried ballistic missile hardware, as early failures documented. Like their ballistic missile progenitors, current expendable rockets are launched for the first, last and only time. In this context a reusable launcher is simply an expendable with some parts reused a few times. Thus neither the USA nor the former USSR have ever realized a truly commercial approach to space travel, although the former USSR was close to achieving a first step with the Energia/Buran system. Energia flew first on its first flight with a cargo pod installed. Energia/Buran flew only once after that. The several Energia launchers and the two Buran hypersonic gliders were eventually scrapped or sent to museums. The roof of the assembly building at Baikonur collapsed in the late 1990s and perhaps the most ambitious, fully recoverable launcher and glider system to have been built was no more. Both the United States and the former USSR have generated a large number of concepts that could fly directly to space and return on a sustained, frequent, and scheduled basis.

The subject of this book is space propulsion; however, in exiting the Earth's atmosphere, the propulsion system and configuration are inexorably linked. An aircraft that is a hypersonic glider exits the atmosphere on either rocket boosters or a first stage of a two-stage-to-orbit aircraft. As such it exits the atmosphere quickly, and the key exit design considerations are the high aerodynamic and mechanical loads encountered in the exit trajectory. Whether a new launcher or the Space Shuttle, the phenomenon is the same, the peak mechanical loads occurring during exit in the region around Mach 1. In this case the exit aerodynamics are important but not vital. The vital aerodynamics and thermodynamics (aerothermodynamics) are in the entry glide, where thermal loads are a maximum and must be controlled. The vehicle must always be controlled in flight so that its attitude and direction are within limits set by aerothermodynamics. The angle of attack limits are very close for high-performance hypersonic gliders, as their glide angle of attack is 11° to 15°, not the 40° of the US Space Shuttle. Even the Russian Buran had a lower glide angle of attack than that of the Shuttle. The Russian Central Aerodynamics Institute (TsAGI) reports show that it is about 30° to 35° [Neyland, 1988]. Like Buran, the high-performance glider is best controlled by an automatic integrated flight control system that monitors the thermodynamic state of the vehicle as well as the aerodynamic and trajectory states. The sensor array provides real time information to the control system that can maintain the correct attitude in a manner a human controller would not be able to accomplish. So it is this phase of the flight that 'designs' the vehicle. Since staging, that is separation from its first stage launcher, occurs in the Mach 8 to 12 range, the propulsion system is usually a hydrogen/oxygen rocket. That means that the configuration is designed for entry, and that propulsion does not determine the configuration.

An aircraft that uses airbreathing propulsion to exit the atmosphere has the same entry issues as the hypersonic glider. However, the capture of atmospheric air to create thrust by chemical combustion is an additional and different issue, as it must configure the underside (aerodynamic compression side) as an integrated propulsion system that produces more thrust than drag and that also produces lift. For the propulsion system to function efficiently the dynamic pressure and air mass flow per unit area must be higher than in a rocket exit trajectory, as it is the airflow that enables the propulsion system to produce thrust in excess of drag so the vehicle can accelerate. Thus in this case we have a propulsion-configured vehicle. Neither the shape of the vehicle nor the trajectory it flies are arbitrary. The airbreather does not exit the atmosphere quickly, as the rocket does, but stays in the atmosphere to the point where the transition to rocket propulsion occurs (usually Mach 8 to 12). The airbreathing propulsion system mechanical, aerodynamic, and thermal loads act longer and are of greater magnitude than the rocket-powered vehicle. In fact the dynamic pressure, that is the pressure of the air impacting the vehicle, is about ten times greater than the entry dynamic pressure of the hypersonic glider. In this case the principal thermal load is encountered during exit from the atmosphere, and the vehicle *must* be configured to generate sufficient thrust to exceed sufficiently drag to provide a strong acceleration. So an airbreather configuration is different from the hypersonic glider, because the hypersonic glider has not been configured to fly extensively in the atmosphere and produce thrust from a captured airflow. Like the hypersonic glider, this vehicle needs the same glide performance at entry. However, with the thermal protection designed by the high exit loads, the entry design is one of detail in maintaining stability and control, and achieving a comparable lift-to-drag ratio while gliding. There is one exception, that is, as we will see in later chapters, there is an airbreathing/rocket-powered hypersonic rocket that operates at a lower Mach number (compared to orbital Mach number of 25 plus) and can accommodate a retractable inlet working up to about Mach 5.

The question is always, why bother with airbreathing at all if it is that much of a challenge. The answer is twofold. (1) Oxidizer carried is heavy, and requires more engine thrust to lift it into space. A hydrogen/oxygen rocket, vertical-launch vehicle with a 7,000 kg payload has a gross weight in the 450,000 to 500,000 kg range and has a 50,000 kg operational empty weight, that is, with the payload loaded. The engine thrust for a vertical takeoff is about 5,950 kilonewtons to 6,620 kilonewtons. A modest performance combined-cycle airbreather that transitions to rocket at about Mach 12 has the same empty weight with payload installed, but a gross weight in the 200,000 to 225,000 kg range. The engine thrust for a vertical takeoff is about 2,650 kilonewtons to 2,980 kilonewtons. Most of the gross weight reduction is from the lesser amount of oxidizer carried and the lighter propulsion system weight. So the installed thrust is about one-half, and the volume is less. An advanced airbreathing system has the potential to reduce the gross weight to the 125,000 to 150,000 kg level (the attributes of different propulsion systems and their impact on size and weight are discussed in Chapter 4). (2) An operational system is sought that is capable of a large number of flights per year. Less resources required for launch means that the system can operate at greater ease and has the potential to operate from more bases. Glebe Lozino-Lozinski had a concept for a spacecraft with a seven metric ton payload carried atop an Antonov An-225, with a second aircraft carrying the liquid hydrogen, launch facilities and staff [Plokhikh, 1989]. It could literally launch a satellite from any facility that could accommodate a B-747 or MDC-11.

1.3 OPERATIONAL REQUIREMENTS

The United States was not the only nation to think beyond rockets. Figure 1.1 shows a spectrum of different launcher concepts investigated by different launcher concept designs from the 1956 to 1981 time period [Miller, 1993]. Numbers in Table 1.1

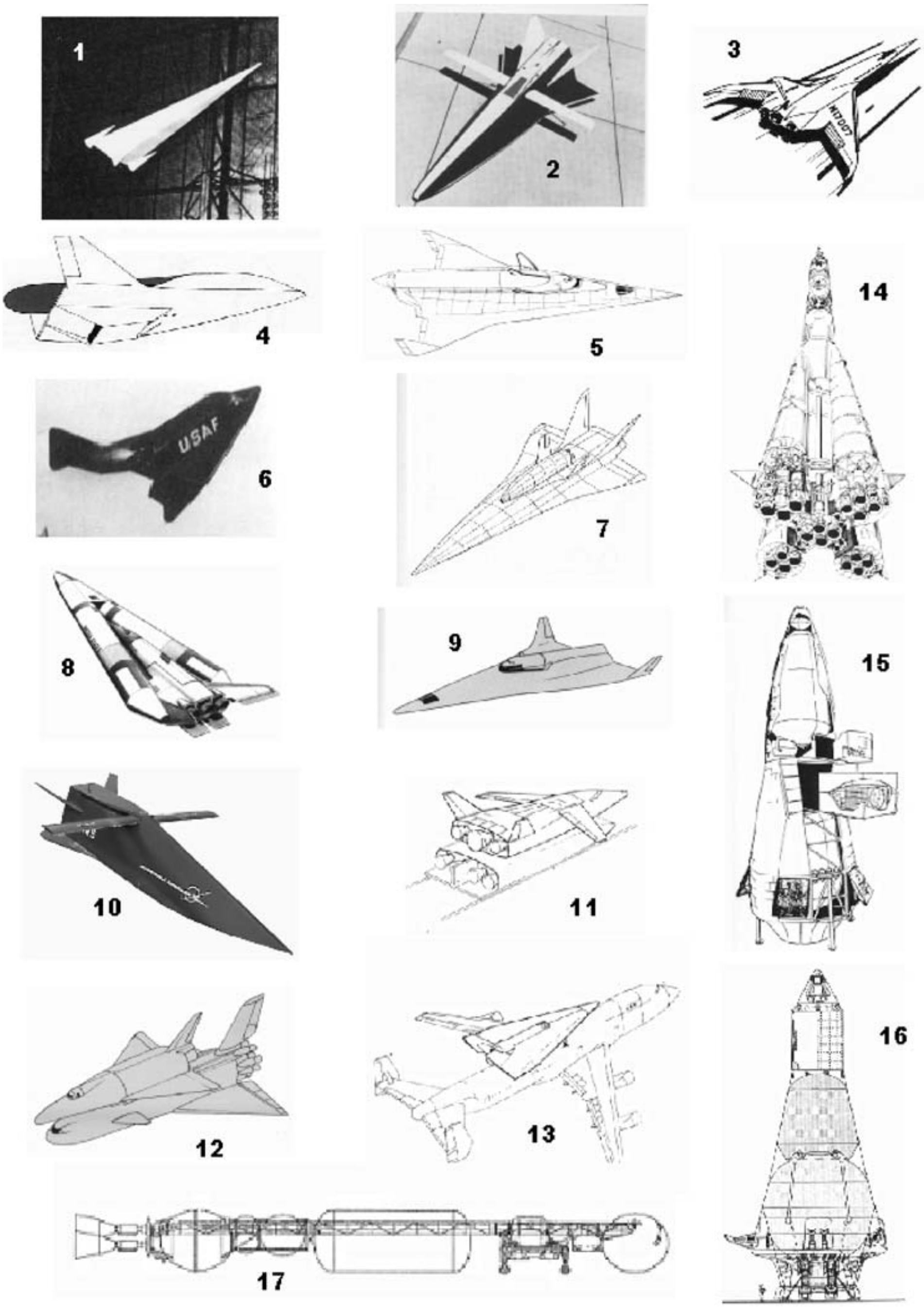

Figure 1.1. Spectrum of launchers/spacecraft from 1956 to 1981.

Table 1.1. Identification of configurations in Figure 1.1.

#	System	#	System
1	HYARDS, USAF, 1956	10	McDonnell Douglas FDL-7MC/MRS
2	Hyper III, NASA, 1964	11	USAF, General Dynamics, 1981
3	G. Harry Stine, 1957	12	Martin Marietta, 1971
4	USAF Spaceplane, 1960	13	USAF, General Dynamics, 1981
5	Mig/Lozinski 50/50, 1962	14	A-1, Vostok, 1961
6	USAF/Boeing, DynaSoar-X-20 1959	15	MDC, Delta Clipper, 1990
7	MBB, Sanger II, 1984	16	GD, Millennium Express, 1991
8	Lockheed Star Clipper 1964	17	Boeing Mars Mission, 1991
9	Dassault, Star-H, 1984	18	

identify the configurations. Examining the images of the launchers and spacecraft we find an excellent cross-section of the past 50 years. There are three configurations that have variable-geometry features employing retractable straight wings for improved landing and takeoff, i.e., numbers 2, 10 and 11. All of the spacecraft are delta planforms, except for Harry Stine's horizontal takeoff and landing concept, number 3. Configurations 5, 7 and 9 are two-stage-to-orbit (TSTO) concepts that are very similar. The German 'Saenger' configuration (7) by MBB employs a hypersonic glider that carries onboard the propellant necessary to achieve orbit, maneuver and return. Lozinski (5) and Dassault (9) both have a different philosophy from MBB with respect to the propellant to reach orbit. In their studies it was more economical to carry the ascent propellant in an expendable rocket and to carry maneuver and return propellant on board the spacecraft. In fact, the question of propellant has many answers, depending on flight rate, and has yet to be determined today. If the flight rate postulated as needed in 1965 were real (74 flights per year) the answer would probably favor the MBB approach. All three of these designs had the idea to use the first stage (which staged the second stage at Mach number from 6 to 7) for a Mach 4.5 to 5 hypersonic cruise aircraft. If sub-cooled liquid methane were substituted for the hydrogen, with the same total energy content, the methane would occupy only 36% of the hydrogen tank volume. The 64% of the hydrogen tank would now make a perfectly well insulated cabin for either carrying cargo or human passengers. The useful range of such an aircraft would easily be in the 6,500 nautical mile (12,040 km) category.

Of the vertical launch rockets in Table 1.1, one is expendable, the Vostock launcher from the former USSR. The Vostock launcher is designated SL-3. The growth version of this launcher is the SL-4, the Soyuz launcher. It is in fact from the former USSR, as the companies that supply the hardware and launch facilities for the Soyuz are now in separate nations. However, it is show because Soyuz has achieved the launch rate required to support the 1965 space station (it is noteworthy that in 1991 there were 92 launches from the three Soyuz pads at the Baikonour launch facility). The other two, the MDC Delta Clipper and the GD Millenium Express are intended to be sustained use vehicles, although not at the rate required to support the 1965 space station. Reusable vertical launch vehicles are important because they can lift heavy payloads to orbit when required by the mission, such as orbital assembly of space stations, or of the deep space and Mars vehicles represented by configuration 17.

We have now established that the launchers and propulsion to get to Earth's orbit is neither beyond current capability (nor was it beyond 1965 capability!) nor limiting in establishing a space transportation system or infrastructure. So now it is to the future to achieve the dreams of the past generation.

Still in the context of reusable versus 'throwaway' launchers, it is a fact that the expediency of launching another expendable rocket historically has always won over the will to develop a commercial, sustained-use, multiple-launch spacecraft. As a consequence, the current 'progressive' path is still an expendable rocket, albeit with some parts reusable. In October 1999 at the International Astronautics Federation (IAF) Congress in Amsterdam, an IAF paper reported that US-Russian cooperation resulted in a hydrogen/oxygen rocket engine (the RD-0120, in the Russian classification) for the Energia launcher that had been fired on a test stand for 80 simulated launches and returns, with a throttle up during ascent to 135% rated thrust (the US Shuttle engine, the SME, throttles up to about 109% rated thrust). A manager from one of the US rocket launcher companies exclaimed, 'This is terrible, we would have lost 79 launcher sales!' [Davis, 1999]. That explains why sustained operational use spacecraft never developed. The rocket launcher organizations never proceeded along a path analogous to that taken by the Douglas Aircraft Company with the DC-3, DC-4, DC-6, DC-7 and DC-8 commercial transport family, to cite one example. From 1934 to 1974 this series of commercial transports went from reciprocating engines with propellers, with 150 mph speed and 1000 miles range, to gas-turbine-powered jet aircraft, flying for 7,000 miles at 550 mph. In the 40 years from the first artificial satellite (Sputnik) the launcher is still the liquid-rocket-powered ballistic missile of the late 1950s. The aerospace establishment has forgotten the heritage of its pioneers and dreamers. It has forgotten to dream, preferring to rely on a comfortable (and certainly perceived safer by shareholders) status quo. These historical motivations and current perceptions will have to be reassessed if man is to travel in space for longer distances than those typical of the near-Earth environment. A synthetic description of distances and time in our Solar System and our galaxy will illustrate this point.

1.4 OPERATIONAL SPACE DISTANCES, SPEED AND TIMES

Envisioning the time and space of our Solar System, our Milky Way galaxy, and intergalactic space is a challenge for anyone. In terms of our current best space propulsion systems, it takes over one year to travel to our planetary neighbor, Mars. It can take up to 12 minutes for a microwave signal to reach Mars from Earth. Consider a rover on Mars that is approaching an obstacle or canyon. When the picture of that is received on Earth it is already 12 minutes behind actuality. By the time a stop signal reaches the rover, between 24 and 30 minutes

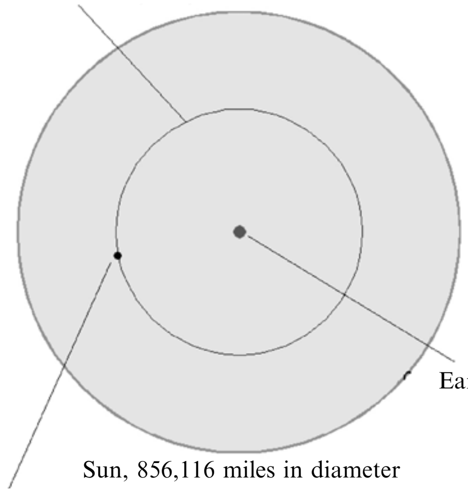

Figure 1.2. Diameter of the Sun compared with the Moon's orbital diameter.

have elapsed, depending on the speed of the project team. It is another 12 minutes, or a 36 to 42 minute elapsed time, before the project team knows whether the rover was saved, stalled, damaged or destroyed. With the control center on Earth, the time interval is too long to assure the rover remains operational, so an independent intelligent robot is a necessity. Traveling to our remotest planetary neighbor, Pluto, requires a daunting 19 years. In terms of light speed, it is a mere 5 hours 13 minutes, at Pluto's average distance from Earth. And this is just the outer edge of our planets, not our Solar System. To the edge of our Solar System, the boundary between our Solar System and the oncoming galactic space medium, the Heliopause, the light time is 11.5 hours. Envisioning the size of our Solar System is also a challenge. For example, our Sun is 109 times the diameter of the Earth and 1.79 times the diameter of the Moon's orbit around Earth, as depicted in Figure 1.2, and the Sun represents the single most massive object in our Solar System. From the Sun, we can proceed outward to the outer edge of our Solar System and our nearest star, Proxima Centauri. Proxima Centauri is a very dim star; its slightly more distant neighbor, Alpha Centauri is instead very bright, but they are near the Southern Cross and only visible from the Southern Hemisphere. A cross-section of our local galactic space is presented in Figure 1.3. Remember that an astronomical unit (AU) is the distance to an object divided by the Earth's distance from the Sun, so Jupiter is 5.20 AU from the Sun means that Jupiter is 5.2 times further from the Sun than Earth is. Figure 1.3 spans the space from the Sun to our nearest star, Proxima Centauri. The space is divided into three zones. The first zone contains the terrestrial planets; those are planets that are rocky, Earth-like in composition. These are Mercury, Venus, *Earth*, Mars and a band of rocky debris called the Asteroid Belt. The second zone contains the Jovian planets; those are planets that are essentially

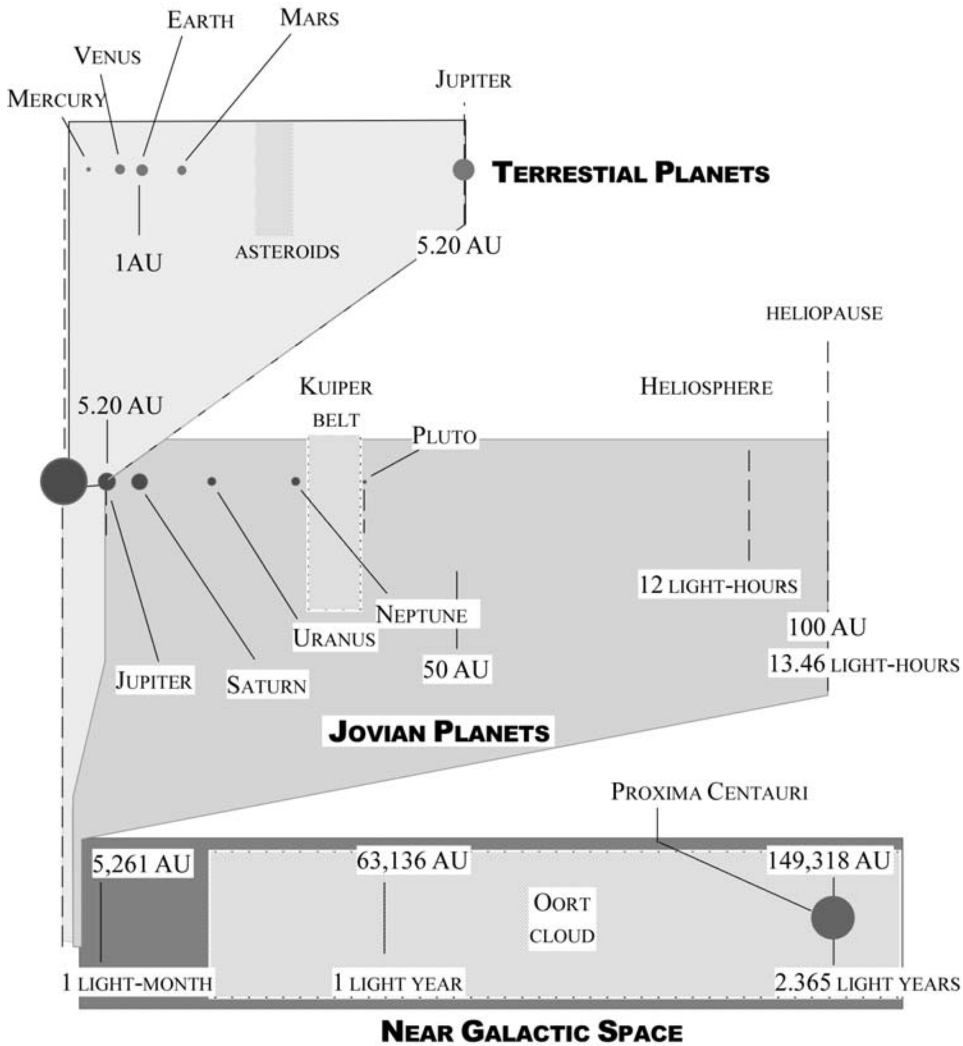

Figure 1.3. Sun to near galactic space in three segments.

gas planets without a rocky core, but could have cores of liquefied or frozen gases. Within this band are the gas giants of Jupiter (11.1 times the diameter of Earth), and Saturn (9.5 times the diameter of Earth). Uranus and Neptune are 4 and 3.9 times the diameter of Earth respectively. Jupiter is so massive that it is almost a sun. The radiation associated with Jupiter is very intense and without massive shielding would be lethal to any human in the vicinity. The second zone extends to the boundary of our Solar System and the galactic medium, the Heliopause. The third zone spans the distance from the Heliopause to the vicinity of Alpha Centauri. In this zone you can see the Jovian planets and the terrestrial planets compressed into two narrow bands.

That is, the size of our Solar System (100 AU) compared to the distance to our nearest star (149,318 AU) is very small indeed. The near galactic space contains a spherical shell about 140,000 AU thick that contains icy and rocky objects of differing sizes. Because the objects appear dark they are very difficult to resolve in visible light. It is from this shell of objects that most long-term comets (such as Halley's) appear to originate. The volume of space encompassed by our Solar System traveling through the galactic medium is called the Heliosphere. Note that between the Heliopause boundary that defines the volume of space encompassed by our Solar System traveling through the galactic medium, and the nearest star, space is essentially devoid of any substantial objects. Even the Oort Cloud begins at a distance some 100 times greater then the Heliopause. If we look at distances measured in light travel time these dimensions are reaffirmed. The outermost planet Pluto is 38.9 AU distant from the Sun. Even with these figures in mind, it is still difficult to visualize the size of our local space. That is important because it is the size of space that determines the character of the propulsion system needed.

The Sun is a logical reference point for visualizing size and distance. One approach to permit visualization of our Solar System is to scale down the system to comprehensible object sizes and distances. To do that, visualize the Sun not as a sphere 856,116 statute miles (1,377,800 km) in diameter, but as a 400 mm diameter (14.75 inch) soccer ball. Doing so means the diameter of the Earth (7927 miles or 12,757 km) is about the diameter of a pea some 43 meters from the soccer ball. Table 1.2 gives the diameter (mm) and distances (m or km) of the objects listed, from our Sun to our nearest galaxy.

In this analogy, Pluto is about one-half the diameter of the Earth, and on this scale is at 1.7 kilometers from the soccer ball. To illustrate now the snail's pace of our travels, traveling to Pluto directly, e.g., without gravity assists from the massive planets, with our current chemical and future nuclear-electric or nuclear-thermal propulsion systems, would take 19 years, at the blinding speed of 220 mm per day on this scale. We truly move at a snail's pace in the dimensions of our Solar System! If we are to move faster, it is propulsion that will enable that greater speed. Over 19 years the true average speed to Pluto using conventional propulsion mentioned, is 32,326 ft/sec (9.853 km/sec). Of course that is an average, i.e., if the spacecraft flew along a radial path from Earth, through the Sun and on to Pluto as if they were all aligned. That is not the case, and the actual path is actually a curve longer than a radius, so the actual speed should be faster. If we wanted the spacecraft to reach Pluto in one year, its average speed would have to be 19 times faster, or 614,100 ft/sec (187.2 km/sec). To obtain the incremental speed, the specific impulse of the propulsion system (the performance index defined in the Introduction) would have to be not the 300 sec of current chemical boosters, or the 3000 sec (2,942 m/sec) of electric thrusters, but 5,509 sec (54,025 m/sec). This number is well beyond our current capability.

In one popular space travel television show it is merely specifying the warp speed and pronouncing, 'engage' that (within several minutes or hours) transport the crew of the Enterprise to their destination. In reality nothing could be further from reality, as we know it today. The Heliopause (the boundary between our Solar System and

Table 1.2. Scale of diameters and distances to objects in space.

	Diameter (mm)	Distance	Distance units
Sun	400	0.00	m
Mercury	1.395	16.79	m
Venus	3.486	30.99	m
Earth	3.670	43.04	m
Mars	1.945	65.42	m
Asteroids		116.2	m
Jupiter	41.10	223.8	m
Saturn	34.50	410.6	m
Uranus	15.41	825.5	m
Neptune	14.68	1,293	m
Kuiper Belt		1,291	m
Pluto	1.834	1,696	m
Heliopause		**4.304**	**km**
Oort Cloud		4.304	km
Oort Cloud		43.04	km
One light-year		**2,717**	**km**
Proxima Centauri		11,443	km
Magellanic Cloud		5.437×10^8	km
(M-31) Andromeda		5.981×10^9	km

the oncoming galactic space medium our Solar System travels through space in the Milky Way) is 4.3 kilometers on the soccer ball scale. One light-year is some 630 times farther, at some 2,717 km from the soccer ball. That is the distance between St. Louis and Washington DC. Still on this scale, the nearest star in our Milky Way Galaxy would be 11,433 kilometers distant, or 2,660 times more distant than Pluto. If Proxima Centauri were in Tokyo the soccer ball (Sun) would be in London! At our snail's pace of 220 mm per day, that is over 1,400 centuries away! To reach Proxima Centauri within one year we would have to travel at about 2.5 times the speed of light. The galactic center is 13,500 times more distant than the nearest star [Harwit, 1973; Kaufmann, 1993] so if we could reach Proxima Centauri in one year at 2.5 times light speed, then it would still take 13,500 years to reach the galactic center! If we were to reach the galactic center within one year we would have to fly at 33,000 the speed of light—or, in Mr Spock's language, 'warp 5.5' (this assumes the speed of light is warp 1.0). The nearest galaxy-like structures are the small and large Magellanic Clouds. They are almost 85,000 times farther away than the nearest star, so to reach the Magellanic Clouds in one year, we would have to fly a fantastic 212,500 times faster than the speed of light, 'warp 6.3'. The nearest spiral galaxy M-31, Andromeda, is 930,000 times farther than our nearest star, and to reach Andromeda in one year, we would have to fly a mind-bending 2,325,000 times faster than the speed of light, at 'warp speed' 7.4. If the desire is to travel the distance in one month, a quantity of 1.07 would have to be added to the warp speed. For a one-week travel time, 1.7 would have to be added, and for one day

2.6 would have to be added. So even at the speed of light we are trapped within the area bounded by the nearest stars; see also Chapter 8. As we shall see, Einstein's concept of space-time as a four-dimensional space becomes an essential factor to comprehend and perhaps overcome this limitation.

Unless we are able to harness some other form of energy (perhaps, vacuum energy) and accelerate at unheard of accelerations, we will be forever confined to the region of our solar system. In order to accelerate at these unheard of accelerations we must discover not anti-gravity but anti-inertia. Otherwise our resistance to change speed or direction will result in us being flattened to nothingness. Nick Cook in *Jane's Defense Weekly* describes GRASP (Gravity Research for Advanced Space Propulsion) as a project with a similar goal, carried on by the partnership between The Boeing Company, 'Phantom Works' and Evgeny Podkletnov of Russia for a propellant-less propulsion system [Cook, 2001].

1.5 IMPLIED PROPULSION PERFORMANCE

In determining the limits imposed by a conventional thermal (chemical or even nuclear) propulsion systems we will consider two options. The *first* is a two-way mission where the spacecraft accelerates to escape speed, or greater, departing low Earth orbit (LEO) along a trajectory that will intercept its destination object. When the spacecraft reaches the maximum speed allowed by the mass ratio and the propulsion system performance, it then coasts until the spacecraft must decelerate to match its destination velocity requirements. After deceleration, the spacecraft then does a propellant burn to place it in orbit around the destination object. The spacecraft releases a probe to gather data about the target object. After a predetermined period of exploration, the spacecraft accelerates to escape velocity from its destination object, then to its maximum speed determined again by the mass ratio and the propulsion system. It coasts at that speed until it must decelerate to be finally captured in Earth orbit. Figure 1.4 illustrates this notional round trip.

The *second* is to just do a one-way mission and launch a probe or lander to the target object, letting the orbiting spacecraft relay data back to Earth. As we shall see, in Einstein's space-time domain this may not be a viable option for the earth-bound

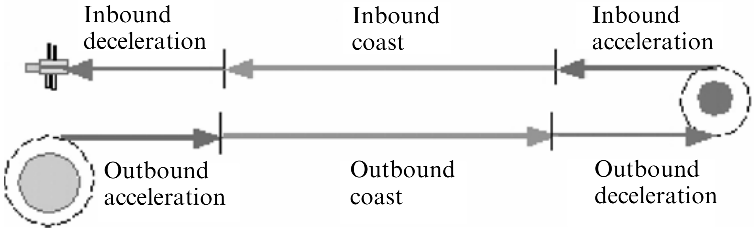

Figure 1.4. Notional round trip to space destination from Earth involving four plus and minus accelerations used to establish mission mass ratios.

Table 1.3. Mass ratios for space exploration mission.

MR per acceleration	*2.0*	*3.0*	*4.0*	*5.0*	*6.0*
One-way	4.86	11.3	20.6	33.1	49.1
Two-way	21.2	114	382	986	2,163

Table 1.4. Current expendable and partially reusable rocket launchers.

Launcher	Nation	Payload (tons)	Gross wt/Payload	Number of lifts
Shuttle	USA	20.4	100	10
Titan IV	USA	17.7	48.9	12
Ariane V	France	17.9	39.6	6
Proton	Russia	20.0	35.1	11
Zenit	Russia	13.7	33.4	15
LM-3B	China	13.6	31.8	15

mission managers. The critical element is the mass ratio for each acceleration and equal deceleration. Table 1.3 gives the total mass ratio from LEO for a one-way and a two-way mission. Included are the mass ratios for orbital transitions in the vicinity of Earth or the target object. It is assumed that, after each major acceleration, the empty propellant tanks are discarded to minimize future propellant expenditures. The propellant tanks weigh approximately 1.5% of the consumed propellant. The probe has a reference mass of 0.25 units and is launched from a spacecraft with a dry mass of 1.0 unit. That one mass unit does not include the expendable propellant tanks or the probe. In the two-way mission, the one mass unit spacecraft is returned to the Earth's surface. The spacecraft one unit dry mass may be in the 5 to 50 tons range for a practical deep-space spacecraft. The mass ratio (MR) shown is from LEO to the end of the mission, either back to Earth or orbiting forever the destination object, as given in Table 1.3. The mass ratio for the two-way mission includes the departing the destination object and entering an Earth orbit on arrival in the vicinity of Earth, so the multiplying factor is somewhat larger than the mass ratio per acceleration squared.

The mass ratio required to lift the spacecraft from the earth's surface to LEO must multiply the mass ratios in Table 1.3. What determines the mass ratio is, *one* a practical limit, and *two* the propulsion system specific impulse. If a 10-ton spacecraft was to be sent to space on a one-way mission, then spacecraft and propellant system mass in LEO would be 206 tons (454,230 lb) for a mass ratio four per each acceleration phase. An Energia configuration with six strap-on boosters could lift 230 tons to LEO in an all cargo configuration, and could lift the 206-ton spacecraft in one lift, as could Saturn V. But since we are now without these superb heavy-lift machines, the lift must be done in multiple launches, as shown in Table 1.4, and assembled in orbit using astronauts/cosmonauts and space walks.

From the data in Table 1.4, the number of lifts for a 206-ton spacecraft to LEO could be a few as six and as great as 15, considering the heavier payload launchers. For a future Combined Cycle Propulsion System the ratio of launcher mass to spacecraft mass (the launcher payload) can be reduced to about 21. That would reduce the launcher mass, but would not reduce the number of lifts to LEO unless the payload was increased. For deep space mission and assembly of structures in orbit nothing can replace an economical, fully reusable heavy-lift launcher, such as the Russian Energia was intended to be. The challenge is greatest for a two-way mission, and includes preservation of the propellant after a long stay in the space environment. The mass ratio for a two-way mission is daunting, as it multiplies the one-way mass ratio by 18.5, from 20.6 to 382. For the same 10-ton spacecraft returned to Earth, the LEO mass that must be delivered into orbit is now 3,820 tons (8,423,100 lbs). Even with the six-booster configuration for Energia, that would require 17 lifts to orbit. Without a reusable heavy-lift booster, such as Energia was intended to be, the viability of such missions is in serious doubt, as even the best, the Russian Proton, would require 191 trips to orbit! We have said nothing yet as to the performance of the propulsion system (in terms of its I_{sp}), only estimated a reasonable value for the mass ratio required to move the spacecraft out of LEO and to its distant space destination. Any change in magnitude of the speed or in the change in the direction of its vector is represented as an incremental velocity (ΔV). For example, to change an LEO orbital plane by 13.5° requires a ΔV of 6,000 ft/sec (1,829 m/sec). A 90-degree orbital plane change corresponds to a 90-degree turn in space and requires 35,666 ft/sec (10,871 m/sec), that is, 1.39 times the velocity increment as achieving LEO from an Earth! An aircraft can accomplish a modest load factor, 90-degree turn with only 20% more fuel consumed than flying level. Going to geosynchronous orbit from LEO can require as much propellant as achieving Earth orbit. Thus moving about in space requires a very large amount of propellant.

We have already spoken of specific impulse, I_{sp}, as an index of the propulsion performance in the Introduction. I_{sp} is the thrust the propulsion system generates per unit of propellant mass flow consumed. When measured in seconds, it is also the time a unit weight of propellant can sustain itself against gravity. An I_{sp} of 455 seconds (4462 m/sec) means that one kilogram per second of propellant flow generates 455 kilograms of thrust or 4,462 newtons. That is:

$$I_{sp} = \frac{\text{Thrust}}{\dot{w}_{ppl}}\left(\frac{\text{lbf}}{\text{lbm/sec}} = \text{sec} \quad \text{in imperial units}\right)$$

$$g\,I_{sp} = c^{*}\left(\frac{\text{newtons}}{\text{kg/sec}} = \frac{\text{m}}{\text{sec}} \quad \text{SI units}\right) \tag{1.1}$$

There are just two principal elements that determine the incremental velocity (ΔV), specific impulse (I_{sp}) and mass ratio (MR). For the one-way mission there are two accelerations, the first a positive acceleration to maximum speed and a second, and equal, opposite acceleration (deceleration) from maximum speed to the spacecraft's initial speed. For the two-way mission there are four accelerations, two on the outbound leg and two on the inbound leg.

Table 1.5. Current chemical and nuclear rocket propulsion characteristics.

Fuel	Oxidizer	I_{sp} (sec)	Sp. gr. I_{sp}	O/F	MR
UDMH	$\mathbf{N_2O_4}$	**319**	**390**	**1.23**	**2.82**
Hydrazine	$\mathbf{H_2O_2}$	**304**	**375**	**2.04**	**2.97**
Hydrazine	$\mathbf{N_2O_4}$	**312**	**365**	**2.25**	**2.88**
JP-4	LOX	329	330	2.40	2.73
Nitromethane	—	*273*	*308*	*monoprop.*	*3.36*
Methyl alcohol	LOX	297	282	1.15	3.05
Methane	LOX	329	247	2.33	2.73
Hydrazine	—	*218*	*219*	*monoprop.*	*4.56*
Hydrogen	N_2O_4	349	207	11.5	2.56
Hydrogen	LOX	455	170	6.00	2.07
Hydrogen	—	2,000	149	nuclear	1.15
Hydrogen	—	1,200	90.0	nuclear	1.32

Whether changing the magnitude of speed or changing direction, the only source of motive force is propulsion. Since there is no lift, the propulsion system must provide all of force required. Because there is no atmosphere, the spacecraft must carry not only fuel but also the oxidizer required to burn the fuel. The total propellant load, i.e. fuel and oxidizer, is many times greater than the fuel for an aircraft flying in Earth's atmosphere. Because rockets must carry oxidizer, the propellant weight (oxidizer + fuel) just to achieve LEO from Earth is from 7 to 15 times the unfueled weight of the spacecraft. It is for this reason that for spacecraft the measure of the total propellant carried is the 'mass ratio, MR', or the total vehicle mass divided by the unfueled mass of the spacecraft. Table 1.5 gives for a number of current propellants their I_{sp}, density I_{sp} = propellants specific gravity times I_{sp}, oxidizer to fuel ratio (O/F) and mass ratio MR required to accelerate from LEO orbital speed (25,656 ft/sec or 7.820 km/sec) to Earth escape speed (36,283 ft/sec or 11.059 km/sec) i.e. a velocity increment of 10,633 ft/sec or 3.241 km/sec.

Nuclear-powered electric propulsion sould be used in low Earth orbit, resulting in an improved mass ratio for a given incremental velocity. In Table 1.5 propellants in **bold** are hypergolic, that is they combust (or even detonate) on contact. Hypergolics have the advantage that they are storable in space and have the highest density specific impulse. Those in *italics* are monopropellants that use the heat of a catalyst bed to decompose the liquid to a high temperature gas, and have the lowest specific impulse. Hydrogen propellant used in nuclear rocket systems results in a low value for density specific impulse. The propellants are ranked in order of density times I_{sp} (Sp.Gravity $\times I_{sp}$), where the bulk density of the propellant is expressed as bulk specific gravity; generally, the higher this value, the less propellant volume required.

Figure 1.5 shows the Specific Impulse (I_{sp}) required to achieve a given velocity for a mass ratio of four. The velocity is given in terms of statute miles/sec with benchmarks in terms of the ratio to the speed of light. This chart has no relativistic effects included in the calculations. At 10% of the speed of light, the relativistic effect

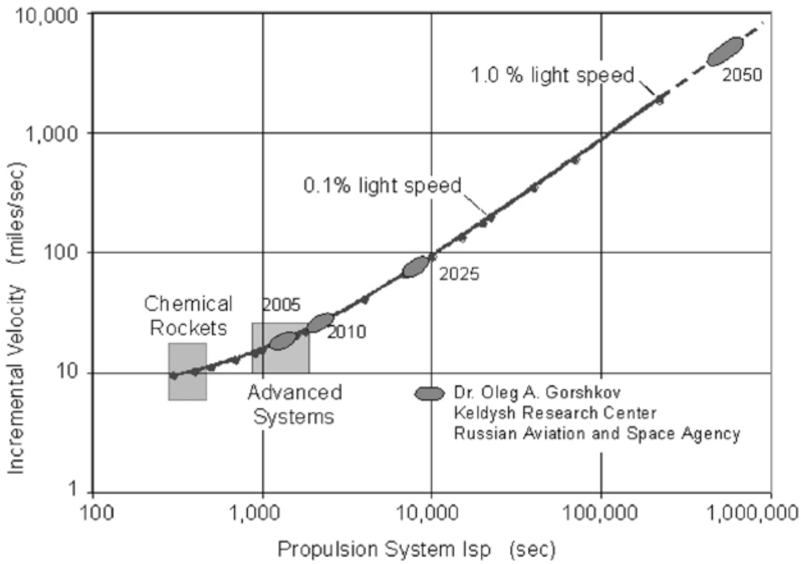

Figure 1.5. Required specific impulse as a function of spacecraft speed with some projections.

is 5.4%. The lowest value on the graph is Earth escape velocity, 36,283 ft/sec or 11.059 km/sec; the greatest speed is 4.85% light speed for the 2050 ellipse. The current hypergolic and cryogenic rockets and U.S. and European advanced systems are indicated. From a talk given by Dr Oleg A. Gorshkov of the Keldysh Research Center, the four capabilities that the center is working toward are indicated in Figure 1.5 with the approximate year of availability. The specific impulse required to reach 1% of light speed is at least two orders of magnitude greater than our expected advanced systems. Another two orders of magnitude are required if we are to attain light speed, i.e., four orders of magnitude greater than our expected advanced systems. That means achieving specific impulses of the order of one to ten million seconds. That means that each kilogram per second of propellant flow produces one to ten million kilograms of thrust (9.8 to 98 Mega-Newtons). We have yet to speak of superluminal speeds, that is, traveling faster than light speed, but superluminal speed cannot be achieved until at least light speed is achieved. Assuming we can achieve the speed enabled by the specific impulse (I_{sp}) in Figure 1.5, the question is , how long is the travel time?

Figure 1.6 shows the Earth time to travel one-way to within our Solar System, beginning with Mercury and ending with the Heliopause (the shaded circles) and beyond. The assumption is we can achieve 0.1% light speed. To achieve 0.1% of light speed (983.580 ft/sec) with a mass ratio of 4, an I_{sp} of 14,700 sec is required. This figure illustrates the staggering challenge of traversing space to objects in nearby Galactic space. With a propulsion system at least 10 times better than our projected advanced propulsion systems the outer planets are readily accesible. Our nearest star, Proxima Centauri is 4.2 light-years distant. So it will take an authomatic

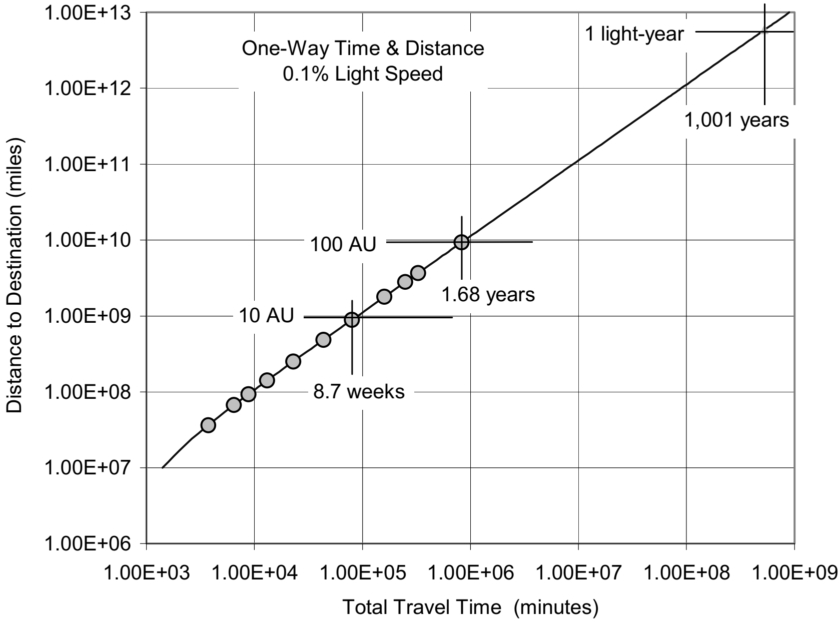

Figure 1.6. One-way distance and travel time in Earth time.

spacecraft over 2,500 years to reach Proxima Centauri. With the possible propulsion systems of Dr Gorshkov, the nearest star falls at the 250 year travel time. The 7 nearest stars to our Solar System are within 10 light-years. That is another order of magnitude greater travel time. In terms of reaching the nearest galaxy, Andromeda, the time is 22 million Earth years. So, for the present we cannot even reach our nearby stars' neighborhoods, much less the nearest galaxy. We are confined to our Solar System, and in the future we may be able to reach only our nearest neighbor star. Unless travel at greater that the speed of light is possible, we are as isolated as a culture in a petri dish. Note, however, that these time are for Earth-based observers, not for the crew of the spacecraft. Relativistic speeds create a sharp difference between these two times; see Chapter 9.

1.6 PROPULSION CONCEPTS AVAILABLE FOR SOLAR SYSTEM EXPLORATION

In the previous section it was shown how I_{sp} and mass control space travel and missions. If human exploration of our Solar System is the goal, then there are some time constraints to consider given the current knowledge of shielding from high-energy particles and radiation in space. There is a limit to the mass of shielding that can be incorporated into a spacecraft and yet retain a practical mass to accelerate from LEO. In addition, the ability to warn the space travelers is limited to radiation that encounters Earth. From other sources and directions the spacecraft will have to have a basic protection level plus a short-term safe house for more intense radiation. Since the first warning may be the arrival of the radiation, the danger is that the first encounter may be a lethal one so the entire crew space may be required to be in a safe house. The best insurance against this occurring is to minimize the travel time. Statistically a trip of less than a year is relatively safe and a trip of over two years is not. Exploring the Solar System by manned missions means ideally the total travel time is on the order of one year to minimize the exposure of a human crew to hard space radiation, even with a shielded spacecraft. Three years time is (right now, at least) a possible way to have an acceptable and recoverable level of damage from the effects of cosmic radiation and loss of bone mass. Russian experience with seven orbital stations, however, shows that even a 2-year mission in microgravity may generate irrecoverable damage. One solution is to provide a minimum level of acceleration, perhaps one-fifth of Earth's gravity (approximately $2\,\mathrm{m/sec^2}$), and a weak magnetic field (at least 0.3 gauss) analogous to Earth's magnetic field. The real limitation is that with current systems a one-way travel time to the Heliopause (100 AU) that appears feasible is 9.5 years. This is too long for a human-carrying spacecraft, and we do not know how to construct spacecraft and supply resources for humans for a total of 19 years. So these missions will of necessity be robotic missions.

The requirements for the propulsion can be determined for a specific distance as a function of spacecraft weight with values selected for just two parameters, the total one-way travel time and the average acceleration of the spacecraft. The equations for the speed increment required over orbital speed (ΔV) for the spacecraft to achieve its destination in the selected time, the spacecraft mass ratio (MR) in Earth LEO for a one-way or two-way mission, the average specific impulse required to achieve the required ΔV, the acceleration time from orbital speed to orbital speed plus ΔV (t_a), and the thrust required to provide the selected acceleration follow:

$$\begin{aligned}
\Delta V &= \frac{\text{Path length}}{\text{Mission time}} \approx \frac{\pi \text{ Radial distance}}{t_\mathrm{m}} = \left(\frac{\mathrm{m}}{\mathrm{sec}}\right) \\
\mathrm{MR} &= \text{one-way mass ratio} = 4 \\
I_\mathrm{sp} &= \left(\frac{\Delta V/g_\mathrm{o}}{\ln \mathrm{MR}}\right) = 0.7213\frac{\Delta V}{g_\mathrm{o}} \\
t_\mathrm{a} &= \frac{\Delta V}{N_x\, g_\mathrm{o}} = (\text{seconds}) \\
N_x &= \text{axial acceleration (`}g\text{'s)} \\
T_\mathrm{sc} &= N_x\, g_\mathrm{o}\, m_\mathrm{spacecraft} = (\text{newtons}) \qquad (1.2)
\end{aligned}$$

where g_o is the surface acceleration on Earth.

Newton's Third Law-based propulsion will enable Solar System exploration within the previously discussed travel times only if there is sufficient specific impulse and thrust. In range of distances from 5 to 100 AU the mass ratio for a one-way mission is 4 and a two-way mass ratio is 16. This determines the I_sp for the

Table 1.6. Propulsion performance for mission to the Heliopause and nearer.

One-way mission time (years)	Acceleration ('g')	Acceleration time (hours)	ΔV^{a} (km/sec)	I_{sp} (sec)	Thrust (N) one-way	Thrust (N) two-way
9.5	0.10	0.4069	1.4366	32.209	3.923	15.69
1.5	0.50	0.5542	9.7829	219.33	19.61	78.45
0.5	1.00	0.8390	29.620	664.08	58.84	235.4

[a] From low Earth orbit.

spacecraft departing from LEO the performance of the propulsion system. The performance for a specific distance traveled can be determined from Table 1.6. To escape the gravity of Earth, the ΔV must be at least 3.238 km/sec to provide an escape speed of 11.056 km/sec.

For the assumed mass ratio in LEO, the propulsion system thrust required (in newtons) is about numerically equal to the I_{sp} for a 1000 kg spacecraft and an 82 AU mission. The thrust and specific impulse values required increase inversely with the travel time. The 1.5-year mission required I_{sp} is 6.3 times the 9.5-year mission and the 0.5-year mission required I_{sp} is 20.6 times the 9.5 year mission. That would put the propulsion capability in the 'future system' capability, as shown in Figure 1.5. The shortest mission time would be in the 'possible systems' that researchers are expecting to be available much later in this century. The challenge will be the thrust versus operating time required as the mission time decreases. Probably the Russian rocket chemical rocket engines hold the record for the longest continuous engine operation as achieved with the Kuznetzov NK-31 engine being used for the proposed Kistler low-cost rocket.

To illustrate the magnitude of the propulsion performance required to achieve a rapid transit to a particular distant destination, a one-way mission to Pluto (39.4 AU average distance from the Sun) will serve as an example. The propulsion system performance required is given in Table 1.7. The mass ratio is four for the one-way trip and the spacecraft mass is 1000 kg. For the shortest mission to Pluto, the propulsion system must generate 15 times the thrust and operate twice the duration. That is a serious challenge, given today's industrial capability in non-chemical space propulsion. Today's non-chemical space propulsion engine thrust is measured in tens and perhaps a hundred newtons. Chemical rockets have operated for perhaps an hour on the test stand, but to 17 or 20 hours continuously; then a restart a year later is a daunting challenge. So the spacecraft today are based on our current launch motor capability of high thrust over a relatively short operating time. What is needed is a new development of deep space propulsion that has both higher thrust and longer operating times and that is capable of ready storage over long deep-space missions.

The thrust can be reduced, but there is a corresponding increase in the acceleration time, that is, the duration the propulsion system must operate. Depending on

Table 1.7. Propulsion performance for mission to Pluto for a 1000-kg spacecraft.

One-way mission time (years)	Acceleration ('g')	Acceleration time (hours)	ΔV* (km/sec)	I_{sp} (sec)	Thrust (N) one-way
9.5	0.10	16.03	56.60	1,270	3,923
1.5	0.50	21.84	385.4	8,640	19.610
0.5	1.00	33.06	1,167	26,170	58,850

Table 1.8. Engine thrust as a function of acceleration for mission to Pluto for 1000-kg spacecraft.

Acceleration ('g')	Acceleration time (hours)	Thrust (N)	I_{sp} (sec)
0.100	16.03	3,923	1,270
0.070	22.90	2,746	1,270
0.032	50.09	1,260	1,270
0.010	160.3	392.3	1,270

the engine providing the thrust, there are limits to the duration a particular engine can provide thrust. The engine must operate to accelerate the vehicle as well as decelerate the vehicle at the end of the trip. So for the 9.5-year one-way mission the engine must be in storage for 9 years before it is needed again to decelerate the vehicle. For the two-way mission there are two 9-year storage periods in sequence. For this mission the acceleration, acceleration times and thrust are given in Table 1.8.

One of the rules of thumb in space operations within the Solar System is that 1000 sec specific impulse and 1000 newtons are in the correct ratio for a proper system. You can see this is the case for the lower acceleration of 0.032 'g' (0.314 m/sec^2) and a travel distance less than the distance of Pluto, about that to Neptune. The 1000/1000 criterion applied to Pluto means that the travel time would be 12.1 years, not 9.5 years. These criteria pose a challenge to existing propulsion technology (basically, chemical, with electric propulsion playing a relatively minor role in satellite propulsion). At the same time, in-orbit assembly of spacecraft and propulsion systems may ease the single lift to orbit requirement but assembly in space adds to the complexity and uncertainty of the mission. Structures of future spacecraft assembled in space may be made much lighter, without the need to withstand launch loads completely assembled.

One of the difficulties of space is that there is no atmosphere—it is not possible to convect rejected heat to a gaseous medium. Operating thermal propulsion and support systems in space without convection means that waste heat associated with thermal propulsion, human beings, and equipment must be disposed of using radiation from large radiators. The Space Shuttle operates with its payload doors open because these contain integral radiators that reject the waste heat from the Shuttle. Some of the waste heat can be used as an energy source to generate electrical and fluid power, but there remains a significant quantity to dispose of. The spacecraft or orbital station is essentially an isolated thermal capacitor. Like an electrical capacitor, the greater the electrical charge the higher the voltage. For the thermal capacitor the greater the thermal energy stored the higher the temperature. An important parameter is the size of the radiator needed to reject the thermal energy to space by radiation. The Stefan law for radiated thermal energy is a function of the surface emissivity (that the efficiency of the radiating surface, an e of 0.9 means that the surface is radiating 90% of the maximum possible energy) and the surface temperature raised to the fourth power. This is a very powerful function, if the absolute temperature is raised just 10% the total radiated energy is increased by 46%. One approach is to operate the radiators at the maximum possible temperature based on the radiator material and the heat transfer fluid used to pump the thermal energy to the radiators. For a fixed maximum temperature (dictated by the melting point of the materials available) large waste heat fluxes q_R need an adequate radiating surface area, as indicated by the Stefan Law:

$$
\begin{aligned}
Q_{\text{rejected}} &= 1_{\text{Radiated}}\, S = \varepsilon\sigma S T^4 = (\text{watts}) \\
q_R &= \varepsilon\sigma T^4 = (\text{watts/m}^2) \\
S &= \frac{Q_{\text{rejected}}}{\varepsilon\sigma T^4} = \text{radiator area}
\end{aligned}
\tag{1.3}
$$

Propulsion system options meeting the 1000/1000 criterion and using Newton's Third Law are 'nuclear' and 'electric', or their combination. Conventional (thermal) nuclear propulsion (NP) has been tested through the 1970s (NERVA engine), resulting in an $I_{sp} \sim 900$ sec and thrust $\sim 9 \times 10^5$ N, more than sufficient for a booster or launcher, but not quite adequate for long interplanetary travel. This type of nuclear propulsion (as will be shown in Chapters 3 and 5) is perfectly suited for RLV upper stages lifting heavy payloads to orbit, and also for lifting payloads from LEO to geostationary Earth orbit (GEO), powering, for instance, a 'space-tug'. Direct heating of a propellant gas by the fission fragments (FF) has been proposed by C. Rubbia. In principle at least, the melting point of material problem is bypassed. This should indeed produce a combination of specific impulse and thrust in the range desired for Solar System travel. A somewhat similar concept uses nuclear power to heat inductively a propellant, as done in wind tunnels using a Plasmatron (for instance, in the Von Karman Institute PWT facility).

Electric propulsion (EP) comes in many varieties. Common to all, however, is a typical low thrust per unit mass, and, for some, even the thrust per unit cross-section of the device, while the specific impulse may be more than adequate: for instance, commercial ion thrusters are now capable of 4000 sec. To achieve the specific impulse and thrust combination already mentioned, magneto-plasma-dynamic (MPD) thrusters are now considered the best choice. They accelerate a plasma by the Lorentz force $F = j \times B$, where j is the current flux and B the magnetic induction.

MPD propulsion still needs large power to achieve a thrust of approximately 1000 newtons. Proposed solar power arrays would need acres of photovoltaic cells to harvest it and feed it to a MPD thruster, say, for a manned Mars mission. The combination nuclear power/MPD looks instead very appealing. Belonging to this same family is the so-called VAriable Specific Impulse Magneto-plasma-dynamic Rocket, or VASIMR, in which the concept is further refined so that for a fixed power the product $F \times I_{sp}$ is fixed, and either low F and high I_{sp}, or vice versa, can be obtained. This feature makes simpler an interplanetary trajectory from a LEO. Thus, either direct nuclear propulsion perhaps of the Rubbia type, or a combination nuclear power plus electric propulsion are the current candidate propulsion systems for Solar System exploration; see Chapter 7. The Rubbia concept could also function as a nuclear generator, and could be alternative to VASIMR. In any event, about half of the nuclear power of any nuclear-powered system would be wasted and must be radiated away or recycled. A recycling application could consist in converting the waste power into electric power for a downstream electric propulsion thruster, or to boost the performance of the main electric propulsion thruster.

Although sketchy, these considerations show the importance of detailed energy and power budgets in planning efficient propulsion systems from basic concepts. A relative newcomer technology that will help MPD propulsion is superconductor (SC) technology. Large B fields imply large and heavy conventional coils. Ohmic heating of the coils limits the B fields in ground applications to 1 tesla (T) at most. On a space vehicle lack of convective cooling would pose even more severe limitations. If, however, coils are made of materials kept superconductive either by active cooling or by using a cryogenic propellant such as LH_2, the magnetic field could be raised to as much as 10 tesla with a drastic reduction in mass and volume. Superconductivity will likely play a large role in future propulsion fed by nuclear power.

Two alternatives to the nuclear and electric propulsion systems should be mentioned, although they are incapable at the moment of satisfying the travel time requirement of even a few years at most. They are the solar sail, and the magnetic sail. They look appealing, largely because they do not need, especially the former, complex hardware, and certainly very little or no power generation.

Solar sails exploit the radiation pressure of photons (light) emitted from the Sun to push a large surface (the 'sail'), properly oriented in space (Poynting vector) much in the same way as the wind on Earth pushes a sailboat. The thrust level available is exceedingly small, decreasing with the square of the distance from the Sun. This limits the usefulness of the solar sail to Mars or the inner planets. Contrary to what is intuitively assumed, the radial direction of the thrust can still be used to sail 'against the wind' and be used for interplanetary missions to the inner planets. Structural mass and low thrust rule out this propulsion concept for manned missions.

Magnetic sails work similarly, but the effect exploited is the solar wind (mostly ions) also radiating away from the Sun. However, instead of using their weak pressure on a physical sail, the spacecraft would generate a 'frozen' magnetic B field inside a plasma cloud emitted from the spacecraft. The interaction between solar wind (i.e., the solar current) and the B field creates a Lorentz force. This is the force that is used for propulsion. Widely publicized recently, this propulsion concept is definitely capable of Solar System missions, but the weak thrust at this time and in the foreseeable future, as in the case of the solar sail concept, makes it incapable of meeting the travel-time criterion.

Unfortunately none of the discussed systems are capable of anything approaching light speed. As stated, these propulsion systems confine us to our Solar System and long-duration missions (10 years or longer to Pluto). Chapter 9 will discuss some of those possibilities that might let us travel beyond our solar system, that is reach the speed of light quickly and travel in 'hyperspace' to our distant destinations.

1.7 BIBLIOGRAPHY

Aviation Week and Space Technology (2001), MIR Deorbit, *www.aiaa.org/aerospace/achives.cfm?ArchiveIssuesid=13*

Cook, N. (2001) *The Hunt for Zero Point*, Random House, London.

Cosmonaut (1984) Private communication with respect to Salyut repair, at the AIAA Space Conference, Los Angeles.

Davis, R. (1999) Private communication at the IAF Congress, Amsterdam.

Hansson, A. (1987, 1991, 1993) Private communications with respect to Soviet biomedical program.

Harwit, M. (1973) *Astrophysical Concepts*, Wiley, New York.

Jenkins, D.R. and Landis, T.R (2003) *Hypersonic – The Story of the North American X-15*, Speciality Press, North Branch, MN.

Kaufmann, III, W.J. (1993) *Discovering the Universe*, 3rd edn, W.H. Freeman, New York, Ch. 17 and Appendix 4.

Miller, R. (1993) *The Dream Machines: An Illustrated History of the Spaceship in Art, Science and Literature*, Krieger Publishing Company.

Miller, J. (2001) *The X-Planes X-1 to X-45*, Midland Publishing, Hinkley, UK.

Neyland, V.Ya. (1988a) Private communication, TsAGI, Moscow.

Neyland, V.Ya. (1988b) *Engineering Problems and Methods of Preflight Development of Orbiters*, unpublished TsAGI report, Moscow [in Russian].

Plokhikh, V.P. (1989) Sensitivity analysis of SSTO reuseable vehicle paramers. IAF Paper IAF-89-223, presented at the IAF Congress, Malaga, Oct. 5–11.

Stafford, T. (General USAF Retd) (1970) Personal communication at McDonnell Aircraft, St. Louis.

Stafford, T. (General USAF Retd) (1990) Personal communication, Paris Air Show, Le Bourget

2

Our progress appears to be impeded

2.1 MEETING THE CHALLENGE

Prior to the 1930s flying in aircraft was costly and potentially dangerous. There were fewer passengers and less cargo than required for profitability without government subsidy. The Douglas Aircraft Company design team took the train to New York City to meet with TWA officials rather than fly the airliners of the day, as there just had been a series of accidents including the one that Knute Rockne, the Notre Dame football coach, had perished on. Gene Raymond, the Chief Engineer for Douglas used the newly dedicated GALCIT wind tunnel at California Institute of Technology (CalTech) to experimentally verify the aerodynamics of the new aircraft. Raymond used the latest aluminum stressed skin structure developed by Jack Northrop for the Lockheed's aircraft fuselages. The engines were the new Wright Cyclones radial air-cooled engines that developed 900 horsepower. So Gene Raymond integrated the three principal elements for a successful aircraft from the newly demonstrated 'industrial capability'. In 1932, the Douglas Aircraft Company introduced the DC-2, and in 1934 the DC-3. The result was a commercial airliner that offered speed, distance and safety to the passenger and profitability to the airlines without subsidy. The aircraft was a sustained-use vehicle that flew hundreds of times per year and therefore at an affordable price. By 1939 the DC-3 was flying tens of thousands of passengers for the airlines worldwide.

Like the DC-3, there were other aircraft built from the available state of the art. One such aircraft was the operational Mach 3-plus SR-71 developed by Clarence (Kelly) Johnson's 'Skunk Works'® team at the Lockheed Burbank plant. The other aircraft was the North American X-15 research aircraft developed to investigate speeds up to Mach 6. The extensive wind tunnel testing established the aerodynamic characteristics of both. The structure was high temperature nickel–chrome alloys for the X-15 and beta-titanium for the SR-71 in a structure analogous to a 'hot' DC-3. The rocket engine for the X-15 was developed from earlier rockets and developed to a level not yet installed on an aircraft. The turbo-ramjet propulsion for the SR-71 has yet to be duplicated 45 years later. For the X-15 the challenging goal was the flight control system that had to transition from aerodynamic control to reaction jet control at the edge of space. For the SR-71 the challenge was to design an integrated control system for both the engine inlets and the aircraft, and from high supersonic speeds to low landing speeds. This had not been done before, and it was accomplished before the era of integrated circuits and digital control. The goal for the X-15 was an approach to fly to space as frequently as could be expected of an aircraft-launched experimental vehicle. By 1958 the X-15 was approaching 300 successful flights. The X-15 was achieving flight speeds at almost Mach 6, and could briefly zoom to the edges of near-Earth space. Rockets of the day were single use and costly, with numerous launch failures. These aircraft were developed by engineers that did not ask, 'What is the technology availability date?' but rather, 'Where can we find a solution from what we already know or can discover?' And in both the X-15 and the SR-71, solutions that were not previously known were discovered and used to solve the problems in a timely manner. That spirit enabled the Apollo team to fabricate a Saturn V rocket of a size that was previously inconceivable, and succeed.

2.2 EARLY PROGRESS IN SPACE

Also in 1957, during the International Geophysical Year (IGY), the USSR lofted the first artificial Earth satellite (Sputnik I) into low Earth orbit. Suddenly the focus was on catching up, and the space flight centered on vertical launch, expendable rockets and the experimental aircraft experience and capability were discarded. The USSR adapted a military intercontinental ballistic missile, the SS-6 Sapwood, to be the first launcher [Clark, 1988]. That launcher had the growth potential to become the current, routinely launched Soyuz launcher. The first Sputnik weighed 150 kg, while the payload capability of the launcher was about 1,500 kg. This is launch margin! The President of the United States rejected the suggestions coming from many sides to adapt military ballistic missiles, and insisted on developing a launcher sized specifically for the IGY satellite; that launcher, Vanguard, had almost no margin or growth potential. There was only about a 4-kg margin for the payload weight. After a series of failures, the first United States Army military IRBM, the Jupiter missile, was modified into a satellite launcher and Explorer I was successfully launched. Since then, the former USSR, Russia, and all the other launcher-capable nations have focused on expendable launchers with the same strategy in ballistic missile utilization, that is they are launched for the first, last and only time.

As discussed in Chapter 1, during the 1960s there was an enthusiasm to reach space together with a very intense effort to obtain the necessary hardware. Technical developments were ambitious yet technically sound and based on available or adapted/modified industrial capability. The difficulty was that the most capable vehicle configuration development, system designs, boosters and spacecraft were associated with a military establishment, primarily the US Air Force. One goal was to have an on-demand global surveillance with either a hypersonic glider with an Earth circumference range capability or a hypersonic cruise vehicle with a half-Earth circumference range capability. Another goal was to establish a manned orbital laboratory to assure a human presence in space and enable space-based research and earth/space observations. The spacecraft launchers proposed had the capability for frequent scheduled flights to support an orbital station with a 21 to 27 crew complement, crewmembers being on six months rotating assignments. With the government's decision that space is not to be military but civilian, a civilian space organization must develop its own hardware and cannot use military hardware. Unfortunately most of the very successful system design efforts by the military organizations were discarded by the civilian organizations, with the result that the civil system never achieved the performance capability offered by the military systems.

Before the Saturn V/Apollo Moon missions, the Apollo–Soyuz rendezvous and the short-lived Skylab experiment, the United States did have a dream to establish a space infrastructure and operational space systems. With the demise of the Apollo program and the elimination of the Saturn V heavy lift capability in view of a future, yet to be realized vehicle, there followed a 12-year period in which no crewed space missions were conducted, as all waited for the Space Shuttle to enter into operation. The dreamers, engineers, scientists and managers alike, with visions of future possibilities, were put indefinitely on hold; the subsequent developments became myopic and focused on day-to-day activities requiring decades in development, and larger and longer funding profiles for minimal performance improvements. Armies of paper-tracking bureaucrats replaced small, dedicated, proficient teams.

The United States is not the only nation that considered a space structure to establish an operational space infrastructure. In Figure 2.1 there is shown a diagram the author drew during discussions with V. Legostayev and V. Gubanov during the IAF Congress in Brighton, England, in 1985, illustrating the USSR vision of a space infrastructure. The sketch remains as drawn, with only the handwritten call-outs replaced by typed captions. This sketch shows a total space exploration concept, with certain capabilities unique to the Russian concept. One capability is a ground-based power generator–transmitter with the capability to power satellites, Lunar and Mars bases, and space exploration vehicles directly and also, via relay satellites, capable of powering other surface sites. In the 1930s Nikolai Tesla stated that, with his wave-based transmission system, a Mars base or spacecraft traveling to Mars could be powered from Earth with less than 10% energy losses. With many years spent translating Tesla's notes and reports in the Tesla Museum in Belgrade, the Russians conducted many experiments (e.g., Gulkin and Chenetski in 1970) using the cathode tubes that Tesla developed. One of the authors (PC) saw such a tube when visiting the Tesla Museum in Smylan, Croatia, in 1980. The remaining elements of the Russian vision in 1985 are in common with other space plans. Their concept is built around an orbital station and free-flying manufacturing factories (manned space stations have too many gravitational disturbances, 'jitter', in the microgravity jargon, to be considered truly 'zero-gravity'). The space facilities are

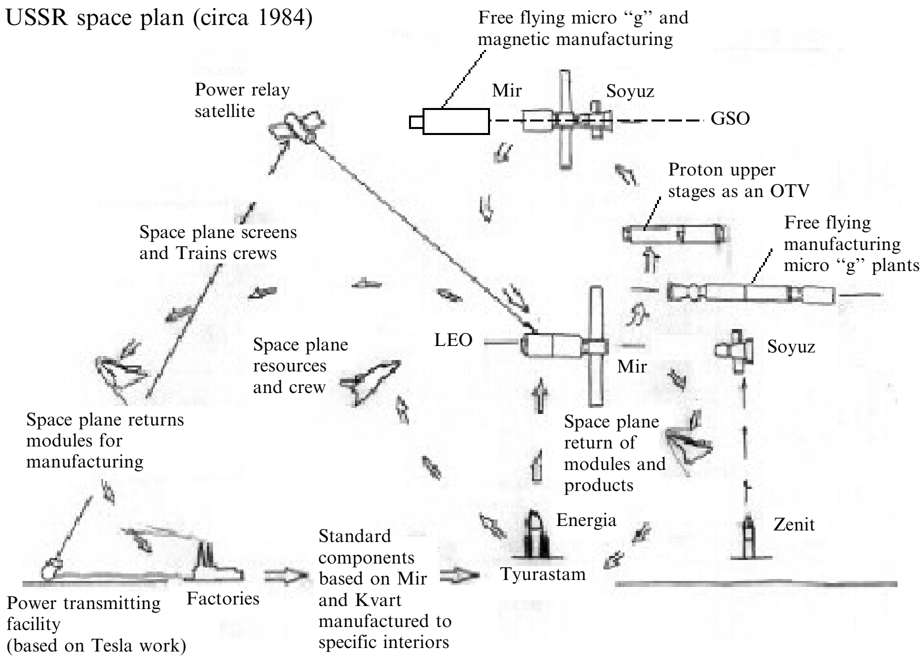

Figure 2.1. A look to the future space infrastructure envisioned by Boris Gubonov and Viktor Legostayev of the former USSR, based on having Energia operational, circa 1984.

in low Earth orbit (LEO) and in geostationary orbit (GSO). So an integral part of the Russian space plan is an orbital transfer vehicle (OTV) to provide movement of satellites and resources to and from LEO. Deep space exploration and establishing a permanent Moon base was also part of the total space plan (see Chapter 6). The important part of the Russian concept is that it is based on hardware capability that they already had in use or was in development. The key difference from other space plans is that their Energia launcher is a heavy-lift system that could launch either cargo payload vehicles (up to 280 tons) or a manned glider (Buran), see Figure 2.7. Energia was to provide a fully reusable heavy-lift system (Energia) and an aeroSpace plane (Buran) to support the orbital station and other human crewed systems.

There was a space transportation vehicle in work at TsAGI [Plokhikh, 1983, 1989] that could be considered analogous to the US National Aerospace Plane. This would be an orbital station resource supply vehicle, with Energia the workhorse of heavy-lift capability. The goal for the Russian and Ukrainian space groups was to greatly reduce the source of space debris, that is, inoperative satellites and third (spent) stages that remain in orbit [Legostayev and Gubanov, 1985]. Their approach would be to use Buran and the aerospace plane to return non-operative satellites to Earth from LEO for remanufacture. The orbital transfer vehicle would return non-functional satellites from GSO to LEO. The unique difference is the addition of beamed power from earth via orbital relay to satellites, orbital stations

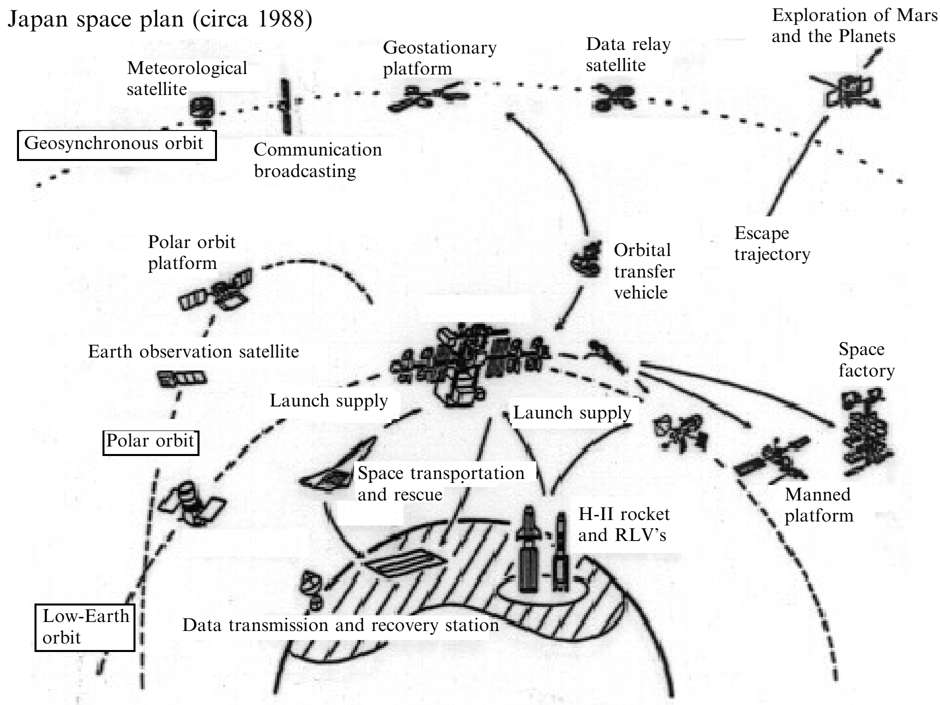

Figure 2.2. A Japanese look to the future space infrastructure based on their development of an Aerospace Plane and significant orbital manufacturing assets, circa 1988.

or a ground power station. The power generation and transmission is based, as said, on concepts developed by the late Nikolai Tesla, with a reported progression of transmitted power up to 10 MW and efficiency over 75% from ground station to ground station. This historical database is archived also in the Tesla Museum in Belgrade, Serbia, as well as at Smylan.

Just as the United States and the former Soviet Union had plans to develop space, so did Japan. In Figure 2.2 is a representation of an analogous plan presented by Japan's space organizations as they considered the future. As with the Russian concept the Japan Space Organizations' concept is built around an orbital station and free-flying manufacturing factories, again independent from the station because of microgravity jitter. Their plan is very comprehensive and indicates a desire to establish commercial space operations. There are large space facilities in LEO, Earth observation platforms in polar/Sun synchronous orbit and a variety of platforms in GSO. Integral to their space plan is an orbital transfer vehicle (OTV) to provide movement of satellites and resources to and from LEO. Deep space exploration and establishing a permanent Moon base was also part of the total space plan. The Moon base was presented during a European Space Conference in Bonn, Germany, in 1985. There was a space transportation vehicle in work at NAL [Yamanaka, 2000] that could be considered also to be analogous the US National Aerospace Plane.

Figure 2.3. Aerospace Plane concept from Japan National Aerospace Laboratories (NAL).

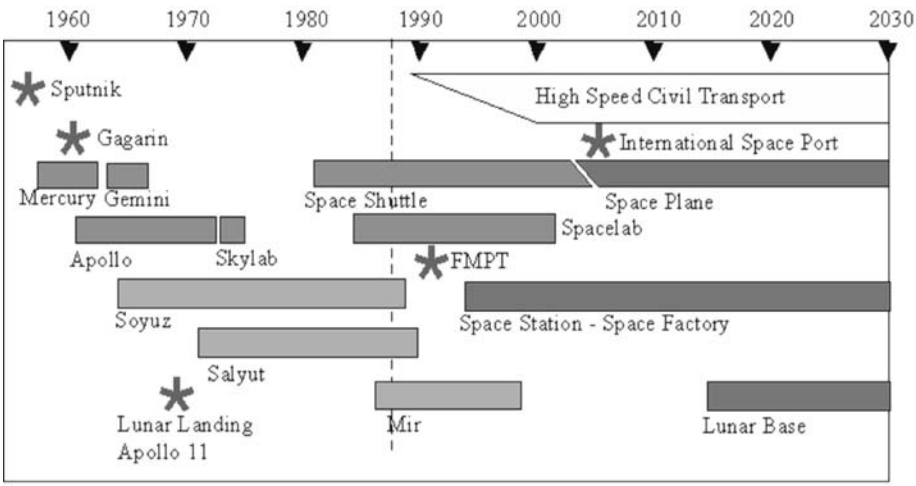

Figure 2.4. International space plans as presented to the Space Advisory Council for the Prime Minister of Japan in 1988.

During the NASP project team visit to Japan in 1988 the Japanese concept was given significant print coverage and presented to the NASP team in considerable detail. Figure 2.3 shows an artist's rendition of the Aerospace Plane. The configuration is a slender wing-body with sharp leading edges and nose, required to minimize the low lift drag and improve the glide lift-to-drag ratio for Earth return. The plane is powered by a rocket based combined cycle (RBCC) propulsion system. The details are technically correct and indicate a competent design team working actual problems. When the NASP team visited Japan they received the view of the Space Advisory Council of the international space activities, as shown in Figure 2.4. Note that this puts into the Japanese perspective the world space plans, as they existed in 1988. In fact, the Japanese plan indicates that in 1988 there was a multinational perspective of establishing a functional space infrastructure that benefited each nation. This future is build around an orbital stations and free-flying manufacturing factories in LEO and in GSO. Deep space exploration spacecraft were planned to the Moon and planets. However problems with the engines for their H-II launcher and the downturn in their national economy put much of the Japanese vision on hold—or their vision was stretched out in time.

So have many concepts envisioning the future, but the pioneers that expanded the scope of aviation are no longer there to make the dream reality. All that remains, it seems, are the skeptics, who say it is too expensive, or too dangerous, or impractical, or irrelevant.

2.3 HISTORICAL ANALOGUES

Experience with expendable vehicles is not limited to rockets, as Figure 2.5 illustrates. In the 1800s, St. Louis, Missouri, was the 'Gateway to the West' and hundreds of thousands of pioneers passed through on their way to the West over a 70-year period. There is no record of how many Conestoga wagons that departed St. Louis in the early and mid-1800s ever returned: it was a one-way trip. (The exception is one of three super-sized wagons sent to Santa Fe to return Spanish gold to St. Louis that returned empty.) Unlike the Space Shuttle Center Tank, the wagons were reused as construction materials at their final destinations. A significant space infrastructure could be constructed from empty center tanks [Taylor, 2000]. At best there are some expendable launcher parts that can be refurbished, as in

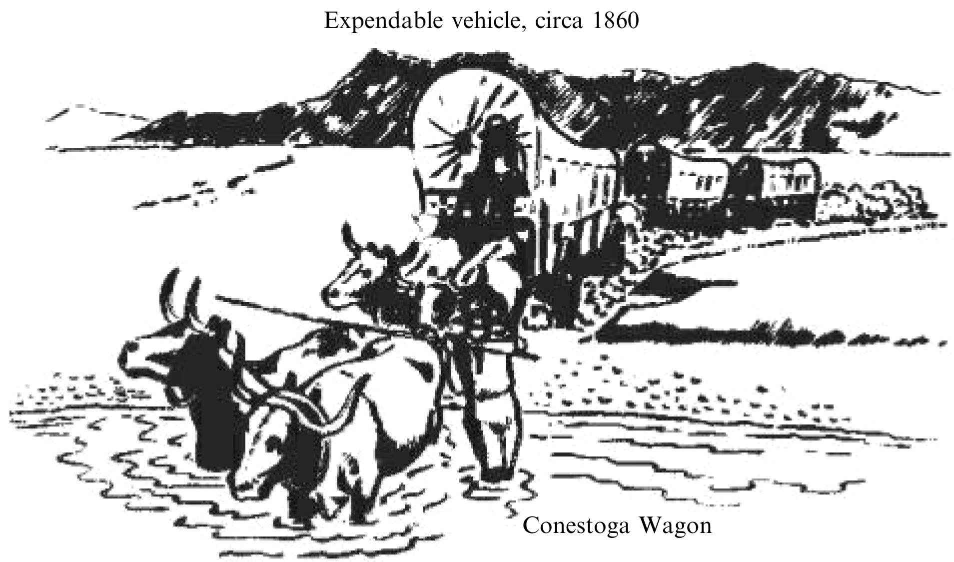

Figure 2.5. Expendable vehicles are for pioneers to open up new frontiers and establish a one-way movement of people and resources.

Sustained-use vehicle, circa 1860

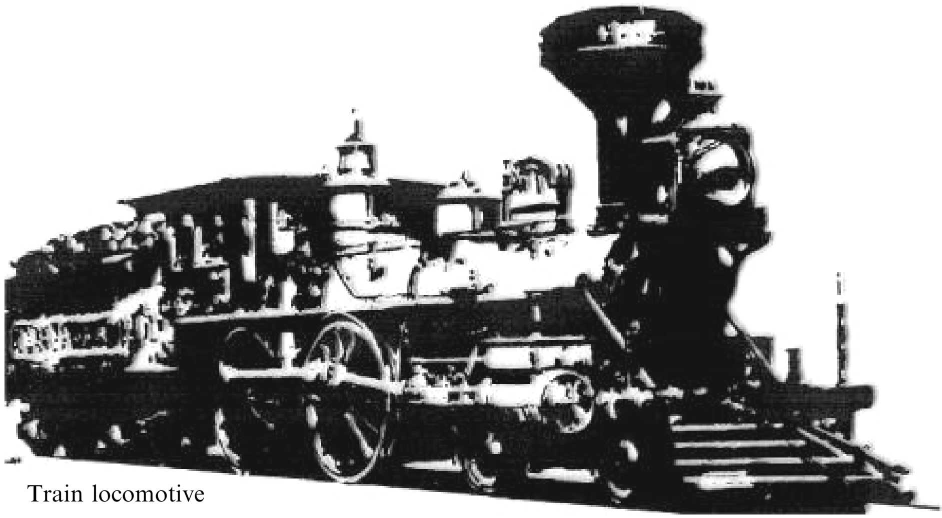

Train locomotive

Figure 2.6. Sustained-use vehicles industries used to open up new economic frontiers and establish scheduled, regular, sustained two-way flows of people and resources.

Reusable Launch Vehicle (RLV) and Highly Reusable Launch Vehicle (HRLV) concepts, but this is a far cry from the sustained-use, long-life aircraft represented by the DC-3. The fact that each expendable launcher is launched for the first, last and only time punctuates our failures. The expendable launcher market is limited, and so is the potential to justify further developments. All of the nations that launch satellites followed the same path, in a sort of 'follow the leader' mindset. The dream of a space transportation system was never permitted to become reality, unlike that of an airline transportation system.

The difficulty is that few transportation systems began with an already existing, or ready-made customer base, whether the first coal transport to the coast from York, England, in the early 1800s or the United States Transcontinental Railroad [Ambrose, 2000]. In the 1870s most of the customers came only after the transportation system was established and two-way commerce could begin. As depicted in Figure 2.6, the railroad enabled the two-way transit necessary for the development of an economic frontier. According to the historical records, between 75% and 80% of the businesses founded in the westward expansion did not exist at the time the railroad began. In the 6 years (1863 to 1869) that it took to build the transcontinental railroad an enormous quantity of men and materials were consumed. Stephan Ambrose's book, *Nothing Like It in the World*, documents the dedication of the dreamers, surveyors, tracklayers, graders, engineers and laborers that made the transcontinental railroad possible [Ambrose, 2000]. Compared to the task of designing, surveying and building the United States Transcontinental Railroad, developing and launching the first sustained use aerospace plane appears to be less labor-intensive and less of a challenge. The current approach of analyzing a future market based on present concept of operation demonstrates that no market exists. The result is the conclusion that the status quo is either sufficient or even over-capacity. Planning a future transportation system to that non-existent market will not yield a satisfactory system now, nor would it have in the 1850s for trains or in the 1930s for aircraft.

2.4 EVOLUTION OF SPACE LAUNCHERS FROM BALLISTIC MISSILES

During the International Geophysical Year (IGY), the USSR lofted the first artificial earth satellite (Sputnik I) into low Earth orbit by adapting a military ICBM, the SS-6 (Figure 2.7), to become their first launcher [Clark, 1988]. That can be defined as typical of Russian design procedures. The United States has achieved its expendable and partially reusable launchers in a similar manner. The US Army Redstone IRBM was the vehicle to launch the First US astronaut (Alan Shepherd) into space on a

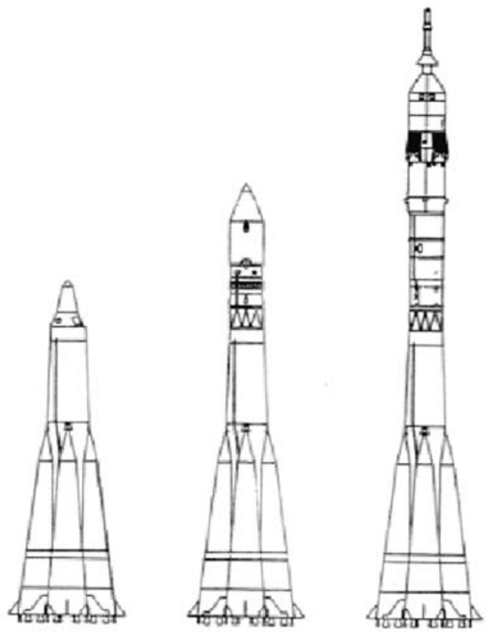

System	SPUTNIK	VOSTOK	SOYUZ
Launch Weight	267 t	287	316
Payload Weight	1.55 t	6.7	8.8

Figure 2.7. The conventional path for launcher development is the adaptation of a military ballistic missile (SS-6 'Sapwood') to a space launcher. 'Sputnik' is an almost unmodified SS-6. 'Soyuz' is a very capable, very reliable space launcher with hundreds of launches (over 90 per year).

ballistic trajectory. The USAF Titan ICBM became the mainstay of the McDonnell Douglas Gemini manned spacecraft program. The McDonnell Douglas Delta launcher began its career as the Unites States Air Force Thor IRBM. The Thor core continues to serve even now, as the Boeing Delta II and Delta III launchers. The Convair Atlas launcher began as the USAF Atlas ICBM, and was the launcher that put John Glenn into the first US astronaut Earth orbit in the Mercury capsule. It keeps on living today, with Russian-derived RD-170 rocket engines, as the Atlas V. Even in Europe, ESA launchers have an industrial rocket hardware base to build on that is military-derived (e.g., the future VEGA launching system).

In fact, in order to begin, this was about the only alternative in existence. What it did, though, was to instill an operational concept of the expendable system as the most cost-effective approach, and with its low launch rate, to assure a continuing manufacturing base. Consider, for instance, the consequences if the first launchers were capable of just 10 launches before overhaul. In the early years, that might have meant only one or two launchers being fabricated, instead of 20. The aircraft scenario was different because there were customers for all of the DC-3s that could be built, and literally hundreds of thousands of potential and actual passengers. For space activities to change, there has to develop a similar customer base requiring hundreds of flights per year, rather than eight to twelve.

In this context, the former USSR came the closest. When one of the authors visited Baikonur in 1990, the civil Soyuz launch complex had launched 90 Soyuz in the previous 1-year period. The launch and countdown was based on a military counter-strike philosophy. There were about seven Soyuz and Soyuz payload in active storage. These could be launched in about 12 hours. On the day the author witnessed the Soyuz launch, the Soyuz arrived, transported horizontally on a train, at about 05:30 h. By 07:00 h the Progress spacecraft (Progress is a Soyuz manned capsule reconfigured as a propellant and materials re-supply vehicle) was horizontally integrated into the Soyuz launcher. It was then taken by rail to the launch site and erected. After 10:00 h the propellant loading and countdown of the Soyuz launcher was executed by a neural network system of computers. The computer system 'remembered' the Soyuz launch history over its several hundred launches. If any feature in the countdown matched a previous problem or potential problem, a service crew was sent to the launch pad to check the launcher. During this checking time the countdown continued, with only the item in question on hold. When the item status was confirmed as 'OK' that item was re-inserted into the count. According to the Soviet Launching Officer on site, only one in fourteen launches have holds past the scheduled launch time for more than 15 minutes. The Soyuz and Progress capsule was launched at 17:05 h that afternoon (Figure 2.8). In spite of the accomplishments of the Soyuz program, it remained an expendable launcher [Karashtin et al., 1990].

The heaviest lift launcher available in the former USSR was the Proton. The Proton was the result of an uncompleted intercontinental ballistic missile program. The Proton is powered by a hypergolic propellant rocket engine, the RD-253, in a unique arrangement. That is, a central larger diameter oxidizer tank is surrounded by six smaller fuel tanks, each with an RD-253 engine installed, as shown in

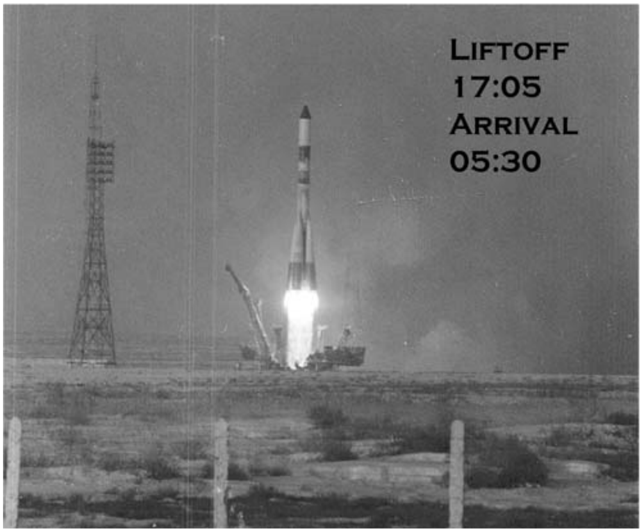

Figure 2.8. 'Soyuz' launch with 'Progress' re-supply capsule at 17:05 h on April 1999, from Baikonur Space Center, Tyuratam, Kazakhstan (Photo by the author).

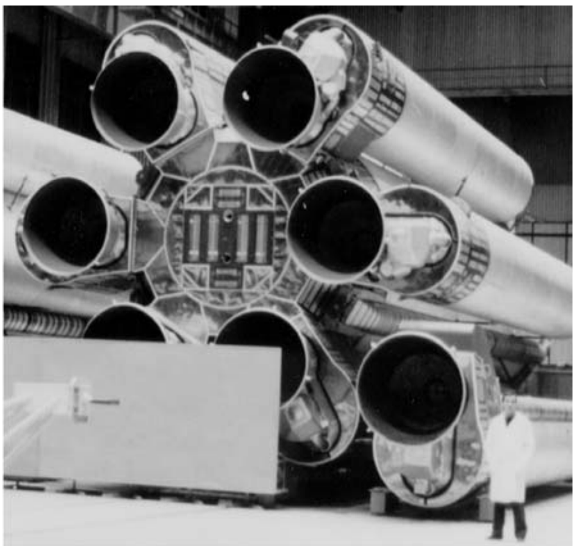

Figure 2.9. Proton first stage in Moscow plant.

Figure 2.9. The hypergolic propellant driven turbopumps start up so abruptly, that the sound is almost like an explosion! The launcher is one of the more reliable launchers available for heavier payloads, but like Soyuz, it is completely expendable. The Proton continues to be produced today, offered as a reliable heavy-lift launcher

by a consortium that includes Lockheed Martin. It is an important element in the construction of the International Space Station. The Russian space organization wanted a launcher that was recoverable, that was reusable, and that was capable of heavy lift to orbit for a spectrum of missions, going from the support of facilities in LEO to deep-space missions [Gubanov, 1984]. With the United States initiation of the 'Star Wars' space defense program (SDIO) and the Space Shuttle, the Soviet military was convinced they needed to counter a new military threat. They perceived (correctly) 'Star Wars' as a system to destroy their warheads and warhead delivery systems. But they also perceived the Space Shuttle program as a disguise to create a direct attack, fractional orbit 'Space Bomber'. This perception would merge into what was to produce eventually the fully reusable heavy-lift vehicle 'Energia' and the fully automatic military space plane 'Buran'. By whatever method of calculation, the Soviets concluded that the Space Shuttle initiative was sufficiently important to build seven vehicles [Legostayev, 1984]. After NASA fielded the three operational shuttles, the Soviets were convinced that 'the missing four' were hidden someplace, ready to launch at the Soviet Union in a manner similar to the ICBMs in missile silos [Lozino-Lozinski, 1986]. In fact, strange as it may seems, it was reported that just seven Buran airframes were fabricated, in a tit-for-tat response to the US shuttle program [Lozino-Lozinski, 1990]. Buran was derived from Lozino-Lozinski's work on the 'BOR' series of hypersonic gliders that began in the 1960s, analogous to the Unites States Air Force Flight Dynamics Laboratory efforts [Buck et al., 1975]. According to Lozinski, he had launched at least 24 test vehicles of the BOR family using scrapped ballistic missile stages. The United States Air Force Flight Dynamics Laboratory had launched several 'Asset' hypersonic glider test vehicles in the 1960s, but that is the limit of the US experience [Buck et al., 1975].

The result of these Russian efforts was a heavy launcher capable of launching either cargo or a spacecraft to space that was fully recoverable in its operational form. In its principal operational version, 'Energia' was equipped with a side-mounted cylindrical cargo carrier that could be configured as a heavy-lift package to LEO, or a satellite to GSO, a payload to be delivered to the Moon or Mars, and a deep space probe. Unlike the United States Shuttle, the primary propulsion engines were mounted on the center main tank on the space plane. In fact because of the emphasis on astronauts with a design that can never be flown without astronauts, the Shuttle has no heavy-lift canister or heavy-lift capability. The author drew Figure 2.10 during a lengthy discussion with Boris Gubanov at a Space Conference in Bonn, Germany, in 1984. This figure clearly shows the concept of operation. There were few disposable parts. The side canister could be configured with just sufficient propulsion to reach LEO, or with sufficient propulsion (and less payload) for a Moon, Mars or a deep-space mission. The Zenit-based strap-on boosters were equipped with lifting parasail parachutes at the front and rear of the booster. The intent was to glide in the vicinity of the launch site for recovery. Since the boosters were liquid boosters (equipped with Energomash RD-180 rocket engines), there was little refurbishment, unlike the US solid propellant strap-on boosters. These solid boosters cost as much to refurbish as to build new. The Buran center tank has a very low ballistic coefficient, and using a Lockheed concept to reduce the heating with the

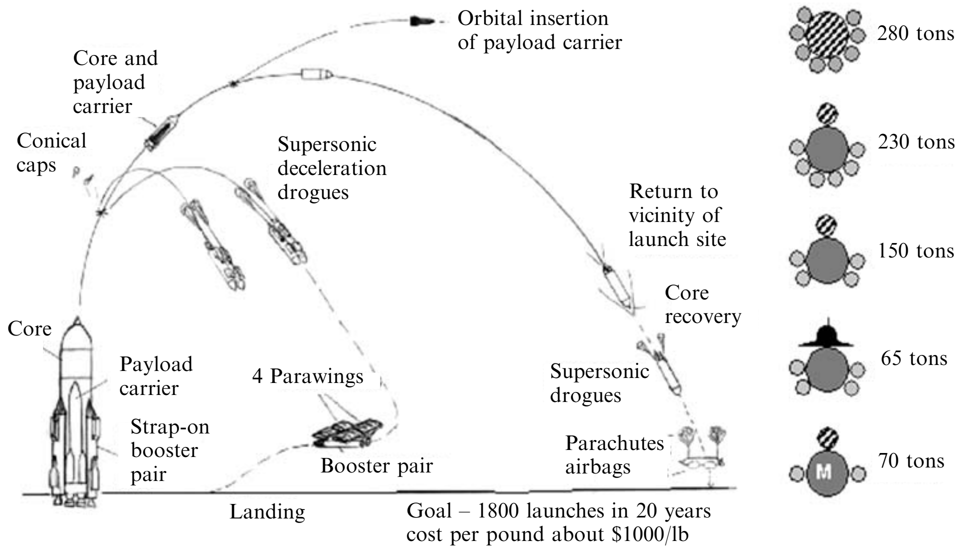

Figure 2.10. Energia was an approach to achieve a fully reusable (all major components recoverable), extended-life launcher (at least 50 launches without overhaul) with a Saturn V heavy-lift capability that the United States discarded. Right side shows strap-on booster configurations and payload to LEO. Energia M was in development in 1990.

thermal and antistatic coating applied to the booster, the entry into the atmosphere could be relatively easy. The center tank did a fractional orbit and was recovered in the vicinity of the launch site. Although never implemented in the first two test flights, the eventual operational capability planned was to recover all major components. Said otherwise, Energia was to be the USSR's fully recoverable Saturn V. The booster configurations on the right side of Figure 2.10 show the payload to LEO for the different strap-on booster configurations. For the four pair configuration, the payload was carried in tandem with the center tank in a special powered stage. For the two pair configuration, two payloads are shown, the canister and the Buran. The Energia M was a two strap-on booster arrangement for a lesser payload. The author saw Energia M in the Energia assembly building in 1990 (there is no reported flight of this version). Note the intended fly rate from three launch complexes: 1800 flights in 20 years, for an annual fly rate of 90, about the same as from the Soyuz launch sites. If the cost is the same for Shuttle, $US 1.32 billion for five flights and $US 100 million for each additional flight, then with a mix of Buran and canister payloads, the payload cost to LEO is in $US 450 to 650 per payload pound. So frequent flights of cargo-configured vehicles lowers costs: the Energia would have been a wise investment. The Russians thought very highly of Saturn V, and were dismayed that the United States would summarily discard a heavy-lift vehicle capable of lower cost to orbit (about $US 5700 per pound payload in the 1980s) than the Space Shuttle.

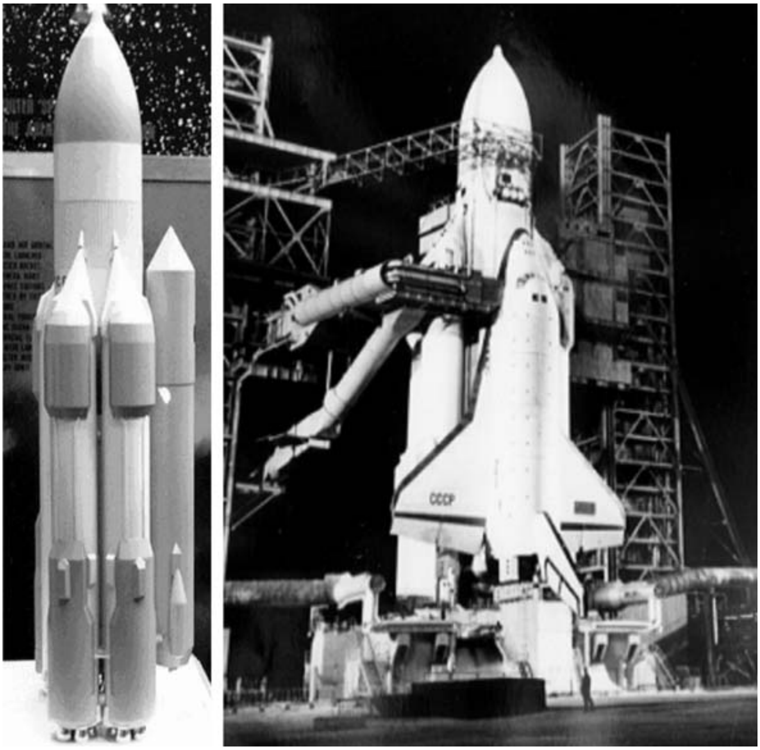

Figure 2.11. A model of the 'Energia' showing the strap-on booster parachute packs and cylindrical payload container (left) and the Buran space plane on the Baikonur launch complex (right). The RD-0120 engines are on the center tank, which is recoverable.

The Energia had several launch configurations to optimize different size payloads for different orbits. The Zenit (SS-16)-derived strap-on boosters were assembled together in pairs. The standard configuration was two coupled pairs, for a total of four individual strap-on boosters. In this configuration the Energia could deliver 150 tons to LEO in the cargo canister configuration and 60 to 80 tons when carried in Buran. With three Zenit pairs, Energia could place 230 tons in LEO with the side-mounted cargo canister. If an in-line cargo section were added to the center tank in lieu of the side-mounted canister, then up to 280 tons could be delivered to LEO, an astonishing figure nowadays (the US Shuttle can deliver less than 4% of this payload to LEO). It was this latter configuration that was the counter-'Star Wars' configuration. Figure 2.11 shows a model of Energia (left) from an AIAA technical meeting display, with the side cargo canister mounted. Clearly visible are the forward and aft parachute packs on each of the strap-on boosters. Utilizing the Zenit launcher as the strap-on booster meant that this part of the system was already an operational launch system, and a reliable component. On the right is a night picture of Energia with Buran mounted and being prepared for launch [Gubanov, 1998]. The gray horizontal cylindrical tube is the crew access

Figure 2.12. Fly-back version of the strap-on as an alternative to lifting parachutes.

to Buran. The angled tube is an escape path to an underground bunker, in the event of a launch mishap. The two horizontal tubes in the lower part of the figure are ducting that lead to the rocket exhaust chute under the vehicle. These are attached to about eight vacuum cylinders on each side, equipped with compressors and a vent stack. When the hydrogen flow is initiated to the rocket engines, this system is opened and any vented hydrogen is drawn off, compressed and burned in a vent stack. The original design was to construct three launch sites in close proximity, so that nine Energia/Buran and Energia/canister configured vehicles could be launched within three days in case of a Space Shuttle/Star Wars attack. None of this was ever accomplished. The Russian Space organization wanted also to replace Proton with a reusable vehicle. When the author visited Baikonur in 1989 there was an Energia M being assembled that has just two Zenit strap-on boosters instead of four. It was their intent to make this the medium-lift launcher replacing Proton. With the side payload placement Energia M could accommodate a payload canister or a smaller hypersonic glider, such as a crew rescue vehicle based, for instance, on the BOR vehicles.

Figure 2.12 shows a modification to the Zenit strap-on booster so that it has a skewed-axis wing instead of four sets of lifting parachutes (Figure 2.11) and a turbojet with a nose inlet in the front of the booster for a powered return; it was shown in an American Institute of Aeronautics and Astronautics technical meeting in 1992.

For readers who may wonder, ‘Buran’ is not a US Space Shuttle, or a copy of it. Its intent is very different. The author visited the Buran II assembly building at

Baikonur in 1989. The glide angle of attack for maximum lift to drag ratio is 10° to 15° less than the US Shuttle. Buran is a fully automatic vehicle with a neural network-based control system. It landed for the first, last and only time at the specially constructed runway at Baikonur without any human intervention. This took place during a snowfall and with significant 90° crosswind; it touched down within a few meters of the planned touchdown site [Buran Site Director, 1989]. As with all Soviet spacecraft, it was never intended to be controlled by human pilots, except in a dire emergency. Its thermal protection system was (and still remains) unique and capable of handling lost surface tiles without damaging the airframe structure [Neyland, 1989].

The reported maneuver Buran did on landing was much discussed in a 2002 article in *Air & Space* but it was not a poorly executed automatic landing: in fact, it was strictly the result of the neural network flight-control computer developed by the USSR Academy of Sciences, Siberian Branch, in Krasnoyarsk in the 1980s [Bartsev and Okhonin, 1989] and built by a company in the Ukraine. The flight-control system had determined that in the entry, the actual lift to drag ratio (L/D) had exceeded the estimates used in the pre-planned flight trajectory. As a result, the aerodynamic heating Buran encountered during re-entry was greater than expected, and due to the control surfaces deflections required to trim Buran near to its expected L/D. So, Buran entered the approach pattern much faster than anticipated. If Buran was to land successfully the excess speed had to be bled off. The neural network controller, without any input from ground control, executed a 540-degree turn, rather than the planned 180-degree turn, to bleed off the excess speed [Lozino-Lozinski, 1990]. Then, Buran touched down on its planned landing point with the correct speed.

Figure 2.13 is a photograph taken from the Buran display in the Moscow Space Museum. It shows conclusively that Buran is more closely related to the United States Air Force Flight Dynamics Laboratory hypersonic glider designs than to the Shuttle. In order for the leading edge vortex (a main source of lift) not to burst, the angle of attack would have been in the 25° to 30° angle of attack range, not the 40° to 45° planned for the United States Shuttle. In many aspects this is a very revealing photograph, as it documents the similarity of Buran with the high-performance *military* hypersonic gliders that Draper, Buck, Neumann and Dalhalm developed at the Flight Dynamics Laboratory in the 1960s. The burn marks on the elevon indicates that the elevon deflections were greater than anticipated and the heating more severe. Pictures in the Moscow Space Museum show the underside of Buran I after flight and there are white streaks emanating from the gaps in the tiles. This is indicative that the tile/aluminum interface temperature would have exceeded 100°C had not the tile adhesive/phase-change material been present and active. This Russian adhesive incorporated a phase-change material that in the event a tile was damaged or lost was capable of maintaining the interface with the aluminum structure at no more than 100°C for several minutes at peak heating conditions, to prevent thermal damage. The intentional gap in the tiles permitted the vapor from the phase-change material to escape. V. Neyland, one-time Deputy Director of the Russian oldest gasdynamic center TsAGI, tested this strategy in one of TsAGI wind

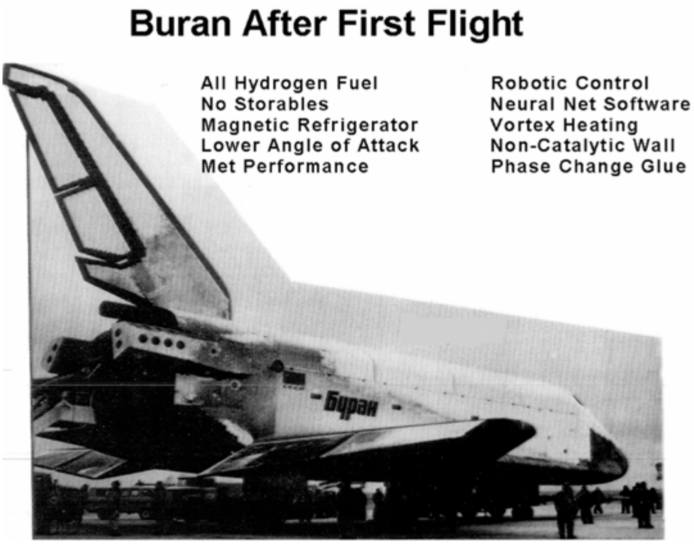

Figure 2.13. Buran after landing on its first, last and only flight. Note the vortex heating emanating from the juncture of wing and fuselage. This matches the thermal mapping test at TsAGI, and proves the angle of attack was sufficiently low that it did not burst, as it does on Shuttle. The burned spot on the inboard elevon is the vortex core location.

tunnels (one of these authors has a copy of the data report [Neyland, 1990]). The thermal protection tiles the Buran employed are structurally strong. During a 1988 visit to Russian research institutes, at Komposit OKB, the author (PC) saw a Buran tile heated to white heat with an oxy-hydrogen torch and then dropped into water, with no damage to the tile. The Buran tiles were intentionally gapped with plastic spacers and were mounted with the unique adhesive described above, that acted as a thermal safety layer.

So, at the beginning of 1990, Russia had the hardware in test for a family of fully recoverable and reusable rocket-powered vehicles for medium and heavy lift. Ten years later, by the beginning of the 21st century, neither the Unites States nor Russia had a heavy-lift launcher on the order of Saturn V any longer. Shuttle was limited to about 11 tons, and Proton was probably in excess of 20 tons. So it fell to the Proton to accomplish lifting the heaviest ISS payloads. Thus with both the United States Saturn V discarded in lieu of the Space Shuttle, and the demise of Energia, unfortunately there is no longer an affordable heavy-lift launcher available to either the United States or the Russian Republic.

2.5 CONFLICTS BETWEEN EXPENDABLE ROCKETS AND REUSABLE AIRBREATHERS

The fundamental question always posed is: ‘Why airbreathers?’ One observation is that specific energy (energy/mass) is a function of speed squared. So if an airbreather

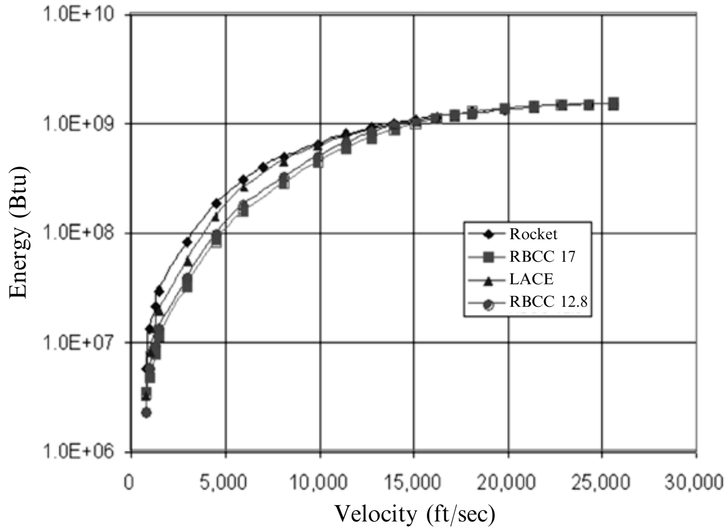

Figure 2.14. Total vehicle energy approaches a constant. Mass is being lost as fast as kinetic energy is increasing for all propulsion systems.

only flies to 12,000 ft/sec rather than orbital speed of 25,573 ft/sec it achieves only 22% of the orbital energy. For specific energy this is correct. However, the launcher is much heavier at launch than when entering orbit. So the total energy (Btu or MJ) is a very different value. Figure 2.14 shows the total energy for launch vehicles with four different propulsion systems. The value of total energy at 12,000 ft/sec (3,658 m/sec) is 70% of the orbital value, a much more significant value. Note also all of the different propulsion system curves converge to a single total energy curve above 15,000 ft/sec (4,572 m/sec) or an energy of 10^9 Btu (1.055×10^9 kJ). The energy does not continuously increase as the square of the velocity because the rocket engines are consuming the mass almost as fast as the specific energy is increasing. However consistent the energy levels are, the weight (mass) levels are not. Figure 2.15 shows the weight (mass) along the trajectory is a unique characteristic of each propulsion system. The weight/time history during the ascent to orbit is given for four different propulsions systems as a linear function of the logarithm of flight path energy. All have essentially the same on-orbit weight (a correctly selected propulsion system has little impact on the vehicle empty weight). For the three airbreathing concepts, once the ‘all rocket propulsion’ stage is reached, the weight histories are essentially identical. Even a simple airbreathing rocket (LACE or Deeply-Cooled) that operates only to Mach 5 or 6 makes a substantial reduction in liftoff weight. In fact increasing the airbreathing speed to Mach 17 from Mach 12 has much less impact than moving from Mach 6 to 12. What the propulsion system directly affects is the oxidizer to fuel ratio at the beginning of the flight when the thrust required is the greatest and a reduction in the oxidizer-to-fuel ratio has the greatest effect, as shown by the liftoff weights on the left-hand ordinate.

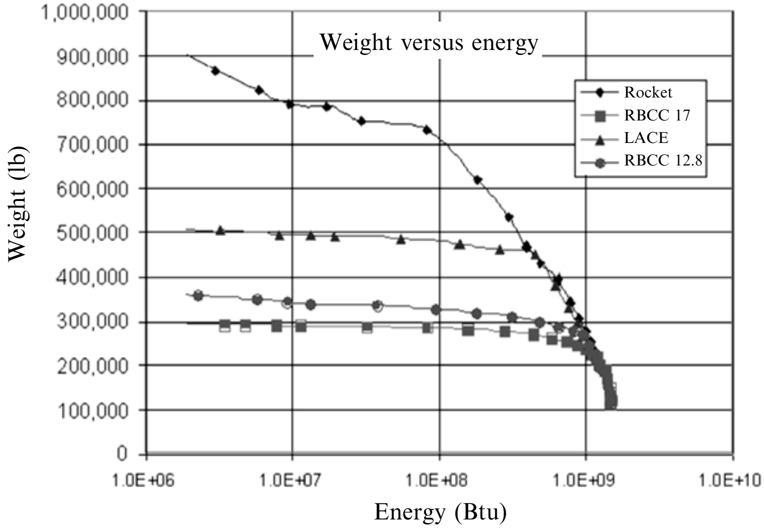

Figure 2.15. Adding the weight history shows the differentiation of the propulsion systems in terms of initial (lift-off) weight and the convergence to a single on-orbit value.

As developed in this chapter, systems studies with what appear to be rational assumptions such as turbojet low-speed propulsion or a combination of engines, doom the airbreathing launcher from its inception. A combined cycle propulsion system in which a single propulsion system can transition from one mode to another is the key to the success of the airbreathing launcher. As Figure 1.1 implies there continued an effort to design and build an aircraft-like hypersonic vehicle that could fly to space [HyFac, 1970; Lockheed Horizons, 1966]. However as many valid programs that were initiated, there were as many programs seeking to discredit the airbreathing vehicle effort. Figures 2.16 and 2.17 show one such example of the conflict as presented in a briefing in the 1970s. The three aircraft shown in Figure 2.16 are, from top to bottom, an all-rocket single-stage-to-orbit (SSTO) launcher, a Boeing B-747-100, and an airbreather/rocket SSTO powered by a combination of 35 turbojet, ramjet, scramjet and rocket engines. So at any one time, three-fourths of the installed propulsion system was being carried as dead weight. As correctly depicted it is a very large airbreathing/rocket SSTO because of the inert weight carried in the non-operating engines. The turbojet is a very poor acceleration propulsion system and can consume more fuel than a rocket in some flight regimes. To many, this was a legitimate comparison considering the low launch rate of rocket launchers, the non-existence of a viable civil need to increase the launch rate, and, for the rocket advocate, the absence of a good reason to replace the rocket.

However, the advocates of an integrated, combined cycle airbreathing/rocket SSTO were proposing a very different system, based on the integration of several different engines into a single combined propulsion system that recovered rejected heat and converted most of the recovered heat as propulsion system thrust or system

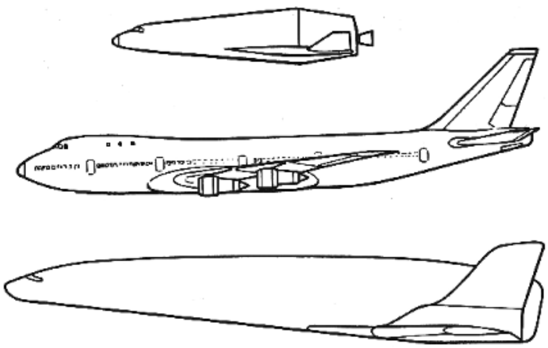

Figure 2.16. The goal is a launcher that flies regularly to space. The all-rocket SSTO launcher (top) is smaller but heavier than the B-747 (center). The airbreather launcher powered by a combination of 35 engines of four different types is larger and heavier than the B-747, discouraging the airbreather concept.

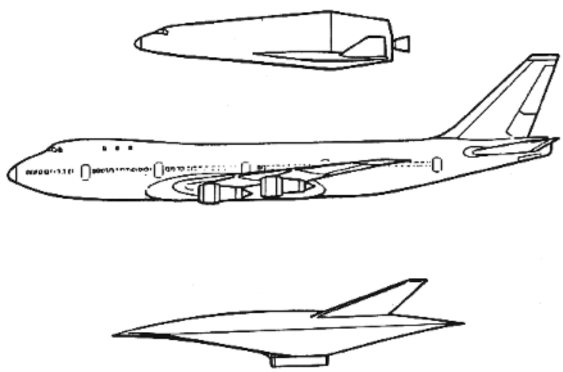

Figure 2.17. The goal is a launcher that flies regularly to space. The all-rocket SSTO launcher (top) is smaller than the B-747 (center). The airbreather launcher powered by a combined cycle ejector ram–scramjet is smaller and lighter than both, but is never pursued as a launcher or hypersonic cruiser.

work. The three aircraft depicted in Figure 2.17 are, from top to bottom, the all-rocket single-stage-to-orbit (SSTO), the Boeing B-747-100, and an integrated combined-cycle airbreather/rocket SSTO vehicle. The aircraft depicted is from McDonnell Douglas Corporation, McDonnell Aircraft Company, St. Louis, Missouri, as presented by the United States Air Force Flight Dynamics Laboratory (AFFDL). The combined cycle propulsion system integrated thermally and physically into one system the rocket, ramjet and scramjet (see Chapter 4) so that there is one and only one *propulsion system* operating. The result is a vehicle with slightly less volume and empty weight than the all-rocket and about one-third the gross weight. The airframe and propulsion system were designed for at least 100 flights before overhaul. At the flight rate anticipated in 1968 that was sufficient for 8 to 10 years'

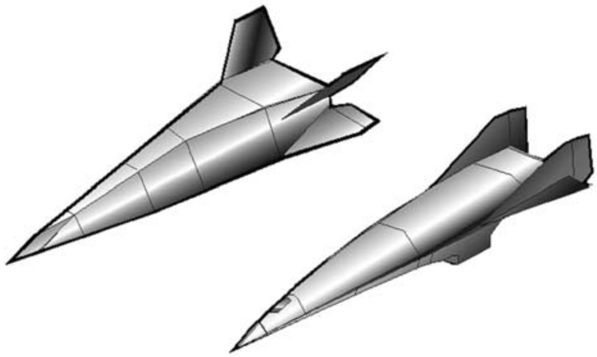

Figure 2.18. Airbreather/rocket, single-stage-to-orbit configuration (left) and a rocket-derived hypersonic glider, single-stage-to-orbit configuration (right).

operation with inspection and maintenance as now accomplished on commercial aircraft. The perception was that the simpler and increasingly reliable rocket was the least costly for the low launch rate required at the time. The launch rate could not be increased because of the selection of the rocket launcher as the primary space launcher system and the payloads that required a high launch rate never appeared, justifying the selection. So the expendable rocket launchers prevailed, and none of the expectations of the hypersonic engine and aircraft of the late 1950s and early 1960s were ever realized. Historically, much of the work done on these vehicles was for highly classified military programs with very limited access and is now lost or shredded. References (such as [Stephens, 1965; McAIR, 1966a,b; Lockheed, 1967]) are the program references that document a small portion of what was accomplished.

The other great debate was single-stage-to-orbit versus two-stage-to-orbit. Both have advantages and disadvantages depending on operational concept and geographical location. It is the operational requirements that make the decision. For the support of an orbital station, as discussed in Chapter 3, with a very specific payload requirement and specific launch sites to a given orbital inclination and altitude, then a SSTO makes a good minimum operational equipment choice. If the operational mission is to deliver both crew and crew supplies in addition to large orbital payloads from different launch sites for different orbital inclinations and altitudes then the TSTO offers a wider range of versatility. Figure 2.18 shows two SSTO configurations based on an airbreathing-rocket propulsion system and a hypersonic glider based on a rocket propulsion system. Nominally these are in the 7 to 10 metric ton internal payload class. Chapter 3 provides a discussion of the rocket propulsion hypersonic glider that was proposed in 1964 to support the Manned Orbiting Laboratory with a 7-ton crew or supplies payload. Except for the configuration, the concept was analogous to the Russian Soyuz-Progress capsule. Although many concepts were analyzed and designed, these concepts were not able to displace an expendable rocket for any mission role.

For operational mission that deliver both crew and crew supplies in addition to large orbital payloads from different launch sites for different orbital inclinations

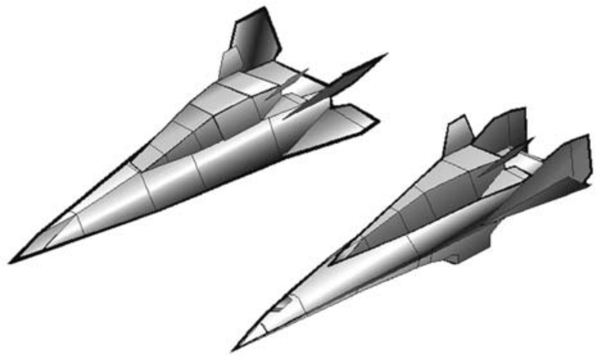

Figure 2.19. Airbreather/rocket, two-stage-to-orbit configuration with all-rocket second stage (left) and an all-rocket hypersonic glider, two-stage-to-orbit configuration with all-rocket second stage (right).

and altitudes then the TSTO offers a wide range of versatility. As shown Figure 2.19, there are two TSTO concepts. As shown, these have rocket-powered hypersonic gliders for second stages. Just as is shown for Energia in Figure 2.10, a faired payload canister can be substituted for the hypersonic glider. If the nominal payload of the second stage returnable hypersonic glider is 7 metric tons, then the payload for the expendable canister second stage could be as large as 23 metric tons or a space station component approaching 28 metric tons. So the payload capability to orbit spans a four-to-one range. With the flying capability of an airbreathing propulsion first stage, considerable offset is available to reach different latitude than the launch site or to expand the launch window by flying either east or west to intercept the orbital launch plane. With this versatility to provide launch capability to different worldwide sites, the TSTO makes an excellent choice for a commercial space launcher. Note that the upper stage can have either a pointed nose or the spatular two-dimensional nose. The latter reduces the nose shock wave drag by as much as 40% [Pike, 1977]. Pike began his work on minimum drag bodies in the mid-1960s. The spatular nose can be used on almost any hypersonic configuration whether SSTO or TSTO, first stage or second stage. Even though some excellent designs were originated in Germany, France, Russia, and the United States based on available hardware with very capable performance to LEO, none were ever able to displace the expendable rocket. The launchers remained as they began, as ballistic missiles.

The hypersonic first stages can require more runway than what is available at airports worldwide. V. Plokhikh and the late Lozino-Lozinski have proposed a TSTO based on the Antonov An-225, an An-125 large cargo aircraft modified to carry a space launcher atop the fuselage. The second stage can weigh up to 300 metric tons. In this case the fuselage of the An-225 can carry a portion of the launch crew and equipment. A second An-225 has sufficient volume to carry the liquid hydrogen required for the space launcher. In this case the An-225 is more of a mobile launch platform than a first stage. With the range of the An-225, and the low-

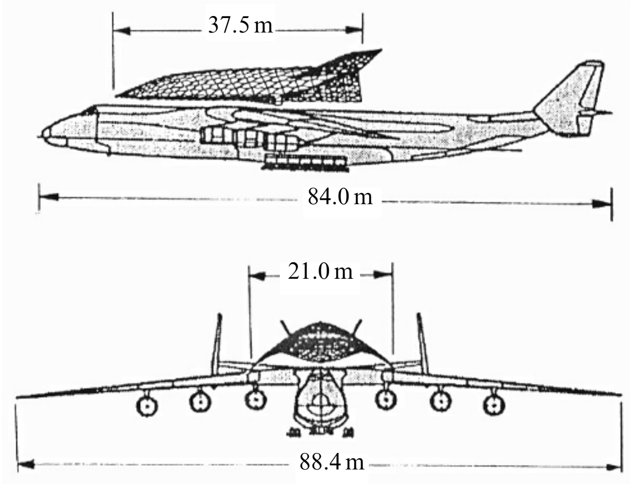

Figure 2.20. Large aircraft-based two-stage-to-orbit configuration with a combined cycle powered waverider second stage.

noise operation of the six turbofans that power it, the An-225 can make almost any commercial international airport a launch site. In Figure 2.20 the An-225 is shown with a combined cycle ram–scramjet-powered waverider mounted on top. The payload capability of the launcher is 7 metric tons. This particular approach has the An-225 operating on hydrogen fuel, and is equipped with an air collection and enrichment system in the cargo hold. That is, the hydrogen that is used to power the engines liquefies air and then separates the oxygen and nitrogen. The oxygen is liquefied and pumped into the launcher oxidizer tank (the launcher has no liquid oxygen in its oxidizer tank at takeoff, only the liquid hydrogen tank is filled). This means that the two aircraft are heaviest not on takeoff but near the launcher separation point [Czysz and Little, 1993]. Although a very straightforward approach, the only attempt to utilize the concept was for the BAe (Space Systems) HOTOL [BAe, 1991]. This was fraught with problems, for unlike the airbreathing combined cycle powered waverider in Figure 2.20 the HOTOL carried six to one liquid oxygen/hydrogen on board and the 300 metric ton payload capacity for the An-225 was easily exceeded. A LACE or deeply cooled powered HOTOL would have solved the problem (see Chapter 4). Again this was a very good concept for commercialization of a worldwide satellite launch service to any country desiring to put a satellite in orbit that is launched from that nation and not a foreign site—but one that failed to overcome the rocket disadvantages.

Steve Wurst of Access to Space LLC has recovered some of the historic hardware from the 'bone yard' of The Marquardt Company, as its property was being sold in bankruptcy, and transformed it into a modern combined cycle access to space launcher concept on private financing. Access to space launcher concepts do not fit the preconceived concepts of the government and, short of turning the project into a government-sponsored program with government control, the project remains

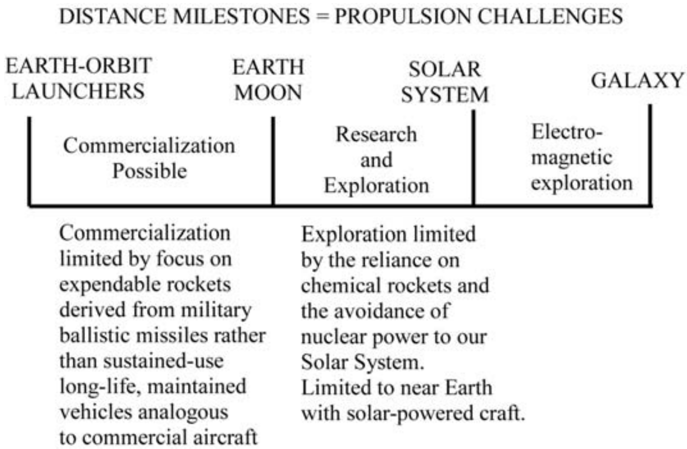

Figure 2.21. The result is that the potentials were never developed and impediments were sufficient to prevent any further hardware development of a truly sustained-use space launcher.

in the shadows. However, the over abundance of nay-sayers and skeptics, and the lack of dreamers continues to prevent the realization of a *transportation system* to space. We are left with Space Conestoga Wagons and have yet to see the 'railroad to Space'. As indicated in Figure 2.21, progress toward the future in both Earth-based launchers and space exploration appears to be impeded by the acceptance of the status quo. The key to breaking this stalemate is a propulsion system integrated into a sustained-use vehicle that can provide routine, frequent flights and advance our space capabilities. The X Series of aircraft proved that even high-speed research aircraft could be operated frequently and safely. And this despite the need to air launch these aircraft from a modified B-50 in the early flight operations and later the modified B-52. Nuclear submarine reactors are reported to outlive the hull, and are without nuclear accident. In space nuclear-electric propulsion is a vital necessity if we are ever to travel significant distances in meaningful time. The missing elements are the dreams, determination and resources analogous to those that were committed to the building of the transcontinental railroad [Ambrose, 2000]. In many respects the challenges are less daunting although the environment is a great deal harsher.

2.6 COMMERCIAL NEAR EARTH LAUNCHERS ENABLE THE FIRST STEP

Incorporation of air breathing offers many propulsion options; however, vehicle design choices are not arbitrary, since requirements and propulsion performance define the practical (technologically and commercially feasible) solution space. *A priori* decisions can doom success before starting on an otherwise solvable problem. One of the difficulties is the identification of need, and this at a time

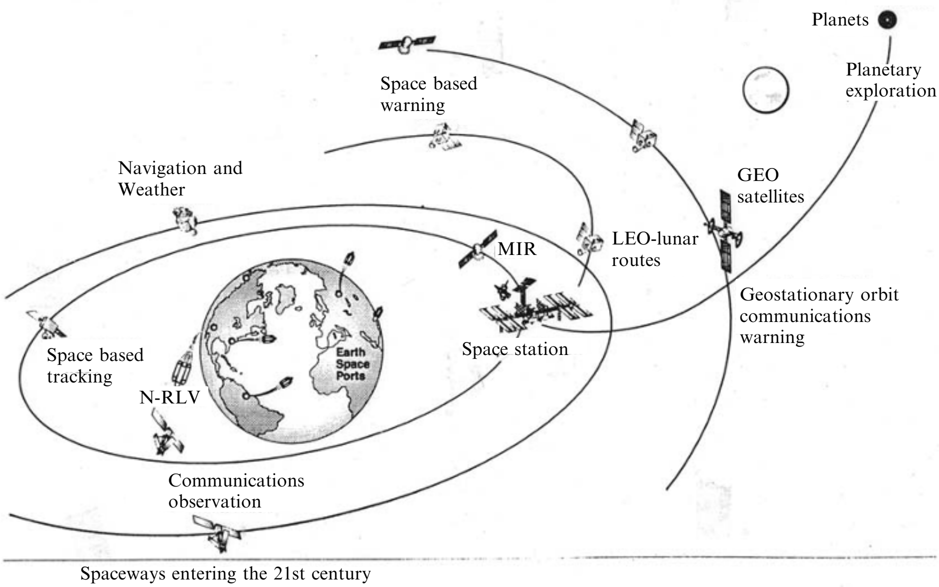

Figure 2.22. Our current space infrastructure, but without MIR is limited to specific LEO and GSO without significant intra-orbit operations. Hubble is in the space-based warning orbit, and is not shown.

when there is an overabundance of expendable launchers that do not have the capability of high fly-rates with the accompanying reduction of payload cost (see Figure 3.1). This issue brings back the Conestoga wagon versus Railroad comparison. Commerce with the Western United States was never possible with the Conestoga wagons, as none ever returned, becoming instead building materials for the settlers. All of projections of future space business for expendable or limited reuse launchers are as valid for future space business as the business projections for the future railroad based on Conestoga wagons. Dr William Gaubatz, formerly of McDonnell Douglas Astronautics and Manager of the Delta Clipper program, has addressed this issue in his briefings on space development. Figure 2.22 represents our current status. Remember, however, that since Dr Gaubatz made his presentation, MIR has deorbited and crashed into the Pacific Ocean and the International Space Station (ISS) has replaced it in 55-degrees inclination orbit. Expendable launchers can of course readily meet the military and commercial need that is suited to expendable launcher. Until a sustained use launch system is operational the payloads that warrant a high launch rate system will remain the subject of design studies only. In other words, without the railroad there will be no railroad-sized payloads for Conestoga wagons. Perhaps if the Space Shuttle main propellant tank was slightly modified to permit its use as a space structure, like the Saturn S-IVB, an infrastructure might begin to build [Taylor, 2000]. However the Shuttle main tank is intentionally not permitted to enter Earth orbit and is deliberately crashed into the ocean.

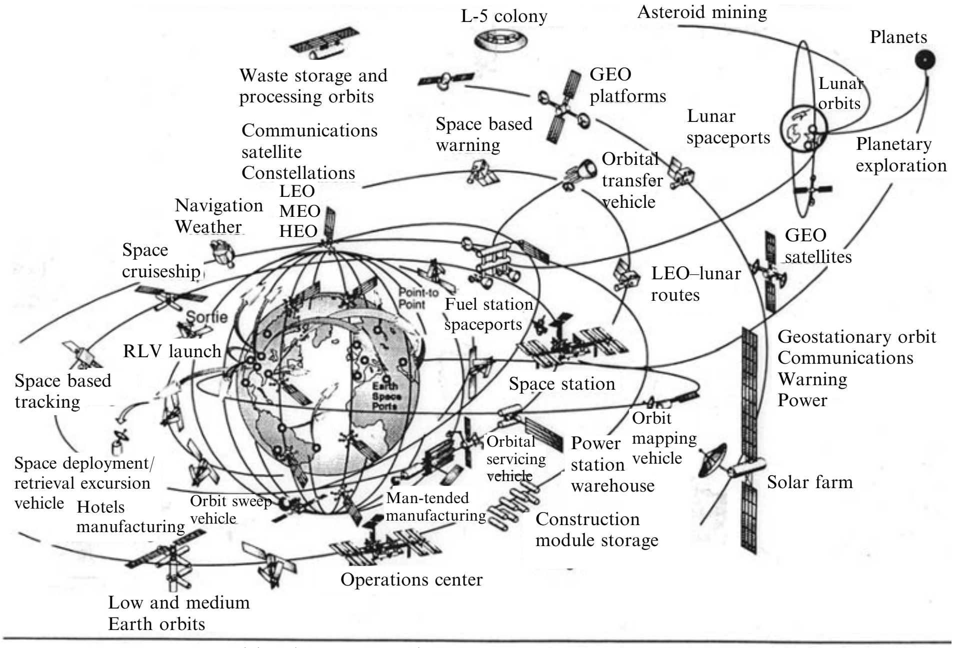

Figure 2.23. One US look to the future space infrastructure that fully utilizes the space potential by Dr William Gaubatz when director of the McDonnell Douglas Astronautics Delta Clipper Program, circa 1999.

For a true space transportation system to exist, a transportation system network has to be built, just as it was for the United States Transcontinental railroad. Dr Gaubatz attempted to anticipate what the future might hold, *if* a space transportation system actually did exist, as shown in Figure 2.23. The future space world envisioned becomes then a crowded, busy place. One of the key enabling space structures is the Fuel Station Spaceport network. Without these Fuel Stations movement between orbital planes and altitudes is limited to specific satellites, such a GSO communication satellites with integral geo-transfer propulsion. Note the Construction Module Storage, that can supply components for orbital, lunar and deep space vehicle assembly in space. The Operations Center and Space Station provide a system to launch and control missions to the Moon, planets and deep space. The Power Station Warehouse provides hardware for the power satellites in Geo-Earth Orbit, that, coupled with an Orbital Servicing Vehicle, can maintain this and other space resources. As in the USSR plan, there are lunar spaceports and lunar orbiting satellites. There are also space deployment and retrieval vehicles as well as a waste storage and processing facility in high orbit. So, Figure 2.23 provides a very comprehensive projection of future space *if* a suitable scheduled, frequent, sustained transportation and heavy-lift capability is available. That is what is needed to plan for the future, not the current status quo.

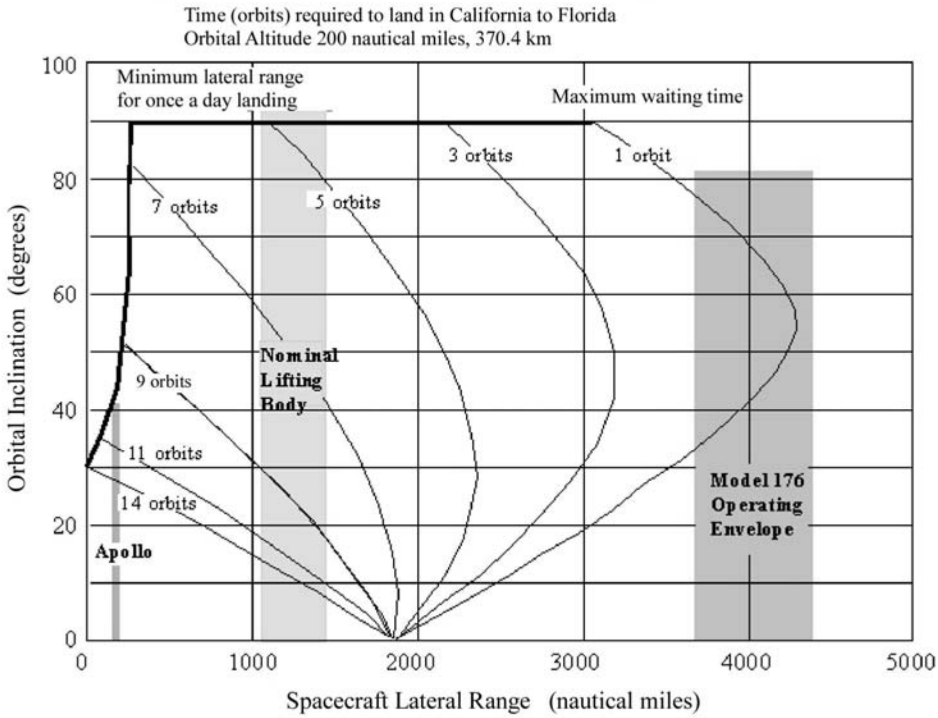

Figure 2.24. Waiting time is costly for commercial space operations.

There is a first step that can be made in propulsion to anticipate the future much as Steve Wurst has done. The key first step is off-loading some of the carried oxidizer by utilizing even partially airbreathing rockets, and designing for sustained operations over a long operational life with normal maintenance, not continuous overhaul and rebuilding. Design space solvable with current industrial capabilities and materials is readily identifiable. A cross-section of propulsion options that are based on available, demonstrated hardware and materials is presented and discussed with its pros and cons in Chapter 3. The propulsion systems that are necessary to reach LEO are evaluated in Chapter 4, including pulse detonation propulsion systems, in terms of takeoff size and weight required for a specified payload.

The focus of the discussion so far has been on a space transportation system. As with the railroad analogy, that implies efficient two-way travel to and from LEO. The vehicle configurations discussed have all had high hypersonic lift-to-drag ratios. The reason for that is the corollary to the argument that if waiting times and launch delays are economically penalizing to commercial launch vehicles, the waiting times and return delays are also economically penalizing. However, the way the continents and national boundaries are distributed on the surface of Earth means that a returning vehicle may have to wait until its landing site comes within the lateral range (cross range) capability. Figure 2.24 shows the waiting time in terms of orbits,

Table 2.1. Return from orbit performance is configuration dependent.

L/D	0.5	1.3	1.7	2.2	2.7	3.2
LR (nautical miles)	200	1,080	1,700	2,600	3,540	4,470
DR (nautical miles)	5,800	9,900	12,900	17,100	21,600	25,900
Waiting time at 28.7° (orbits)	14	11	8	4	1	1[a]

[a] at 55° orbital inclination.

as functions of the spacecraft lateral range capability and orbital inclination. This chart was salvaged from the original 1964 work done for the MOL support vehicle. For Cape Kennedy orbital inclinaion, the waiting times for an Apollo type balistic capsule (with very limited lateral range capability) can be 14 orbits or about 21 hours. For nominal lifting bodies the wait times vary from 11 orbits or about 16.5 hours to 8 orbits and about 12 hours delay. The class of vehicles discussed in Chapter 3 would have no wait times. They could return at any time, any location in the orbit they were in, and land in CONUS (Continental U.S.A). The longest return would be if the spacecraft were directly overhead the landing site: the spacecraft would have to circumnavigate the Earth in space, that is one orbital period of about 1.5 hours. The spacecraft hypersonic aerodynamic performance and its resultant glide performance is shown in Table 2.1 in terms of lateral range (LR) and down range (DR) together with the maximum waiting time.

The implication of commercial operational requirements is to be able to return to the landing site from any orbital location on the current orbit. That requires a high hypersonic lift-to-drag ratio glider. The Space Shuttle had a hypersonic L/D sufficient to land at its intended site after 1 missed orbit, or a 1,500 nautical mile lateral range. The hypersonic lift-to-drag ratio performance of spacraft discussed in Chapter 3 have hypersonic L/Ds of from 2.7 to 3.2, meaning they can land in CONUS from any position on a low Earth orbit (400 nautical miles or less).

So, this class of spacecraft can have a scheduled launch and return capability that minimizes waiting time and, more importantly for commercial passengers and crew, can return in an emergency without waiting time.

The correlation of lateral range and L/D and the resulting down range is given in equation (3.1).

$$LR = 1.667 + 68.016\left(\frac{L}{D}\right) + 706.67\left(\frac{L}{D}\right) - 91.111\left(\frac{L}{D}\right)^3$$

$$\left(\frac{L}{D}\right) = \text{hypersonic lift-to-drag ratio} \tag{3.1}$$

$$LR = \text{lateral range (nautical miles)}$$

$$DR = 4,866.6 + 4.704\,17LR = \text{down range (nautical miles)}$$

For continental Russia, the longitudinal span is twice that of the U.S.A, so the L/D requirement for any time return is less at approximately an L/D of 1.7. Lozino-Lozinski was a strong advocate of no waiting emergency return, and his BOR vehicles were capable of meeting the Russian L/D requirement. He had a forceful way of making his emergency return requirement much as Mr McDonnel had for the MOL support vehicle in 1964.

2.6.1 On-orbit operations in near Earth orbit: a necessary second step

The concept of the train yard as a center of operations for switching, long-haul train assembly, transfer of goods, refueling and repair is applicable to a space marshaling facility. The remoteness of space parallels the remote bases on the Earth's surface where the environment forces significant logistics operations to include propellant, cargo, repair parts, pilot accommodation, structures and support items. The late Frederick ('Bud') Redding formed a company, In-Space Operations Corporation (IOC) to exploit his orbital servicing and crew rescue vehicle (Space Cruiser). As originally conceived in 1980, the Space Cruiser was a low-angle conical hypersonic glider based on the McDonnell Douglas Model 122 (BGRV) experimental vehicle that was flown in 1966. As initially conceived, the Space Cruiser had a length of 26 feet and could be folded to a 13.5 foot length (see Figure 5.26). Redding adapted the design to incorporate an aft plug cluster engine configuration and storable propellants to create 13.3 kN (3,000 lb) of thrust. The 4,453 kg (10,000 lb) vehicle performed a variety of missions using the 8 cubic foot forward payload bay and the 4 cubic foot aft payload bay. The Space Cruiser is capable of atmospheric entry and uses a small drogue parachute at Mach 1 followed by a multi-reefed parafoil to land safely on any flat surface. The Space Cruiser was intended to be operated by a pilot in an EVA suit [Griswold et al., 1982; Redding et al., 1983; Redding, 1984]. In 1983, Redding modified the configuration to an elliptical cross-section thus expanding the propellant quantity, as shown in a McDonnell Douglas Corporation Trans-Atmospheric Vehicle (TAV) artist illustration in 1983, Figure 2.25. This particular configuration is based on a hypersonic glider research vehicle proposed to the United Sates Air Force in 1964. It has sufficient volume and cross range to act as a three-person rescue vehicle. The Space Cruiser is an LEO service vehicle that can utilize the refueling station shown in Figure 5.27. With its hypergolic propellant and small mass ratio, refueling was always a critical issue for the original Space Cruiser size. There were four basic tasks for the Space Cruiser as envisioned by Mr Redding, as a one- or two-seat resource mover between spacecraft or orbital stations in close proximity, a 'Lifecraft' or emergency rescue vehicle, and a movable orbital workshop for repairing or maintaining nearby satellites. In the folded configuration there was a camera mounted in the folded nose to act as a vehicle/satellite scanning system or an ad hoc reconnaissance vehicle free of the space station or shuttle.

For orbital transfer from low Earth orbits (LEO) to geostationary orbits (GSO) and return; collecting for repair or disposal of non-functional satellites in LEO; and GSO refueling of sustained-use satellites, orbital busses and tugs there is a real need for a nuclear-powered tug. This nuclear-electric-powered tug can sustain in-orbit operations and maintain a functional orbital infrastructure, including space habitats, free-flying facilities, and power stations. In Chapter 5 several levels of development are depicted using prior work of Dr William Gaubatz, Tom Taylor

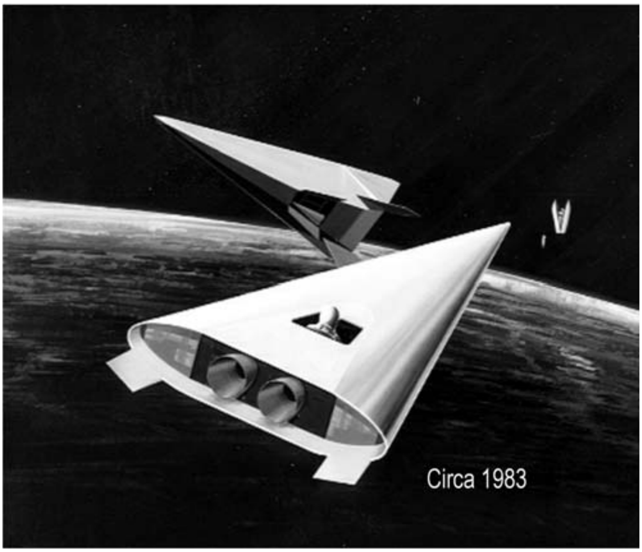

Figure 2.25. 'Bud' Redding Space Cruiser launched from a trans-atmospheric vehicle to accomplish a satellite repair. The Space Cruiser is able also to serve as a three-person rescue vehicle.

and 'Bud' Redding. The most important determination is the quantity of propellant required in LEO to implement the space infrastructure concepts in Figures 2.22 and 2.23 and the enormous quantity of launch propellant required to lift and accelerate the LEO propellant to low Earth orbit unless both airbreathing launchers and nuclear-electric space propulsion are operationally available.

2.6.2 Earth–Moon system advantages: the next step to establishing a Solar System presence

Unlike LEO orbital stations (MIR and International Space Station) the Moon is not devoid of indigenous resources, including gravity. Using Col. Tom Stafford's report to Congress on why we should return to the Moon as a data source, shows the advantages of the Moon compared to an Earth orbital station. This report shows also the advantages of testing and evaluating human operations on a foreign, inhospitable planet before venturing far from Earth, without the capability of easy and fast return. It also identifies the resources that can be obtained from the lunar surface and interior. A mass of liquid oxygen sent to LEO from the Moon may actually cost less than the same mass sent up from the Earth's surface. High-energy material recoverable from the lunar surface can power deep space explorers. Again, as in Earth orbit, the commercialization of sustained operations on it is needed. Chapter 6 discusses General Stafford's Congressional report and the need to return to the Moon.

2.6.3 The need for nuclear or high-energy space propulsion, to explore the Solar System

As discussed in Chapter 1, achieving much higher space speeds than are offered by practical rockets requires high-energy, high-specific-impulse propulsion systems. Chapter 7 presents some specific systems that are under development or in conceptual formulation. Researchers at the high-energy particle research facilities speak of space-available energy in a different way than chemical propulsion engineers. If developments continue in our understanding of energy, we may actually be able to traverse the Solar System nearly as quickly as the Earth–Moon system. If someone had told Donald Douglas Sr that just 30 years after the first DC-3 flew a prototype supersonic transport would cross the Atlantic at Mach 2.0, he would have laughed in disbelief. In fact he delayed the development of the DC-8 because he believed turboprops would hold the commercial market for over a decade before turbojets were commercially and economically practical. Nikolai Tesla, before 1930, stated that with his electromagnetic energy transmitter he could power a base on Mars from Earth (the Russians have done it on an orbiting satellite). Leik Myrabo has done experiments on a laser power vehicle ('LightCraft') at Holloman Air Force Base; see Chapter 6. All these avenues are explored in the attempt to fulfill the need for a high-specific-impulse propulsion system. In planetary exploration the holy grail is a propulsion system enabling a manned round trip to Mars in about 1 year: longer than that, solar flares and re-adaptation to both Mar's and Earth's gravity may be lethal to the human crew. Russia and a European nation are working on such a system. We need also to get to Pluto and the other gas planets in a reasonable time. All of these systems can operate within the acceleration tolerances of the human being and spacecraft structures. For humans to be in a sustained acceleration much greater than one '*g*' is probably untenable. Automatic, robotic spacecraft could accommodate instantaneous accelerations to eight to ten '*g*'s and sustained perhaps to three. This and other issues are explored and discussed in Chapter 7.

2.6.4 The need for very-high-energy space propulsion: expanding our knowledge to nearby galactic space

Researchers at the high-energy particle research facilities may be the source of the propulsion system that enables us to reach the nearby stars. Distances are in the tens and hundreds of light-years. Even the closest stars are farther than a human lifetime away at current chemical rocket speeds, and even fractional light speeds. Concepts based on solid quantum physics and some experiments are pointing the way, *if* we had an operational base on the Moon to mine helium-3. This next step depends on the previous three, and will probably not be realizable until they are accomplished. Nevertheless it is possible to identify propulsion systems that can work and why and how they work. The difficulty in achieving even near light speed is the acceleration required. In this and the next subsection the understanding of mass and inertia are is essential. If these speeds are to be real, then a means to negate mass and inertia are essential. Otherwise the spaceship and its contents will be flattened to a disc by the acceleration. This is discussed in Chapter 8.

2.6.5 The need for light-speed-plus propulsion: expanding our knowledge to our Galaxy

Researchers can now theorize quantum physics approaches to traveling at fractional light speed, and even at greater than light speed. Our Galaxy is about 100,000 light-years in diameter and about 20,000 light-years thick at the center. It might contain up to 100,000 million stars. The Earth is about 32,000 light-years from the center. Without the ability to travel in 'hyperspace', as described in Chapter 1, the galaxy is isolated from our ability to explore it in any other way than by remote sensing. Except for our nearby galactic neighbors, our Galaxy is off-limits. The distances are almost not comprehensible. At 1000 times the speed of light, it would take 32 years for us to reach the galactic center. Yet to consider super light speed is not any more daunting than the prior century researchers considering supersonic travel. There are concepts that are based on solid physics. Many of these are presented at the Annual International Astronautics Federation Congresses. Some will be discussed in Chapter 9 in terms of what might be possible.

2.7 BIBLIOGRAPHY

Ambrose, S. (2000) *Nothing Like It in the World*, Simon & Schuster, New York.

BAe (1991) Antonov DB, BAe Military Aircraft, BAe (Space Systems), Chemical Automatics DB, NPO Molnyia, TsAGI & TsIAM, *An-225/Interim HoTol Launch System Study*, Presentation to the European Space Agency, Paris, June 1991.

Bartsev, S.I., and Okhonin, V.A. (1989) *The Algorithm of Dual Functioning (Back Propagation): General Approach, Versions and Applications*, USSR Academy of Sciences, Siberian Branch, Institute of Biophysics, Preprint IC7B, Krasnoyarsk.

Buck, M.L., Zima, W.P., Kirkham, F.S., and Jones, R.A. (1975), 'Joint USAF/NASA Hypersonic Research Aircraft Study', AIAA 75-1039, AIAA 25th Aircraft Systems and Technology Meeting, Los Angeles, California, August 1975.

Buran Site Director (1989) Discussion during visit to Baikonur, April 1990.

Clark, P. (1988) *The Soviet Manned Space Programme*, Salamander Books, London.

Czysz, P.A. (1992) 'Space Transportation Systems Requirements Derived from the Propulsion Performance', Session: Hypersonic and Combined Cycle Propulsion, 43rd IAF Congress, Washington, DC, September 1992.

Czysz, P., and Little, J. (1993) 'Rocket Based Combined Cycle Engine (RBCC)—A Propulsion Systems for the 21st Century', 5th Aerospace Planes and Hypersonic Technologies Conference and Exposition, Munich, Germany.

Griswold, H.R., Stein, D.S., and Redding, F.W. Jr. (1982) 'Integration of a Crewman Into a High Performance Spaceplane', Twelfth Intersociety Conference on Environmental Systems, Society of Automation Engineers, Inc., San Diego, CA.

Gubanov, V. (1984) Private communication, International Astronautical Federation Congress.

Gubanov, V. (1988) Private communication, International Astronautical Federation Congress.

Gubanov, V. (1998) Photographs in Figure 2.11, Private communication, International Astronautical Federation Congress.

Harpole, T. (2002) 'White elephant', *Air & Space Magazine*, Dec 2002/Jan2003.

HyFAC (1970) Anon., 'Hypersonic Research Facilities Study'. Prepared under NAS2-5458, Vols I–VI, NASA CR 114322–114331, October 1970, Declassified 1982.

Karashtin, V.M., Zemtsov, I.V., and Shulman, L.B. (1990) 'Technology of Rocket and Space Pre-Launch Operations Control Systems Development', IAF-90-186, 41st Congress, International Astronautical Federation, Dresden, Germany.

Legostayev, V. (1984) Private communication, International Astronautical Federation Congress.

Legostayev, V., and Gubanov, V. (1985) Private communication, European Space Conference, Bonn Germany.

Lockheed (1967) Anon., 'A Study of Advanced Airbreathing Launch Vehicles with Cruise Capability', Lockheed Report IR 21042, The Lockheed Aircraft Corporation.

Lockheed Horizons (1966) Anon., *Lockheed Horizons*, Issue 4, first quarter 1966.

Lozino-Lozinski, G.E. (1986) 'BURAN': Its Creation and Prospects of its Usage', White Paper, 1984. Received during the International Astronautical Federation Congress, Malaga, Spain.

Lozino-Lozinski, G.E. (1990) Private communication/brief concerning BOR and Buran vehicles, International Astronautical Federation Congress.

McAIR (1966a) Anon., 'Mission Requirements of Lifting Systems (U), Summary of Significant Results & Figures', McDonnell Aircraft Report B947, prepared under NASA NAS 9-3562 (declassified 1970).

McAIR (1966b) Anon., 'MA188-XAB Baseline Dual Mode Scramjet for the McDonnell/Douglas Reusable Launch Vehicle Application, (U)', Marquardt Letter to MCAIR (Confidential).

Neyland, V.Ya. (1991) 'Scientific and Engineering Problems and Methods of Preflight Development of Orbiters', Draft Original of TsAGI paper.

Pike, J. (1977) 'Minimum Drag Bodies of Given Length and Base Using Newtonian Theory', *AIAA Journal*, Vol. 15, No. 6.

Plokhikh, V.P. (1983) Private communication, IAF Congress. Discussion with respect to his presented paper.

Plokhikh, V.P. (1989) 'Sensitivity Analysis of SSTO Reusable Vehicle Parameters', IAF-89-223, Malaga, Spain, October 1989.

Redding, Fred W., Jr. (1984) 'Spaceplane Technology & Research (STAR!)', DCS Corporation, Final Report, DARPAOrder4913.

Redding, F.W., Jr., et al. (1983) 'Spaceplane Examination', SRI Int'l, Final Report, Contract FO4701-8IK-0001, Managed by the Air Force Space Division, Sponsored by DARP A (Strategic Technology Office).

Stafford, Thomas (Lt. Gen., Retd) (1991) 'America on the Threshold', Synthesis Group, Space Exploration Initiative, Chairman's Report to Congress, Washington DC.

Stephens, R.R. (1965) 'Mission Requirements of Lifting Systems-Engineering Aspects'. Vol. I, 'Condensed Summary', and Vol. II, 'Mission Analysis—Spacecraft Selection—Performance Analysis', McDonnell Aircraft Company Report B831 for NASA Manned Spacecraft Center, contract NAS-9-3562.

Taylor, T.C. (2000) 'Commercial Space Habitation, 2000', Global Outpost, Inc., Lunar Development Conf., Las Vegas, NV, July 2000.

Yamanaka, T. (2000) 'Innovative Breakthroughs to a Reuseable STS', Private commnication.
Yugov, O.K. et al. (1989) 'Optimal Control Programs for Airbreathing Propulsion System or Single-Stage-to-Orbit Vehicles'. IAF-89-308, 40th IAF Congress, Malaga, Spain, October 1989.
Yugov, O.K., Dulepov, N.P., and Harchenvnikova, G.D. (1990) 'The Analysis of Hypersonic and Combined Cycle Engines in the Propulsion System of the SSTO Vehicles', 41st IAF Congress, Dresden, Germany, October 1990.
www.wpafb.af.mil/museum/space_flight (2005) ASSET program.

3

Commercial near Earth space launcher: a perspective

Before there can be any space exploration, there must first be an ability to reach low Earth orbit (LEO) from Earth's surface. The required speed for low Earth orbit is given in Table 3.1. For all practical purposes 100 nautical mile and 200 kilometer orbital altitudes are equivalent.

Whether it is an expendable launcher or a sustained-use, long-life launcher, the launcher must reach the same orbital speed to achieve LEO. From here the spacecraft can move to a higher orbit, change orbital planes or do both. Reaching LEO is a crucial step because, as indicated in Figures 2.5, the current system of launchers is representative of the Conestoga wagons that moved pioneers in the United States in just one direction: west. There is no record of any wagon returning to the east. The cost of traveling west was not reduced until the railroad transportation system was established that could (1) operate with a payload in both directions, and (2) operate frequently on a scheduled basis. Both directions are key to establishing commercial businesses that ship merchandise west to be purchased by western residents, and raw materials and products east to be purchased by eastern residents. The one-way Conestoga wagons could never have established a commercial flow of goods.

Scheduled frequency is the key to making the shipping costs affordable so the cargo/passenger volume matches or even exceeds capacity. The same is true of course for commercial aircraft and even for commercial space. In this context it is worthwhile mentioning that the November 18, 2002, issue of *Space News International*

Table 3.1. Low Earth orbital altitudes and speeds.

Altitude (km)	185.2	**200.0**	370.4
Speed (m/sec)	7,794.7	**7,785.8**	7,687.1
Altitude (nautical miles)	**100**	108	200
Speed (ft/sec)	**25,573**	25,544	25,220

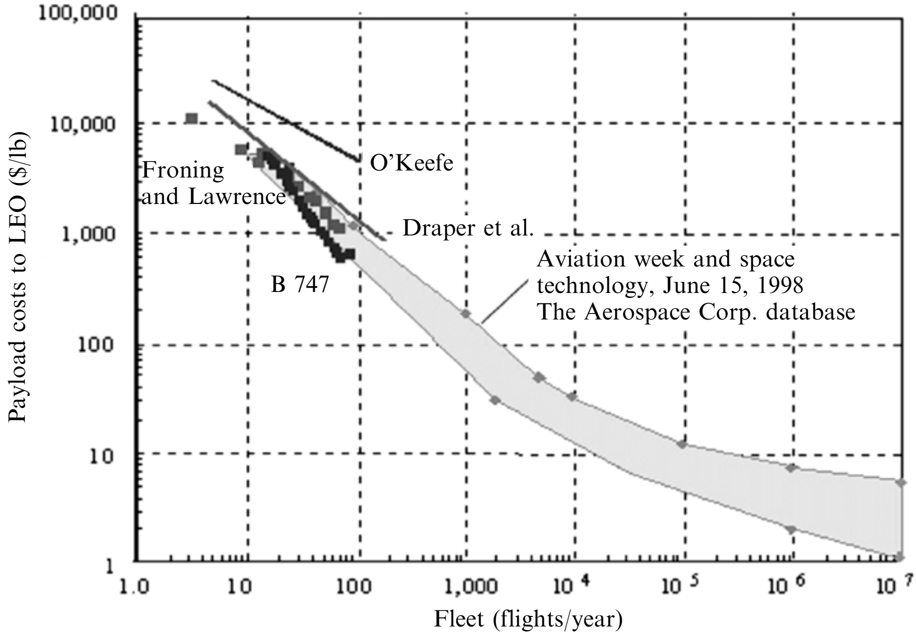

Figure 3.1. Comparison of payload costs to orbit, from 1971 to 2003.

presented an interview with the former NASA Administrator, Sean O'Keefe, that stated the projected cost for the five Space Shuttle launches per year is $US 3.2 billion. That reduces to about $US 29,000 per pound of payload delivered to LEO; for some missions that cost could rise to $US 36,000 per pound. The article stated that an additional flight manifest will cost between 80 and 100 million $US per flight. If the Shuttle fleet could sustain 10 flights per year, the payload cost would reduce to $US 16,820 per pound. If the flight rate were two a month, the cost would be $US 9,690 per pound. *It is really the flight rate* that determines payload costs.

Figure 3.1 shows that the historical estimates of payload cost per pound delivered to orbit were correctly estimated and known to be a strong function of fleet flight rate for over 30 years. In the same figure there are five estimates shown covering the time period from 1971 to Sean O'Keefe's data in 2002. In the AIAA *Aeronautics & Astronautics* article in 1971 [Draper et al., 1971] the projected total costs for a 15-year operating period were given as a function of the number of vehicles. The payload costs were determined with the information provided in the article. This is shown as a solid line. One of the students in the author's aerospace engineering design class obtained the cost of crew, maintenance and storage for 1 year of operation of a B-747 from a major airline. The student used that data to establish for a Boeing 747 operations cost in maintenance, fuel, and personnel for 1-year operation of three aircraft with one in 1-year maintenance. The annual costs are fixed, as they would be for a government operation; then, assuming that same B-747 operating with Shuttle payload weights and flight frequency yields a result shown in Figure 3.1 as the line of black squares. *These results show an infrequently used B-747 fleet is as costly as the Space Shuttle.*

This result shows the airframe or system 'technology' is not the issue, the real issue is the launch rate. This is an important finding, as most of the current new launch vehicle proposals are said to reduce payload costs through 'new and advanced technology', and that may not be correct. For the McDonnell Douglas TAV effort in 1983, H. David Froning and Skye Lawrence compared the cost per pound of payload delivered to LEO for an all-rocket hypersonic glider/launcher and a combined cycle launcher (rocket-airbreather) operated as an airbreather up to Mach 12. Their analysis showed that the total life-cycle costs for both systems were nearly identical, the vast difference in technology notwithstanding, and it was the fleet fly rate that made the payload cost difference. The Froning and Lawrence data is the line of grey squares. In 1988 Jay Penn and Dr Charles Lindley prepared an estimate for a two-stage-to-orbit (TSTO) launcher that was initially an all-hydrogen vehicle and then evolved into a kerosene-fueled first-stage and a hydrogen-fueled second stage. Liquid oxygen was the oxidizer in all cases. They examined a wide spectrum of insurance, maintenance, and vehicle costs and published their analysis in *Aviation Week and Space Technology* in June 1998. This is shown in Figure 3.1 as the light grey area curve. Their analysis merges into the three previously discussed analyses. At the fly rate of a commercial airline fleet the kerosene-fueled TSTO payload costs are in the 1 to 10 $US per payload pound. NASA Administrator O'Keefe's data presented in *Space News International* is shown as a solid line. This most recent Shuttle data is the greatest payload cost data set. As a point of interest, Dr Charley Lindley, then a young California Institute of Technology PhD graduate, worked for The Marquardt Company on Scramjet propulsion for the first Aero Space Plane. The bottom line is, as stated by Penn and Lindley, 'It is not the technology, it is the fly rate that determines payload costs.'

Thus, one way to improve the launch cost issue is to schedule the Shuttle to operate more frequently, or purchase surplus Energia launchers. Given the stated NASA goals of $US 1,000 and $US l00 per pound of payload delivered to LEO by 2020, the solution is launch rate, not specifically or exclusively advanced technology. It is not specifically a technology issue because operational life and number of flights are design specifications: it is they that govern durability, not necessarily technology. Translating the Penn and Lindley data into a single-stage-to-orbit launcher with all hydrogen fuel engines, results are in Figure 3.2. Six categories of cost were adjusted for a SSTO launcher from the Penn and Lindley data: namely Propellant, Infrastructure, Insurance, Maintenance, Production and RDT&E (Research, Development, Technology and Engineering). The costs of hydrogen fuel and oxygen oxidizer are essentially constant with flight rate, as they are new (recurring) for each flight. The one cost that changes the most is the amortized infrastructure cost. However, this cost and the other four costs (Insurance, Maintenance, Production and RDT&E) do not become minimal until high commercial aircraft fleet fly rates are achieved. The corollary is that propellant (in this case hydrogen, not kerosene) does not become the primary cost until fleet flight rates in excess of 10,000 flights per year are achieved. This and larger fleet flight rates are achieved

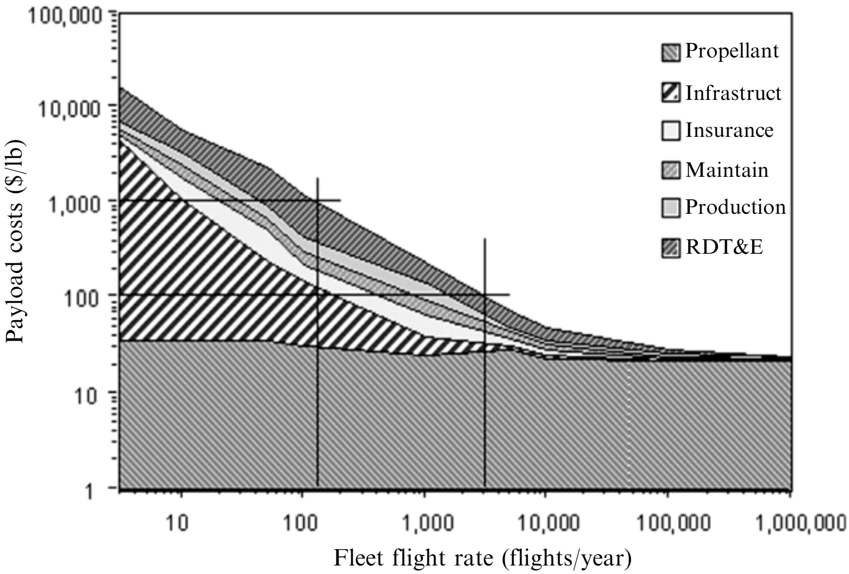

Figure 3.2. Payload costs per pound based on fleet flight rate, after Penn and Lindley.

by commercial airlines, but are probably impractical in the foreseeable future for space operations. From the MOL requirements given in Chapter 1, near-future fleet flight rates will be in the hundreds per year, not hundreds of thousands. NASA goals of $US 1,000 per pound can be met if the fleet launch rate is about 130 per year, or 2.5 launchers per week. For a fleet of seven operational aircraft, that amounts to about 21 launches per year per launcher, assuming an availability rate of 88%. That is about one flight every two weeks for an individual aircraft. At this point the five non-propellant costs are about 30 times greater than the propellant costs. For the NASA goal of $US l00 per pound to LEO requires about a 3,000 fleet flight rate and a larger fleet. Given 52 weeks and a fleet of 33 launchers with an 88% availability rate, the weekly flight rate is 58 launches per week, yielding a fleet flight rate of 3,016 flights per year. Such a fly rate demands an average of 8.3 flights per day! At this point the five non-propellant costs are about three times greater than the propellant costs. That is in the realm of the projected space infrastructure shown in Figure 2.23. Commercial aircraft exceed 1 million flights per year for the aircraft fleet, and that is why the cost for commercial aircraft passengers is primarily determined by fuel cost, not by individual aircraft cost. So, whatever the future launcher system, for the space infrastructure envisioned by Dr William Gaubatz in Figure 2.23 to ever exist, the payload cost to LEO must be low enough and the launch rate high enough to permit that infrastructure to be built.

3.1 ENERGY, PROPELLANTS AND PROPULSION REQUIREMENTS

In today's space initiative there appears to be only one propulsion system of choice, the liquid or solid rocket. In fact since the early 1950s a wide variety of space launcher propulsion systems concepts that were built and tested. These systems had one goal that of reducing the carried oxidizer weight, so a greater fraction of the gross weight could be payload. Another need was for frequent, scheduled launches to reduce the costs required to reach LEO from the surface of Earth. Without that frequency launches would remain a one-of-a-kind event instead of a transportation infrastructure. Figure 3.3 and 3.4 give two representations for the single-stage-to-orbit (SSTO) mass ratio (weight ratio) to reach a 100 nautical mile orbit (185 km) with hydrogen for fuel. In Figure 3.3 the mass ratio is a function of the maximum airbreathing Mach number. Six classes of propulsion systems are indicated: Rocket derived, Airbreathing (AB) rocket, so-called KLIN cycle, Ejector ramjet, Scram-LACE, and Air collection and enrichment systems (ACES). These and others are discussed in Chapter 4 in detail. The trend clearly shows that to achieve a mass ratio significantly less than rocket propulsion (about 8.1) an air-breathing Mach number of 5 or greater is required. This can be calculated by the equations that follow:

$$\begin{aligned}
\mathrm{TOGW} &= \mathrm{WR\,OWE} = \mathrm{OWE} + W_{\mathrm{ppl}} = \mathrm{OWE} + W_{\mathrm{fuel}}\left(1 + \frac{\mathrm{O}}{\mathrm{F}}\right) \\
\mathrm{WR} &= \frac{\mathrm{TOGW}}{\mathrm{OWE}} = 1 + \frac{W_{\mathrm{ppl}}}{\mathrm{OWE}} = 1 + \frac{W_{\mathrm{fuel}}}{\mathrm{OWE}}\left(1 + \frac{\mathrm{O}}{\mathrm{F}}\right) \\
(\mathrm{WR} - 1) &= \frac{W_{\mathrm{ppl}}}{\mathrm{OWE}} = \frac{W_{\mathrm{fuel}}}{\mathrm{OWE}}\left(1 + \frac{\mathrm{O}}{\mathrm{F}}\right) \\
\frac{W_{\mathrm{fuel}}}{\mathrm{OWE}} &= \frac{(\mathrm{WR} - 1)}{(1 + \mathrm{O/F})}
\end{aligned} \tag{3.1}$$

where:

$$\begin{aligned}
\mathrm{TOGW} &= \text{takeoff gross weight} \\
\mathrm{OWE} &= W_{\mathrm{fuel}} + W_{\mathrm{empty}} = \text{operational weight empty} \\
\mathrm{O/F} &= \text{oxidizer to fuel ratio} \\
\mathrm{WR} &= \mathrm{TOGW/OWE} = \text{weight ratio} = \text{mass ratio}
\end{aligned}$$

So the weight ratio, hence the takeoff gross weight, is a direct result of the propellant weight with respect to the operational weight empty (OWE). The propellant weight is a direct function of the oxidizer to fuel ratio (O/F). In Figure 3.4 the mass ratio is a function of the carried oxidizer to fuel ratio. Note that in Figure 3.3 the mass ratio curve is essentially continuous, with an abrupt decrease at about Mach 5. In Figure 3.4 the oxidizer to fuel ratio is essentially constant for the rocket-derived

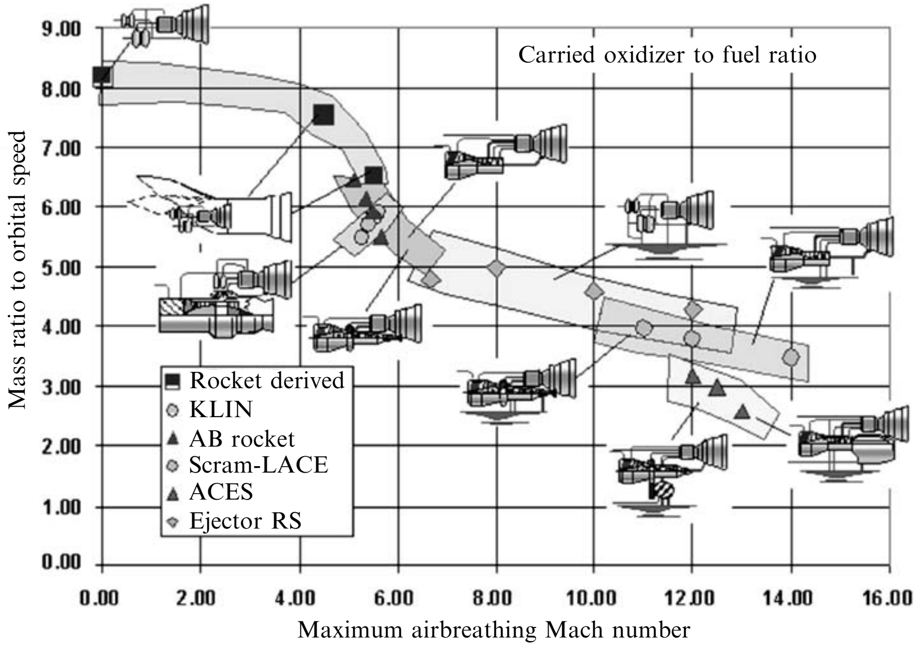

Figure 3.3. Weight ratio to achieve a 100 nautical mile orbit decrease as maximum airbreathing Mach number increases.

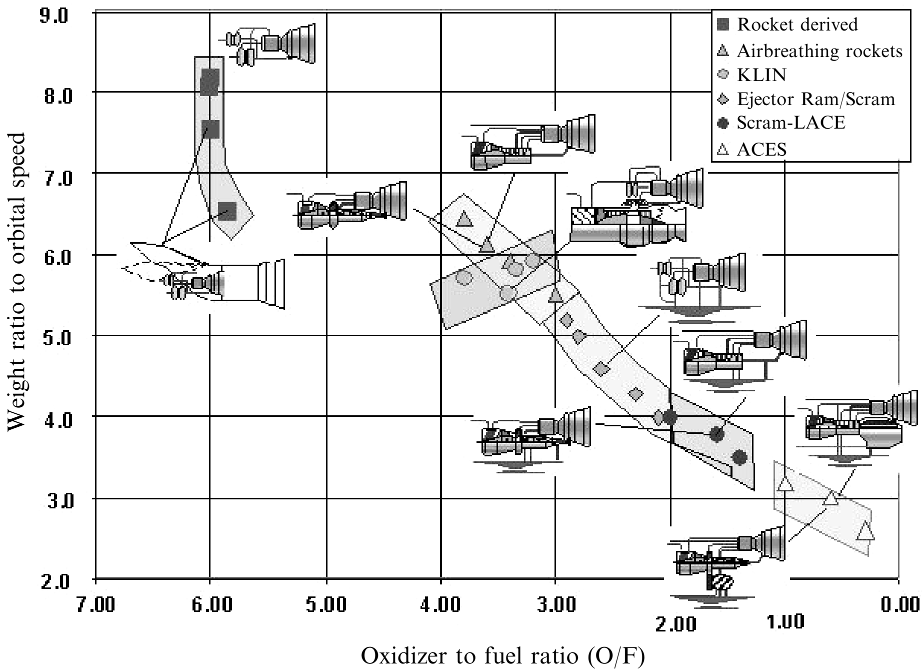

Figure 3.4. The less oxidizer carried, the less the mass ratio.

propulsion (about 6). There is a discontinuity in the oxidizer to fuel ratio curve between rocket-derived propulsion (value of 6) where airbreathing rockets begin, at a value of 4. Based on the definition of fuel weight to OWE in equations (3.1), the values from Figure 3.3 result in a fuel weight to OWE ratio of approximately 1. That is, for all of these hydrogen-fueled propulsion systems, the fuel weight is approximately equal to OWE. The mass ratio is decreasing because the oxidizer weight it decreasing as a direct result of the oxidizer to fuel ratio. So, using hydrogen fuel, an all-rocket engine can reach orbital speed and altitude with a weight ratio of 8.1. An airbreathing rocket (AB rocket) or KLIN cycle can do the same with a weight ratio about 5.5. A combined cycle rocket/scramjet with a weight ratio of 4.5 to 4.0, and an air collection and enrichment system (ACES) needs 3.0 or less. So an airbreathing launcher has the potential to reduce the mass ratio to orbit by one-half. It is clear that results in a significantly smaller launcher, both in weight and size.

What that means is that, for a 100-ton vehicle with its 14-ton payload loaded, an all-rocket requires a gross weight of 810 tons (710 tons of propellant) and a 1,093-ton (10.72-MN) thrust propulsion system. With oxidizer to fuel ratio reduced to 3.5 the gross weight is now 600 tons (500 tons of propellant) and a smaller 810-ton (7.94-MN) thrust propulsion system. If the oxidizer to fuel ratio can be reduced to 2, then the gross weight is now 200 tons (100 tons of propellant) and a much smaller 270-ton (27-kN) thrust propulsion system. For the same 810-ton gross weight launcher with a oxidizer to fuel ratio propulsion system of 2, the vehicle weight is now 405 tons with a 67-ton payload.

SSTO is shown because it requires the least launcher resources to reach LEO. Hydrogen is the reference fuel because of the velocity required for orbital speed: any other fuel will require a greater mass ratio to reach orbit. A two-stage-to-orbit launcher will require two launcher vehicles, and can have a different mass ratio to orbit (depending on fuel and staging Mach number), but the effect of increasing airbreathing speed is similar. Since the ascent to orbit with a two-stage vehicle is in two segments, the lower-speed, lower-altitude segment might use a hydrocarbon fuel rather than hydrogen. The question of SSTO versus TSTO is much like the aerospace plane versus Buran arguments. The former is very good at delivering valuable, fragile cargo and crew to space complexes, while the TSTO with the option of either a hypersonic glider or a cargo canister can have a wide range of payload types and weight delivered of orbit. It is important to understand that they are not mutually exclusive, and in fact in all of the plans from other nations and in those postulated by Dr William Gaubatz both SSTO and TSTO strategies were specifically shown to have unique roles.

3.2 ENERGY REQUIREMENTS TO CHANGE ORBITAL ALTITUDE

Having achieved LEO the next question is the energy requirements to change orbital altitude. The orbital altitude of the International Space Station (ISS) is higher than the nominal LEO by some 500 km, so additional propellant is required to reach

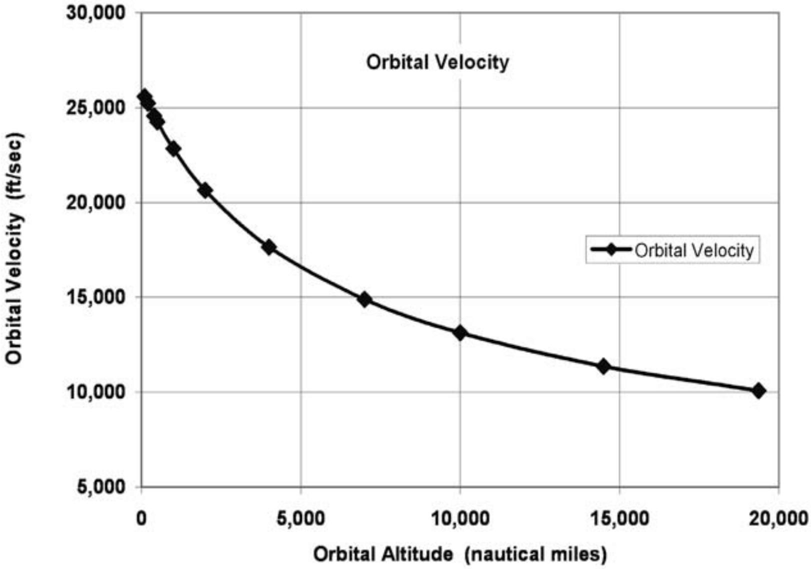

Figure 3.5. Orbital velocity decreases as altitude increases.

ISS altitude. The ISS is also at a different inclination than the normal United States orbits (51.5 degrees instead of 28.5 degrees) and the inevitable increment in propellant requirement will be discussed in Chapter 5 when describing maneuvering in orbital space. As orbital altitude is increased, the orbital velocity required decreases, with the result that the orbital period is increased. However, because the spacecraft must first do a propellant burn to accelerate to the elliptical transfer orbit speed, and then it must do a burn to match the orbital speed required at the higher altitude, it takes a significant energy expenditure to increase orbital altitude. Figure 3.5 shows the circular orbital speed required for different orbital altitudes up to the 24-hour period GSO at 19,359 nautical miles and 10,080 ft/sec (35,852 km and 3,072 m/sec). Figure 3.6 shows the circular orbital period as a function of orbital altitude, and at GSO the period is indeed 24 hours. Translating this velocity increment requirement into a mass ratio requirement calls for specifying a propellant combination. The two propellant combinations most widely used in space are the hypergolic nitrogen tetroxide/unsymmetrical dimethyl-hydrazine and hydrogen/oxygen (see Table 1.4 in Chapter 1). The hypergolic propellants are room-temperature liquids and are considered storable in space without any special provisions. Hydrogen and oxygen are both cryogenic and require well-insulated tanks from which there is always a small discharge of vaporized propellants. Both the United States and Russia have experimented with magnetic refrigerators to condense the vaporized propellants back to liquids and return them to the storage tanks. Had Buran continued development, the author saw a magnetic refrigerator to be used for the all hydrogen/oxygen propellant maneuvering and station-keeping systems used for Buran. The resulting mass ratios for the two propellants are shown in Figure 3.7. The propellant for this orbital altitude change must be carried to orbit

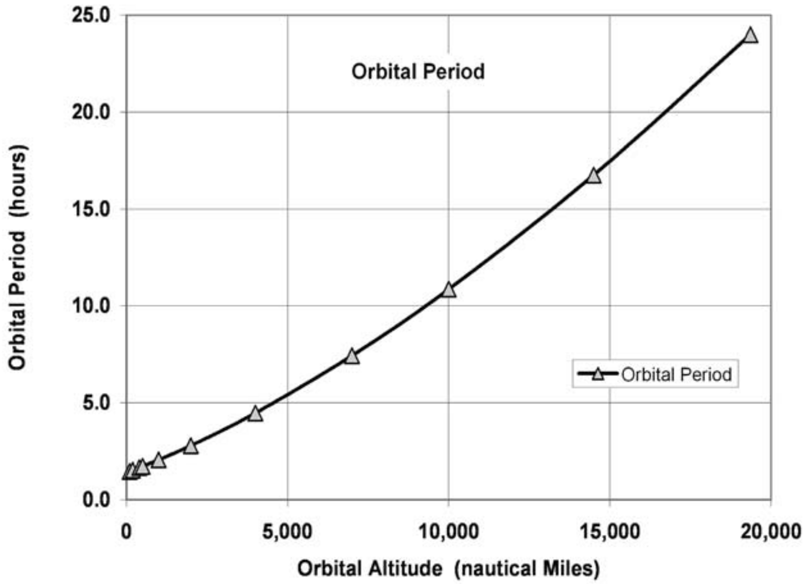

Figure 3.6. Slower orbital speed means longer periods of rotation.

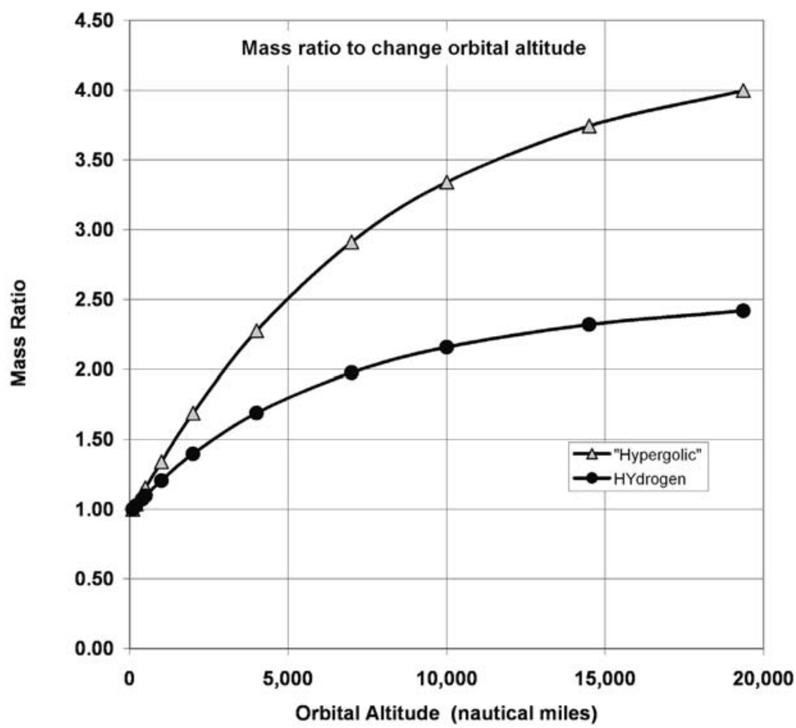

Figure 3.7. To achieve a higher orbit requires additional propellant.

from Earth, as there are no orbital fueling stations now in orbit (see Figure 2.23 for future possibilities). So if the weight of the object to be delivered to higher orbit is one unit, then the mass of the system in LEO times the orbital altitude mass ratio is the total mass of the system required to change altitude.

To achieve GSO from LEO with a hypergolic propellant the mass ratio is 4, and for hydrogen/oxygen it is 2.45. As an example, a 4.0-ton satellite to GSO requires orbiting into LEO a *16.0-ton spacecraft as an Earth launcher payload*. If that payload represents a 14% fraction of the launcher empty weight, then the launcher empty weight is 114.3 tons and, with the typical mass ratio to reach LEO of 8.1 for an all rocket system, the total mass at liftoff is 925.7 tons. So it takes about 57.8 tons of an all rocket launch vehicle to put 1 ton in LEO using an all rocket launcher system, and 231 tons of the same all rocket vehicle to put 1 ton in GSO.

To achieve GSO from LEO with a hydrogen propellant the mass ratio is 2.45, so a 4.0-ton satellite to GSO requires orbiting into LEO a *9.8-ton spacecraft as an Earth launcher payload*. If that payload represents a 14% fraction of the launcher empty weight, then the launcher empty weight is 70.0 tons. For an ejector ram/scramjet-powered launcher that flies to Mach 12 as an airbreather, the mass ratio to reach LEO is 4.0 and the total mass at liftoff is 280.0 tons. So it takes about 28.6 tons of launch vehicle to put 1 ton in LEO for an ejector ram/scramjet-powered launcher that flies to Mach 12 as an airbreather and about 70 tons of the same ejector ram/scramjet-powered vehicle to place 1 ton in GSO.

The advantage of airbreathing propulsion is than it requires a launcher that has an empty weight 39% less than the rocket launcher, and a gross takeoff weight that is 70% less for the same payload. The primary reason is rather obvious, since the airbreathing launcher carries some 210 tons of propellant rather than the 811 tons of propellant the all-rocket carries to achieve LEO speed and altitude; it does not use the large mass of oxidizer needed by an all-rocket system, replacing most of it with external air. The advantage of airbreathing propulsion is that less propellant and vehicle resources are required.

3.3 OPERATIONAL CONCEPTS ANTICIPATED FOR FUTURE MISSIONS

For current concepts of expendable systems the configuration choice of cylinders is practical. At best the solid boosters for the Unites States Space Shuttle are recovered from a low Mach number separation close to the Florida shore. However, for reusable vehicles and long-life, sustained-use vehicles the requirements for glide range become important enough to shape and even determine the configuration of the launcher and launcher components. As discussed in Chapter 2, the first example is that of a more conventional launcher designed from the start for 100% recoverable elements, and 80 flights between overhaul/refurbishment. Information about this launcher comes from a briefing on Energia that V. Legostayev and V. Gubanov supplied to one of the authors (PC) concerning the Energia operational concept (designed but never achieved, as Energia was launcher for the first, last and only time in 1991). The second example is that of a hypersonic glider/launcher that was intended to be operated over 200 launches before scheduled maintenance. This is from work from one of the authors' (PC) experience at McDonnell Douglas Corporation, McDonnell Aircraft Company including hypersonic gliders based on the USAF Flight Dynamic Laboratory FDL-7 glider series, the McDonnell Douglas model 176 Manned Orbiting Laboratory Crew and Resource re-supply/rescue vehicle, and the hypersonic cruise vehicle work done for the NASA-sponsored Hypersonic Flight Research Vehicle Study (HyFAC) in the 1965 to 1970 time period.

To recapitulate the observations from Chapter 2, Figure 2.10 shows the goals of the Energia operational concept with all its components recoverable for reuse. The sketch was a result of discussion PC had with Viktor Legostayev and Vladimir Gubanov at several opportunities. The orbital glider, Buran was a fully automatic system that was intended to be recovered at a designated recovery runway at the Baikonur Space Launch Facility at Leninsk, Kazakhstan. (In Kazak, the Baikonur site is called Tyurastam, or coal mine, which is the first facility encountered when entering Baikonur.) Buran has a very different operational envelope than the United States Space Shuttle. In a briefing from Vladimir Yakovlich Neyland when he was Deputy Director of TsAGI, the specific operational design parameters were presented; among its features of interest, Buran's glide angle of attack was said to be between 10 and 15 degrees less than the Shuttle, and its lift to drag ratio to be greater. This because Buran's glide range was intended to be greater than that required for one missed orbit, as is the case with the Shuttle. The center tank used an old Lockheed concept of a hydrogen gas spike (to reduce tank wave drag) and overall very low weight-to-drag characteristics to execute a partial orbit for a parachute recovery at Baikonur. The strap-on booster were recovered down range using parasail parachutes or returned to Baikonur by a gas-turbine-powered booster with a switchblade wing. It is important to point out that the basic design of Energia was to have all of the components recoverable at the launch site, in this case Baikonur.

In a 1964 brief, Roland Quest of McDonnell Douglas Astronautics, St. Louis, presented a fully reusable hypersonic glider, the model 176, intended to be the crew delivery, crew return, crew rescue, and re-supply vehicle for the Manned Orbiting Laboratory (MOL) crew. One vehicle was to be docked with the MOL at all times as an escape and rescue vehicle. It could accommodate up to 13 persons, and as with Buran, all components were recoverable. Given the space infrastructure of the 21st century, it is important to recall that rescue and supply of the manned space facilities requires the ability to land in a major ground-based facility at any time from any orbit and orbital location. The cross- and down-range needed to return to a base of choice also requires high aerodynamic performance. Unlike airbreathing propulsion concepts limited to Mach 6 or less, an excellent inward-turning, retractable inlet can be integrated into the vehicle configuration derived from the FDL series of hypersonic gliders developed by the Flight Dynamics Laboratory [Buck et al., 1975] and the work of the McDonnell Douglas Astronautics Company. The hypersonic work between the McDonnell Douglas Astronautics Company and the McDonnell Aircraft Company, McDonnell Douglas Corporation, and between the USAF

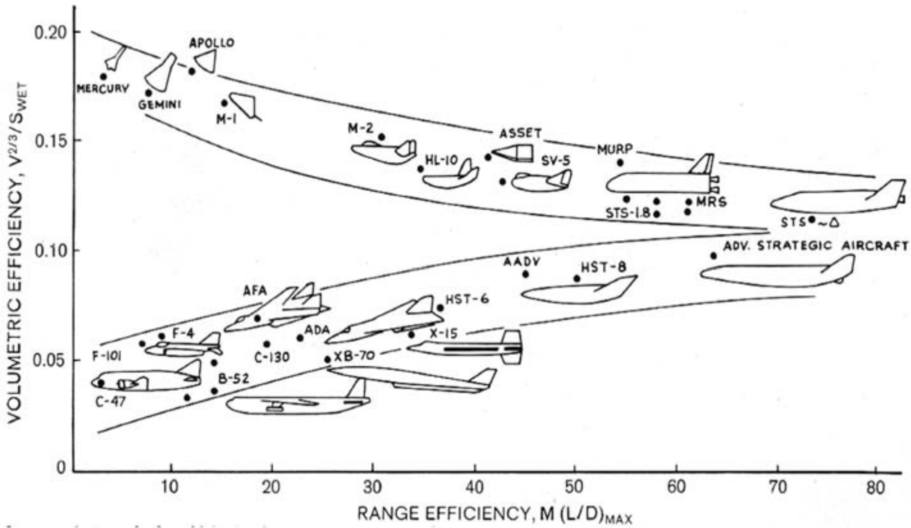

Figure 3.8. Space and atmospheric vehicle development converge, so the technology of high-performance launchers converges with the technology of airbreathing aircraft. M = Mach number.

Flight Dynamic Laboratory and McDonnell Douglas Astronautics Company provided a basis to converge the space and atmospheric vehicle developments to a common set of characteristics. As shown in Figure 3.8 [Draper et al., 1971] that convergence was published in the AIAA Aeronautics and Astronautics publication in January 1971. The correlating parameter is the 'total volume' raised to the 2/3 power divided by the 'wetted area'. The converged center value is 0.11 ± 0.03. The importance of this convergence is that the space configurations were moving from blunt cylinders and atmospheric configurations were moving from wing-cylinders to blended lifting bodies, without any clearly defined wing (although there were large control surfaces, these primarily provided stability and control). This convergence of technical paths remained unrecognized by most, with only AFFDL and two or three aerospace companies (McDonnell Douglas being one of those companies) recognizing its importance to future space launchers and aircraft. As a result today we still launch single expendable or pseudo-expendable launchers one at a time, for the first, last and only time.

3.4 CONFIGURATION CONCEPTS

At McDonnell Aircraft Company the author was introduced to a unique approach to determining the geometric characteristics required by hypersonic configurations with different missions and propellants. Figure 3.9 shows the approach. Normally, to increase its volume a vehicle is made larger, as in photographic scaling. That is, all dimensions are multiplied by a constant factor. This means that the configuration

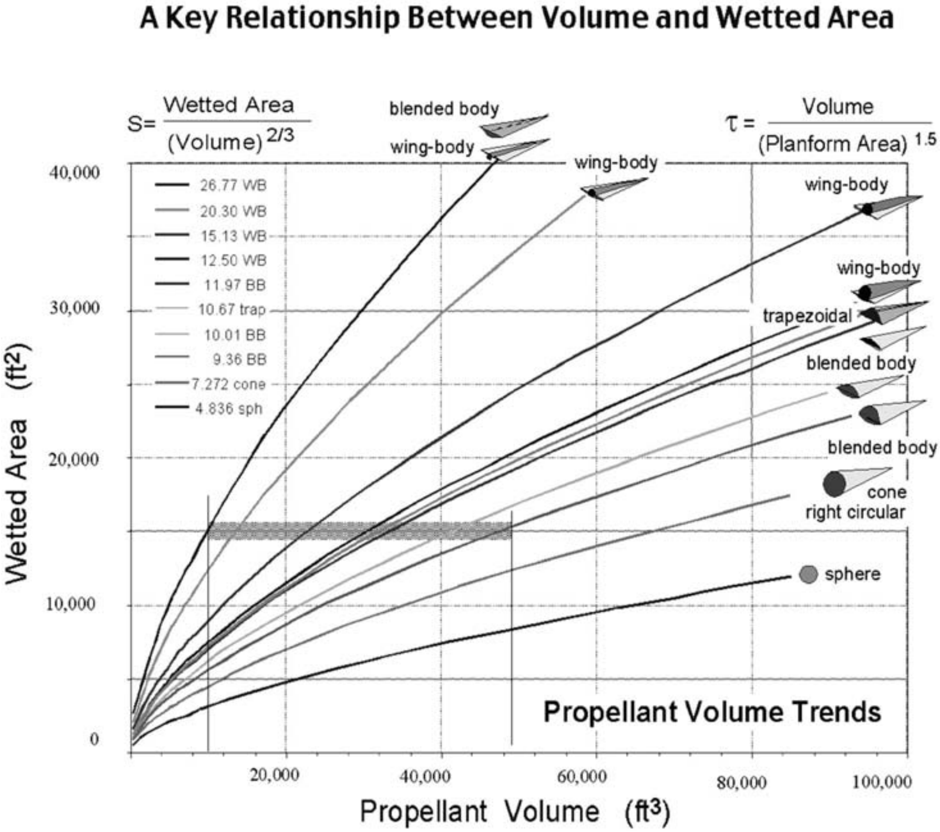

Figure 3.9. Controlling drag, that is skin friction resulting from wetted area, is the key to higher lift-to-drag ratios.

characteristics remain unchanged except that the vehicle is larger. The wetted area is increased by the square of the multiplier, and the volume is increased by the cube of the multiplier. This can have a very deleterious impact on the size and weight of the design when a solution is converged. The McDonnell approach (and as probably practiced by Lockheed and Convair in the 1960's) used the cross-section geometry of highly swept bodies to increase the propellant volume without a significant increase in wetted area. As shown in Figure 3.9 the propellant volume is plotted for a number of geometrically related hypersonic shapes as a function of their wetted area. The correlating parameter is 'wetted area' divided by the 'total volume' raised to the 2/3 power and it is the reciprocal of the AFFDL parameter in Figure 3.8. The corresponding range of this parameter is 10.5 ± 2.0. As this parameter reduces in value, the wetted area for a given volume reduces. The most slender configuration is characteristic of an aircraft like Concorde. If a 78-degree sweep slender wing-cylinder configuration ($S = 26.77$) were expanded to stout blended body ($S = 9.36$) the propellant volume could be increased by a factor of 5 without an increase in wetted area. If the original configuration were grown in size to the same propellant volume, the wetted area would be three times greater. So the friction drag of the $S = 9.36$ configuration is approximately the same, while the friction drag of the photographically enlarged vehicle is at least three times greater. Moving to a cone, the propellant volume is 6.8 times greater for the same wetted area. That is why the McDonnell Douglas Astronautics Corporation, Huntington Beach, Delta Clipper Experimental vehicle was a cone. It could accommodate the hydrogen–oxygen propellants within a wetted area characteristic of a kerosene supersonic aircraft

The correlating parameters with the area in the numerator and a volume raised to the 2/3 power in the denominator are characteristically used in the United States. The European correlating parameters associated with Dietrich Küchemann have volume in the numerator and area raised to the 1.5 power in the denominator [Küchemann, 1960]. The two approaches can be related as in the following equation set.

$$S = \frac{S_{\text{wet}}}{(V_{\text{total}})^{0.667}} = \frac{K_{\text{w}} S_{\text{plan}}}{(V_{\text{total}})^{0.667}} \qquad T = \frac{S_{\text{plan}}}{(V_{\text{total}})^{0.667}}$$

$$\sigma = \frac{V_{\text{total}}}{(S_{\text{wet}})^{1.5}} = \frac{V_{\text{total}}}{(K_{\text{w}} S_{\text{plan}})^{1.5}} \qquad \tau = \frac{V_{\text{total}}}{(S_{\text{plan}})^{1.5}}$$

$$K_{\text{w}} = \frac{S_{\text{wet}}}{S_{\text{plan}}} \qquad S = \frac{K_{\text{w}}}{\tau^{0.667}} \tag{3.2}$$

The Latin letters indicate United States parameters in which the area is in the numerator. These parameters have values greater than one. The European parameters are indicated with Greek characters. These parameters have values less than one.

Figure 3.9 shows the value of S for a broad spectrum of hypersonic configurations. The values of S corresponding approximately to those in Figure 3.8 are 12.5 through 8.3. This shows that the preferred configurations are all pyramidal shapes with different cross-sectional shapes that includes a stout wing-body, trapezoidal cross-sections, and blended body cross-sections. Figure 3.10 shows that the value of S can be uniquely determined from Küchemann's tau for an equally wide variety of hypersonic configurations, including winged cylinders. So whether for hypersonic cruise configurations, airbreathing launchers, rocket-powered hypersonic gliders, or conventional winged cylinders, Küchemann's tau can be a correlating parameter for the geometric characteristics of a wide range of configurations. This means that specific differences in configurations are second-order to the primary area–volume characteristics. Supersonic cruise configurations using kerosene (such as Concorde) are in the 0.03 to 0.04 range of tau. Supersonic cruise configurations using methane are in the 0.055 to 0.065 range of tau. Hypersonic cruise configurations are in the tau = 0.10 vicinity. Airbreathing space launchers are in the range of 0.18 to 0.20. Rocket-powered hypersonic gliders are in the range of 0.22 to 0.26 tau. A correlating equation provides a means of translating Küchemann tau into the S parameter,

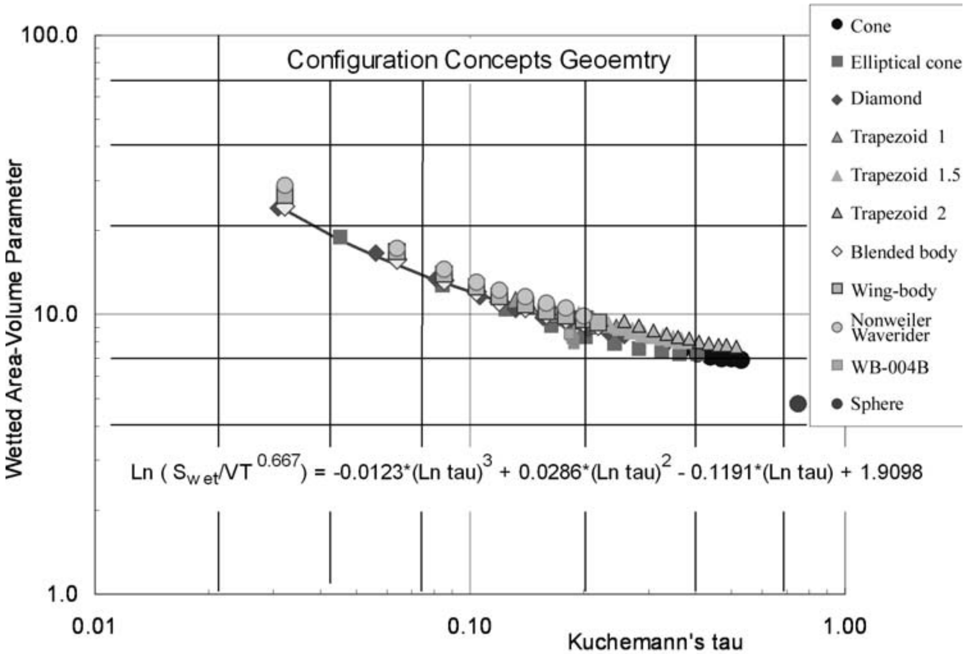

Figure 3.10. Wetted area parameter from Figure 3.9 correlates with Küchemann's tau yielding a geometric relationship to describe the delta planform configurations of different cross-sectional shape.

$S_{wet}/V_{total}^{0.667}$. As implied in Figure 3.10, as tau increases, the value of S decreases, meaning that the volume is increasing faster than the wetted area—crucial for a hypersonic aircraft, as skin friction is a significant part of the total drag. Later in the chapter this parameter will be related to the size and weight of a converged design as a function of the industrial capability to manufacture the spacecraft.

There are a wide variety of configurations possible. *But* if the requirements for a transportation system to space and return are to be met, the configurations spectrum is significantly narrowed [Thompson and Peebles, 1999]. Two basic configurations types are selected. One is for all-rocket and airbreathing rocket cycle propulsion systems that can operate as airbreathing systems to about Mach 6. For the rocket propulsion and airbreathing rocket propulsion concepts that are limited to Mach 6 or less, a versatile variable capture, inward-turning inlet [DuPont, 1999] can be integrated into the vehicle configuration derived from the FDL series of hypersonic gliders (see Figure 3.14) developed by the Flight Dynamics Laboratory [Buck et al., 1975] and the work of the McDonnell Douglas Astronautics Company. Because of the mass ratio to orbit, these are generally vertical takeoff and horizontal landing vehicles (VTOHL). This is the upper left vehicle in Figure 3.11. The second is for airbreathing propulsion systems that require a propulsion-configured vehicle where the underside of the vehicle is the propulsion system. The thermally integrated air-

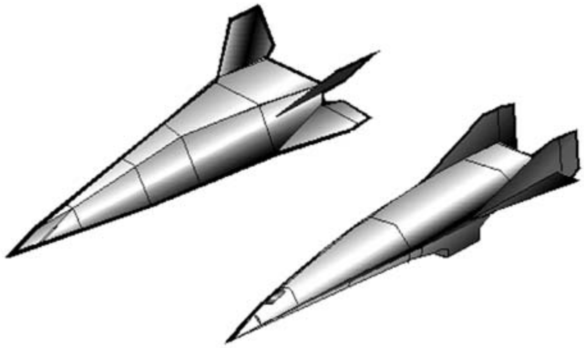

Figure 3.11. Hypersonic rocket powered glider for airbreathing Mach <6 and hypersonic combined cycle powered aircraft for airbreathing Mach >6.

breathing combined cycle configuration concept is derived from the McDonnell Douglas, St. Louis, Advanced Design organization. This is family of rocket hypersonic airbreathing accelerators and cruise vehicles [HyFac, 1970]. Depending on the mass ratio of vehicle these can take off horizontally (HTOL) or be launched vertically (VTOHL) and always land horizontally. The initial 1960s vehicle concept was propulsion configuration accelerated by a main rocket in the aft end of the body. Today it can retain this concept or use a rocket-based combined cycle propulsion concept. In any case, individual rockets are usually mounted in the aft body for space propulsion. This is the lower right vehicle in Figure 3.11. Both are functions of tau, that is for a given planform area, the cross-sectional distribution is determined by the required volume.

Both this hypersonic glider based on the FDL-7C and the hypersonic airbreathing aircraft in Figure 3.11 have hypersonic lift-to-drag ratios in excess of 2.7. That means un-powered cross-ranges in excess of 4500 nautical miles and down-ranges on the order of the circumference of the Earth. So these two craft can depart from any low-altitude orbit in any location and land in the continental United States (CONUS) or in continental Europe (CONEU). Both are stable over the entire glide regime. The zero-lift drag can be reduced in both by adding a constant width section to create a spatular configuration. The maximum width of this section is generally the pointed body half-span. The pointed configurations are shown in Figure 3.11. No hypersonic winged-cylindrical body configurations were considered as these have poor total heat load characteristics and limited down-range capability. As a strap-on booster the configuration is acceptable. The key to achieving the NASA goals of reduced payload to orbit continues to be flight rate and, as in the case of the transcontinental railroad, the scheduled services were supplied when as little at 300 statute miles of track (out of 2,000) had been laid [Ambrose, 2000]. So our flights to Earth orbit need to be as frequent as they can be scheduled.

Vertical fin configuration has presented low-speed stability problems for many hypersonic glider configurations such as X-24A, M2/F2, HL-19 and others. The high

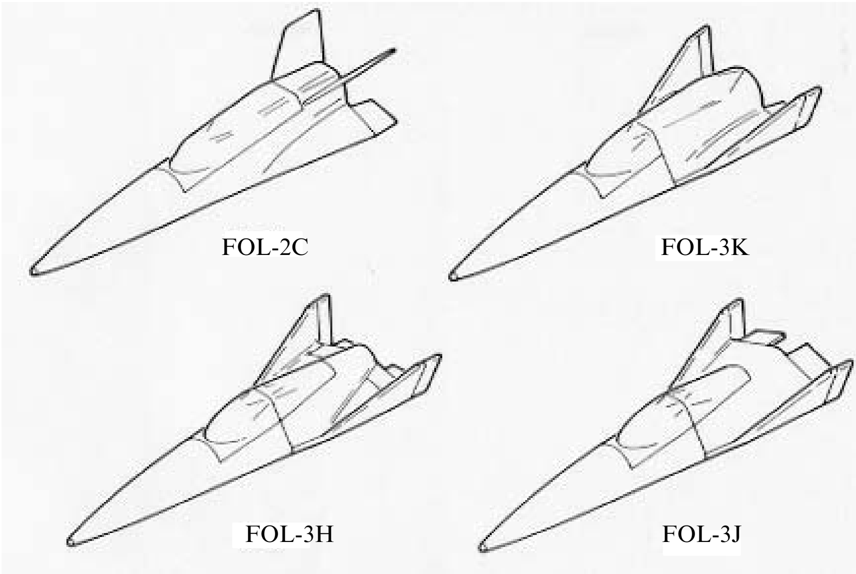

Figure 3.12. Wind-tunnel model configurations for tail effectiveness determination over hypersonic to subsonic speed regime (Mach 22 to 0.3).

dihedral angle verticals for three of the four configurations in Figure 3.12 are representative of the vertical fin orientation. The 'X' fin configuration was the result of an extensive wind-tunnel investigation by McDonnell Douglas and the AFFDL that covered Mach 22 to Mach 0.3. A total of four tail configurations were investigated over the total Mach number range and evaluated in terms of stability and control; they are shown in Figure 3.12. All of the configurations, except the first 'X' tail configuration had serious subsonic roll–yaw instabilities at lower speeds. The 'X' tail configuration has movable trailing edge flaps on the lower anhedral fins, and upper surfaces are all movable pivoting control surfaces at approximately 45 degrees dihedral angle. This combination provided inherent stability over the entire Mach number range from Mach 22 to landing.

The FDL-7 derived hypersonic gliders have a higher lift-to-drag ratio configuration than those similarly developed by Mikoyan and Lozinzo-Lozinski in Russia as the 'BOR' family of configurations because of operational requirements. Some of the first studies performed for NASA by McDonnell Aircraft Company and Lockheed [Anon, McDonnell, 1970; Anon, Lockheed, 1967] identified as a need, the ability to evacuate a disabled or damaged space station immediately, returning to Earth without waiting for the orbital plane to rotate into the proper longitude (see Chapter 2). Unfortunately, many of these studies were not published in the open technical literature and were subsequently destroyed. For a Shuttle or CRV configuration that waiting might last seven to eleven orbits, depending on inclination, or, in terms of time, from 10.5 to 16.5 hours for another opportunity for entry: that might be too long in a major emergency. In order to accomplish a 'no waiting'

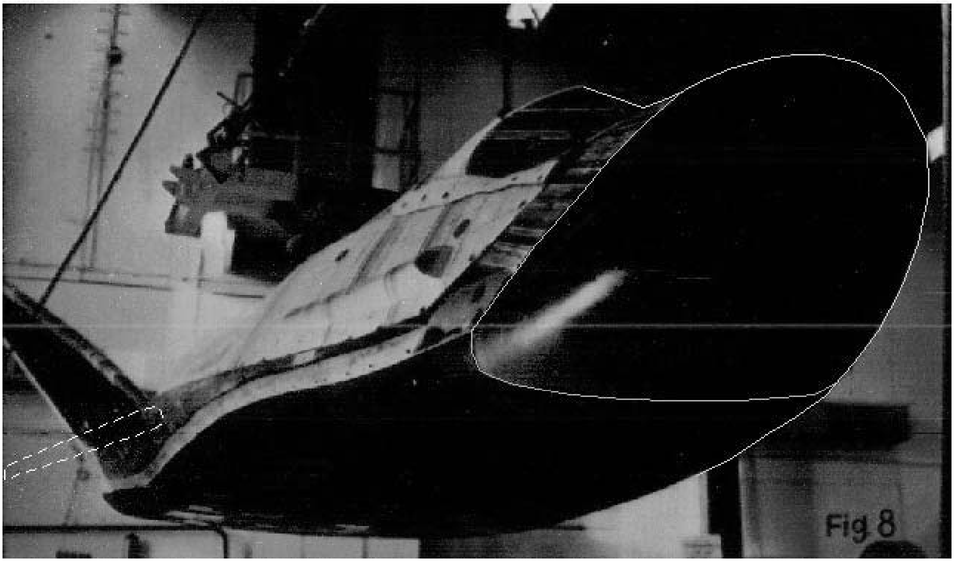

Figure 3.13. BOR V after return from hypersonic test flight at Mach 22. The one-piece carbon–carbon nose section is outlined for clarity. The vertical tails are equipped with a root hinge, so at landing the tails are in the position shown by the dashed line. Thus BOR V is stable in low-speed flight. If the variable dihedral were not present, BOR V would be laterally and directionally unstable at low speeds.

descent with the longitudinal extent of the United States, that requires a hypersonic lift-to-drag ratio of 2.7 to 2.9. The hypersonic gliders based on the FDL-7 series of hypersonic gliders have demonstrated that capability. Given the longitudinal extent of the former USSR, that requirement translates into a more modest hypersonic lift-to-drag ratio of 1.7 to 1.9. So Lozino-Lozinski BOR hypersonic gliders meet that requirement to land in continental Russia without waiting. This hypersonic lift-to-drag ratio means that, if the deorbit rocket retrofiring is ground-controlled, Russian spacecraft could be precluded from reaching the United States. The BOR class of vehicles is now being realized not in Russia but in the United States, as the CRV is in fact an adaptation of the BOR V vehicle. Such a BOR vehicle is shown in Figure 3.13 after recovery from a hypersonic flight beginning at about Mach 22 [Lozinski, 1986]. The BOR V picture was given to the author by Glebe Lozino-Lozinski at the IAF Congress held in Malaga, Spain. Lozinski was very familiar with the subsonic lateral-directional instability for this high dihedral angle fin configuration, and in the 1960s constructed a turbojet powered analog that investigated this problem. The solution was to make the aft fins capable of variable dihedral (a power hinge was mounted in the root of each fin) so that at high Mach numbers the fins were at about plus 45 degrees, as shown in Figure 3.13. However, when slowing down to transonic and subsonic Mach numbers, the dihedral angle was decreased, so that at landing the fins were at a minus 10 degrees, as shown by the dashed outline in Figure 3.13. So the BOR class of vehicle was a variable geometry configuration that could land in

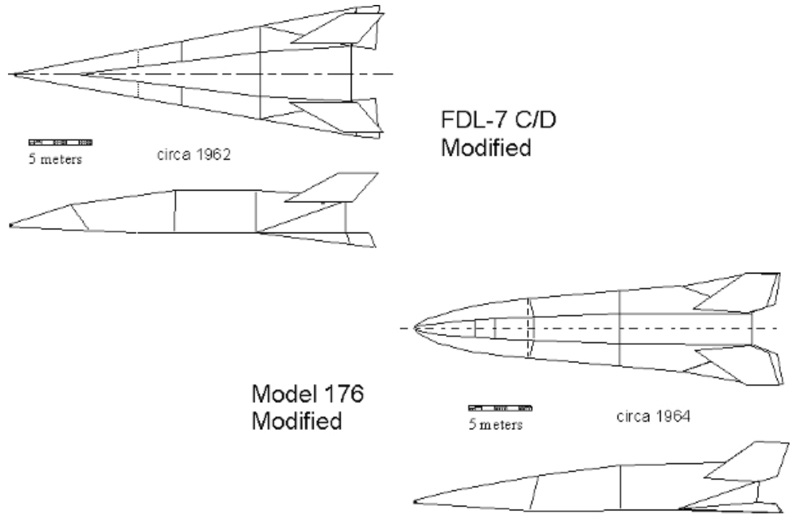

Figure 3.14. FDL-7 C/D (top) compared to Model 176 (bottom).

continental Russia; its stability could be maintained over the entire flight regime, from Mach 22 to zero.

The Model 176 began with the collaboration of Robert Masek of McDonnell Douglas and Alfred Draper of AFFDL in the late 1950s on hypersonic control issues. After a series of experimental and flight tests with different configurations the 'X' tail configuration and the FDL-7C/D glider configurations emerged (Figure 3.12) as the configuration that was inherently stable over the Mach range and had Earth circumferential glide range. The result was the FDL-7MC and then the McDonnell Douglas Model 176. Figure 3.14 compares the two configurations. In the early 1960s both configurations had windshields for the pilots to see outside (see Figure 3.19). However, with today's automatic flight capability visual requirements can be met with remote viewing systems. The modified FDL-7 C/D configuration was reshaped to have flat panel surfaces, and the windshield provisions were deleted, but it retains all of the essential FDL-7 characteristics. To assure the lift-to-drag ratio for the circumferential range glide, the Model 176 planform was reshaped for a parabolic nose to increase the lift and decrease the nose drag. A spatular nose would have also provided the necessary aerodynamic margin; however, the original configuration was retained, with just the windshield provisions (Figure 3.16) deleted. The Model 176 was proposed for the Manned Orbiting Laboratory (MOL) described in Chapter 2. It was a thoroughly designed and tested configuration with a complete all-metal thermal protection system that had the same weight of ceramic tile and carbon–carbon concepts used for the US Shuttle, but was sturdier. A wind-tunnel model of the McDonnell Douglas Astronautics Company Model 176 installed in the McDonnell Aircraft Company Hypervelocity Impulse Tunnel for a heat transfer mapping test is shown in Figure 3.15. Note that conforming to the piloting

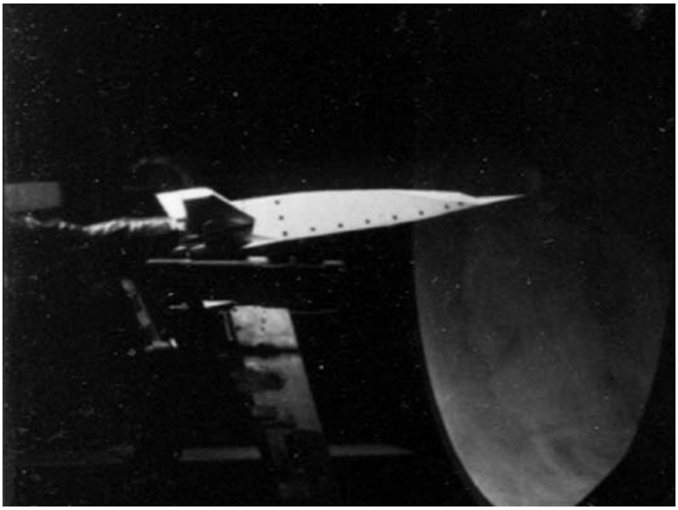

Figure 3.15. Model 176 in the McDonnell Douglas Hypervelocity Impulse Tunnel (circa 1964).

concepts of the 1960s it has a clearly distinct windshield that is absent from the configuration concept in Figure 3.14. The model is coated with a thermographic phosphor surface temperature mapping system [Dixon and Czysz, 1964]. This system integrated with semiconductor surface temperature heat transfer gauges [Dixon, 1966] permits the mapping of the heat transfer to the model and full-scale vehicle. The model permitted accurate thermal mapping to the heat transfer distribution on the body and upper fins. From this data the full-scale surface temperatures for a radiation shingle thermal protection system could be determined and the material and thermal protection system appropriate for each part of the vehicle determined.

The important determinations that resulted from these heat transfer tests are that the sharp leading-edge, flat-bottomed, trapezoidal cross-section reduced the heating to the sides and upper surfaces. The surface temperatures of the thermal protection shingles are shown in Figure 3.16. In the range of angles of attack corresponding to maximum hypersonic lift-to-drag ratio the sharp leading-edge corner separates and reduces the upper surface heating. Because of the separation, the isotherms are parallel to the lower surface and to 2,100 to 2,400°F (1,149 to 1,316°C) cooler than on the compression surface. The upper control fins are hot, but there are approaches and materials applicable to control surfaces. The temperatures shown are radiation equilibrium temperatures. The temperatures with asterisks are the radiation equilibrium temperatures if not employing thermal management. Thermally managed with nose water transpiration cooling (demonstrated in flight test in 1966) and heat pipe leading edges (demonstrated at NASA Langley in 1967–68) these temperatures of the nose and leading edges are 212°F and 1,300°F (100°C and 704°C) respectively.

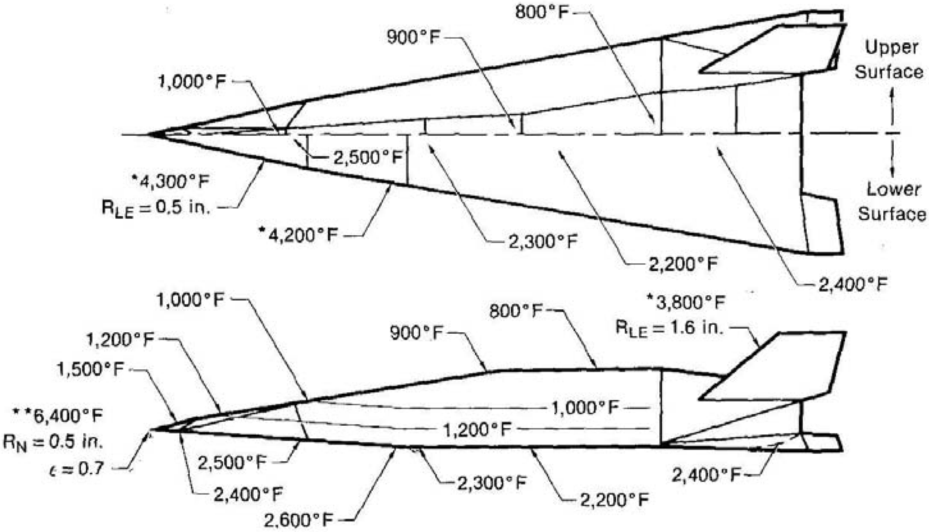

Figure 3.16. FDL-7 C/D, Model 176 entry temperature distribution. Upper surface heating minimized by cross-section geometry.

Except for the tail control surfaces, the vehicle is a cold aluminum/titanium structure protected by metal thermal protection shingles. Based on the local heat transfer and surface temperature, the material and design of the thermal protection system was determined, as shown in Figure 3.17. It employs a porous nose tip with about a one-half inch (12.3 mm) radius, such the Aerojet Corporation's diffusion bonded platelet concept. In arc-tunnel tests in the 1960s, a one-half-inch radius sintered nickel nose tip maintained a 100°C wall temperature in a 7200 R (4,000 K) stagnation flow for over 4300 seconds utilizing less than a kilogram of water. The one-half-inch (12.3 mm) radius leading edges and the initial portion of the adjacent sidewall forms a sodium-filled, Hastelloy X heat pipe system that maintains the structure at approximately constant temperature. Above the heat pipe, sidewall are insulated Inconel honeycomb shingles, and above those and over the top, are diffusion-bonded multicell titanium. The compression side (underside) is coated columbium (niobium) insulated panels or shingles similar to those on the compression side of the X-33, that protect the primary structure shown in Figure 3.18. The upper all-flying surfaces and the lower trailing flap control surfaces provide a significant challenge. Instead of very high temperature materials that can still have sufficient differential heating to warp the surfaces significantly, the approach was to adapt the heat pipe concept to heat pipes contained within honeycomb cells perpendicular to the surface. In that way the control surfaces are more isothermal reducing thermal bending and reducing the overall material temperature.

The structure of Model 176 was based on diffusion bonding and superplastic forming of flat titanium sheets. Forty years ago the method was called 'roll bonding' and executed with the titanium sealed within a stainless steel envelope and processed

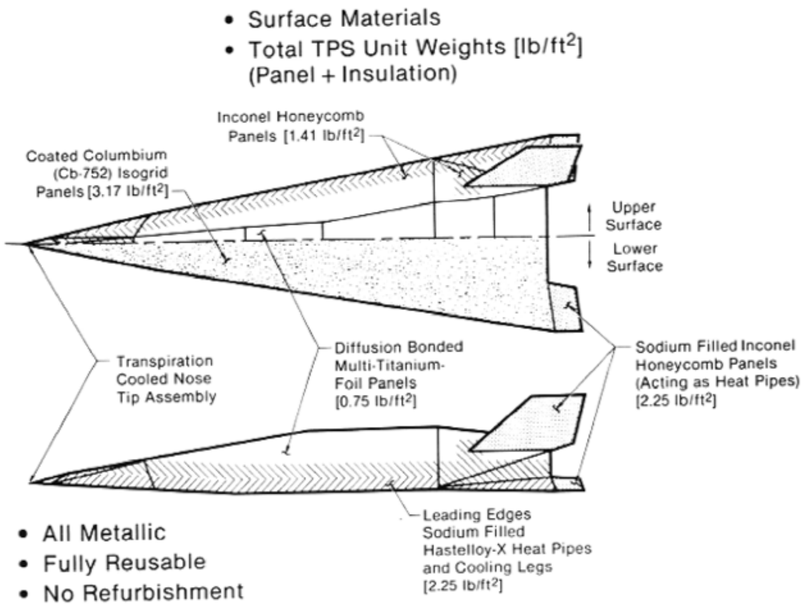

Figure 3.17. FDL-7 C/D, Model 176 materials, termal protection systems distribution based on temperature profile in Figure 3.16.

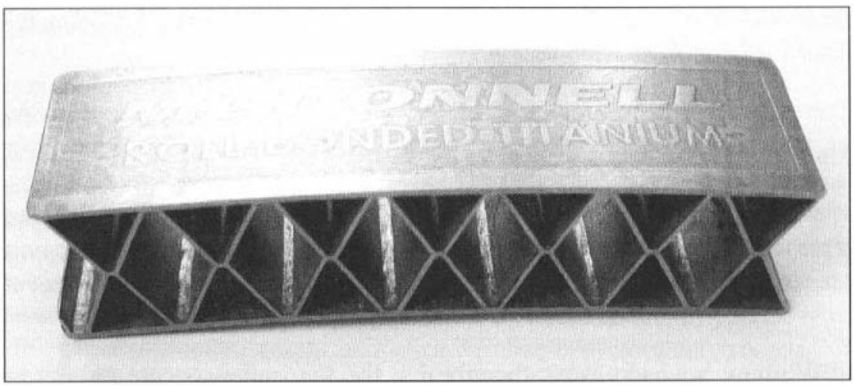

Figure 3.18. McDonnell Aircraft Company Roll-Bonded Titanium Structure (circa 1963), from *Advanced Engine Development at Pratt & Whitney* SAE [Mulready, 2001]. Today this structure would be super-plastically formed and diffusion-bonded from RSR titanium sheets.

in a steel rolling plant. With a lot of effort and chemical leaching the titanium part was freed from its steel enclosure. All of that has been completely replaced today by the current titanium diffusion bonding and superplastic forming industrial capability. The picture in Figure 3.18 is from a Society of Automotive Engineers (SAE) publication entitled *Advanced Engine Development at Pratt & Whitney* by Dick

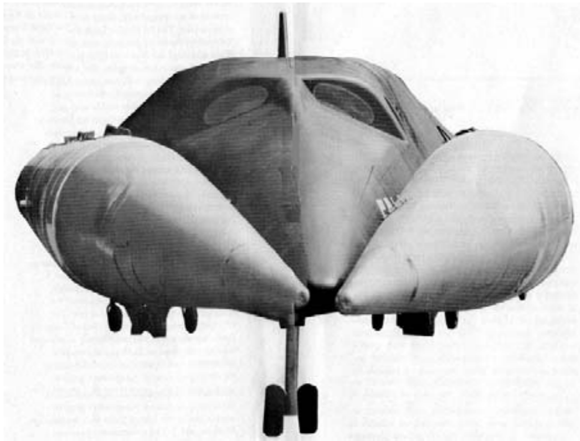

Figure 3.19. USAF FDL-7C/Model 176 scale model of a stage and one-half depicted in Figure 3.11. (Reproduced from *Astronautics and Aeronautics* [Draper, 1971].

Mulready. The subtitle is 'The Inside Story of Eight Special Projects 146-1971.' In Chapter 6, 'Boost glide and the XLR-129—Mach 20 at 200,000 feet'. The McDonnell Douglas boost-glide strategic vehicle is mentioned, together with the key personnel at McDonnell Aircraft Company. Low thermal conductivity standoffs set the metal thermal protection insulated shingles off from this wall so that there is an air gap between them. The X-33 applied the metal shingle concept but with significant improvement in the standoff design and thermal leakage, in the orientation of the shingles, and in the thickness and weight of the shingles. This is one aspect of the X-33 that can be applied to future spacecraft for a more reliable and repairable TPS than ceramic tiles. The titanium diffusion bonded and super-plastically formed wall was both the primary aircraft structure and the propellant tank wall. The cryogenic propellants were isolated from the metal wall by a metal foil barrier and sealed insulation on the inside of the propellant tank.

The United States Air Force Flight Dynamics Laboratory fabricated a half-scale mock-up of the stage and one-half Model 176 configuration [Draper et al., 1971] shown on the right side of Figure 3.14, and presented in Figure 3.19. The strap-on tanks provided propellants to about Mach 6 or 7 and then the mission continued on internal propellants. Note the windshields installed in this 1960s mock-up. This was a vertical launch, horizontal landing configuration, as shown in Figure 3.19. The intent was to provide the United States Air Force with an on-demand hypersonic aircraft that could reach any part of the Earth in less than a half-hour and return to its launch base or any base within the continental United States (CONUS). However, in a very short period of time after this mock-up was fabricated, the path the United States took to space detoured and most of this work was abandoned and discarded.

The ultimate intent was to begin operational evaluation flights, with the Model 176 launched on a Martin Titan IIIC, as shown in Figure 3.20. In 1964, the estimated

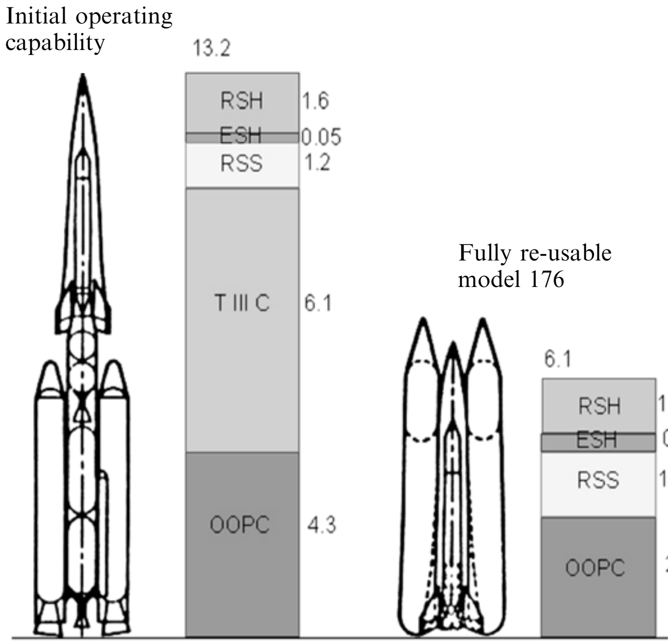

Figure 3.20. Individual Model 176 launch costs for a 100-launch program, as projected in a McDonnell Douglas Astronautics Corporation 1964 brief. RSH, reusable spacecraft hardware; ESH, expendable spacecraft hardware; RSS, reusable spacecraft spares; OOPC, other operational costs; T IIIC, Martin Titan III C cost.

cost was $US 13.2 million per launch for a 100-launch program, or about $US 2,700 per payload pound. As the system was further developed, two strap-on liquid hydrogen–liquid oxygen propellant tanks would be fitted to the Model 176 spaceplane for a fully recoverable system, as shown on the right side of Figure 3.20. The estimated 1964 cost of this version was $US 6.1 million per launch for a 100-launch program, or about $US 1,350 per payload pound. The launch rate for which the launch estimate was made has been lost in history, but to maintain the MOL spacecraft, launch rates on the order of one per week were anticipated for both re-supply and waste return flights. The latter flights could exceed the former in all of the studies the author is familiar with.

One of the most practical operational aspects of the FDL-7 class of hypersonic gliders was that the lifting body configuration forms an inherently stable hypersonic glider. Based on work by McDonnell Douglas Astronautics on control of hypersonic gliders, the FDL-7 as configured by McDonnell Douglas incorporated an integral escape module. As shown in Figure 3.21, the nose section with fold-out control surfaces was a fully controllable hypersonic glider capable of long glide ranges (though less than the basic vehicle, but greater then the Space Shuttle). So the crew always had an escape system that was workable over the entire speed range.

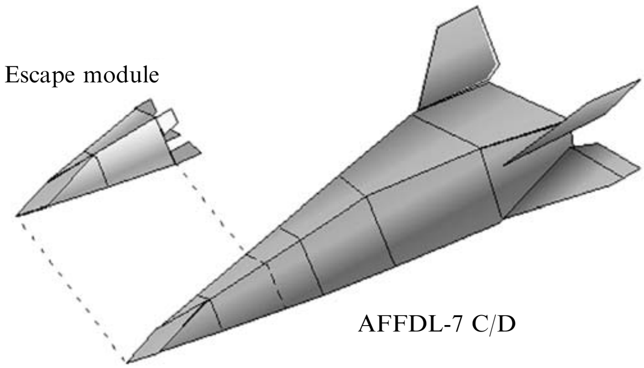

Figure 3.21. USAF FDL-7C as configured by McDonnell Douglas with an escape module capable of controlled hypersonic flight..

As shown the fold-out control surfaces are representative of a number of different configurations possible.

3.5 TAKEOFF AND LANDING MODE

The switchblade wing version of the FDL-7C (that is, the FDL-7MC) was the preferred version for the 1964 studies. A switchblade wing version of the McDonnell Douglas Model 176 configuration, without a windshield, is presented in Figure 3.22. This was part of the McDonnell Douglas TAV (Trans-Atmospheric Vehicle) effort; that vehicle was powered by either an Aerojet, Sacramento, Air Turboramjet or an airbreathing rocket propulsion system. The inward-turning, variable capture area inlet [DuPont, 1999] provides the correct engine airflow from landing speeds to Mach 5 plus. The propellant tanks were cylindrical segment, multi-lobe structures with bulkheads and stringers to support the flat metal radiative thermal protection shingles (similar to those planned for the now defunct X-33). The nose was transpiration-cooled with a low-rate water-porous spherical nose. The sharp leading edges (the same leading edge radius was used for the nose tip) were cooled with liquid metal heat pipes. This approach was tested successfully during the 1964 to 1968 time frame, and found to be equal in weight and far more durable than a comparable ceramic tile/carbon–carbon system. Whenever the landing weights were heavier than normal, the switchblade wing provided the necessary margin for these operations.

For an aircraft the takeoff mode is not an issue: it is a runway takeoff and runway landing. However for a space launcher the issue is not so clear-cut. With mass ratios for launchers much greater than for aircraft (4 to 8, compared to less than 2 for aircraft) runway speed may be impractical for some launchers with high mass ratios. So the principal option is vertical takeoff (VTO), with horizontal landing (HL) remaining viable. However, in some launcher studies, the study

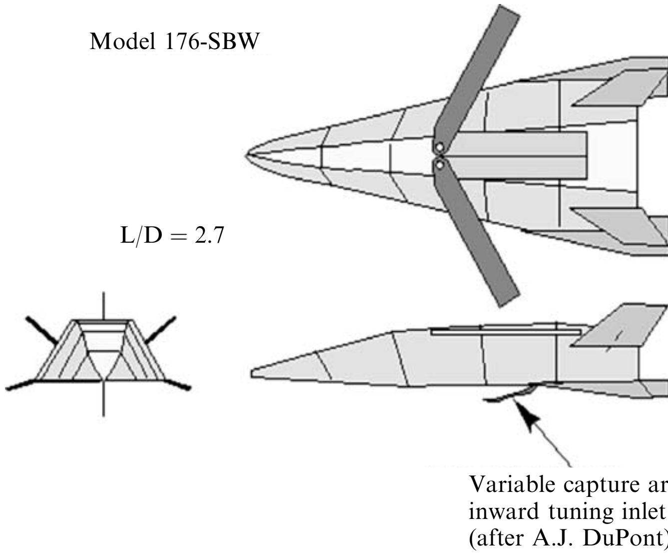

Figure 3.22. USAF FDL-7C/Model 176 equipped with a switchblade wing and retractable inward-turning inlet for airbreathing rocket applications.

directives mandate horizontal takeoff whatever the mass ratio. Many launcher studies have been thwarted by this *a priori* dictate of horizontal takeoff. In reality, horizontal or vertical takeoff, like the configuration concept, is less a choice than a result of the propulsion concept selected. Horizontal takeoff requires that the wing loading be compatible with the lift coefficient the configuration can generate and the maximum takeoff speed limit. For high sweep delta planforms, such as that of the Model 176, the only high-lift device available is the switchblade wing and a retractable canard near the nose of the vehicle.

The basic FDL-7C/Model 176 was not designed for horizontal takeoffs. As presented in Figure 3.23, the takeoff speed, as a function of the SSTO launcher mass ratio to orbital speed, is very high for the basic delta lifting body, even for low mass ratio propulsion systems (squares). With the lowest mass ratio, the takeoff speed is still 250 knots (129 m/sec) and that is challenging for routine runway takeoffs. Landing and takeoff speeds are for minimum-sized vehicles, that is, values of tau in the range of 0.18 to 0.20, where the gross weight is a minimum. Adding the switchblade wing provides a reasonable takeoff speed for all mass ratios (triangles). This takeoff speed with the switchblade wing deployed is approximately also the landing speed with the wing stowed. All of the launcher vehicles have very similar empty plus payload weight (operational weight empty); the landing speeds are essentially constant for all configurations and propulsion systems, corresponding to the lower mass ratio values. With this approach the landing and takeoff speeds are essentially equal, adding a degree of operational simplicity. Landing and takeoff speeds correspond to those of current military aircraft and civil transports, at least for the lower mass ratios (five or less). However, the landing speeds do increase with

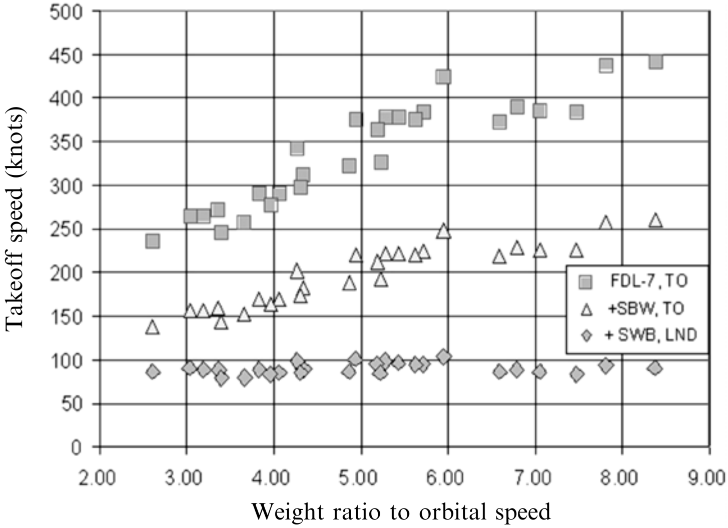

Figure 3.23. Takeoff and landing speeds of minimum-sized launchers.

takeoff mass ratio, since the operational empty weight of the vehicle increases with mass ratio. An approach to make the landing speed approximately constant and a lower value is to deploy the switchblade wing for landing (diamonds). Then the landing speed becomes very modest, even lower in most civil transports and military aircraft.

Takeoff speeds for blended bodies in the 200- to 230-knot ranges were postulated in the 1960s by using a very large gimbaled rocket motor to rotate upwards causing the body to rotate, lifting off the nose wheel and eventually the entire vehicle with a thrust-supported takeoff. This concept was not implemented in an actual system. If the takeoff speed is too high for the propulsion system chosen (because of weight ratio) then the only way to decrease the takeoff speed is to increase the planform area for the system volume, that is, to reduce the Küchemann tau. This unfortunately introduces a cascade of incremental mass increases that result in an exponential rise of the takeoff gross weight. This is illustrated in Figure 3.24.

Figure 3.24 begins with a solution map of vertical takeoff launchers, as represented by the shaded area in the lower part of the figure. All of this data is for converged solutions, where the SSTO mission requirements are met and the mass and volume of each solution are converged. These solution areas represent a spectrum going from all rocket systems (far right) to advanced airbreathing systems (far left). These solution area are for vertical takeoff, horizontal landing (VTOHL) with thrust to weight ratio at takeoff (TWTO) of 1.35 and tau equal to 0.2. For comparison, the gross weight trends are shown for five different takeoff wing loadings. The horizontal takeoff, horizontal landing (HTOL) solutions for constant wing loading are shown for values of tau from 0.2 to 0.063. The point at which the VTOHL and HTOL modes have the same gross weight is then the maximum weight

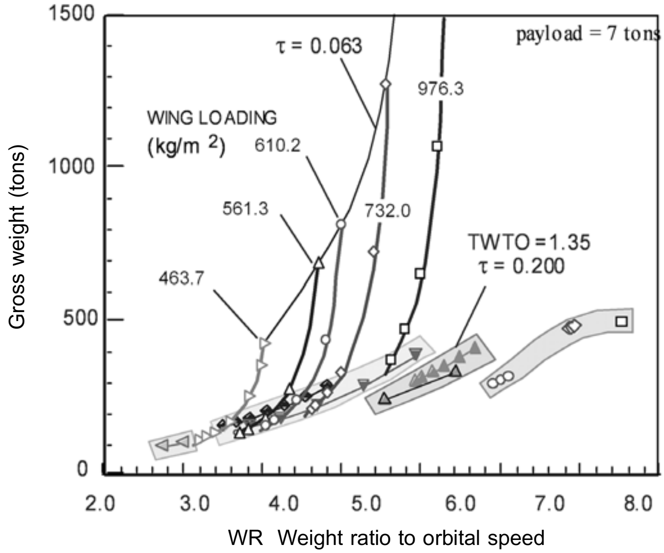

Figure 3.24. Imposed horizontal takeoff requirement can radically increase takeoff gross weight unless the weight ratio is less than 4.5.

ratio for which there is no penalty for horizontal takeoff. For example, at a takeoff wing loading of 973 kg/m^2 (200 lb/ft^2) this weight ratio is 5.5, or an airbreathing speed of Mach 6 ± 0.3. For a takeoff wing loading of 610 kg/m^2 (125 lb/ft^2) the VTOHL/HTOL boundary is now a weight ratio 4.3, or an airbreathing Mach 10.5 ± 0.5. This wing loading is also correct to air launch, horizontal landing (ALHL) in the Mach 0.72 at 35,000 ft region. For a takeoff wing loading of 464 kg/m^2 (95 lb/ft^2) the VTOHL/HTOL boundary is now a weight ratio 3.4, or an airbreathing Mach 13 ± 1.0 or an ACES propulsion system. This latter wing loading is the wing loading that would represent the maximum airbreathing speed practicable and consistent with commercial transports. For an airbreathing rocket, a mass ratio of 5.0 is achievable. That results in a gross weight of about 230 tons. This is less than half the 480 tons for an all-rocket case. However, if a horizontal takeoff requirement is imposed *a priori*, the lowest wing loading for which a practical solution exists is 610.2 kg/m^2. At that point, the gross weight for the horizontal takeoff solution is about 800 tons, almost twice the all-rocket value. If the study team is not aware of the comparison to vertical takeoff, the improper conclusion might be drawn that it was the propulsion system that caused the divergent solution. For lower wing loading, the solution curve becomes vertical, and the solution will not converge. The conclusion is that, if the weight ratio is greater than 4.5, the best vehicle configuration is vertical takeoff or an air-launched configuration (all of the vehicles have a horizontal landing mode). Again, it is important to let the characteristics themselves of the converged solution determine the takeoff and landing modes, if the lowest gross weight and smallest size vehicle is the goal.

3.6 AVAILABLE SOLUTION SPACE

So far the mass ratio required to reach LEO from the surface, the mass ratio to reach higher orbits, the impact of how often these systems operate on the cost of delivering payloads to orbit have been discussed. The next step is to use this material to establish where a solution exists for the combination of propulsion system, geometry, and mission. The AIAA book, *Scramjet Propulsion*, [Curran and Murthy, 2000] discusses the approach in Chapter 16, 'Transatmospheric vehicle sizing' by J. Vandenkerckhove and P. Czysz. Then, using a very minimum of information on the capability of the aerospace industry to manufacture air vehicles together with the propulsion system description and the basic geometry trends of hypersonic vehicles, the solution space can be identified. The two principal relationships are: (1) the industrial capability index (ICI) and (2) the operational weight empty (OWE), as functions of the propulsion system, geometry, size and material/structures manufacturing capability of industry, as given in equations (3.3). These two equations are solved simultaneously for planform area and ICI given a specific payload and tau.

$$\mathrm{OWE} = 10\,\frac{I_\mathrm{p}}{I_\mathrm{str}}\,f(\mathrm{geo})\,\frac{1 + r_\mathrm{use}}{S_\mathrm{p}^{0.7097}}$$

$$\mathrm{OWE} = W_\mathrm{empty}\,(1 + r_\mathrm{use}) = K_\mathrm{v}\,\tau\,I_\mathrm{p}\,S_\mathrm{p}^{1.5717} \tag{3.3}$$

The equation elements are defined in equations (3.4).

$$f(\mathrm{geo}) = \frac{K_\mathrm{w}}{K_\mathrm{str}K_\mathrm{v}\tau} = f(\tau)$$

$$K_\mathrm{v} = \frac{V_\mathrm{ppl}}{S_\mathrm{p}^{0.0717}}$$

$$r_\mathrm{use} = \frac{W_\mathrm{pay} + W_\mathrm{crew}}{W_\mathrm{empty}}$$

$$\mathrm{ICI} = 10\,\frac{I_\mathrm{p}}{I_\mathrm{str}} \qquad I_\mathrm{p} = \frac{\rho_\mathrm{ppl}}{\mathrm{WR} - 1}$$

$$I_\mathrm{str} = \frac{W_\mathrm{str}}{S_\mathrm{wet}} \tag{3.4}$$

The two principal terms in determining size are $f(\mathrm{geo})$ and ICI. The $f(\mathrm{geo})$ is given in Figure 3.25 as a function of tau. As for previous geometric correlations (Figure 3.10) the different hypersonic configurations map (collapse) into a single trend line. There are two correlating equations, one for values of tau less than 0.24, and one for values greater than 0.24. The shaded rectangle represents typical SSTO solution space for both rocket and airbreathing propulsion systems. The reason the solution space is so narrow is that, whatever the propulsion system, the quantity of hydrogen fuel is approximately the same, and therefore the volumes for the different propulsion systems are quite similar. With liquid oxygen 15.2 time more dense than liquid

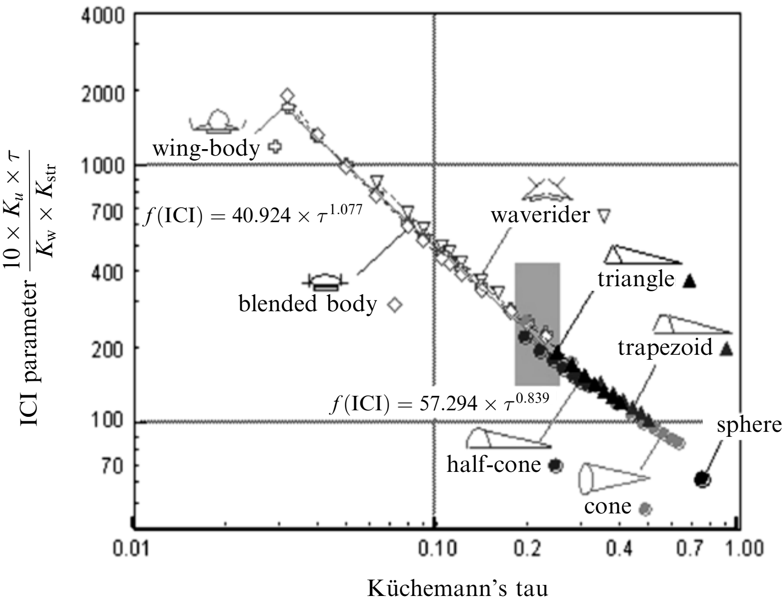

Figure 3.25. Size-determining parameter group correlates with Küchemann's tau.

hydrogen, the presence or absence of liquid oxygen has a significant weight impact, but a lesser volume impact. The K_v term is a function of tau and the configuration concept and details of this formulation can be found in [Curran and Murthy, 2000]. Nominally K_v has a value of 0.4 for a wide range of tau and configurations. The K_v term is a correlation term that defines the maximum volume available for propellant as a function of vehicle size as defined by the planform area. The correlation is based on analyzing the results of hypersonic design studies from the author's experience that spans from 20 tons to 500 tons gross weight vehicles.

The ICI term consists of two elements, the propulsion index (I_p) and the structural index (I_{str}), see equation (3.4). For an entire spectrum of propulsion systems the I_p depends mainly on turbopumps: the I_p value for a given turbopump level of performance is almost constant. Assuming a Space Shuttle main engine (SSME) propulsion system, the propulsion index for an SSTO vehicle is 4.3. For a spectrum of propulsion systems from the SSME to an airbreather that must operate to Mach 14, and that must be installed on SSTO vehicles, the propulsion index is 4.1 ± 0.2. The structural index is the total structural weight divided by the wetted area of the vehicle. This index is remarkably consistent over the passage of time. In 1968, the projected 1983 weight of an insulated, aluminum structure that is, both the structure and the propellant tank, was 3.5 lb/ft^2 (17.1 kg/m^2) [HyFac, 1970]. In 1993, NASA's estimated weight of an insulated, aluminum structure for a hypersonic waverider aircraft, that is, both the structure and the propellant tank, was 3.5 lb/ft^2 (17.1 kg/m^2) [Pegg and Hunt, 1993]. Using these values, the estimated range for the current value of ICI is 9 to 11. This then gives us a boundary to

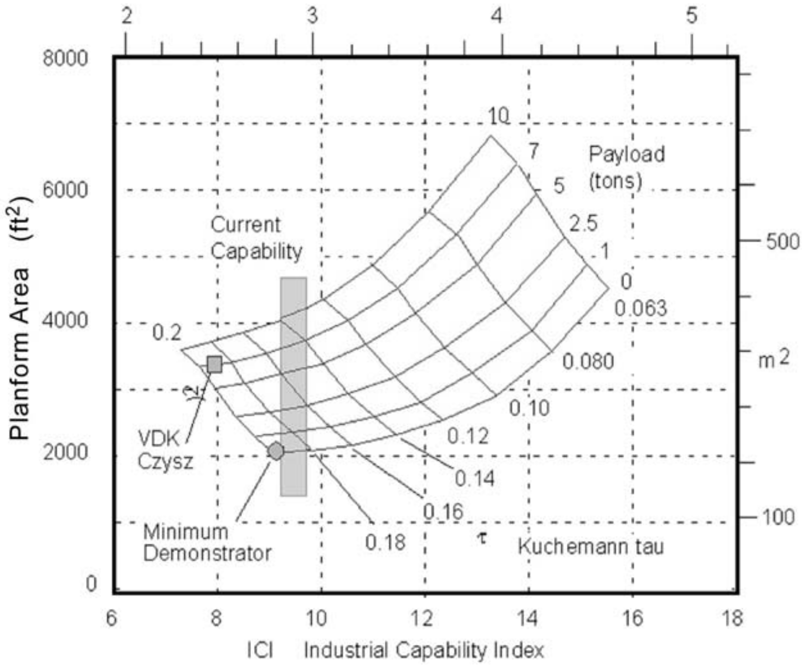

Figure 3.26. All-Rocket available design space is limited.

establish the practicality of SSTO vehicles with today's industrial capability. If the value ICI is 9 to 11 or less, the concept is practical in terms of current industrial capability. If the value of ICI of a configuration/propulsion system is greater than the boundary value, then it is doubtful the concept is practical in terms of the current industrial capability The distance the concept under consideration is from the ICI boundary is a measure of the margin, or lack of margin, with respect to the current state of the art, perhaps more meaningful than less quantitative indices such as the popular 'technology readiness level'.

Based on these definitions, the solution space is presented graphically as a function of planform area (on the ordinate), and ICI (on the abscissa), with lines of constant payload and tau forming the graphical results map. Three propulsion systems are presented for the SSTO to LEO mission (100 nautical miles or 200 km orbital altitude), with payloads varying from zero to 10 metric tons. Küchemann's tau ranges from 0.063 to 0.20. The two propulsion systems evaluated are:

(1) All-rocket, topping cycle similar to the P&W XLR-129 or the US SSME. For hydrogen/oxygen propellants is a hypersonic glider analogous to FDL-7C/D, Figure 3.26.
(2) Rocket plus ejector ram/scramjet operating as an airbreathing system to Mach number 8, then transitioning to rocket to orbit. For hydrogen/oxygen propellants, the airbreather configuration shown in Figure 3.27.

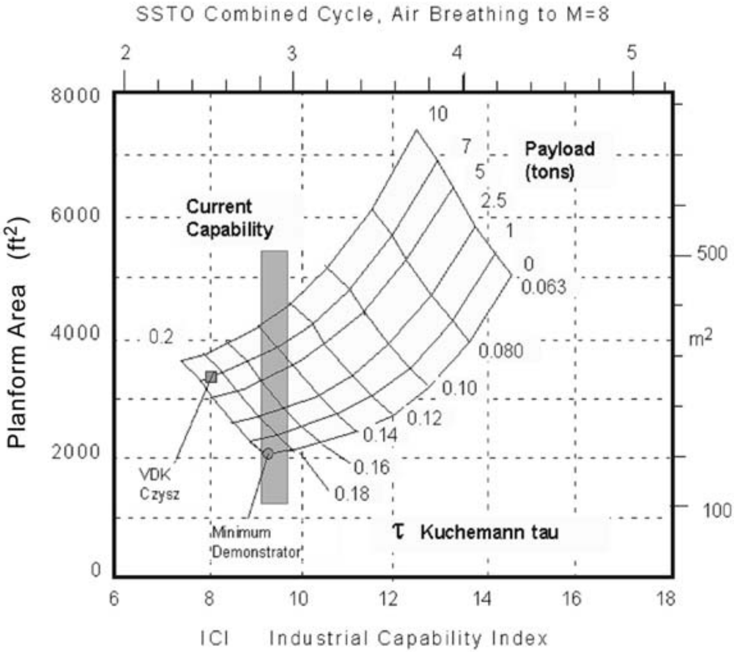

Figure 3.27. The Mach 8 combined cycle launcher is also limited.

(3) Rocket plus ejector ram/scramjet operating as an airbreathing system to Mach number 12 then transitioning to rocket to orbit. For hydrogen/oxygen propellants, the airbreather configuration shown in Figure 3.28.

Figure 3.26 presents the solution map for the all-rocket configuration. The bottom scale is for ICI in English units for I_p and I_{str} and the top scale is for ICI in SI units. The left scale is in English units and the right scale is in SI units for the planform area. The vertical bar is the ICI boundary for the all-rocket, topping cycle similar to SSME. Note that most of the design space is to the right of the ICI boundary at 9.0 to 9.5, that is, beyond the current state of the art. A kerosene-fueled supersonic cruise vehicle like Concorde has a low value of tau, about 0.035. A hydrocarbon-fueled hypersonic cruise vehicle would have a larger value of tau, about 0.063. If the designer of a SSTO chose to pattern the design after a cruise vehicle, with a low value of tau, the design would not converge, no matter what resources were expended. Note that as the payload increases, the available design space increases. One of the dilemmas of hypersonic vehicle design is illustrated in Figure 3.27. Using reasoning based on subsonic aircraft, a smaller aircraft should be easier to fabricate and operate than a larger one. However, for a SSTO demonstrator, that is, a demonstrator that can actually achieve orbital speed and altitude, the opposite is the case. The minimum sized, zero payload demonstrator is on the ICI boundary, and at the maximum value of tau. A operational vehicle with a 7.0-ton payload, as analyzed by

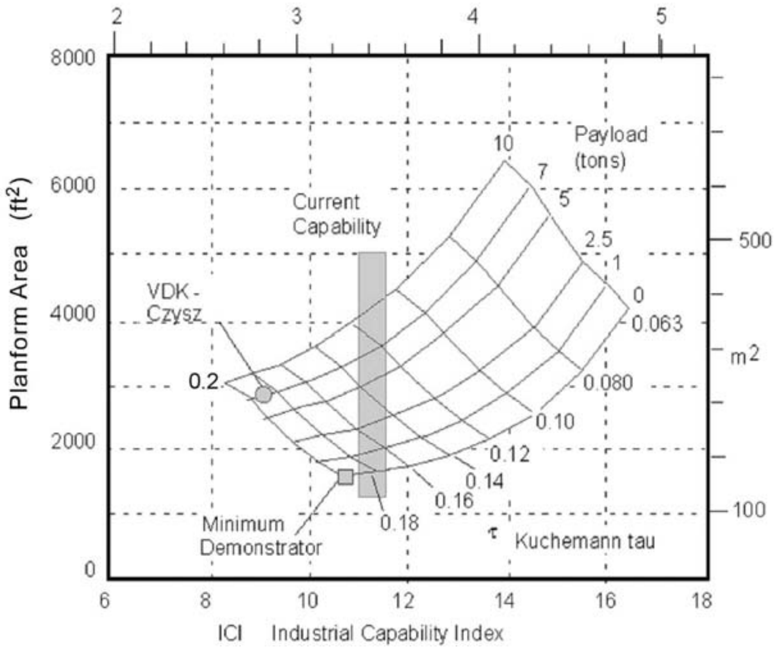

Figure 3.28. The Mach 12 combined cycle launcher is also limited.

Vanderckhove and Czysz, has a significant reduction of the ICI value needed. As the payload increases, the tau value at the ICI boundary decreases, so that for a 10-ton payload the minimum value of tau is 0.14. Please note it would be possible to build a hypersonic demonstrator that could achieve Mach 12 for, say, just 5 minutes flight time, but the mass ratio for that mission might be on the order of 1.8, far from the 8.1 ratio required to reach orbital speed and altitude.

Figure 3.27 presents the solution map for the rocket plus ejector ram/scramjet operating as an airbreathing system to Mach number 8. The bottom scale is for ICI in English units for I_p and I_{str} and the top scale is for ICI in SI (IS) units. The left scale is in English units and the right scale is in SI units for the planform area. The vertical bar is the ICI boundary for the rocket plus ejector ram/scramjet operating as an airbreathing system to Mach number 8 and it is at the 9.0 to 9.5 value, the same as for the all-rocket launcher. In terms of industrial capability required, this analysis points to an equality of requirements. As with the previous case, most of the design space is to the right of the ICI boundary, that is, beyond the current state of the art. Both the operational example and the demonstrator example have the same ICI value as the previous rocket case. So the Mach 8 airbreather is about equal, in terms of technical challenge, to the all-rocket.

Figure 3.28 presents the solution map for the rocket plus ejector ram/scramjet operating as an airbreathing system to Mach number 12. The bottom scale is for ICI in English units for I_p and I_{str} and the top scale is for ICI in SI units. The left scale is

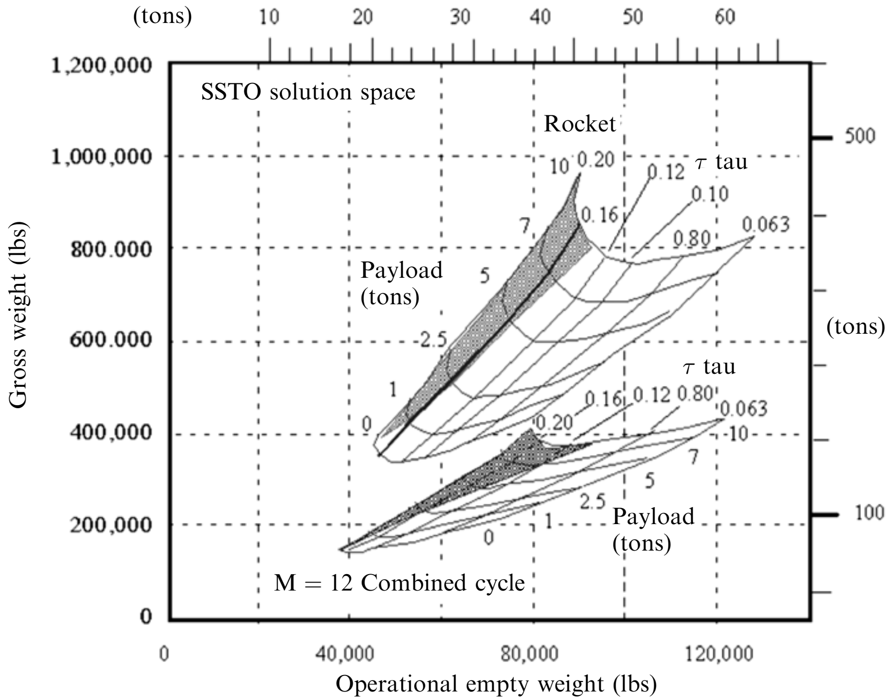

Figure 3.29. The combined cycle propulsion has the advantage.

in English units and the right scale is in SI units for the planform area. The vertical bar is the ICI boundary for the rocket plus ejector ram/scramjet operating as an airbreathing system to Mach number 12 is to the right of the previous two cases at a value in the 11 to 11.5 range. That is a greater industrial capability fraction of the design space is available for converged designs, but those designs require a higher value of the ICI. As with the two previous cases, most of the design space is to the right of the ICI boundary, that is, beyond the current state of the art. Both the operational example and the demonstrator example have a greater ICI value than the previous two cases. So the Mach 8 airbreather is about equal, in terms of technical challenge, to the all-rocket, but the Mach 12 airbreather is a greater challenge, especially in propulsion, as the value for the structural index can be assumed to be the same for all three cases presented.

Again, it is important to note, that the conventional aircraft design wisdom puts SSTO designs out of reach of current industrial capability. Secondly, the SSTO challenges are similar for all-rocket and airbreather, but increasingly difficult as the Mach number at which airbreathing propulsion must transition to rocket propulsion increases beyond Mach 8. Given the similarity of the industrial challenge, the question is, what are the differences in weight for the airbreather compared to the all-rocket vehicle. Figure 3.29 presents answers to this question. For approximately the same empty weight, the gross weight of the rocket vehicle is at least twice heavier than the combined cycle vehicle.

3.7 BIBLIOGRAPHY

Ambrose, S. (2000) 'Nothing Like It in the world', Simon & Schuster, New York.

Anon, McDonnell (1970) 'Mission Requirements of Lifting Systems (U), Summary of Significant Results & Figures', McDonnell Aricraft Report B947 prepared under NASA NAS 9-3562, August 1965. (Declassified 1970.)

Anon, Lockheed (1967) 'A Study of Advanced Airbreathing Launch Vehicles With Cruise Capability', Lockheed Report IR 21042, The Lockheed Aircraft Corporation.

Buck, M.L., Zima, W.P., Kirkham, F.S., and Jones, R.A. (1975) 'Joint USAF/NASA Hypersonic Research Aircraft Study', AIAA 75-1039, AIAA 25th Aircraft Systems and Technology Meeting, Los Angeles, California, August 1975.

Curran, E.T., and Murthy, S.N.B. (2000) 'Scramjet Propulsion', *Progress in Astronautics and Aeronautics*, Vol. 189, American Institute of Astronautics and Aeronautics, Reston, VA.

Dixon, W.P. (1966) 'Precise Heat Transfer Measurement with Surface Thermocouples', Paper presented at the 8th Annual Rocky Mountain Spectroscopy Conference, Denver, CO.

Dixon, W.P., and Czysz, P. (1964) 'Quantitative Heat Transfer Measurement Using Thermographic Phosphors', *Society of Photo-Optical Instrumentation Engineers Journal*, Vol. 7, No. 3, p. 77.

Draper, A.C., Buck, M.L., Goesch, W.H. (1971) 'A Delta Shuttle Orbiter', *Astronautics & Aeronautics*, Vol 9, No. 1, pp. 26–36.

DuPont, A.A. (1999) 'Further Studies of Optimized Inlets for Hypersonic Turbine Engines', ISABE 99-7039, 14th International Symposium for Air Breathing Engines (ISABE), Florence, Italy, September 1999.

HyFac (October 1970) Anon., 'Hypersonic Research Facilities Study', Prepared under NAS2-5458, Vol I–VI, NASA CR 114322–114331. (Declassified 1982.)

Küchemann, D. (1960) *Aircraft Shapes and Their Aerodynamics for Flight at Supersonic Speeds*, RAE TM Aero 674.

Lozino-Lozinski, G.E. (1986) 'BURAN: Its Creation and Prospects of Its Usage', White Paper, 1984. Received during the International Astronautical Federation Congress, Malaga, Spain.

Mulready, D. (2001) *Advanced Engine Development at Pratt & Whitney (The Inside Story of Eight Special Projects 1946–1971)*, SAE International, Warrendale, PA. ISBN: 0-7680-0664-3.

Pegg, R.J., Hunt, J.L. and Peebles, C. (1999) *Design of a Hypersonic Waverider-Derived Airplane*, AIAA Paper 93-0401, AIAA Aerospace Scienced Conference, Reno, NV, January 1993.

Thompson, M.O., and Peebles, C. (1999) *Flying without Wings: Before the Space Shuttle: Testing NASA's Wingless Aircraft*, Crécy Publishing, Manchester, NH.

4

Commercial near Earth launcher: propulsion

As presented in Chapter 2, airbreathing propulsion advocates fought a losing battle to change the space launcher paradigm from expendable rockets, that are launched for the first, last and only time, to sustained-use launchers that were more like military airlift transports with long and frequent usage [Anon., Lockheed, 1967]. Chapter 3 has details of the debate that took place in the US, following which even a sustained-use rocket launcher proposed to support the military Manned Orbiting Laboratory (MOL) was discarded, as was MOL, as not having relevance in a purposely designated 'civilian' space fleet. As a result most, if not all, of the military high-performance hypersonic gliders design and performance data was forever lost, together with the benefits of these high-performance systems to the civilian space organization. The challenge of airbreathing propulsion, based on what were indeed rational assumptions, but applying only to rockets, resulted (and to many, still results now) in large, ponderous and too costly vehicles. Even though that was challenged, as shown in Figures 2.16 and 2.17, lasting impressions were that airbreathers were too large and too expensive, and they required too long a development period when compared to rocket-launching systems. This is factually contrary to the actual rocket record, an example being total lack of manned launches during the 12-year period the Space Shuttle was being developed. Chapter 3 also shows that, when propulsion systems are put on a common basis, and the lifting body configurations are used, there are indeed differences in weight between rocket and airbreathing propulsion, but no significant size or industrial capability index differences. So, the fact remains, if we are to transition from the status quo today, as illustrated in Figure 2.22, into the commercial space scenario of Figure 2.23, something has to change to support the flight rate such a commercial infrastructure would require. However, it must be said that this particular status quo is comfortable, and profitable, for the telecommunications and launcher companies.

In order to achieve a transportation system to space analogous to the transcontinental railroad, i.e., that can support a commercial space infrastructure, the shift must be to include an airbreathing launcher to meet the high flight rate requirements. The MOL was designed for 20 to 27 persons. The support spacecraft would carry 9 to 12 persons or materials to re-supply the station. For that goal the payload planned was a 7 metric ton payload (15,435 lb). An airbreathing launcher would be at least one-half the weight of the rocket vehicle in Figure 3.20, requiring one-half the resources. The MOL study identified that each replacement person would have a 994-lb (450-kg) resource supply payload to accompany each crewmember. For a 12-person crew replacement mission, that makes the crew replacement payload 15,228 lb, well within the 7-ton payload capacity. The operating parameters for the station were a nominal 21-person crew. The same study determined that 47,000 lb (21,315 kg) of resources were required per crewmember per year. For one year, with a 21-person complement, that means 448 metric tons (987,000 lb) of supplies needs to be lifted to the station for crew support, not counting propellants to maintain the station orbit. With 21 crewmembers, there are four flights per year required to meet the 6-month assignment requirement. To lift the crew supplies to the station would require 64 flights per year, not counting propellant and hardware replacement missions that may require another five to six flights per year. The number of flights to a large station is then at least 74 flights per year. From a military mission analysis, that would require a fleet of 10 aircraft (14, counting in operational spares) that flew seven times a year for 15 years, and a 100-flight operational life [Czysz, 1999; Zagaynov and Plokhikh, 1991]. Using instead the present rocket launchers, that becomes a total of 1,050 launches by 1,050 rockets. To the MOL designers of 1964 it was instead a fleet of 10 to 14 sustained-use vehicles operated over a 15-year period, plus repair and maintenance. That vast difference in outlook between the aircraft manufacturers and the ballistic missile manufacturers remains today. Sustained-use remains as a poor competitor to expendable rocket rather than being a necessity for the future of commercial space.

Just as ground transportation has railroad trains, over-the-road tractor-trailers, cargo trucks, busses, and automobiles, so space must have a variety of transportation vehicles with different payload capacities and fly rates. The United States is still lacking a heavy-lift capability as we once had with Saturn V. There is yet to be constructed a dedicated space exploration system. We need the capability of sending heavy payload to the gas giants such as Jupiter and Saturn; moderate payloads to the outer planets; and modest payloads to the boundaries of our Solar System [Anfimov, 1997], all in comparable travel times. Airbreathing propulsion will not help us in space, but it can enable lighter, sustained-use launchers that increase the frequency to orbit and reduce the cost to an economically practical value that will enable more space infrastructure and space exploration.

4.1 PROPULSION SYSTEM ALTERNATIVES

Incorporation of airbreathing can provide many propulsion options; however, vehicle design choices are not completely arbitrary as requirements and propulsion performance define practical solution space, as discussed in Chapter 3. *A priori* decisions such as horizontal versus vertical takeoff can doom success before starting on an otherwise solvable problem. From the governing equations, the two keys appear to be off-loading some of the carried oxidizer, and designing for sustained operations over a long operational life with maintenance, not continuous overhaul and re-building. As illustrated in Figures 3.27, 3.28 and 3.29, the design space solvable with current industrial capabilities and materials is readily identifiable. New discoveries and industrial capabilities are always important, but, as was clearly demonstrated in the 1960s, neither discovery of new technologies nor the identification of technology availability dates (TADs) are *necessary* to fabricate an operational space flight system with more capability than the current hardware. Even a cursory review of the North American X-15, or Lockheed and Kelly Johnson's SR-71 would show that the presence of bureaucratic roadblocks such as TADs would have meant neither aircraft would have been built or flown. It was curiosity, resourcefulness, skill and knowledge that enabled the North American and Lockheed teams to succeed. Governmental planning had little to do with their success. The teams adapted what was available and created what was not, only if and when necessary. The latter is the late Theodore von Karman's definition of an engineer [Vandenkerckhove, 1986], contained as a personal note to Jean, one of von Karman's last graduate students: 'scientists discover what is; engineers create that which never was'.

There is an excellent documented example of what just written above in a book published by the Society of Automotive Engineers (SAE) entitled *Advanced Engine Development at Pratt & Whitney* by Dick Mulready. The subtitle is 'The Inside Story of Eight Special Projects 1946–1971.' In Chapter 6, 'Boost glide and the XLR-129—Mach 20 at 200,000 feet' two McDonnell Aircraft Company persons are named, Robert (Bob) Belt and Harold Altus (sic). The spelling should be Altis. The former was known to lead the 'belt driven machine.' Figure 4.1 comes from Figure 6.7 in that book and compares the development testing of the XLR-129 turbopump to its design value of 6705 psia, with that of the NASA 350K turbopump that became later the main SSME component. In the last paragraph of the chapter the sentence is: 'The liquid oxygen turbopump was the next component in line. However, before it was funded, NASA had started the Space Shuttle campaign, and the Air Force gave the XLR-129 program to NASA, granting free use of the existing hardware to Pratt & Whitney. NASA promptly canceled the liquid oxygen turbopump because it would be unfair to our competitors to fund it. I bet there were times when NASA wished it had continued the program.' And with it disappeared a rocket engine with a run record of 42 simulated flights (in the test chamber) without any overhaul or repair.

Applying this viewpoint, a cross-section of propulsion system options based on available, demonstrated hardware and materials are discussed with both pros and cons. Airbreathing propulsion can be beneficial over at least a part of the flight trajectory. Historically, there are three broad categories of airbreathing propulsion:

(a) A combination of individual engines operating separately (sometimes in parallel, sometimes sequentially) that can include a rocket engine [The Aerospace Corporation, 1985].

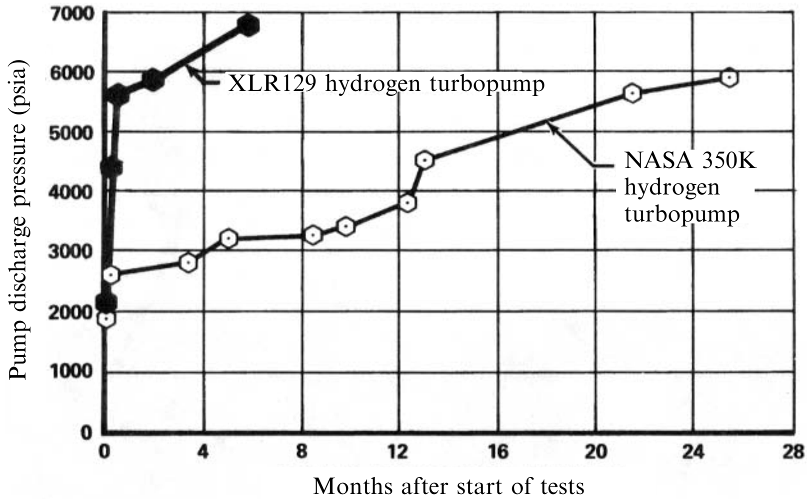

Figure 4.1. Comparison of XLR-29 qualification (circa 1965) with that of the Space Shuttle main engine (SSME) (circa 1972).

(b) An individual engine (usually a rocket engine) operating in conjunction with an engine that can operate in more than one cycle mode [Tanatsugu et al., 1987, 1999; Nouse et. al., 1988; Balepin et al., 1996], or a combined cycle engine.
(c) A single combined cycle engine that operates in all of the required cycle modes, over the entire flight trajectory [Maita et al., 1990; Yugov et. al., 1989; Kanda et al. 2005].

4.2 PROPULSION SYSTEM CHARACTERISTICS

For a combination of individual engines, to transition from one engine to another means that one has to be shut down and another started while maintaining flight speed. If the engine is airbreathing, then the flow path has to be changed also. In the past switching the flow path from one engine to another has always been this system downfall. For a rocket engine operating in conjunction with another engine system, the operation is relatively straightforward. The key challenge is to control the fuel path to the engines. For the single combined cycle concept, the engineering challenge is transitioning from one cycle to the next within a single engine. The transition from one engine cycle operation to another must be made efficient (on First Law basis that means the total energy losses must be minimized) and effective (on Second Law basis that means when the available energy is available for recovery as useful work, the energy conversion must be accomplished then or become unrecoverable). An engine of category (c) is designed for the minimum entropy rise across the cycle. The scope and limitations of these engines are discussed in detail in references [Escher, 1994; Czysz, 1993a,b], and there are several advantages to such a scheme that have been identified. In the case of most airbreathing propulsion systems the transition from one cycle to another is not a showstopper. For airbreathing propulsion the two most important considerations are: the flow energy compared to the energy the fuel can add to the flow through combustion, and the internal flow energy losses due to internal drag of struts, injectors and skin friction and fuel/air mixing.

4.3 AIR FLOW ENERGY ENTERING THE ENGINE

With a rocket, all of the fuel and oxidizer are carried onboard the vehicle, so other than atmospheric vehicle drag and the nozzle exit pressure compared to atmospheric pressure, the vehicle's relative speed with respect to the atmosphere does not determine the propulsion system performance. The specific impulse is the thrust per unit propellant mass flow per second. So, if more thrust is required more engine mass flow is required, i.e. a larger engine or increased chamber pressure to increase the mass flow. With an airbreathing propulsion system just the opposite is true. Because for the airbreathing engine air enters the vehicle via an inlet, Figure 4.2, the ability of the inlet to preserve energy, as the flow is slowed down in the inlet (for instance, by passing through a series of shock waves), is absolutely critical. The magnitude of the flow kinetic energy recovered at the end of the inlet determines

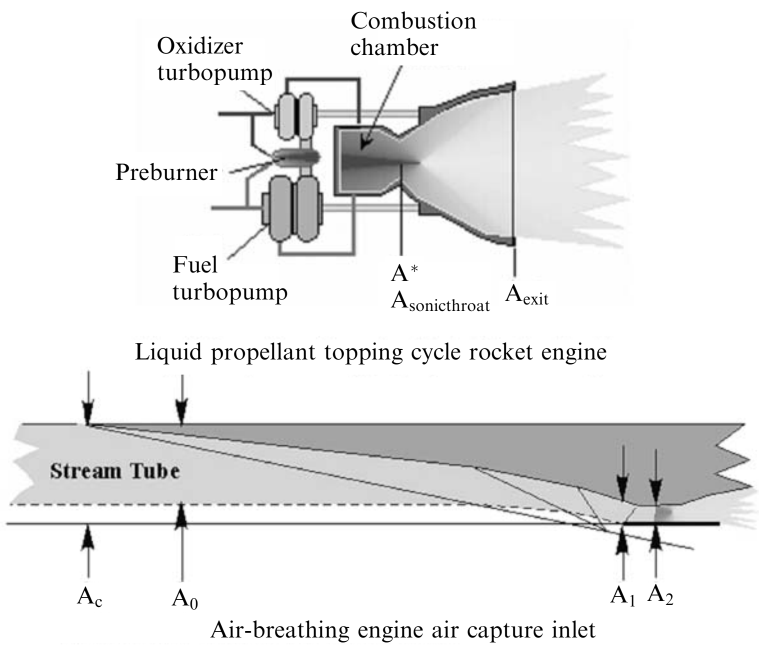

Figure 4.2. Liquid rocket engine carries its fuel and oxidizer onboard. By contrast an air-breathing engine carries only fuel onboard and the oxidizer is atmospheric air captured by the inlet.

how much of the fuel combustion energy is available to be converted into thrust. Because the oxidizer is the oxygen in the air, there is a maximum energy that can be added per unit mass flow of air. The capture area of the inlet and flow speed relative to the vehicle determines how much total energy the burned fuel can add to the air stream. Ultimately, it is the difference between the energy lost in the inlet and the combustion energy that determines the thrust. The energy of the air is a function of two quantities, the energy of the air in the atmosphere (static enthalpy, in kJ/kg) and the kinetic energy of the air stream (kinetic energy, in kJ/kg). In equation form the relationship is:

$$\text{Total energy} = \text{Static enthalpy} + \text{Kinetic energy}$$

$$h_\mathrm{t} = h_0 + \frac{V_0^2}{2} = \left(\frac{\mathrm{kJ}}{\mathrm{kg}}\right) \qquad V_0 = \mathrm{m/s}$$

$$h_\mathrm{t} = 232.6 + \frac{V_0^2}{2{,}000} = \left(\frac{\mathrm{kJ}}{\mathrm{kg}}\right) \tag{4.1}$$

The static enthalpy is almost a constant over the altitude range over which the airbreathing propulsion system operates. The total energy is essentially a function of the kinetic energy of the air stream. However the energy added to the air by the combustion of a fuel is approximately a constant for each fuel. Thus:

$$Q_\mathrm{c} = \text{Heat of combustion} = \left(\frac{\mathrm{kJ}}{\mathrm{kg}}\right)_{\text{fuel}}$$

$$Q = \text{Brayton cycle heat addition} = \left(\frac{\mathrm{kJ}}{\mathrm{kg}}\right)_{\text{air}}$$

$$Q = \left(\frac{\text{fuel}}{\text{air}}\right) Q_\mathrm{c} \tag{4.2}$$

In an actual combustion, 100% of the fuel energy is not available to increase the energy of the air stream. The *first* non-availability results because the atmospheric air is not at absolute zero. That loss of available energy is called a Carnot loss. Typically the Carnot loss is about 21% of the input energy, that is 79% *is* available. The *second* non-availability in the combustor results from the temperature gradient in the combustor from the center of the combustor to the cooler wall. Typically for metal walls in gas turbine engines and other airbreathing engines that loss is about 10%, so now 69% of the available combustor energy is available to produce thrust. The *third* non-availability results from the energy required to mix the fuel and air at high combustor flow speeds [Swithenbank, 1969]. This latter energy loss is a function of the kinetic energy of the fuel entering the combustor compared to the kinetic energy of the air stream. These three non-availabilities are due to basic thermodynamics and gas dynamics. Nothing at this point has been included in terms of friction and shock wave losses in the engine module. The ratio of the kinetic air stream energy to the hydrogen–air combustion heat addition is presented in Figure 4.3 for the three energy non-availabilities.

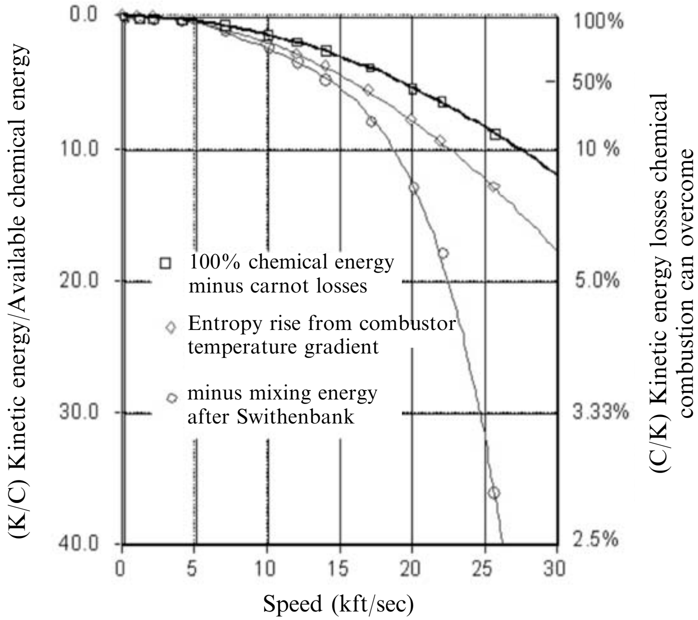

Figure 4.3. Airflow energy compared to available chemical energy.

Remember 25,573 ft/sec is orbital speed at 100 nautical miles. At orbital speed and with Carnot losses the ratio of kinetic energy to energy added by burning hydrogen is about 9. That means the kinetic energy of the air stream is nine times the fuel combustion heat addition, an astonishing number. So if the air stream was to lose 11% of its energy (for instance, through friction), combustion of hydrogen fuel could not make up the deficit and there would be *no net positive thrust*. Adding losses caused by non-uniform combustion, that 9 ratio becomes about 12. So the loss limit for the air kinetic energy is now more stringent, about 8%. Adding energy required to mix the fuel with the high-energy air the ratio is about 38. So the loss limit for the air kinetic energy is now 2.6%. That means that *all* of the internal inlet-combustor-nozzle losses must be less than 2.6% just to maintain thrust equal to drag, with no acceleration. That is very challenging. The qualitative conclusion is that for a hypersonic airbreathing propulsion system the task is *not so much maximizing combustion efficiency* but *minimizing air stream energy losses*. So hypersonic airbreathing propulsion becomes an energy conservation problem, and that encompasses the entire vehicle. For instance, the heat energy that enters the airframe is normally discarded, and that process is called cooling. If instead a portion of that heat energy could be recovered as useful work and converted to thrust that could represent a heat addition corresponding roughly to 30% of the hydrogen fuel heat of combustion [Novichkov, 1990]. Considering the loss limits discussed above, that is a very large energy addition.

Each fuel has a unique heat of combustion (energy per unit mass of fuel) and fuel air ratio that burns all of the oxygen in the air, called the 'stoichiometric fuel/air

Table 4.1. Representative fuel properties.

Fuel	Q_c	Q	Q Carnot loss	Q Carnot + non-uniform	$Q_c \cdot$Sp. gr.
Hydrogen	51,500	1,504	1,188	1,038	3,648
	119.95	3,498	2,763	2,414	8,485
Kerosene	18,400	1,247	985.1	860.4	14,360
(JP-4)	42.798	2,900	2,291	2,001	33,402
Methane	21,500	1,256	992.2	866.6	8,927
	50.009	2,921	2,308	2.015	20,765
	Btu/lb	Btu/lb	Btu/lb	Btu/lb	Btu/lb
	MJ/kg	kJ/kg	kJ/kg	kJ/kg	kJ/kg

ratio', f_s, see Table 4.1. When the heat of combustion and the fuel/air ratio are multiplied together the result is the Brayton cycle heat addition, that is the energy added per unit mass of air. For the Brayton cycle heat addition there are essentially two families of values of heat addition using conventional fuels: hydrogen and acetylene, at 3,498 kJ/kg, and hydrocarbons at $2{,}954 \pm 92$ kJ/kg. There are indeed some exotic fuels at higher values, but these are very unstable or spontaneously ignite on contact with air. Since the total energy of the air (energy per unit mass of air) is a constant plus the square of the speed, there comes a point when the energy of the air equals the energy added to the air by burning fuel. So, the faster the aircraft flies, the smaller the fraction fuel heat addition becomes of the kinetic energy: the ratio of the total enthalpy to the fuel heat addition ratio increases, as shown in equation set (4.3) for the fuel combustion energy (without any losses):

$$\frac{h_t}{Q} = \frac{232.6}{Q} + \frac{500.0\,V_0^2}{Q} \qquad V_0 = \text{km/sec}$$

$$\left(\frac{h_t}{Q}\right)_{\text{hydrogen}} = 0.0665 + \frac{V_0^2}{6.995} \qquad V_0 = \text{km/sec}$$

$$\left(\frac{h_t}{Q}\right)_{\text{hydrocarbon}} = 0.0787 + \frac{V_0^2}{5.907 \pm 0.18} \quad V_0 = \text{km/sec} \tag{4.3}$$

From hydrocarbons to hydrogen, the Brayton cycle heat addition with Carnot losses equals the air kinetic energy between 2,160 m/sec and 2,351 m/sec (7,087 ft/sec to 7,713 ft/sec). From hydrocarbons to hydrogen, the Brayton cycle heat addition with Carnot *and* non-uniform combustion losses equals the air kinetic energy between 2,196 m/sec and 2,019 m/sec (6,623 ft/sec to 7,208 ft/sec). So, for any speed above these speeds, the air kinetic energy is greater than the fuel combustion energy addition to the air stream. Second Law available energy losses make the problem a bigger problem because they limit the actual heat energy added to the air to less than the maximum values in equation sets (4.2) and (4.3). For hydrocarbons there is a range in the heat of combustion, so there is a ± 0.18 range on the value in the denominator. There is a practical limit to the combustion energy's ability to offset internal flow and frictional losses that can be determined from first principles. At that point the airbreathing propulsion system can no longer accelerate the vehicle.

If we look at the other energy losses added to the Carnot loss, we see how much greater the air stream kinetic energy is compared to the fuel addition energy. This is what limits the application of airbreathing propulsion to space launchers. In terms of practical operational engines, the maximum flight speed is probably about 14,000 ft/sec and perhaps as much 18,000 ft/sec for research engines. The latter figure is one-half the specific kinetic energy (energy per unit mass) required to achieve orbit. So, to achieve orbital speed with an airbreather propulsion system a rocket for final speed in the trajectory and space operations is required.

4.4 INTERNAL FLOW ENERGY LOSSES

The performance of an airbreathing engine is governed principally by the state properties of air and from vehicle characteristics that include: the captured inlet air mass flow, the entry air kinetic energy, the energy released to the cycle by combustion of the fuel, and the internal drag and energy losses through the engine flowpath [Yugov et al., 1990]. The energy losses in the air stream, the internal wave drag and friction drag of the engine module can be a dominant factor. Evaluating these factors permits the establishment of performance boundaries based on first principles. The result is an altitude–speed representation of performance potential and constraints for Brayton cycle airbreathing engines defined by two parameters, altitude and velocity. Performance is constrained by an altitude boundary (based on the entropy state of exhaust gas) and a velocity boundary (based on the air kinetic energy to combustion energy ratio). In order to define these boundaries we need to first establish the magnitude of the engine internal flow losses.

Energy input into the combustion chamber must overcome all the losses that are a result of the external drag of the vehicle, energy losses associated with the internal engine flow, and irreversible losses in the thermodynamic cycle plus supply the excess thrust minus drag required for acceleration to orbital speed. As shown in Figure 4.3, as the flight speed in increased, the kinetic energy becomes increasingly greater than the energy added by the fuel. As the flight speed is increased, the internal drag of the engine increases more rapidly than the airframe drag, so there is a point where the total drag is just equal to the thrust potential of the airbreathing propulsion system (which is decreasing with increasing speed because the fuel added energy is becoming a smaller fraction of the kinetic energy). That is the maximum speed of the air-breathing engine. The losses are represented as a fraction of the flight kinetic energy. The drag losses are given as drag areas referenced to an area related to the propulsion system (see Figure 4.2). Drag area is a universal way to represent drag energy losses. Multiplying the drag area by the local dynamic pressure, q, yields the total drag

$$\text{Drag} = C_{\text{D}}Sq = C_{\text{D}}S\,\frac{\rho V^2}{2}$$

$$\frac{D}{q} = C_{\text{D}}S \tag{4.4}$$

The losses as fractions of the flight kinetic energy are listed in equation set (4.5) for engine internal drag losses, fuel–air mixing losses (after Swithenbank), aircraft total drag, and the kinetic energy added to the combustor flow by the hot gaseous fuel injection (not applicable for cold liquid-fuel droplet injection).

$$\text{Combustor drag losses}\quad \left(\frac{\Delta E}{\text{KE}}\right)_{\text{comb}} = -\left(\frac{V_{\text{c}}}{V_0}\right)^2\left(\frac{C_{\text{D}}S}{A_1}\right)_{\text{eng}} \tag{4.5a}$$

$$\text{Fuel mixing losses}\quad \left(\frac{\Delta E}{\text{KE}}\right)_{\text{mix}} = -k_{\text{mix}}\left(\frac{V_{\text{c}}}{V_0}\right)^2 \tag{4.5b}$$

$$\text{Aircraft drag losses}\quad \left(\frac{\Delta E}{\text{KE}}\right)_{\text{vehicle}} = -\left(\frac{C_{\text{D}}S}{A_{\text{c}}}\right)_{\text{vehicle}} \tag{4.5c}$$

$$\text{Fuel injection energy gain}\quad \left(\frac{\Delta E}{\text{KE}}\right)_{\text{fuel}} = +\phi f_{\text{s}}\left(\frac{V_{\text{fuel}}}{V_0}\right)^2 \tag{4.5d}$$

In equation (4.5d) ϕf_{s} is the equivalence ratio.

The only positive term that adds to the available energy is the kinetic energy of the injected fuel. If the temperature of the fuel (in this case hydrogen) is scheduled so that the injected fuel velocity is equal to the flight speed, and the fuel injection angle is in the 6° to 10° range, then the injected fuel energy to air stream kinetic energy ratio is 0.0292ϕ. For an equivalence ratio of six, this provides an energy addition of 17.5% of the air stream kinetic energy. So recovering normally discarded energy as thrust is as critical as burning fuel in the engine. This will be discussed further on in this chapter, when identifying the operational zone for Brayton cycle propulsion systems.

The principal culprit in the drag energy loss inside the combustion chamber (equation (4.5a)) is the wetted area of the engine referenced to the engine module cowl cross-sectional area, and the shock and wake losses from struts and injectors in the combustor flow. To keep the wetted area, and therefore skin friction loss, to a minimum, the combustor cross-sectional shape and length are critical. Cross-sectional shape is generally driven by integration consideration with the aircraft, and have only limited variability. The combustor length used is based on both experimental data [Swithenbank, 1966, 1969] and Computational Fluid Dynamics (CFD) analyses with Second Law (available energy) losses considered [Riggins, 1996]. From both sources, the combustor length for maximum energy efficiency is 0.40 meters (15.7 inches). Swithenbank's measurements in a shock tube combustor test facility verified that for methane, atomized hydrocarbons, and hydrogen the

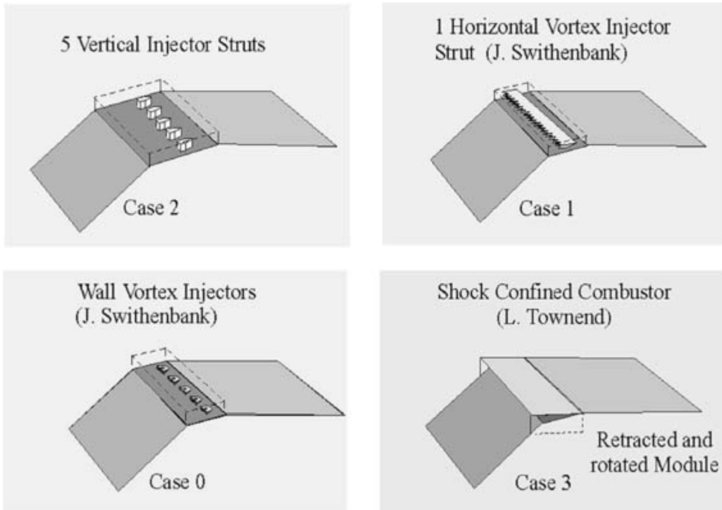

Figure 4.4. Four representative ram/scramjet module configurations. For clarity the aircraft is compression side up with the airflow from right to left.

combustion time was 35 microseconds ±5 microseconds over the combustor gas speed range of 6,000 to 12,000 ft/sec (1,828 to 3,658 m/sec) [Swithenbank, 1984].

With the wetted area minimized, the remaining task is to identify the shock wave and wake losses. This was done for four combustor configurations in Figure 4.4 [Czysz and Murthy, 1991]. The total internal drag area for four internal combustor geometries are shown in Figure 4.5. In addition to the work by Murthy and Czysz, these were analyzed by students in the Parks College Hypersonic Propulsion and Integration class with the same results. Case 2 is a set of five vertical struts with fuel or rocket injectors in the strut base to produce wake turbulence mixing that is characteristic of many ram/scramjet designs. Case 1 is from Professor James Swithenbank of Sheffield University and is a single horizontal strut with a line of trailing-edge triangles inclined a few degrees to the flow to form a lifting surface that creates a trailing vortex for mixing. The fuel injection is in from the strut base and at the base of each triangular ‘finger’. The trailing-edge angle is sufficient to produce a subsonic trailing edge in the Mach 4 to 5 combustor flow. The trailing-edge vortex mixing is that produced by a subsonic trailing edge on a lifting surface and was developed via experiments in the late 1960s. Case 0 is an adaptation of the Swithenbank vortex mixing concept to a wall injector configured as a surface inclined to the wall with a subsonic trailing-edge angle [Swithenbank et al. 1966, 1969; Swithenbank, 1984]. The subsonic trailing edge produces the mixing vortex. The author (PC) was shown these injectors by Professor Swithenbank in 1988. The concept of a trailing-edge vortex on a lifting surface was also proposed by Leonard Townend [Townend, 1986]. Case 3 is a shock-confined combustion zone formed between the body and the low-angle body shock wave when the engine module is retracted. With Mach numbers on the order of 10 or greater the resistance

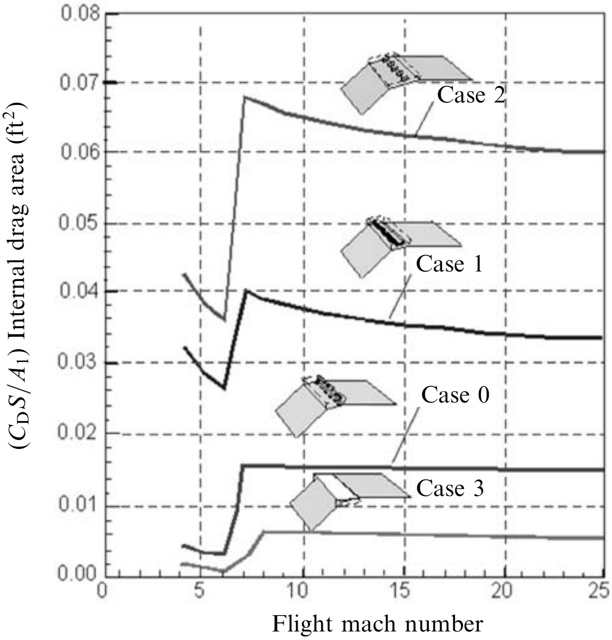

Figure 4.5. Four very different internal drags for the four module configurations.

of the shock system to normal flow is as great as a physical wall. This concept was successfully tested in an RAE facility by Leonard Townend in 1966, and offers the lowest losses of any configuration. It was also a configuration developed at McDonnell Aircraft under the leadership of H.D. Altis [Czysz, 1999, Figure 15]. For each of these cases the internal drag area based on skin friction and shock wave drag ($C_D S$) was determined and referenced to the engine module cowl area $(C_D S/A_1)_{eng}$ for each of the four engine module combustor configurations in Figure 4.4 as a function of flight Mach number. Note that as supersonic combustor through-flow begins (that is, scramjet operation begins) there is a sharp increase in the internal drag. The stronger the shock waves and shock interference associated with the internal geometry, the sharper the drag rise.

With this information the magnitude of the internal engine drag can be compared to the external aircraft drag. The ratio of engine drag to aircraft drag can determined using the relationship in equation set (4.6). The value for the aircraft drag area referenced to the geometric capture area $(C_D S/A_0)_{air}$ is essentially a constant for the supersonic through-flow operation of the engine above Mach 6 and has a value of approximately 0.090. The engine airflow contraction ratio (A_0/A_2) depends on whether the engine is operating in supersonic through-flow mode or subsonic through-flow mode. Table 4.2 compares the combustor entrance conditions for the flight speed of 14,361 ft/sec (4,377 m/sec). Once supersonic through-flow is established, the combustor static pressure and temperature remain essentially constant, as determined by Builder's thermodynamic analysis

Table 4.2. Combustor entrance geometry and conditions for 19,361 ft/sec flight speed.

$V_0 = 14{,}361$ ft/sec $Z_0 = 124{,}000$ ft $q_0 = 1{,}122$ lb/ft^2

$V_0 = 4{,}377$ m/sec $Z_0 = 37{,}795$ m $q_0 = 57.72$ kPa

Combustor conditions	A_0/A_2	V_c	P_c	T_c	ρ_c
Supersonic through-flow	28.4	12,972 3,954	1.10	1,756	0.152
Subsonic through-flow	76.5	4,495 1,370	34.4	5,611	1.325
		ft/sec m/sec	atmosphere[a]	K	amagat[b]

[a] Referenced to sea level pressure and density at 14.696 psia and 59°F analogous to one atmosphere pressure
[b] One amagat is local density divided by density at 14.686 psia and 0°F, 0.002 662 slugs/ft^3

[Builder, 1964]. At 19,350 ft/sec (5,898 m/sec) the contraction ratio for supersonic through-flow is 32 and for subsonic through-flow is 128. So, as the vehicle accelerates, the supersonic through-flow engine geometry and combustor are almost constant. For the subsonic through-flow engine the combustor height becomes rapidly smaller and more intensely heated.

The pressure and temperature are very high for the subsonic through-flow engine, to the point of being impractical to impossible to operate in a flight weight combustor built from known materials. Given the combustor conditions, the ratio of engine module drag to aircraft drag can be determined from equation set (4.6).

$$\frac{\text{Engine drag}}{\text{Aircraft drag}} = \frac{\left[\left(\dfrac{C_D S}{A_1}\right)_{\text{eng}} + k_{\text{mix}}\right]\left(\dfrac{q_c}{q_0}\right)}{\left(\dfrac{C_D S}{A_0}\right)_{\text{air}}\left(\dfrac{A_0}{A_1}\right)}$$

$$\left(\frac{q_c}{q_0}\right) \le \frac{A_0}{A_2}\frac{V_c}{V_0}$$

$$\frac{A_0}{A_1} \approx \text{constant} \approx 7.0 \tag{4.6}$$

The drag ratio for the four different combustor configurations of Figure 4.4 are shown in Figure 4.6. Because the flow entering the engine represents a streamline flow tube of the free stream, the mass flow is constant, and the density, velocity and flow area are consistent with that constant mass flow. The result is that the dynamic pressure of the flow, that is the ability of the flow to generate force, is greatly increased, just as predicted by equation (4.6). That increase can be from 3 to 12 times the free stream value. That also means the internal drag of the engine can exceed the external drag of the aircraft, and explains why internal drag losses are so vital to the operation of the scramjet vehicle as shown in Figure 4.6. This is a key

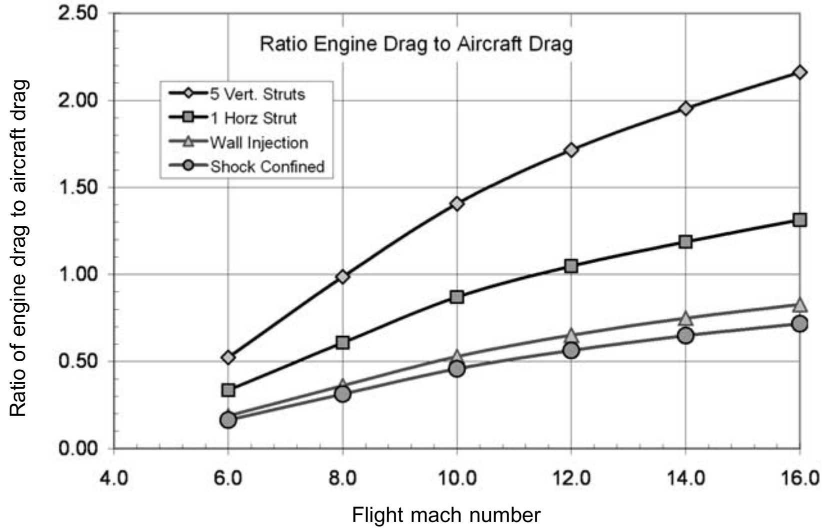

Figure 4.6. Module configuration significantly affects performance.

result, because it quantifies how serious the engine drag can be as flight speed is increased and why some historical engine programs struggled to exceed the Mach 10 to 12 regime. With a retractable vertical strut, it is possible to shift from the strut injector configuration to the wall injector configuration to maintain aircraft acceleration. If this configuration change is impossible, or is not made, accelerating much beyond Mach 10 is unlikely. It is therefore clear why engines with retractable strut concepts [Baranovsky, 1992a,b; and Vandenkerckhove and Czysz, 2001] are essential to high Mach number operation. The adaptation of the Swithenbank center strut to a wall-mounted vortex mixing injector represented a significant improvement. Swithenbank developed the single horizontal strut with the trailing-edge delta fingers so that a fixed strut had the potential to reach Mach 12. Townend's early pioneering in shock-confined combustion offered a significant reduction is propulsion system drag [Townend, 1966, 1985]. Ashford, and Emanuel, have compared ejector ramjet to the Oblique Detonation Wave Engine (ODWE). The ODWE can be one operating regimes of a combined cycle propulsion system [Townend and Vandenkerckhove, 1994], when internal drag of the engine module become so large as to significantly diminish a thrust to drag ratio at high hypersonic speeds. The result is that propulsion acceleration specific impulse, or effective specific impulse, based on thrust minus drag, is the important parameter for accelerating vehicles, not specific impulse alone.

We now have nearly everything necessary to determine what speed a scramjet-powered vehicle can reach based on available energy and thrust minus drag. There is one element missing, and that is altitude. Altitude is not limiting in the sense that combustion cannot be maintained; it can be limiting based on the value of the nozzle expansion entropy. Entropy is a thermodynamic quantity that relates to how much of the energy in the system is irreversible. That is, if energy (pressure) is expended to accelerate an airflow to supersonic speeds, then to slow it down the air must be passed through a series of shock waves. The entropy increase across the shock train determines how much of the initial pressure can be recovered. The greater the entropy rise, the larger the fraction of the initial pressure becoming unrecoverable (irreversible pressure loss). The same is true for any Brayton cycle engine (ram/scramjets and turbojets are Brayton cycles). One characteristic of the atmosphere is that, as altitude is increased, pressure decreases. As pressure decreases, entropy increases; therefore for any propulsion cycle, the higher the altitude the higher the initial entropy in the atmosphere. Most Brayton cycles have a constant increment of entropy across the cycle, therefore the higher the altitude the higher the expansion nozzle entropy. That entropy level determines how much of the chemical energy added to the air molecules through combustion can be recovered as exhaust velocity. The reason the combustion energy cannot be recovered as flow kinetic energy of the gas bulk motion (or flow velocity) is that the entropy limits the internal energy of the gas (temperature) that can be transmitted to the gas molecules by collisions. The burnt expanding gas is said in this case to be 'frozen', and will be colder compared to a gas in the opposite state ('equilibrium'), a state where molecular collisions, can indeed transform internal energy into velocity. Equation (4.7) gives the critical entropy value based on the physical size of the nozzle and its expansion nozzle half-angle [Harney, 1967]. In the equation, (S/R) is the non-dimensional entropy, θ is nozzle half-angle, r^* is the radius of an equivalent sonic throat that would give the nozzle mass flow and static pressure and temperature at the combustor exit, and r^*_{ref} is one inch (25.4 mm).

$$\left(\frac{S}{R}\right)_{\text{nozzle}} = \Sigma - 0.4\ln\left(\frac{\tan\theta}{r^*/r^*_{\text{ref}}}\right)$$

$$\begin{aligned} \text{If:}\quad & \Sigma = 30 \text{ then there is no 'frozen' energy} \\ & \Sigma = 32 \text{ then about 3\% of the energy is 'frozen'} \\ & \Sigma = 34.6 \text{ then about 10\% of the energy is 'frozen'} \end{aligned} \tag{4.7}$$

If 10% of the chemical energy is 'frozen' and cannot be recovered, there is a serious drop in exhaust gas velocity and a loss of thrust. Remember that in an airbreathing engine for thrust to be generated the exhaust nozzle exit speed must be greater than the flight velocity. For the case presented in Table 4.2 the exhaust gas speed is just 9.7% greater than flight speed for the supersonic through-flow case and only 3.5% greater than flight speed for the subsonic through-flow case, so any loss of velocity producing energy is critical at this speed. For a particular engine, given the initial entropy of the atmosphere and the entropy increment of the engine, the onset of 'frozen' flow can be identified.

With this understanding, and putting everything we now have together, the operating spectrum of a ram/scramjet can be determined.

4.5 SPECTRUM OF AIRBREATHING OPERATION

As the speed increases, the engine performance becomes characterized by energy conservation rather than by combustion: energy conservation is far more important than chemistry [Ahern, 1992]. The result is a spectrum of operation over the speed regime developed by Czysz and Murthy [1991] and shown in Figure 4.7. This figure illustrates the extent to which the kinetic energy of free stream air entering the vehicle inlet capture area and the fuel mass and internal energy become gradually more significant and critical as the flight speed increases. Thus the operating limits of the airbreather can be clearly identified.

Figure 4.7 shows flight altitude versus flight speed, in kft/sec. The corridor, labeled 'acceleration', that begins at zero speed and extends across the figure to nearly orbital speed (20 kft/sec) is the flight corridor for airbreathing vehicles to reach orbital speed. This corridor is based on the dynamic pressure limits of accelerating airbreathing vehicles. The lower limit is based on structural weight and skin temperatures. The upper limit is based on having sufficient thrust to accelerate efficiently to orbital speed. The narrow corridor cutting across the acceleration corridor, labeled 'cruise', is the corridor for hypersonic cruise vehicles to achieve maximum range. The vertical shaded area identifies the flight speeds at which a subsonic through-flow engine (ramjet) should transition to a supersonic through-flow engine (scramjet). The shaded area between 5 and 7 kft/sec is the transition

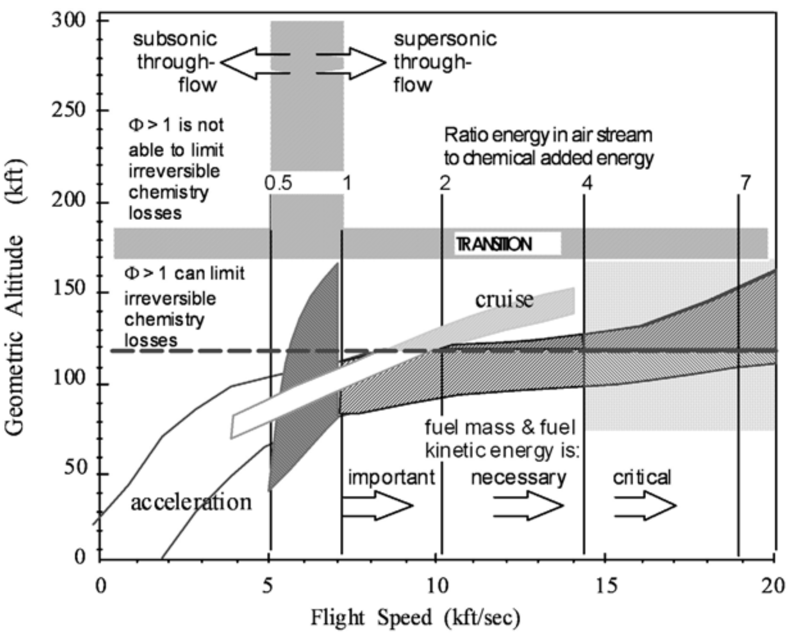

Figure 4.7. Operating boundaries of Brayton cycle engines based on enthalpy and entropy analyses.

region defined by Builder for hydrogen and hydrocarbon fuels as the region where kinetic compression to subsonic speeds ahead of the combustor alone yields optimum enthalpy compression ratio [Builder, 1964]. To the left of this area the mechanical compression ratio is too large, reducing engine efficiency. In this area the engine must limit the enthalpy compression by limiting the diffusion, so the speed ahead of the combustor is supersonic. Analysis of the Second Law of Thermodynamics by Builder documented that the engine design enthalpy compression ratio (rather than the design pressure ratio) and the fuel define the cycle efficiency. Hydrocarbon fuels are to the left side of the shaded area and hydrogen is to the right side of the area. The vertical lines identified with the numbers 0.5, 1, 2, 4, and 7 represent the ratio of flight kinetic energy to the available fuel energy accounting for Carnot losses. As indicated by the arrows, to the left of the vertical shaded area engines are subsonic through-flow, and to the right of the vertical shaded area engines are supersonic through-flow. As pointed out in equation (4.5d), the kinetic energy of the injected, hot, gaseous fuel is a source of energy very useful to overcome the internal drag and mixing losses. As indicated by the arrows and text adjacent to the vertical lines, this energy addition becomes more critical to engine operation as the speed increases.

The speed regime to the right of the 4 energy ratio line is questionable for an operational vehicle. It is totally possible for a research vehicle to investigate this area but, as we shall see, at the 4 energy ratio boundary the airbreathing vehicle has achieved a significant fraction of the benefits from incorporating airbreathing in terms of the propellant required to achieve a given speed increment. As the energy ratio increases, the scramjet-powered vehicle thrust-to-drag ratio decreases. As the thrust-to-drag ratio decreases the acceleration (effective) $I_{sp} = I_{spe}$ decreases to the point where the high thrust-to-drag rocket uses less propellant for a given speed increment than the scramjet. At that point the rocket engine is clearly a better accelerator than the airbreathing engine. So, from an energy viewpoint, a practical maximum airbreathing speed is about 14,200 ft/sec (4.33 km/sec). To the right of this line the payoff achieved compared to the resources required reaches diminishing returns. That is, the velocity increment produced per unit propellant mass and volume flow is less for the airbreather: beyond this point a hydrogen/oxygen rocket requires less propellant mass flow per velocity increment and less vehicle storage volume than the airbreathing engine. So, in terms of available energy and of the propellant required to produce a given velocity increment, the airbreather is outperformed by a hydrogen/oxygen rocket. This is a result of the fact that the thrust-to-drag ratio of the airbreather is diminishing as speed and altitude are increased, while the thrust-to-drag ratio for rocket is increasing. So the acceleration (effective) I_{spe} of the airbreather falls below that of the rocket.

Returning to the consideration of entropy and applying the criteria from equation (4.7), the loss of exhaust velocity begins at about 120,000 ft (36,576 m), shown as a horizontal dashed line. The altitude regime above 120,000 ft altitude produces a degradation of thrust because the increasing entropy levels limit the internal molecular energy that can be converted into kinetic energy and exhaust gas velocity. Dr Frederick Billig of APL/JHU advocated the introduction of excess hydrogen in the flow to act as a molecular collision third body. In equation (4.5d) excess hydrogen means the equivalence ratio (ϕ) is greater than 1. For a phi of 1 the fuel burns all of the oxygen available in the air. Excess hydrogen provides abundant third bodies for the dissociated air molecules to recombine [Billig, 1989; Czysz and Murthy, 1991]. The hydrogen molecule dissociates into two hydrogen atoms, but unlike the other diatomic gases, atomic hydrogen has about 90% of the velocity potential as molecular hydrogen. And being a low-molecular-weight gas, it is a better working fluid than air, and pound per pound produces more thrust. However, again due to entropy, this only works up to a point. In terms of altitude, that point is about 170,000 ft (51,816 m). Between 120,000 and 170,000 ft the excess hydrogen ameliorates the energy 'frozen' in the non-equilibrium gas chemistry. Above that altitude, the entropy levels are such that, even with the third body collisions provided by the hydrogen, the irreversible energy cannot be recovered and it is improbable that a Brayton cycle engine can produce sufficient thrust. If excess hydrogen fuel is used in Brayton cycle engines below 150,000 feet and at less than 14,500 ft/sec, it can convert a fraction of the aerodynamic heating into net thrust via injection of the heated hydrogen into the engine at velocity corresponding to flight speed. Note that cruise engines operate at greater cycle entropy levels than acceleration engines and thus may require a larger excess hydrogen flow than the acceleration engines.

Up to this point, we have used first principles to determine that the vehicle will be stout, and not too small if it is to be built from available industrial capability, see Figures 3.22 to 3.24. We have also established it is not practicable for an operational vehicle to exceed 14,200 ft/sec in airbreathing mode, and apparently 12,700 ft/sec would be less challenging while retaining the benefits of airbreather operation.

4.6 DESIGN SPACE AVAILABLE—INTERACTION OF PROPULSION AND MATERIALS/STRUCTURES

We have now established the most likely operational region for an airbreathing operational launcher from a first principles approach. The next question is: 'Are there materials available to operate in the Brayton cycle operating region?' The approach taken was first used in the 1968–70 Hypersonic Research Facilities Study (HyFAC) for NASA [Anon., HyFAC, 1970]. The interest was in identifying operational regions for different materials used on the compression side of hypersonic vehicles, near the nose, where radiation-cooled structures begin. Specifically, the heat transfer rate and surface temperature determined at a point 5 ft aft of the nose were computed for the vehicles in Figure 3.11 as a function of Mach number, altitude, angle of attack and load factor, and are shown in Figure 4.8. The load factor is the lift divided by the weight: in level flight it is exactly 1. In a maneuver such as a vertical turn, or horizontal turn, or change in flight path angle, the normal load factor can be in the 2 to 3 range. The normal load factor is defined as the ratio of lift to weight and is usually expressed in units of '*g*', the gravitational acceleration constant on ground (9.81 m/s^2). The angle of attack range was selected from 1 to 20

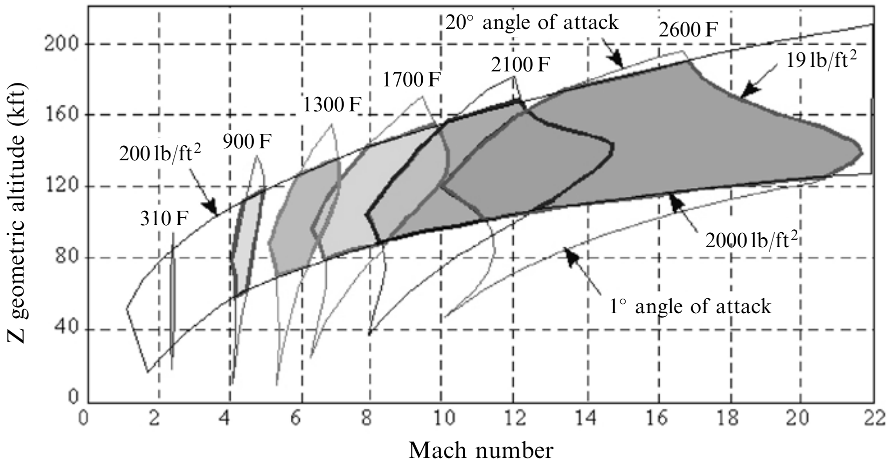

Figure 4.8. Operational areas for six different materials for a point 5 ft from the nose.

degrees, since this class of hypersonic aircraft develops their maximum lift-to-drag ratio at less than 20 degrees. This range is not like the one planned for Space Shuttle or Dynasoar configurations, that typically have glide angles in the 40- to 45-degree range. The database generated was cross-correlated to arrive at a area plot of altitude versus Mach number for a particular material temperature, with load factor and angle of attack as parameters.

Figure 4.8 shows the area plots for six representative radiation equilibrium temperatures [Anon., HyFAC, 1970]. Since 1970 the availability of materials has changed, so not all of the materials identified in the reference are available today. One notable example is thoria dispersed nickel (TD nickel). Thoria is mildly radioactive and what was thought acceptable in 1967 is no longer acceptable 25 years later. TD-nickel was not considered for either Copper Canyon or the National Aerospace Plane (NASP). So for a given material the operational envelope and maximum speed for an aircraft was determined as a function of angle of attack and load factor. Each operational region for a particular material is bounded by four limits. The right side limit each area is a lift loading of 19 lb/ft^2 (92.75 kg/m^2). Lift loading is defined as:

$$\frac{L}{S_{\text{plan}}} = N_Z \frac{W}{S_{\text{plan}}} \quad (N_Z \text{ is the normal load factor}) \tag{4.8}$$

Where S_{plan} is the wing planform area.

The upper boundary of each area is 20 degrees angle of attack, and the lower boundary is 1 degree angle of attack. The left boundary is not the same for each temperature area, as the aircraft becomes lighter while propellant is consumed and the aircraft accelerates toward orbital speed or cruise speed. The materials associated with each surface temperature and the magnitude of the maximum lift loading for each is given in the Table 4.3.

Table 4.3. Material selections and maximum lift loading boundary for Figure 4.8.

Temperature						
(°F)	310	900	1,300	1,700	2,100	2,600
(°C)	154	482	704	927	1,149	1,427
Material	Aluminum	Titanium	RSR titanium[a] Inconel	RSR titanium[a] Hastelloy 1700	RSR MMC[a]	Coated niobium C–C C–Sic
Left boundary limit	350 lb/ft^2 1.71 ton/m^2	250 lb/ft^2 1.22 ton/m^2	210 lb/ft^2 1.03 ton/m^2	210 lb/ft^2 1.03 ton/m^2	180 lb/ft^2 878 kg/m^2	155 lb/ft^2 757 kg/m^2

[a] These materials are hot isostatically pressed, rapid solidification rate (RSR) titanium powders and metal matrix composites (MMC) made from RSR titanium powder with either silicon carbide fiber or Tyranno fiber reinforcement. Tyranno fiber and coating are patented materials of the UBE Corporation, Tokyo, Japan.

Remember that the left and right boundaries are lift loads. If a maneuver of 3 '*g*' is required (and that is not impossible or unlikely for a hypersonic aircraft flying at high dynamic pressure) then the wing loadings corresponding to the left lift loading in Table 4.3 are (from the left) 117, 83.3, 70.0, 70.0, 60.0 and 51.7 lb/ft^2 respectively (569, 407, 343, 343, 293 and 252 kg/m^2). So if a margin for an emergency maneuver is the operational requirement, then the maximum speed must correspond to the emergency lift load, not the 1 '*g*' acceleration load. The importance of lift loading in determining the maximum speed for a given surface temperature is not to be minimized. If a vehicle is flying near its lift loading Mach limit, and for some reason the angle of attack, that is, the lift loading, must be changed, it may be mandatory to slow down before executing that maneuver. For an accelerating air-breather at 1500 lb/ft^2 (7.32 ton/m^2) dynamic pressure, the 1 '*g*' level-flight lift loading can be doubled by a 2-degree change in angle of attack, a very significant effect. Near a speed boundary that could 'over temperature', in pilot parlance, i.e., overheat, the compression surface (lower surface). Similarly a reduction of the angle of attack to near 1-degree angle of attack could 'over temperature' the expansion surface (upper surface). For high-speed hypersonic flight it seems the straight and narrow is the best path. With either the hypersonic glider or the airbreathing hypersonic aircraft possessing a glide range approximately equal to the circumference of the Earth, it may be better to continue around and land at the launch site rather than attempting to turn back and overheat the structure.

Scramjets accelerate by increasing their angle of attack to increase the inlet mass capture and therefore thrust. An afterburning turbofan engine can increase its thrust by 42% by advancing the power lever to the afterburner position: additional fuel is then injected into the afterburner downstream of the turbine. This maneuver increases thrust by burning the oxygen left in the exhaust gas flow, at the expense of increasing specific fuel consumption by 2.5 times (the I_{sp} is 40% of non-afterburning I_{sp}). Scramjets instead can easily double their thrust by an angle of attack increase of only a few degrees, at almost constant I_{sp}, by simply capturing more air flow. So while the afterburning turbofan in afterburner produces 1.42 times the thrust at 3.55 times the fuel flow, the scramjet produces 2.0 times the thrust at 2.1 times the fuel flow. So, when a pilot flying a scramjet-powered vehicle chooses to accelerate, when he/she advances the throttle the aircraft *increases its angle of attack* and accelerates! This can produce very different reactions in human pilots, not accustomed to see the angle of attack increase as the power lever is advanced. However, doing so can never give the automatic pilot any concern.

From Figure 3.16 for the hypersonic glider, the maximum compression-side wall temperature is 4600°F (1,427°C). This means that any vehicle achieving orbital speed with a vehicle in the FDL-7 class of performance must have materials capable of the same *thermal* performance on its compression side, whether rocket- or airbreather-powered to orbital speed. In Figure 4.8 the maximum temperature material is 4600°F (1,427°C) for an airbreathing vehicle either cruising or accelerating to orbital speed. So a vehicle capable of orbital speed must be built of the right materials to potentially achieve airbreathing operation in the Mach 12 to 18 speed regime. Whether it is possible for the airbreather to operate in this range, considering what already said on the Second Law energy losses, remains to be seen. The P. Czysz and J. Vandenkerckhove collaboration early in 1984 established a practical maximum for operational airbreathing launchers [Czysz, 1992] at 3.9 km/sec (12,700 ft/sec) with the possibility to reach 14,000 ft/sec (4.27 km/sec) from a vehicle sizing, compression side materials, and minimum dry weight approach [Czysz, 1995]. Many vehicles may not require operations above Mach 12. TSTO launchers concepts usually 'stage' (i.e., release the second stage) in the Mach 6 to Mach 10 range, although some concepts stage at Mach 12. Hypersonic cruise vehicles are historically in the Mach 8 to Mach 12 range because of the engine limitations, and also due to the very practical fact that flying faster does not improve the block time, because of the longer climb and descent time and distances. For these cases current titanium material systems match up well with the acceleration and cruise requirements.

Figure 4.9 shows two of these operational areas for two representative radiative equilibrium surface temperatures at 5 ft (1.52 m) aft of the nose, i.e., 1700°F (927°C) and 2100°F (1149°C). These two temperatures are characteristic of hot isostatically pressed, rapid solidification rate (RSR) titanium powders, and of metal matrix composites (MMC) made from RSR titanium powder with silicon carbide fibers or Tyranno fibers/cloth reinforcement. These operational zones are from Figure 4.8, with three values of lift loading shown. The lift loading lines have the same value in both operational areas. If the leading edges are thermally controlled by transpiration cooling, or heat-pipe thermal pumping, then the materials shown are applicable for the primary metal thermal protection shingles. The control surfaces will have to be fabricated with carbon–carbon or silicone carbide–carbon ceramic matrix materials because of their flow environment and also because of their thinness, as indicated in Figure 3.16. Note in Figure 4.8 that the cruise corridor corresponds to the highest flight Mach numbers for a given material. For instance, if an aircraft is flying at Mach 14 with a 1 '*g*' wing loading of 19 lb/ft^2 (92.5 kg/m^2) and there is an operational problem that requires returning to base, note that unless the aircraft is slowed to about Mach 11 before attempting to climb,

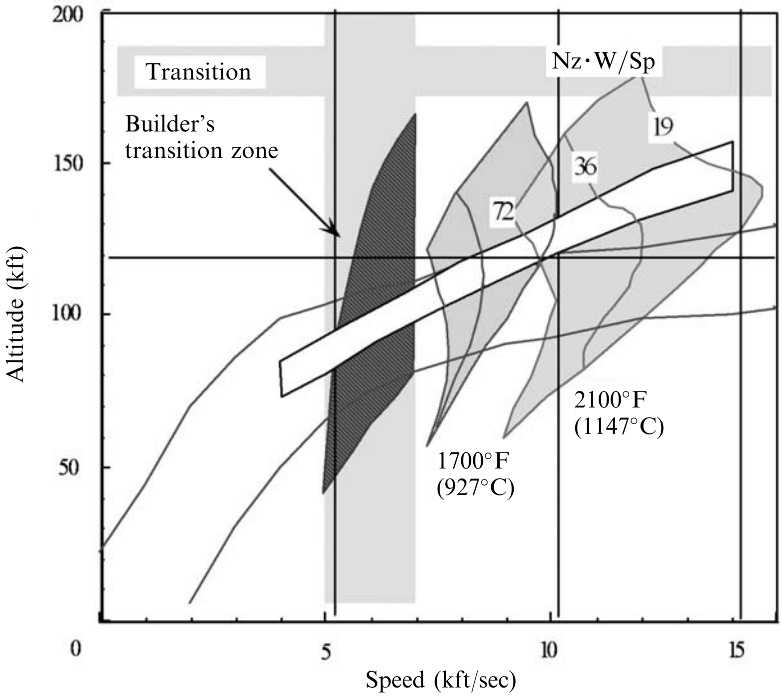

Figure 4.9. Materials and engine operating regimes compared. The ratio (Nz·W/Sp) is normal acceleration times wing loading in lb/ft^2.

dive or execute a 2 '*g*' turn (lift loading now 38 lb/ft^2 (185 kg/m^2)) this maneuver will end in 'over-temperaturing' the vehicle. This is one reason for automatic controls, because actions instinctive in subsonic or low supersonic aircraft are fatal in hypersonic aircraft. So whether accelerating or cruising, any deviation from straight-ahead can be a source of 'over-temperaturing' the thermal protection system.

4.7 MAJOR SEQUENCE OF PROPULSION CYCLES

There are a significant number of propulsion system options that have been studied and reported. In this chapter 14 different classes of propulsion systems are discussed that are suitable for either hypersonic flight or space launchers. The authors have focused on those that are applicable to SSTO transatmospheric vehicles and hypersonic cruise vehicles. If the rocket ascent to orbit is deleted from the analysis then a SSTO that uses airbreathing propulsion to Mach 10 is essentially the first stage of a TSTO vehicle. At the end of this chapter there is a comparison between SSTO and TSTO vehicle sizing that is the work of the late Jean Vandenkerckhove in collaboration with the authors. The intent is to define the SSTO weight ratio and the on-board oxygen ratio carried by the vehicle. As we have seen in Chapter 3 the less the weight ratio and the oxygen-to-fuel ratio, the smaller the size and gross weight of the vehicle. In terms of mass ratio to orbital speed and of oxidizer-to-fuel ratio, the authors examined six principal propulsion categories with hydrogen as fuel, as shown in Figures 3.3 and 3.4. The term 'thermally integrated' is used in the description of these categories: that means the hydrogen fuel passes through both engines in the combined cycle and collects available thermal energy normally discarded as 'cooling heat', turning that energy into useful work. How to do that could be by driving closed-loop power extraction units [Ahern, 1983], or expansion turbines, or by converting heat into thrust. The combined cycle concept dates back 40 years [Escher, 1998] and goes to The Marquardt Company. Marquardt had a propulsion concept that could go hypersonic using a single engine) [Escher, 1994, 1996]. One of The Marquardt Company's concept incorporated folding rotating machinery [Escher et al., 1993] into their cycle; however, it was still a single engine that could go from takeoff to hypersonic speed.

(1) The first category is the liquid propellant, chemical rocket and rocket-derived air-augmented propulsion where the primary propulsion element is a rocket motor. Solid rockets and hybrid rockets are not included as they are inherently expendable, limited-use propulsion not applicable to sustained-use vehicles.
(2) The second category is airbreathing rocket where the propulsion elements are a rocket motor and an air/fuel heat exchanger that supplies the rocket motor with atmospheric air as oxidizer over part of its trajectory. The British HOTOL concept developed by Alan Bond was such a propulsion system.
(3) The third category is the thermally integrated rocket–ram/scramjet engine as a combined cycle propulsion system where the principal element is a rocket ejector ramjet/scramjet. The rocket ejector provides both thrust and low-speed compression. The rocket ejectors in the ram/scramjet are fuel ejectors when the thrust/compression augmentation is not required. Jean Vandenkerckhove 'Hyperjet' was this class of engine.
(4) The fourth category is a combined cycle based on a thermally integrated rocket and turbojet (often cited in the literature as 'KLIN' cycle). In this case thermal integration provides the turbojet precompressor cooling for higher Mach number operation and greater thrust, and the thermal energy recovered from the turbojet improves the rocket expander cycle operation. Invented by V.V. Baliepin, formerly at the Russian center TsIAM, it is the only know such thermally integrated, turbine based, combined cycle propulsion system.
(5) The fifth category is a combined cycle consisting of an airbreathing rocket thermally integrated with a rocket ejector ram/scramjet. This system was first reported by A. Rudakov and V. Baliepin in 1991 at an SAE Aerospace America Conference in Dayton, Ohio.
(6) The sixth category is the thermally integrated engine combined cycle propulsion analogous to the fifth category, except the thermally processed air is separated into nearly pure liquefied oxygen (so-called 'enriched air') and oxygen-poor nitrogen, with the liquid-oxygen-enriched air stored for later use in the rocket engine. The oxygen-poor nitrogen is introduced into the ramjet engine creating a

by-pass ramjet. With the greater mass flow and reduced exhaust velocity the propulsion efficiency is increased.

(7) There is a seventh category spanning the above categories. In fact, the engines discussed in the above are all *continuously* running engines. In World War II the V-1 flying bomb was powered by a pulsejet, or pulse detonation engine (PDE). This engine is an *intermittently* firing engine, consisting of an acoustically tuned pipe fed an explosive mixture inside that, when ignited, sends the combustion products wave traveling down the pipe. After the products exit the tube, the tube is effectively scavenged, new fuel is then injected and a new mixture forms, sort of reloading the tube. The ignition process is then repeated, starting a new cycle. This periodic operation gives the PDE a characteristic cyclic rate and the characteristic sound that, in the V-1's case gained it the nickname of 'buzz bomb'. Three PDE versions of the continuous operation engines are included in the discussion at the end of this chapter. The first is a pulse detonation rocket (PDR) and the remaining two are PDE-ramjet and PDE-scramjet combined cycles. As a reminder, thermal integration means that the fuel passes through both rocket and the scramjet to scavenge rejected heat and convert it into useful work before entering the combustion chambers, increasing the specific impulse.

There is a discussion of each engine cycle in this chapter. But before proceeding with it, there are operational considerations giving additional insight into the application of the propulsion system to a launcher, that are presented in Table 4.4. There are three general performance groups. One that has no airbreathing capability, another that can reach Mach 5 to 6 airbreathing, and the last group that can reach Mach 6 to 14, again in airbreathing operation. The nominal *SSTO mass ratios* to orbital speed and the *normal airbreathing speeds* at their transition to rocket propulsion are given in the top rows. As with all launchers, until the mass ratio is less than four, horizontal takeoff is not possible and vertical takeoff, horizontal landing (VTOHL) will be the *takeoff and landing* mode assumed.

In Table 4.4 the term '*Abortable on launch*' is the capability of the launcher to safely abort the mission while being *on launch* and to *return* to the launch site. This does not just consist in an escape rocket firing and a payload capsule being recovered. It means, in aircraft terms, that the system aborts the launch and returns intact and functional to the launch or adjacent alternate site. The only vertical launch rocket that aborted its launch after an engine failure and landed vertically and safely on its launch pad was the McDonnell Douglas Astronautics experimental rocket, the Delta Clipper. The late astronaut Pete Conrad was flight director, and Dr William Gaubatz was program manager. Other than current aircraft, no other space launcher has ever demonstrated that capability. One of the limitations to achieving abort on launch is indeed the mass of the oxidizer carried. The Delta Clipper had only a mass ratio of about 2.5. Had it been an operational orbital vehicle with a mass ratio of about nine, it may not have been abortable. If commercial space is to happen, it will be a necessity to recover the launcher, functional and intact, in the authors' opinions, and this capability is dramatically influenced by the oxidizer mass carried. It should be remembered that the

Table 4.4. Comparison of continuous operation propulsion cycles.

Characteristics	Continuous operation propulsion system concepts						
Propulsion concept	Rocket	Rocket-derived	Airbreather rocket	Turbojet rocket combined cycle	Ejector rocket combined cycle	Airbreather rocket combined cycle	ACES
Candidate cycles	Topping, expander cycle	air augmented or ram rocket	LACE or deeply cooled	KLIN	strutjet or ram/scram and rocket	LACE, or deeply cooled and ram/scram	LACE, deeply cooled and ram/scram
Category	first	first	second	fourth	third	fifth	sixth
SSTO mass ratio (LEO)	8.0 to 9.0	6.5 to 7.5	5.0 to 6.2	5.0 to 5.5	4.0 to 5.4	3.2 to 4.2	2.5 to 3.5
Airbreathing speed	0	~5.0	5.0 to 6.0	~5.5	6.0 to 14	6.0 to 14	6.0 to 14
Abortable on launch	improbable	possible	possible	possible	likely	yes	yes
Reuse/sustained operation	no	possible	yes	yes	yes	yes	yes
Flights before overhaul	100[a]	100	200	200	300	500	600
On-board oxidizer	maximum	90%	55%	55%	40%	30%	< 10%
Applicable to TSTO	possible	possible	yes	yes	yes	yes	yes
Basing	fixed	fixed	fixed	multiple	multiple[b]	multiple	multiple
Takeoff/landing	VTOHL	VTOHL	VTOHL	VTOHL	VTOHL	HTOHL option	HTOHL
Configuration concepts	external tank + glider	external tank + glider	hypersonic glider	hypersonic glider	integrated airbreather	integrated airbreather	integrated airbreather

[a] 80+ flight ground test without overhaul demonstrated by RD-0120.
[b] Operates from numerous non-space launcher bases.
All can carry personnel or payload, but are automatic, autonomous vehicles.

oxidizer mass is always many times greater than the fuel mass: it is the oxidizer that affects the mass of propellants the most.

Reuse and sustained operations implies that the returned vehicle is ready for another flight after an inspection. With today's rocket engines this is improbable, because they are designed for minimum weight and not for sustained use, as aircraft engines are. Designing rocket engines for sustained use would require readopting the philosophy in place for the XLR-129. *Flights before overhaul* is indicative of an operational system that has sustained operational capability and need not be refurbished after every launch. In 1964 the goals for the vehicle to support the Manned Orbiting Laboratory (MOL) and the XLR-129 was 100 flights before overhaul.

One of the serious impediments to commercial operations is that there is only one *launch site* available per launcher. This may be acceptable for the commercial communications satellite organizations, just as operations from one coal mine was acceptable for the first commercial railroad train in York, England. A commercial space transportation system will have to have the characteristics of a UPS or Federal Express system to be truly commercial. Until the launchers are designed for a lower mass ratio, say, four or less, that will not be practicable. When a mass ratio of four or less is achieved the entire concept of operations will change, because with the correct hypersonic configuration and propulsion system the time-consuming vertical assembly, fueling and month-long count-down will be eliminated. Runway operations will become the norm, opening more launch and return sites for distributed operations. Orbital plane change and offset maneuvers will be far more economical whether executed in ascent and not from orbit.

Another item in the table is *applicable to TSTO*. This is an important consideration. Most of the analyses discussed in this chapter were done for SSTO because this requires only one vehicle, offers the best approach for sustained operations, and is the most challenging. SSTO, however, can look, and be, too much like a one-size-fits-all solution. The advantage of a TSTO solution is the payload to orbit flexibility. An SSTO with a 7 metric ton (15,435 lb) payload to orbit is a hypersonic vehicle with an empty weight (OEW) about 70 metric tons (154,300 lb) and a gross weight (TOGW) of about 380 metric tons (837,900 lb). That is a mass ratio to orbit of 4.9. The payload to Earth orbit is 10% of the vehicle empty weight that carries it. This means whether people or support supplies, the payload is always 7 tons. However a hypersonic glider, that is the second stage of a TSTO, with a 7 metric ton payload can be carried by a first stage that stages at Mach 11 and that has an OEW of about 35 metric tons. So the payload to Earth orbit is 20% of the vehicle empty weight that carries it. The first stage OEW is about 38 tons, for a total empty weight of 73 tons (161,000 lb). The total gross weight of the two stages is about 210 tons (463,000 lb), with the second stage gross weight at about 94.5 tons (208,500 lb). That means a total mass ratio of 5.0. If the second stage were a cargo-only, expendable cylinder, then for the same gross second stage weight the payload would be about 17.5 tons (38,600 lb). The payload to Earth orbit is 50% of the vehicle empty weight that carries it. The gross weight is the same, so the mass ratio is the same. Thus there is much more flexibility in the payload variety and weight that can be delivered to Earth orbit. In addition the offset or orbital plane maneuver would be carried by the first stage flying as an aircraft in the atmosphere, not the stage reaching orbital speed and altitude [Czysz and Vandenkerckhove, 2000]. The propulsion conclusions apply to TSTO as well as SSTO.

4.8 ROCKET-DERIVED PROPULSION

Rocket-derived propulsion systems begin with the liquid propellant rocket. Propellants are injected into a combustion chamber to burn at high pressure and temperature then exit via a sonic throat into an expansion nozzle that is designed to match the nozzle exit static pressure to the ambient atmospheric pressure, as shown in Figure 4.2. For maximum performance the nozzle exit pressure should be equal to the surrounding ambient pressure. However atmospheric pressure ranges from 14.696 psi (101.3 kPa) at the surface to zero in space. Normally the nozzle size is specified by the area ratio, i.e., the exit area divided by the sonic throat area. The area ratio determines the ratio of the nozzle exit pressure to the chamber pressure. Once the chamber pressure is determined, then the exit pressure is determined. If the nozzle exit pressure is higher than the ambient pressure the nozzle is termed 'under-expanded' and the result is the nozzle flow suddenly expands upon exiting the nozzle. When you see a picture of a rocket at high altitude or in space and see the exhaust blossoming into a large plume, this is an under-expanded nozzle. If the nozzle exit pressure is lower than the ambient pressure, the nozzle is termed 'over-expanded' and the nozzle flow separates from the nozzle wall at a location that yields the approximate correct area ratio for the ambient pressure. If you see a picture of a rocket lifting of from a launching pad, you can see the flow exiting the nozzle is smaller in diameter than the actual nozzle diameter, a sign that this is an over-expanded nozzle. Engines such as the Pratt & Whitney RL-10-3 have a two-position nozzle. At lower altitudes the nozzle area ratio is small (10 to 20). As the altitude is increased and the area ratio becomes too small, a nozzle extension slides over the nozzle increasing the area ratio (50 to 60). Thus there are two altitude regions where the engine is matched to the ambient pressure. For most high-thrust rockets the propellants are a fuel and an oxidizer. For some space maneuver and station-keeping rockets the fuel is a *monopropellant*, that is decomposed by a catalyst into gaseous products.

Rocket-derived propulsion involves installing the rocket as a primary nozzle in an air ejector system. The rocket induces airflow in the secondary air system increasing the total mass flow through the system. These systems are generally operated up to Mach 6 or less because of pressure and temperature limits of the air induction system. At Mach 6 the inlet diffuser static pressures can typically equal 10 to 20 atmospheres and 3,000°R (1,666 K). These propulsion systems can offer major advantages when applied to existing rocket launchers [Czysz and Richards, 1998].

1. Chemical rocket. Figure 4.10 represents a typical turbopump-fed liquid propellant rocket. A turbopump is generally a centrifugal compressor to pressurize the fuel, coupled to an expansion turbine driving the pump. The turbopump pressurizes the propellant feed system to the pressure required for engine operation. For the

Figure 4.10. Rocket-derived propulsion.

turbopump to function some fuel and oxidizer are burned in a separate combustion chamber to generate the hot gases necessary to power the turbine, powering in turn the pump. Because this burned propellant does not contribute to the primary thrust of the rocket engine, the turbopump cycle rocket (such as Rocketdyne J-2 for Saturn V) has the lowest specific impulse (I_{sp}) for a given propellant combination. A hydrogen/oxygen high-pressure engine has an I_{sp} of about 430 sec. In the so called 'Topping cycle' (such as in the Rocketdyne SSME) the turbopump exhaust, which is still rich in fuel, is introduced into the rocket motor, contributing to the engine total thrust. A hydrogen/oxygen high-pressure engine using this cycle has an I_{sp} of about 455 sec. In an 'expander cycle' (such as Pratt & Whitney RL-10) a liquid fuel, such hydrogen, is vaporized and raised in temperature by passing through the engine cooling passages. The hot gases then drive an expansion turbine to drive the turbopump before being introduced into the combustion chamber. This engine has the highest I_{sp} for a specific propellant. A hydrogen/oxygen high-pressure engine has an I_{sp} of about 470 sec. Some representative propellants are given in Table 4.5 with hypergolic propellants in bold. *Hypergolic propellants* are those that spontaneously ignite on contact with each other, monopropellants are in italics.

The chamber pressure assumed in Table 4.5 is 1000 psia (about 68 atmospheres),

Table 4.5. Representative propellants and their characteristics.

Fuel	Oxidizer	I_{sp} (sec)	Sp. gr. $\cdot I_{sp}$ [a]	O/F
UDMH	$\mathbf{N_2O_4}$	**319**	**390**	**1.23**
Hydrazine	$\mathbf{H_2O_2}$	**304**	**375**	**2.04**
Hydrazine	$\mathbf{N_2O_4}$	**312**	**365**	**2.25**
JP-4	LOX	329	330	2.40
Nitromethane	—	*273*	*308*	*monoprop.*
Methyl alcohol	LOX	297	282	1.15
Methane	LOX	329	247	2.33
Hydrazine	—	*218*	*219*	*monoprop.*
Hydrogen	N_2O_4	349	207	11.5
Hydrogen	LOX	455	170	6.00

[a] The product of specific impulse and the specific gravity of the propellant is termed density specific impulse and was used by the late V. Gleshko of the GDL OKB to show the performance advantages of hypergolic propellants.

yielding the specific impulse values given in a nozzle with optimum area ratio. The I_{sp} is the thrust developed per unit mass flow and per second (lb/(lb/sec)) or kg/(kg/sec)). The I_{sp} is a function of the combustion temperature, chamber pressure, and the thermodynamics of the products of combustion. Since the thrust per unit mass flow is constant, the rocket engine thrust is a function of the total mass flow. Given the combustion temperature, the mass flow depends on chamber pressure and engine throat area. To obtain more thrust either the pressure can be increased for the same size engine, or the size of the engine can be increased. The rocket motor is necessary for space propulsion because it is independent of any atmosphere. Although a turbopump rocket engine is shown, for some, if not most, space applications the propellant tanks are pressurized to feed propellant into the engine and there are no turbopumps. This is to clarify that the question of airbreather engines versus rocket applies only to flight in the Earth's atmosphere and concerns the large weight of oxidizer required by rockets, which increases the gross weight of the vehicle and increases the thrust of the rocket engines accordingly. Thinking along these lines, it appears intuitive that one way to increase the thrust of the rocket, for the same propellant flow, is to make it an 'air augmented' rocket.

2. **Air augmented rocket**. Figure 4.10 employs the rocket motor as a primary ejector [Harper and Zimmerman, 1942; Nicholas et al., 1966] so some of the external airstream can be mixed with the rocket exhaust to increase mass flow and thrust and increasing the specific impulse. These systems are generally operated up to Mach 6 or less because of pressure and temperature limits of the air induction system. At Mach 6 the inlet diffuser static pressures can typically equal 10 to 20 atmospheres and 3,000°R (1,666 K). The rocket motor operates on its normal oxidizer-to-fuel ratio. The reduction of the mass averaged exhaust velocity increases propulsion efficiency. This simple concept is not designed to burn the oxygen in the entrained air. The weight ratio is reduced for an SSTO from 8.1 to 7.5. The sketch in Figure 4.10 is notional, but the use of an inward-turning inlet with a variable capture area offers high mass capture tailored to the Mach number and provides high-pressure recovery. The retractable feature eliminates inlet drag at higher Mach numbers. True, the external air inlet system adds empty weight, but with a mass ratio reduction of 0.60, the air induction system weights less than the rocket, if the inlet system is less than 8% of the dry weight.

3. **Ram rocket**. Figure 4.10 is an air augmented rocket cycle where the rocket is operated at a fuel-rich oxidizer-to-fuel ratio, so the oxygen in the entrained air can now burn the excess fuel at the normal airbreathing air/fuel ratios for the fuel used. Scherrer gives an excellent evaluation of the air augmented rocket and the ram rocket based on ONERA research [Scherrer, 1988]. The external airstream is mixed with the rocket exhaust to increase mass flow and with the combustion of the excess fuel thrust and specific impulse increase at lower Mach numbers ($M < 6$). The weight ratio is reduced for an SSTO from 8.1 to 6.5. The sketch in Figure 4.10 is notional, but the use of an inward-turning inlet with a variable capture feature offer high mass capture tailored to the Mach number and provides high-pressure recovery.

The retractable feature eliminates inlet drag at higher Mach number. The external air inlet system adds empty weight. But with a mass ratio reduction of 1.6, the air induction system weights less than the rocket if the inlet system is less than 24% of the dry weight. This is the better operational mode than the air augmented rocket.

Neither of these latter two rocket configurations has found any significant applications yet, because of the opinion that the air induction system is too heavy for the benefit provided. That is very close to true for the air augmented rocket but it is not true for the ram rocket. A significant reduction in mass ratio can be realized for about a 5% increase in empty weight. Aircraft such as the Saab-Scania Viggen, in fact, employ this method to increase the thrust of the gas turbine engine. The exhaust nozzle is an ejector nozzle, where the primary gas turbine exhaust induces ambient air into a secondary nozzle-mixer flow.

4.9 AIRBREATHING ROCKET PROPULSION

Airbreathing rocket-derived propulsion systems are generally operated up to Mach 6 or less because of pressure and temperature limits of the air induction system [Miki et al., 1993]. At Mach 6 inlet diffuser static pressures can typically equal 20 atmospheres and 3,000°R (1,666 K). Airbreathing rocket propulsion concepts employ a method to reduce the temperature of air entering the inlet system so it can be compressed to rocket chamber operating pressures with reduced power requirements. There are two options. One option is to deeply cool the air just short of saturation and use a turbocompressor to compress the cold gaseous air to the rocket chamber pressure and inject it into the combustion chamber. The second option is to liquefy the air and use a turbopump to pump the liquid air to rocket chamber pressure, then gasify it for injection into the rocket chamber, see Figure 3.3. The rocket motor operates at nearly normal oxygen-to-fuel ratios, except that there is now a large mass of nitrogen also introduced into the combustion chamber. Again the mass average exhaust velocity is reduced and the total mass flow increased, increasing thrust and propulsion efficiency.

4. Liquid air cycle engine, LACE rocket. Figure 4.11 is the rocket part of the Aerospace Plane propulsion concept developed by The Marquardt Company in the mid- to late-1950s. LACE (from Liquid Air Cycle Engine) is a concept developed in Russia [Rudakov et al., 1991; Balepin and Tjurikov, 1992; Balepin et al., 1993, 1995] Japan [Aoki et al., 1991; Togawa et al., 1992], [Miki et al., 1993; Ogawara and Nishiwaki, 1989] and India [Anon., Hyperplane, 1991; Gopalaswami et al., 1990]. The thermodynamic principle of LACE is that a significant fraction of the energy required to liquefy the hydrogen is recoverable as available energy that can be converted to useful work. For a hydrogen-fueled aircraft atmospheric air is an enormous source of energy. Via a hydrogen/air heat exchanger, atmospheric air can be cooled as the liquid hydrogen is boiled, requiring no energy expenditure from the aircraft's systems. Ahern [Ahern, 1992, 1993] was associated with the development of

Figure 4.11. Airbreathing rockets.

the first LACE system in the United States when working with the Scramjet team at The Marquardt Company in 1958. As part of that work Ahern proposed a closed helium heat pump that avoided the problem of having two phase changes in the hydrogen/air heat exchanger (air being liquefied as hydrogen is gasified) and of having a hydrogen heat exchanger in the air inlet. To the authors' knowledge this concept has never been developed beyond the laboratory. Ahern also had a concept of recovering the aircraft aerodynamic heating in the hydrogen flow to the engine and use that energy to create useful work (electrical, hydraulic and air handling work) and engine thrust (thrust from supersonic hydrogen fuel jet, injected into the scramjet). This will be discussed in the section on ram/scramjets.

As depicted in Figure 4.11, this cycle employs a hydrogen/air heat exchanger in the air inlet to capture the inlet air kinetic energy from the incoming air and cools it to nearly saturation. The cooled air is then pressurized to a few atmospheres and then flows into the pressurized liquefying heat exchanger. The total thermal energy collected from the incoming air and hydrogen combustion chamber is used to drive an expansion turbine, which in turn drives a turbopump that pumps liquefied air into the rocket motor. A rocket motor combustion chamber heat exchanger is necessary to provide sufficient energy to drive the turbomachinery [Tanatsugu, 1987]. In effect the rocket becomes an airbreathing rocket for Mach number less than 6. In this concept there is no need for another airbreathing engine. This cycle reduces the mass ratio to the 5.0 to 5.8 range and the oxygen to fuel ratio to about 3.5.

5. Deeply cooled rocket. As depicted in Figure 4.11 this cycle employs a hydrogen/air heat exchanger in the air inlet to capture the inlet air kinetic energy from the incoming air and cool it to nearly saturation. Unlike the LACE cycle, the next step is to compress the cold air via a turbo-compressor. This controls the air temperature entering the compressor, and limits the work of compression and the compressor corrected speed. The warmed hydrogen then enters the rocket combustion chamber to recover additional energy. The total thermal energy collected from the incoming air and hydrogen combustion chamber is then used to drive an expansion turbine, which in turn drives a turbocompressor that compresses the cooled inlet air. That air can be cooled to nearly saturation by the hydrogen flow, then compressed to rocket operating pressures and introduced into the combustion chamber. This cycle was independently developed at TsIAM [Rudakov and Balepin, 1991a] and by Alan Bond for HOTOL. A rocket motor combustion chamber heat exchanger is necessary to provide sufficient energy to drive the turbomachinery in an expander

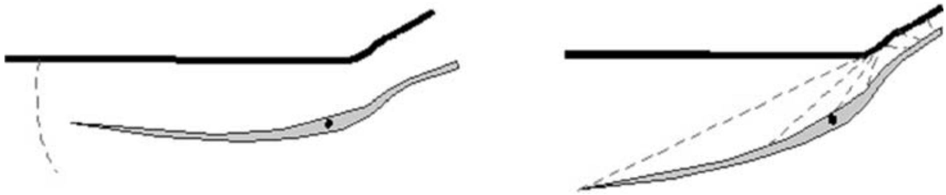

Figure 4.12. Variable capture area, inward-turning inlet.

cycle. Both Rudakov and Balepin of TsIAM and Tanatsugu of JAXA, Japan, employ heat exchangers in their rocket combustion chamber. Alan Bond did not for the HOTOL engine, as it could have adversely affected its performance at higher Mach numbers. In effect the rocket becomes an airbreathing rocket for Mach numbers less than 6. In this concept no other airbreathing engine is required. This cycle reduces the mass ratio to the 5.2 to 6 range and the oxygen to fuel ratio to about 3.4. There is a significant discussion of whether a liquefying system is equivalent in weight to a deeply cooled gaseous system. In most studies the authors are aware of, it is an even trade-off and other considerations should be used to make the selection.

With a suitable inlet system, airbreathing rockets can be integrated into flat-bottomed hypersonic glider configurations (Figure 3.14), as the forebody compression system required by a ramjet/scramjet (Figure 4.2) is not needed. Figure 4.12 shows such an inlet, an inward-turning, variable capture area inlet [DuPont, 1999] that has been wind-tunnel tested to Mach 5 plus. The mechanical details are not shown, but the mechanical actuation and integration is similar to the movable ramps on current supersonic military fighters. The movable lower inlet can be designed to retract even with the lower surface when not in use. Since the outer surface of the lower cowl is the only surface that experiences entry heating, this system is much lighter than an outward-turning inlet. Note that in the low-speed position, the exit of the lower ramp flow is parallel to the lower vehicle moldline. Thus all of the inlet structure is inside the fuselage moldlines, except the lower movable ramp. The inlet has the advantage of turning the flow inward, so there is no bulge in the moldline produced by an outward-turning inlet, such as the half-conical inlets on the Dassault Mirage aircraft. It also has the advantage of changing capture area to match the increasing corrected airflow requirement as speed is increased. The inlet meets or exceeds the Military Inlet Recovery Specification over the entire Mach range.

This class of propulsion systems can be airbreathers to Mach 5.5, and it is not necessary to have a fully developed airbreather configuration (Figure 4.36). A variable capture, inward-turning inlet [DuPont, 1999], Figure 4.12, integrated into the hypersonic glider configuration provides a satisfactory system [Balepin and Hendrick, 1998]. Figure 4.13 shows an inward-turning inlet incorporated into a hypersonic glider configuration with the engine system represented in Figure 4.11, the LACE or deeply cooled rocket propulsion system. The rocket is installed much as it would be for an all rocket configuration.

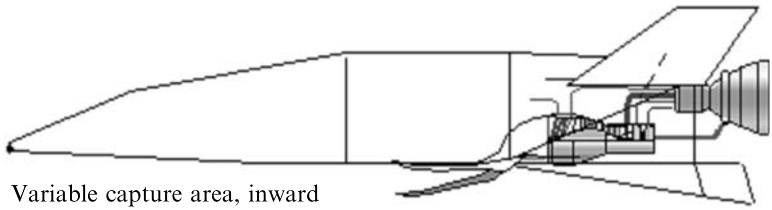

Figure 4.13. Airbreathing rocket configuration concept.

4.10 THERMALLY INTEGRATED COMBINED CYCLE PROPULSION

As the Mach number increases, the kinetic energy of the air increases by the square of the speed. As we saw in Figure 4.3, the kinetic energy of the air rapidly exceeds the thermal energy available to be transferred to the engine working fluid, air. The fraction of the combustion energy rejected as unavailable for conversion to useful work is also significant. In a modern turbojet engine only about 23% of the fuel combustion energy is actually converted to thrust, and 44% is discarded out of the exhaust nozzle unused except to make a hot atmosphere [Kroon, 1952]. With commercial high bypass ratio engines, about 31% is converted to thrust. It is critical then to examine what part of the energy that has been carried on board the aircraft has not converted to useful work or thrust. Any increase in the useful work conversion ratio reduces the propellant carried on board and thus the gross weight. The result of this analysis and of many efforts was the thermally integrated combined cycle propulsion system. The combined cycle engine concept's fundamental element began as a rocket ejector ramjet-scramjet [Stroup and Pontez, 1968], thermally integrated into a rocket propulsion system, and that has a long history in hypersonics. An excellent discussion of the subject, by one who was already working in supersonic combustion engines in 1958, is by E. T. Curran, [Curran, 1993]. Another early pioneer, Dr Frederick Billig, has added many insights into the advantages of thermal integration [Billig, 1993]. Other nations were also working on thermally integrated concepts and one excellent source is from TsAGI [Lashin et al., 1993]. In the class of integrated ejector ram-scramjet propulsion, the integral rocket ejectors provide both thrust and compression at lower Mach numbers. [Buhlman and Siebenhaar, 1995]. The combination of a *separate* ramjet and turbojet results in a poor acceleration. However, the introduction of a deeply cooled turbojet thermally integrated with an expander rocket (KLIN cycle) [Balepin and Hendrick, 1998] is analogous to the rocket ejector ram-rocket-ramjet, with an additional benefit of excellent low-speed performance.

6. Deeply cooled turbojet-rocket (KLIN cycle). Figure 4.14 is an adaptation of Rudakov and Balepin's deeply cooled rocket ramjet into a deeply cooled turbojet-rocket. The turbojet and expander cycle rocket are thermally integrated

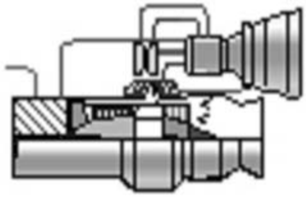

Figure 4.14. KLIN cycle, thermally integrated turbojet-rocket.

[Balepin and Hendrick, 1998]. Unlike the ramjet, the pre-cooler on the turbojet keeps the compressor air inlet temperature low to reduce required compressor work and to increase mass flow and thrust. With the pre-cooler, the turbojet does not see the inlet temperature associated with higher Mach number flight, so it 'appears' to be at lower flight speed. The pre-cooled turbojet provides a significant increase in transonic thrust. Even with the increased transonic thrust, the turbojet remains a poor transonic accelerator. So the KLIN cycle operates with the rocket as a team. Whenever the turbojet thrust is not adequate to maintain a higher value of effective specific impulse, the rocket engine operates to add additional thrust and increases the effective specific impulse, as defined below:

$$I_{sp} = \frac{\text{Thrust}}{\text{Propellant flow}} = \frac{T_{\text{rocket}} + T_{\text{airbreather}}}{\dot{w}_{\text{rocket}} + \dot{w}_{\text{airbreather}}}$$

$$I_{spe} = \frac{\text{Thrust} - \text{Drag}}{\text{Propellant flow}} = I_{sp}\frac{T/D - 1}{T/D} \tag{4.9}$$

Because of its lower thrust, a hydrogen-fueled turbojet is about equivalent in effective specific impulse in the transonic region to a hydrogen–oxygen rocket. In afterburner operation, the rocket outperforms the turbojet. Thermally integrated together the combination is better that the sum of individual engines, as demonstrated in Figure 4.16. The thermal energy from both the rocket and turbojet is used to power the expansion turbines that drive the propellant turbopumps. If there is remaining excess energy it can be added to a heat exchanger upstream of the turbojet combustor. The pre-cooled turbojet provides operation from takeoff to Mach 5.5 with rocket thrust augmentation when required, such as in the transonic region. Above Mach 5.5 turbomachinery is shut down and the rocket operates as a conventional cryogenic rocket.

7. LACE rocket-ram-scramjet. Figure 4.15 is the engine family in Figure 4.11 integrated with a ramjet. As in Figure 4.16, the results with a LACE rocket will be similar to the deeply cooled rocket. The airbreathing rocket operates only to Mach 6 or less, so the companion engine is a subsonic through-flow ramjet. In this cycle the thermal energy from the incoming air and hydrogen combustion is used to drive an expansion turbine that in turn drives a turbopump. A rocket motor combustion chamber heat exchanger is necessary to provide sufficient energy to drive the turbomachinery. After leaving the expansion turbine, the hydrogen is introduced

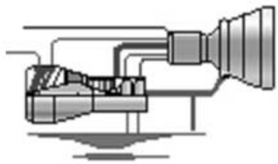

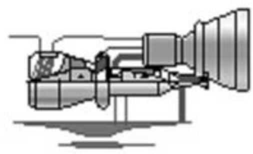

Figure 4.15. Airbreathing rocket thermally integrated combined cycle.

into the ramjet combustion chamber. The inlet air is cooled to nearly saturation by an air–hydrogen heat exchanger, and then pressurized to a few atmospheres. It then flows into the pressurized liquefying heat exchanger. The turbopump pressurizes the liquid air to rocket operating pressures so it can be introduced into the rocket combustion chamber. After exiting the turbomachinery, the hydrogen is introduced into the ramjet combustion chamber. At Mach 6 or less, the rocket is essentially an airbreathing rocket operating in parallel with a ramjet. The ramjet can convert to supersonic through-flow engine (scramjet) at Mach number above 6, but the rocket is now a conventional cryogenic rocket, not an airbreathing rocket. Above Mach 6, the rocket is normally not used when the scramjet is operating. After scramjet shutdown the rocket operates as a conventional expander cycle cryogenic rocket.

8. Deeply cooled rocket-ram-scramjet. Figure 4.15 is the integration of the deeply cooled cycle developed by Rudakov and Balepin at CIAM and Alan Bond for HOTOL [Anon., BAC, 1991] with a subsonic through-flow ramjet. In this cycle the recovered thermal energy from the incoming air and hydrogen combustion in both the rocket and ramjet is used to drive an expansion turbine, which in turn drives a turbocompressor. The incoming inlet air is cooled to nearly saturation in an air–hydrogen heat exchanger, and then compressed to rocket operating pressures by the turbocompressor so it can be introduced into the rocket combustion chambers. A rocket motor combustion chamber heat exchanger is necessary to provide sufficient energy to drive the turbomachinery. After leaving the expansion turbine, the hydrogen is introduced into the ramjet combustion chamber. At Mach 6 or less, the rocket is essentially an airbreathing rocket operating in parallel with a ramjet. Above Mach 6, the rocket is normally not used, and the ramjet operates as a supersonic through-flow ramjet (scramjet). After scramjet shutdown the rocket operates as a conventional cryogenic rocket.

4.11 ENGINE THERMAL INTEGRATION

When discussing propulsion, hypersonic flight or atmospheric entry, the question of cooling is always prominent: cooling implies discarding the rejected energy [Ahern, 1983, 1992]. Thermal management implies that a fraction of the rejected energy creates useful work or thrust [Barrère and Vandenkerckhove, 1993]. The concept of thermal management begins typically with two separate engines that are thermally

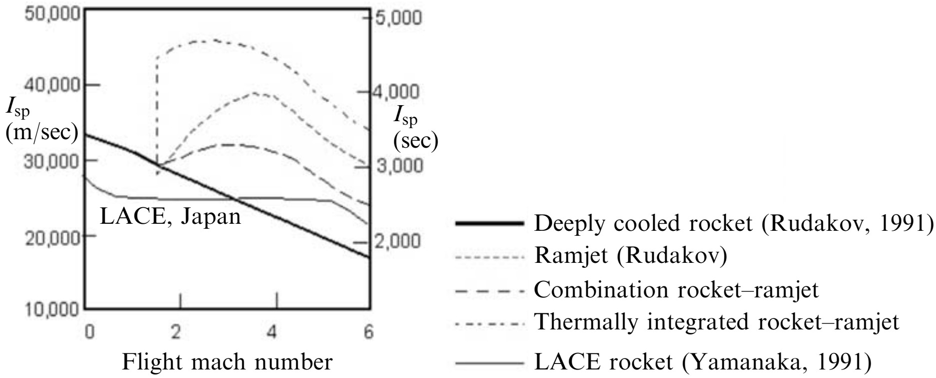

Figure 4.16. Benefits of thermal integration (from Rudakov and Balepin, [1991]).

integrated by having the fuel (in this case hydrogen) flows through both engines before a portion of the collected thermal energy is extracted as useful work. This first example is limited to an airbreathing Mach number of 6 and the airframe is not a part of the thermal integration concept.

Figure 4.16 is from [Rudakov and Balepin, 1991] and shows performance of a Japanese LACE rocket with a pressurized liquefier, as part of a scram–LACE system [Aoki and Ogawara, 1988; Aoki, et al., 1991; Yamanaka, 2000, 2004], and of a Russian deeply cooled rocket, integrated with a ramjet [Rudakov and Balepin, 1991]. The solid line identifies the deeply cooled rocket, by Rudakov. The central dashed line identifies a hydrogen ramjet by Rudakov. When simply operated independently, the combined thrust and fuel flow produces about a 500 sec I_{sp} increase, as indicated by the lower dashed line identified as combination of rocket/ramjet. When thermally integrated, the fuel flows through both engines, collecting thermal energy, from both the rocket and the ramjet, that is used to power the expansion turbines that drive the turbocompressor; thus, the same two engines, when thermally integrated, provide a 1,500 sec increase in I_{sp} over the combination of rocket/ramjet, as indicated by the top dashed line. Thus between Mach 2 and 6 it is possible to have the thrust of a rocket and the specific impulse of a military subsonic turbofan, e.g. 4,500 to 4,000 sec (specific fuel consumption from 0.8 to 0.9 kg/sec per kg of thrust). This concept could be preceded by the development of the airbreathing rocket, that does produce a tangible benefit for operational launchers based on existing rocket engines and hardware technology. This initial step could deliver an interim operational capability in terms of a sustained-duration-use rocket launcher, in parallel with the development of the ramjet engine to be incorporated later into this propulsion system, eventually developing into a scramjet version of the ramjet. When these principles are applied to SSTO and TSTO launchers, size and weight are reduced (both dry and gross weight).

These three propulsion systems could profoundly affect the size and weight of both SSTO and TSTO launchers if they were applied. Their advantage is that they are fabricated of existing tested and demonstrated hardware and use current industrial capability. Alan Bond and Alexander Rudakov were pioneers in the construction of actual hardware with operational potential. Unfortunately the status quo environment prevailing in aerospace propulsion steadfastly maintained rockets were known solutions, and better than new concepts based on the very rockets they advocated to the exclusion of all else.

4.12 TOTAL SYSTEM THERMAL INTEGRATION

When discussing propulsion, hypersonic flight or atmospheric entry the question of cooling must be examined in the context of the total energy management or integration. In the case of the SR-71 the aerodynamic heating was mostly absorbed by the structure, and the surface ran at radiative equilibrium temperature. So the SR-71 was a hot structure vehicle and therefore it required a material that maintained its strength at high temperature (i.e., in the 660°C range) and that was beta-titanium. The thermal energy had to be removed from the crew compartment and equipment bays. That thermal energy plus the thermal energy rejected by the engine was transferred to the fuel. Discussions of the SR-71 design state that the fuel temperature entering the engine was over 600°C. In this case all of the thermal energy was discarded as hot fuel and that hot fuel provided no useful work or engine thrust. With a high-temperature hydrocarbon as fuel this was a rational approach as there was hardly any option to extract the recovered energy from the liquid hydrocarbon.

With a fuel that is a good heat transfer medium, the structural concept is unlike the SR-71 hot structure, but more like a cold structure protected by a combination of radiation shingles, radiating about 95% of the aerodynamic heating back to space, and a structural thermal management system that converts about half of the thermal energy entering the airframe into useful work and thrust. Figure 4.17 illustrates a systems level thermal integration approach [Ahern, 1992]. The skin panels in the nose region, engine ramps and nozzle region, and the combustion module are one side of a heat exchanger system that pumps aerodynamic heating into an energy extraction loop. The very cold hydrogen passes through a skin panel that absorbs the

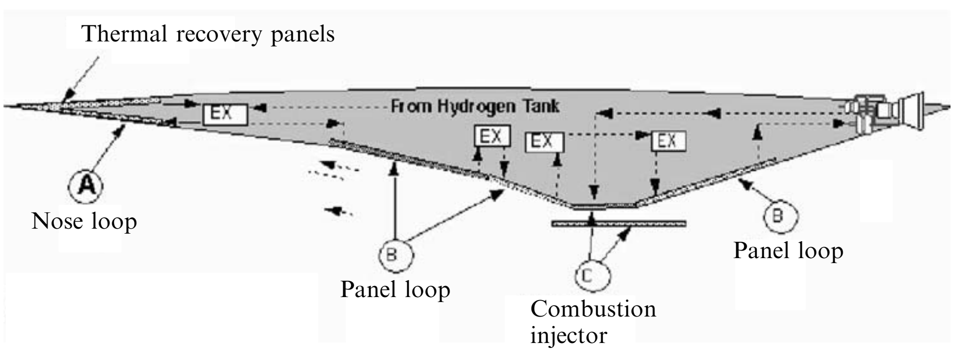

Figure 4.17. System thermal integration.

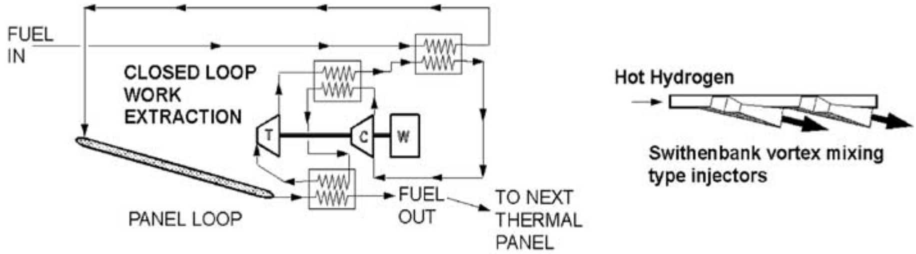

Figure 4.18. Closed cycle heat pump (after Ahern) and combustor fuel injection.

incoming aerodynamic heating. The energy extraction loop lowers the hydrogen temperature and then passes it to another heat exchanger panel. Thus the hydrogen goes through a series of net energy additions until it reaches the combustion chamber where is injected as a hot gas (Figure 4.18). This concept goes back to the original aerospace plane for the United States Air Force to which The Marquardt Company was a contractor. At that time John Ahern worked with Charles Lindley, Carl Builder and Artur Magar, who originated many of these concepts.

Figure 4.18 depicts a typical closed-loop heat pump loop identified in Figure 4.17 as a rectangle with 'EX' inside and the fuel wall injection system. This particular loop is for one of the inlet ramps ahead of the engine module. The three heat exchangers form a closed-loop system where thermal energy extracted from the skin panels is used to power an expansion turbine that drives the working fluid compressor. The net work exacted can be used to power electrical generators, hydraulic pumps, refrigeration units or fuel boost pumps. With hydrogen as fuel, the vehicle is independent of ground power sources and can self-start as long as there is hydrogen in the fuel tanks. Eventually the fuel reaches the engine module where it picks up the heat transferred to the combustor walls. When the hydrogen reaches its maximum temperature it is injected into the combustion chamber via series of Mach 3 nozzles at a low angle to the wall. The size of the nozzles can be small and approach the equivalent of a porous wall. The result is that the hydrogen acts as film cooling for the wall, reducing the wall friction and heat transfer rate. For a Mach 3 wall nozzle the kinetic energy of the injected fuel also creates thrust, and the thrust per unit fuel flow, I_{sp}, is given in equations (4.10) for hydrogen.

$$\text{Fuel } I_{sp} = 9.803\, T^{0.5197} \text{ (sec)} \qquad T \text{ is in Rankine}$$

$$\text{Fuel } I_{sp} = 13.305\, T^{0.5197} \text{ (sec)} \qquad T \text{ is in Kelvins} \tag{4.10}$$

At 2,000 R (1,111 K) the hydrogen specific impulse is 509 sec, or better than a hydrogen/oxygen rocket. For a scramjet engine with an equivalence ratio greater than one, this can produce 30% or more of the engines net thrust [Novichkov, 1990]. Applying this approach using Builder's Second Law approach, the impact of fuel temperature injected through Mach 3 nozzles in the combustor wall (Figure 4.19) can be assessed.

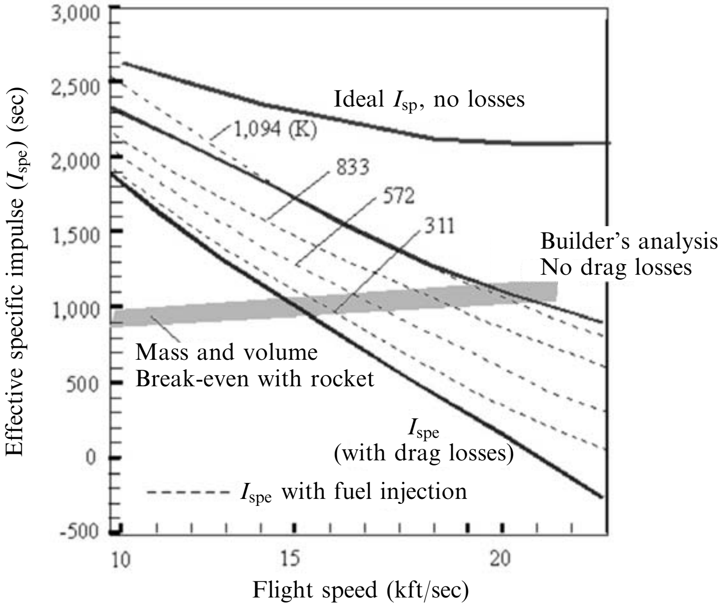

Figure 4.19. System thermal integrated specific impulse.

One measure of airbreathing engine performance is the energy conversion efficiency (θ). The definition is:

$$\theta = \frac{VT}{Q_c \dot{w}_{\text{fuel}}} = \frac{VI_{sp}}{Q_c} = \frac{VT}{Q\dot{w}_{\text{air}}}$$

$$I_{sp} = \frac{\theta Q_c}{V} \tag{4.11}$$

At hypersonic speeds the value of θ is almost constant, ranging between 0.55 and 0.60 from the Second Law analysis [Builder, 1964]. That means that as speed (V) is increased, the specific impulse must decrease with increasing speed. Figure 4.19 shows three I_{sp} values, decreasing from upper left to lower right. The top solid line is for an ideal engine with no internal losses. The middle solid line shows the I_{sp} from Builder's analysis including the losses from Swithenbank's injector system (Case 0, Figure 4.4). This is the value of the I_{sp} if the vehicle were in cruise mode; that is, thrust equal to drag, with no acceleration. The bottom solid line shows the effective or acceleration I_{sp} based on engine net thrust minus aircraft drag; this is the I_{sp} for an accelerating aircraft that must have thrust greater than drag. If there is no acceleration (that is, thrust minus drag is zero) then the value of effective I_{sp} is zero. The gray band is the sizing breakeven I_{sp} for a hydrogen/oxygen rocket and a hydrogen fueled airbreather. Since the bulk volume of 100 kg of 6 to 1 liquid oxygen–hydrogen is 0.26 cubic meters, and that of 100 kg of sub-cooled liquid hydrogen is 1.34 cubic meters, the breakeven I_{sp} is a function of volume and I_{sp} together. As Mach 12 is approached the propulsion system efficiencies become similar. That is, the propellant masses required to achieve a unit change in velocity are equal. For some airbreathing systems, the rocket propellant mass required to achieve a unit change in velocity is less than for the airbreathing system and so the volume requirements for the rocket propellant is about one-fifth that for the airbreather system. For the Swithenbank injectors that breakeven speed is Mach 15.0. However, at the breakeven speed the airbreather is just equal to the rocket, and even if no higher speed is sought, a higher I_{sp} is always welcome. That higher I_{sp} comes through system thermal management.

The impact of thermal management is illustrated in Figure 4.19 by the four dashed lines for the specific impulse of the thermally integrated system. The temperature of the injected hydrogen is given in Kelvin. As the injected fuel temperature increases, the injected fuel energy offsets a greater fraction of the internal drag losses. If the injected hydrogen temperature can reach 1,094 K (1970 R) then all of the internal drag losses generated by the Swithenbank injector concept have been eliminated (in fact, compensated for). The airbreathing engine energy and entropy limitations presented in Figure 4.7, are still in effect. At Mach 15 flight speed, the effective I_{sp} can be increased by over 600 sec. It requires a detailed engine analysis to quantify a specific value for a given system, but the general trend is correct. Recovered thermal energy can be converted into useful work and thrust to increase performance [Ahern, 1992; Barrére and Vandenkerckhove, 1993; Novichkov, 1990].

9. Ejector ram-scramjet-rocket. Figure 4.20 is an ejector ramjet thermally integrated with a rocket. The ejector may be a hot gas ejector and/or a rocket ejector. Remember, if the ramjet is a subsonic through-flow engine, then the scramjet is simply a supersonic through-flow engine. The maximum airbreathing speed can be selected to be from Mach 6 to at least Mach 14.5. At Mach less than 2, the system is an ejector ramjet analogous to a ram rocket system, except the rocket ejectors are distributed in the struts inside the ramjet engine module [Stroup and Pontez, 1968]. At Mach number greater than 2 the engine is a conventional ramjet with the rocket injectors now functioning as hot hydrogen injectors. Subsonic thrust is generated in the same manner as a ramjet, and the supersonic hydrogen injection acts as an aerodynamic isolator. Above Mach 6 it is a conventional scramjet engine with variable configuration injectors to minimize internal drag as discussed earlier in this chapter [Gounko et al., 2000].

This propulsion concept was the backbone of the effort to create an airbreathing launcher and hypersonic cruiser discussed in conjunction with Figure 3.11 and represented the Marquardt effort to achieve the first aerospace plane for the United States Air Force, and the effort of the Applied Physics Laboratory, Johns Hopkins University, to achieve a scramjet missile for the United States Navy. In all cases the rocket community overcame the advantages of airbreathing propulsion and an all-rocket solution was adopted in every case.

There have always been, and still remain, arguments that scramjets will not work, and that the analogy is with trying to light a match in a supersonic wind tunnel. However, Professor James Swithenbank of Sheffield University has the correct analogy, and that is lighting a match in a Concorde traveling at Mach 2.

Figure 4.20. Integrated ejector ram-scramjet rocket.

Both the surrounding air and match are at the same speed if hot hydrogen is injected into the engine via the injection devices and if the airflow velocity and hydrogen velocity can be the same. For the Mach 14 case shown in Table 4.2, the hydrogen injection velocity would be the same as the combustor through-flow speed at a gas temperature of 660°C (933 K, 1,246°F). For a slower Mach 8 case, the combustor through-flow speed is 7,100 ft/sec (2,164 m/sec) and the hydrogen gas temperature required is a modest 293°C (566 K, 585°F). In reality then, traveling with the air stream, the fuel and air are essentially at static conditions with very little differential speed. So the scramjet *is* like lighting a match on Concorde.

When one of the authors (PC) was a young engineer at Wright Patterson Air Force Base he was assigned as Chief Engineer for the High Temperature, Hypersonic Tunnel at Hypervelocity Branch, Aircraft Laboratory, Wright Air Development Division. The High Temperature, Hypersonic Tunnel was a nominal Mach 4 wind tunnel heated with a Zirconia pebble bed. Nominal air temperatures were in the range 2,500 to 1,500 K (4,500 to 2,700 R). The pressure, temperature, and velocity in the test section were very close to those of a scramjet operating at a Mach 8 flight conditions. The Aero-Propulsion Laboratory assigned Paul Ortwerth and then, Squadron Leader E. Thomas Curran to investigate the possibility of testing a scramjet combustor in the High Temperature, Hypersonic Tunnel. Squadron Leader Curran was familiar with the work Professor James Swithenbank was doing in a similar facility in Montreal, Canada. The result was an experiment that used the test section of the High Temperature, Hypersonic Tunnel as a scramjet combustor. A 7.6 cm wide flat plate model 19 cm long with five hydrogen injection ports placed one-fourth of the model length from the model nose was placed in the 12.7 cm test section [Burnett and Czysz, 1963]. The model was installed on an injection system, so the duration of the time in the test section could be controlled. There were a series of pressure taps running down the model centerline. The gas plenum chamber in the model was equipped with thermocouples to measure the hydrogen temperature. Both color Schlieren and infrared ciné film recording of the flow field were made. The infrared film was filtered to center on the high-temperature water emission radiation. Figure 4.21 (see the color section) shows two of only a few surviving photographs from the test. The left picture is a color Schlieren with a horizontal knife-edge, so above the model red indicates a reduction in density, and green/blue an increase in density. The shock waves from the model and gas injection are clearly visible. The red hydrogen injection is also clearly visible. The model plenum chamber thermocouple gave a hydrogen temperature of 300°C ± 15°C (573 K ± 15 K) so the test section air and hydrogen speeds were very similar. From Table 4.2, the 7,100 ft/sec test section speed corresponds to a flight speed of 8,000 ft/sec as does the 2,500 K stagnation temperature. The picture on the right is from the infrared film camera and clearly shows the water formation approaching the hydrogen injection holes. So combustion delay was minimal. Professor Swithenbank's data correlations for over 1,000 test runs give a time to complete combustion of 35 ± 5 microseconds for gaseous fuels; at this airflow speed the distance traveled is about 2.98 inches ± 0.4 inches (6.6 to 8.6 cm) and is very close to the data from the pictures. A later analysis showed a very close correlation between the schlieren and infrared pictures and confirmed the combustion distance from pressure measurement [Czysz, 1993b]. So indeed hydrogen will burn very well in a scramjet.

4.13 THERMALLY INTEGRATED ENRICHED-AIR COMBINED CYCLE PROPULSION

These cycles are thermally integrated combined cycle propulsion analogous to the *LACE rocket-ram-scramjet* and the *deeply cooled rocket-ram-scramjet* except the thermally processed air is separated into nearly pure liquefied oxygen (Liquid Enriched Air, LEA; LACE stands for Liquid Air Cycle Engine; and ACES for Air Collection Enrichment System) and gaseous nitrogen (Oxygen-Poor Air, OPA). This is possible because the boiling point of liquid oxygen is 90.03 K and the boiling point for liquid nitrogen is 77.2 K. Just as in a fractionating tower for hydrocarbons, where hydrocarbons of different boiling points can be separated, the oxygen can be liquefied while the nitrogen remains gaseous. This means that most of the oxidizer carried on-board the launcher was not loaded at takeoff but loaded during the flight to orbit. The result is that the carried oxidizer-to-fuel ratio at takeoff is less than for a non-ACES system. Thus the takeoff gross weight and engine size are reduced. Whether also the volume (size) of the launcher is reduced depends on the volume of the ACES system [Bond and Yi, 1993]. The maximum weight of the launcher is then near the ascent climb to orbital speed and altitude, rather than at takeoff. The process is executed in steps, through temperature gradients where a fraction of the oxygen is liquefied at each step. As in all chemical processes, the difficulty increases as the oxygen purity increases, and for a flight weight system there is a practical limit. The liquid-enriched air has purity in the 85% to 90% oxygen range and is stored for use in the rocket engine during the rocket ascent portion of the ascent trajectory. The oxygen-poor air contains 2% to 5% oxygen and is introduced into the ramjet, creating the equivalent of a mixed flow by-pass turbofan. That is, the mass-averaged exhaust velocity is reduced but the specific impulse, engine mass flow and thrust are increased. Thermal integration means that the fuel passes through both rocket and scramjet to scavenge rejected heat and convert it into useful work before entering the combustion chambers, increasing the specific impulse at the same time oxidizer is being stored for the ascent to space. Just as for the LACE and deeply cooled rocket, both rocket and scramjet must operate as an acceleration system until efficient ramjet operation is reached. So the Mach number for air separation and collection is usually in the Mach 3 to 5 region. This is a very good cycle for launchers that require a launch offset to reach an optimum launch latitude and time window, for instance, when the vehicle must cruise some distance to the ascent to orbit point. The approach is applicable to SSTO vehicles. ACES has more significant payoffs for TSTO launchers that must fly an offset because the air separation plant is in the first stage, not in the stage that flies to orbit. A good example of this is reaching the ISS 55-degree orbital inclination from Cape Canaveral, at 28.5 degrees latitude. The Space Shuttle loses a significant fraction of its payload because of the propellant required to move the orbital plane during a rocket ascent. To rotate the orbital plane 26.5 degrees requires a significant weight ratio increase to achieve low earth orbit (this will be discussed in Chapter 5). However, a first stage *flying* in the atmosphere can achieve this with a small fraction of the propellant required to do the plane change by rocket thrust, because the first stage accomplishes the turn simply using aerodynamics. The rocket in its acceleration-turning flight has thrust at least twice its weight with an effective I_{sp} of perhaps 400 sec, while the aircraft has the thrust of one-sixth its weight with a specific impulse about 10 times greater (Figure 4.12). This expands the launch window because the launcher can fly to intercept the ascending node of the desired orbit and not be confined to when the ascending node and launch site latitude coincide. The figure of merit for these systems is the weight of LEA collected per weight of hydrogen. A practical value is 6 kg of LEA per kg of hydrogen; for more details see [Czysz and Vandenkerckhove, 2000]. Examples of the thermally integrated enriched-air combined cycle propulsion are:

10. ACES-LACE ejector ram-scramjet-rocket. Figure 4.22 is an air collection and enrichment system [Ogawara and Nishiwaki, 1989] added to Propulsion System 6. The liquid air is not pumped to the rocket immediately, but passed through a liquid fractionating system to separate the oxygen component as liquid-enriched air (LEA contains 80% to 90% oxygen) and nitrogen component as liquid oxygen poor air (OPA contains from 2% to 5% oxygen) [Balepin, 1996]. The oxygen component is then stored for use in the rocket ascent portion of the flight. The oxygen-poor nitrogen component is injected into the ramjet, to create a hypersonic by-pass engine that increases engine mass flow, thrust and reduce the mass-averaged exhaust velocity. The hardware development in the 1960s was undertaken by the Linde Corporation under Air Force contract. Sufficient hardware was fabricated to design the operational system and confirm performance. ACES most significant penalty was the volume required for the fractionating separator. For hydrogen-fueled hypersonic and space launchers volume is a critical parameter, and increasing it comes at a significant size and weight penalty. At takeoff this propulsion strategy can significantly reduce the takeoff perceived noise. It is done for the same reasons a conventional mixed flow by-pass gas turbine was invented. ACES was originally proposed by the Air Force Aero-Propulsion Laboratory for the space plane of the

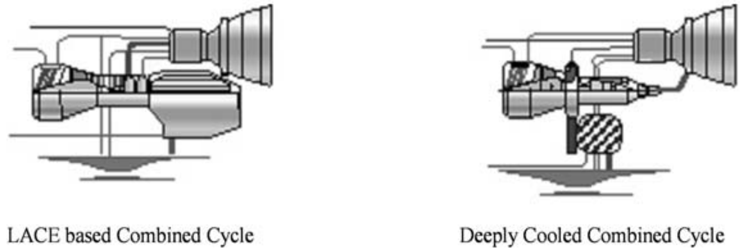

Figure 4.22. Air collection and enrichment cycle (ACES).

late 1950s [Leingang, 1988; Maurice et al., 1992]. and was the subject of intense investigation in the 1960 to 1967 time period [Leingang et al., 1992]. Most of the original Air Force work was for a TSTO vehicle although application to SSTO was investigated. For airbreather operation to the 12,000 to 14,000 ft/sec range, its cycle can achieve weight ratios less than 3 with oxygen-to-fuel ratios approaching one-half.

11. ACES-deeply cooled ejector ram-scramjet-rocket. Figure 4.22. is an ACES option added to Propulsion System 7. Even in the 1950s, the paramagnetic properties of liquid oxygen were noted by the LACE and ACES investigators [Leingang, 1991]. Patrick Hendrick was a graduate student under the late Jean Vandenkerckhove in 1988 who observed that Siemens sold an exhaust gas analyzer measuring gaseous oxygen based on the magnetic properties of oxygen. The magnetic susceptibility of oxygen at its boiling point (90.03 K) is 7699×10^{-6} in cgs units, that is, as large as some chromium and nickel compounds. During a visit to Jean Vandenkerckhove at his Brussels residence, Patrick Hendrick [Hendrick, 1996] discussed his concept of gaseous air separation using the magnetic properties of oxygen. Collaboration with Vladimir V. Baliepin resulted in the addition of a vortex tube pre-separator based on the small temperature difference in the liquid temperature of nitrogen and oxygen. The result was a new approach to the ACES concept with much lower total volume requirements than the liquid fractionating equipment. The deeply cooled gaseous air is not pumped to the rocket immediately, but passed first through a vortex tube initial separator (at this stage the LEA contains about 50% oxygen) [Lee et al., 2003], and then into a cryogenic magnetic oxygen separator. The oxygen component is then liquefied as LEA (LEA contains 80% to 90% oxygen) and stored for use in the rocket ascent portion of the flight. The gaseous nitrogen component of oxygen- poor air (OPA) contains from 2% to 5% oxygen. The oxygen-poor nitrogen component is injected into the ramjet, to create a hypersonic by-pass engine that increases engine mass flow, thrust and reduce the mass-averaged exhaust velocity. At takeoff this can significantly reduce takeoff noise, for the same reasons a conventional mixed flow by-pass gas turbine was invented. This system is in laboratory testing and studies but has not as yet been developed as propulsion hardware. At this point in time it has potential to significantly reduce the volume and weight required for an ACES system, but is not yet proven. For airbreather operation to the 12,000 to 14,000 ft/sec range, this cycle can achieve weight ratios less than 3 with oxygen to fuel ratios approaching one-half.

4.14 COMPARISON OF CONTINUOUS OPERATION CYCLES

To compare the continuous operation cycles Figure 3.4 is repeated as Figure 4.23. In Figure 4.23 weight ratio to LEO, that is the takeoff gross weight divided by the on-orbit weight, is represented for different engine cycles as a function of the net oxidizer to fuel ratio. These divide into two distinct groups. The rocket-derived propulsion represented by cycles: rocket, air augmented rocket and ram rocket. For the rocket-derived cycles the oxidizer-to-fuel ratio is essentially constant at a value of 6. As a ram rocket, the weight ratio of LEO decreases from 8.1 to 6.5. There is only a minimal payoff for the air augmented rocket as without burning the oxygen in the air, there is insufficient thrust boost to make a significant difference in weight ratio. There is a discontinuity in the oxidizer-to-fuel ratio curve between the rocket-derived propulsion value of 6 and where airbreathing propulsion begins, at a value of 4. The airbreathing propulsion cycles move down to the right, reducing in weight ratio and oxidizer-to-fuel ratio to values 2.5 and 0.5, respectively. From equation (3.1) we have the relationship in equation (4.12a). Equation (4.12a) directly links the weight ratio to orbit to a function of the oxidizer-to-fuel ratio and the weight of fuel

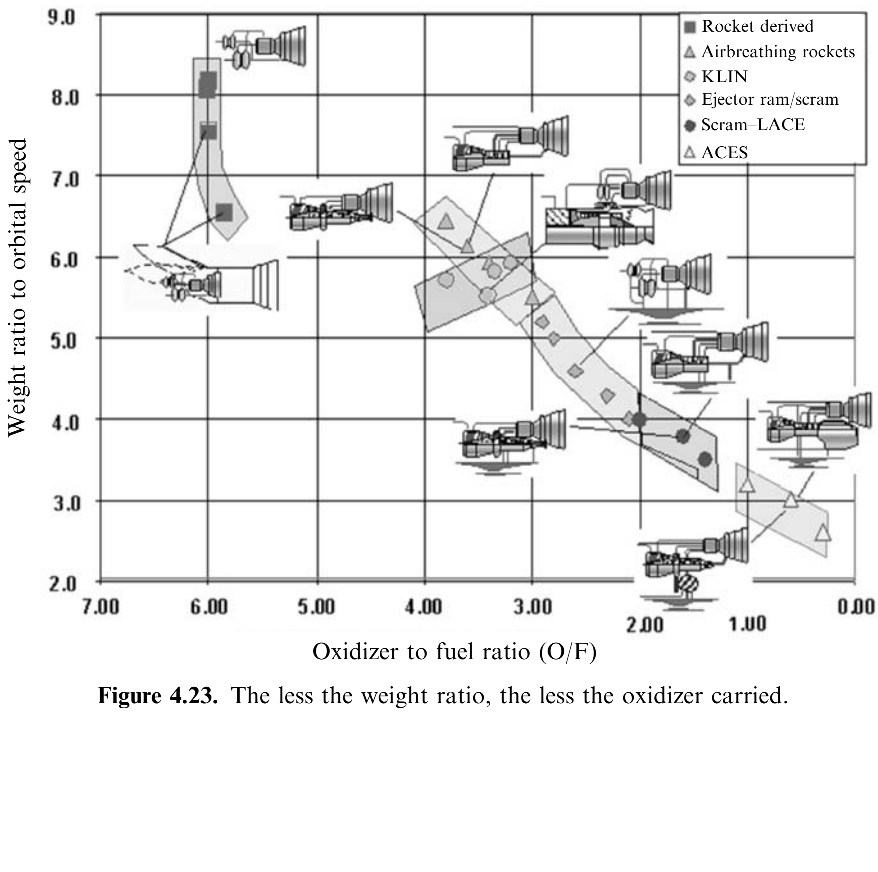

Figure 4.23. The less the weight ratio, the less the oxidizer carried.

divided by the operational weight empty (dry weight plus trapped fluids, crew and payload). So the fuel-to-OWE ratio is multiplied by one plus the oxidizer-to-fuel ratio to produce the weight ratio. If the fuel-to-OWE ratio is approximately constant, then there is a direct benefit to incorporating airbreathing propulsion. The gross weight is reduced and the total engine thrust is reduced greatly reducing the size, complexity and cost of the propulsion system. If the fuel-weight-to-OWE ratio is approximately constant then increased engine and turbopump size and weight is a consequence of continuing with rocket propulsion systems.

$$\mathrm{WR} = 1 + \frac{W_{\mathrm{ppl}}}{\mathrm{OWE}} = 1 + \frac{W_{\mathrm{fuel}}}{\mathrm{OWE}}\left(1 + \frac{\mathrm{O}}{\mathrm{F}}\right)$$

$$\mathrm{TOGW} = \mathrm{WR}\cdot\mathrm{OWE} = \mathrm{OWE}\left[1 + \frac{W_{\mathrm{fuel}}}{\mathrm{OWE}}\left(1 + \frac{\mathrm{O}}{\mathrm{F}}\right)\right] \tag{4.12a}$$

Rearranging equation (4.12a) we have equation (4.12b). Remember in this equation the oxidizer/fuel ratio is the oxidizer/fuel ratio carried on the launcher with the associated weight ratio, not the rocket engine oxidizer-to-fuel ratio. The importance of equations (4.12a,b) and of the graph is that it shows the gross weight is a function of one airframe parameter, OWE, and of two propulsion parameters and that the gross weight is directly proportional to the carried oxidizer-to-fuel ratio. Reduce the carried oxidizer and the gross weight and resultant engine thrust decrease proportionately. Beginning with the rocket point in Figure 4.23 at a weight ratio of 8.1 to the ACES weight ratio of 3.0 a straight line constructed between these points has all of the hydrogen-fueled propulsion system lying along that line, except the air augmented rocket and ram rocket. The reason these two do not lie on the curve is that the engine oxidizer-to-fuel ratio is essentially unchanged and the reduction in weight ratio comes from the air entrained in the ejector system.

$$\frac{W_{\mathrm{fuel}}}{\mathrm{OWE}} = \frac{(\mathrm{WR} - 1)}{(1 + \mathrm{O/F})} \tag{4.12b}$$

Analyzing the data in Figure 4.23, the result is a value for $W_{\mathrm{fuel}}/\mathrm{OWE}$ equal to 1.05 ± 0.06. So, regardless of the propulsion system, the quantity of fuel carried by a hydrogen-fueled launcher that achieves LEO lies between 99% and 111% of the OWE. This only holds true only for a hydrogen/oxygen propulsion system with a six-to-one oxygen/fuel ratio and a stoichiometric air/fuel ratio of 35.4 to one. A hydrogen/oxygen rocket with a seven-to-one oxidizer/fuel ratio will have a different value. This is an important result of the governing equations, as it fixes the fuel weight regardless of the propulsion system and focuses on the real problem, the weight of the oxidizer carried. As shown by Equation (4.12a), the launcher weight ratio is only a function of the carried oxidizer-to-fuel ratio and the weight ratio is determined by the propellant combination. From the propellant combinations in Table 4.5, the value of $W_{\mathrm{fuel}}/\mathrm{OWE}$ for the different rocket propellant combinations was calculated and given in Table 4.6. Note that hydrogen carries the least fuel per OWE. With an oxidizer-to-fuel ratio of 6, that means the propellant load is 7.3 times the OWE. The hydrocarbons are five times greater and with an

Table 4.6. Fuel weight to operational weight empty for propellant combinations from Table 4.5.

Fuel	Hydrogen	Hydrogen	Kerosene	Methane	Hydrazine	UDMH[a]
Oxidizer	O_2	N_2O_4	O_2	O_2	N_2O_4	N_2O_4
Relative fuel volume	14.83	16.24	6.51	13.47	6.20	10.73
Relative oxidizer volume	5.25	7.73	2.09	2.05	1.52	0.819
W_{fuel}/OWE	1.05	1.15	5.02	5.12	6.20	8.42
W_{ppl}/OWE rocket	7.35	14.4	17.0	17.1	20.2	18.7

[a] UDMH = Unsymmetrical Dimethyl Hydrazine

oxidizer to fuel ratio about 2.35, the propellant load is 17 times the OWE. The hypergolic propellants propellant load ranges from 19 to 20 times OWE. From Table 4.6 you can see why one of the famous Russian rocket designers, V. P. Glushko, chose the room temperature liquid UDMH and N_2O_4 for Proton and the submarine-launched ballistic missiles.

The importance of this relationship is that with minimal information a reasonable estimate of the fuel and propellant weight compared the OWE is available. Hydrogen provides the least weight ratio to orbit. Because the density of hydrogen is low, the volume required is the greatest.

The weight ratio is decreasing because the oxidizer weight is decreasing as a direct result of the oxidizer-to-fuel ratio. So from Figure 4.23, using hydrogen fuel, an all-rocket engine can reach orbital speed and altitude with a weight ratio of 8.1. An airbreathing rocket (AB rocket) or KLIN cycle can do the same with a weight ratio about 5.5. A combined cycle rocket/scramjet with a weight ratio of 4.5 to 4.0, and an ACES has weight ratio of 3.0 or less. So an airbreathing launcher has the potential to reduce the mass ratio to orbit by 60%. It is clear that results in a significantly smaller launcher, both in weight and size, and presumably also less expensive. To achieve this operationally, the design goal must be, 'reduce the carried oxidizer'. It is more difficult if not impossible to achieve this progression of propulsion systems with fuels other than hydrogen. Methane is a cryogenic fuel, but it does not have the thermal capacity to liquefy or deeply cool air, so the hydrocarbon equivalent of a LACE or deeply cooled cycle is not possible. Ramjet/scramjet engine are possible with most of the liquid fuels, although for hydrocarbons the decomposition into free carbon will limit the temperature, and therefore the maximum speed is limited by the hydrocarbon thermal decomposition.

Examining the operational regions for each cycle concept we can make several observations.

(1) *Chemical rocket, air augmented rocket and ram rocket* maintain essentially a constant oxidizer-to-fuel ratio, with the weight ratio to achieve orbit decreasing because of the increased thrust produced by the air ejector system. For a vehicle for a rocket OWE equal to 76 metric tons and assuming the OWE of other

propulsion systems at 76 t (plus any differential weight for the propulsion system), the TOGW for the three systems is:

WR	WR	O/F	TOGW	Savings[a]
Rocket	8.10	6.00	616 t	0
Air augmented rocket	7.50	6.00	616 t	0
Ram rocket	6.50	5.80	543 t	73 t

[a] With respect to an all-rocket SSTO launcher.

For the same liftoff weight of 616 t the payload for the three systems is 7.0, 6.0, and 15.4 tons respectively. As is usually the case for the air augmented rocket, the increased system weight is not offset by the increase in thrust unless the oxygen in the secondary air is burned. For the ram rocket the payload is more than doubled. The ram rocket is not any kind of technology challenge, as many afterburning turbojet engines have ejector nozzles (such as the mentioned Saab J-35 Viggen). The ram rocket is a simple way to increase payload to orbit using the same rocket engine, or to reduce the size and cost of the rocket engines for a fixed payload.

(2) *LACE rocket, deeply cooled rocket and cooled turbojet-rocket (KLIN cycle)* are other propulsion system concepts that build onto the basic rocket engine for increased performance. This propulsion system creates an airbreathing rocket operating to about Mach 5.5. All of the hardware required for the thermodynamic processing of the air has been built in one form or another over the last 45 years. No differentiation in weight is made for the liquid air cycle versus the deeply cooled. Historical data suggests that these two systems are essentially equal in total system weight. One of authors (PC) saw a 1 m^3 liquid hydrogen/air heat exchanger operate for 1 min at Mitsubishi Heavy Industries in 1988 at outside air conditions of 38°C and 90% relative humidity without any water condensation on the heat exchanger tubes. The runtime was short because the container capturing the liquid air was overflowing and running down the ramp. So again this is not a technology issue, but (rather disappointingly) simply a decision-to-proceed issue. The KLIN cycle has the advantage of thrust for landing without the operation of a heat exchanger to provide the rocket with airbreathing capability. For a rocket vehicle with OWE equal to 76 metric tons and assuming the same OWE for other propulsion systems plus any system-specific differential, the TOGW for the two systems is:

WR	WR	O/F	TOGW	Savings[a]
LACE–deeply cooled rocket	6.40	3.85	476 t	140 t
LACE–deeply cooled rocket	6.00	3.60	443 t	173 t
LACE–deeply cooled rocket	5.50	3.10	404 t	212 t
KLIN cycle	5.70	3.40	432 t	184 t

[a] With respect to an all-rocket SSTO launcher.

Even considering the weight of the heat exchangers, the conversion of the rocket to an airbreathing rocket to Mach 5.5 offers considerable savings in weight and engine thrust. This straightforward improvement to the rocket engine offers major cost reductions [Czysz and Richards, 1998]. For the same liftoff weight of 616.2 t the payload for the airbreathing rocket systems and the KLIN cycle is between 24 and 38 tons. Had the Delta Clipper program survived and, had an airbreathing rocket been considered, the payload could have been increased and the gross weight reduced.

(3) *LACE rocket-ram-scramjet, and deeply cooled (DC) rocket-ram-scramjet* have the advantage of providing a weight saving equal to the ejector ram-scramjet but with an intermediate step. For the ejector ram-scramjet propulsion system the benefits cannot be realized until an operational scramjet is developed and qualified for flight operations. The advantage of the airbreathing rocket is that it can be an effective first step based on existing hardware arranged in a different manner and that can achieve approximately 60% of the eventual scramjet benefit without any new engine development. An operational system can be operating and realizing this benefit while the scramjet is being developed at its own pace, to be integrated later into the airbreathing rocket system (as A. Rudakov envisioned) to realize the final 40% improvement. During that time the airbreathing rocket system and the air vehicle have been proven in operation. No differentiation in weight is made for the liquid air cycle versus the deeply cooled. Historical data suggests that the systems are essentially equal in total system weight. For a vehicle for a rocket OWE equal to 76 metric tons and the OWE of other propulsion systems also fixed at 76 t, plus any differential for the propulsion system, the TOGW for the two systems is:

WR	WR	O/F	TOGW	Savings[a]
LACE rocket-ram-scramjet	4.00	2.00	283 t	334 t
LACE-DC rocket-ram-scramjet	3.50	1.40	245 t	372 t

[a] With respect to an all-rocket SSTO launcher.

Integration of the ram-scramjet into the airbreathing rocket system realizes the gains Rudakov reported in Figure 4.12 and reduces the gross weight by more than half. We are now approaching the weight of a vehicle that can safely abort on launch. With a weight ratio of 4 or less, the potential for horizontal takeoff becomes a real possibility, and a true, safe abort-on-launch capability could be reality.

(4) *Ejector ram-scramjet-rocket* operational area overlaps the airbreathing rocket and airbreathing rocket-ram/scramjet operational areas, so the complete spectrum for the ejector ram-scramjet-rocket is given below. At the higher weight ratios, the ejector ram-scramjet overlaps the airbreathing rockets. The advantage of the latter is that it can be developed from existing hardware and does not require the development of a new engine, the scramjet, for operational application. So there is a clear advantage for the application of airbreathing

rockets to launcher before the application of scramjets. The lower weight ratios overlap the airbreathing rockets integrated with the ejector ram-scramjet engine. Again, the initial operating capability offered with the airbreathing rocket is built onto, rather than being replaced by, a new system. Building on the airbreathing rocket offers the advantages of expanding the capability of a proven operational system rather than introducing a new vehicle, an important advantage for this propulsion system. If the scramjet were a developed propulsion system, beginning with the airbreathing rocket might not be the path of choice. However, attempts to take this path began in the late 1950s and have yet to yield even a small-scale operational weight engine. Recent developments are encouraging (*Aviation Week*, July 2003). But as of today there is neither an operational size scramjet nor research and development size scramjet that has the necessary maturity to apply them to an operational vehicle. Considering all of the scramjet programs canceled, perhaps there should have been an operational scramjet engine, but that is history, not an operational engine. With rocket ejectors, the ejector ram-scramjet has low-speed thrust and does not require an additional propulsion system for takeoff and low-speed acceleration. If propellant remains after entry, the engine can provide landing and go-around thrust.

For a vehicle for a rocket OWE equal to 76 metric tons and the OWE of other propulsion systems also at 76 t, plus any differential for the propulsion system, the TOGW for these systems is:

WR	WR	O/F	TOGW	Savings[a]
Ejector ram/scramjet-rocket	5.50	3.40	396 t	220 t
Ejector ram/scramjet-rocket	5.20	3.00	372 t	244 t
Ejector ram/scramjet-rocket	5.00	2.80	365 t	260 t
Ejector ram/scramjet-rocket	4.50	2.50	317 t	299 t
Ejector ram/scramjet-rocket	4.23	2.00	296 t	320 t
Ejector ram/scramjet-rocket	4.00	1.75	278 t	338 t
Ejector ram/scramjet-rocket	3.50	1.40	241 t	375 t

[a] With respect to an all-rocket SSTO launcher.

The ejector ram-scramjet operating to airbreathing Mach numbers from 6 to 14 offers the ability to reduce the gross weight by more than half.

(5) *ACES–LACE ejector scramjet-rocket, ACES–deeply cooled ejector scramjet-rocket* is another concept that dates back to the late 1950s, and, like the scramjet, has not proceeded beyond the ground test phase. This concept did have much more full-sized, flight-weight hardware built and tested very successfully in the 1960s. The difficulty has always been the sensitivity of SSTO space launchers to volume demands. This propulsion system is very attractive for TSTO launchers, with the air collection and separation system in the first stage [Rudakov et al., 1991b,c]. A number of these have been designed, but none have proceeded beyond the concepts stage. This will be discussed later in

the chapter dealing with mission-sized launcher systems. If indeed there is a problem with this propulsion system concept, it is the volume required for the liquid air separator. For volume-limited applications the size and weight of the airframe increases. It remains to be designed and demonstrated that the volume reduction potential of the deeply cooled gaseous separation is real [Lee et al., 2003]. As a result both systems are being treated as equal size, weight and performance systems.

For a vehicle for a rocket OWE equal to 76 metric tons and the OWE of other propulsion systems also 76 t, plus any differential for the propulsion system, the TOGW for the this systems is:

WR	WR	O/F	TOGW	Savings[a]
ACES-scramjet	2.90	0.50	252 t	364 t

[a] With respect to an all-rocket SSTO launcher.

Even though the weight ratio is less than for the ejector ram-scramjet-rocket, the gross weight is not, and that is result of the air separation system volume.

4.15 CONCLUSIONS WITH RESPECT TO CONTINUOUS CYCLES

Carl Builder was one of The Marquardt Company team that developed the Air Force Scramjet Program. Builder, Charles Lindley [Lindley, 1963] and John Ahern were responsible for developing the thermodynamic analysis for the scramjet. The standard approach for the ramjet and its extension to scramjets was based on an isentropic stagnation conditions analysis where First Law inefficiencies were evaluated in terms of stagnation pressure losses and an aerodynamic analysis of the engine flow path based on local Mach numbers and aerodynamic characteristics. For a subsonic through-flow engine (ramjet) where the heat addition is done at subsonic speeds, and where maximum pressure and temperatures do not exceed (typically) 20 atmospheres and 1,800 K, this type of approach is very acceptable. However for supersonic through-flow engines (scramjet) the heat addition is at supersonic Mach numbers and the Fanno and Rayleigh solution characteristics change sign [Scott and Riggins, 2000]; the isentropic stagnation pressure and temperature can reach 1000 atmospheres and 6,000 K. For this case a different approach was sought, and it was based on static conditions, not stagnation, the cycle being analyzed using a Second Law approach based on un-recovered (lost) available energy and entropy increases [Builder, 1964]. The original work was done in the late 1950s. By 1960 the Air Force Scramjet program associated with the aerospace plane began falling apart and this group sought employment elsewhere. Builder joined the Rand Corporation in the strategic planning department, giving up on further scramjet work because his work had been so close to completing a successful program and yet it was to be scrapped arbitrarily in favor of rockets. At the urging of The Marquardt Company scramjet manager, Artur Magar, Builder finally published a partial description of the approach in 1964. One of the authors (PC) and a colleague from Douglas Aircraft Company, Gordon Hamilton, visited Builder in 1984 to discuss the unfinished portion. As a result a paper was prepared that documented the complete approach [Czysz, 1988]. Although the original paper is now over 40 years old, the conclusions reached by Builder are as applicable today as then. In fact in reading this book the reader should come to the same conclusions. The tragedy is that in the intervening 45 years there has been no change in the space launchers propulsion systems, design or fabrication. Forty years after the Wright Brothers' first flight, jet power aircraft were flying in both Britain and Germany and by 50 years the first commercial jet transport was approaching operational status in Britain. As in the past, each rocket flies for the first, last and only time. The following paragraphs are Builder's conclusions from 1964, verbatim.

> Before summarizing, it would be well to note that the analyses and figures presented are based upon an ideal gas analysis. It is well recognized that the behavior of air is not ideal at high temperatures, above about 3500 or 4000°R. However. this analysis is restricted to the static conditions throughout the cycle, so the errors due to non-ideal behavior may not be as large as they would if stagnation conditions were being used. For example, the optimum compression enthalpy ratios determined in this analysis are generally under ten, which means that the temperatures at the end of the compressive device would be under 4000°R, because of this, it is believed that the trends and characteristics which have been presented for the Brayton Cycle family are quite valid, even if the specific values or curves are subject to adjustment for non-ideal gas effects.
>
> What conclusions can be drawn from this treatment of the Brayton Cycle family of airbreathing engines? First: we should note that a thermodynamic analysis on Mollier coordinates for the static gas conditions provides a consistent treatment of the complete spectrum of engines in this family.
>
> Second: an optimum amount of compression can be defined which depends only upon the overall processing efficiency of the heat-energy input of the cycle. That optimum amount of compression is compared to that available from ram stagnation of the engine airflow, a clearer insight is gained into the factors, which are common to the natural evolution of the turbojet, the conventional ramjet, and the supersonic combustion ramjet.
>
> Third: the energy conversion efficiency of the Brayton Cycle appears to continuously improve with speed, even approaching orbital velocities. It has been shown that the amount of compression is an important consideration in determining the energy conversion efficiency. Thus, we should not be overly preoccupied with the efficiency of compressive devices or the attainment of the maximum amount of compression possible. It is over-compression which causes the drop-off of conventional ramjet efficiencies above 10,000 fps.
>
> Finally, what does this analysis tell us with respect to potentially new engines lurking in the spectrum of chemical airbreathing propulsion? The turbojet, conventional ramjet, and super sonic combustion ramjet are clearly the dominant occupants of the three distinct regions of desired compression: mechanical, stagnation, and partial diffusion. However, we seem to lack engines for the transition regions. The turboramjet is a hybrid, which spans two of the three regions, but is probably not the best possible choice for the region in-between. In the Mach 3 to 5 regime, an engine

> having very modest mechanical compression with high processing efficiencies might be very attractive. In a sense, a fan-ramjet might be a suitable name for such a cycle; .the duct-burning turbofan and the air-turborocket could be considered close cousins to this hypothetical engine. At the higher speed end, around Mach 10, we can postulate a very efficient engine called the transonic combustion ramjet. There is still another important class of possibilities offered just outside the confines of the Brayton Cycle family: engines with non-adiabatic compression and expansion processes as a result of heat exchanges between the air and fuel. We might find a complete new spectrum of such engines awaiting our discovery.

At the time Builder wrote the AIAA-64-243 paper a major effort was underway to develop, in a single engine, the characteristics of both a turbojet and ramjet. The concept was called a turboramjet [Doublier et al., 1988; Escher, 1966a].

4.16 PULSE DETONATION ENGINES

4.16.1 What is a pulse detonation engine?

A pulse detonation engine (PDE) is a cyclical operation engine analogous to the World War II pulse jets. This engine fires *cyclically* resulting in an *intermittent* firing engine. The engine consists of an acoustically tuned pipe fed a detonatable mixture inside that, when ignited, sends the combustion products wave traveling down the pipe ahead of a detonation wave. After the products exit the tube, the tube is effectively scavenged, new fuel is then injected and a new mixture forms, sort of reloading the tube. The ignition process is then repeated, starting a new cycle. This periodic operation gives the PDE a characteristic cyclic rate and the characteristic sound that, in the V-1 case, gained it the nickname of 'buzz bomb'. A comparison of the pulse detonation rocket engine (PDRE) or pulse detonation engine (PDE) with today's standard rocket and turbojet cycles can show the potential of this propulsion system. A PDRE is a cylindrical tube with a defined length. The PDRE is an intermittent internal combustion/detonation engine with three strokes, namely injection, detonation, and exhaust, as shown in Figure 4.24 (see the color section). The PDRE is characterized by mechanical simplicity, and high compression ratio compared to continuous combustion engines. PDE/PDREs have the potential to significantly reduce the cost and complexity of today's liquid-propellant rocket engines. PDE/PDREs present novel alternatives to current gas turbine and/or rocket engines. The PDE/PDRE has the potential to provide dramatic improvements in both costs and performance for space propulsion applications. This is due primarily to the fact that detonations provide a more efficient mode of combustion over the conventional constant pressure approach of current engine technology. Large reductions in pumping, plumbing, and power requirements would also be possible with the PDE/PDRE. The self-compressing nature of the detonation combustion would dramatically reduce the need for massive oxidizer/fuel turbopumps. Pump pressure is 10 atmospheres not 300 atmospheres. Corresponding reductions in plumbing structural requirements and pumping power would be available with the

PDE/PDRE. Practical engineering issues and subsystem technologies need to be addressed to ensure that this potential is realized.

The PDE/PDRE possesses a significantly higher power density than conventional rocket designs. Detonation combustion produces large pressure increases in the combustion chamber (over and above those produced by pre-combustion turbopumps), creating large thrust forces at the chamber thrust wall. The result would be a very high thrust for an engine of equivalent dimensions as today's state-of-the-art propulsion systems, provided of course that the repetition rate were sufficiently high. Alternatively, an equivalent amount of thrust could be generated with a more compactly designed PDE/PDRE. Because additions in PDE/PDRE load-bearing structure do not increase proportionally with gained chamber thrust forces, the PDE/PDRE also would possess a much higher thrust-to-weight ratio than current chemical rocket engines. As shown in Figure 4.24 (see the color section) the basic cycle has one detonation wave traveling down the tube. One way to increase the thrust is make a multiple-tube engine [Norris, 2003] as is being developed by Pratt & Whitney. Note in the referenced article the detonation wave tubes are shown alone, which is satisfactory for sea-level testing. In all of the work done on PDEs for this chapter they were equipped with expansion nozzles just as a rocket engine would be, as shown in Figure 4.26. Another approach is to operate the detonation wave tube so there are multiple pulses traversing the tube [Norris, 2003].

The flow characteristics in a pulse detonation engine have been modeled previously using a variety of methods including zero-dimensional, one-dimensional, and two-dimensional unsteady analyses. All three of these levels are useful, but provide different types of information. Zero-dimensional analyses provide fast, global parametric trends for the unsteady operation of a PDE. One-dimensional models provide a first indication of the dominant wave processes and the manner in which they couple with the overall engine/vehicle system at a cost that is intermediate between zero- and two-dimensional models. Two-dimensional models have the capability of identifying the dominant multi-dimensional effects and their level of importance. However, multi-dimensional modeling requires a substantial investment of computational resources. Some specific areas of PDE/PDRE operation are inherently dominated by multi-dimensional phenomena and the only way to address these phenomena is by modeling the entire multi-dimensional process.

4.16.2 Pulse detonation engine performance

Analysis of engine flowpath physics, anchored to available experimental and CFD data, has shown this performance gain to be dependent on the propellant combination of choice, the chosen feed system, and other design parameters. It is only through detailed component energy balancing, coupled with unsteady detonation analysis and loss modeling that accurate estimates of the PDE/PDRE performance may be obtained. Three key parameters that determine performance are, *nozzle length* compared to the detonation tube length, *fill fraction* (i.e. whether there are multiple detonation waves present in the engine), and *detonation frequency*.

The first factor is *nozzle length*. Nozzle lengths can double the I_{sp} for a hydrocarbon-fueled, PDRE [Kailasanath, 2002]. The data from [Daniau, 2002] indicates that a divergent nozzle does not adversely affect the cycle time. Detonation frequencies in the 140 Hz range for hydrogen-oxygen and 110 Hz for hydrocarbon-oxygen mixtures are possible [Daniau, 2002]. The importance of the information, is that for a fully airframe integrated PDE with the aft-body forming the nozzle, a beta parameter in the 5 to 6 range enhances the PDE performance. Beta is the ratio between nozzle length and combustion chamber length. The combustion chamber length is not the entire tube length, the forward part of the tube being where the combustion is initiated, as shown in Figure 4.24 (see the color section).

The second factor that affects the performance of the PDE is the *fill fraction*. In an ideal detonation wave tube, Figure 4.24, the products of combustion exit the tube and the tube is purged before the next charge is introduced. An option is to introduce a new charge into the tube before the cycle is complete. In this case the fill fraction is less than 100%. That is, only a fraction of the tube receives a new charge. A reduction in the fill factor directly affects the I_{sp} of the engine, no matter at what frequency. In this chapter a 100% fill and a 60% fill fraction were used. The partial fill case provides 38% greater I_{sp} than the full fill case. The former is referred to a full fill and the latter is referred to a partial fill in the propulsion characteristics and sizing results.

The third factor affecting performance is the *detonation frequency*. In a chart shown by [Kailasanath, 2002], the real difference in the performance of the PDE versus the ramjet is governed by the detonation frequency of the PDE. The chart depicts experimentally determined thrust versus frequency for the PDE compared to a ramjet. For the PDE, as the frequency is increased the thrust increases almost linearly. For a modest frequency PDE operating at one-half the maximum frequency of 35 Hz, the thrust is 2.25 times the ramjet thrust. Since the reason for rocket-driven ejectors in the ramjet engine is to obtain greater thrust at low-speed, the pulse detonation engine has significant potential to increase low-speed performance over that of a ramjet. For this chapter a thrust of twice the subsonic through-flow ramjet engine was used (Figure 4.25).

In the low-speed flight regime, there is insufficient kinetic energy to produce a static compression enthalpy ratio (Ψ) sufficient to sustain ramjet operation. The rocket ejector ramjet is a means of providing sufficient nozzle enthalpy and pressure ratio to have an efficient ramjet at speeds lower than Mach 2.5. The PDRE does not depend on ram pressure: with the PDE ejector it has sufficient pressure ratio to operate at zero flight speed as either a pulse detonation rocket or as an airbreathing pulse detonation engine analogous to the rocket ejector ramjet. So, the question was to predict its potential performance using Builder's analysis.

The original Brayton cycle analysis by Builder [Builder, 1964] was based on the static enthalpy rise within the engine. Builder called the term (Ψ) the static enthalpy compression ratio. Extension of Builder's original work by Czysz [Czysz, 1988] continued that nomenclature. [Heiser and Pratt, 2002] and [Wu et al., 2002] use static temperature ratio for the value of (Ψ) so there is about one unit difference between the two definitions of Ψ in the 5,000 to 6,000 ft/sec range, with the temperature ratio definition being the lower value. The comparison in performance

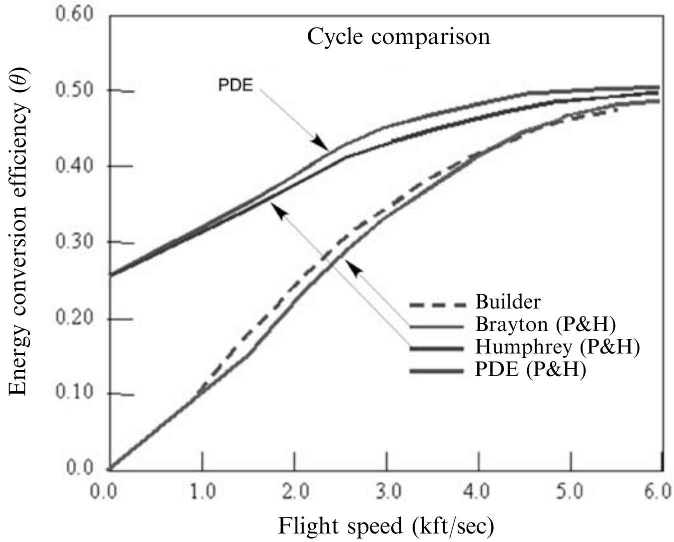

Figure 4.25. The pulse detonation engine (PDE) cycle compared to the Brayton cycle.

is made using the energy conversion efficiency (θ), that is, what fraction of the input fuel energy is converted into useful thrust work.

The energy conversion efficiency is defined as:

$$\theta = \frac{VT}{Q_c \dot{w}_{\text{fuel}}} = \frac{VI_{\text{sp}}}{Q_c}$$

$$\theta = \frac{VT}{\text{Fuel/Air} \cdot Q_c \dot{w}_{\text{air}}} = \frac{VT}{Q\dot{w}_{\text{air}}} = \frac{VT_{\text{sp}}}{Q}$$

$$I_{\text{sp}} = \frac{\theta Q_c}{V} \qquad T_{\text{sp}} = \frac{\theta Q}{V} \tag{4.13}$$

It is important to observe that as velocity is increased both the specific impulse, I_{sp} (thrust per unit fuel flow) and specific thrust, T_{sp} (thrust per unit air flow) decrease inversely proportional to velocity, even though θ may increase with velocity to a plateau value. Making a direct comparison between the energy conversion efficiency of Builder (θ) using the enthalpy ratio Ψ and the temperature ratio definition of Ψ by Yang and Heiser and Pratt did not produce a clear cut conclusion. The comparison for θ between Builder and Heiser & Pratt is rather good, considering that the values for Builder were independently done prior to 1964 using a Second Law approach that minimized the cycle entropy rise. Nevertheless the clear advantage in the lower speed range for the PDE is shown in Figure 4.25. The Humphrey cycle is a cycle that has been used as a surrogate for the pulse detonation cycle to estimate performance. As is shown it provides a good representation of the PDE energy conversion efficiency. The energy conversion efficiencies were converted into I_{sp} values (equation (4.11)) and compare the PDEs to conventional ram-scramjets.

Figure 4.26. Pulse detonation rocket engine (PDRE).

The more informative parameter for an acceleration-dominated SSTO application can be obtained from a comparison of effective specific impulse, that is, the acceleration specific impulse using the T-D difference rather than thrust, T, alone. For I_{spe} estimations the aircraft drag was determined from historical data for the two configurations of interest [Anon., HyFAC, 1970].

12. Pulse detonation-Rocket (PDR). Figure 4.26 depicts a *rocket PDE (or PDRE)*. The PDRE usually is charged with a near stoichiometric mixture of fuel and oxidizer, and they can be any detonatable fuel and oxidizer. For estimating the performance of launchers, only hydrogen was used as a fuel. The primary advantage of this system is less complexity and weight in the propellant fluid pressurization systems. The PDR is charged with fuel and oxidizer to generally less than 10 atmospheres. The resulting pressure behind the detonation wave can exceed 1000 atmospheres. The very uniform pressure behind the detonation wave yields a constant thrust pulse. In one of the Research Institutes located outside Beijing, China, and at the Aeronautical Research Laboratory at the University of Texas, Arlington, there are high-performance shock tube wind tunnels driven by a detonation wave tube, rather than the conventional hydrogen/oxygen combustion driver. The result is a very uniform driven pressure, with greater run time. The advantages are that the charge to the driver tube is a few atmospheres rather than the conventional tens to a hundred atmospheres. The detonation wave does the compression and heating rather than a mechanical pump. The PDR is such a device, made flight weight and operating at cyclic rate rather than with single firing. It can be installed in any rocket-powered aircraft or launcher, just as the rocket engine was installed, with the expansion nozzles located at the same place.

13. Pulse detonation rocket/ramjet engine. The evolution of a PDRE/PDE-based combined cycle engine is reported as a Russian concept [Kailasanath, 2002]. This Russian concept can operate over a range of flight conditions going from takeoff to hypersonic flight. The PDE can be integrated into an airframe in the same manner as a rocket and ram-scramjet. For the low-speed flight regime, and until there is sufficient kinetic energy to produce a static temperature ratio (Ψ) sufficient to sustain PDE operation, a strut-integrated PDRE is very much as a rocket ejector strut, except with less complexity and high-pressure fluid systems. Figure 4.27 shows a Russian concept for a *PDRE/ramjet PDE* that is equivalent to a rocket-ramjet system and can operate as an airbreathing system up to Mach 6, as described in [Kailasanath, 2002]. In the first operating region, to about Mach 2.3, the engine operates as a pulse detonation rocket ejector ramjet with the PDR replacing the

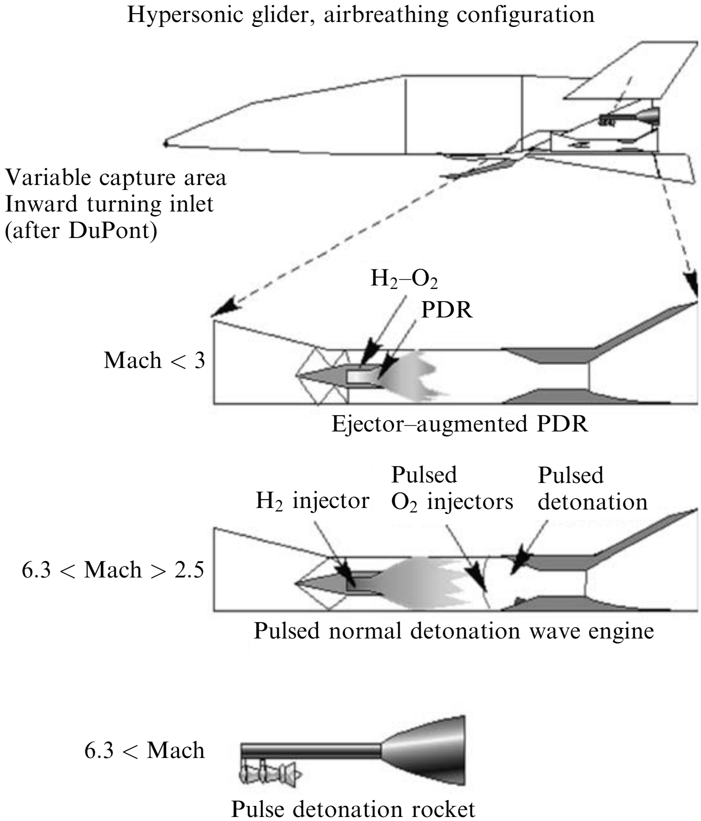

Figure 4.27. Integrated PDRE ramjet combined cycle.

rocket ejector. Above Mach 2.5, the PDR acts as an ejector and is a hydrogen ejector, with a downstream-pulsed oxygen injection which stabilizes an oscillating detonation wave in the engine ahead of the nozzle contraction. So the ramjet nozzle is driven by a detonation wave process. The shock system around the PDR ejector and the ejected hydrogen pressure isolate the detonation process from the inlet, and prevent regurgitation of the shock system. Above Mach 6 the PDR is the propulsion system, analogous to the airbreathing rocket or ejector ramjet-rocket. A representative installation is shown in a hypersonic glider at the top of the figure.

14. Pulse detonation rocket/ramjet-scramjet engine. Figure 4.28 shows a Russian concept for a *PDE/ramjet/ODWE* equivalent to a rocket-ram-scramjet system as described in [Kailasanath, 2002]. The PDE module is shown integrated into a blended body airbreathing configuration much as a rocket ejector ramjet-scramjet is integrated. Except for the pulsed nature of the ejector strut operation, the engine is essentially a rocket ejector ramjet. The PDRE operation is confined to the strut in low-speed phase of the operation. The engine spans the operational envelope from

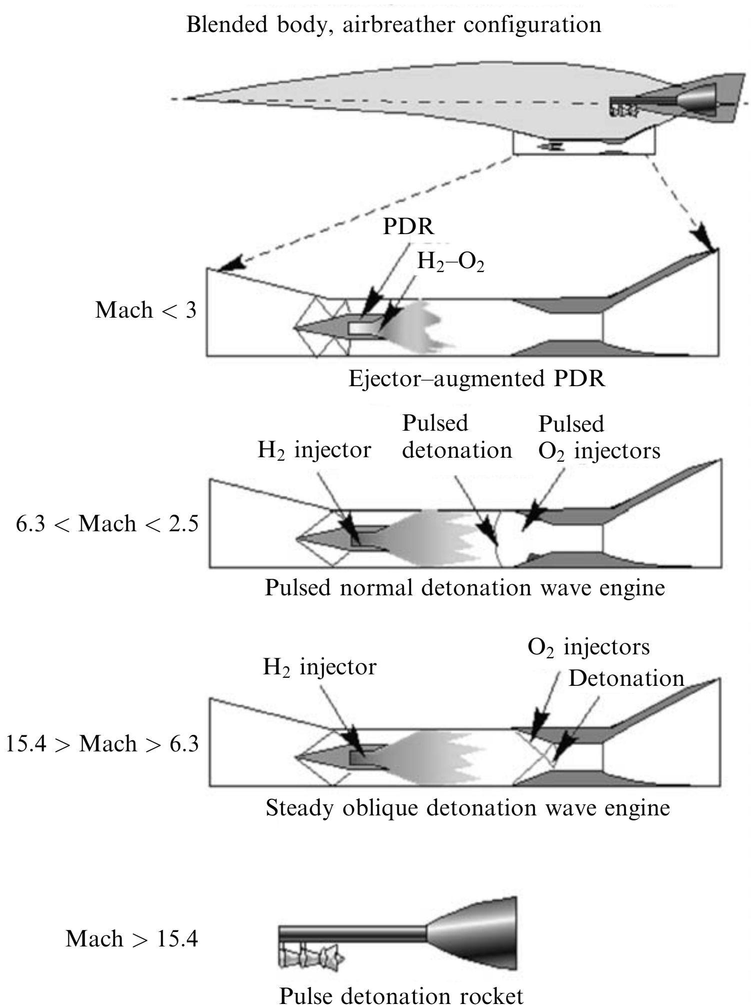

Figure 4.28. Integrated PDRE ram-scramjet combined cycle.

takeoff to perhaps a little above Mach 15. For the PDE engine above Mach 6 flight the propulsion configuration is an airbreathing PDE that incorporates elements of the rocket PDE, with the kinetic compression of the rocket ejector ramjet producing a pulsed detonation wave within a steady flow device. This concept is equivalent to a LACE or deeply cooled airbreathing rocket. For speed greater than Mach 6, the propulsion converts to a steady-state operation as an oblique detonation wave engine (ODWE), as it is necessary to transition the detonation wave from an oscillation detonation wave structure to a steady oblique detonation wave structure. In this operating mode it is equivalent to a scramjet [Kailasanath, 2002]. In this latter mode the engine operates in a continuous detonation process and is now a steady-state engine. Above the maximum airbreathing speed the PDR provides the thrust to orbital velocity. A representative installation in an airbreathing configuration is shown at the top of Figure 4.28. Externally there is little difference in the configuration from the conventional scramjet configuration except for perhaps a longer engine cowl.

The pulse detonation propulsion systems offer considerable promise in reduced weight and propellant pumping challenges. The PDRE are in a period of experimentation and development. The question remains: Can the eventual operational hardware developed capture the promise shown in the analytical studies? In this chapter we assume the operational hardware has captured the promised performance so a valid measure of the potential is presented.

4.17 CONCLUSIONS WITH RESPECT TO PULSE DETONATION CYCLES

The three pulse detonation engine systems are compared in a single table in similar manner to the continuous engine cycles. For a vehicle powered by a conventional continuous rocket engine, the OWE is 76 metric tons; the equivalent PDR OWE is 70 metric tons because of the lesser total vehicle volume and the lesser propellant pumping hardware and weight. The assumption made was that the engine weight is the same as an equivalent thrust conventional rocket engine. This is yet to be demonstrated with operational engine weights, but it is a reasonable expectation considering the much less complicated hardware required. With these considerations, the OWE of 70 metric tons is equivalent to the conventional all-rocket. For other propulsion systems the OWE is 70 tons plus any differential weight for the propulsion system. The TOGW for the three systems is:

WR	WR	O/F	TOGW	Savings[a]
Pulse detonation rocket	8.10	6.00	567 t	49 t
Pulse detonation rocket/ramjet	5.10	4.60	357 t	259 t
Pulse detonation rocket/ram/scramjet	3.20	1.80	224 t	392 t

[a] With respect to an all-rocket SSTO launcher.

Perhaps the PDEs are the beginning of the Builder conclusion some 40 years ago, 'There is still another important class of possibilities offered just outside the confines of the Brayton Cycle family: engines with non-adiabatic compression and expansion processes as a result of heat exchanges between the air and fuel *and engines with non-steady operation* (italics by the authors). We might find a complete new spectrum of such engines awaiting our discovery.'

4.18 COMPARISON OF CONTINUOUS OPERATION AND PULSED CYCLES

Adding the PDEs to the results in Figure 4.23, the result is Figure 4.29 that gives the SSTO mass ratio (weight ratio) to reach a 100 nautical mile orbit (185 km) with hydrogen for fuel as a function of the maximum airbreathing Mach number for both continuous and cyclic operation engines. Seven classes of propulsion systems are indicated: rocket-derived, airbreathing (AB) rocket, so-called KLIN cycle, ejector ramjet, scram-LACE, air collection and enrichment systems (ACES) and pulse detonation derived engines (PDR/PDRE). As in Figure 4.23, there is a discontinuity in the results. If the mass ratio to orbit is to be significantly reduced the carried oxidizer to fuel ratio (oxygen and hydrogen) must be reduced to 5 or less. That means at least an airbreathing rocket or airbreathing PDR to achieve that threshold.

The weight ratio, hence the takeoff gross weight, is a direct result of the propellant weight with respect to the OWE. The propellant weight is a direct function of the oxidizer-to-fuel ratio (O/F).

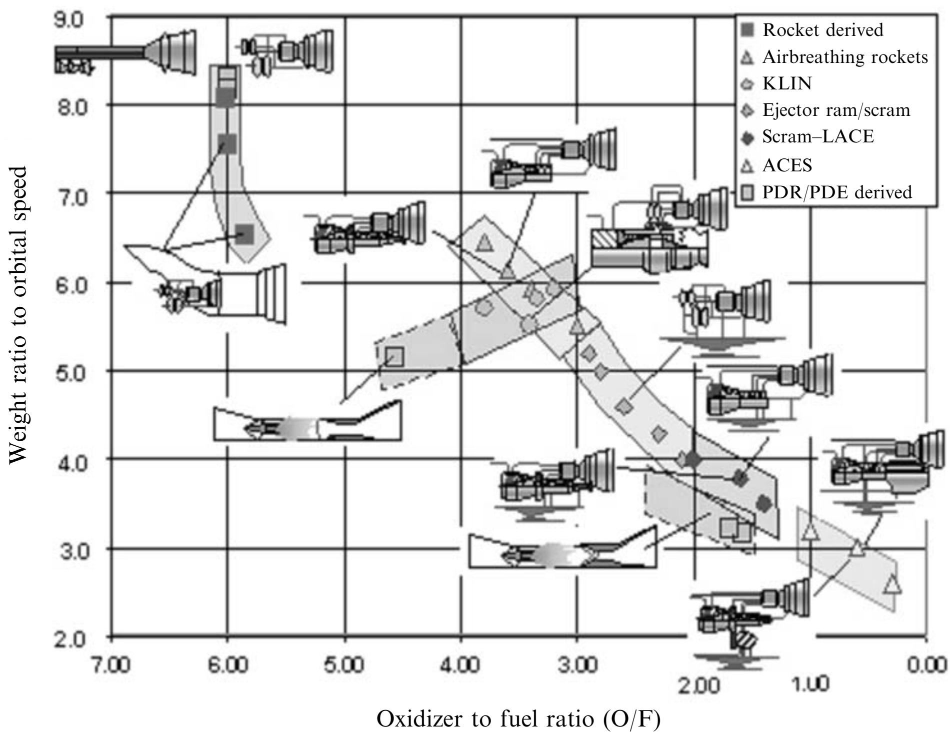

Figure 4.29. The PDE improves the total weight ratio.

$$\mathrm{WR} = 1 + \frac{W_{\mathrm{ppl}}}{\mathrm{OWE}} = 1 + \frac{W_{\mathrm{fuel}}}{\mathrm{OWE}}\left(1 + \frac{\mathrm{O}}{\mathrm{F}}\right)$$
$$\mathrm{TOGW} = \mathrm{WR/OWE} = \mathrm{OWE}\left[1 + \frac{W_{\mathrm{fuel}}}{\mathrm{OWE}}\left(1 + \frac{\mathrm{O}}{\mathrm{F}}\right)\right]$$
$$\frac{W_{\mathrm{fuel}}}{\mathrm{OWE}} = \frac{(\mathrm{WR} - 1)}{(1 + \mathrm{O/F})} \tag{4.14}$$

This equation set (4.14) is equations (4.12a) and (4.12b) repeated. Remember in this equation the oxidizer/fuel ratio is the oxidizer/fuel ratio carried on the launcher with the associated weight ratio, not the rocket engine oxidizer/fuel ratio. The importance of the graph is that the gross weight is a function of one airframe parameter, OWE, and two propulsion parameters, and that the gross weight is directly proportional to the carried oxidizer to fuel ratio. Reduce the carried oxidizer and the gross weight and resultant engine thrust decrease proportionately. Beginning with the rocket point in Figure 4.29 at a weight ratio of 8.1 to the ACES weight ratio of 3.0, a straight line constructed between these points has all of the continuous hydrogen-fueled propulsion system lying along that line. Except for the PDR, the PDEs lie below the continuous propulsion curve, hence their fuel weight to OWE ratio is *less than one*.

The PDR is essentially equivalent to the rocket in terms of weight ratio to orbital velocity. The PDE/ramjet is equivalent to a rocket-ramjet system and lies inline with the thermally integrated KLIN cycle at a higher oxidizer-to-fuel ratio and lower weight ratio. So the PDE/ramjet has an oxidizer-to-fuel ratio about one unit greater than the KLIN cycle and about one-half unit less in terms of weight ratio. In terms of characteristics the PDE/ramjet appears to be more like a thermally integrated rocket/turbojet than the airbreathing rocket propulsion systems. In terms of the impact on operational systems, the next set of charts will size launchers to the same mission and payload so these propulsion system differences can be evaluated in terms of launcher system size and weight.

The PDE/ram-scramjet jet is equivalent to the thermally integrated airbreathing rocket-ram-scramjet systems and lies to the left (greater O/F ratio) of the thermally integrated ram-scramjet cycles at a slightly lesser weight ratio to orbital speed near the RBCC propulsion systems of Yamanaka (scram-LACE), Builder (ejector ram-scramjet) and Rudakov (deeply cooled-ram-scramjet). From the cycle analysis the PDE appears to have performance advantages and disadvantages with respect to the continuous cycles (lesser weight ratio but greater oxidizer-to-fuel ratio) that must be evaluated on launcher-sizing programs. These three propulsion configurations were evaluated in detail. When deciding the thrust-to-weight ratio, cost of development, and payload capability for all these various configurations must be examined without bias to determine the best overall configuration to build. These ideas require further parametric investigation to finalize the comparison.

So, while most conventional propulsion systems have fuel weight approximately equal to the OWE, the PDE propulsion systems have fuel weights that are less than the OWE, hence the advantage of PDE systems. This is a simple and fundamental relationship to judge hydrogen/oxygen propellant SSTO results. As shown in Table 4.6 for other fuels, the ratio will not be one.

In determining the launcher size for each propulsion system concept, an important parameter is the installed engine thrust-to-weight ratio. A non-gimbaled (that is fixed and not steerable by pivoting the engine) rocket engine for space operation could have an engine thrust-to-weight ratio as large as 90. For a large gimbaled engine, such as the Space Shuttle main engine (SSME) that value is about 55 for the installed engine. And this value will be the reference value. The liftoff thrust generally determines the maximum engine thrust for the vehicle. For a given vehicle thrust-to-weight ratio at liftoff or takeoff, the weight of the engines is a function of the required vehicle thrust-to-weight ratio at liftoff, the thrust margin, the weight ratio and the OWE. Thus:

$$W_{\text{engine}} = \text{WR} \cdot \text{TWTO} \cdot \text{OWE}/\text{ETWR} \tag{4.15}$$

TWTO = vehicle thrust-to-weight ratio at takeoff; ETWR = engine thrust-to-weight ratio; WR = weight ratio to achieve orbit speed; OWE = vehicle operational weight empty.

The weight ratio is the total mission weight ratio including all maneuvering propellant. For vertical liftoff the launcher thrust-to-weight ratio is at least 1.35. For horizontal takeoff the launcher thrust-to-weight ratio is in the 0.75 to 0.90 range. Usually if the horizontal takeoff thrust-to-weight ratio exceeds one, there is a significant weight penalty (Czysz and Vandenkerckhove, 2000). The engine thrust-to-weight ratio has been a constant source of controversy and discussion for airbreathing engines. One approach to avoid the arguments before the sizing procedure begins, and that has stopped the sizing process in the past, is to find a suitable relationship for determining the engine thrust-to-weight ratio. For the authors' efforts, that procedure is to assume the total installed engine weight is a constant equal to the all-rocket launcher. The resulting engine thrust-to-weight ratio for all other propulsion systems can then be determined as:

$$\text{ETWR} = \left(\frac{\text{WR}}{\text{WR}_{\text{Rkt}}}\right)\left(\frac{\text{TWTO}}{\text{TWTO}_{\text{Rkt}}}\right)\left(\frac{\text{OWE}}{\text{OWE}_{\text{R}}}\right)\text{ETWR}_{\text{Rkt}}$$

$$\text{ETWR} = \left(\frac{\text{WR}}{8.1}\right)\left(\frac{\text{TWTO}}{1.35}\right)\cdot(1)\cdot 55 = 5.0\cdot\text{WR}\cdot\text{TWTO} \tag{4.16}$$

Evaluating equation (4.16) for the data in Figure 4.29 results in Figure 4.30, engine thrust-to-weight ratio as a function of weight ratio to orbital speed with minimum maneuver propellant. There is one calibration point in the open literature from 1966. William J. Escher completed the testing of the SERJ (supercharged ejector ram jet) to flight duplicated engine entrance conditions of Mach 8, the maximum airbreathing speed for SERJ. In those test, the flight weight engine would have had an installed thrust-to-weight ratio of 22, had it been installed in an aircraft. From Figure 3.3, the mass ratio for an airbreathing speed of Mach 8 is 5. From

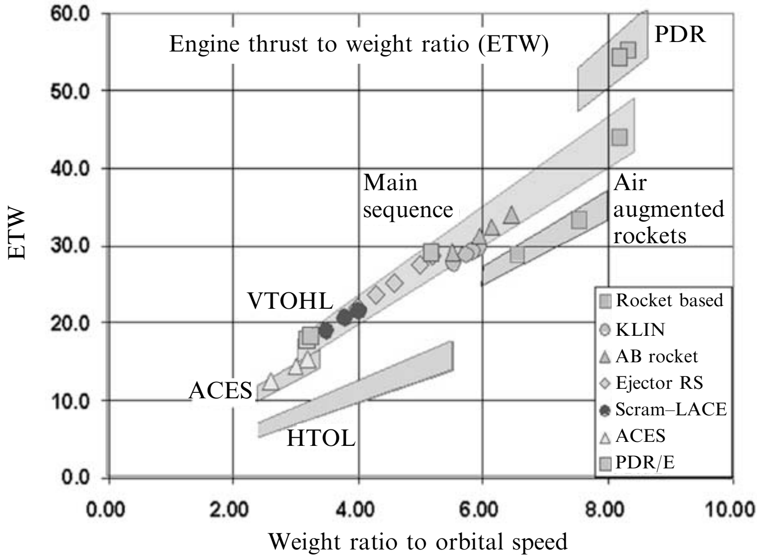

Figure 4.30. Engine thrust-to-weight ratio decreases with weight ratio.

Figure 4.30 the range of values for a weight ratio of 5 is 25 to 27. So the SERJ engine would have had a weight just slightly greater than the assumed all-rocket engine weight. This is a simple approach to estimate the operational weight of an arbitrary propulsion system. However, a word of caution: this approach is to estimate the installed engine thrust-to-weight ratio for an integrated propulsion system. It will not estimate the weight of the engine airbreather approach shown in Figure 2.14, as that is an impracticable system by any standard. It is very easy to have estimates that destroy an airbreathing approach in that, to some, they appear perfectly reasonable when they are in fact based on misinformation. The relationship given in equation (4.16) will give an obtainable value, given the industrial capability available today and the history of actual integrated airbreathing cycles.

Figure 4.30 shows that air augmented rockets and ram rockets have lower engine thrust-to-weight ratios because of the secondary air duct weight. ACES has a lower engine thrust-to-weight ratio because of the weight of the air separation hardware. And, as postulated, PDEs have a higher engine thrust-to-weight ratio because the pumping hardware is lighter than the conventional rocket turbopumps, with a lower required launcher takeoff thrust to weight ratio. One of the advantages of wing-supported horizontal takeoff is an acceptable lower engine thrust-to-weight ratio. So as discussed earlier in conjunction with Figure 3.24, if the mass ratio permits horizontal takeoff without serious weight penalty, it has the operational advantage to open up more launch sites, and also the advantage of less strenuous engine thrust-to-weight requirements.

4.19 LAUNCHER SIZING WITH DIFFERENT PROPULSION SYSTEMS

The real measure of a propulsion system's performance is when, installed in a vehicle and sized to a defined payload and mission, it is then compared to other propulsion systems. For the evaluation of the propulsion systems in this chapter the reference mission is an SSTO mission, launching into 200 km orbit with a 28.5-degree inclination and carrying a 7 metric ton payload with a carried net density of 2.83 lb/ft^3 (100 kg/m^3). The sizing was accomplished using the sizing program described in [Cyzsz and Vandenkerckhove, 2000] using the configurations in Figure 3.11. Hypergolic propellants were carried for in-orbit maneuvering, corresponding to a ΔV of 490 m/sec that resulted in a weight ratio for in-orbit maneuvering of 1.1148. The orbital maneuvering propellant includes propellant to circularize the orbit and a retro-burn to deorbit the vehicle. All of the weight ratios presented in this chapter include the orbital maneuvering weight ratio of 1.1148, assumed constant for all propulsion systems. That is, a weight ratio of 8.1 for the all-rocket includes the 1.1148 weight ratio, so the actual weight ratio just to achieve orbital velocity is 7.2659. The sizing equations are given below. For details of the range of values, and the definition of the terms, see [Czysz and Vandenkerckhove, 2000]. The equations are solved simultaneously for the planform area and Küchemann's tau; then the other vehicle characteristics can be determined for that specific solution. The approach was originally developed for application to 'Copper Canyon' and the National Aerospace Plane programs. It was used in the Phase 1 screening of 32 high-speed civil transport concepts for the effort NASA sponsored with Douglas Aircraft Company. The solution was adapted to MathCad by a Parks College graduate student, Ignacio Guerro, for use in the Senior Cap Stone Aerospace Design Course. Douglas Aircraft checked the solutions against a number of subsonic transports, and the author (PC) checked the solutions against the hypersonic aircraft concept of McDonnell Aircraft Advanced Engineering and the comparisons between this approach and specific converged design data were very close.

$$W_{\text{dry}} = \frac{\left[I_{\text{str}} K_{\text{w}} S_{\text{plan}} + C_{\text{sys}} + W_{\text{eprv}} + \dfrac{\text{TWTO}\cdot\text{WR}}{\text{ETWR}}(W_{\text{pay}} + W_{\text{crew}})\right]}{\left[\dfrac{1}{(1+\mu_{\text{a}})} - f_{\text{sys}}\cdot\dfrac{\text{TWTO}\cdot\text{WR}}{\text{ETWR}}\right]}$$

$$W_{\text{dry}} = \text{OWE} - (W_{\text{pay}} + W_{\text{crew}}) - W_{\text{trapped fluids}} - W_{\text{consumed fluids}}\,\text{OEW} \tag{4.17}$$

$$W_{\text{dry}} = \frac{\tau S_{\text{plan}}^{1.5}(1 - k_{\text{vv}} - k_{\text{vs}}) - (V_{\text{pcrw}} + k_{\text{crw}})N_{\text{crw}} - W_{\text{pay}}/\rho_{\text{pay}}}{\dfrac{(\text{WR}-1)}{\rho_{\text{ppl}}} + k_{\text{ve}}\cdot\text{TWTO}\cdot\text{WR}} - W_{\text{pay}} - f_{\text{crw}} N_{\text{crw}} \tag{4.18}$$

Three key determinants of the airframe empty weight are the total volume, the total surface area, and the structural index. The first two are geometry-determined, and the latter is the total airframe structure (no equipment) divided by the total wetted area. Table 4.7 gives data on 10 different structural approaches developed

Table 4.7. Specific weights of structures, structural indices.

	Source	I_{str} Structural index (metric)	I_{str} Structural index (Imperial)	Operational weight empty
1	NASA, active, 1993 [Pegg et al., 1993]	13.8 kg/m^2	2.83 lb/ft^2	33.3 tons
2	NASA, passive, 1993 [Pegg et al., 1993]	16.6 kg/m^2	3.40 lb/ft^2	43.4
3	HyFAC, passive, 1970 1970 projection to 1985	17.1 kg/m^2	3.50 lb/ft^2	45.5
4	VDK, passive, FUTURE	18.0 kg/m^2	3.68 lb/ft^2	49.6
5	VDK, passive, CURRENT	21.0 kg/m^2	4.30 lb/ft^2	65.8
6	HyFAC, passive, 1970 1970 industrial capability	22.0 kg/m^2	4.50 lb/ft^2	72.1
7	HyFAC, passive, 1970 1966 industrial capability	22.7 kg/m^2	4.66 lb/ft^2	76.7
8	HyFAC, passive, 1970 non-integral tank	25.4 kg/m^2	5.20 lb/ft^2	96.5
9	HyFAC, passive, 1970 1970 hypersonic demonstrator	29.3 kg/m^2	6.00 lb/ft^2	130.6
10	HyFAC, hot structure, 1970 non-integral tank	32.5 kg/m^2	6.66 lb/ft^2	163.4

over the past 35 years and their impact on the empty weight of a launcher with a 7-ton payload and a weight ratio of 6. They are listed in increasing weight per unit wetted area. Except for structures 8 and 10, all are cold primary structure constituted by an internally insulated cryogenic integral propellant tank, protected by internally insulated, metal thermal protection shingles that stand off from the structure/tank wall and provide an insulating air gap. The metal shingles are formed from two sheets of metal with a gap filled with a high-temperature insulation. The edges are sealed so a multilayer, vacuum insulation can be employed, if needed. Structure 8 has the same thermal protection system, but the propellant tank and primary structure are separate, that is, a non-integral tank. Structure 10 is a non-integral tank concept with an external hot structure, separated from the propellant tank by insulation and air gap (like the fuselage of the X-15). The SR-71 and X-15 wings were hot structures that were not protected by insulation, and the structure and fuel were heated by the absorbed aerodynamic heating. In these cases the determining structural parameter was the hot strength and stiffness of the material. In all other cases the determining structural parameter was the cold strength and stiffness of the material. All the concepts protect the structure or tank with passive insulation, except concept one that uses propellant (fuel) to pump heat away from the structure and convert it into useful work (Figures 4.17 and 4.18).

4.20 STRUCTURAL CONCEPT AND STRUCTURAL INDEX, ISTR

Structures 1 and 2 (Table 4.7) are from reasonably recent reports (1993) concerning metal thermal protection systems (TPS) with current advanced titanium and metal matrix composite materials. Structures 3, 6, 7, 8, 9 and 10 are from the Hypersonic Research Facilities Study (HyFAC) conducted for NASA by McDonnell Aircraft Company, Advanced Engineering Department, from 1968 to 1970. One of the authors (PC) was the Deputy Study Manager for that program. Except for structure 3, which anticipated the developments of advanced titanium, metal matrix composite materials and high-temperature plastic matrix materials, the other concepts employed high-temperature chrome–nickel alloys, and coated refractory metals for the thermal protection shingles that enclosed vacuum multilayer insulation. Structure 9 was an effort to minimize the cost of a short flight time research vehicle (5 min) at the expense of increased weight by using more readily available high-temperature materials.

Structures 4 and 5 were the work of the late Jean Vandenkerckhove (VDK) and the author to characterize the high-temperature metal and ceramic materials available in Europe. Carbon/carbon, silicone carbide/carbon and silicone carbide/silicone carbide structural material from SEP, Bordeaux (now SAFRAN/SNECMA, Bordeaux), and metal matrix composites from British Petroleum, Sudbury, along with the conventional aircraft materials were characterized from material supplied by the major aerospace manufacturers in Europe. At that time no materials from the former Soviet Union were included. Notice that they center on the HyFAC structural data. These values were used in most of the work done by the authors.

The two structural indices used by J. Vandenkerckhove result in an OEW, for a weight ratio 6 launcher, of 49.6 t employing VDK FUTURE and 65.8 t employing VDK CURRENT. The same vehicle using 1970 McDonnell Douglas structural index is 72.1 tons, and 45.5 tons projected to 15 years in the future, to 1985. Assuming the current availability of materials and manufacturing processes is equivalent to 1970, then the vehicle empty weight is from 65.8 to 72.1 metric tons. Assuming the current availability of materials and manufacturing processes is equivalent to the 1985 projection, and from what the authors saw at SEP, Bordeaux, BP, Sudbury, and NPO Kompozit, Moscow, then the vehicle empty weight is from 45.5 to 49.6 metric tons. These values should span what is possible today much as Saturn V was constructed from what was available in 1965. The non-integral structural concepts are not competitive, resulting in an OEW of 96.5 tons for a passively insulated tank, and 163.4 tons for a hot structure concept. The 1993 results from Pegg and Hunt show some improvement in the passive structural concept (about a 5% reduction), not a critical item. The focus on future launcher must be durability over a long period of use, not one-time lightness. The design, build and operations philosophy must be akin to the Boeing B-52, not an ICBM.

The cold, insulated integral tank structural concept employed in these studies remains appropriate and valid. The concept has withstood the test of many challenges, but remains the lightest and lowest-cost approach to high-temperature, hypersonic aircraft structure that was established by practice as reported in [Anon., HyFAC, 1970]. The primary structure is principally aluminum with steel and titanium where strength is a requirement. The aerodynamic surface is made by interleaved smooth shingles with standoff and insulation material that provide a high-temperature radiation surface to dissipate most of the incoming aerodynamic heating to space. Less than 3% of the incoming aerodynamic heating reaches the aluminum structure. The HyFAC data is circa 1968 and based on the materials and insulation available then. With advanced rapid solidification rate (RSR) materials and superplastic forming with diffusion bonding, together with silicon carbide and carbon fiber reinforcements to fabricate metal matrix composites (MMC) the values in Table 4.7 should be conservative.

The active TPS values are from a recent source, as given by [Pegg and Hunt, 1993]. Depending on the duration of the flight that heat can be absorbed in the airframe thermal capacitor or removed by an active thermal management system (Figures 4.17 and 4.18). For some short duration (10 min or less) research flights and some orbital ascent flights, no active thermal management system is necessary. For a long-duration cruise flight some means of moving the incoming thermal energy to a site where it can be disposed of or used to perform mechanical work is required. The original concept in the 1970s was implemented using high-temperature refractory metals such as columbium (niobium), tantalum, molybdenum, and Réne 41 and other refractory alloys, which have densities greater than steel (9 to 17 kg/m^3). Today rapid solidification rate (RSR) titanium, RSR metal matrix composites (MMC), titanium aluminide, carbon/carbon, and silicon carbide/silicon carbide composites can achieve the same temperature performance at much less weight. The weight estimates based on scaling of the 1970 data are therefore very conservative. The concept uses conventional aircraft construction techniques for most of the aircraft; the shingles are well within the current manufacturing capabilities considering the hot isostatic pressing, superplastic forming, and diffusion bonding available in the gas turbine industry. For longer-duration flights required for long-range cruise, the advantages of active thermal management is clear. With current materials, whether actively thermally managed for cruise, or passively thermally managed for exit and entry, it should be possible in 2005-plus to build a structure for a hypersonic aircraft that is between 3.0 and 4.0 lb/ft^2 (14.6 and 19.5 kg/m^2) using materials and processes available now.

The OWE is a function of the structural index (I_{str}) and a weak function of the weight ratio to orbit (Figure 4.32). There is a 15% margin on the OEW assigned by the sizing equations. The OWE for a structural index other than the structural index for structural concept 5, VDK CURRENT, of 21 kg/m^2 that applies to the sizing results in this book is as given in equation (4.19).

$$\mathrm{OWE} = 65.8[0.003226(I_{str})^2 - 0.04366 I_{str} + 0.4943](0.02369 \cdot \mathrm{WR} + 0.8579) \quad (4.19)$$

4.21 SIZING RESULTS FOR CONTINUOUS AND PULSE DETONATION ENGINES

For the evaluation of the different propulsion systems, structural concept 5, VDK CURRENT, at 21.0 kg/m^2 was used. The propulsion systems (Figure 4.29) were installed in the appropriate configuration concept, and sized to the mission. Figure 4.31 presents the gross weight and OWE as a function of oxidizer-to-fuel ratio, and Figure 4.32 presents the gross weight and OWE as a function of weight ratio. Each of these presentations provides different perspectives of the sizing results and the characteristics of the propulsion systems. Whenever presenting results as a function of oxidizer-to-fuel ratio, Figure 4.31, there is always the discontinuity between the rockets and the airbreathing systems. For the rocket-derived systems, the all-rocket is not the top point, but the second from the top. The air augmented rocket is heavier than the all-rocket because the thrust increase and reduced oxidizer-to-fuel ratio does not offset the weight of the ejector system. In Figure 4.32 this is clearly shown, as the Air Augmented rocket is at a mass ratio of 7.5 and heavier than the all-rocket. Below that point, the OWE value is on top of the correlation line indicating a heavier empty weight. The ram rocket, in which the oxygen in the ejector secondary air is burned, is a different case and the weight and oxidizer-to-fuel are less than the all-rocket. The ram rocket has a gross weight similar to the PDE. The difference is the ram rocket is at the end of its improvement capability while the PDE is just at the beginning of its potential improvement cycle. The pulse detonation

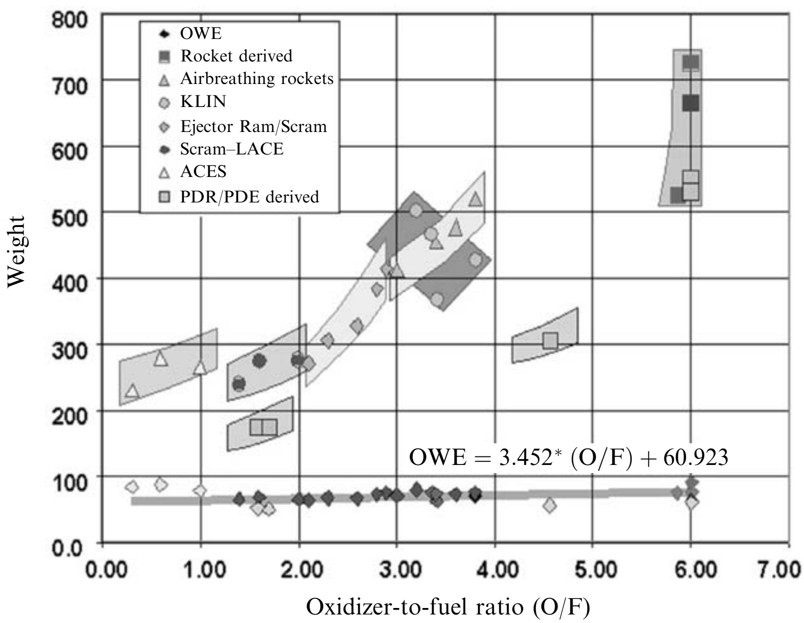

Figure 4.31. Gross weight decreases significantly as oxidizer-to-fuel ratio decreases. Operational weight empty (empty weight plus payload) is nearly constant.

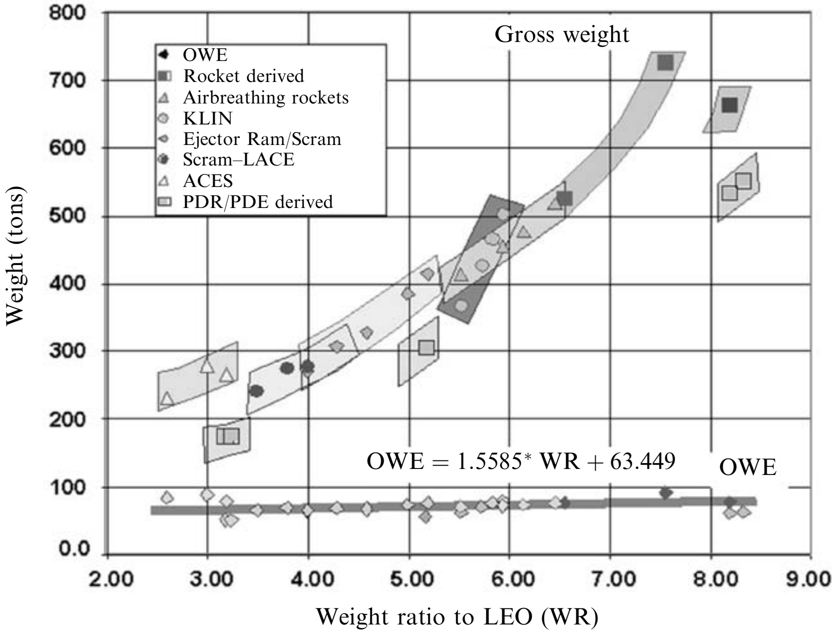

Figure 4.32. Gross weight decreases significantly as weight ratio decreases. Operational weight empty is almost constant.

rocket (PDR) has a gross weight similar to the ram rocket, with much less complexity. The important result is that either can reduce the gross weight by 200 metric tons! This is comparable to the highest values of the airbreathing rockets and the KLIN cycle. So the incorporation of some airbreathing in the rocket, whether an ejector burning fuel in the secondary air stream (ram rocket) or by direct airbreathing rocket (LACE, deeply cooled rocket or KLIN cycle) results in a significant advantage in gross liftoff weight and engine size and thrust reduction (28% reduction).

Direct airbreathing rockets (LACE, deeply cooled rocket or KLIN cycle) form a grouping in the center of each graph, in the 3 to 4 oxidizer-to-fuel ratio and in the 5.5 to 6.5 weight ratio area. These propulsion cycles form the first steps in airbreathing propulsion and are capable of reducing the gross weight from nearly 700 metric tons to 400 to 500 metric tons. There maximum airbreathing Mach number is in the 5 to 6 range. The important factor is that this is a beginning capability that, with adaptation to further airbreathing (scram LACE), can achieve gross weights in the 200 to 300 metric ton range. As shown in Figure 3.3, as the airbreathing speed is increased, both the oxidizer-to-fuel ratio and mass ratio decrease. As Mach 12 airbreathing speed is reached, further increases in airbreathing speed do not result in additional decreases in the mass ratio. This results from the fact that, as shown in equation (4.11), both the thrust and specific impulse for an airbreathing system are decreasing inversely proportional to speed and the drag could be increasing. When the effective specific impulse (based on thrust minus drag) falls below the effective specific impulse of a rocket, the rocket is a better accelerator. So attempting to fly to orbital speed with an airbreather will result in a larger vehicle that requires more propellant.

Air collection, enrichment and separation (ACES) began being recommended for TSTO launcher. As discussed in Chapter 2 and later in the chapter, for that application the ACES has significant advantages. However, for SSTO the added volume in the orbital vehicle can have penalties, depending on the system design. Even though the ACES has both a lower weight ratio and oxidizer-to-fuel ratio, its gross weight is about the same as the ejector ram-scramjet and the scram-LACE and scram–deeply cooled. In both plots, the OWE is heavier than the correlation line, as was the air augmented rocket.

What does fall below the OWE correlation line are the PDE points. That is for two reasons: less volume required and lower-weight propellant pumping systems. In Figure 4.32 it is almost possible to envision a new main sequence of PDEs parallel and lower than the continuous operation engines. As this class of engine is developed into operational systems the potential exists for this class to reduce both rocket and airbreathing classes in gross and empty weight. What is not clear is whether the cyclic engine can have the equivalent to the airbreathing rocket and its ACES derivative. These latter engines may remain as continuous operations engine cycles only.

If we take the OWE results and subtract the 7-ton payload to yield the OWE, then it is possible to see how volume affects the magnitude of the empty weight. Figure 4.33 shows the empty weight value as a function of the total vehicle volume. The correlation is rather good. First notice that the triangles representing the ACES

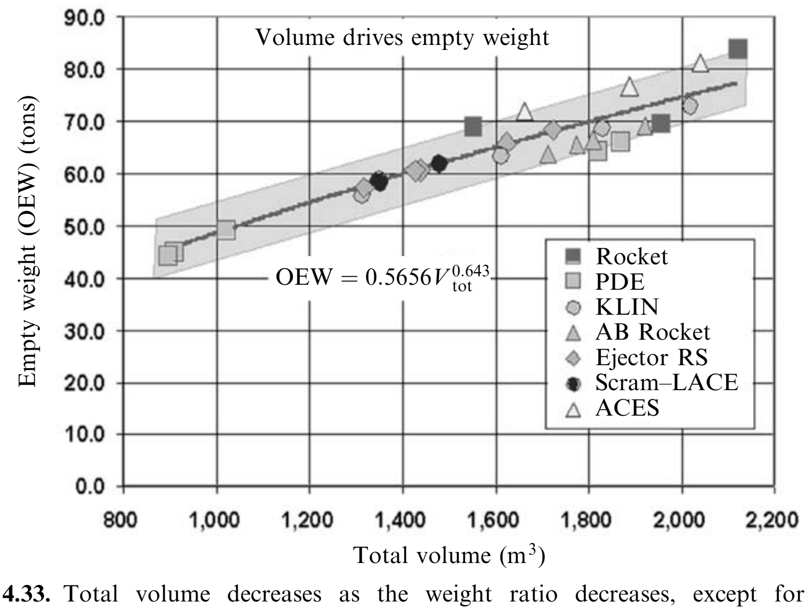

Figure 4.33. Total volume decreases as the weight ratio decreases, except for ACES propulsion system.

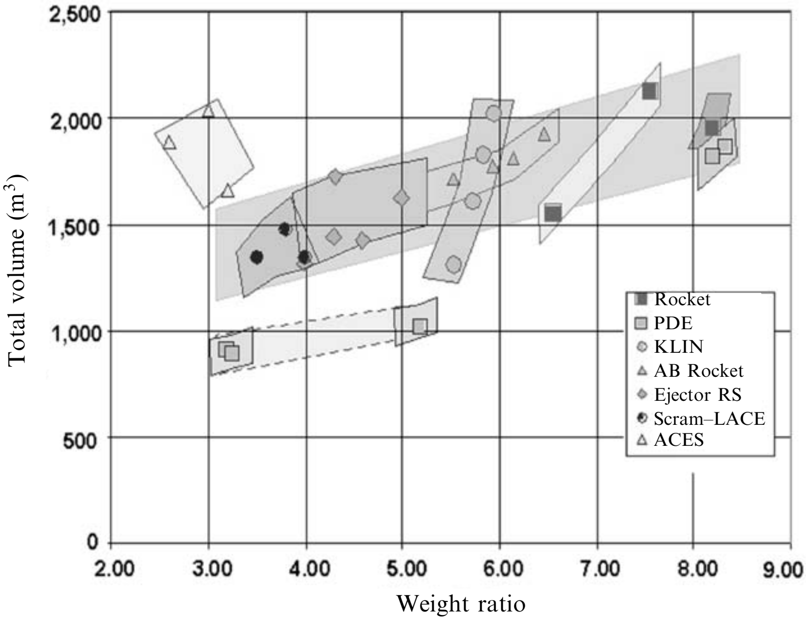

Figure 4.34. Empty weight is less if total volume is less. ACES is heavier because volume is greater.

propulsion system have almost the largest volumes. The largest is the air augmented rocket. This clearly explains the OWE values in the previous two graphs where the OWE values were greater than the correlation curve through the other cycles. It is also clear that the PDEs have some of the lowest volume values for the propulsion systems presented. So the variation in empty weight can primarily be explained by variation in total volume. The OEW is also a function of the structural index and the weight ratio to orbit (Figure 4.32). As given in equation (4.19), the mean OEW for any other structural index than the VDK CURRENT at 21.0 kg/m^2 and any mass ratio can be determined.

Representing the data in Figure 4.32 in terms of total volume rather than weight, results in Figure 4.34. Clearly the ACES lies above the main sequence of propulsion systems (large shaded area) and the PDEs lie below the main sequence of propulsion systems. Whether the PDE-ramjet and PDE-scramjet areas can be connected remains to be seen, but there should be no technical reason why future PDE systems would not span that area.

What we can conclude so far is:

(1) The structural concept for an insulated cold primary structure is an important decision that can have a significant impact on vehicle empty weight. For launchers passive thermal protection is more than adequate. However, for a cruising vehicle passive insulation permits too much of the aerodynamic

heating to reach the cryogenic tanks, and an active heat removal scheme is required. Pegg and Hunt employed fuel as the heat transfer agent. Others include water, water-saturated capillary blankets, and other phase-change materials between the backside of the shingle and the integral tank structure outside surface. All of these are appropriate for most of the structure for a blended body or all-body configurations. The leading edges are based on sodium heat pipes that move the thermal energy to a lower temperature area or a heat exchanger. Control surfaces are a case-by-case basis and each is designed based on configuration and local flow conditions. In terms of the total vehicle and an advanced concept initial sizing, these have minimal impact on the final size and weight. But if the reader wishes to refine the estimate, the values in Table 4.7 can be improved by the following first-order correction that assumes the leading edges are 10% of the total surface area, and the control surfaces are 15% of the total surface area. These corrections are based on values from [Anon., HyFAC, 1970] for an operational vehicle.

$$I_{\mathrm{str}}\ 5.87 + 0.75(I_{\mathrm{str}})_{\mathrm{Table\ 4.7}} \tag{4.20}$$

So the VDK CURRENT structural index would become 21.6 kg/m^2.

(2) Given the thermal protection system and structural concept, the next most important determinant of the empty weight is the total volume of the vehicle (Figure 4.33). In some cases the total volume is a response to the change in oxidizer-to-fuel ratio; in other cases it is the inherent volume of the propulsion concept (ACES and PDE systems) as shown in Figure 4.34.

(3) The gross weight is a direct result of the weight ratio to orbit (Figure 4.32), which is determined by the propulsion system oxidizer-to-fuel ratio (Figure 4.29).

(4) The threshold value for the oxidizer-to-fuel ratio and weight ratio that clearly separate airbreathing systems from rocket-derived vehicles are 3.9 and 6.5, respectively (Figures 4.31 and 4.32). At these values the OWE for a launcher with a 7-ton payload is 71.48 tons and the gross weight is 510 tons, less than the 690 tons for the all-rocket.

(5) The ACES system for an SSTO will have a greater volume than a corresponding ejector ram-scramjet propulsion system: even though the weight ratio and oxidizer-to-fuel ratio are less, some of the weight ratio and oxidizer-to-fuel advantages may be offset (Figures 4.31 and 4.34).

(6) Because of the reduced pumping system weights and the lesser installed volumes, the pulse detonation propulsion systems will have a lesser volume and less weight than a corresponding sustained operation propulsion system.

(7) Propulsion system weight was assumed to be a constant, equal to that for the all-rocket with a gross weight of 690 tons, liftoff thrust of 932 tons, and a propulsion system weight of 16.9 tons. The exceptions were the air augmented rocket in which an ejector structure was added to the airframe, the ACES system in which the air separation system was added to the LACE or deeply cooled air-breathing rockets, and the PDEs where the conventional turbopumps were replaced by lower-pressure-ratio turbocompressors (Figure 4.30).

4.22 OPERATIONAL CONFIGURATION CONCEPTS, SSTO AND TSTO

For the rocket-derived vehicles, the configuration is the hypersonic glider derived from the Air Force Flight Dynamics Laboratory FDL-7 C/D. This configuration is depicted accelerating to orbit in Figure 4.35. As depicted it is powered by either a LACE or a deeply cooled airbreathing rocket. Although sized as an SSTO vehicle it could also represent the second stage of a TSTO accelerating to orbital speed. At the altitude shown, the Mach number is greater than 6, so the inward-turning inlet is retracted. As the Model 176, the McDonnell Douglas version for MOL, it was designed in 1964 for a fleet of 10 vehicles to fly between 75 and 90 flights per year with an individual aircraft flights between overhaul of 200 and an operational life of 25 years.

For the airbreathing vehicles, the configuration is derived from the McDonnell Blended Body, as shown in Figure 4.36. The configuration is depicted in an accelerating climb with a combination of rocket and ramjet power as the vehicle accelerates through the transonic flight regime. It is depicted climbing from an air launch from a C5A, but it could just as easily have separated from an An225. If this were a TSTO vehicle, a smaller version of the vehicle in Figure 4.35 would be on top, and separation would be in the Mach 8 to 14 region. As one of the reference operational vehicles for the 1970 HyFAC study, this airbreathing launcher was the first stage of the TSTO vehicle that staged at Mach 10 to 12. Later, as the CFD (Computational Fluid Dynamics) verification model for Copper Canyon and the subsequent NASP program, it was a SSTO configuration. Again the design goals were for frequent

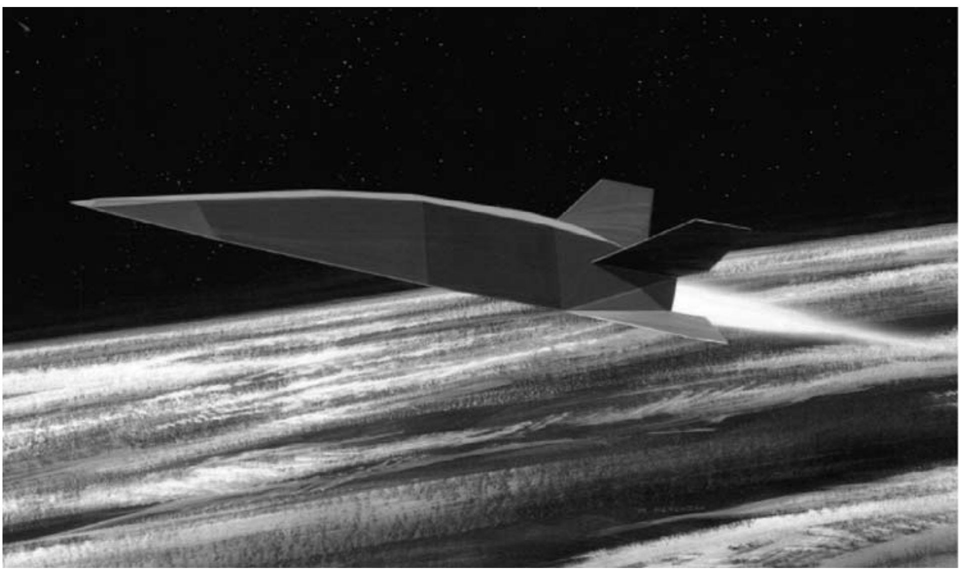

Figure 4.35. LACE rocket powered VTOHL SSTO with a gross weight of 450 tons, a weight ratio of 5.5 and an oxidizer/fuel ratio of 3.5.

HYFAC M12

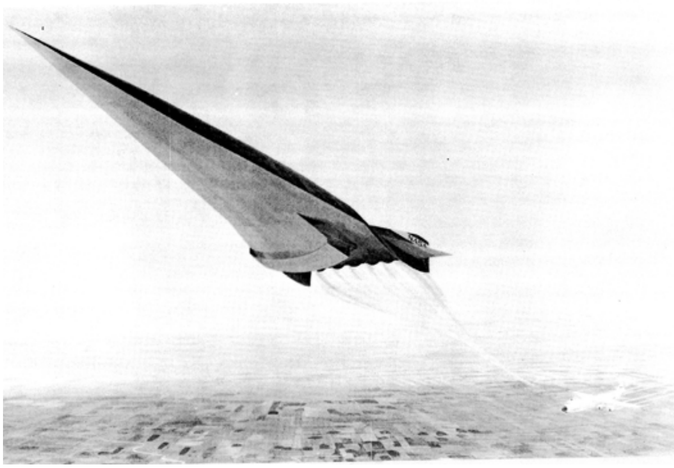

Figure 4.36. Ejector ram-scramjet powered HTOL SSTO with a gross weight of 300 tons, a weight ratio of 4.3 and an oxidizer/fuel ratio of 2.2.

flight spanning a long operational life with significant flights between overhaul, as for the Model 176. Unfortunately no actual goal numbers survive.

For a versatile and payload-flexible launcher, in the authors' opinion a TSTO vehicle offers the best options. And there were some elegant and practical TSTO launchers designed, but unfortunately never built. Figure 4.37 shows two of those launchers, the MBB Sänger (upper) and the Dassualt Aviation Star-H (lower). The MBB Sänger program was directed by Ernst Hogenhaur, who conceived of the first stage as also being constructed as a hypersonic transport carrying over 200 passengers. This highly refined blended wing-body was developed through extensive wind tunnel testing, including the detailed testing of the second stage separation at Mach 7 in the Ludwig tube facility at the Goettingen DLR Institute in Germany. For the MBB Sänger the second stage was a flat-bottomed hypersonic glider that carried the ascent propellant and payload to orbit. It was designed as an automatically piloted vehicle. Considering that the net density of a passenger cabin is about 80 kg/m^3 and that of sub-cooled hydrogen is 76 kg/m^3 a hydrogen tank makes a perfect cabin for a weight of passengers equal to the weight of the hydrogen, with much less thermal insulation requirements. Switching the fuel to sub-cooled methane means that there is volume for both the passengers and methane, replacing the hydrogen and oxygen for the launcher.

Dassault Aviation Star-H used a different approach for the second stage. Since the thermally protected second stage glider is the most costly, the Dassualt Aviation Star-H approach is to minimize its size and carry payload only, and provide for the propellant and thrust in a separate expendable rocket. This reduces the size of the hypersonic glider, in this case depicted as the Hermes. This was also the philosophy of Glebe Lozino-Lozinski in the Mig 50-50 concept that dated back to 1968. Both

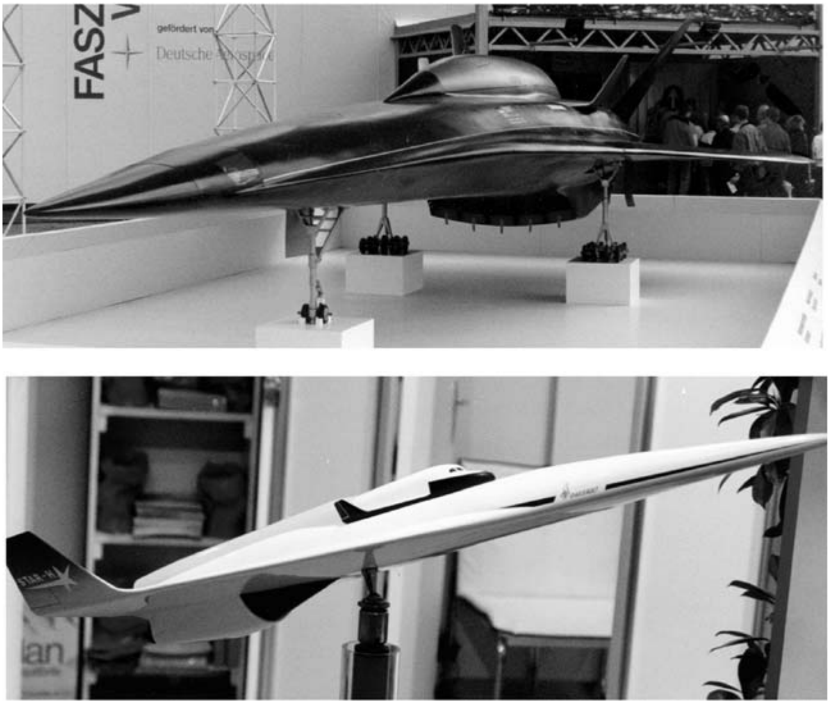

Figure 4.37. Two elegant TSTO designs. The MBB Sänger (top) and Dassault Aviation Star-H (bottom).

the MBB Sänger and the Dassualt Aviation Star-H are elegant designs that would have been successful had they been built. However, both suffered from a propulsion community mistaken assumption that the turbojet was the best accelerator for lower-speed operation (Mach 2.5 to 3.0). The resultant massive over-under turbojet/ramjet propulsion system of the MBB Sänger and the turboramjet propulsion of the Dassualt Aviation Star-H appear to be their downfall. A rocket ejector ramjet or airbreathing rocket would have provided excellent acceleration capability. In [Czysz and Vandenkerckhove, 2000] a TSTO with a rocket ejector ramjet is compared to a TSTO powered by a turboramjet. Both TSTO launchers were sized to deliver a 7-ton payload to 463 km in a 28.5-degree inclination orbit. The staging Mach number was 7 (same as the MBB Sänger). The turboramjet launcher consisted of a second stage weighing 108.9 tons, carried by a 282.7-ton first stage for a total liftoff weight of 393.0 tons. The rocket ejector ramjet launcher consisted of a second stage weighing 118.4 tons, carried by a 141.6-ton first stage for a total liftoff weight of 261.0 tons. The reason for the difference is the ejector ramjet thrust is nearly constant from transonic to staging speeds, while the turboramjet at staging speed is only 25% of the transonic thrust. The turboramjet will have significantly more thrust at takeoff but that is not as important as maintaining a constant supersonic acceleration. The result is the turboramjet launcher suffers a 50% gross weight penalty at takeoff compared to the ejector ramjet.

If a commercial hypersonic transport version of the first stage was contemplated, then the propulsion system would have to be changed to a cruise-focused system, replacing the acceleration-focused system of the launcher. The acceleration-focused system must maximize thrust minus drag and minimize zero lift drag. The cruise-focused system must maximize aerodynamic efficiency (lift-to-drag ratio) and propulsion efficiency (energy conversion efficiency). This change in focus almost precludes a single system from doing both missions. The exception might be Rudakov's combined cycle with the performance shown in Figure 4.16. The attempt to get one gas turbine based propulsion system to do both is the weakness of most of these TSTO programs. Yet TSTO launchers are an excellent option, and with a suitably powered TSTO a substantial saving in gross weight can be realized together with significant payload flexibility.

P. Czysz and the late Jean Vandenkerckhove extensively examined in the 1990s the SSTO compared to the TSTO based on rocket ejector ram-scramjet propulsion. That work later became part of an AIAA Progress in Aeronautics and Astronautics book [Czysz and Vandenkerckhove, 2000; Vandenkerckhove, 1991, 1992a,b, 1993]. Figure 4.38 compares the takeoff gross weight (TOGW) results, and Figure 4.39 compares the dry weight (OEW) results. Nine comparisons are made as given

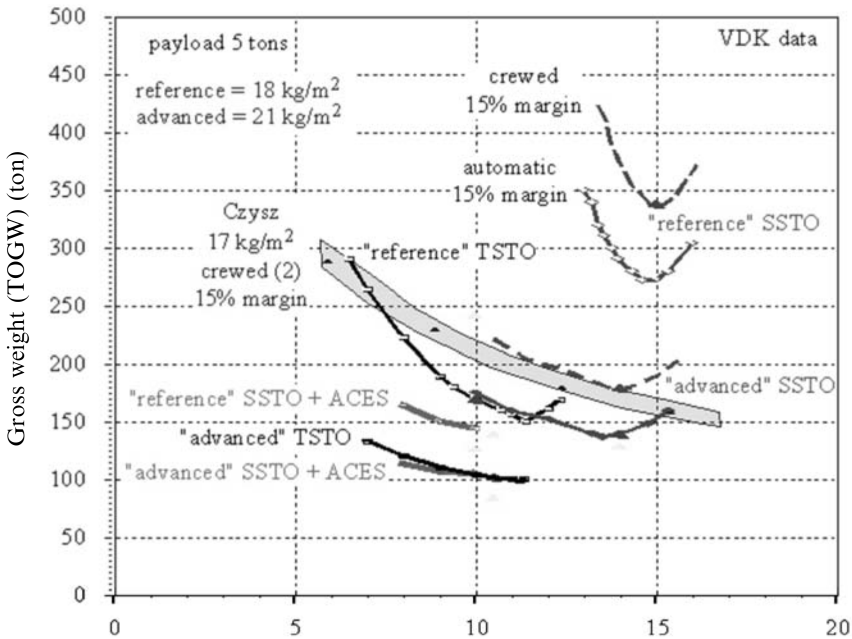

Figure 4.38. Comparison of SSTO and TSTO results for TOGW.

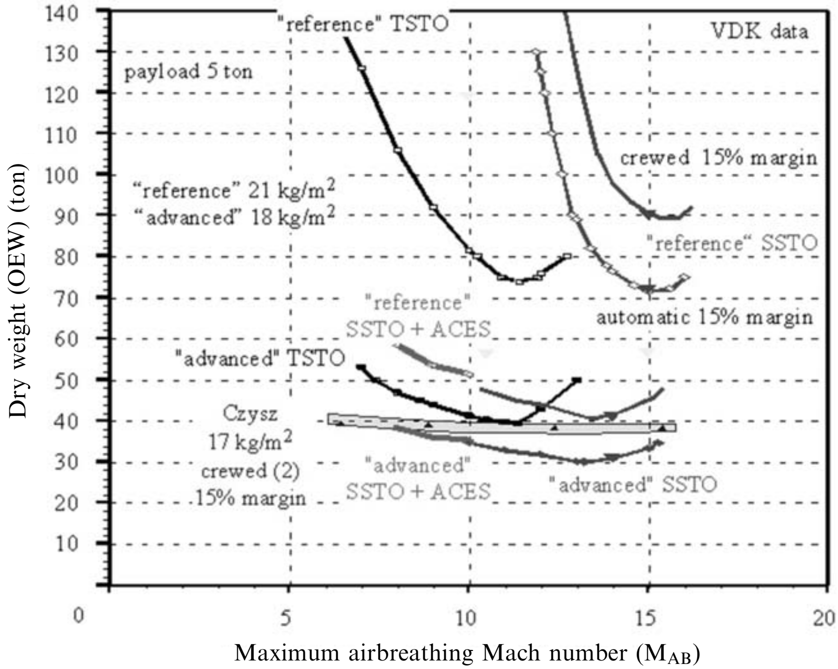

Figure 4.39. Comparison of SSTO and TSTO results for OEW.

below. Note that any crew for space operations or crew rotation on an orbital station are considered payload, not crew, that is, pilots.

(1) SSTO with VDK CURRENT structural concept (reference 21.0 kg/m^2) with 15% dry margin and crewed (piloted) by two crew members with provisions for orbital stay, powered by ejector ram-scramjet of VDK design, HYPERJET Mk #3 [Vandenkerckhove, 1993a].
(2) SSTO with VDK CURRENT structural concept (reference 21.0 kg/m^2) with 15% dry margin and piloted by automatic flight control system, powered by ejector ram-scramjet of VDK design, HYPERJET Mk #3 [Vandenkerckhove, 1993a].
(3) SSTO with VDK FUTURE structural concept (advanced 18.0 kg/m^2) with 15% dry margin and crewed (piloted) by two crew members with provisions for orbital stay, powered by ejector ram-scramjet of VDK design, HYPERJET Mk #3 [Vandenkerckhove, 1993a].
(4) SSTO with VDK FUTURE structural concept (advanced 18.0 kg/m^2) with 15% dry margin and piloted by automatic flight control system, powered by ejector ram-scramjet of VDK design, HYPERJET Mk #3 [Vandenkerckhove, 1993a].
(5) SSTO with Czysz structural concept from McDonnell HyFAC Study (17.0 kg/m^2) with 15% dry margin and piloted by automatic flight control system

powered by engines with maximum airbreathing Mach numbers from 6.0 to 12.0 from the engine sequence in Figure 3.3.

(6) TSTO with VDK CURRENT structural concept (reference 21.0 kg/m^2) with 15% dry margin and piloted by automatic flight control system powered by ejector ram-scramjet of VDK design, HYPERJET Mk #3 [Vandenkerckhove, 1993a].
(7) TSTO with VDK FUTURE structural concept (advanced 18.0 kg/m^2) with 15% dry margin and crewed (piloted) by two crew members with provisions for orbital stay, powered by ejector ram-scramjet of VDK design, HYPERJET Mk #3 [Vandenkerckhove, 1993a].
(8) SSTO with VDK CURRENT structural concept (reference 21.0 kg/m^2) with 15% dry margin and piloted by automatic flight control system, powered by ejector ram-scramjet of VDK design with ACES (air collection, enrichment and collection).
(9) SSTO with VDK FUTURE structural concept (advanced 18.0 kg/m^2) with 15% dry margin and piloted by automatic flight control system, powered by ejector ram-scramjet of VDK design with ACES (air collection, enrichment and collection).

Because this is a specific engine design, the results have much sharper minimums than generic engine concepts. In Figure 4.37 we can see the impact of piloted (crewed) systems for both 'reference' SSTO and 'advanced' SSTO launchers. For the reference the gross weight increment is almost 90 tons. The minimum gross weight occurs at Mach 15 maximum airbreathing speed for the 'reference' structural concept, and Mach 14 for the 'advanced' structural concept. The gross weight is driven by the difference in empty weight shown in Figure 4.38. In this figure the 90 tons difference in OEW is clearly seen for the 'reference' structural concept. The results from 'hypersonic convergence' [Czysz, 1989] is close to the results for VDK 'advanced' solutions. The difference is the family of combined cycle propulsion yields a design point at each Mach number whereas the VDK results are for a particular ejector ramjet engine configuration.

Examining the TSTO results there are two interesting observations. The first is that the minimum empty weight of both TSTO stages is about the same as the single SSTO stage for both the 'reference' and 'advanced' structural concepts. This means that other than design and engineering costs, the airframe cost based on weight should be quite comparable. Note that the design, engineering and production costs are not the driving costs in launcher operations (see Figure 3.2). The second is that the gross weight for the 'reference' TSTO is only slightly greater than the 'advanced' SSTO, and that the 'advanced' TSTO is one of the lowest gross weights. This is due to the fact that much less mass (second stage only) must be delivered to orbit for the TSTO compared to the entire SSTO vehicle. So TSTO can have an acquisition and cost advantage over SSTO. If both vehicles are automatic then crew costs are not a factor.

The last comparison is the addition of ACES (air collection, enrichment and collection) to the SSTO propulsion system. This permits the SSTO to have an offset capability analogous to the TSTO as it collects the enriched air oxidizer for ascent into orbit. Jean Vandenkerckhove and Patrick Hendrick wrote the complete ACES performance code themselves rather than depend on 1960s programs. The performance of the hardware came primarily from two sources, John Leingang in the United States and N. Maita and his colleagues with the National Aerospace Laboratories (now: JAXA) in Japan. The results show that the addition of ACES to SSTO results in the SSTO weight now being equivalent to TSTO. The results are different that those from Figures 4.31 and 4.32, but the Vandenkerckhove results are based on a detailed system analysis of individual hardware items, while the other results are based on correlated results. However, the results are not that dissimilar in that both suggest that an SSTO with ACES is as light as an advanced SSTO.

Examining Figures 4.31 and 4.32 there are a number of options that yield very similar results. Considering the 'advanced' SSTO with automatic flight controls for a maximum airbreathing Mach number of 14, and the 'reference' TSTO with automatic flight controls for a maximum airbreathing Mach number of 12, and the 'reference' SSTO plus ACES with automatic flight controls for a maximum airbreathing Mach number of 10, we have three different systems, two of which use current materials and fabrication capability, with essentially the same gross weight and different empty weights. Considering the 'advanced' TSTO with automatic flight controls for a maximum airbreathing Mach number of 12, and the 'advanced' SSTO plus ACES with automatic flight controls for a maximum airbreathing Mach number of 10 we have two different systems with essentially the same gross weight and similar empty weights. So there are two approaches to reach minimum weight launchers. One way is to focus on TSTO with inherent payload size and weight flexibility or focus on SSTO with ACES and a more focused payload capability, such as discussed for the Model 176 resupply and crew rescue vehicle for the MOL.

4.23 EMERGING PROPULSION SYSTEM CONCEPTS IN DEVELOPMENT

This section will discuss two propulsion systems that operate in a manner different from conventional airbreathing chemical combustion systems.

The first originated in the former Soviet Union, probably in the 1970s, as a total energy concept that coupled aerodynamic forces with electromagnetic forces and required a local plasma flow to exist for the system to work. The Russian name for the system is 'Ayaks', or Ajax, and is described as a magneto-hydro-dynamic (MHD) energy bypass system. If the flow inside (or even around) the aircraft is sufficiently ionized, i.e. a plasma, then the MHD system equivalent to an induction generator can remove energy (velocity) from the flow as an electrical current, with minimal aerodynamic diffusion [Tretyakov, 1995]. This reduces the energy lost through the shock waves in conventional inlet aerodynamic deceleration. If that electrical power is transmitted to the equivalent of an induction motor (a Lorentz force accelerator) then electromagnetic interaction with the plasma can add energy (velocity) back to the flow. The motivation for the MHD system is the realization that the electromagnetic energy transfer suffers less of an entropy rise (irreversible energy loss) than aerodynamic diffusion and expansion, so the net thrust is greater. If the flow field around the aircraft is a plasma, flow [Gorelov et al., 1995] energy can be removed at the nose by an MHD generator that alters the shock wave structure around the vehicle, reducing the total drag [Batenin et al, 1997]. Again, because the flow is ionized, the flow in the propulsion inlet system can be turned by MHD Lorentz forces instead of physical inlet ramps (a form of morphing). That may dramatically reduce the weight and mechanical complexity of the inlet/nozzle system. In this chapter the focus is on the energy bypass system.

The second is creating heated air to produce thrust not by combustion, but by the interaction of the air and intense electromagnetic radiation (either by a LASER or by a microwave beam). The advantage is that only some working fluid to produce thrust is needed (usually water), which can be dense when stored and produce a low-molecular-weight gas when heated. It needs not to be combustible. Since the energy is remote from the vehicle, a directed energy beam on Earth, the Moon, a space station or wherever must provide the power to the vehicle to produce thrust. This vehicle is termed the 'Lightcraft' by its inventor, Professor Leik Myarbo of Rennselaer Polytechnic Institute.

Ajax

The initial Ajax system information came from two sources [Novichokv, 1990a, 1990b]. One was from a Russian document and the other an article 'Space Wings of Russia and the Ukraine' in the September 1990 magazine *Echoes of the Planet/Aerospace*. The article states that the project originates in the State Hypersonic Systems Scientific Research Enterprise (GNIPGS) in St Petersburg, which is (or was) headed by Vladimir Freishtadt. The article goes on to state the cooperation of industrial enterprises, Technical Institutes, the VPK (Military Industrial Commission) and RAN (Russian Academy of Sciences). All the discussions with individuals about Ajax stress both the global range capability at hypersonic speeds and the directed energy device for peaceful purposes. Use as a space launcher is not mentioned. In the Russian and Ukrainian literature, beginning in 1990, there were articles about a new long-range aircraft named Ajax, whose development had begun at least 10 years earlier, that cruised at hypersonic speeds. Its propulsion system employed a coupled magneto-hydro-dynamic (MHD) element that (reportedly) significantly increased the performance of and decreased the size of this hypersonic vehicle. With the available literature and discussions by the authors with Russian and Ukrainian citizens there was sufficient information to use first principles to analyze the system and determine whether the concept provided a real advantage. In September 1996, as part of the Capstone Design Course, AE P 450-1, and the Hypersonic AeroPropulsion Integration Course, AE P 452-50 a student design team took on the task of analyzing Ajax. The resulting performance increase reduced the size and weight of the performance-sized aircraft [Esteve et al., 1977].The student team members were Yago Sanchez, Maria Dolores Esteve, Alfonso Gonzalez, Ignacio Guerrero, Antonio Vicent, Jose Luis Vadillo. Professor Mark A. Prelas,

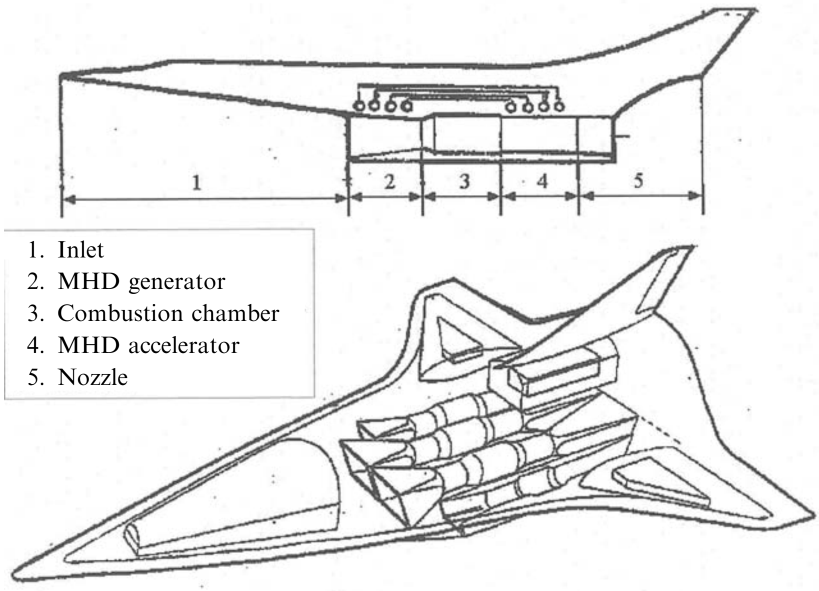

Figure 4.40. Ajax from article by *Space Wings Over Russia and the Ukraine*.

Department of Nuclear Engineering, University of Missouri-Columbia, was an advisor to the student team. After touring a number of Russian nuclear facilities, he provided first-hand knowledge of the ionization devices that are reported to be key components of the Ajax system.

From Novichokv [Novichokv, 1990a], comes a sketch of the propulsion system concept with the coupled MHD generator-accelerator showing the energy bypass concept, Figure 4.40. The simple sketch gives a cross-section similar to any totally integrated propulsion system in which the bottom of the vehicle hosts the propulsion system, and the forebody is indeed the front part of the inlet. Figure 4.40 clearly shows the energy bypass concept associated with the Ajax propulsion system. Also from Novichokv [Novichokv, 1990b] are the features of the Ajax system and reasons the Ajax system was developed. They are as follows:

(1) *Energy bypass*: via a coupled MHD generator-accelerator system [Gurianov and Sheikin, 1996; Carlson, 1996; Lin and Lineberry, 1995], a portion of the free stream *kinetic energy* bypasses the combustion chamber to reduce the entropy rise associated to aerodynamic diffusion and to the combustion process.
(2) *Reforming of hydrocarbon* fuel via a thermal decomposition process followed by an electrical arc process into a high hydrogen fraction fuel, with about 20,200 Btu/lbm heat of combustion. It is assumed that the products are gaseous hydrogen, ethylene and other combustible species, and possibly carbon monoxide. The quantity of water used or the disposal of the excess carbon for this process is unclear (experimental data and analyses from

various sources, including Russian, support qualitatively the relevance of this feature).

(3) *Ionization* of the airflow at the nose of the aircraft and of the airflow entering the engine, probably generated by the Russian-developed Plasmatron. One of these Plasmatron devices is operating as a plasma test facility at the von Karman Institute (VKI) in Brussels. The former may alter the shock system surrounding the aircraft to reduce drag and to permit the MHD nose generator to extract kinetic energy from the flow. The latter permits the MHD generator-accelerator to function with the magnetic field strengths possible with superconducting magnets and the flow velocities present within the engine module to produce a flow energy bypass system [Tretyakov, 1995; Gordon and McBride, 1993; Gorelov et al., 1995, 1996], (Russian information supported by analysis and available databases.)
(4) *Powering of the fuel reforming process* by an MHD generator in the nose of the vehicle [Batenin et al., 1997], that with a particle beam generator in the nose, produces a plasma cloud at the vehicle nose and results in a *reduction* of the vehicle total *drag* [Gurijanov and Harsha, 1996; Tretyakov, 1995; Zhluktov, 1996; Gorelov et al., 1996, 1995; Smereczniak, 1996]. (Russian information with experimental data obtained, under an Italian research collaboration effort with the Russian Academy of Sciences (RAS)-Novosibirsk).
(5) *Increase in the combustion efficiency* within the engine by means related to injection of plasma or hydrogen ahead of the fuel injector struts [Tretyakov et al., 1995]. (Russian information with experimental data obtained under Italian collaboration research effort with RAS-Novosibirsk.)
(6) *Diversion* of the bypassed energy to a directed energy device on an intermittent basis for peaceful purposes. Purposes listed are: reduction of the ice crystal formation over Antarctica to reduce the size of the ozone hole, space debris burning, ionosphere and upper atmosphere research, ozone generation, communication with artificial satellites, water surface and atmosphere ecological conditions diagnostics, ore deposits prospecting, earth vegetation research and monitoring, seismic conditions and tunnel monitoring, ice conditions and snow cover monitoring, and long-range communication and navigation.

In January 2001, Alexander Szames of *Air et Cosmos* interviewed Nikolai Novitchkov and Vladimir L. Freishtadt [Szames, 2001]. The article states that the project originated in the State Hypersonic Systems Research Institute (GNIPGS) in St Petersburg. Vladimir Freishtadt was the OKB Director, with members Viktor N. Isakov, Alexei V. Korabelnikov, Evgenii G Sheikin, and Viktor V. Kuchinskii. It is clear in the literature that Ajax is primarily a global range hypersonic cruise vehicle. All the discussions with individuals about Ajax stress both the global range capability at hypersonic speeds and the directed energy device for peaceful purposes. When the illustration (Figure 4.41) was published in Paris in December 1999 it showed a vehicle concept that corresponded to correct hypersonic design criteria, and a flow field significantly modified by MHD interaction. A paper presented in the IAF Congress held in Turin, Italy, provided details of an axisymmetric MHD nose

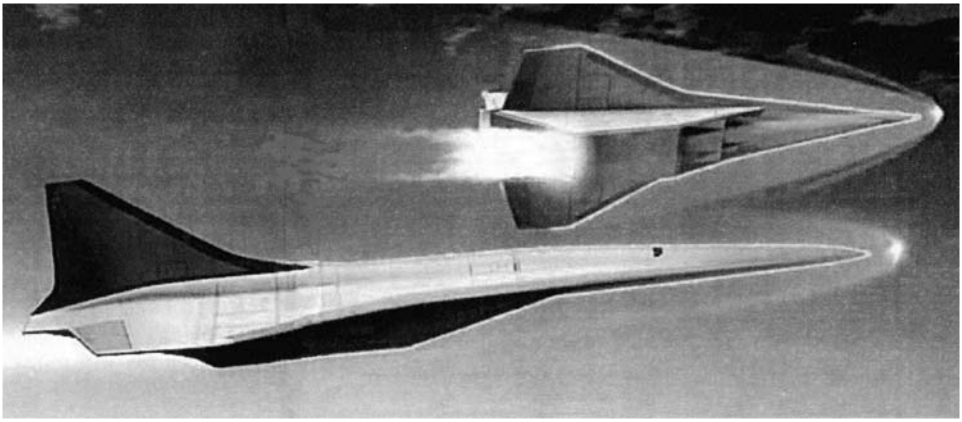

Figure 4.41. Ayaks illustration by Alexandre Szames from information obtained from Vladimir Freistat, the Program Director of AYAKS in *Air and Cosmos*.

generator. Its intent is to drive the device that creates plasma ahead of the nose. Researchers from Novosibirsk have stated such tests have been conducted in their hypersonic, high-temperature wind tunnels and presented very similar pictures. An AIAA paper by Dr J. Shang of the Air Force Research Labs has similar data. One of the difficulties with the MHD propulsion system analysis is the only analyses possible are for aircraft in a free stream flow field without any ionization. As the Szames illustration shows, and Russian researchers have stated, the propulsion system and aircraft operate as if they were in a modified Mach number and gas flow field. In fact the flow around the aircraft and entering the engine is a plasma flow. None of the aircraft or propulsion analyses these authors have done have considered this plasma flow field. The plasma effect is not the same as a simple thermal modification of the gas properties. Since the atmosphere ahead of the aircraft has the lowest density, MHD interaction with the flow field ahead of the aircraft is the greatest and covers the greatest extent. An IAF paper presented in Turin, Italy, describes the nose MHD device that reportedly powers a fuel-reforming process of unknown description [Batenin et al., 1997].

The reported performance includes a 13,812 km (7458 nautical miles) range at Mach 8 and 33 km altitude, and the mission time, 129 minutes. Cruise speed is then 8,005 ft/sec. From historical aircraft performance correlations, the climb and descent time and distance are 46 min and 1250 nautical miles, respectively. With ground operation, that yields a cruise distance of 6,208 nautical miles (11,497 km) and a mission time of 130 minutes. For a fuel fraction of 50% the range factor is 16,590 km (8,960 nautical miles). The sketch of Ajax (Figure 4.41) indicates a Küchemann's tau of about 0.10. That yields an aerodynamic lift-to-drag ratio (L/D) of 4.1. The integrated propulsion system and gravity relief results in a final L/D of 4.7. The reported heat of combustion for Russian reformed kerosene is about 30,000 Btu/lbm. With a 50% propulsion energy conversion efficiency the $V I_{sp}$ is 1,920 nautical miles (3,557 km) and the I_{sp} is 1,457 sec. The resulting range factor is 9,024 nautical miles

(16,712 km). If low-level ionization were employed to reduce the cruise drag, then the mission range would be 25,309 km (13,666 nautical miles) in 204 minutes. So the reported Ajax performance is an Earth-circling range in three and one-half hours [Bruno et al., 1998].

For a cruise system the total heat load can be an order of magnitude greater than for an atmosphere-exit trajectory, so some form of continuous energy management is required to prevent the airframe thermal capacitor from absorbing excess energy [Anon., 1970]. The heat capacity of some of the reformed hydrocarbon fuels can be greater than hydrogen. From the Szames article the heat of formation is given as 62,900 kJ/kg or 59,620 Btu/lb for the case of reformed methane. In the case of Ajax the thermal energy is not discarded but used to create thrust. As indicated in the Introduction, the Ajax system is an energy management system that minimizes the shock losses (entropy rise of the total aircraft system in hypersonic flight) and makes converted kinetic energy available for applications. The fraction of the thrust energy provided by the recovered aerodynamic heating reported in the Russian references, 30%, is in agreement with prior analyses [Czysz, 1992; Ahern, 1992].

MHD flows are governed by the interaction of aerodynamic and electromagnetic forces. As a result the key MHD parameter contain elements of both. The seven most important considerations and parameters are **cyclotron frequency and collision frequency**, the **MHD interaction parameter**, the load parameter, the Hall parameter, the Hartmann number, and the **gas radiation losses**; they characterize and also constrain the performance of a MHD system. The bold-faced parameters are the four discussed in this chapter. One of the authors (CB) provided information related to the impact of each of these parameters. Four of them are critical to the operation of the MHD generator and accelerator in determining the existence and intensity of the Lorentz force [Bottini et al., 2003]. That is the force that accelerates or decelerates the airflow via electromagnetic energy interaction with the ions in the flow. If the Lorentz force is not present, there is no electromagnetic acceleration of the gas.

Cyclotron frequency and collision frequency

Consider the motion of a single charged particle in a magnetic field B. A single charged particle spirals around the B field lines with the electron cyclotron frequency. The charged particle of an ionized gas is thus guided ('confined', in plasma parlance) by the magnetic field (and thus can be separated by ions and create an E field and a voltage), but only on condition its mean free path (the distance a particle travels between collisions) is greater than the cyclotron radius. If this were not the case, after a collision with another particle, the particle would be scattered away from its spiral trajectory and 'diffuse' across the field lines. This condition is the same as saying that the collision frequency must be less than the cyclotron frequency. The condition for guidance, accounting for collision frequency and cyclotron frequency, scales with B, pressure and temperature as the following equation:

$$10^{-3}\left[\frac{BT^{1.5}}{p(1-\alpha)}\right] \gg 1 \tag{4.21}$$

where $B =$ magnetic field strength (in tesla), $T =$ gas static temperature (K), $p =$ static pressure (atm) and $\alpha =$ ionization fraction. Since the numerical factor in front of equation (4.21) is on the order of 10^{-3}, it is clear that this condition requires very high B or very low pressure. Very high (nonequilibrium) electron temperature T_e can satisfy this condition, provided B is on the order of 1 tesla or greater, and pressure is on the order of 0.1 atmosphere. This puts a stringent condition on the operation of an MHD device. It is clear that this rules out equilibrium ionization for all practical purposes (the equilibrium temperature would be unrealistically high, many thousand K), and that extraction can work efficiently after a certain amount of dynamic compression, but not inside combustion chambers where pressure is of the order of 1 atm for a supersonic though-flow combustor and 10 to 20 atmospheres for subsonic through-flow combustor. This condition favors hypersonic cruise vehicles, as their typical dynamic pressure (hence internal pressures) are at least one-third that of an accelerating launcher.

MHD interaction parameter (S)

It defines the strength of the interaction between the magneto-hydro-dynamic energy and the airflow.

$$S = \frac{\sigma B^2 L}{\rho u} = \text{MHD interaction parameter} \tag{4.22}$$

with $\sigma =$ flow electrical conductivity (mho/m), $\rho =$ gas density (kg/m^3), $u =$ gas velocity along MHD device (m/sec) and $\rho u =$ mass flow per unit area (kg/m^2/s).

The mass flow per unit area along a vehicle increases by 25 or more from the nose to the engine area as the flow is compressed. This means that the Russian installation of a nose MHD device and plasma generator, to drive the hydrocarbon fuel arc reforming process and alter the surrounding flow field to reduce drag, is using the basic physics to advantage. Again the nose mass flow per unit area is about an order of magnitude less for a hypersonic cruise vehicle compared to an accelerating space launcher, favoring the application of MHD to cruise vehicles. For the cruise vehicle the pressure is less and the ionization potential to create a plasma much greater than for an accelerator (see Figure 4.7). Note that the magnetic field strength (B) is squared, so a doubling of the B field increases the interaction by a factor of 4. The mass flow per unit area inside the combustor is too large to have a significant interaction at moderate magnetic field strengths. That is why the MHD generator and accelerator are placed where the local Mach number is higher and the mass flow per unit area and pressure are less. The B field for the MHD generator and accelerator usually is greater than that required for the nose device because of the larger mass flow per unit area.

Radiative losses

The plasma transport equations include energy transport. In terms of temperature, T, the energy transport is the left side of equation (4.23):

$$\frac{\partial kT}{\partial t} + \frac{2}{3} kT \vec{\nabla \nu_{\mathrm{i}}} = \left(\frac{D_{\mathrm{ric}}}{\sqrt{T}} + D_{\mathrm{Brem}} \sqrt{T} \right) \alpha N_{\mathrm{i}} \tag{4.23}$$

where on the right hand side, the two terms are the radiation heat transfer due to recombination of electrons and ions (D_{rec}), and the brehmsstrahlung radiation contribution (D_{Brem}). The number of ions (N_{i}) and the degree of ionization (α) multiply the radiation heat transfer terms. Again there needs to be a compromise on α and to consider different T scaling.

MHD summary

The four MHD parameters discussed, cyclotron frequency and collision frequency, the MHD interaction parameter, and gas radiation losses, provide the minimum criteria for an MHD system to operate successfully. It is critical that any system seeking to operate as an MHD system meet the criteria for the Lorentz force to exist. Although appearing to be applicable to space launchers, the MHD energy bypass system is limited by the internal pressure in the propulsion system. The result is that an MHD system that has significant potential for a global range cruise aircraft has only minimal potential for the space launcher [Bottini, 2003], The MHD interaction with the external flow to reduce drag and permit electromagnetic deflection of the airflow (instead of a physical ramp) is applicable to both cruise aircraft or space launcher because the external flow pressure is low in both cases.

Lightcraft

One of the limitations of the space launcher it the quantity of propellant that must be carried to achieve orbital speed. Even the most optimistic airbreathing system has a mass ratio of 4, so the propellant is three times the operational weight empty. During the 1984 International Astronautical Congress held at Brighton, England, Viktor Legostayev approached the author to discuss space developments in the Soviet Union [Legostayev, 1984]. Part of the material presented was an experiment where a vertical launch rocket used water as a propellant and the energy to vaporize the water and produce thrust was provided by a focused microwave generator. An altitude of about a kilometer was achieved. Material was also presented from the Nikolai Tesla museum in Belgrade, Yugoslavia. In the translated Tesla manuscripts there was a discussion of projected electromagnetic energy with minimum transmission losses. Tesla's claim was that a base on the Moon or Mars could be powered by a suitably located generator on Earth. Legostayev presented some data to the effect that experiments projecting energy from Siberia to an orbiting satellite re-transmitting it to Moscow achieved the transmission efficiencies Tesla had predicted. The picture of the power generating tube Legostayev showed was identical to the tube the

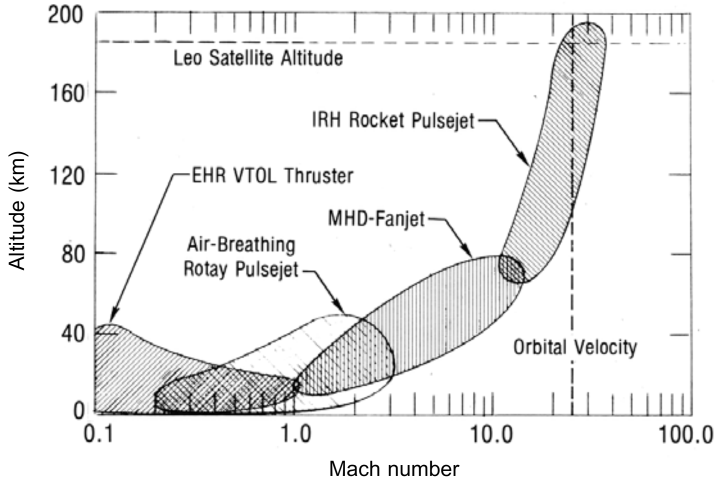

Figure 4.42. Laser/microwave heated MHD spacecraft operating envelope enabled by a series of propulsion configuration adaptations.

author saw at the small museum at Tesla's birthplace in Smilyan, Serbia. In both cases the evidence supported that a remote-powered vehicle was possible.

Professor Leik Myrabo, of Rensselaer Polytechnic Institute, Troy, New York, has been developing a spacecraft based on focused electromagnetic energy (laser or microwave) for at least the last 20 years [Myrabo, 1982, 1983; Myrabo et al., 1987, 1998; Myrabo, 2001]. In this case the vehicles are toroidal, the toroid forming a mirror to focus the received electromagnetic energy to vaporize and ionize water and air. Thus the propulsion system becomes an MHD-driven space launcher. Myrabo has recently demonstrated with USAF support a scale model propelled by a laser at Lawrence Livermore Laboratory, as shown in an *Aviation Week* article [*Aviation Week and Space Technology*, 2002]. The importance of the Myrabo concept is that is truly a combined cycle concept. Through a series of propulsion configuration adaptations, the single spacecraft becomes four different MHD propulsion systems, all powered by projected power that can, in principle, reach low Earth orbital speed and altitude (Figure 4.42). The power projecting system can be on Earth or in orbit. If there is an orbital power generator, spacecraft can be powered to the Moon (see Chapter 6), or a satellite can be powered to geosynchronous orbit with a minimum of earthbound resources. If the power generator is placed on the Moon, then the system can provide propulsion to the nearby planets and moon systems. This concept is very interesting because it has the least onboard propellants of any system and hence the lightest weight.

The vehicle is a rotational symmetric vehicle and begins its liftoff under beamed power, in this case from an orbiting laser, as shown in Figure 4.43. Selective illumination of the laser windows provides lateral thrust, so sideways translation movement is possible as well as vertical. In this liftoff phase the propulsion system is configured for vertical takeoff or landing. Although forward acceleration to high

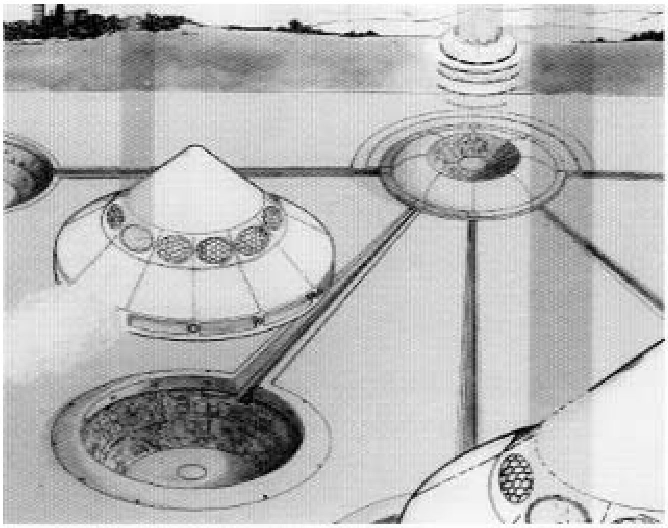

Figure 4.43. Laser/microwave heated MHD spacecraft by Leik Myrabo of Rensselaer Polytechnic Institute, Troy, New York.

subsonic speed is possible, the propulsion system soon transitions to the airbreathing rotary pulsejet mode. In this case the rotating outer ring provides linear acceleration by ejecting an air plasma from an MHD engine segment. As speed increases, the entire vehicle acts as an MHD airbreathing fanjet to cover the supersonic and hypersonic speed regimes. In its final configuration the pulsejet configuration now operates as a rocket, for instance with water as a working fluid (see Myrabo references for details). Since its inception, the concept has proceeded through a number of evolutionary steps, but the basic axisymmetric shape with toroidal mirrors to focus the radiated energy to produce a plasma remains.

Variable cycle turbo ramjet

Repeating part of the conclusion from Builder's 1964 report, there is an observation about a hypothetical engine (at that time), the air turboramjet. To quote,

> In a sense, a fan-ramjet might be a suitable name for such a cycle; the duct-burning turbofan and the air-turborocket could be considered close cousins to this hypothetical engine. At the higher speed end, around Mach 10, we can postulate a very efficient engine called the transonic combustion ramjet. There is still another important class of possibilities offered just outside the confines of the Brayton Cycle family: engines with non-adiabatic compression and expansion processes as a result of heat exchanges between the air and fuel. We might find a complete new spectrum of such engines awaiting our discovery.
>
> [Builder, 1964]

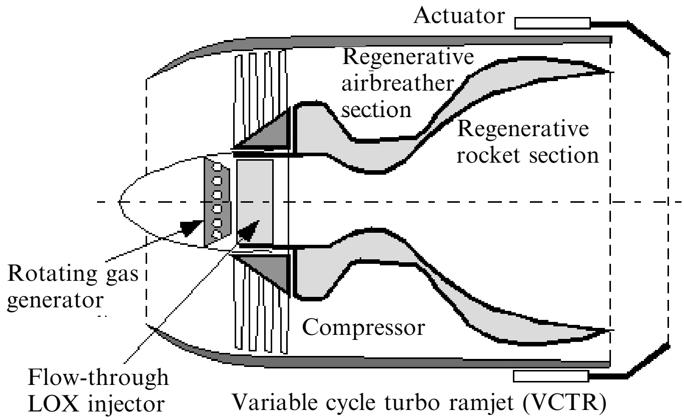

Figure 4.44. Sketch of variable cycle ramjet based on Rocketdyne SSME, circa 1983.

Such engines were discovered and unfortunately never pursued. In Figure 4.44 there is a thumbnail insert of an original sketch of a variable cycle turboramjet based on the Rocketdyne SSME sketched sometime in the early 1980s. Unfortunately the identity of the sketch's source has long been lost. But it shows the ingenuity that was routinely discarded in favor of the rocket status quo. Although the details of the engine's operation are also lost, the originality in adapting an existing fixed cycle rocket engine with a fixed specific impulse to a variable cycle, airbreathing turboramjet/rocket is evident. As shown in the enlarged drawing based on the sketch, a rotating gas generator provided the power for the low-pressure ratio compressor. The engine operated as rocket-based turboramjet at lower Mach numbers and then could transition to a conventional rocket for the higher Mach numbers. With the flow through a LOX injector, if the airbreather thrust could not provide sufficient low speed acceleration, the rocket could be ignited to provide an additional boost. Who knows what the launchers of today would be like if innovations like this, based on current operational hardware, had been allowed to proceed.

It is not a lack or ideas or hardware concepts, or the lack of technology that confines us to low-performing rockets today, but a lack of imaginative and decisive leadership to implement those ideas.

4.24 BIBLIOGRAPHY

Ahern, J.E. (1983) Briefing for Robert Williams on Second Law Thermodynamics, DARPA Copper Canyon manager, Washington, DC.

Ahern, J.E. (1992) 'Thermal Management of Air-Breathing Propulsion Systems', AIAA 92-0514, 30th Aerospace Sciences Meeting, Reno, Nevada, January 1992.

Anfimov, N.A. (1997) 'In Searching for an Optimal Concept of Future Russian Reusable Space Transportation System', Proceedings of the International Workshop on Spaceplane/RLV Technology Demonstrators, March 1997, Tokyo Japan, pp. 67–96.

Anon. HyFAC (1970) 'Hypersonic Research Facilities Study, Prepared under NASA contract NAS2-5458. NASA CR 114324, October 1970.

Anon. BAC (1991) 'An-225/Interim HOTOL Launch System Study', British Aircraft Company Presentation to the European Space Agency, Paris, 21 June 1991.

Anon. Lockheed (1967) 'A Study of Advanced Airbreathing Launch Vehicles with Cruise Capability', Lockheed Report IR 21042, The Lockheed Aircraft Corporation, circa 1967.

Anon. Hyperplane (1988) 'Hyperplane' 39th International Astronautical Federation Congress, October 1988, Bangalore, India.

Aoki, T., and Ogawara, A. (1988) 'Study of LACE Cycle for SSTO Space Plane', IAF-88-252, 39th Congress of the International Astronautical Federation, October 1988, Bangalore, India.

Aoki, T., Ito, T. et. al. (1991) 'A Concept of LACE for SSTO Space Plane', AIAA-91-5011, AIAA 3rd International Aerospace Planes Conference, December 1991, Orlando, Florida.

Balepin, V.V. (1996) 'Air Collection Systems', *Developments in High-Speed-Vehicle Propulsion Systems*, edited by S.N.B. Murthy and E.T. Curran, AIAA Progress in Aeronautics, Vol. 165, Washington, DC.

Balepin, V.V. and Hendrick, P. (1998) 'Application of the KLIN Cycle to Vertical Take-Off Lifting Body Launcher', AIAA-98-1503.

Balepin, V.V. and Tjurikov E.V. (1992) 'Integrated Air Separation and Propulsion System for Aerospace Plane with Atmospheric Oxygen Collection', SAE-92-0974, Aerospace Atlantic Conference, April 1992, Dayton, OH.

Balepin, V.V., Harchermikova, G.D., Tjurikov, E.V., and Avramenko, A.Ju. (1993) 'Flight Liquid Oxygen Plants for Aerospace Plane: Thermodynamic and Integration Aspects', SAE chapter, 1993 SAE Aerospace Atlantic Conference and Exposition, April 1993, Dayton, OH.

Balepin, V.V., Yoshida, M., and Kamijo, K. (1994) 'Rocket Based Combined Cycles for Single Stage Rocket', SAE 941166.

Balepin, V.V., Czysz, P.A., Maita, M., and Vandenkerckhove, J. (1995) 'Assessment of SSTO Performance with In-Flight LOX Collection', AIAA-95-6047, AIAA 6th International Aerospace Planes Conference, Chattanooga, TN.

Balepin, V.V., Maita, M., Tanatsugu, N., and Murthy, S.N.B. (1996) 'Deep-Cooled Turbojet Augmentation with Oxygen—Cryojet for an SSTO Launch Vehicle', AIAA 96-3036, 32nd AIAA/ASME/SAE/ASEE Joint Propulsion Conference, July 1996, Lake Buena Vista, FL.

Baranovsky, S.I. et al. (1992a) 'Combustion Chamber of Ramjet for Aerospace Plane', Proceeding of the 9th World Energy Conference, Vol. 3, pp. 1583–1591, June 1992, Paris.

Baranovsky, S.I. et al. (1992b) 'Experimental Study of the Hydrogen Supersonic Combustor', Proceeding of the 9th World Energy Conference, Vol. 3, pp. 1699–1720, June 1992, Paris.

Barrère, M. and Vandenkerckhove, J. (1993) 'Energy Management', ISABE 93-7016, 11th International Symposium on Air Breathing Engines, September 1993, Tokyo, Japan (published as CDROM by AIAA, Reston, VA).

Batenin, V.M., Bityurin, V.A., Ivanov, G.S. Inozemzev, N.N., and Gorozhankin, P.A. (1997) Institute of High Temperatures of Russian Academy of Sciences Moscow, Russia. 'Electromagnetic Complex Concept for the Horizontal Start and Landing of a Reusable Air-Space Aircraft', 48th International Astronautical Congress, October 6–10, Turin, Italy.

Billig, F.S. (1989) 'Hypersonic Vehicles II', 1989 Purdue Short Course on Engine Airframe Integration, Purdue University.

Billig, F.S. (1993) 'The Integration of the Rocket with a Ram-Scramjet as a Viable Transatmospheric Accelerator', Proceedings of the XI ISABE, Tokyo, Published by AIAA, pp. 173–187.

Bond W.H. and Yi A.C. (1993) 'Prospects for Utilization of Air Liquefaction and Enrichment System (ALES) Propulsion in Fully Reusable Launch Vehicles', AIAA-93-2025, AIAA/SAE/ASME/ASEE 29th Joint Propulsion Conference, Monterey, June 1993.

Bottini, H., Bruno, C. and Czysz, P.A. (2003) 'Is The MHD Scramjet Really An Advantage?' AIAA 2003-5046, 39th Joint Propulsion Conference, Huntsville, Alabama, July 2003.

Bruno, C., Golovitchev, V.I. and Tretyakov, P.K. (1998) 'New Trends in Improving Hypersonic Vehicles Aerodynamics and Propulsion Flow Control by External Energy Supply', Paper 98-0-1-08V, 21st international Symposium on Space and Technology (ISTS), Omiya, Japan, May 1998.

Builder, C.H. (1964) 'On the Thermodynamic Spectrum of Airbreathing Propulsion', AIAA 64-243, 1st AIAA Annual Meeting, Washington, DC, July 1964.

Buhlman, M. and Siebenhaar, A. (1995) 'The Strutjet: The Overlooked Option for Space Launch', AIAA 95-3124, 31st AIAA Joint Propulsion Conference, San Diego, CA, July 1995.

Buhlman, M. and Siebenhaar, A. (1995) 'The Strutjet: Exploding the Myths Surrounding High Speed Airbreathing Propulsion', AIAA 95-2475, 31st Joint Propulsion Conference, San Diego, CA, July 1995.

Burnett, D. and Czysz, P. (1963) 'Hydrogen Combustion Studies', AEDC-TDR-63, Aerodynamic Division, Directorate of Engineering Test, Air Force Systens Command, Wright-Patterson AFB, Ohio, April 1963.

Carlson, C.P., Kessler, R. and Schmitt, E.W. (1996) Textron Defense Systems, Everett, Massachusetts, 'Magnetohydrodynamic Generator Design for a Combined-Cycle Demonstration Powerplant', *Journal of Propulsion & Power*, Vol. 12.

Curran, E.T. (1993) 'The Potential and Practicality of High Speed Combined Cycle Engines', Hypersonic Combined Cycle Propulsion, AGARD Conference Proceeding N0.479, AGARD, Neuilly-sur-Seine, pp. K1–9.

Czysz, P.A. (1988) 'Thermodynamic Spectrum of Airbreathing Propulsion', SAE Technical Paper 881203, Future Transportation Technology Conference and Exposition, San Francisco, CA, August 1988.

Czysz, P.A. (1988) 'Air Breather vs. Rocket: Is the rocket the only reliable, demonstratable space propulsion system?' SAE Aerospace Atlantic Conference & Exposition, Dayton, OH, April 1993.

Czysz, P.A. (1989) 'Hypersonic Convergence', Text for Hypersonic AeroPropulsion Design Course, AE-P-450-52, Parks College of Engineering and Aviation, Saint Louis University, St. Louis, Missouri.

Czysz, P.A. (1992) 'Space Transportation Systems Requirements Derived from the Propulsion Performance Reported in the *Hypersonic and Combined Cycle Propulsion Session* at the IAF Congress'. IAF-92-0858, 43rd IAF Congress, Washington, DC, September 1992.

Czysz, P.A. (1993a) 'Rocket Based Combined Cycle (RBCC) Propulsion Systems Offer Additional Options', Proceedings of the XI ISABE, Tokyo, Published by AIAA, New York, pp. 119–137.

Czysz, P.A. (1993b) 'Hydrogen Combustion Studies—Revisited', 1993 JANNAF Conference, Albuquerque, NM, February 1993.

Czysz, P.A. (1995) 'Interaction of Propulsion Performance with the Available Design Space', Proceedings of the XII International Symposium on Air Breathing Engines (ISABE), Melbourne, Australia, September 1995.

Czysz, P.A. (1999) 'Combined cycle propulsion—is it the key to achieving low payload to orbit costs', ISABE Paper 99-7183, XIV International Symposium on Air Breathing Engines (ISABE), Florence, Italy, September 1999.

Czysz, P.A. and Froning, H.D. (1995) 'A Propulsion Technology Challenge—Abortable, Continuous Use Vehicles', IAF-95-S.2..03, 46th IAF Congress, Oslo, Norway, October 1995.

Czysz, P.A. and Little, M. (1993) 'Rocket-Based Combined Cycle Engine (RBCC)—A Propulsion System for the 21st Century', AIAA-93-5096, Munich, Germany.

Czysz, P.A. and Murthy, S.N.B. (1991) 'Energy Analysis of High-Speed Flight Systems', *High-Speed Flight Propulsion Systems*, AIAA Progress in Astronautics and Aeronautics, Vol. 137, edited by E.T. Curran and S.N.B. Murthy, AIAA, Washington, DC, pp. 183–186.

Czysz, P.A. and Richards, M.J. (1998) 'Benefits from Incorporation of Combined Cycle Propulsion', AIAA-98-S.5.10, 48th IAF Congress, Melbourne, Australia, October 1998.

Czysz, P.A. and Vandenkerckhove, J. (2001) 'Transatmospheric Launcher Sizing', *Scramjet Propulsion*, editors E.T. Curran and S.N.B. Murthy, Progress in Astronautics and Aeronautics, Vol. 189. AIAA, Reston, VA.

Czysz, P.A., Froning, H.D., and Longstaff, R. (1997) 'A Concept for an International Project to Develop a Hypersonic Flight Test Vehicle', Proceedings of The International Workshop on Spaceplanes/RLV Technology Demonstrators. Tokyo, Japan, March 1998.

Czysz, P.A., Bruno, C. and Kato, K. (2001) 'Interactions between Propulsion Systems and the Configuration Concepts Defines the Design Space', AIAA-2001-1924, 10th International Space Planes and Hypersonic Systems and Technologies Conference, Kyoto, Japan, April 2001.

Daniau, E. (2002) 'Pulse detonation engine, concept, performance and applications', ISU/AAAF Short Course, Versailles, France, May 2002.

Der, J.Jr. (1991) 'Characterizing Ejector Pumping Performance', *AIAA Journal of Propulsion & Power*, May–June 1991.

Doublier, M., Pouliquen, M. and Scherrer, D. (1988) 'Combined Engines for Advanced European Launchers', IAF-88-251, 39th IAF Congress, Bangalore, India, October 1988.

DuPont, A. (1999)'Further studies of optimized inlets to hypersonic turbine engines', ISABE-99-7039, 114th International Symposium for Air Breathing Engines (ISABE), Florence, Italy, September 1999.

Escher, W.J.D. (1994) 'Motive Power for Next Generation Space Transports: Combined Airbreathing + Rocket Propulsion', private communication.

Escher, W.J.D. (1996a) 'A Winning Combination for Tomorrow's Spaceliners', *Aerospace America*, American Institute of Aeronautics and Astronautics, Washington, DC, pp. 38–43.

Escher, W.J.D. (1996b) 'Rocket-Based Combined Cycle (RBCC) Powered Spaceliner Class Vehicles Can Advantageously Employ Vertical Takeoff and Landing (VTOL)', AIAA 95-6145, 6th International Aerospace Planes and Hypersonic Technologies Conference, Chattanooga, TN, April 1996.

Escher, W.J.D. (1998) 'A History of RBCC Propulsion in the U.S.—A Personal Recounting', White Paper, Kaiser Marquardt, Van Nuys, CA.

Esteve, M.D. et al. (1977) 'ODYSSEUS, Technology Integration for a Single Stage to Orbit Space Transport Using MHD Driven Propulsion', Senior Design Study, Parks College of Aerospace and Aviation, Saint Louis University, St. Louis, MO.

Gorelov, V.A., Gladyshev, M.K., Kireev, A.Yu., Korolev, A.S., Nikol'sky, V.S., Byzov, V.N., Fedosov, B.M. and Zhukovsky L.II. (1995) 'Ionization Near Hypersonic Vehicles: The Experience of Numerical, Laboratory and Flight Investigations', AIAA 95-1940, 26th AIAA Plasmadynamics & Lasers Conference, San Diego, CA, June 19–22, 1995.

Gorelov, V.A. Gladyshev, M.K. Kireev, A.Y. Korolev, A.S., Yegorov, I.V., and Byzov, V.N. (1996) 'Computational and Experimental Investigations of Ionization near Hypersonic Vehicles', *Journal of Spacecraft & Rockets*, Vol. 33, No. 6.

Gopalaswami R., Gollakota S., Venugolapan P., Nagarathinam M., and Sivathanu P.A. (1990) 'Concept Definition and Design of a Single-Stage-To-Orbit Launch Vehicle HYPERPLANE': IAF-88-194, 39th IAF Congress, Bangalore, October 1990.

Gounko, Yu.P., Kharitonov, A.M., Latypov, A.F., Mazhul, I.I. and Yaroslavtsev, M.I. (2000) 'Technique for Determination of Heat Fluxes and Force Characteristics of Ramjet/Scramjet Models in a Hot-Shot Wind-Tunnel', Institute for Theoretical and Applied Mechanics SB RAS, Novosibirsk.

Gurijanov, E.P. and Harsha, P.T. (1996) 'AJAX, New Directions in Hypersonic Technology', AIAA Paper 96-4609.

Harney, J. (1967) 'Similarity of Nonequilibrium Expansion in Hypersonic Nozzles', FDM-TM-67-1. Air Force Flight Dynamics Laboratory, Wright-Patterson AFB, Ohio, May 1967, AD664084.

Harper, R.E. and Zimmerman, J.H. (1942) 'An Investigation of Rocket Engine Thrust Augmentation with a Nozzle-Ejector System', AEDC Report TRD-62-42.

Heiser, W.H. and Pratt, D.T. (2002) 'Thermodynamic Cycle Analysis of Pulse Detonation Engines', *AIAA Journal of Power*.

Hendrick, I.P. (1996) 'SSTO and TSTO LOX Collection System Performances: Influence of LOX Plant Architecture', ICAS-96-3.8.3.

Kailasanath, K. (2002) 'Recent Developments in the Research on Pulse Detonation Engines' (Invited), AIAA 2002-0470, 40th AIAA Aerospace Sciences Meeting & Exhibit, Reno, NV, January 14–17, 2002.

Kanda, T., Tomioka, S., Ueda, S., Tani, K and Wakamatsu, Y. (2005) 'Design of Sub-scale Rocket-Ramjet Combined Cycle Engine Model, Paper 1AC-05-C4.5.03. Presented at the 56th International Astronautical Congress, Oct. 16–21, Fukuoka, Japan.

Kroon, R.P. (1952) Turbojet Performance Manual, Engineering Department, Dept. A-1200, Westinghouse Electric Corporation, Aviation Gas Turbine Division.

Lashin, A.I., Kovalevski, M.M., Romankov, O.N. and Tjurikov, E.V. (1993) 'Combined Propulsion System for Advanced Multipurpose Aerospace Plane (ASP)', IAF-93-S.4.479, 44 IAF Congress, Graz, Austria, October 1993.

Lee, Y.M., Nikolic-Tirkas, B., Tarrant, G., Balepin, V., Petley, D. and Czysz, P.A. (2003) 'Vortex Tube Air Separation Applications for Air Collection Cycle Hypersonic Vehicles', 41st AIAA Aerospace Sciences Meeting and Exhibit, Reno, NV, January 2003.

Leingang, J.L. (1991) Personal communication, Dayton, OH.

Leingang, J.L., Maurice, L.Q., and Carreiro, Captain L.R. (1992) 'Space Launch Systems Using Collection and Storage', IAF 92-0664, 43 IAF Congress, Washington, DC, September 1992.

Legostayev, V. (1984) Private communication, IAF Congress Brighton, UK, October 1984.

Lin, B.C. and Lineberry, J.T. (1995) ERC, Incorporated, Tullahoma, TN, 'An Assessment of T-Layer MHD', AIAA 95-1933, 26th AIAA Plasmadynamics & Lasers Conference, San Diego, CA, June 19–22, 1995.

Lindley, C.A. (1963) 'Performance of Air Breathing and Rocket Engines for Hypervelocity Aircraft', Fourth Congress of the Institute of Aeronautical Sciences.

Maurice, L.Q., Leingang, J.L. and Carreiro, L.R. (1992) 'The Benefits of In-Flight LOX Collection for Air Breathing Space Boosters', AIAA paper, 4th International Aerospace Planes Conference, Orlando, FL, December 1992.

Mierau, A.N., Derevyanko, V.A. and Vasilyev, E.N. (2000) 'Numerical Simulation the Periodic Operating Regime of Hypersonic Ramjet with MHD-Control', Krasnoyarsk State University and Institute of Computational Modeling SB RAS, Krasnoyarsk.

Miki, Y., Togawa, M., Tokunaga, T., Eguchi, K., and Yamanaka, T. (1991) 'Advanced SCRAM-LACE System Concept for SSTO Space Plane', IAF-91-272: 42nd Congress of the International Astronautical Federation, Montreal, October 1991.

Myrabo, L.N. (1982) 'A Concept for Light-Powered Flight', AIAA 78-698, AIAA Joint Propulsion Conference, Cleveland, OH, June 1982.

Myrabo, L.N. (1983) 'Advanced Beamed-Energy and Field Propulsion Concepts', BDM Corporation publication BDM/W-83-225-TR, Final Report for the California Institute of Technology and Jet Propulsion Laboratory under NASA contract NAS7-1000, Task Order RE-156.

Myrabo, L.N. (2001) 'World Record Flights of Beam-Riding Rocket Lightcraft: Demonstration of 'Disruptive' Propulsion Technology', AIAA paper 2001-3798, 37th AIAA Joint Propulsion Conference, Salt Lake City, UT, July 2001.

Myrabo, L.N. et. al. (1987) 'Apollo Lightcraft Project', Final Report, prepared for NASA/USRA Advanced Design Program, 3rd Annual Summer Conference, Washington, DC, June 1987.

Myrabo, L.N., Messit, D.G. and Mead, F.B. (1998) 'Flight and Ground Tests of a Laser-Boosted Vehicle', AIAA 98-3735, 34th AIAA Joint Propulsion Conference and Exhibit, Cleveland, OH, July 1998.

Nicholas, T.M.T. et al. (1966) 'Mixing Pressure-Rise Parameter for Effect of Nozzle Geometry in Diffuser-Ejectors', *AIAA Journal of Propulsion & Power*, Vol. 12, No. 2, pp. 431–433.

Norris, G. (2003) 'Pulse Power', *Flight International*, Vol. 163, No. 4887, pp. 50–52.

Novichkov, N. (1990a) 'Space Wings of Russia and the Ukraine', *Echo of the Planet/Aerospace*, Moscow, September.

Novichkov, N. (1990b) Private communication, IAF Congress, Graz, Austria.

Ogawara, A. and Nishiwaki, T. (1989) 'The Cycle Evaluation of the Advanced LACE Performance', IAF-89-313, 40th IAF Congress, Malaga, Spain, October 1989.

Pegg, J., Hunt, L. and Petley, D.H. (1993) *Design of a Hypersonic Waverider-Derived Airplane*, AIAA Paper 93-0401, AIAA Aerospace Sciences Conference, Reno, NV, January 1993.

Riggins, D.W. (1996) 'Brayton cycle engine/component performance assessment using energy and thrust-based methods', AIAA1996-2922. 32nd AIAA Joint Propulsion Conference, Lake Buena Vista, FL, July 1996.

Rudakov, A.S. (1993) 'Cryogenic Propellant Rocket Engine Problems; Liquid Air Rocket Engines & Some Perspective of Engines', unpublished.

Rudakov, A.S. and Balepin, V.V. (1991) 'Propulsion Systems with Air Precooling for Aerospaceplane', SAE 911182, SAE Aerospace Atlantic, Dayton, OH, April 1991.

Rudakov, A.S., Gatin, R.Y. et al. (1991b) 'Analysis of Efficiency of Systems with Oxidizer Liquefaction and Accumulation for Improvement of Aerospace Plane Performance', IAF-91-279, 42nd IAF Congress, Montreal, Canada, 1991.

Rudakov, A.S., Gatin, R.Y., Dulepov, N.P., Koralnik, B.N., Harchevnikova, G.D., and Yugov, O.K. (1991c) 'Analysis of Efficiency of Systems with Oxidizer Liquefaction and Accumulation for Improvement of Spaceplane Performance', IAF-91-270, 42nd Congress of the International Astronautical Federation, Montreal.

Scherrer, D. (1988) 'Evaluation du Concept de Fusee-Statoreacteur pour la Propulsion Hypersonique', ONERA Activities, ONERA Paris, France, April, 1988.

Scott, T. and Riggins, D.W. (2000) 'Work Interaction in Quasi-One Dimensional Flows', *Journal of Propulsion & Power*, Vol. 16, No. 6, pp. 1053–1059.

Smereczniak, P. (1996) 'Electromagnetic Drag Reduction (EMDR) Program', Developed for Aeronautical Systems Center Planning Directorate (ASC/XR), Contract F33657-96-D-2004-0002.

Stroup, K.E. and Pontez, R.W. (1968) 'Ejector Ramjet Systems Demonstration', The Marquardt Corporation final report under USAF Contract AF33(615)-3734, report AFAPL-TR-67-118.

Swithenbank, J. (1984) Oral presentation on scramjet research at Sheffield University, May 1984.

Swithenbank, J. and Chigier, N.A. (1966) 'Hypersonic Airbreating Propulsion', Progress in the Aero. Sciences, Volume 8, Pergamon Press, NY, pp. 229–294.

Swithenbank, J. and Chigier, N.A. (1969) 'Vortex Mixing for Supersonic Combustion', Proceedings of !2th Symposium (International) on Combustion, The Combustion Institute, pp. 1153–1182.

Szames, A. (2001) 'Enquete sur une enigme avion hypersonique Ajax', *Air et Cosmos*, No. 1777, pp. 22–24.

Tanatsugu, N. (1987) 'Analytical Study of Space Plane Powered by an Air-Turbo Ramjet with an Intake Air Cooler', IAF-87-264, IAF Congress, Brighton, UK, October 1987.

Tanatsugu, N. (1999) 'Thermal management of precooled ATREX engine with expander cycle', ISABE Paper 99-7026, XIV International Symposium on Air Breathing Engines (ISABE), Florence, Italy, September 1999.

Togawa, M., Aoki, T. and Hirakoso, H. (1991) 'A Concept of LACE for SSSTO': IAF-91-5011: 3rd International Aerospace Planes Conference, Orlando, FL, December 1991.

Townend, L. (1986) Oral presentation to NASP technical team on scramjet test in 1966, Hampshire, UK, April 1986.

Townend, L. and Vandenkerckhove, J. (1994) 'External Afterburning and Shock-Confined Combustion in Supersonic Flow', APECS-VDK 001/94, ESA contract 120285.

Tretyakov, P. (1995) 'Supersonic Flow around Axisymmetric Bodies with External Supply of Mass and Energy', Institute of Theoretical and Applied Mechanics SB RAS, Russia.

Tretjakov, P.K., Golovitchev, V.I. and Bruno, C. (1995) 'Experimental and Numerical Study of Counterflow jet Flame Stabilization in a Supersonic Air Stream', XII ISABE, Melbourne, Australia, September 10–15, 1995.

Vandenkerckhove, J.A. (1986) Personal communication with respect to Von Karman at CalTech, March 1986.

Vandenkerckhove, J.A. (1991) 'A First Assessment of Scramjet-Propelled Single-Stage-To-Orbit (SSTO) Vehicles', VDK System S.A., WLC Phase 5, WP 260, chapter 1, Brussels, Belgium.

Vandenkerckhove, J.A. (1992a) 'SSTO Configuration Assessment', VDK System S.A., WLC Phase 5, WP 260, chapter 2, revision 1, Brussels, Belgium.

Vandenkerckhove, J.A. (1992b) 'A Peep Beyond SSTO Mass Marginality', IAF-92-0656, 43 IAF Congress, Washington, DC, September 1992.

Vandenkerckhove, J.A. (1993a) 'HYPERJET Mk #3, a rocket derived combined engine': a VDK System report.

Vandenkerckhove, J.A. (1993b) 'Comparison between Ejector-Ramjets and Turbo-Ramjets for TSTO Propulsion', Fifth International Aerospaceplanes Conference AIAA-93-5095, Munich, November 1993.

Wu, Y., Ma, F., and Yang, V. (2002) 'System Performance and Thermodynamic Cycle Analysis of Air-Breathing Pulse Detonation Engines', AIAA 2002-0473, 49th AIAA Aerospace Sciences Meeting 7 Exhibit, Reno, NV, January 2002.

Yamanaka, T. (2000) 'Innovative Breakthroughs to a Reusable STS', private communication.

Yanamanka, T. (2004) 'Fundamentals of Airbreathing Rocket Combined Cycle (ARCC) Engine and Design of an ARCC Engine Powered Single-Stage-To-Orbit (SSTO) Vehicle', Beyond the atmosphere CDROM, July 2004.

Yugov, O.K. et.al. (1989) 'Optimal Control Programs for Airbreathing Propulsion System or Single-Stage-to-Orbit Vehicles'. IAF-89-308, 40th IAF Congress, Malaga, Spain, October 1989.

Yugov, O.K., Dulepov, N.P., and Harchenvnikova, G.D. (1990) 'The Analysis of Hypersonic and Combined Cycle Engines in the Propulsion System of the SSTO Vehicles', 41st IAF Congress, Dresden, Germany, October 1990.

Zagaynov, G.I., and Plokhikh, V.P. (1991) 'USSR Aerospace Plane Program', AIAA-91-5103, 3rd International Aerospace Planes Conference, Orlando, FL, December 1991.

5

Earth orbit on-orbit operations in near Earth orbit, a necessary second step

Although not in the frontline technical or popular press, a critical element in reaching space beyond Earth is establishing the space infrastructure around the planet Earth. The concept of this infrastructure as a train marshalling and switching yard is appropriate. The rail control center serves as a center of operations for switching, long-haul train assembly, transfer of goods, refueling and repair. Likewise the orbital stations serve as centers for switching payloads between carrier and the required orbit, long-haul space exploration vehicle assembly, transfer of goods to human habitats and manufacturing facilities, and return, refueling and repair coordination. This is no trivial activity, and it will take a commitment as dedicated as the Apollo program to achieve. In a step-by-step discussion we will document the resources necessary to supply what is needed by this space infrastructure as a function of the propulsion systems.

Chapter 4 shows there are propulsion systems with which we can effectively build reduced oxidizer-to-fuel ratio launchers that are lighter and smaller than conventional expendable rockets. In fact, the remotely powered, directed electromagnetic energy system of Professor Leik Myrabo requires even less carried on-board propellants, a huge advantage in resource-absent space. As long as the principal launchers are expendable launchers for military and commercial needs, the available payloads will be those suitable for infrequent, expendable rocket launches. In the context of Chapter 2, the payloads will remain consistent with Conestoga wagons until there is an operational railroad. Until a sustained-use launch system is operational, the payloads that warrant a high launch rate system will remain the subject of design studies only. Until sustained-use launch system is operational the flight rate is insufficient to build the global space infrastructure needed to support space operations. If the Space Shuttle main propellant tank was slightly modified to permit its use as a space structure, like S-IVB, an infrastructure might begin to build [Taylor, 1998]. However the Shuttle main tank is intentionally crashed into the ocean, wasting a valuable asset.

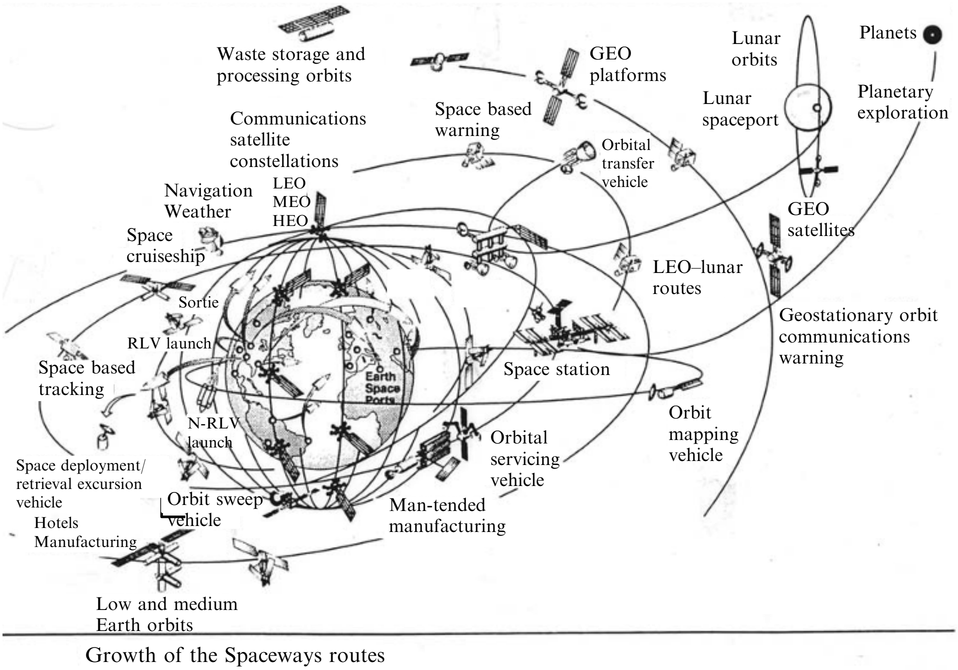

Figure 5.1. Future space infrastructure by Dr William Gaubatz. If there is a space transportation system and in-space operations system to support the infrastructure.

Assuming the capability existed for sustained space launches to establish an operational near-Earth orbit space infrastructure, there are serious performance and propellant refueling challenges that need to be immediately addressed. Because of the activity required by the elements of the near-Earth orbit infrastructure the quantity of propellant required in space and, more importantly, the quantity launcher propellant required to lift that very propellant into low Earth orbit (LEO) is truly prodigious, unless a non-chemical rocket is used. For a true space transportation system to exist, a transportation system *network* has to be built, just as it was for the United States transcontinental railroad. Dr William Gaubatz, formerly of McDonnell Douglas Astronautics (and former director of the Delta Clipper program) attempted to anticipate what the future might hold, *if* a space transportation system actually did exist, as shown in Figure 5.1. Dr Gaubatz shows the elements necessary to build the infrastructure, but unfortunately does not address the assets required to establish and sustain that infrastructure.

Table 5.1 lists systems and functions of the infrastructure shown in Figure 5.1. Future global space is a crowded and busy place. The key enabling space structures are the fuel station spaceports and orbital servicing vehicles. Without these vehicles movement between orbital planes and altitudes is limited to specific satellites, such as GSO communication satellites with integral geo-transfer propulsion. With servicing centers equipped with construction module storage they can supply components for

Table 5.1. Space infrastructure vehicles and missions, from Figure 5.1.

	Orbital system	Function	Orbit
1	Sustained-use launcher	High frequency, modest payloads	LEO/MEO
2	Expendable launcher	Low frequency, heavy payloads	LEO
3	Point-to-point transfer	Points on Earth or orbit	
4	Operations center/space station	Operations coordination/research	LEO/MEO
5	Orbital servicing vehicle	Maintains in-orbit vehicles	All
6	Fuel station spaceport	Refuels orbital vehicles	LEO
7	Space-based manufacturing	Human based low '*g*' manufacturing	LEO
8	Man-tended manufacturing	Robot based micro '*g*' manufacturing	LEO/GEO
9	Orbital sweep vehicle	Orbital clean-up vehicle	All
10	Waste storage and processing vehicles	Processes and disposes human and manufacturing wastes	HEO
11	Navigation/weather	Supports travel network	LEO/MEO
12	Orbital mapping vehicle	Measures resources and geography	LEO/MEO
13	Space-based warning	Military and asteroid warning	HEO/GEO
14	Space-based hotel	Space tourist facilities	LEO/MEO
15	Spacecruiser vehicle	Human transport and rescue	LEO
16	Communication satellite constellations	Supports telecommunication systems	All
17	Orbital transfer vehicle	Orbital altitude/plane change	All
18	LEO–lunar vehicle	Transport to Moon and return	LEO
19	Space deployment retrieval vehicle	Recovers spent vehicles Replaces spent vehicles	All
20	Space excursion vehicle	Placement of new systems	LEO
21	GEO platforms/satellites	Micro '*g*' and magnetic field space	GEO
22	GEO communications and warning vehicles	Fixed equatorial position	GEO
23	Lunar spaceport system	Lunar transportation/research hub	Lunar
24	Lunar orbital vehicles	Support lunar activities	Lunar
25	Planetary exploration vehicles	Near- and deep-space vehicles	LEO/Lunar

orbital, lunar and deep-space vehicle assembly in space. The operations center/space station provides a system to launch and control missions to the Moon, the planets and deep space. Like the USSR plan, there are lunar spaceports and lunar orbiting satellites. There are space deployment and retrieval vehicles as well as a waste storage and processing facility in high orbit. So this pictures provides a very comprehensive projection of future space if a suitable scheduled, frequent, and sustained transportation and heavy-lift capability is available. That is what is needed to plan for the future, not the current status quo. A functional orbital infrastructure, including space habitats, free-flying facilities, and power stations and several levels of development, is depicted using prior work of Dr Gaubatz. A list of the orbital vehicles and platforms and their functions shows their diversity.

What is not shown in the Gaubatz Figure 5.1 is a solar power station that beams power to the Earth's surface or space assets or a power station warehouse that provides hardware for the power satellites in geo-Earth orbit. It remains to be seen if a solar power satellite has energy conversion efficiency to provide affordable energy to Earth or space assets comparable to nuclear power stations. A source of excellent information on solar power stations is from reports by H.H. Koelle formerly at the University of Berlin [Koelle, 1993]. In fact the singular reliance on solar cell electric generation may doom all power stations until a more efficient and more durable conversion system can be identified. As proven by the NASA LDEF materials evaluation satellite, space is a very hostile environment and we have yet to identify slowly deteriorating or non-deteriorating materials and construction concepts. Nicholai Anfimov, of the Russian TsNIIMash, in a private communication, had stated that the hub of the Russian MIR orbital station (that stayed 15 years in orbit) was so riddled with solar particles that it was beginning to leak, even though there were no visible holes. The complexity and extensive nature of the space infrastructure means that a significant commitment of human and monetary resources is necessary if we are to go beyond a solitary orbital station with limited capability.

5.1 ENERGY REQUIREMENTS

The concept of train yard as a center of operations for switching, long-haul vehicle assembly, transfer of goods, refueling and repair is not unrealistic for the space infrastructure. As we shall see the energy requirements are greater for mobility in the vicinity of Earth than to reach LEO. There is a clear need for a nuclear powered tug for orbital transfer to LEO to geostationary orbits (GSO) and return, see Chapter 7. There is a need also for collecting, for repair or disposal, non-functional satellites in LEO and GSO; refueling of sustained-use satellites; orbital busses and tugs; and, generally speaking, for sustained in-orbit operations and maintenance. As we shall see, this implies a first step that must be taken as far as propulsion to anticipate the future, much as Steve Wurst has done for a space launcher.

5.1.1 Getting to low Earth orbit: energy and propellant requirements

At non-relativistic speed all of the classical orbital mechanics from near-Earth to the edge of our solar system and beyond are based on Newton's fundamental law of gravitational attraction. The assumption is that the gravity force, F_g, acts throughout the universe in the same way. Newton's law of universal gravitation is:

$$F_g = \text{Universal gravitational force between two bodies}$$

$$F_g = \frac{mMG}{d^2}$$

where m, M = mass of the two bodies, G = universal gravitational constant $= 6.67 \times 10^{-11}\ \mathrm{m^3\,kg^{-1}\,s^{-1}}$, and d = distance between the center of masses of the two bodies.

Gravity is probably one of the most mysterious forces in the universe. In fact, while our everyday experience of gravity is commonplace, our understanding is very limited. The law has been well tested on Earth and in the vicinity of the Earth. However, when astronomers attempt to use Newton's fundamental law of gravitational attraction to predict the motion of stars orbiting the center of the Galaxy, they get the wrong answers. The most distant man-made objects are *Pioneer 10*, launched in 1972 and *Pioneer 11*, launched in 1973. *Pioneer 10* is now more than 8 billion miles from Earth. On January 23, 2003 the tracking stations picked up the last feeble transmission from the probe's radioactive isotope (plutonium) powered transmitter [Folger, 2003]. As *Pioneer 10's* feeble signal faded from detection, the spacecraft seemed to be defying Newton's law of gravity because it was slowing down as if the gravitational attraction from the Sun was growing stronger the farther away it traveled. *Pioneer 11* also slowed down in a similar manner. The Ulysses spacecraft, which has been orbiting the Sun for 13 years, has also behaved in a manner characteristic of an unknown force slowing it down. This chapter will not attempt to explain the behavior, but there is scant but growing evidence that perhaps gravity does not act in the same way on a galactic scale. Our Galaxy makes one rotation in about the time from when dinosaurs began to inhabit the Earth to now. Perhaps on that time and distance scale gravity acts differently. Until more is known, we will continue with the traditional assumption of gravity acting the same throughout the universe, but also acknowledge that the farther we travel and the longer we are in space we may be departing slightly from the expected.

The law of gravity rules the attraction between two masses. When we put them into motion, then the laws that govern the two-body problem (that is, a large central body and a moving smaller body) yield Kepler's three laws of motion. Although these laws can be formulated for N number of bodies, the only analytic (closed-form) solutions found are for $N = 2$. Numerical solutions are possible, but these involve the use of the largest computers and are used only when the two-body problem is suspect (such as a Mercury orbiter) or high navigational accuracy is required [Brown, 1988]; the Keplerian circular orbit between two bodies is as given below [Koelle, 1961].

$$V_{\text{circular}} = \sqrt{\frac{MG}{r}} = \sqrt{\frac{\mu}{r}} = \sqrt{\frac{\mu}{R_0 + h}} \quad \text{km/sec}$$

$$\text{Period} = 2\pi\sqrt{\frac{r^3}{\mu}} = 2\pi\sqrt{\frac{(R_0 + h)^3}{\mu}} \quad \text{sec} \tag{5.1}$$

where μ = gravitational constant = MG, M = mass of the central body, r = radius from the spacecraft center of mass to the center of mass of the central body, R_0 = planet radius, and h = altitude above surface.

The gravitational parameters and the orbital speeds for a 200-km orbit and escape are given in Table 5.2 for selected bodies.

From equation (5.1), the orbital velocity decreases and the orbital period increases as the spacecraft altitude is increased (see Figures 3.5 and 3.6). The two-body equations assume non-rotating masses. If the central body is rotating, then its rotation can add a velocity vector increment to the launcher vehicle depending on the

Table 5.2. Gravitational characteristics of nearby planets and Earth's Moon.

	Venus	Earth	Moon	Mars	Jupiter
μ (km^3/sec^2)	324,858.8	398,600.4	4,902.8	42,828.3	126,711,995.4
R_0 (km)	6,061.8	6,378.14	1,737.4	3,397	71,492
V_{200} (km/sec)	7.203	7.784	1.680	3.551	42.10
V_{esc} (km/sec)	10.187	11.008	2.376	5.022	59.538

latitude of the launch site and the launch azimuth. Figure 5.2 shows the required velocity increment from the Earth's surface to the orbital altitude (in nautical miles).

Both the non-rotating Earth and rotating Earth (launch site at the Equator) velocity *increments* required are shown. These are not velocity in orbit, but the velocity increment (energy increment) that determines the mass ratio to reach simultaneously the given orbital altitude and required orbital speed. The speed of the Earth's surface at the Equator is 1,521 ft/sec. That reduces the launch speed increment (ΔV) to 24,052 ft/sec if the launcher is launched due east (90° from true north) at the Equator. If the launcher is launched due west, then the launcher must cancel out the easterly motion, so the launch speed increment (ΔV) is 27,094 ft/sec. For a true east launch, the launch velocity increment as a function of the launch site latitude is:

$$V_0 = V_{\text{circular}} - 1521 \sin(La)$$
$$La = \text{latitude of the launch site} \tag{5.2}$$

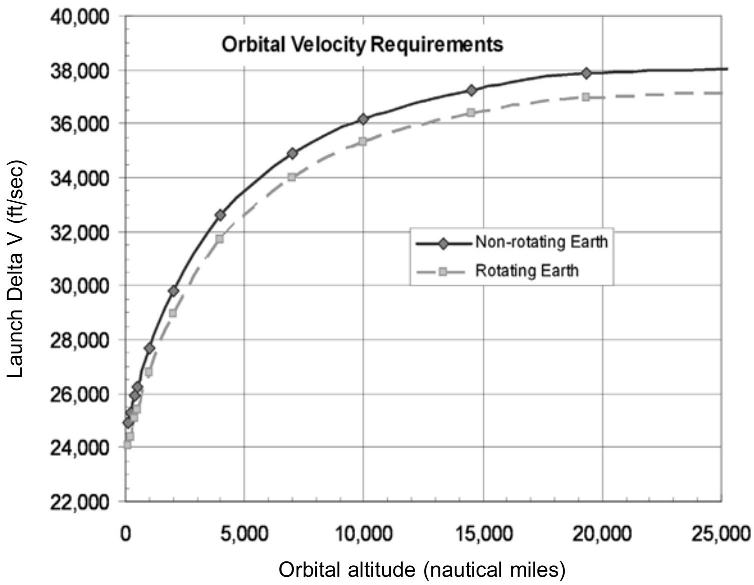

Figure 5.2. Launch velocity increment to reach Earth orbit.

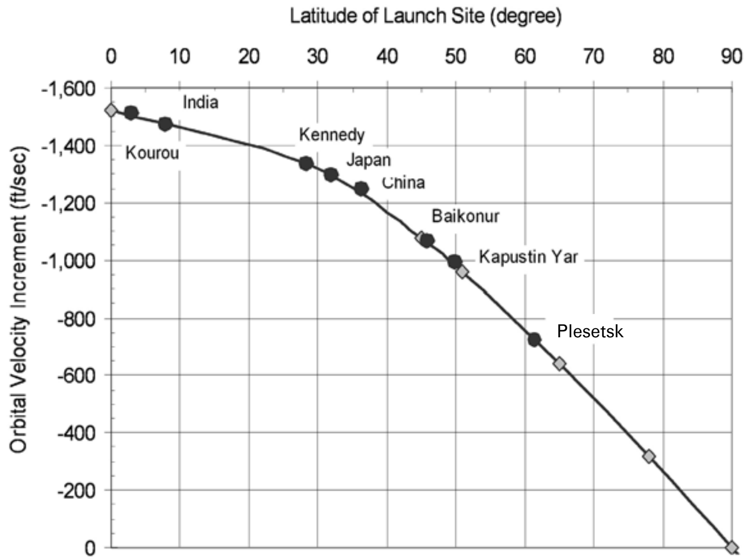

Figure 5.3. Velocity increment to 200 nautical mile orbit for orbital inclination. Some launch centers indicated.

For a due east launch, the inclination of the orbit is equal to the latitude of the launch site. Figure 5.3 shows the velocity increment for the launch ΔV as a function of the launch site azimuth for a due east launch with a number of launch sites indicated. In reality the launch azimuth will not always be due east. The launch azimuth for a non-rotating Earth at a given orbital inclination and launch site latitude is:

$$\sin A_z = \frac{\cos i}{\cos(La)}$$

$$A_z = \text{launch azimuth from true north}$$

$$i = \text{orbital inclination} \tag{5.3}$$

Equation (5.3) defines the minimum inclination for an orbit as the latitude of the launch site and a true east or west launch (90° or 270°). For the rotating Earth case a correction to the launch azimuth and velocity must be made by the vector addition of the eastward velocity of the Earth and the launch velocity vector. But equation (5.3) will give the minimum azimuth and a good first-order value. For a Sun-synchronous orbit (98°) from a launch site at 45° latitude this value is $-11.4°$ degrees or an azimuth of 348.6°. For a space station orbit (55°) from Kennedy (28.5°), the azimuth angle is 40.7° or just north of northwest. So if Shuttle launches from Kennedy, the spacecraft must roll so the wing plane is perpendicular to 40.7°, and then proceed along its launch trajectory.

Given the incremental velocity required to achieve a circular orbit, the next step is to determine the quantity of launch propellant required to place a given quantity of propellant into LEO for inter-orbit maneuvering.

5.2 LAUNCHER PROPULSION SYSTEM CHARACTERISTICS

Section 3.1 provides the governing equations and methodology for determining launcher size to achieve a given velocity increment with a given payload mass. The sizing process is the same. The difference is that, for a fixed-volume payload bay, each propellant combination has a different bulk density and therefore a different tank volume occupied for a fixed propellant mass. The role of the propellant delivery vehicle is analogous to that of an Air Force Tanker. Its role is to deliver fuel to in-flight operational vehicles on demand, and on a sustained operational basis. In this case the role of the LEO tanker is to routinely deliver propellant to an orbital refueling station in LEO. Being a dedicated tanker, the cargo container is a propellant tank, with provisions for transferring propellant in orbit. In micro-gravity special design considerations are necessary, e.g., that the propellant is adjacent to the transfer pumps, but this has been accomplished for some time in space and is a known design approach. In all cases, the LEO tanker is an automatic vehicle, that has sustained, frequent use and routinely exits and enters the atmosphere, and in not an expendable or a reusable expendable vehicle. So the configuration of the LEO tanker is that of a hypersonic glider or airbreathing launcher, as shown in Figures 2.16 and 2.17, and Figures 4.34 to 4.36. Four different launcher propulsion systems were evaluated for the tankers to LEO:

(1) Hydrogen/oxygen rocket, based on the Pratt & Whitney XLR-129.
(2) Hydrogen/oxygen LACE rocket based on the Pratt & Whitney XLR-129.
(3) Rocket ejector ram-scramjet airbreathing to Mach number 10, transitioning to a hydrogen/oxygen rocket, based on the Pratt & Whitney XLR-129.
(4) Rocket ejector ram-scramjet airbreathing to Mach number 12, transitioning to a hydrogen/oxygen rocket, based on the Pratt & Whitney XLR-129.

The design payload is 19 tons (41,895 lb) of propellant with a bulk density of 999.4 kg/m^3 (62.4 lb/ft^3). A launcher for the design payload was sized for each propulsion system. For different propellant densities, the size and weight of the launcher is different, and these corrections are discussed later in this chapter and are given in Figure 5.6.

5.2.1 Propellant ratio to deliver propellant to LEO

The propellant ratio is defined here as the propellant mass burned by the launcher to achieve LEO, divided by the propellant load carried to LEO. Both the mass of propellant and the density of the propellant affect the size of the launcher, and this sensitivity was evaluated. The launchers were sized using the methodology of

Table 5.3. Launchers sized to deliver 19 tons of propellant to LEO.

	H_2/O_2 rocket FDL-7C/D	LACE rocket FDL-7C/D	RBCC Mach 10 airbreather	RBCC Mach 12 airbreather
Planform area	600 m^2	370 m^2	301 m^2	268 m^2
Weng	27.95 tons	11.85 tons	11.13 tons	8.92 tons
OEW	97.86 tons	57.9 tons	46.73 tons	40.18 tons
OWE	116.9 tons	76.9 tons	65.73 tons	59.18 tons
W_{ppl}	892.9 tons	379.2 tons	235.2 tons	181.0 tons
TOGW	1,010 tons	456.1 tons	300.9 tons	240.1 tons
Propellant ratio	47.0	20.0	12.4	9.53

Design payload is 19 tons (41,895 lb) of propellant with a bulk density of 999.4 kg/m^3 (62.4 lb/ft^3).

Vandenkerckhove–Czysz described in Chapter 4 and not repeated here. The vehicle assumptions were the same as Chapter 4 except that a permanent propellant tank replaced the accessible payload bay. For the design payload and payload density, the sizing results are given in Table 5.3.

The propulsion system selection determines the key parameter for an orbital tanker, the propellant burnt to lift the orbital maneuver propellant, divided by the propellant delivered. The LACE rocket is an adaptation of an existing, operational rocket engine, and requires good engineering design and testing, but it is *not* a technological challenge. The LACE rocket offers a greater than 50% reduction in the propellant required to deliver the design 19 tons of propellant to LEO, as shown in Table 5.3 and Figure 5.4. Because of the LACE rocket's greater thrust/drag ratio, the propellant ratio is slightly better than a rocket ejector ramjet utilizing atmospheric air up to Mach 6. A piloted vehicle is a disadvantage for an orbital tanker in that the provisions for the pilot increases the propellant required to deliver the orbital propellant to LEO. Transitioning to an airbreather vehicle and propulsion configuration offers the potential to reduce the propellant required to deliver the orbital maneuver propellant by 38% and 52% respectively. Proceeding beyond an airbreathing Mach number of 12 results in an increase in the propellant required to deliver the orbital maneuver propellant.

The important conclusion from this analysis is that a first step, based on an existing rocket motor (LACE rocket) offers a 57% reduction in the propellant required to deliver the orbital maneuver propellant. And that step does not require a technological breakthrough but only an adaptation of an existing operational propulsion system. The important observation is that even with the best propulsion system for the launcher, it requires 10 pounds of launcher propellant to deliver 1 pound of orbital maneuver propellant to LEO, so the orbital maneuver vehicle needs to be a very efficient user of orbital propellant.

In this exercise the design payload was 19 metric tons. If that payload mass is *increased*, there is a gradual decrease in the *percentage* of the propellant required to deliver the orbital maneuver propellant, as shown in the top graph of Figure 5.5. However, if the payload is *decreased* the propellant required to deliver the orbital

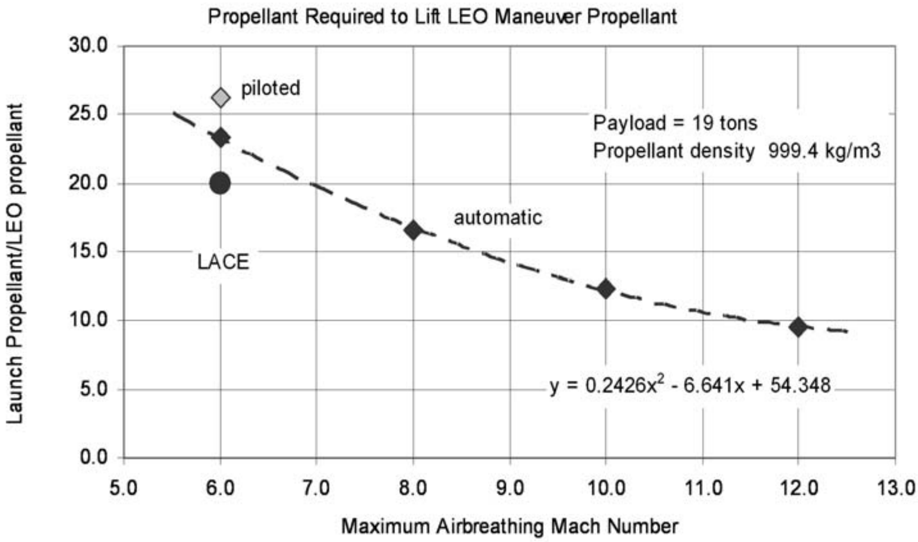

Figure 5.4. Launch propellant required to lift orbital maneuver propellant to LEO by a rocket ejector ramjet. All-rocket ratio = 47.

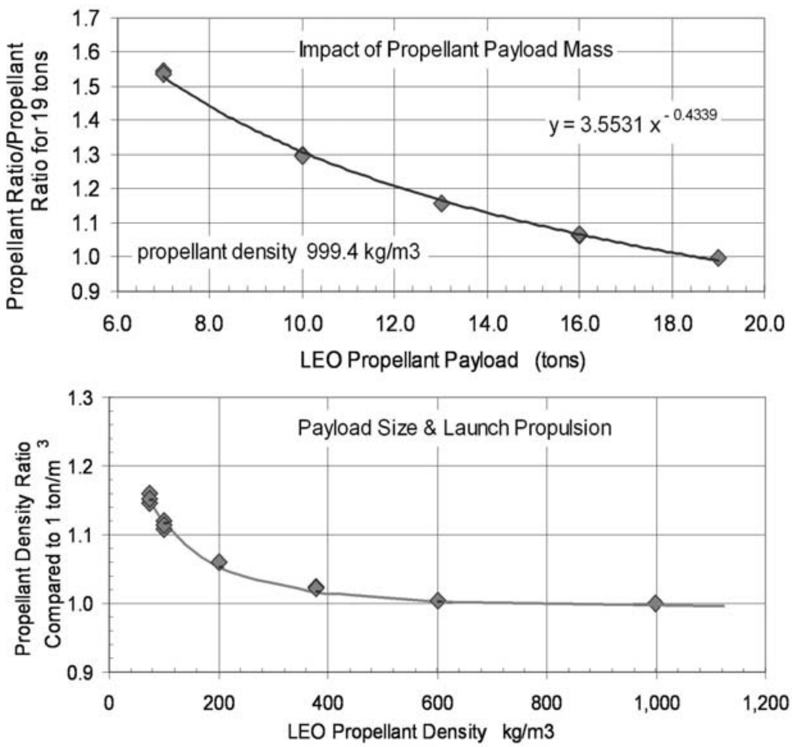

Figure 5.5. Propellant required parametrics with respect to payload mass and density.

Table 5.4. Characteristics of space propulsion systems for orbital maneuvering vehicles.

	Hypergolic rocket	Hydrogen/oxygen rocket	Solar electric	Nuclear electric
Fuel	Hydrazine	Hydrogen	Lithium	Lithium
Oxidizer	Nitrogen Tetroxide	Oxygen	none	none
Bulk density (kg/m^3)	1,229	378.0	533.7	533.7
I_{sp} (sec)	290	460	3,200	9,000
Density I_{sp} (sec)	357	174	1,705	4,797

maneuver propellant increases quickly. At 7 metric tons the propellant required to deliver the orbital maneuver propellant is 50% greater than for 19 tons. The correlating curve fit is:

$$\frac{\text{Launcher propellant}}{\text{LEO propellant}} = 3.5531\,(W_{\text{payload}})^{-0.4339} \tag{5.4}$$

Orbital maneuvering vehicles (OMV) are powered by a mix of propulsion systems and propellants, so a parametric sizing effort established the variability of the ratio of launcher propellant to propellant payload with payload propellant bulk density and payload mass. A representative set of orbital maneuver propulsion systems is given in Table 5.4. This is only meant to span possible systems and is by no means all-inclusive or comprehensive. The density I_{sp} (specific gravity times I_{sp}) is a measure of the relative volume taken by the propellant system. In that respect the hypergolic propellants take always less volume than a hydrogen-fueled system.

For propellant bulk densities greater than 700 kg/m^3 (43.7 lb/ft^3) there is no change is the propellant/payload ratio. That is, the propellant payload volume does not influence how much propellant is required to deliver the orbital maneuver propellant, the payload mass does. For propellant bulk densities less than 700 kg/m^3 (43.7 lb/ft^3) there is an increase in the propellant required to deliver the orbital maneuver propellant. That is, now *both* the propellant mass *and* the volume of the orbital maneuver propellant determine the size and volume of the launcher. The result is an increase in propellant required to deliver the orbital maneuver propellant as shown in the bottom graph of Figure 5.5. The correlation curve fit for propellant bulk densities less than 700 kg/m^3 (43.7 lb/ft^3) is:

$$\frac{\text{Launcher propellant}}{\text{LEO propellant}} = 2.189 - 0.3524X + 0.0263X^2$$

where

$$X = \ln(\text{LEO propellant density})\ (\text{kg/m}^3) \tag{5.5}$$

The range of launcher propellant required to lift one mass unit of orbital maneuver propellant into LEO is from 47 to 9.5. Compare this to a Boeing 767-200 carrying 216 passengers over a 5,800 km distance: the fuel consumed is 2.6 mass units per one mass unit of payload. The oxidizer-to-fuel ratio for the airbreather to Mach 12 is 3.14, and the resulting fuel-to-payload ratio is 3.02. That implies that the airbreathing launcher is only about 16% less efficient in its propulsion system flying to Mach 12 as a Mach 0.85 transport. Concorde, flying 100 passengers at Mach 2.04 over a 6,300 km distance consumes about 8.3 mass units of fuel per unit mass unit of payload. So in fact the airbreathing launcher is more efficient than Concorde in terms of fuel use. Given the propellant required to lift the orbital maneuver propellant to LEO, the task remains to establish how much orbital maneuver propellant is required.

5.2.2 Geostationary Orbit satellites sizes and mass

The first step is to examine a number of geostationary orbit (GSO) satellites from the open literature and determine a representative reference value. The goal is to generate a 'reference GSO satellite' that is heavy enough to represent future satellites and provide a reasonable estimate of the orbital propellant required. Table 5.5 gives the dimensions of the satellite main body, with all antennas folded. The mass ratio determined by the 'beginning-of-life' mass and the 'empty' mass is the propellant required for maintaining the GSO orbit and station-keeping due to orbital precession.

Referring to *Aviation Week and Space Technology* of 31 October 2003, the cover has a picture of the Boeing Satellite Systems 601B for broadcast and broadband multimedia services. This is not unlike the reference satellite in Table 5.5. Given a reference satellite, how much propellant is required to change its altitude and orbital inclination?

Table 5.5. Characteristics of a number of GSO satellites [Karol, 1997].

System	Length (m)	Width (m)	Height (m)	Volume (m^3)	Beginning-of-life (BOL) mass (kg)	Empty mass (kg)
ASTRA-1F	4.51	3.41	2.80	43.2	1,803	1,279
EHF-7	3.35	3.35	3.35	37.7	1,224	868
INTERSAT 707	4.69	2.41	2.19	27.2	3,649	1,760
APSTAR 1A	6.58	2.16[a]	2.16[a]	24.1	584	414
CHINSAT 7	6.58	2.16[a]	2.16[a]	24.1	557	395
N-STAR-B	3.05	2.40	2.20	27.3	1,617	2,057
INMARSAT III	2.10	1.80	1.71	16.7	1,098	778
AMOS-1	1.22	1.68	1.92	10.5	579	410
Reference	3.40	2.80	2.80	26.7	2,267	1,608

[a] Diameter, cylindrical configuration.

5.3 MANEUVER BETWEEN LEO AND GEO, CHANGE IN ALTITUDE AT SAME ORBITAL INCLINATION

The nominal LEO is 100 nautical miles (185.2 km) or 200 km (108 nautical miles). To reach a higher-altitude orbit is usually a two-step process, as shown in Figure 5.6 for GSO for example. For a general elliptical orbit the lowest altitude is the periapsis and the highest is the apoapsis. Specifically for selected bodies:

General	Sun	Earth	Moon
Periapsis	Perihelion	Perigee	Perilune
Apoapsis	Aphelion	Apogee	Apolune

The first step is an elliptical transfer orbit to the orbital altitude desired, which requires a propulsion burn to leave the low-altitude orbit; the second step is a propulsion burn to match the circular orbital velocity at the desired higher orbital altitude. This process to return to the low orbital altitude requires a burn to match the elliptical orbital speed at the higher altitude, then a second propulsion burn to match the lower circular orbit speed. This is a minimum energy transfer orbit, or a Hohmann transfer. Equation (5.1) provides the magnitude of the circular orbital velocity at the desired altitude.

Figure 5.6 shows the geometry for an elliptical transfer orbit from LEO to GSO, as an example. The information needed is the elliptical orbit velocities for the lowest

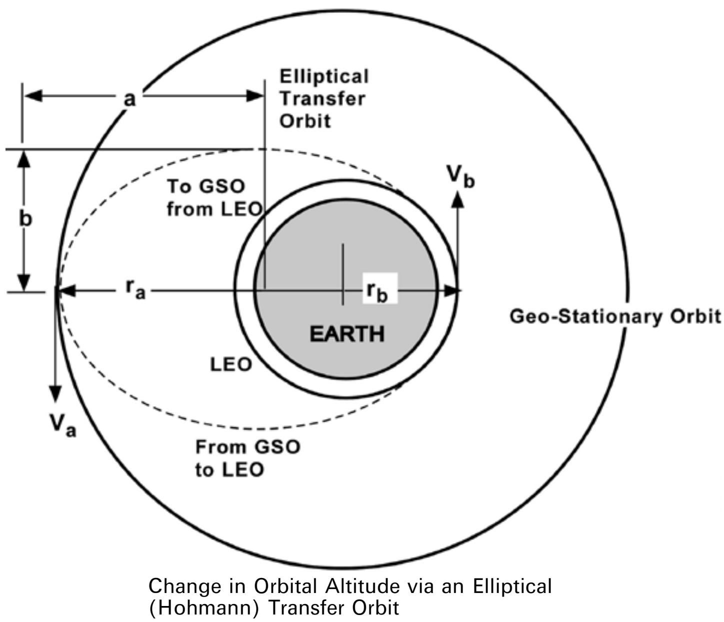

Figure 5.6. Transfer ellipse to change orbital altitude.

orbital altitude (periapsis) and the highest orbital altitude (apoapsis). Equation set (5.6) provides the orbital parameters for Keplerian elliptical orbits.

$$V_{\mathrm{p}} = \text{Velocity at periapsis}$$
$$V_{\mathrm{p}} = \sqrt{\frac{2\mu}{R_0 + h_{\mathrm{p}}} + \frac{\mu}{a}}$$
$$V_{\mathrm{a}} = \text{Velocity at apoapsis}$$
$$V_{\mathrm{a}} = \sqrt{\frac{2\mu}{R_0 + h_{\mathrm{a}}} - \frac{\mu}{a}}$$
$$h_{\mathrm{a}} = \text{Apoapsis altitude}$$
$$h_{\mathrm{p}} = \text{Periapsis altitude}$$
$$a = \text{Semi-major axis of transfer ellipse}$$
$$\mathrm{a} = [(R_0 + h_{\mathrm{a}}) + (R_0 + h_{\mathrm{p}})]/2$$
$$\mathrm{e} = \text{Eccentricity (defines the shape of the orbit)}$$
$$\mathrm{e} = (r_{\mathrm{a}} - r_{\mathrm{p}})/(r_{\mathrm{a}} + r_{\mathrm{p}})$$
$$\text{Period of ellipse} = 2\pi\sqrt{\frac{a^3}{\mu}} \tag{5.6}$$

The Keplerian orbits are conic sections. In this general sense an orbit is a path through space defined by a conic section. There are two closed orbital solutions (circular and elliptical) and two open (not returning) orbital solutions (parabolic and hyperbolic). For a circular orbit the eccentricity (e) must be equal to zero. For an elliptical orbit, eccentricity (e) must be less than one. For a parabolic orbit, eccentricity (e) must be equal to one. For a hyperbolic orbit, eccentricity (e) must be greater than one.

The velocity increments to achieve an orbital altitude change are then

Increasing orbital altitude	Decreasing orbital altitude
$\Delta V_1 = V_{\mathrm{p}} - V_{\mathrm{circular,\,p}}$	$\Delta V_1 = V_{\mathrm{circular,\,a}} - V_{\mathrm{a}}$
$\Delta V_2 = V_{\mathrm{a}} - V_{\mathrm{circular,\,a}}$	$\Delta V_2 = V_{\mathrm{circular,\,p}} - V_{\mathrm{p}}$ (5.7)

So to increase orbital altitude there is a propulsion burn at periapsis to accelerate to elliptical orbit speed, then at apoapsis there is a propulsion burn to increase the spacecraft speed to circular orbit speed at the higher altitude. To decrease orbital altitude there is a propulsion burn at apoapsis to slow the spacecraft to elliptical orbit speed, then at periapsis there is a propulsion burn to decreases the spacecraft speed to circular orbit speed at the lower altitude. Specifically, in transferring from a 100 nautical mile (185.2 km) LEO to a 19,323 nautical mile (35,786 km) GSO orbit (refer to Figure 5.6 for the geometry of the transfer maneuver and the location of the velocities called out) the orbital velocity for a 100 nautical mile (185.2 km) circular orbit is 25,573 ft/sec (7,795 m/sec). For an elliptical transfer orbit, the orbital velocity at the 100 nautical miles (185.2 km) perigee is 33,643 ft/sec (10,254 m/sec) and 5,235 ft/sec (1,596 m/sec) at the 19,323 nautical miles (35,786 km) apogee. The orbital velocity for a 19,323 nautical miles (35,786 km) circular orbit is 10,088 ft/sec (3,075 m/sec).

5.3.1 Energy requirements, altitude change

Referring to Figure 5.6, to initiate the transfer maneuver the spacecraft must be 180 degrees away from the desired point in the GSO orbit. A that point, a rocket burn is required to increase the spacecraft velocity from 25,573 ft/sec to 33,643 ft/sec, an incremental velocity of 8,070 ft/sec (2,460 m/sec). The spacecraft is now in an elliptical trajectory towards the 19,323 nautical miles (35,786 km) apogee. When apogee is reached, the elliptical orbital velocity is 5,235 ft/sec (1,596 m/sec). That is slower than the 10,088 ft/sec (3,075 m/sec) required for a GSO circular orbit. So at apogee a rocket burn provides a 4,853 ft/sec (1,479 m/sec) velocity increment necessary to circularize the orbit, otherwise the spacecraft will continue along its elliptical trajectory. The *total* velocity increment is 12,923 ft/sec (3,939 m/sec). To return to LEO, the opposite sequence of events is necessary. Again at the orbital location opposite the location point in the LEO orbit, a retro-burn of minus 4,853 ft/sec (1,479 m/sec) velocity is necessary to slow the spacecraft to the elliptical orbit apogee velocity of 5,235 ft/sec (1,596 m/sec). When approaching the 100 nautical mile altitude, the elliptical orbit speed is approaching 33,643 ft/sec (10,254 m/sec). In order to achieve a 100 nautical mile circular orbit, a retro-burn of minus 8,070 ft/sec (2,460 m/sec) is necessary to reach the 100 nautical mile circular orbit speed of 25,573 ft/sec (7,795 m/sec). For a round trip a total of four rocket firings are required for a total incremental velocity of 25,846 ft/sec (7,878 m/sec), or greater than the incremental velocity to reach LEO!

So, to change orbital altitude requires the expenditure of energy. The amount of the energy depends on the altitude change desired. The incremental velocity to move from a 100 nautical mile or 200 km orbital altitude is given in Figure 5.7. The incremental velocity curve is very non-linear. A 6,000 ft/sec (1,829 m/sec) incremental velocity will permit an altitude change of about 3,000 nautical miles (5,556 km). However a burn of twice the velocity increment, 12,000 ft/sec (3,658 m/sec) will permit an altitude change of about 13,000 nautical miles (24,076 km), or 4.3 times greater.

5.3.2 Mass ratio required for altitude change

The previous section provides the methodology to determine the magnitude of the incremental velocity to achieve a given orbital altitude change, in a fixed orbital inclination. The propulsion systems described in Table 5.3 provide the specific

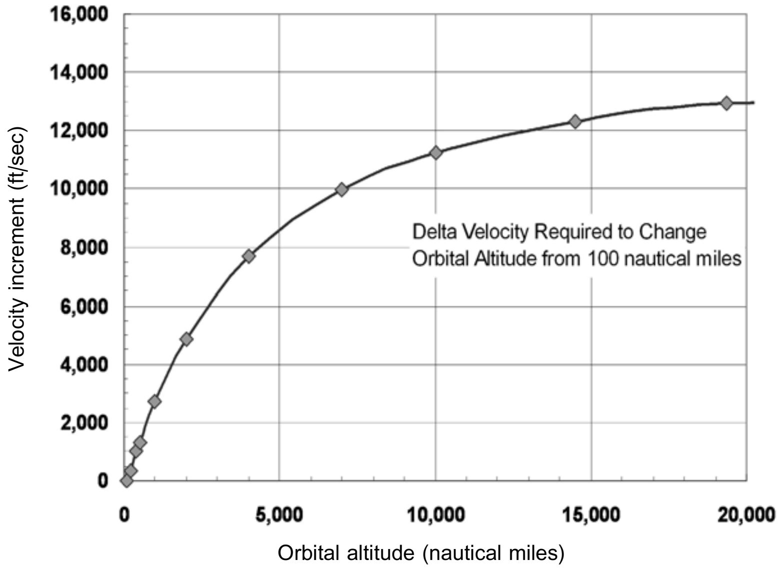

Figure 5.7. Velocity requirement to change orbital altitude can approach one-half of the orbital speed.

impulse (I_{sp}) for each of four systems. In space there is no atmospheric drag, so the ideal weight ratio equation (5.8) applies:

$$\mathrm{WR} = \frac{\Delta V}{g\, I_{sp}} \tag{5.8}$$

Translating the incremental velocity data and specific impulse data into weight ratio yields Figure 5.8. The weight ratio for the four propulsions systems described in Table 5.3 is indicated in the legend. The weight ratios for the LEO to GSO orbital altitude change are: 4.00 for the hypergolic engine, 2.39 for oxygen/hydrogen, 1.55 for solar electric and 1.11 for nuclear electric. The acceleration specified for the chemical rocket powered OMV is 0.5 '*g*'. For the electric thruster-powered OMV the acceleration is 0.1 '*g*'. The gross weight of the one-way OMV is straightforward, and the sizing program balances the propellant required versus the capacity of the propellant tank that determines the operational empty weight (OEW). The sized OMV for each of the propulsion systems transporting a 5,000-lb (2.268-ton) satellite given in Table 5.6 that follows. The gross weight for the one-way mission is:

$$\begin{aligned} \text{Gross weight} &= \mathrm{WR}\,(\mathrm{OEW_{OMV}} + W_{\text{satellite}}) \\ W_{\text{propellant}} &= (\mathrm{WR} - 1)(\mathrm{OEW_{OMV}} + W_{\text{satellite}}) \end{aligned} \tag{5.9}$$

Note that the Operational Empty Weight (OEW) is essentially constant. It is greater for the electric propulsion configurations because of the solar panels for the solar electric and radiators for the nuclear electric. As in the case for the launchers, the

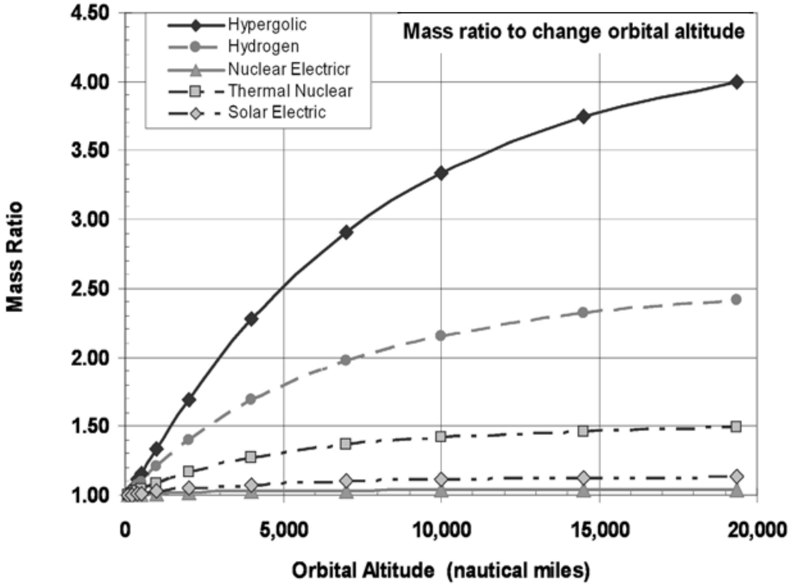

Figure 5.8. Mass ratio required to change orbital altitude is very dependent on the propulsion system performance (I_{sp}).

primary difference in the weights and thrusts is a result of the carried propellant. The propellant mass for the hypergolic rocket is 34 times greater that for the nuclear electric rocket. The propellant load is reduced by the increasing specific impulse of the propulsion system, and the reduction in mass and thus engine thrust and propellant flow rate. Unlike the space launcher, where the payload is about one-seventh the OEW, for the Orbital Maneuver Vehicle the payload is greater than the OEW. The OEW differs from 'empty' or 'dry' weight in that all of the fluid lines are filled and any trapped fluids or propellants are included in the OEW. The operational weight empty (OWE) is the OEW plus the payload. That is it is the vehicle operationally ready but without the propellants loaded. The satellite (payload) weight for the OTV is 2.268 tons. The Russian Progress capsule can deliver 3.5 tons to LEO and the Projected European Space Agency (ESA) Automated Transfer Vehicle (ATV) is being designed for 7.5 tons [Snead, 2003]. If the OMV in Table 5.6 is extended for

Table 5.6. Sized orbital maneuver vehicles for one-way mission from LEO to GSO.

Propulsion	Gross mass (tons)	Propellant (tons)	OWE (tons)	OEW (tons)	One-way mass ratio	Thrust (kN)
Hypergolic	12.01	9.00	3.01	0.738	3.996	58.67
H_2/O_2	7.14	4.16	2.98	0.716	2.418	35.02
Solar electric	4.80	1.59	3.21	0.945	1.134	4.71
Nuclear electric	3.60	0.345	3.25	0.985	1.046	3.53

Table 5.7. Payload size versus OMV for a hypergolic propulsion system with a one-way mass ratio of 4.

Payload (tons)	Gross mass (tons)	Propellant (tons)	OEW (tons)	OWE (tons)	Thrust (kN)
2.268	12.01	8.991	0.735	3.02	58.7
3.50	18.32	13.71	1.106	4.61	89.9
3.650	19.08	14.28	1.148	4.80	93.6
4.00	20.86	15.61	1.245	5.24	102
4.50	23.38	17.50	1.380	5.88	115
5.50	28.40	21.25	1.641	7.14	139
6.50	33.36	24.97	1.891	8.39	164
7.50	38.28	28.65	2.130	9.63	188

different payloads masses for hypergolic propulsion, the size and mass trends can be established, as given in Table 5.7.

For payloads greater than 4.9 tons, the 19 tons of propellant payload delivered to LEO by the tanker launcher is insufficient for a LEO to GSO mission. This is shown for hypergolic propulsion because as advanced propulsion enters orbital operations, the propellant requirement will substantially reduce, even for the heavier payloads. The propellant load scales as the mass ratio minus one, so for nuclear electric the propellant load for the 7.5-ton payload OMV is only 1.07 tons and for the solar electric it is 4.71 tons. But as long as the principal orbital maneuver propellant of choice is hypergolic, the orbital propellant requirements will steadily increase. The ESA ATV meets a current need. With the Space Shuttle again grounded, a more substantial thrust OMV is required to re-boost the International Space Station (ISS) and some mechanism to provide service capability to the Hubble Telescope is necessary. If Hubble were to be placed at the same orbital inclination as ISS, but at a higher altitude, Hubble could be serviced from ISS without an operational Shuttle.

The gross weight of the two-way OMV is more complex because the OMV must carry the return-to-LEO propellant to GSO. The sizing program balances the total propellant required versus the capacity of the propellant tanks that determines OEW. The sized OMVs for each of the propulsion systems transporting a 5000-lb (2.268-ton) satellite is given in Table 5.8 that follows. The gross weight for the two-way mission is:

$$\begin{aligned}
\text{Gross weight} &= [\mathrm{WR}(\mathrm{OEW}_{\mathrm{OMV}}) + W_{\mathrm{satellite}}]\,\mathrm{WR} \\
&= \mathrm{OEW}_{\mathrm{OMV}}\cdot\mathrm{WR}^2 + \mathrm{WR}\cdot\mathrm{W}_{\mathrm{satellite}} \\
(W_{\mathrm{propellant}})_{\mathrm{to\ LEO}} &= (\mathrm{WR}-1)(\mathrm{OEW}_{\mathrm{OMV}}) \\
(W_{\mathrm{propellant}})_{\mathrm{to\ GSO}} &= [\mathrm{WR}(\mathrm{OEW}_{\mathrm{OMV}}) + \mathrm{W}_{\mathrm{satellite}}](\mathrm{WR}-1) \qquad (5.10)
\end{aligned}$$

As would be expected the to-GSO and return OMV is significantly larger than the one-way vehicle, Table 5.8. Other than being larger, the same comments apply to the

Table 5.8. Sized OMVs for two-way mission from LEO to GSO to LEO.

Propulsion	Gross mass (tons)	Propellant (tons	OWE (tons)	OEW (tons)	Two-way mass ratio	Thrust (kN)
Hypergolic	27.07	23.70	3.37	1.10	16.00	119.5
H_2/O_2	10.98	7.79	3.19	0.925	5.71	53.83
Solar electric	5.99	2.59	3.39	1.12	2.22	5.87
Nuclear electric	3.79	0.494	3.30	1.03	1.23	3.72

two-way OMV as the one-way OMV. In launches to GSO with the current multi-stage rockets, the propellant in the upper stage (usually third stage) contains the propellant for the elliptical geo stationary transfer orbit and the GSO circularization propellant is carried in the GSO satellite. Sizing the one-way mission gives some indication of the upper stage propellant mass required to place the payload into GSO transfer orbit. Given the function of the OMV, the two-way mission is the logical sizing mission.

With a conventional rocket-powered OMV, rocket engines of approximately the correct thrust are available. For example, a hypergolic restartable rocket in the 50 to 60 kN range is available from the Ukrainian Yuzhnoye organization and is the YUZ-U-29 rocket propulsion system for the Tsyklon launcher. The specific impulse is 289 sec for a total installed engine thrust-to-weight ratio 49.1, and with a thrust of 56 kN. The hydrogen/oxygen rocket in the 35 kN range is available both from the United States and from the former USSR. The collaboration of Energomash and Khimki has produced an in-development engine of the correct thrust level, the ENM-C-36. The specific impulse is 461 sec. The Pratt & Whitney RL-10 is also a candidate. As the RL-10 is an expansion turbine cycle, its potential operational life is very long compared to a conventional rocket engine.

Electric-powered engines for the solar electrical and nuclear electrical are a challenge in that there are no engines or group of engines in the thrust class required. The largest electric thrusters are in the former Soviet Union and are about 1 N in gross thrust! At one-tenth '*g*' acceleration the total velocity increment of 12,923 ft/sec (3,939 m/sec) is achieved in 1.11 hours. At one-hundredth of a '*g*' the time required is 11.16 hours, and this choice of acceleration would reduce the thrust to the 5 to 6 kN range. The only future electric thruster that appears capable of such thrust levels is the VASIMR engine (see Chapter 7) [NASA/ASPL site, 2000]. It may not be possible to fabricate solar panels of the size necessary to drive an electric thruster in the 5 to 6 kN thrust level, given the low energy conversion efficiency of the solar panels. A 0.57 N thruster with a 50% energy conversion efficiency would require an input from the solar panels of about 30 to 40 kW. A 5,700 N thruster, by analogy, would require an input of some 300 to 400 MW, an unheard of power level for solar panels. The largest multimedia communication satellites have total solar panel power of from 5 to 6 kW. This would be 1,000 times greater. At that power level, to reach an incremental velocity of 12,923 ft/sec (3,939 m/sec) the acceleration time is 46.5 days, slow, but still operationally practicable for some GSO operations. An order of magnitude increase in thrust to 5.7 N would reduce the transit time to 4.6 days, a more acceptable level. So that may be the first objective in developing thrusters for the solar electric OMV.

We now have both the quantity of launcher propellant required to deliver the OMV propellant to LEO, and the OMV propellant required in each of three orbital maneuver missions. So we can now determine the total mass units of propellant (launcher and OMV) required per unit mass of the satellite for each of the four space propulsion systems.

5.3.3 Propellant delivery ratio for altitude change

In Figure 5.9 the ratio of the total mass units of propellant (launcher and OMV) required per unit mass of the satellite is presented for the four space propulsion systems and the four launcher propulsion systems, namely those in Table 5.9.

Figure 5.9 shows the dramatic reduction in the total propellant mass (launcher and OMV) required per unit mass of the satellite, for all of the OMV propulsion systems, by advancing the performance of the launcher propulsion system. By incorporating a LACE system into an existing hydrogen/oxygen rocket the propellant required to deliver 1 mass unit of propellant to LEO is reduced by 56%. Proceeding to a Mach 12 ram/scramjet produces another 50% reduction in the required propellant to deliver 1 mass unit of propellant to LEO. So instead of the 190.5 mass units of propellant required, LACE reduces that number to 83.1 and a Mach 12 ram/scramjet reduces that to 41.8 propellant mass units required to deliver

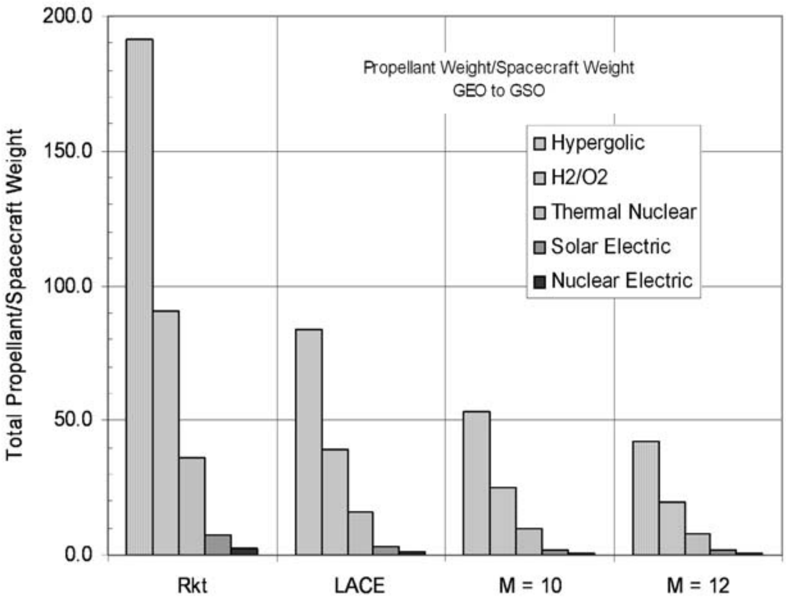

Figure 5.9. Ratio of total propellant weight/satellite weight.

Table 5.9. Launcher and OMV propulsion options.

Launcher propulsion	OMV propulsion
Hydrogen/oxygen rocket based on the P&W XLR-129	Hypergolic, restartable, long-life rocket closed turbopump cycle rocket
LACE rocket based on the P&W XLR-129	Hydrogen/oxygen restartable, long-life expander or closed-cycle rocket
Rocket ejector ram/scramjet to $M = 10$ + hydrogen/oxygen rocket	Electric MHD thruster with lithium fuel powered by solar panels
Rocket ejector ram/scramjet to $M = 12$ + hydrogen/oxygen rocket	Electric MHD thruster with lithium fuel powered by nuclear reactor

1 mass unit of propellant to LEO. However, the real advances occur when both the launcher and the OMV propulsion is improved.

Figure 5.10 focuses in on the electric propulsion for the OMV and the more efficient launcher propulsion systems. Now the propellant required to deliver 1 mass unit of propellant to LEO is between 4.5 and 2. Now it becomes practicable to deliver propellant to LEO as the propellant cost is no more than the propellant to deliver a unit mass of payload in a commercial transport. Although it is nearly prohibitive in terms of hypergolic space rockets and conventional launch rockets to deliver significant quantities of orbital maneuver propellant to LEO (the actual

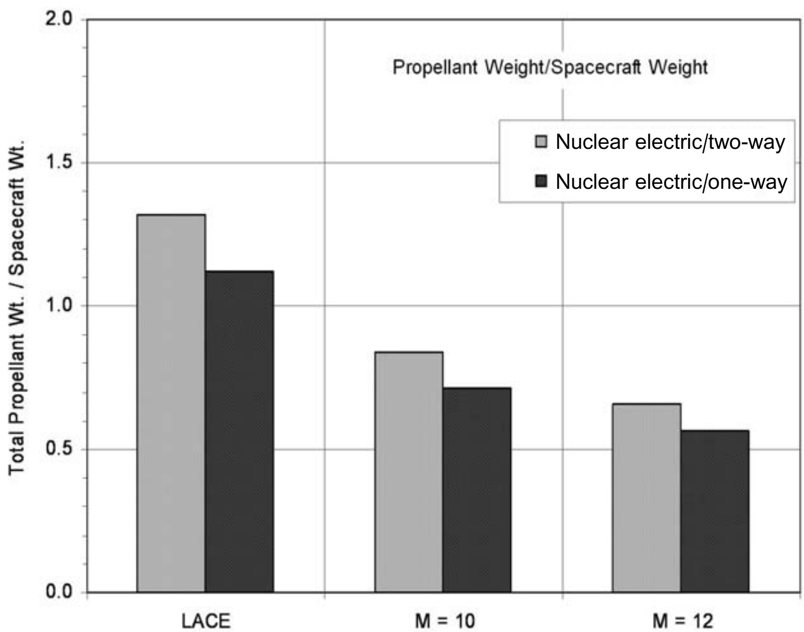

Figure 5.10. Ratio of total propellant weight/satellite weight for nuclear electric propulsion.

figure is 190.5 kg of propellant per kilogram of LEO propellant delivered), the future holds a dramatic reduction in that quantity by a factor about 20 just by using hydrogen/oxygen propulsion in space, and using a combination of hydrogen/oxygen rocket and airbreathing propulsion for the launcher. With space electric propulsion and hydrogen/oxygen rocket plus airbreathing propulsion for the launcher that ratio can be reduced to 2 or 3 kg of burnt propellants per kg delivered to orbit. The orbital tanker is now competitive with a KC-135 or modified B-767 for refueling missions.

5.4 CHANGES IN ORBITAL INCLINATION

Orbital plane change is a challenging propulsion space maneuver. It requires a large expenditure of energy to achieve a small change in the orbital plane. A propulsive plane change is an impulse turn, and is executed with the thrust line perpendicular to the orbital path and in the direction of the plane change. The equation for the incremental velocity for an impulse turn is given in equation (5.11) for a non-rotating Earth.

$$\Delta V_{\text{pc}} = 2\sqrt{\left(\frac{\mu}{R_0 + h}\right)} \sin\left(\frac{\alpha}{2}\right)$$

$$\mu = 1.407645 \times 10^{16} \ \frac{\text{ft}^3}{\text{sec}^2} \text{ Earth}$$

$$R_0 = 3442.5 \text{ nautical miles}$$

$$h = \text{orbital altitude from surface}$$

$$\alpha = \text{plane change angle} \tag{5.11}$$

As indicated by equation (5.11), the higher the orbital altitude the less the incremental velocity for a given plane change. To travel to that higher orbital altitude requires propellant, as we have just seen in the previous section. So there is an opportunity for a trade-off as to whether the change in orbital altitude propellant plus the reduced plane change propellant is less than the lower altitude plane change. From equation (5.11), the incremental velocity per 1-degree change in orbital plane is about 446 ft/sec (135.9 m/sec) at an orbital altitude of 100 nautical miles. So a 5-degree plane change requires an incremental velocity of 2,230 ft/sec (679.7 m/sec).

The right sketch in Figure 5.11 depicts an orbital plane change in LEO, and a higher-altitude elliptical orbit to execute the plane change at a higher orbit. To accomplish this a rocket burn is required to put the spacecraft into the elliptical orbit, then at apoapsis a rocket burn to rotate the orbital plane, and finally a final rocket burn to return the spacecraft to the lower-altitude circular orbital speed. As we shall see, there is an angle above which this procedure requires less incremental velocity than a lower orbital altitude plane change.

The left sketch in Figure 5.11 depicts an orbital plane change in LEO performed

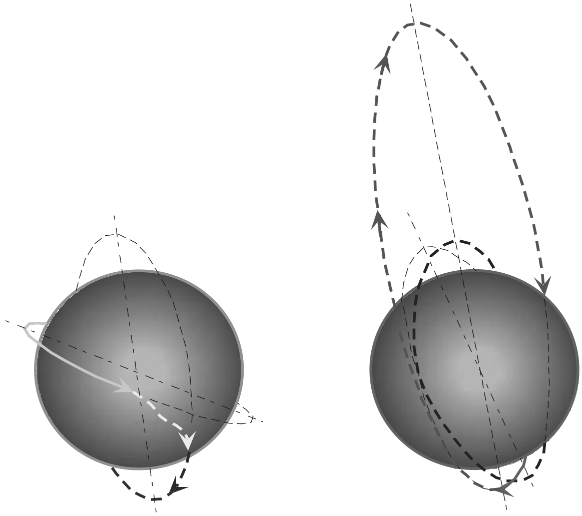

Orbital plane change at 218,000 ft with an aerodynamic turn in the atmosphere from a 200 nautical mile orbit

An impulse orbital plane change from a 200 nautical mile orbit via an elliptical transfer orbit to GSO altitude

Figure 5.11. Orbital plane change via an aerodynamic turn in the upper atmosphere (Left) and an impulse turn executed during an elliptical transfer orbit to 22,400 nautical mile orbit.

by entering the Earth's upper atmosphere with a high lift-to-drag ratio hypersonic glider and executing a thrust-equals-drag aerodynamic turn at maximum L/D. This maneuver requires a hypersonic glider, but it enables a much larger orbital plane change for the same propellant consumed. With conventional rocket propulsion, this method of changing the orbital plane is always a lesser energy approach. This was first analyzed and presented by Dr Wilbur Hankey in 1959 when at the Air Force Flight Dynamics Laboratory at Wright-Patterson Air Force Base, Ohio, now with Wright State University in Dayton, Ohio.

5.4.1 Energy requirements for orbital inclination change

Using equation (5.11), the variation in incremental velocity with altitude as a function of plane change angle is given in Figure 5.12 for five orbital altitudes, from 100 nautical miles (185.2 km) to 19,323 nautical miles (35,786 km). For a 90-degree plane change at 100 nautical mile orbital altitude the incremental velocity is just over 35,000 ft/sec (10,668 m/sec). Compare that to the incremental velocity for the orbital altitude change from 100 nautical miles to 19,323 nautical miles of 12,900 ft/sec (3,992 m/sec) in Figure 5.7. So the incremental velocity requirements for a orbital *plane* change are much more demanding than an orbital *altitude* change. For an incremental velocity of 12,900 ft/sec an orbital plane change of about 29

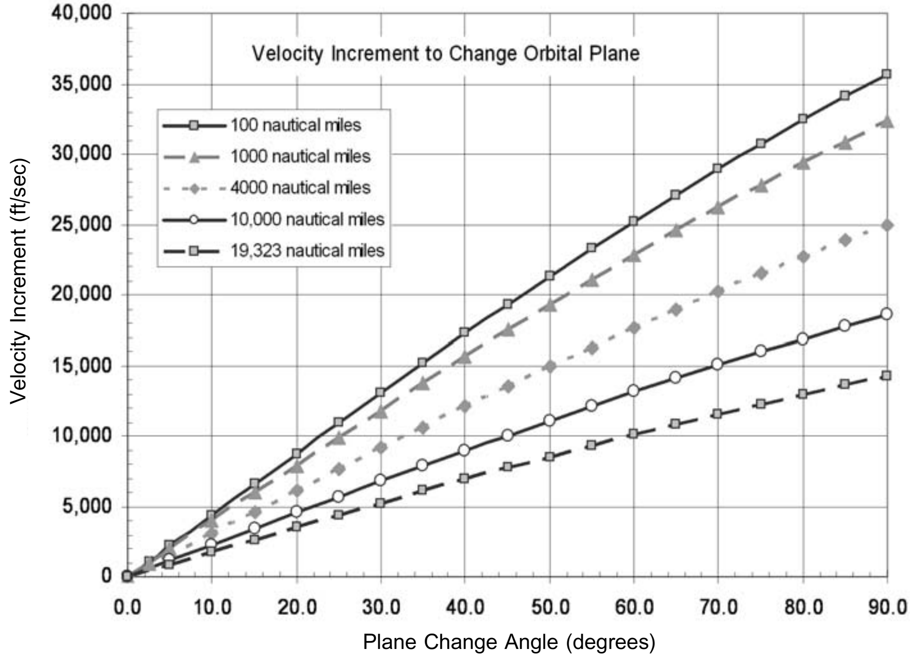

Figure 5.12. Velocity increment to rotate orbital plane for different orbital altitudes. Higher altitude requires less energy.

degrees is possible. That is, less plane change than required to move from the latitude of NASA Kennedy to the latitude of the International Space Station.

Shown in Figure 5.13 is an impulse turn made from the GSO orbital altitude of 19,323 nautical miles (35,786 km), which requires about 11.5 hours to execute. This is one of the lower-energy solutions for the plane change. Increasing the altitude for the impulse turn to 36,200 nautical miles (67,042 km) decreases the incremental velocity to about 1,000 ft/sec (304.8 m/sec) but increases the mission time to 24 hours. As shown, the breakeven orbital plane change is 50 degrees. So if the orbital plane change is less than 50 degrees, it is best made from the spacecraft's orbital altitude, without any orbital altitude change. However, there remains the interesting possibility of using aerodynamics to change orbital plane.

The aerodynamic plane change requires slowing the hypersonic glider to about 22,000 ft/sec (6,706 m/sec) so it can enter the upper atmosphere between 240,000 and 260,000 ft (73,152 to 79,248 m) altitude. At that point the rocket engines are ignited, and a thrust-equals-drag turn at the lift coefficient corresponding to maximum lift-to-drag is initiated, turning through the orbital plane change angle desired. The aircraft is then leveled at the correct orbital heading and the engines ignited to regain orbital velocity. For the class of hypersonic gliders evaluated, this maneuver requires an incremental velocity of about 1,022 ft/sec (311.5 m/sec) to decrease the orbital altitude to the maneuver altitude and speed, and then to

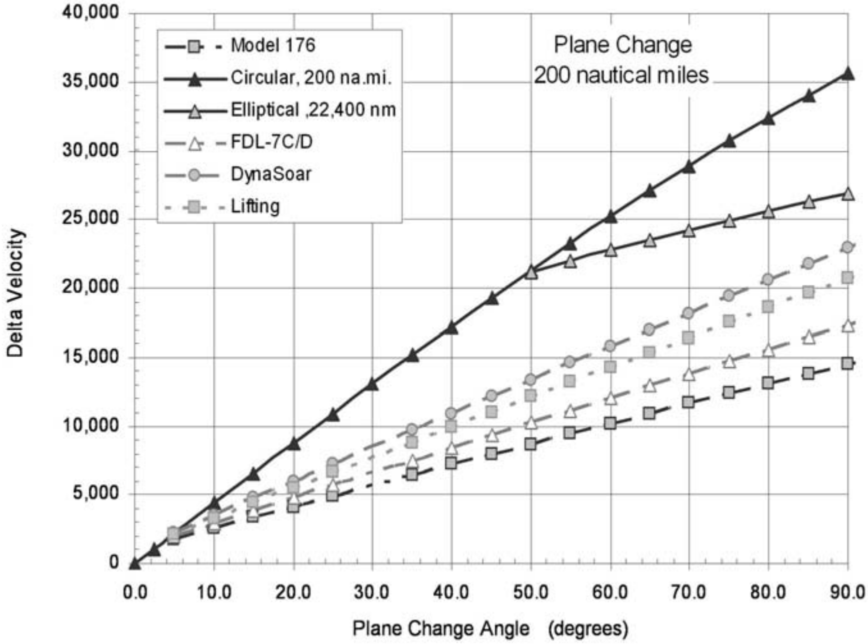

Figure 5.13. Velocity increment as a function of turn method.

return to the initial orbital altitude and speed. The incremental velocity required to execute the orbital turn is a function of the lift-to-drag ratio, as presented in Figure 5.13. The lift-to-drag ratio at Mach 22 varies from 1.88 to 2.95 for the four hypersonic gliders presented. This performance can be represented as a curve fit as follows:

$$\Delta V_{\text{turn}} = 1022 + C(L/D) - 0.0883(L/D)^2$$
$$C = 2317.2 - 2545.6(L/D) + 1040.9(L/D)^2 - 144.45(L/D)^3 \qquad (5.12)$$

As shown in Figure 5.13, the aerodynamic plane change requires much less energy than the impulse turn. For the Model 176 hypersonic glider configuration the incremental velocity required is about 40% of the impulse turn requirement. Even a rather modest Dynasoar lift-to-drag ratio of 1.88 offers a plane change requirement of order 60% of the incremental velocity required by an impulse turn. The current Space Shuttle has a lift-to-drag ratio of about 1.5, and the Russian Buran had a lift-to-drag ratio of about 1.7. It is the blunt leading edges and nose plus the winged configuration that reduces their lift-to-drag ratio.

The aerodynamic plane change is executed by slowing the hypersonic glider to about 22,000 ft/sec (6,706 m/sec) so it can enter the upper atmosphere between 240,000 and 260,000 ft (73,152 to 79,248 m) altitude. At that point the rocket engines are ignited, and a thrust equals drag turn at the lift coefficient corresponding to lift-to-drag ratio is initiated to turn through the orbital plane change angle

Figure 5.14. Arodynamic turn at 245,000 ft at 22,000 ft/sec.

desired. The aircraft is then leveled at the correct orbital heading and the engines ignited to regain orbital velocity. Figure 5.14 depicts an USAF Flight Dynamics Laboratory FDL-7 C/D glider making a plane change to rendezvous with another orbital vehicle in the distance. In actuality the rocket engines would be firing, but the artist omitted the engine plume to clarify the orientation of the maneuver. The hypersonic glider is generally a second stage of a TSTO vehicle sized as an automatic OMV, specifically for plane change maneuvers. The design payload is the same as for the space OMV, a 2,268 kg (5,000 lb) payload. The OMV cannot enter the Earth's atmosphere, so it is limited to space operations. The glider has the capability to enter the atmosphere if needed to operate as a rescue vehicle. The glider has an Earth's circumference glide range and can return to Earth without any prior preparation or waiting in orbit. With a payload bay of 36.5 m^3 (1,289 ft^3) capacity it could accommodate nine to twelve persons in pressure suits in an emergency situation.

The propulsion systems described in Table 5.3 provide the specific impulse (I_{sp}) for each of four systems OMVs. In space there is no atmospheric drag, so the ideal weight ratio equation applies, equation (5.8). For the hypersonic glider there is a about an 8% reduction in the specific impulse due to atmosphere drag during the turn maneuver. Translating the incremental velocity data and specific impulse data into weight ratio yields Figure 5.15.

5.4.2 Mass ratio required for orbital inclination change

Figure 5.15 presents the weight ratio for the four propulsions systems described in Table 5.3 and the four hypersonic gliders indicated in the column headings. With the

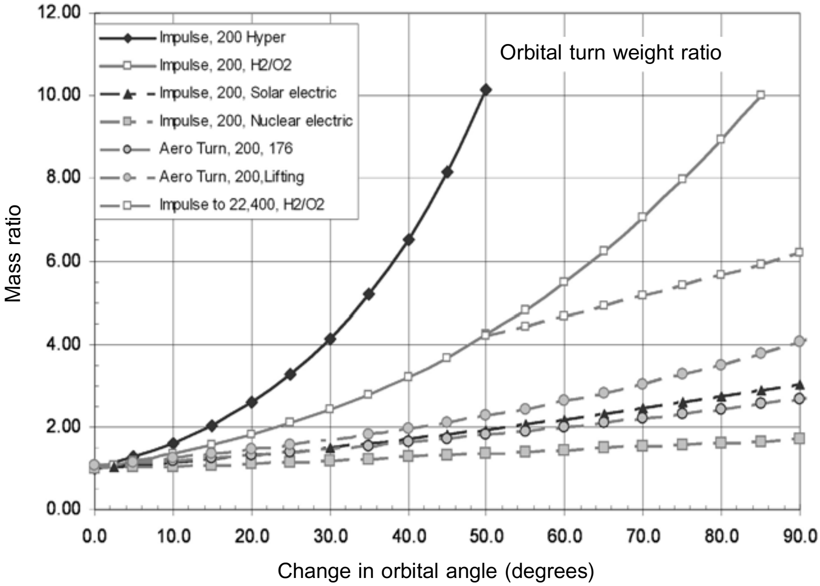

Figure 5.15. Mass ratio requirements for orbital plane change.

hypergolic propellant, the mass ratio quickly becomes impracticable. The curve was terminated at a mass ratio of 10 and a 50-degree plane change. With a hydrogen/oxygen rocket the same mass ratio permits an 85-degree plane change. Extending the time for the plane change by transitioning to an elliptical transfer orbit and executing the plane change at 19,323 nautical miles (35,786 km) GSO orbital altitude reduces the mass ratio to 6 at a 90-degree plane change. The solar electric and nuclear electric together with the aerodynamic plane change vehicles provide the only practicable mass ratios for an operational infrastructure. The mass ratios for a 90-degree orbital turn are between 11 and 5. The weight ratios for the 32-degree orbital plane change for the impulse turn are: 4.53 for the hypergolic engine, 2.62 for oxygen/hydrogen, 1.15 for solar electric and 1.05 for nuclear electric, as shown in Table 5.10. The acceleration specified for the chemical rocket powered OMV is 0.5 '*g*'. For the electric thruster powered OMV the acceleration is 0.1 '*g*'.

The gross weight of the plane change OMVs is straightforward, and the sizing program balances the propellant required versus the capacity of the propellant tank that determines OEW. The sized OMVs for each of the propulsion systems transporting a 5000-lb (2.268-ton) satellite given in Table 5.10. The gross weight for a single mission is:

$$\text{Gross weight} = \text{WR}(\text{OEW}_{\text{OMV}} + W_{\text{satellite}})$$

$$W_{\text{propellant}} = (\text{WR} - 1)(\text{OEW}_{\text{OMV}} + W_{\text{satellite}}) \tag{5.13}$$

Note that the operational empty weight (OEW) of the OMV is essentially constant. It is greater for the electric propulsion configurations because of the

Table 5.10. Sized OMV for 32-degree plane change at 200 km for a 2,268 kg satellite.

Propulsion	Gross mass (tons)	Propellant (tons)	OWE (tons)	OEW (tons)	Mass ratio	Thrust (kN)
Hypergolic	13.83	10.78	3.05	0.786	4.529	67.8
H_2/O_2	7.82	4.80	3.02	0.716	2.619	38.3
Solar electric	5.38	1.91	3.47	1.20	1.147	10.6
Nuclear electric	3.82	0.397	3.42	1.15	1.050	7.49

solar panels for the solar electric and radiators for the nuclear electric. As in the case for the launchers, the primary difference in the weights and thrusts is a result of the carried propellant. The propellant mass for the hypergolic rocket is 27 times greater that for the nuclear electric rocket. The propellant load is reduced by the increasing specific impulse of the propulsion system, and the reduction in mass and thus engine thrust and propellant flow rate. Unlike the space launcher, where the payload is about one-seventh the OEW, for the OMV the payload is greater than the OEW. The OEW differs from empty or dry weight in that all of the fluid lines are assumed filled, and any fluids or propellants trapped there are included in the OEW. The OWE is the OEW plus the payload. That is, it is the vehicle operationally ready but without the propellants loaded.

The hypersonic glider for plane change maneuvers is usually a second stage of a TSTO vehicle sized as an automatic OMV, and specifically for plane change maneuvers. The design payload is 2.268 tons (5,000 lb). With a mass ratio of 1.603 the OMV is sized for a 32-degree plane change capability, the same as the impulse turn OMV. The size and mass characteristics are given in Table 5.11. At Mach 22 the glider has a L/D of 2.70. It is in orbit acting as a plane change orbital maneuver vehicle. An alternate design is shown with a design payload to accommodate the heaviest satellite in Table 5.5, that is, 3,650 kg. The vehicle scales as the square-cube law as the ratio of masses, 1.609, is just slightly greater than the ratio of areas 1.354 raised to the 3/2 power, that is 1.576. As would be expected, the OEW ratio 1.362 scales with the area ratio.

Because the glider is a hypersonic glider and not just a space structure, it requires more resources to construct and operate. However, it is the only OMV with a true escape and rescue capability for an orbital facility crew. It might be better to design the glider to more demanding requirements so it can have a more versatile opera-

Table 5.11. Hypersonic glider (FDL-7 C/D) for 32-degree plane change at 200 km.

Satellite weight (tons)	Gross mass (tons)	Propellant (tons)	OEW (tons)	OWE (tons)	Planform area (m^2)	Thrust (kN)
2.268	8.33	3.13	2.93	5.20	42.33	40.8
3.650	12.15	4.61	3.99	7.64	57.33	60.1

Table 5.12. Hypersonic glider (FDL-7 C/D) for variable-degree plane change at 200 km and 2.268-ton satellite.

Plane change	Mass ratio	Propellant (tons)	OEW (tons)	OWE (tons)	Gross mass (tons)	Planform area (m^2)
90.0	3.228	14.69	4.33	6.60	21.29	59.59
62.0	2.313	7.57	**3.49**	**5.76**	13.13	**49.29**
32.0	1.603	3.13	2.93	5.20	8.33	42.33
32.0	1.603	3.47	**3.49**	**5.76**	9.23	**49.29**

tional life. Table 5.12 gives the sizing of a hypersonic glider with a 2,268-kg payload for three plane change capabilities. To increase the plane change capability from 32 to 62 degrees (+93.8%) the OEW increases just 19.1%. OEW and dry weight determine the cost of the spacecraft. Gross weight determines the operational cost. In this case the gross weight is 57% greater. Designing for a larger plane change capability (62 degrees), but operating at a 32-degree plane change, has only a minimal increase in the resources required over a spacecraft specifically designed for a 32-degree plane change, see the last two rows of Table 5.11. It would be practicable to design for the greater operational capability. Since the hypersonic gliders are designed to operate with hydrogen/oxygen propellants, the availability of engines is not critical, and a number of engines from either the United States or Russia are suitable.

We now have both the quantity of launcher propellant required to deliver the OMV propellant to LEO, and the OMV propellant required in each of three orbital maneuver missions. So we can now determine the total mass units of propellant (launcher and OMV) required per unit mass of the satellite for each of the four space propulsion systems.

5.4.3 Propellant delivery ratio for orbital inclination change

For the impulse turn OMV, Figure 5.16 shows the dramatic reduction in the total propellant mass (launcher and OMV) required per unit mass of the satellite by advancing the performance of the launcher propulsion system. Incorporating a LACE system into an existing hydrogen/oxygen rocket, the propellant required to deliver one mass unit of propellant to LEO is reduced by 56%. Proceeding to a Mach 12 ram/scramjet produces another 50% reduction in the required propellant to deliver one mass unit of propellant to LEO. So instead of the 228.2 mass units of propellant required to deliver one mass unit of propellant to LEO, LACE reduces that number to 99.6 and a Mach 12 ram/scramjet reduces that further to 50.0 propellant mass units. However, the real advances occur when *both* the launcher *and* the OMV propulsion systems are improved.

Similarly to Figure 5.10, Figure 5.17 focuses in on the electric propulsion for the OMV and more efficient launcher propulsion systems (now the propellant required

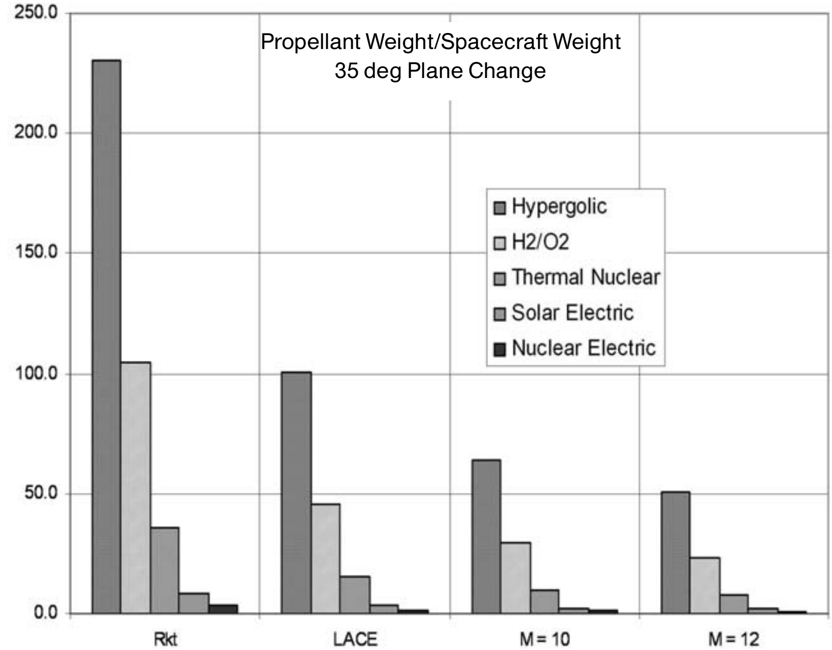

Figure 5.16. Ratio of total propellant weight to satellite weight.

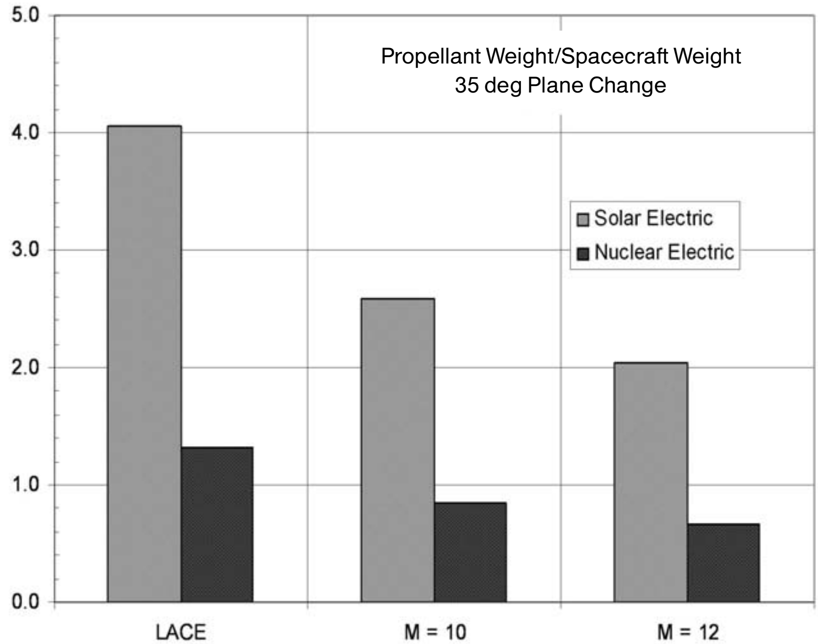

Figure 5.17. Ratio of total propellant weight to satellite weight for solar and nuclear electric propulsion.

Table 5.13. Ratio of total propellant weight to satellite weight for an FDL-7 C/D hypersonic glider with a 32-degree plane change capability and two satellite weights.

	Launcher propulsion			
Satellite weight	Rocket	LACE	M = 10	M = 12
3,650 kg	60.6	26.5	16.9	13.3
2,268 kg	73.5	32.1	20.5	16.1

to deliver one mass unit of propellant to LEO is between 4.5 and 2, and delivering propellant to LEO is no longer impracticable, as the cost of propellants burnt is comparable with that to deliver a unit mass of payload in a commercial transport). Although using conventional hypergolic space rockets and conventional launch rockets to deliver significant quantities of orbital maneuver propellant to LEO is still prohibitive (228.2 kg of propellant per kilogram of LEO propellant delivered) a substantial reduction by about 20 just by using hydrogen/oxygen propulsion in space, also (as already seen) using hydrogen/oxygen rocket in combination with airbreathing propulsion for the launcher. With the application of electric propulsion in space and hydrogen/oxygen rocket and airbreathing propulsion for the launcher that ratio can be reduced to a figure about 3 or maybe 2. The orbital tanker is now competitive with a KC-135 or modified B-767 for refueling missions.

Since the hypersonic glider is part of a TSTO vehicle, the first stage is used only once, that is to launch the glider. After that the space propellant tankers are used to replenish its operational propellants. Table 5.13 gives the propellant to satellite weight ratio for a FDL-7 C/D glider and two satellite weights. The Model 176 would have a lesser value of the ratio, and the Dynasoar and lifting body would have a larger value of the ratio. This table corresponds to the values in Table 5.11.

The hypersonic glider is more readily adaptable to larger plane changes; for, as we saw in Table 5.12, the increase in capability is possible for a reasonable investment in vehicle size. This table corresponds to the values in Table 5.11 for three levels of design for the plane change hypersonic glider. As in Table 5.12, the last row in Table 5.14 is for the 62-degree orbital plane change design spacecraft operating in a 32-degree plane change. Observations on the OMV results: it is clear that the better the propulsion system of the orbital tanker, the less resources required to transport the propellant to LEO. There is a clear advantage for an airbreathing launcher when considering sustained space operations.

Compared to the impulse turn OMV, the hypersonic glider needs less total propellant to accomplish its mission, requiring only about 65% of the impulse turn OMV propellant, as shown in Table 5.15.

So for performing orbital plane changes hypersonic gliders have a clear advantages. Even the hypersonic glider designed for a 62-degree plane change and flying a 32-degree plane change (last row of Figure 5.13) requires less propellant than an impulse OMV. The hypersonic gliders require less propellant to be lifted to orbit, *and* offer an escape and rescue capability not available with impulse turn OMVs.

Table 5.14. Ratio of total propellant weight to satellite weight for FDL-7 C/D hypersonic glider and three plane change angles for four launcher propulsion systems.

	Launcher propulsion			
Plane change	Rocket	LACE	M = 10	M = 12
90 degrees	310.9	135.7	86.7	68.2
62 degrees	160.2	70.0	44.7	35.1
32 degrees	66.2	28.9	18.5	14.5
32 degrees[a]	73.5	32.1	20.5	16.1

[a] Sized for 62° plane change operated over a 32° plane change.

Table 5.15. Ratio of total propellant weight to satellite weight for FDL-7 C/D hypersonic glider compared to the hydrogen/oxygen propellant OMV designed for a 32-degree plane change for four launch propulsion systems.

	Launcher propulsion			
Plane change	Rocket	LACE	M = 10	M = 12
Hypersonic glider	66.2	28.9	18.5	14.5
H_2/O_2 OMV	101.7	44.4	28.3	22.2

5.5 REPRESENTATIVE SPACE TRANSFER VEHICLES

Each OMV has approximately the same OEW as indicated in Figures 5.6, 5.7 and 5.9. But each has a different configuration that is determined by the characteristics of the individual propulsion system, as depicted in Figure 5.18. The two chemical rocket-powered OMVs are similar and conventional. Although having different gross weights, they are similarly sized. The satellite attaches to an equipment module mounted on the front end of the propellant tank, where the guidance and control systems and all subsystems are housed. There would be a stowed communications antenna and solar panels for power in the equipment module (not shown). The solar electric propulsion system would require much larger solar panels than shown. Current communications satellites have solar panels in the 25 to 30 m (82 to 98 ft) total span for thrusters with less than one-tenth the thrust required for the solar electric OMV. Some of the limitations of this system are the current low thrust levels; the continuously degrading solar panel output; and the unwieldy size of the solar panels for such a vehicle. Nuclear electric has the same problem as the solar electric in that current thrusters have less than one-tenth the thrust required for the nuclear electric OMV. This system does have the advantage that the power output is sufficient and constant. There is a requirement for large radiators to dissipate the rejected thermal energy from the reactor to space. Their exact size depends on the nuclear

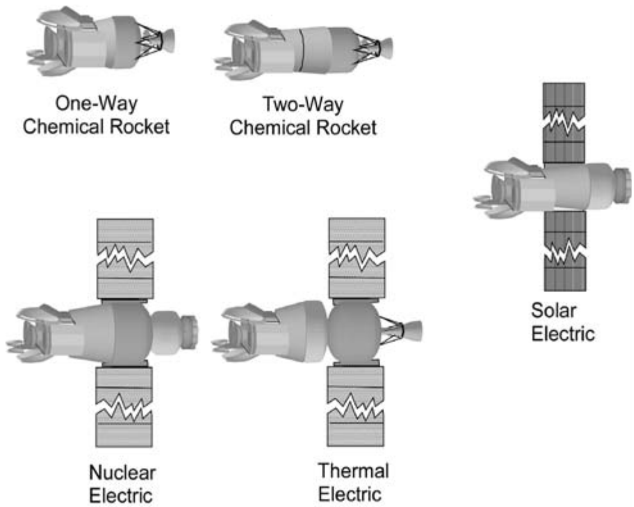

Figure 5.18. Relative size and general configuration of OMVs.

system chosen and the thermodynamic cycle to power the electric generators. The nuclear reactor will be a space-designed reactor and not based on Earth-based nuclear power stations. A most likely candidate is some type of gas-cooled reactor.

A round trip operational OMV that travels from LEO to GSO and returns is shown in Figure 5.19. The solar panels are just sufficient to power the system electronics and other electrical subsystems. A communications link to Earth and space-based ground stations is indicated. Because the intended life is years, and recalling the damage one of these authors (PC) witnessed on the LDEF satellite, a

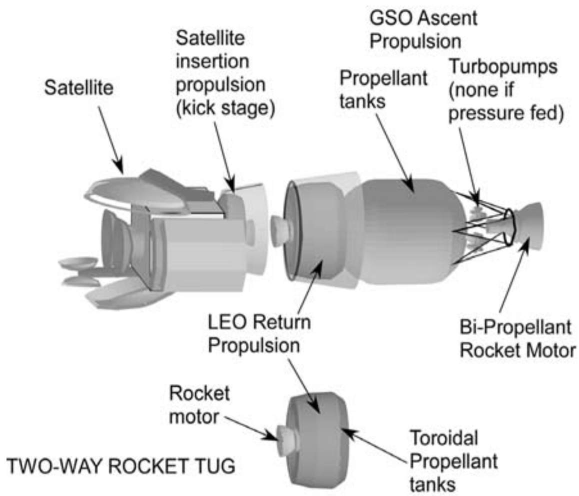

Figure 5.19. LEO–GSO–LEO two-way OMV with shield.

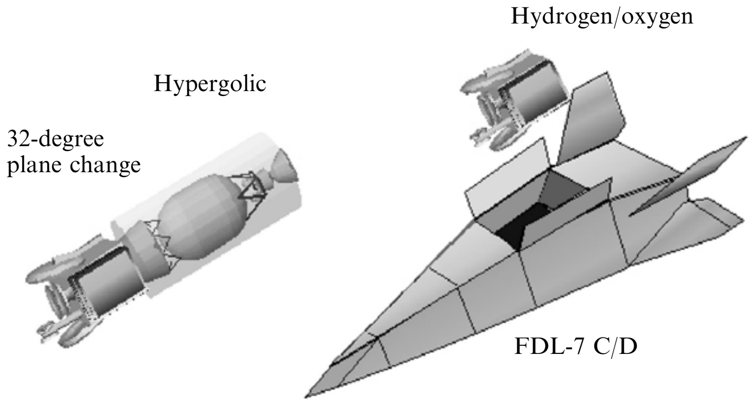

Figure 5.20. OMV for impulse turn and hypersonic glider for aerodynamic turn.

shield over the tank structure and engine is necessary, as shown in phantom. The equipment module can be made robust enough not to require a separate shield. As with the MIR orbital station, the solar panels on an operational OMV will probably have to be replaced within its lifetime.

The orbital plane change OMV can change the orbital plane by an impulse turn in orbit or an aerodynamic turn in the upper atmosphere. The impulse plane change OMV is very similar to the OMV shown in Figure 5.19 and is shown in the left side of Figure 5.20. The aerodynamic plane change OMV is shown in the right side of Figure 5.20. Both are sized for a 32-degree plane change with a 2,268 kg (5,000 lb) satellite. The OMV cannot enter the Earth's atmosphere, so it is limited to space operations. The glider has the capability to enter the atmosphere to operate as a rescue vehicle. The glider has a glide range equal to the Earth's circumference and can return to Earth without any prior preparation or waiting in orbit. With a payload bay of 36.5 m^3 (1,289 ft^3) capacity it could accommodate nine to twelve persons in pressure suits in an emergency situation.

5.6 OPERATIONAL CONSIDERATIONS

Given the characteristics of the OMVs, the question is how to make these spacecraft an operational infrastructure and what is required, in addition to the OMVs, to build an operational infrastructure. The next five subsections will attempt to put the needs for an operational infrastructure into perspective. In fact, one of the most critical issues, if not *the* most critical, is the orbital propellant resources required to sustain an operational infrastructure. The availability of infrastructure hardware and configuration is important, but without propellant all grinds to a standstill. The infrastructure will probably be configured in some type of constellation so that resources are available over the infrastructure shell around the Earth. Resources are scarce, so the operators of the infrastructure must be a frugal group, not wasting any reusable resource or hardware. And, finally, with the infrastructure populated with human beings that are not pilots, but workers with identified tasks and tourists hoping to see and experience space, a viable and readily available rescue and return capability is necessary.

5.6.1 Missions per propellant delivery

It is worth repeating, the critical issue is the orbital propellant resources required to sustain an operational infrastructure. As the results given in previous figures have shown, the existing rocket launcher systems and hypergolic propellant space rockets force a level of launcher performance and activity that makes any but limited space operations impractical. Figures 5.9 and 5.10 with Figures 5.16 and 5.17 show the rocket launcher–hypergolic rocket OMV spends over 200 kg of propellant to deliver 1 kg of OMV propellant to LEO. The solution anticipated is to use airbreathing launchers and nuclear electric powered OMVs. Then the requirement reduces to a figure of the order of 2 or 3 to deliver the propellant to LEO, and of the order of 5 to deliver to LEO propellant required for orbital plane changes. It would appear that the operational infrastructure envisioned by Dr Gaubatz in Figure 5.1 must wait for the operational deployment of the correct propulsion systems for both the space launcher and the OMV.

The next critical issue is the following: given the propellant is delivered to LEO in 19-ton (41,895 lb) increments, how many missions can the OMVs complete from a single delivery? Figure 5.21 and Table 5.16 give the number of missions for the

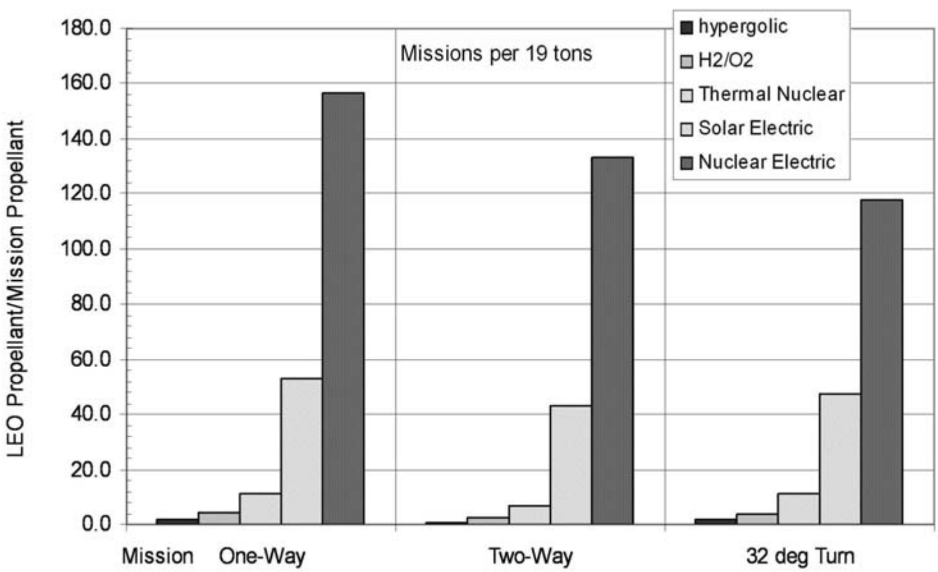

Figure 5.21. Orbital maneuver missions per 19 t propellant payload for five different OMV propulsion systems.

Table 5.16. Number of orbital missions per 19 metric ton propellant payload for 2,268 kg satellite payload for the OMV.

	Launcher propulsion				
Mission	Hypergolic	H_2/O_2	Solar electric	Thermal nuclear	Nuclear electric
Impulse OMV LEO to GSO and return	0.71	2.3	4.3	6.8	133
Impulse OMV 32-degree plane change	1.7	3.8	4.7	11	118
Hypersonic glider 32-degree plane change		5.5			

impulse OMVs executing two different missions, and the aerodynamic turn mission for the FDL-7 C/D hypersonic glider with a lift-to-drag ratio of 2.7.

Although heavier than the impulse OMV's, the efficiency of the aerodynamic plane change maneuver permits the hypersonic glider to have 45% greater mission capability from the same orbital tanker propellant load. Solar electric and nuclear electric are not appropriate propulsion systems for vehicles that fly in the upper atmosphere, because of the solar panels and radiators associated with those systems.

5.6.2 Orbital structures

The concept of spaceways depicted in Figure 5.1 is dependent on a capability to manufacture space structures as standard items on a limited production line, much as for aircraft. Although the United States, Japan and Europe have manufactured individual modules for the Space Station over 5 to 10 years construction time, these are one-of-a-kind items, hand-built at great expense. The only nation known to manufacture space structures with standardized components on a limited production line is the former Soviet Union. Figure 5.22 shows one picture of one of a number of orbital station major components being manufactured in a factory in the Moscow area. In this picture the orbital station module is being integrated with its PROTON launcher, at the manufacturing plant, so interface problems can be addressed during the manufacturing process, not later on the launch stand. Each of the modules/components had different functions, but, like automobiles and aircraft, each was tailored to a specific mission based on installed equipment and a common structural core. The costs and time to manufacture the components were minimized. The organization of the manufacturing line, and the use of standardized components that was gleaned from the plant pictures was quite impressive. The pictures of this plant are now 16 years old. It is not known if the plant or manufacturing capability

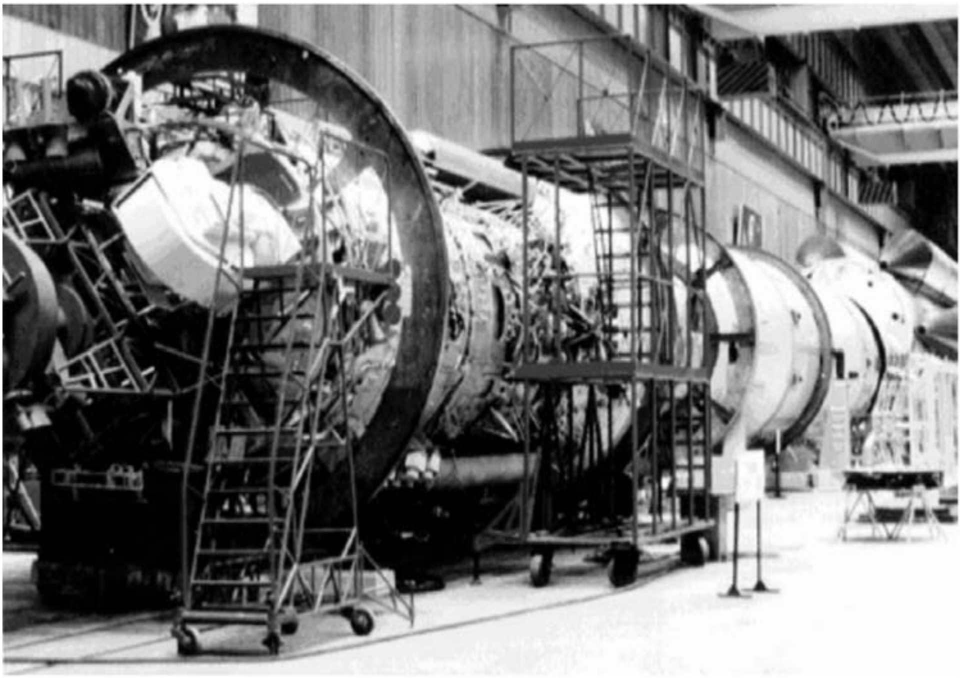

Figure 5.22. Large orbital station in final assembly and integration with its PROTON launcher. Moscow factory, circa 1989.

remains in the present Russia. This is the only plant of its kind known to the authors, and it should be the model for manufacturing components for an operational space infrastructure instead of relying on building single, one-of-a-kind custom components. One of the very important observations of the Russian approach to space payloads is that the payload and delivery stage are integrated as a part of the manufacturing process and not left to cause future delays on the launch pad.

5.6.3 Orbital constellations

One of the senior Capstone design course project teams at the University of St. Louis, USA, looked at the near-Earth infrastructure postulated by Dr William Gaubatz and chose to analyze what would constitute the first step in the development of that infrastructure as their design project. The title of their project was 'Space-based satellite service infrastructure' [Shekleton et al., 2002]. Among results found was that, as the number of structures in space continually increases, the need for a space-based service infrastructure continues to grow. The increasing human presence in space calls for newer and newer support and rescue capabilities that would make space an 'easier' and safer frontier. In addition, over 2000 unmanned satellites populate Earth's orbits. These include a variety of commercial, military,

Figure 5.23. Student design team results for requirements in terms of orbital systems hardware.

weather, and research satellites, many of which require servicing or removal from orbit. As a first step the team determined that significant space facilities were necessary to achieve support of an initial infrastructure. As shown in Figure 5.23 there was a requirement for distributed facilities [Shekleton et al., 2002]. The primary facility was a twin propellant tank arrangement with living quarters, repair shop, and a parts storage straddling the two propellant tanks. A much larger, modified version of the elliptical Space Cruiser shown in Figure 5.26, was the primary OMV. The elliptical cross-section hypersonic glider was modified to a captured shock cross-section (wave-rider) based on the work of Mark J. Lewis of the University of Maryland [Lewis, 2002]. The OMVs were deployed from the service facilities on an as-needed basis for non-routine maintenance and repair, and on a scheduled basis for operational satellites and facilities. The gliders have limited facilities as habitats but have sufficient provisions for 3- to 5-day deployments away from the main service facility. The space station was not chosen as a support base because of the large quantity of propellant stored and the large inventory of spare parts and repair facilities required. One of the service facilities could be in orbital proximity to the space station if that was operationally required. The propellant storage would accommodate about 100 tons of propellant or up to five propellant tanker payloads. The propellant tanks were segregated to accommodate hypergolic and hydrogen/oxygen propellants separately. The hypersonic gliders were capable of escape and rescue missions for up to 15 persons. This constellation was considered the foundations on which to build an operational space infrastructure.

5.6.4 Docking with space facilities and the International Space Station

Examining Figure 5.1, we see a variety of space structures (facilities) that are unique to each facility's function. In time that is probably the norm for space facilities. In reality we are just beginning because there is no existing space infrastructure. At best there are specific mission to specific orbital assets (such as a shuttle mission to Hubble). As published in the aerospace literature, the current European (Columbus Laboratory) and Japanese (Japanese Experimental Module, kimbo) laboratory modules for the Space Station needed over 5 years to complete and large financial expenditures [NASA, 2003b]. These are waiting for the Space Shuttle to deliver them to the Space Station. The Columbus Laboratory is a 4.5 m (14.75 ft) diameter cylinder 8 m (26.25 ft) in length, and has an 11,000 kg (24,500 lb) mass on orbit. The JEM is similar in size and mass, and has an additional feature, a ramp extension exposed to the space environment for space experiments. Existing orbital facilities are expensive and require visiting vehicles to conform to standards and requirements based on vehicle and facility idiosyncrasies. There is not a consistent set of standards and requirements in sync with the commercial industries. Eventually the transportation vehicles will provide the requirements for the orbital facility, including support of the transportation cycle like airports do. Commercial platform markets include transportation-related support services, habitation and in-space service industry support.

The most economical space facility ever flown was the United States Skylab. It was a Saturn S-IVB stage modified for habitation and launched empty. Instead of being the prototype of future space structures for the initial phase of infrastructure building, it was summarily and unwittingly permitted to decay from orbit and burn up in the atmosphere. Skylab was put into a 435 km (235 nautical mile) orbit at an inclination of 50 degrees [NASA, 2003a]. Skylab was in orbit from 14 May 1973 to 11 July 1979 (6 years, 5 months and 25 days). It was launched empty, and was sent crews via a Saturn rocket and an Apollo capsule. There were three missions to crew Skylab: Skylab 2 for 28 days, Skylab 3 for 59 days, and the final Skylab 4 for 84 days, for a total of 171 days occupied. The last crew departed Skylab on 8 February 1974, just 8 months and 26 days after being put into orbit. So Skylab remained unused for over 5 years. Unfortunately there was no mechanism to maintain Skylab in orbit, and on 11 July 1979 it entered the atmosphere over Australia. Again, instead of being a prototype for an economical first step into orbital stations it was a one-of-a-kind only. The next philosophical path taken was then to create an 'optimum' space station, the 'perfect' creation of NASA, that took almost 26 years before another American astronaut crewed a United States orbital station. In that time period the former Soviet Union placed seven orbital stations into orbit, ending with the orbital station MIR.

There exists an analogous situation today. The Space Shuttle external tank is a giant cylinder 154 ft (46.7 m) in length and 27.5 ft (8.4 m) in diameter containing 73,600 ft^3 (2,083 m^3) of propellants. That is about 369,600 lb (167.63 tons) at a six-to-one oxygen/hydrogen ratio by mass. The new lithium–aluminum external tank weighs 58,250 pounds dry. Each Space Shuttle mission discards the external tank

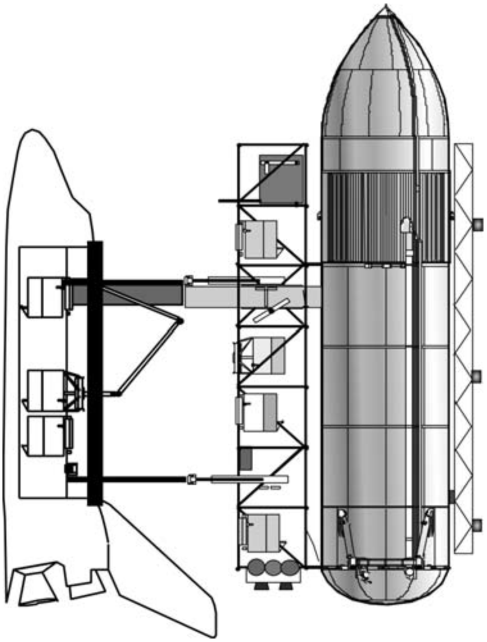

Figure 5.24. An orbital infrastructure station fabricated from discarded Shuttle main propellant tanks with a Space Shuttle docked for resupply.

after it has achieved 99% of full orbital velocity. This means significant energy is invested in the external tank, only about 260 ft/sec (79 m/sec) short of orbital velocity. With a very small investment the external tank could be placed into orbit, and become the building block for orbital facilities *other than* the International Space Station, at a fraction of the cost. At one time the government was encouraging organizations to put this empty space asset to a useful application [*Commerce Business Daily*, 1988]. One of the individuals taking this seriously was Thomas Taylor, CEO of Global Outpost. He and his company have championed the salvage of the external tank for over two decades, [Taylor, 1980, 1998; Gimarc, 1985]. Global Outpost developed a salvage method using the Space Shuttle with NASA assistance. Global Outpost has won the right to 'five ET's in orbit at no cost' and has worked out a salvage procedure with NASA [Global Outpost Inc., 1993]. The concepts shown in Figures 5.24, 5.25 and 5.27 are based on concepts developed by Thomas Taylor and Global Outpost Inc.

There are several possibilities for the empty external tank:

(1) The external tank could be used as it was intended to be used, as a hydrogen/oxygen propellant storage facility, using the orbital refueling launchers to supply propellants on a scheduled basis. The tank could accommodate 8.8 19-ton propellant deliveries by the orbital propellant tanker.
(2) The aft dome of the external tank could be cut to provide a 10.3 ft (3.14 m)

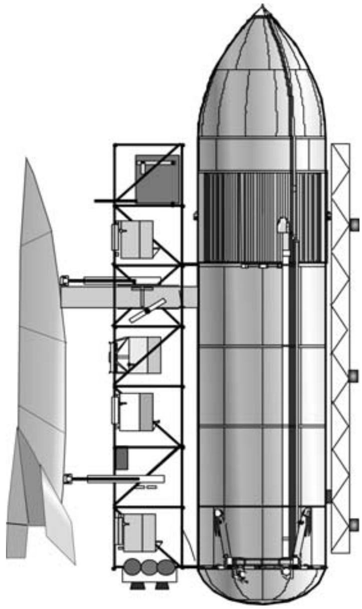

Figure 5.25. An orbital infrastructure station fabricated from discarded Shuttle main propellant tanks with a hypersonic glider resupply spacecraft analogous to MDC model 176.

diameter hole permitting the use of 55,00 ft^3 (1,557 m^3) of the interior as a hangar for the OMVs.

(3) Just as with the Saturn S-IVB stage, the external tank could be launched, with some modifications so that at least one external tank could accommodate human habitat. This modification is the basis for the sketches in Figures 5.24, 5.25 and 5.27.

(4) An inflatable habitation structure is possible using the TransHab Consortium 8 m (26.25 ft) diameter 8.2 m (26.90 ft) long inflatable structure [Internet, 2000], to fabricate a volume transported uninflated in a sustained-use space launcher described in Chapter 3 and inflated on orbit. The habitat is capable of resisting high-speed particle impact and providing environmental controlled life support interior [Internet, 2003a, 2003b].

Habitation requires cargo and passenger services. Each new industry will require cargo in both directions. The change from one type of transportation to another has always evolved into major commercial centers of industry such as harbors and airports. Emerging commercial spaceways expand the capabilities around the Earth and then to the Moon. Transportation is a major factor. The cost reduction stimulates the accelerated growth and expansion. Harbors start small, grow and reach out to their customers with docks and wharfs; the space harbor is no exception.

The external tank modified for crewed habitation and an equipment and parts storage facility as conceived by Tom Taylor [Taylor, 1980] is shown with the NASA Space Shuttle docked with the crew transfer structure deployed between the Shuttle air lock module and the external tank (Figure 5.24). This mission could be for an equipment/parts resupply mission, for crew rotation, or as a mission adjunct. However the Shuttle has a limited useful operational life and must be replaced by a sustained flight rate spacecraft. The one actually designed for that purpose (for the USAF MOL in 1964) was the Air Force Flight Dynamics Laboratory FDL-7 C/D and the McDonnell Douglas derivative, the Model 176. The modified external tank shown in Figure 5.24 is shown docked with the crew transfer structure deployed between the FDL-7 C/D or MDC Model 176 air lock module and the external tank (Figure 5.25). As before, this could be an equipment/parts resupply mission, crew rotation, or as a mission adjunct.

The concept of a Space Cruiser introduced in Chapter 2, Figure 2.27, enables the external tank to take on the role of a maintenance, repair and orbital transfer center, much as that developed by the Parks College design team [Shekleton et al., 2002]. The Space Cruiser dates back over 20 years. The authors first were aware of the concept when one of the authors was manager of the McDonnell Douglas Aerospace Vehicle Group in 1983. Mr Redding visited the author and briefed him on the Space Cruiser concept. As originally conceived in 1980, the Space Cruiser was a low-angle conically shaped hypersonic glider similar to the McDonnell Douglas Model 122 (BGRV) experimental hypersonic vehicle that was flown in 1966. As initially conceived, the Space Cruiser length was 26 feet and could be folded to a 13.5 feet length (see Figure 5.27). Redding adapted the design to incorporate an aft plug nozzle cluster configuration and storable propellants to create 13.3 kN (3,000 lb) of thrust. The 4,453-kg (10,000-lb) vehicle was to perform a variety of missions using the 8 cubic foot forward payload bay and the 4 cubic foot aft payload bay. The Space Cruiser is capable of atmospheric entry and uses a small drogue parachute at Mach 1 followed by a multi-reefed parafoil to land safely on any flat surface. The Space Cruiser was intended to be operated by a pilot in a space suit [Griswold et al., 1982]. In 1983 Redding modified the configuration to an elliptical cross-section thus expanding the propellant quantity, as shown in a 1983 McDonnell Douglas Corporation Trans-Atmospheric Vehicle (TAV) artist illustration (Figure 2.26) [Redding et al., 1983; Redding, 1984]. Mr Redding formed an organization shortly before his death to preserve the work on the Space Cruiser and seek future development, the In-Space Operations Corporation (IOC).

The external tank modified for crewed habitation and an equipment and parts storage facility as conceived by Tom Taylor [Taylor, 1980] is shown with several space maneuvering vehicles docked to the support structure in Figure 5.27. From the top-right there is a round trip to GSO rocket transfer vehicle (Figure 5.19); center-right, a solar electric orbital transfer vehicle (Figure 5.18). At bottom-right, there is a folded Space Cruiser with a satellite for transfer to another facility. At top-left there is a hypersonic glider aerodynamic plane change vehicle, and at bottom-left a full-length Space Cruiser. The space cruisers shown in this figure are 2.4 times larger than the original Space Cruiser (62 ft or 18.9 m in length) and have 13.5 times more

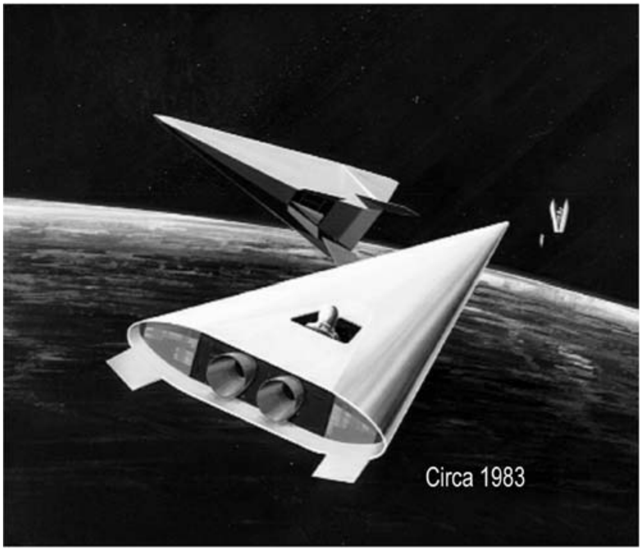

Figure 5.26. 'Bud' Redding Space Cruiser launched from a trans-atmospheric vehicle to accomplish a satellite repair.

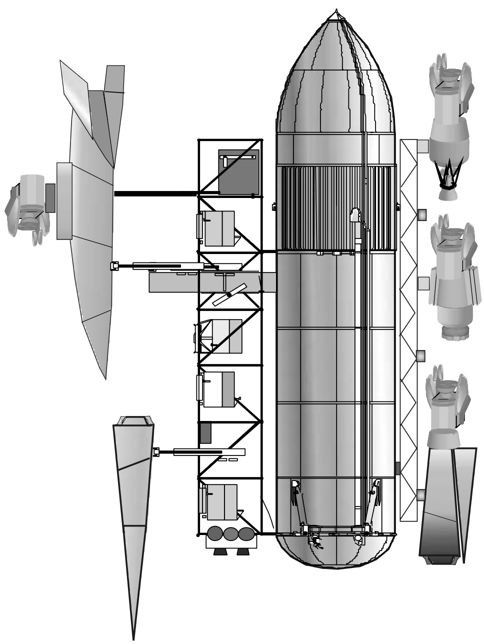

Figure 5.27. An orbital infrastructure station fabricated from discarded Shuttle main propellant tanks with docked In-Space Operations Corporation (IOC) Space Cruiser, a hypersonic orbital plane change vehicle and OMVs.

volume and greater capability because the propellants are now cryogenic hydrogen and oxygen with magnetic refrigerators to all but eliminate propellant losses. These, like all the orbital maneuver vehicles are automatic control vehicles that can carry crewmembers when necessary. In this figure, the salvaged external tank is an operations center for orbital maneuver vehicles necessary to move satellites, provide on-site repair and maintenance and non-functioning satellite removal.

5.6.5 Emergency rescue vehicle with capability to land within continental United States

Whether it is the orbital facilities support vehicle (Figure 5.25), the hypersonic glider aerodynamic plane change vehicle, or the Space Cruiser, these vehicles can serve as an immediately available escape and rescue vehicle in case of an emergency. With these vehicles recovering in the continental United States (CONUS), or continental Europe, is possible without waiting in orbit for the correct orbital position to reach these locations with a limited cross- and down-range vehicle. The orbital facilities support vehicle has the capability to accommodate nine to thirteen crew, depending on the medical circumstance (litter patients or ambulatory). This means that with a fleet of these vehicles, the space facilities need not be partially manned or be without a safe return. These vehicles were designed in the past to be able to generate 75 to 90 flights a year, and to be launched in less than 24 hours. This provides a true capability to build an operational infrastructure as envisioned by Dr William Gaubatz in Figure 5.1.

5.7 OBSERVATIONS AND RECOMMENDATIONS

This chapter has demonstrated the very large resources required to support the delivery of propellant for an operational infrastructure if conventional rocket launchers are used with conventional hypergolic rockets for space operations. It is required that sustained-use airbreathing launchers and nuclear space propulsion be developed into an operational system if an operational space infrastructure is ever to exist. The key to achieving an initial operating capability with an infrastructure is not to throw away valuable, and reusable, assets in lieu of very costly and long-delivery-time optimum solutions that have little tolerance or durability when encountering off-design conditions and unexpected events. Some of the uses a salvaged Shuttle main external tank can be put to have been identified by Thomas Taylor, namely:

(1) The emerging reusable launch vehicles will bring cost-effective transportation and commercial ventures to LEO.
(2) Salvaged hardware in orbit will provide commercial opportunities and transportation markets in LEO.
(3) Human-operated commercial services in orbit will emerge as the lower costs emerge.

(4) The transportation node in LEO is important to the commercial world, because the mode of transportation changes in LEO.
(5) The cost for countries interested in positioning on the trade routes of the future is lower than ever and will be commercial.
(6) A new method of cooperation between government and the private sector must be found.

5.8 BIBLIOGRAPHY

Commerce Business Daily (1988) President Reagan's Space Policy and Commercial Space Initiative of Feb. 11, 1988, encouraged private sector use of External Tanks by making available 'the expended external tanks of the Shuttle fleet at no cost to all feasible U.S. commercial and non-profit endeavors, for uses such as research, storage and mfg. in space', CBD announcement, June 1, 1988.

Folger, T. (2003) 'Nailing Down Gravity', *Discover Magazine*, Vol. 24, No. 10, pp. 34–40.

Gimarc, J.A. (1985) 'External Tank Applications in Space Manufacturing, Space Mfg 5—ngineering with Lunar and Asteroida', 7th Princeton/AIAA Conference on Space Manufacturing, October 1985, AIAA.

Global Outpost Inc. (1993) 'Global Outpost Inc. and NASA Enabling Agreement', No. 1564-001-00A, Rev. 3, 20 April 1993, included a cash deposit for five external tanks on orbit.

Griswold, H.R., Stein, D.S. and Redding, F.W.Jr. (1982) 'Integration of a Crewman into a High Performance Spaceplane', Twelfth Intersociety Conference on Environmental Systems, Society of Automation Engineers, Inc., San Diego, CA.

Internet (2000) http://www.universitytoday.com/html/special/tanshab.html

Internet (2003a) http://www.astronautix.com/craft/tradule.htm

Internet (2003b) http://www.lunar-reclamation.org/transhab/html

Karol, J.M. (1997) '1996 Space Launch Activities', ANSER Report SAD 97-1, ANSER, Arlington, VA.

Koelle, H.H. (ed.) (1961) *Handbook of Astronautical Engineering*, McGraw-Hill, New York.

Mobley, T. (1979) 'ET Applications in Space', study contract for Martin Marietta Corporation, Final Report, Taylor & Associates, Inc., December 1979.

NASA (1980) NASA external tank informational website, http://www.NASA.gov/

NASA (1999) NASA Habitat Module Commercialization Conference, August 1999, Houston, website, http://technology jsc.nasa.gov/habconference/

NASA (2003a) http://www_pao.ksc.nasa.gov/kspao/history/skylab

NASA (2003b) http:// www.scaperef.com/news/viewpr.html

Redding, F.W.Jr. (1984) 'Spaceplane Technology & Research (STAR!)', DCS Corporation, Final Report, DARPA, Order 4913, August 1984.

Redding, F.W.Jr. et al. (1983) 'Spaceplane Examination', SRI International, Final Report, Contract FO4701-8IK-0001, February 1983, Managed by the Air Force Space Division, Sponsored by DARP A (Strategic Technology Office).

Shekleton, M., Patel, M., Muravyeva, I. and Steele, K. (2002) 'Space-Based Satellite Service Infrastructure', Parks College of Engineering and Aviation, Senior Course Design Project Final Report, Saint Louis University, St. Louis, MO.

Taylor, T.C. (1980) 'Commercial Operations for the External Tank in Orbit', Eighteenth Goddard Memorial Symposium, March 1980, Washington, DC, AAS 80-89.

Taylor, T.C. (1981) 'A Commercial Construction Base Using the External Tank', 2nd AIAA Conference on Large Space Platforms, February 2–4, 1981, AIAA-810460.

Taylor, T.C. (1998) 'Salvage Hardware Apparatus and Method for Orbiting Objects', United States Patent 5,813,632, inventor: Taylor, Thomas C. (Las Cruces, NM).

Taylor, T.C. (2000) 'Commercial Space Habitation, 2000', Global Outpost, Inc., Lunar Development Conference, July 2000, Las Vegas, NV.

Taylor, T.C. and Cema, P.J. (1988) 'Aerospike for Attachment to Space Vehicle System', United States Patent 4,790,499, issued 3 December 1988.

6

Earth–Moon system: establishing a Solar System presence

The Earth's Moon is a natural satellite that the evidence suggests was created by a Mars-sized body that crashed into the Earth very early in the history of the Earth, about 4.5 billion years ago. The latest sky surveys give an age of our Solar System of about 4.7 billion years. With the Soviet and American lunar mapping satellites, the Soviet automatic rovers, and the Apollo landings a significant amount of information has been gained about the Moon, [Spudis, 2003]. Even with this information, there is much more to be learned from exploring the Moon and understanding its geology and structure. During the 1960s there were plans to use the Apollo system for lunar exploration. ALSS, Apollo Logistics Support Systems and LESA (Lunar Exploration System for Apollo) were efforts within NASA to define the equipment and operational requirements to explore the Moon. Unfortunately none of these plans ever reached realization. Using the 1991 report to Congress entitled *America on the Threshold*, Thomas P. Stafford, former Apollo astronaut and Lieutenant-General USAF (Retd), as Chairman of the Synthesis Group, Space Exploration Initiative [Stafford, 1991] assembled a number of documents reasoning that we should return to the Moon. Figure 6.1 (see the color section) shows the cover and inside page from that report. Note that the Moon is shown in front of the planet Mars with the Solar System in the background. General Stafford provides the argument for the Moon as a stepping-stone to Mars and space. So the Moon is very important as a base of operations for space exploration. The Moon can be a launching point for vehicles to explore our Solar System and nearby space. A non-rocket launcher that has difficulty being justified on Earth can readily provide lunar escape speed. Equipment, rovers, and habitats can be developed on the Moon for use on Mars. With the resources of an operational base, equipment that needs modification can be accomplished on the Moon without having to return the equipment to Earth. Systems can be modified until successful operation on the Moon provides high confidence of successful operation on Mars. One of the critical features of this natural satellite is that there are no propulsion requirements to keep it in stable orbit, unlike LEO orbital stations (MIR and International Space Station). Also unlike artificial orbital stations, the Moon is not devoid of indigenous resources, including gravity. It is possible to show the advantages of the Moon compared to an Earth orbital station.

6.1 EARTH–MOON CHARACTERISTICS

The Moon, at least on the side we can see, is characterized by bright, rugged, heavily cratered highlands and large sparsely cratered, level dark areas called by Galileo Galilei 'maria', or 'seas' in Latin, as shown in Figure 6.2. The Moon has a mass of 1/81.3 Earth masses. Analysis of the lunar rocks returned by the Apollo astronauts indicates an age of about 4.5 billion (4.5×10^9) years. The orbit of the Moon around Earth is nearly circular, the eccentricity, e, being only slight ($e = 0.0549$); its inclination to the plane of the ecliptic is 5.145 degrees. The plane of the ecliptic is the plane containing most of the planets orbiting the Sun (except the planet Pluto). The Earth–Moon distance ranges from 406,700 km to 356,400 km from Earth, with a mean of 379,700 km (252,711 statute miles to 221,456 miles from Earth, with a mean of 235,934 miles). Nominal orbital speed is much lower than Earth, 1,656 m/sec (5,433 ft/sec), and nominal escape speed is 2,342 m/sec (7,683 ft/sec). The acceleration of gravity at the Moon surface is 1.618 m/sec^2 (5.308 ft/sec^2). So the Moon's gravitational acceleration is about one-sixth that of the Earth.

In Figure 6.3, for the Earth–Moon distance of 384,400 km (238,854 statute miles) the center of gravity (and rotation) of the Earth–Moon system is offset from the Earth's Center by 4,671 km (2,902 miles), that is, at 379,729 km (235,952

356,400 km perigee
379,700 km mean
406,500 km apogee

$$V_{\text{orbit}} = 1,656\,\text{m/sec}$$
$$V_{\text{escape}} = 2,432\,\text{m/sec}$$
$$g_0 = 1.618\,\text{m/sec}^2$$
$$\text{Moon mass} = \text{Earth mass}/81.3$$

Figure 6.2. Orbital parameters of the Moon and distances from Earth.

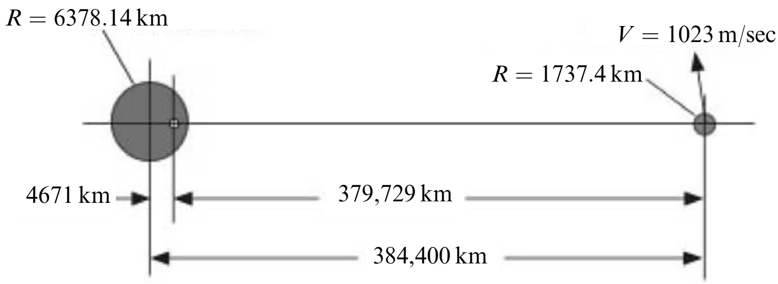

Orbital inclination with respect to the ecliptic = 5.145 deg.
Orbital eccenticity = 0.0549
Earth mass/Moon mass = 81.3
Lunar sphere of influence radius = 66,183 km
Lunar gravitational parameter, $\mu = 4902.8\,\mathrm{km^3/s^2}$
Earth sphere of influence radius = 924,000 km
Earth gravitational parameter, $\mu = 398{,}608.4\,\mathrm{km^3/s^2}$

Figure 6.3. The Earth–Moon system revolves about the barycenter some 4,600 km from the center of the Earth. The Moon rotates about that center at an average speed of 1,023 m/sec, so any vehicle traveling from Earth must match that speed to orbit the Moon.

statute miles) from the Moon. That center of rotation is called the barycenter. The gravitational sphere of influence of the Moon, when it is at 384,400 km (238,854 statute miles) from Earth, is 66,183 km (41,124 statute miles). At that distance the gravitational influence of the Moon will be greater than that of the Earth and will therefore control the motion of approaching spacecraft. So in calculating the trajectory when the lunar sphere of influence is crossed, a conical patch is required to approximate the Moon approach trajectory. Since the conical patch is an approximation, the correct trajectory solution must be obtained by numerical analysis. The Moon travels around the Earth in a counter-clockwise direction at 1,023 m/sec (3,356 ft/sec), and added to the Moon's orbital velocity, nominally 1,655.9 m/sec (5,433 ft/sec) for a 50 km (31.07 miles) orbital altitude, this is the velocity that a spacecraft must possess to capture a stable lunar orbit. The Moon covers about 13.177 degrees per day (0.54904 degrees per hour) in its orbit, so the travel time to the Moon gives the lead angle at injection to the lunar transfer trajectory.

A typical lunar trajectory is shown in Figure 6.4 and this is not unlike the Apollo trajectories. The usual approach in planning an Earth–Moon trajectory is to specify the approach angle to the Moon (λ) and evaluate the resultant lunar trajectory inside the lunar sphere of influence. The approach angle is then varied until the desired lunar orbit is obtained. Remember, the lunar sphere of influence is a function of the distance from Earth to the Moon, as given by the Laplace method:

$$r_s = r_1 \left(\frac{M_{\text{moon}}}{M_{\text{earth}}} \right)^{2/5}$$

$$\frac{M_{\text{moon}}}{M_{\text{earth}}} = \frac{1}{81.3} \tag{6.1}$$

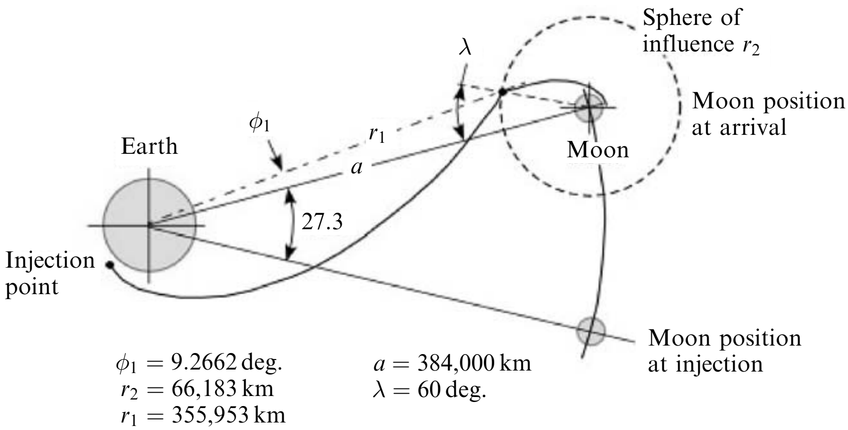

Figure 6.4. Flight path geometry of the representative lunar trajectory.

So the 66,183 km (41,124 statute miles) given in Figure 6.3 is for the 384,400 km Earth–Moon distance. The Earth–Moon distance varies, as said, from 406,700 km to 356,400 km with a mean of 379,700 km, so the lunar sphere of influence ranges from 70,023 km to 61,362 km, with a mean of 65,374 km (43,510 miles to 38,129 miles with a mean of 40,621 miles). The lead angle for launch, in this particular case 27.9 degrees, is a function of the transfer trajectory time from injection to intersection of the Moon's sphere of influence. In all cases the injection speed into an Earth–Moon transfer trajectory is less than the Earth escape speed, 10,946 m/sec (35,913 ft/sec), so all of the lunar transfer trajectories are elliptical orbits. The minimum energy transfer ellipse is represented by a Hohmann transfer ellipse to the Moon's orbit, followed then by a propulsion burn to match the Moon's orbital speed of 1,023 m/sec. This transfer orbit requires the greatest time to reach the Moon's orbit, that is 109.5 hours. The Apollo trajectory was designed to reach the Moon in less than that, that is, 72 hours. Remember the conical patch technique is very simple for planning interplanetary missions, but it is only an approximation for Earth–Moon missions and a precise numerical integration is required for any specific trajectory. However, the approximate approach does not influence the selection of propulsion systems for lunar missions, and is satisfactory for the purposes of this book.

Launching a spacecraft to the Moon for a specific arrival time requires very precise velocity control as shown in Figure 6.5. The Moon travels in its orbit around Earth at 1,023 m/sec (3,356 ft/sec) at an angular rate of 13.177 degrees per day (0.54904 degrees per hour). To achieve the Apollo mission 72-hour transit time, the precision of the injection speed had to be less than 1 m/sec, at least (a difference of 0.01 km/sec, or 10 m/sec, can change the arrival time by 5 hours). The important fact is that all of the trajectories are ellipses and all eventually return to the Earth periapsis after completing a longer or shorter portion of the ellipse. So, errors in the exact trajectory will not 'lose' a spacecraft in space. However, the time to complete an elliptical trajectory matters, and therefore the issue is acquiring the precise point

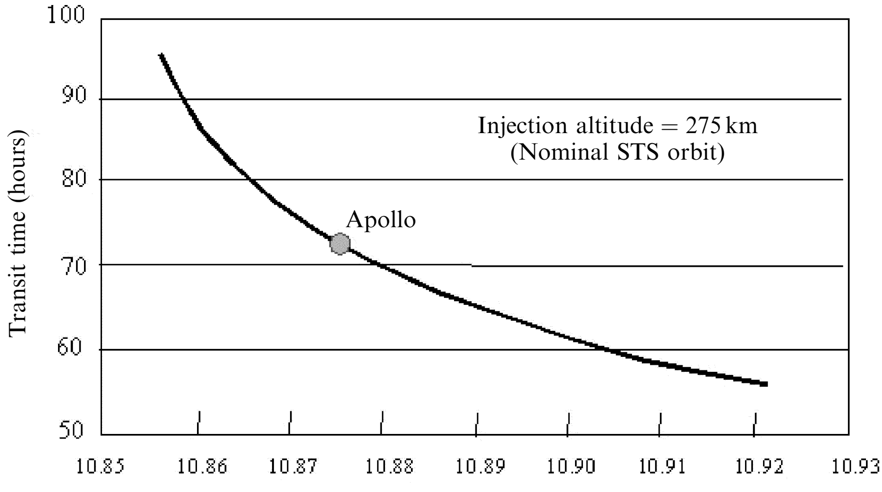

Figure 6.5. Earth orbit injection speed is less than escape speed, so the trajectory to the moon is a transfer ellipse analogous to LEO to GSO transfer ellipse ($V_{esc} = 10.946$ km/sec) [Brown, 1998].

of intersection between the transfer ellipse and the Moon's sphere of influence, as this point sets the rest of the trajectory to the Moon. A 1-sec error puts this intersection over 1 km in error and can have serious impact on the resultant lunar trajectory, so timing is critical. This is not meant to make the lunar trajectory a technology challenge, but only to clarify the requirements. The late 1960s technology was adequate for a at least eight Apollo missions to the vicinity and surface of the Moon.

6.2 REQUIREMENTS TO TRAVEL TO THE MOON

As shown in Figure 6.6, traveling to the Moon is a multi-step process. The first step is to achieve low Earth orbit (LEO), nominally set at 100 nautical miles or 185.3 km. From that orbit spacecraft can achieve higher orbits or be injected into a lunar or planetary transfer orbit. The International Space Station (ISS) is nominally in a 275 km (148.5 nautical miles) orbit. All of the calculations performed in this section for lunar transfer orbits were for a 275 km circular Earth orbit. So the first step is to determine the requirement to reach a circular Earth orbit. For that a single-stage-to-orbit (SSTO) launcher was selected, as this is the most demanding. A two-stage-to-orbit (TSTO) launcher will have lesser mass ratio requirements. Table 6.1 gives the launcher requirements for LEO with a SSTO launcher.

Achieving even a modest airbreathing capability can reduce the liftoff mass of the launcher by a factor of 2, simultaneously reducing vehicle size and propulsion system size. With a lesser oxidizer load and an operational design focus, the possibility of more frequent and lower cost to orbit is a reality. In terms of Moon

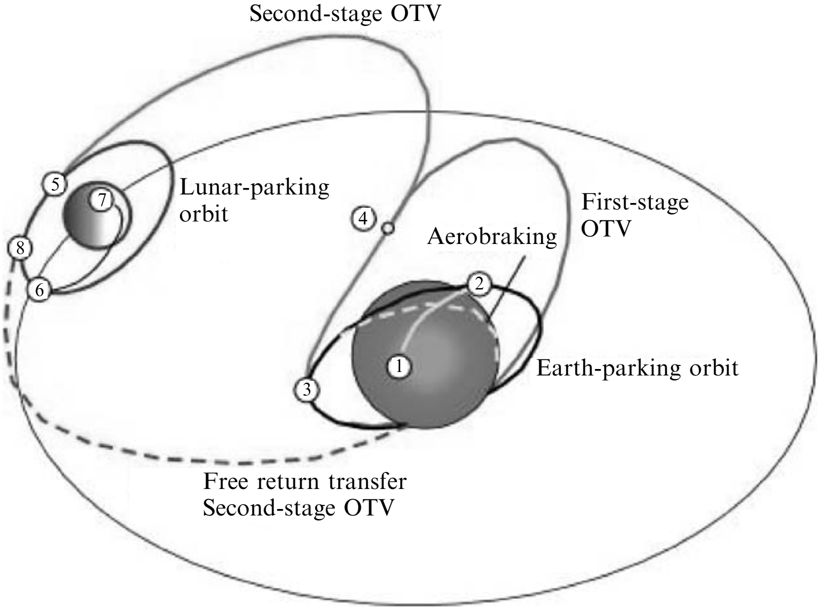

Figure 6.6. Transfer trajectory from Earth orbit to lunar orbit from a brief by V. Gubanov at the European Space Conference in Bonn, Germany, in 1984.

Table 6.1. Launcher requirements to achieve circular low Earth orbit.

Altitude (km)	Altitude (nautical miles)	V_{orbit} (km/sec)	V_{escape} (km/sec)	Mass ratio rocket	Mass ratio combined cycle
185.2	100.0	7.7930	11.021	8.07	4.06
275.0	148.5	7.7403	10.946	8.28	4.16
370.4	200.0	7.6854	10.869	8.37	4.20

missions, the propulsion advances associated with the launcher have the greatest impact. With respect to the in-space operations the options available in the near term are about the same as for the Apollo missions.

Having achieved LEO the next step is to inject the spacecraft into a trans-lunar elliptical transfer orbit. From the data in Figure 6.5 [Brown, 1998], the requirements for the transfer ellipse were determined for a range of travel times, and are presented in Table 6.2. The travel duration of 119.5 hours is the lowest-energy Hohmann transfer ellipse. The shortest time corresponds to a speed approaching escape speed, 10.946 km/sec, in Table 6.2.

If and when a nuclear electric rocket or a nuclear thermal rocket becomes available (see Chapter 7), the reduction of the propellant required for the trans-lunar trajectory will be significant. As with the orbital maneuver vehicles (OMVs)

Table 6.2. Injection speed and transit time to Moon from 275 km circular orbit.

Lunar transit time	Injection speed (km/sec)	ΔV (km/sec)	ΔV (ft/sec)	Mass ratio hypergolic rocket	Mass ratio nuclear rocket
119.5	10.854	3.111	10,207	2.986	1.172
88.0	10.86	3.118	10,230	2.993	1.172
75.0	10.87	3.128	10,263	3.004	1.173
65.5	10.89	3.148	10,328	3.025	1.174
58.5	10.91	3.168	10,394	3.046	1.175
56.0	10.92	3.178	10,427	3.057	1.176
54.0	10.93	3.188	10,460	3.068	1.177

described in Chapter 5, the major hurdle for the nuclear electric propulsion system is thrust and the magnitude of the rejected heat, that determines the space radiator mass. The propellant mass in terms of the operational weight empty (OWE) will reduce from about 2.0 times the OWE to about 0.17 times the OWE, a reduction of some 91.5% in propellant mass. The difficulty with all elliptical transfer orbits is the time it takes to return to Earth if the trajectory is not precisely corrected at the intersection with the lunar sphere of influence. For the Hohmann transfer ellipse, 119.5-hour trip time, the elliptical orbital period is approximately *10 days*, 5 hours. For the 70-hour lunar trip time the injection speed is 10.88 km/sec and the transfer ellipse orbital period is approximately *16 days*, 15 hours. For the 58.5-hour lunar trip time, the transfer ellipse orbital period is approximately *40 days*, 22 hours. And finally, for the 54.0-hour lunar trip time, the transfer ellipse orbital period is approximately *135 days*, 21 hours: the faster you go, the larger the orbit eccentricity and length if the trajectory to the Moon is not precise All of these elliptical trip times are greater than the resources carried by the Apollo spacecraft, so either a redundant or very reliable rocket system, or a sufficient resource reserve is necessary. There is a propellant requirement for the transfer to the lunar sphere of influence trajectory with the proper selection of the arrival angle (λ) that can be almost negligible, or at least sufficiently manageable not to affect too much sizing the total propellant mass. Only a numerical analysis for a specific trajectory will yield that quantity correctly; such analysis does not affect the selection of the propulsion system and therefore need not be done for the purposes of this book. The last table (Table 6.3) deals with the propellant requirements to land on the Moon's surface and to take off from it.

Table 6.3. Arriving or departing the Moon, hypergolic propellant rocket.

Altitude (km)	Altitude (nautical miles)	V_{orbit} (km/sec)	V_{escape} (km/sec)	Mass ratio orbit	Mass ratio escape
50.0	27.0	1.656	2.342	1.756	3.082
122.3	66.0	1.623	2.296	1.820	3.313

Table 6.3 lists the minimum mass ratios to the lunar surface from the lunar parking orbit and back, from the lunar surface to the lunar parking orbit. As for the Apollo lunar ascent module, a hypergolic propellant is a reasonable choice until nuclear rockets or other non-chemical launching systems are operational. The hypergolic rocket requires no igniter and is the most reliable starting engine available, providing the propellant isolation valves DO NOT leak. (If there is a leak, the lunar spacecraft will probably be totally destroyed by a violent explosion. With the demise of clean machine shops with dust and oils contamination controls that existed for the Mercury, Gemini, and Apollo programs, the potential for contaminated surfaces and leaking hypergolic isolation valves remains a concern today). The 112.3-km lunar orbit has a 2-hour period and makes a good lunar holding orbit if a rendezvous in lunar orbit is required. The mass ratio to descend to the surface, with some margin, is about two. A mass ratio of 3.5 is sufficient for the escape maneuver. The spacecraft essentially falls toward Earth once it clears the lunar sphere of influence. As the spacecraft approaches Earth it can be traveling at a speed greater than the lunar injection speed and greater than escape speed, so it is necessary to have braking rocket propulsion or aerodynamic breaking in the upper atmosphere to slow the spacecraft speed so it can be captured in an Earth orbit. In the case of a braking rocket, the returning spacecraft must have available a mass ratio similar to that in Table 6.2. In the case of a spacecraft braking aerodynamically in the upper atmosphere, the attitude is one for maximum drag; and if a lifting body configuration, it may roll upside-down and lift-down to increase the energy dissipated and decrease the heating intensity, as the heating pulse is spread out over a longer time in the upper atmosphere. The actual mission mass ratio will depend on trajectory and configuration specifics, but these tables give the reader an estimate of the propulsion and propellant requirements. From a LEO the round trip to the Moon can require less mass ratio than an out and back mission to GSO.

6.2.1 Sustained operation lunar trajectories

The Apollo trajectories and the Saturn V delivery system provided the necessary transport to the Moon and return in the late 1960s. With a near-Earth-orbit space infrastructure established (see Chapter 5) it is not necessary to have a direct flight to the Moon with expendable hardware. Both Russia and the United States contemplated a Moon base and the systematic flights necessary for its support and staffing. Figure 6.6 is a composite of both approaches, based on briefings and reports from the early 1980s. The figure is from a brief given by V. Gubanov to the space organization of the former Soviet Union, and presented at the 1984 European Space Conference in Bonn, Germany. The original figure is in Cyrillic and has been translated. The presentation by V. Gubanov describes a multi-step approach that begins with an 'artificial' Earth orbital station, then moves to the Moon as the Earth's 'natural' orbital station. After the Moon station is established and operational, the tested and proven Moon facilities are used to design a *Mars* facility, and the Moon is used as a launching platform for the human expedition to Mars. In the original Gubanov brief, there is a single transportation vehicle that moves from LEO to the lunar parking orbit and returns. In the Science Applications International Corporation (SAIC) study from 1984 for an initial operational Moon base, a two-stage transportation system using Orbital Maneuver Vehicles (OMVs) is proposed [SAIC, 1984].

Earth-based launchers deliver the lunar base materials to LEO for integration to an OMV. The first OMV puts the system into an Earth elliptical orbit, and the second stage OMV stages at the correct time for another Earth elliptical orbit that intersects the lunar sphere of influence, Figure 6.4. Both OMVs return to LEO for continued use. There is the option for the lunar payload to be transferred to a lunar surface delivery vehicle in lunar orbit, or to descend directly to the lunar surface, as the mission requirements dictate. Just as the Earth launchers can deliver to LEO, or return lunar payloads from LEO, there is a lunar launcher that delivers and returns payloads from low lunar orbit (LLO). Since the second-stage OMV must execute an aero-braking maneuver in the Earth's upper atmosphere, it must have at least a capsule configuration for braking with a finite lift-to-drag ratio (such as the Apollo heat shield or a Mars aero-braking design with an asymmetric cone configuration). Technologically, here the choice is between reusable heat shields or ablatives, the latter requiring refurbishment or replacement after each re-entry flight.

6.2.2 Launching from the Moon surface

The lunar launcher that delivers and returns payloads from low lunar orbit (LLO) requires propellant to reach LLO and return to the surface. We have said already that nominal orbital speed is much lower than that for Earth, 1,656 m/sec (5,433 ft/sec), and requires a much smaller mass ratio to reach and return from LLO; the nominal escape speed is 2,342 m/sec (7,683 ft/sec), or about one-third of the Earth nominal LEO speed. From Table 6.3, we see that the mass ratio to reach LLO is 1.82, or about 3.5 for a round trip back to the surface. This is a modest mass ratio, but all of the propellants must be delivered from Earth, at a very high cost in expended propellant (see Chapter 5), unless propellants can be manufactured *in situ*. This provides an opportunity for a non-conventional launch capability, solving the difficult operational problem associated with using Earth to function as a launcher to LLO. The lunar surface acceleration of gravity is 1.618 m/sec^2 (5.308 ft/sec^2), so the weight of the equipment is one-sixth what it is on Earth: the force required by construction equipment is less, as it the materials strength requirements. Humans on the Moon will still be limited by having to work in pressure suits when outside, and in environmentally controlled habitats and facilities.

Launching payloads from the Moon surface is thus attractive. With rockets, only a modest amount of propellants is needed. However, given the inherent thermodynamic inefficiency of rockets, the low lunar gravity suggests also alternative means to achieve escape speed, among them magnetic accelerators and laser-driven propulsion. The first practical means of launching payloads/vehicles from the lunar surface to LLO, or to accelerate them to lunar escape speed for deep-space missions, is the 'Magnetic levitation linear induction accelerator', or MagLev driver [Batenin et al., 1997; Loftus, 1999; Post, 1998, 2000]. Such a device must have a straight launch path

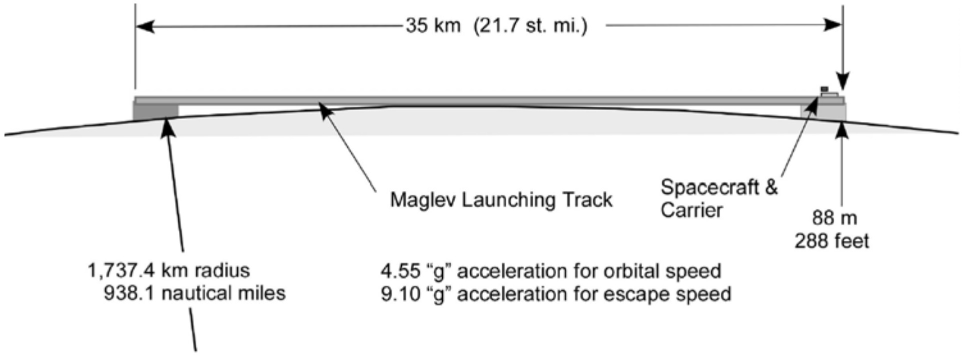

Figure 6.7. Superconducing MagLev launcher on the Moon to provided a non-chemical propulsion means to achieve lunar escape speed.

and cannot follow the curved surface of the Moon; see Figure 6.7 showing a MagLev launcher capable of both lunar orbital and lunar escape speed. The linear accelerator has a substantial advantage on the Moon, as there is no atmospheric drag to overcome. The most significant challenge is to move the quantity of materials to build on the Moon, or to manufacture from *in situ* lunar resources a 35 kilometer-long track that is flat and supported off the lunar surface. The drivers are to reduce as much as possible the need for propellants ferried from Earth or even when manufactured *in situ* (in either case, an expensive solution, although water seems to exist on the lunar south pole). Solar energy is available during the long Moon day, the solar constant there being about 1.35 kW/m^2, some 10% higher than on Earth due to the lack of an atmosphere. In principle, solar energy could be collected more easily and readily than on Earth to generate electricity; this strategy is potentially cheaper than manufacturing or ferrying propellants, and could then provide the energy needed for orbiting payloads with lunar MagLevs.

A variation on the MagLev theme is the 'magnetic lifter', or MagLift. The MagLift accelerates a payload in the same way as the MagLev, that is, using the Lorentz force, while keeping it slightly above the electrically conductive rail(s) to avoid friction. It is not designed to reach escape speed: it replaces only the first stage of a conventional rocket. For instance, installed on the Moon, it could accelerate a single-stage rocket up to half the lunar escape speed. The magnetic lifter or magnetic levitator concepts can significantly affect lunar-based transportation. By levitating the launcher and providing the initial acceleration or boost, fuel weight is eliminated or reduced, enabling larger payloads or/and less costly launches. This strategy to accelerate payload can be self-standing or can complement rocket propulsion. Because it does not need consumables (other than electricity) and has no moving parts, MagLev/MagLift launch-assist technology is inherently geared to high launch rates—power generation aside, these would be limited by the ability to prepare the launcher and carrier (the 'sled') assemblies. The MagLev track and supporting facility is inherently capable of rapid turnaround.

A MagLift-assisted launch would be accomplished by mounting the vehicle, or payload, to launch piggyback on a carrier structure (sled). The sled accelerates along a fixed track as power is fed to embedded magnetic coils by a dedicated power generation or energy storage system. The coils interact with magnets (permanent or not) on the bottom of the sled to provide both levitation and propulsion Lorentz forces necessary to accelerate the assembly. Part, or all, of the final speed needed is obtained in this way. Once the required velocity is attained, for instance, if it is less than the Moon escape or orbital speed, the vehicle's own propulsion system is activated, taking it to final speed and orbit. MagLift/MagLev acceleration is limited by track length and vehicle/payload sturdiness. After the launch vehicle is released, the carrier sled is slowed to a stop, for instance electromagnetically, to recover part of the sled energy and store it, it then is returned to the starting end of the MagLev track for reuse.

Lunar MagLev/MagLift systems are constrained by power available, track length and acceleration. In fact, neglecting for simplicity the lunar gravitational work, the thrust power P to accelerate a mass m to a final velocity V along a track of length L and with a constant acceleration a_o is given by

$$\begin{aligned} P &= m a_o V = \text{Power} \\ L &= \frac{a_o t^2}{2} = \text{Track length} \\ V &= a_o t \end{aligned} \tag{6.2}$$

where t is the time to reach V. From equation set (6.2)

$$\begin{aligned} L g a_o &= \frac{V^2}{2} \\ L &= \frac{V^2}{2a_o} \end{aligned} \tag{6.3}$$

that is, a hyperbola on the (a_o, L) plane, showing that, per unit mass, escape velocity can be reached by using a combination of acceleration and track length so that neither a too intense acceleration nor an excessively long track is necessary. The payload for exploration of the Jovian planets and Mars will require that the magnitude of the acceleration is limited to less than 3 to 5 times the Earth's gravitational acceleration. For insertion into escape orbits the problem is one of track length: for instance, at 3 'g' acceleration (96.52 ft/sec^2 or 29.73 m/sec^2) and for launch speed just exceeding escape, i.e. 8,200 ft/sec or 2.5 km/sec, yields a track length of 348,313 ft or 105.1 km and a acceleration duration of about 85 seconds. At our current stage of Moon supply capability it is totally impracticable to construct a track of that length on the lunar surface. For simply gaining a $\Delta V = 500$ m/s with the same acceleration the squared-V dependence indicates a much more manageable 4.2-km track length.

Energy-wise, the energy E to reach escape speed V is of course independent of a_o and L, that is:

$$E = \frac{mV^2}{2} \tag{6.4}$$

for instance, a one-ton payload needs some 3 GJ (some 3 MJ/kg) to reach the Moon escape speed. This is not a large figure per se (it is equivalent to the heat given off by burning completely 717 kg of gasoline with air), but power may be significant: in fact, since velocity changes during acceleration, the *maximum* power required is:

$$P_{\max} = m(a_o)^{1.5}(2L)^{0.5} = ma_o V \tag{6.5}$$

The power required is a stronger function of the acceleration than L. In the first case examined ($V = 2.5$ km/s, $a_0 = 3$ 'g'), the maximum power is reached at the end of the track, and is 74.3 kW/(kg of payload). This means 74.3 MW/ton, the power of a medium-size gas turbine, except on the Moon there is no air, and the only *in situ* power source is the Sun. At 1.35 kW/m^2 and 12% photovoltaic efficiency the area needed is 458.6×10^3 m^2, or a 677×677 m^2 filled with solar cells. A possible solution to the power problem is to store energy harvested by solar cells, and to release it gradually when needed, or to use nuclear power, that is limited only by materials temperature limitations, see Chapter 7. In the end, a MagLev solution for lunar transportation will depend on the nature of the payloads to be accelerated, i.e., how much acceleration, a_o, they can stand without damage, that controls the track length, and on power available.

A second device that could provide a viable launch system it the LightCraft concept of Professor Leik Myrabo, [Myrabo, 1982, 1983; Myrabo et al., 1987]. This system is shown in Chapter 4 as an Earth launcher, but the LightCraft has a deep space configuration where acceleration can be provided by interaction of the solar wind with the laser/microwave beam. As shown in Figures 4.42 and 4.43, the installation of the laser/microwave projector is much less extensive than for the MagLev device because no track is required.

Laser beams are an attractive means of carrying concentrated power over distance. *In vacuo*, such as on the Moon, their power is not dissipated by interaction with gas molecules, and diffraction cannot take place. Thermal blooming is absent, and the beam (theoretically) stays coherent. These advantages suggest using a laser as a primary power source beamed to a spacecraft to supply power and accelerate it. Atmospheric effects (accounted for by the so-called Strehl ratio, of order 10^{-1}) result in a laser range, R, given by the (approximated) Rayleigh equation

$$R = D\,gd\sqrt{\frac{S_{tr}}{24.4\lambda}} = \text{Laser range} \tag{6.6}$$

where D = diameter of the beaming mirror, d = diameter of the receiving mirror on the spacecraft, S_{tr} = Strehl ratio ≈ 0.1, and λ = laser wavelength.

For instance, a CO_2 laser ($\lambda = 10.6\,\mu$m), beamed by a 5 m diameter mirror could be received by a 1 m diameter mirror at about 140 km, assuming a Strehl factor 0.5. In space this range can be higher, since the Strehl ratio is close to 1. Chemical oxygen–iodine lasers (COIL), with their 1.3-µm wavelength, offer a range almost an order of magnitude longer. Free electron lasers (FEL) may have a range of wavelengths, but operate in the pulsed mode only: the continous wave (CW) or pulsed mode operation is an important issue, since it directly affects thrust.

Once received, the power can be used in a variety of propulsion strategies. A semi-empirical quantity, the 'coupling coefficient C_T', expresses how much of the incident power is converted into thrust. C_T depends on the particular strategy chosen to produce thrust from the power transmitted by the laser beam, and permits analysis of Moon-launching without bothering with the specifics of propulsion. If sufficiently large, or lasting, or both, laser power becomes thrust capable of lifting payload from the Moon and injecting it into orbit. Notice that small thrust lasers are still capable of accelerating (of course, thrust must be at least equal to the lunar weight), but the Rayleigh equation sets a crude distance and time limit on how long acceleration may last. In fact, if a_0 is the acceleration (assumed constant) imparted to the craft, T is the thrust, V the lunar escape speed, t the escape time, neglecting gravity work for simplicity, it must be

$$\begin{aligned} a_o &= \frac{T}{m} \\ R &> \frac{a_o t^2}{2} \\ V &= a_o t \end{aligned} \tag{6.7}$$

and eventually the minimum acceleration a_0 must satisfy the conditions:

$$\begin{aligned} \frac{T}{m} &> \frac{V^2}{2R} \\ \frac{P}{m} &> \frac{V^2}{2C_T R} \end{aligned} \tag{6.8}$$

For instance, a 1000-kg payload accelerated by a CW CO_2 laser beamed by a $D = 5$-m mirror, received by a 1-m focusing mirror and assuming a Strehl coefficient of 0.5 needs an acceleration of about 21 m/s^2 ($T = 21{,}000$ N) to accelerate to lunar escape speed within 140 km of the laser range. The power required, with a coupling coefficient of 1000 N/MW turns out to be $P = 21$ MW, a rather striking figure at this time, but maybe feasible in a few years from now. In any event, equation (6.8) points to the fact that 'shipping' payload from the Moon requires significant installed power. As in the case of MagLev systems, powering the directed energy beam can be a combination of stored solar energy and nuclear power plant electrical energy. With less acceleration and the requirement to illuminate the accelerating spacecraft for longer time periods, stored solar energy alone is probably insufficient. Takeoffs and landings are vertical with minimum surface footprint. The basic concept has been demonstrated [Myrabo et al., 1998; Myrabo, 2001]. In terms of potential for deep space acceleration and launching from the lunar surface, this concept has the most potential and the least acceleration load on the spacecraft.

As with all of these schemes, a significant amount of material must be either fabricated on the Moon or lifted from the surface of the Earth and that requires an even greater mass of propellant to reach LEO and the Moon. So the tradeoff question is, does the propellant saved in lunar launches and the propellant required to deliver that propellant to the Moon (or *in situ* facilities to manufacture the propellant) justify the cost of the facility? With current chemical propellants the answer is no, as we saw how large is the ratio between propellant mass required to deliver a payload to its destination and the payload mass. However, as higher-thrust solar electric and nuclear electric propulsion systems become operational, the cost of propellant will fall dramatically and non-rocket launch facilities on the Moon will in all probability become practical.

6.3 HISTORY

The history of our visits to the Moon are listed as a reminder that we have not returned to the Moon since the last Apollo 17 astronauts departed the surface, more than 40 years ago. In the decade beginning in the mid-1960s there were probes, landers, rovers, lunar satellites and even 12 American astronauts that briefly visited the surface. Since then only Clementine, the Lunar Prospector and the SMART-1 electric thruster-powered probe have orbited or visited the Moon. After the few brief visits to the Moon, subsequent Apollo mission and any sustained exploratory visit to the Moon were scrapped. The very efficient and capable heavy launch system, Saturn V, was discarded as having no future. Today a heavy-lift system to LEO is still missing, although in the process of being planned. The closest to regaining that capability was the Russian 'Energia' launcher that was scrapped after just two successful launches. So the Moon still conceals many mysteries about its past history that remain to be discovered. There are unexplained anomalies in surface composition, there is the massive, violent bombardment of the Moon that occurred about four billion years ago, there is the question of water ice in the shadowed south polar region, and whether ^{3}He (or 'helium-3', a very interesting fusion 'fuel', see Chapter 8), hydrogen and oxygen can be recovered from the surface in a sustained operation. Briefly, past exploration has been by the former Soviet Union and the United States. Now the European Space Agency (ESA), Japan and the United States plan to send more unmanned spacecraft to the Moon in an attempt to resolve some of its unanswered questions. Figure 6.8 shows where the different systems have reached the Moon's surface and some of the lunar orbital systems.

6.3.1 USSR exploration history

- Luna 1, 2 & 3 — Luna 3 returned the first pictures of the near and far side of the Moon
- Luna 9 & 13 — First successful soft landings on the lunar surface
- Luna 16 & 17 — First automatic probe to return samples and have robot rovers to transverse the lunar surface and avoid craters
- Orbiters 1, 2, 3, 4, 5 — All were successful and mapped the lunar surface in detail

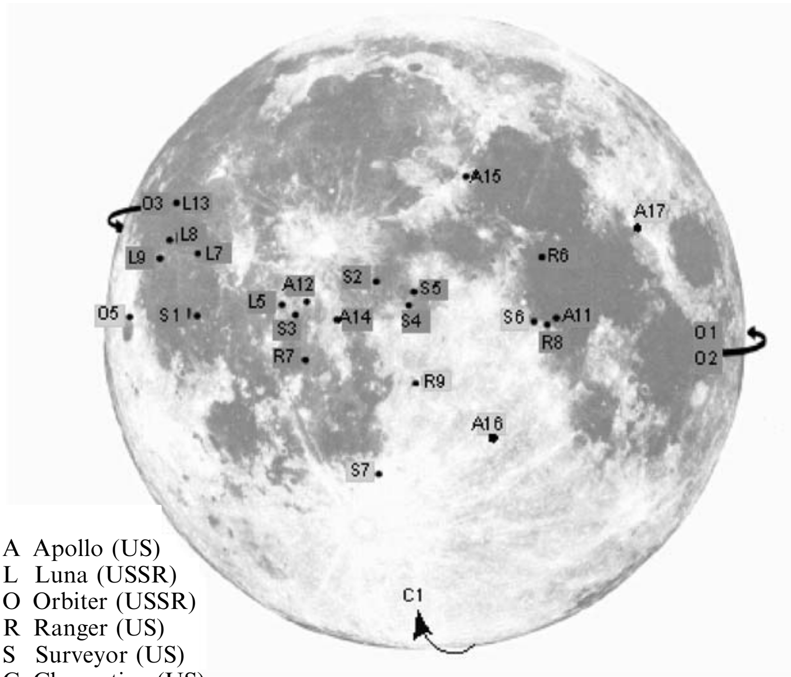

Figure 6.8. We have been there before with probes, landers, orbiters, and human visitors. Apollo was a manned Moon mission beginning with Apollo 10 lunar mapping mission, and ending with Apollo 17. Luna was a USSR robotic lander and rover series, Orbiter was a series of USSR flyby and orbital photographic mapping missions, Ranger crashed into the surface relaying pictures as it did, Surveyor was a lander mission series, and Clementine was an orbital mapping and resources survey mission.

6.3.2 USA exploration history

• Ranger 7, 8 & 9	Nine Rangers were launched; the last three were able to send back pictures of the lunar surface as the probe crashed into the surface
• Surveyors	All successfully landed on the lunar surface and made measurements
• Apollo 11, 12, 14, 15, 16, 17	Human landings on lunar surface, local exploration and mineral (ilmenite) sample collection
• Apollo–Soyuz	First rendezvous and link-up between USA and Russian spacecraft
• Clementine	Lunar mapping and resource survey. First to find evidence of water in southern hemisphere craters
• Lunar Prospector	Lunar mapping and resource survey
• SMART-1	First ESA lunar probe sent from LEO to LLO with an ion electric thruster

This brief listing of the lunar exploration history and probes was given in the hope that these would not be the last. All of these aided in our understanding of the Moon, and have already radically changed our perception of the Moon and its origin. There is much more to the Moon than a nearby object to be explored for its history, natural resources and structure. The most important aspect of the Moon is that it can be a natural orbital station, it can be a staging base for deeper exploration of space, it can be an operational training base and systems development test site for hardware that will eventually permit us to confidently and safely have humans establish a base on Mars. Technically Apollo–Soyuz was not a lunar mission, but it was the precursor to the cooperation that led to the ISS being established in orbit. When one of these authors (PC) visited the Space Museum in Moscow, the centerpiece of the Museum (in 1990) was the Apollo–Soyuz spacecraft joined together and hanging in the rotunda. In the Leninsk Museum outside of Baikonur Space Center there is a tribute to the spacecraft commanders, Tom Stafford and Alexei Leonov. Also within the tribute is some of the space artwork of Leonov, who was quite an accomplished artist. The last Saturn and Apollo moon launch departed Kennedy Space Center on 15 July 1973 at 19:50 GMT and brought to an end the United States exploration of the Moon and an era of accomplishments that, just a few years previously, were thought impossible.

6.4 NATURAL VERSUS ARTIFICIAL ORBITAL STATION ENVIRONMENTS

Tom Stafford provides a very clear view of what might be if we take advantage of the Moon's potentials [Stafford, 1991]. Stafford's synthesis group, in defining the Space Exploration Initiative, placed significant emphasis on the utilization of the Moon as an orbital operational base. Stafford's report goes into significant detail on how this could be accomplished, beginning with a reconstituted, and with upgraded electronics, Saturn V/Apollo program. In discussing the finding with General Stafford at the 1991 Paris Air Show, he related the frustration in the inability of industry to manufacture the Saturn V hardware, especially the Pratt & Whitney J-2 hydrogen/oxygen rocket engine and the Rocketdyne one-million-pound thrust F-1 rocket engine. It was apparent that the human machining and tooling skills had disappeared with the ageing and retiring of skilled craftsmen, and because the computer-controlled machining was not an adequate substitute. Thirty years after the Apollo missions, with all of the technology improvements, the 1960s hardware capability could not be reconstituted. What was thought impossible prior to the Apollo missions now is impossible because the only operational crewed vehicle we have, the Space Shuttle, is incapable of anything approaching a lunar mission.

If we are to take advantage of the Moon as an orbital station it must be with new launcher hardware capable of a lunar mission. At this stage, with President G.W. Bush's Space Exploration Initiative still in planning, it is not clear what that hardware is or should be, but whatever it is, the new hardware must approach the lunar missions from the viewpoint of maintaining a sustained presence with frequent flights, rather than with a few short visits. At the time of writing this book, the heavy lifter proposed by NASA should use a combination of five shuttle liquid engines and four solid rocket motors.

6.4.1 Prior orbital stations

Not to belabor the point, but the most operational experience in an artificial orbital station is still possessed by the former Soviet Union and today's Russia. In discussing that experience with Vladimir Gubanov of the Production Company Energia, it is clear that the Russian engineers and researchers are aware of the limitations of a crewed artificial orbital station. Gubanov's presentations to the Russian government clearly emphasized an operational Moon-based orbital station as a precursor to venturing to Mars, and as a launching platform for automatic spacecraft space exploration. The artificial orbital stations that have been operational are listed below. Salyut 6 was reactivated after a serious hypergolic propellant leak forced evacuation of the station. An innovative adaptation of Earth-based tools to operate in space by a single cosmonaut permitted repair of the propellant system. MIR was in orbit the longest of any station, some 15 years.

- SkyLab, USA civil space station 1972
- Salyut 2 3 & 4, USSR military orbital stations 1973, 1974, 1977
- Salyut 1, 4, 6 & 7, USSR civil orbital stations 1971, 1974, 1977, 1982
- MIR, USSR civil orbital station 1986
- ISS, International Space Station, USA with Russia and European and Japanese participation 1999

6.4.2 Artificial orbital station

An artificial orbital station is an isolated man-made habitat for humans to exist in the inhospitable and hostile environment of space. Figure 6.9 shows MIR in orbit near the end of its 15 years in space and Figure 6.10 shows the International Space Station (ISS) in orbit early in its lifetime. MIR is not as elaborate as ISS, but is was the longest-lived functional orbital station. Its modular design allowed different functional modules to be added as needed. Note that, in the absence of a Unites States supply and rescue vehicle, for both orbital stations the Soyuz capsule is the supply and rescue vehicle. There is a Soyuz attached to the ISS (bottom of Figure 6.10) but there is no Soyuz attached to MIR because the picture was taken by the last crew departing MIR before its entry into the atmosphere. Since both stations had their origins in the Russian station modules, there is a similarity of structure. The characteristics of such a station require its sustained and continual support to sustain a human crew over the operational life of the station, as given below.

The defining characteristics of an artificial Earth satellite/orbital station are:

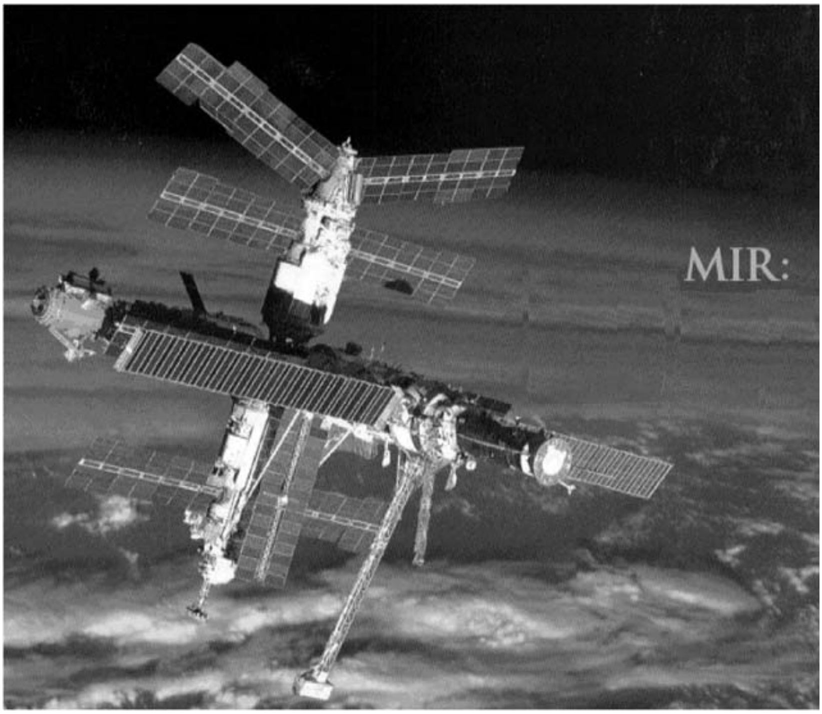

Figure 6.9. Orbital station MIR in its fifteenth and last year of operation.

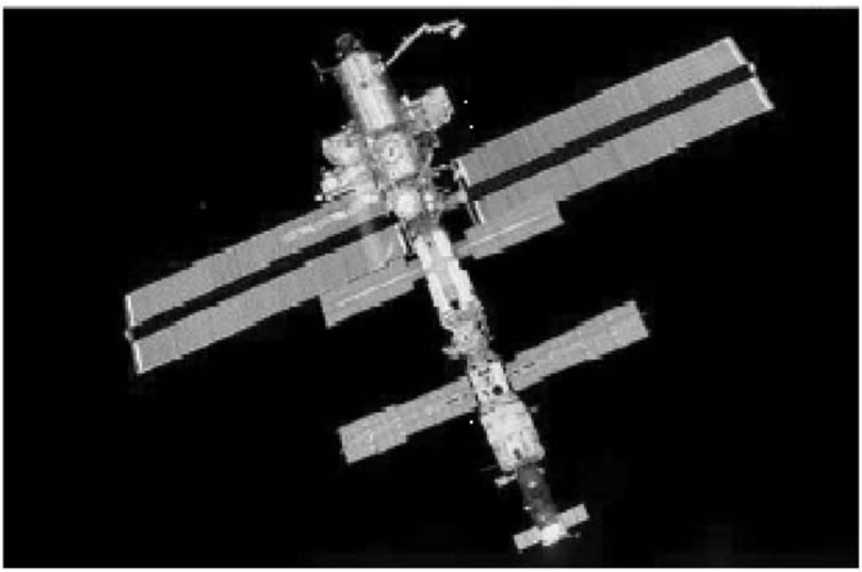

Figure 6.10. International Space Station in orbit.

(1) The station is without any self-sustaining resources, and must be continuously resupplied.
(2) The orbital station is the only inhabitable facility; survival outside the orbital station can be by space-suit only and is limited by life-support resources of the space-suit.
(3) The micro-gravity environment begins to induce significant physiological changes in the human crew for orbital stay times that exceed roughly 6 months.
(4) Solar and space radiation are serious hazards, especially over long orbital stays. A 'safe house' is required for the crew to wait out hazardous solar events (e.g. unpredictable solar flares).
(5) Solar wind and atmospheric drag requires propulsion burns to sustain orbital altitude. Failure to re-boost to operational orbital altitudes can result in atmospheric entry and destruction of the orbital station.
(6) The orbital station must be attitude-controlled to maintain solar panel and antenna orientation.
(7) Solar radiation is currently the sole, sustained, renewable power source via solar cells. Solar driven heat engines (Stirling or Rankine cycles driving generators) and nuclear power systems are yet to be considered or designed, much less tested or implemented.
(8) With human inhabitants, there is a critical requirement for means of rapid evacuation to Earth. This was one of the overriding considerations of the support systems for the 1964 USAF Manned Orbiting Laboratory. Only Russia has implemented a rescue system, sized for the station crew, which is attached to the orbital station whenever the crew is on board the station. Had the former Soviet Union not collapsed, the Lozino-Lozinski BOR 5 hypersonic gliders would be that crew re-supply/escape system, rather than the Soyuz ballistic capsule.

If the orbital station is to be more than a crewed pressurized container, then a sustained support and transportation system must be an integral part of the orbital station system. In terms of ISS that is not the case, even with the Space Shuttle regaining operational status. As discussed in Chapter 5, an LEO infrastructure is a demanding operation because nothing associated with the infrastructure is self-sustaining. Everything must be supplied from the Earth's surface. Secondly, unless some type of gravitational acceleration (of magnitude required to overcome physiological changes, yet to be determined) is generated, long-term human habitation will have serious health risks. Considering these challenges, General Stafford and his synthesis group determined that there is an approach that avoids most of these complications.

6.4.3 Natural orbital station

A natural orbital station is a habitat for humans to exist located on a natural satellite of Earth. It is true the Moon's environment is also an inhospitable and hostile environment. But with the presence of gravity and a soil surface there are options that do not exist for the artificial orbital station. General Stafford's Synthesis Group is not the first to study the Moon as a suitable operational crewed orbital station. Science Applications International Corporation (SAIC) generated such a concept in a 1984 report for the initial operational Moon base [SAIC, 1984]. The characteristic of such a station is that it does not require continual support to sustain a human crew over the operational life of the station, as given below.

The defining characteristics for the natural Earth satellite (Moon) station are:

(1) The lunar station can be self-sustaining for food and water, given construction of pressurized transparent domes and soil-processing equipment. Automated operation can last from 10 to 20 years with nuclear power. This station can be a prototype robotic facility for eventual deployment on Mars [Bayón-Perez, 2002].
(2) Solar and space radiation hazards exist, but underground facilities negate risk, Figure 6.11. habitats near the lunar north pole (near the Peary crater) might be ideal, as they may be permanently illuminated, but enjoy a thermally benign environment [Bussey et al., 2005].
(3) Both external modules and below-surface facilities provide multiple inhabitable locations that undergo less temperature extremes and offer protection from damaging solar radiation, Figure 6.12.
(4) Natural gravity about one-sixth that of Earth provides some gravitational acceleration. Whether it is sufficient to trigger gravity-based beneficial physiological reactions remains to be established. The orbital and escape speeds are lower.

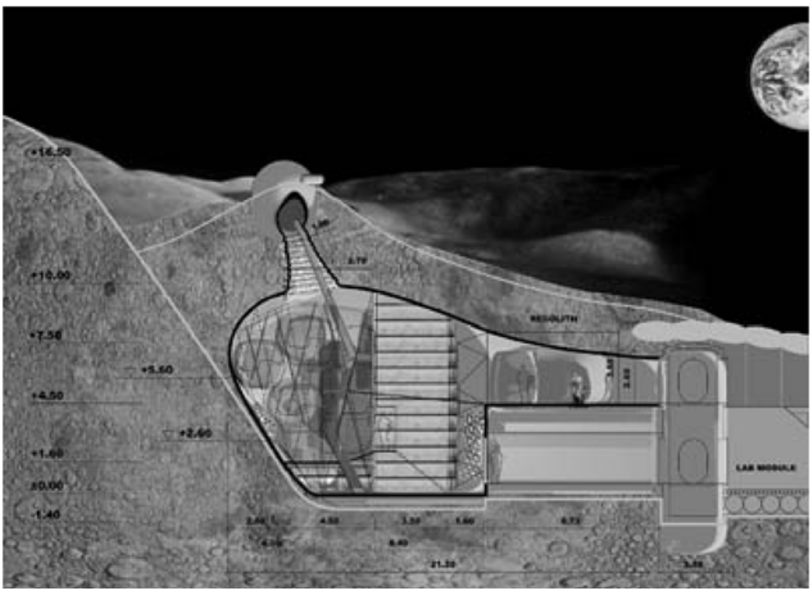

Figure 6.11. ESA concept for underground lunar habitat.

Figure 6.12. ESA concept for long-term lunar structures.

(5) The beam-powered LightCraft and the magnetic levitation (MagLev) accelerator are both options and alternatives to pure rocket launch from the lunar surface.
(6) Possibilities for *in situ* manufacturing of hydrogen and oxygen for rocket propellants from elements in the lunar soil deposited from the solar wind or comets exist. One of the chief components of the solar wind is atomic oxygen. Water seems to be present near the south pole.
(7) Assembling of prefabricated equipment and structures from Earth is possible, Figure 6.12.
(8) No space walks required; surface assembly uses mostly standard construction equipment.
(9) Solar radiation and ^{3}He mining are sources of renewable power.
(10) Lunar facilities inhabitants can evacuate to sub-surface facilities or other surface modules in case of solar flares or other occurrences, Figure 6.11.
(11) Return to Earth is free once lunar escape speed is reached and the spacecraft passes beyond the lunar sphere of influence.

Figures 6.11 and 6.12 show both the underground and surface concept structures being designed by ESA and the Japanese Space Agency. None of these require a technical breakthrough to be built. Available industrial capability in the United States, Europe or Asia can develop the first generation facilities and assembly equipment necessary to establish an initial operational capability (IOC). As more is learned about the lunar environment and surface conditions, systematic improvements can be incorporated. At the European Space Conference in Bonn, Germany, in 1984, where V. Gubanov presented the basis for Figure 6.6, the Japanese Space Agency NASDA (now JAXA) presented a comprehensive plan and an approach for returning to the Moon and establishing a permanent habitat. Unfortunately it had been too long since Apollo, and the engineers that for the first time created that which never was were not in attendance; the audience expressed severe skepticism about whether humans would ever return to the Moon. The approach and plan were well-thought-out and do-able, given significant engineering of practicable and operational Moon facilities. There seemed to be a misunderstanding between what is technically feasible (already demonstrated by Apollo) and what needs to be engineered as operationally practicable with our available industrial capability.

Using the Moon as an operational base makes propulsion choices less costly and easier to make for deep-space missions. Spacecraft speeds on the order of 13,500 m/sec (44,291 ft/sec) are possible with non-chemical rockets with low mass ratios (1.4 with a nuclear rocket, instead of 20 for a hydrogen/oxygen rocket and 98 for hypergolic rockets), a first advantage. There is a clear advantage for testing and evaluating human operations on a foreign, inhospitable planet that is just 70 hours away, before venturing far from Earth without the capability of easy and fast return. General Stafford found that, on a per pound basis, the cost of liquid oxygen sent from the Moon to LEO may actually be less than if the same mass were lifted up from the Earth's surface. High-energy material (^{3}He) recoverable from the lunar surface can power deep-space exploration and Earth-based fusion power plants when cryogenic, magnetic confinement reactors are available (see Chapter 8). For launches into our Solar System and for astronomical observatories on its dark side, the Moon is a natural choice. Using the Moon greatly reduces the magnitude of the resources required from Earth. Again, as in Earth orbit, the commercialization of sustained operations on the Moon is more practicable than if lunar missions are infrequent.

6.5 MOON BASE FUNCTIONS

A permanent operational base on the Moon has many more options than an artificial orbital station. Perhaps one of the most important functions relates to the future exploration of Mars. We left the Moon in a hurry, not even completing the scheduled missions. There is much left un-discovered on the Moon. The lunar mapping satellites *Clementine* and the *Lunar Prospector* have discovered large mineral deposits that can be exploited for fabrication of Moon-launched deep-space missions. As an astronomical observatory it has advantages over Hubble in terms of size and accessibility. Some of the most intriguing features of establishing a permanent lunar foothold are listed and discussed below.

6.5.1 Martian Analog

Figure 6.13 is from General Stafford's report on America's Space Exploration

Initiative [Stafford, 1991]. The figure shows sites on Mars and the Moon that have features in common, and could be used to evaluate facilities and equipment destined for deployment on Mars. Before these are deployed on Mars, they can be put to good use for building a Moon operational base, their performance evaluated and modifications made while in relatively close proximity to Earth. Although the Moon has no atmosphere while Mars has a tenuous atmosphere that can generate massive seasonal dust storms, the key similarities are those associated with the surface features. The Moon has essentially no surface pressure; Mars has a surface pressure that is everywhere lower than 10 millibar. On Earth the pressure of 10 millibar corresponds to an altitude of 29,300 m (96,127 ft), so there is very little atmosphere on Mars. Humans require a full pressure suit over altitudes of 55,000 ft (16,764 m), so in that respect full pressure suits are required on both Mars and the Moon. On Mars the acceleration of gravity is 3.707 m/sec^2 (12.162 ft/sec^2), on the Moon about half of that, that is 1.62 m/sec^2 (5.309 ft/sec^2). On the Martian surface the temperature is approximately 218 kelvin (−67°F) (it depends on the season) and on the Moon approximately 215 kelvin (−73°F). With the surface conditions rather similar, this makes the Moon an excellent Mars evaluation site. With a lesser gravity it will be easier to move about on the Moon and assemble equipment and facilities, but the difference with Mars is not so large that operation of the hardware cannot be established fairly well. One of the uncertainties with Martian operations is that of the density variation of the atmosphere at the time of entry. As a result, the landing ellipses (the set of points of most probable landing location, or elliptical error probability) are quite large. If material is being prepositioned, even if the same landing coordinates are selected, the landing sites

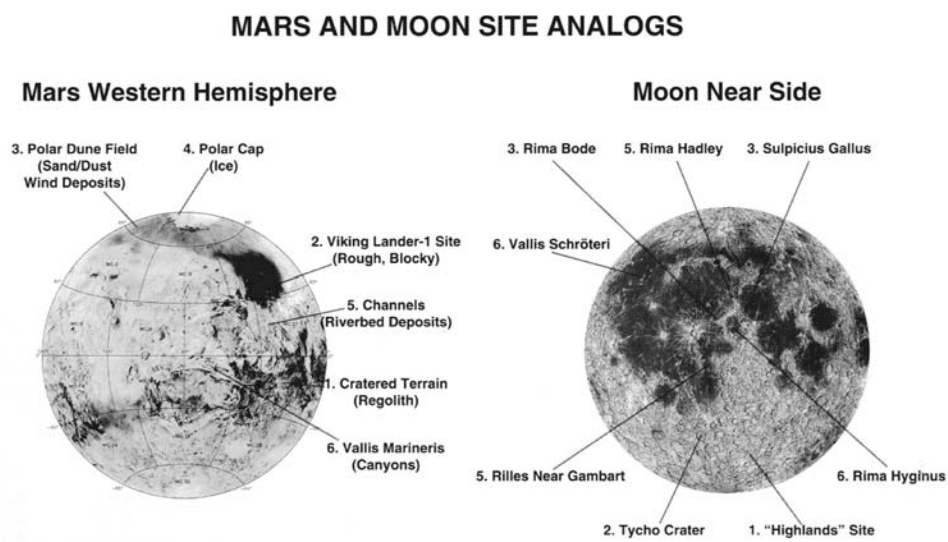

Figure 6.13. From Thomas Stafford's Report to Congress: the comparison of representative lunar sites with representative Martian sites.

could be 5 km (3.1 st. mi.) apart. So part of the Mars equipment evaluation will be the ability of the astronauts to locate and move the equipment to the same location. For a human mission to Mars that may be a truly critical element.

6.5.2 Lunar exploration

Both Russia and the United States left the Moon after a few brief encounters without really exploring it. We do know from the early Luna pictures that the far side of the Moon (the side that is always facing away from the Earth) is far different than the near side. Figure 6.14 is a composite of a near-side photograph with a far-side photograph so the differences can be compared [Berman, 2003]. With the far side always invisible from Earth it will make for a major challenge for human astronauts to explore the area. The maria on the near side were formed at different times. From the lunar samples returned by the Apollo astronauts, the age of the samples vary from 4.5×10^9 to 2.6×10^9 years. There are no maria on the far side, so whatever process produced the large flat areas on the near side was absent. *Clementine* and the *Lunar Prospector* have identified the surface materials on both the near and far side of the Moon and record the elevations, as shown in Figure 6.15 (see the color section) [Spudis, 2003]. Figure 6.15 shows the enormous extent of the South Pole-Aitken basin (purple are on the bottom of the right image) that stretches across some 2,500 km (1553 st. mi.). There are many anomalies that remain unexplained on the surface. The Apollo 11 astronauts returned a very high density, titanium-rich magma

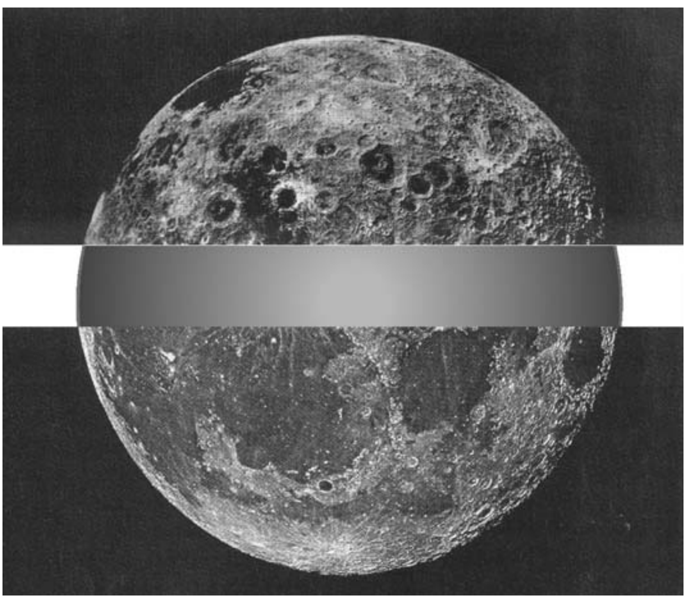

Figure 6.14. The back side of the Moon from Soviet *Luna 3* spacecraft (top) compared to the near side (bottom) (From *Discovery Magazine* [Berman, 2003]).

from the mare basalts. *Clementine* and the *Lunar Prospector* have identified areas with iron-rich soils in the maria on the near side and in the center of the South Pole-Aitken basin. Locations rich in thorium and KREEP (K = potassium, REE = rare earth elements, and P = phosphorus). This indicates that early Moon underwent intense melting and differentiation in which incompatible elements were concentrated in the molten part of an increasingly solid, crystallized system. The highest levels of thorium are in the upper left-hand part of the left image in Figure 6.15 (see the color section). The highest level of thorium, a potential fission fuel, occurs in the Oceanus Procellarum, but the reason, again, is not clear. The *Lunar Prospector* also discovered evidence of water ice at the Moon's north and south poles. The Moon's highlands are dominated by rocks primarily composed of the mineral feldspar. Feldspar is rich in calcium and aluminum. *Clementine* and the *Lunar Prospector* came as close as 7 km (4.3 st. mi) altitude and were able to precisely measure the variations in the Moon's gravity. The result was concentrations of mass ('mascons') higher than the average predicted by gravitational measurements in some of the youngest impact basins.

So, there are wide variations of the Moon's physical and geological characteristics, and there is hardly any symmetry between the near and the far side of the Moon. A great deal of research is clearly necessary to discover how the Moon was formed, what its structure is, and why. Understanding how the Moon was formed may provide insight as to how the inner planets of our Solar System were formed and some of the history of the Earth's development. Because of this diversity in the Moon's geology there are many opportunities to produce engineering materials and possibly propellants *in situ*, as the resources on the Moon are developed, creating an independent operational base that supports exploration of our Solar System.

The Moon has been also proposed as an astronomical observation site. The Hubble space telescope is a tremendous astronomical asset in understanding the development of the universe and in progressing towards resolution of the many uncertainties concerning star formation, quasars, visible and dark matter, and the early time in the universe after the spatial matter became transparent. However Hubble is a high-maintenance item. Not because of its design or manufacture, but because of the way it must be maintained in Earth orbit. If the US Shuttle is not available to transport both crew and materials to Hubble there is no crewed system that will permit Hubble to be maintained or repaired. If Hubble or its equivalent were located on the surface of the Moon, then accessibility to resupply from Earth and availability of a human repair crew would not require any flight to an orbital location and work in zero-gravity. If there is something that does not fit or is broken the mission to the Hubble orbit is aborted, because there are no spares or repair facilities available nearby. On the surface of the Moon instead, all of the necessary facilities could be available for spare parts, parts repair, or part manufacture. The location would have to be located on the Moon for maximum visibility of the space of interest. A lunar surface telescope could supplemement Hubble and replace it when Hubble is no longer maintained in orbit.

6.5.3 Manufacturing and production site

Given the Moon's wide variations in physical and geological characteristics, the opportunity exists to refine *in situ* critical spacecraft structural materials, that is, aluminum, titanium and iron. With the gradual establishment of an infrastructure, Moon-based repair and maintenance facilities could be a part of the total system that enables the traffic and infrastructure envisioned in Chapters 2 and 5 to become reality. As the view of the Earth from the Moon shows, Figure 6.16 (see the color section), one should keep in mind that the Earth and the Moon are the closest natural Solar System objects locally available, and the infrastructure that permits the expansion of our exploration of the Solar System *needs to be established and maintained using these two initial elements as foundation*.

6.6 BIBLIOGRAPHY

Batenin, V.M., Bityurin, V.A., Ivanov, G.S., Inozemzev, N.N., and Gorozhankin, P.A. (1997) Institute of High Temperatures of Russian Academy of Science Moscow, Russia, 'Electromagnetic Complex Concept for the Horizontal Start and Landing of a Reusable Air-Space Aircraft', IAC Paper IAF-97-V.5.10, 48th International Astronautical Congress, Turin, Italy, October 6–10, 1997.

Bayón-Perez, S. (2002) 'Design, Transportation, and Operation of a Food Supply Unit for the First Manned Mission to Mars', Master of Science thesis, Saint Louis University Graduate School, Saint Louis University, St. Louis, MO.

Berman, B. (2003) 'The Worlds Out of Balance', *Discovery Magazine*, Vol. 24, No. 12, p. 38.

Brown, C.D. (1998) *Spacecraft Mission Design*, second edition, AIAA Educational Series, J.S. Przemieniecki series editor-in-chief, American Institute of Aeronautics and Astronautics, Reston, VA.

Bussey, D.B.J., Fristrad, K.E., Schenk, P.M., Robinson, M.S., and Spudis, P.D. (2005) 'Constant Illumination at the Lunar North Pole', *Nature*, Vol. 434, p. 842.

Gubanov, V. (1984) Private communication, European Space Conference, Bonn, Germany.

Loftus, D. (1999) 'Final Report on the MSE Technology Applications, Inc. MAGLIFT Project', MSE-TA Report NASA-28, September 1999.

Myrabo, L.N. (1982) 'A Concept for Light-Powered Flight', AIAA 78-698, AIAA Joint Propulsion Conference, Cleveland, OH, June 1982.

Myrabo, L.N. (1983) 'Advanced Beamed-Energy and Field Propulsion Concepts', BDM Corporation publication BDM/W-83-225-TR, Final report for the California Institute of Technology and Jet Propulsion Laboratory under NASA contract NAS7-1000, Task Order RE-156.

Myrabo, L.N. (2001) 'World Record Flights of Beam-Riding Rocket Lightcraft: Demonstration of "Disruptive" Propulsion Technology' AIAA paper 2001-3798, 37th AIAA Joint Propulsion Conference, Salt Lake City, UT, July 2001.

Myrabo, L.N. et al. (1987) 'Apollo Lightcraft Project', Final report, prepared for NASA/USRA Advanced Design Program, 3rd Annual Summer Conference, Washington, DC, June 1987.

Myrabo, L.N., Messit, D.G., and Mead, F.B. (1998) 'Flight and Ground Tests of a Laser-Boosted Vehicle', AIAA 98-3735, 34th AIAA Joint Propulsion Conference and Exhibit, Cleveland, OH, July 1998.
Post, R.F. (1998) 'Inductrack Demonstration Model', Report UCRL-ID-129664, Lawrence Livermore National Laboratories.
Post, R.F. (2000) 'MAGLEV: A New Approach', *Scientific American*, Vol. 282, No. 1, pp. 64–69.
SAIC (1984) Science Applications International Corporation (SAIC) concept from 1984 report for initial operational Moon base, from the Lunar and Planetary Institute provided by NASA Astrophysics Data System.
Spudis, P.D. (2003) 'The New Moon', *Scientific American*, Vol. 289, No. 6, pp. 86–93.
Stafford, T. (1991) Thomas P. Stafford, Chairman, Synthesis Group, Space Exploration Initiative, 'America on the Threshold', Report to Congress.

Patent literature on MagLev

US4709883, Giuliani et alia.
US5722326, Post.
US5652472, Tozoni.
US5565763, Arrendale et alia.
DE3608499, Schmid.
DE3402755, Theurer.
WO8801245, Newman.

Websites on MagLev

http://www.fra.dot.gov/o/hsgt/fedassist/MagLev.htm
http://www.rtri.or.jp

7

Exploration of our Solar System

7.1 REVIEW OF OUR SOLAR SYSTEM DISTANCES, SPEEDS AND PROPULSION REQUIREMENTS

Distances to places within our Solar System in Chapter 1 (see Figure 7.1) provided a yardstick to measure human ambition. At its speed (about 300,000 km/s), light traveling from the Earth to Pluto would reach it (in the average) in 5.45 hours. The highest speed reached by human handicraft is probably the Cassini-Huygens probe while traveling to Saturn in 2004 at about 40 km/s, or 7,500 times less than the speed of light.

A sense of the times needed to travel within our planetary system using chemical propulsion may be acquired by planning a round trip to the external planets, for instance to Neptune. The average distance, d, of Neptune from Earth is some 30 AU, or 4.5 billion km. Table 7.1 shows that a rocket leaving Earth at its escape speed (about 11.2 km/s), would reach Neptune in a minimum of about 11.7 years, actually longer since Hohmann interplanetary trajectories are ellipses, not straight lines. So a round trip would last more than 23 years. These are extremely impractical times for a manned mission, both because of vehicle mass (to ensure crew sustenance and survival) and cost. It does not take long to conclude that traveling at constant speed in the Solar System becomes feasible only if the speed is higher by at least a factor 10, or if traveling at *constant acceleration*, rather than constant speed. In both cases the spacecraft must be accelerated far more than allowed by chemical propulsion.

It is instructive to see the consequences of shifting to a trajectory strategy, based on constant acceleration. For constant acceleration, a, kept until mid-course, followed by an equal deceleration to Neptune, classical mechanics predicts a one-way time as given in equation (7.1) where S and $S_{1/2}$ are distance and mid-way distance to Neptune, respectively. For $a = 1$ 'g' (the Earth gravitational acceleration or 9.81 m/s^2), the round trip to Neptune would take $15\frac{1}{2}$ days, not 23 years. Such

Object	Mass	Diameter	Distance	Time at c from the Sun	Time at V_{escape}
Sun	332,946	109.0	0.00		
Mercury	0.060	0.38	0.30	2.493 minutes	132.018 days
Venus	0.082	0.95	0.72	5.984 minutes	142.018 days
EARTH	**1.000**	**1.00**	**1.00**	8.311 minutes	0.000 days
Mars	0.110	0.53	1.52	12.633 minutes	215.87 days
Asteroids			2.70	22.440 minutes	1.050 years
Jupiter	317.80	11.20	5.20	43.218 minutes	2.022 years
Saturn	95.17	9.40	9.54	1.321 hours	3.709 years
Uranus	14.60	4.20	19.18	2.657 hours	7.458 years
Neptune	17.25	4.00	30.05	4.162 hours	11.684 years
Pluto	0.100	0.50	39.40	5.458 hours	15.320 years
Kuiper Belt	40.0		30 to 50	5.541 hours	15.553 years
Heliopause			100.00	254.0 days	38.883 years

Note: 1 AU = 1.496×10^8 km (AU) average.

Figure 7.1. Features and average distances of objects from the Sun (1 AU = 1.496×10^8 km is the average distance of Earth from the Sun).

acceleration would be very convenient, freeing a crew from all undesirable effects of micro-gravity ('weightlessness'). Lowering a to 1/10 'g', the round trip would last a factor $\sqrt{10}$ longer, or about 46 days.

$$t = \sqrt{\frac{2S_{1/2}}{+a}} + \sqrt{\frac{2(S_{1/2} - S)}{-a}} = 2\sqrt{\frac{S}{a}} \tag{7.1}$$

These sound like awfully short travel times, but actually depend on whether or not the space ship can keep accelerating at the acceleration a chosen for the trip. Fast travel depends on 'affordable' acceleration, that is, on how long the propulsion system can supply the thrust capable of maintaining it, since acceleration $a =$ thrust F/vehicle mass M. The higher the acceleration, the shorter the trip time, but also the higher the propellant rate of consumption and the vehicle initial mass M, thereby lowering a: in fact, M must include all propellants needed by the propulsion system. The quantitative analysis of this problem is determined by the rocket equation and Newtonian mechanics. The governing equations follow:

$$\begin{aligned}
t_{1/2} &= \sqrt{\frac{2S_{1/2}}{a}} \\
V_{1/2} &= a\,t_{1/2} = a\sqrt{\frac{2S_{1/2}}{a}} \\
\mathrm{WR}_{1/2} &= \exp\left(\frac{V_{1/2} - V_{\text{orbit}}}{g\,I_{\text{sp}}}\right) \\
W_{\text{gross}} &= \mathrm{OWE}(\mathrm{WR}_{1/2})_{\text{from earth}} \qquad \text{fly-by} \\
W_{\text{gross}} &= (\mathrm{OWE}(\mathrm{WR}_{1/2})_{\text{to planet}})(\mathrm{WR}_{1/2})_{\text{from earth}} \qquad \text{rendezvous}
\end{aligned} \tag{7.2}$$

Table 7.1. Neptune mission as a function of acceleration, ***a***.

acceleration	1/100	1/10,000	boost–coast	'*g*'
distance	4.05E + 09	4.05E + 09	4.05E + 09	miles
1/2 distance	2.02E + 09	2.02E + 09	2.02E + 09	miles
time	0.258	2.582	11.284	years
time	94.31	943.14	4,121	days
$V_{1/2}$	799.13	79.91	18.29	km/sec
$V_{1/2}/c$	0.43%	0.043%	0.010%	% light speed
$\mathrm{WR}_{1/2}$	7.52E + 77	1.25E + 07	10.28	

The $\mathrm{WR}_{1/2}$ is the weight ratio either from the Earth to the halfway point or from the halfway point to the orbit of the target planet. Table 7.1 gives the parameters for two constant accelerations and for a boost and coast mission for an I_{sp} of 459 seconds (4,500 m/s). If the mission is a fly-by then only the weight ratio for departing Earth applies. If the mission is a rendezvous mission then the product or the two weight ratios apply. Remember for the rendezvous mission the orbital velocity is for the target planet. For a rendezvous mission with Neptune the boost–coast the total weight ratio is about 15.5.

So a 5,000 kg spacecraft that flies by the target planet (in this case Neptune) would have to have a mass departing Earth orbit of 3.76×10^{78}, 6.25×10^{7} and 51.4 tons, respectively. For comparison, the Saturn V rocket weighed only 2,700 tons. A rendezvous mission with Neptune would require a departing mass of 77.5 tons. A return to Earth for the boost–coast mission would have an Earth-departing mass of 797 tons and require about 24 years time. Traveling within our Solar System with a low I_{sp} and constant acceleration is very expensive! That is why deep-space spacecraft are low-mass vehicles and fly using short bursts of acceleration trajectories. To attempt a Neptune mission with chemical propellants in trans-Mars trip times is impossible in terms of the requirements. Hence the search at the dawn of the rocket age for new propellants, capable of higher I_{sp}.

At that time, in the effort to improve I_{sp}, hundreds of propellant pairs were tested, starting from the liquid oxygen/alcohol the Germans used on the V-2, with $I_{sp} = 290$ sec. In fact, we know now that in chemical propulsion I_{sp} is limited by chemistry, that search pretty much ending with the liquid H_2/O_2 combination capable of $I_{sp} = 450$ sec. Slightly higher I_{sp} are possible, but using propellants that are either too toxic (e.g. fluorine), or too toxic and too expensive (e.g. beryllium). Increasing the I_{sp} decreases the trip time, see Figure 7.2.

A second, no less crucial, consideration is power. In chemical propulsion, propellant consumption is inextricably linked to power, because power is produced by burning propellants. For instance, combustion of H_2 and O_2 produces 13.5 MJ per kg of propellants burned. The 10^6 N thrust assumed in the Neptune trip example corresponds to burning 222 kg/s in the rocket engine: so, the power output is about 3 GW, or that of five large electric utility power generators. Substantial power is no problem in chemical propulsion, but can be obtained only by means of an equally substantial mass consumption.

	years	years	years
Jupiter	2.69	1.70	0.793
Saturn	4.92	3.12	1.45
Uranus	8.14	5.16	2.40
Neptune	11.15	7.07	3.29
Kuiper Belt	11.13	7.06	3.29
Pluto	**13.75**	**8.72**	**4.06**
Kuiper Belt	16.29	10.34	4.81
Heliopause	27.86	17.67	8.22
I_{sp} (sec)	459	1,100	4,590
WR	10.70	7.23	3.38

Figure 7.2. Increased I_{sp} reduces transit time and weight ratio.

Designing high-power chemical rockets is quite possible (blurbs for the Space Shuttle main engine boast about the tens of millions HP developed at takeoff); but as their I_{sp} is limited to less than about 450 sec, chemical power to accelerate a ship for sustained periods of times means huge propellant consumption. Hundreds of tons of propellants are burned in the few minutes of operation of the liquid rocket engines of a space launcher such as the Shuttle or Ariane 5.

In a nutshell, chemical propulsion is capable of large thrust but for very short times, because its propellants consumption is too high. When in 1969 Saturn V took off for its Moon mission, the thrust of its first stage was some 3,400,000 lb, or 15.4 MN, but lasted only for about 10 minutes. Most of the energy expended was not used to carry the Lunar Module and crew re-entry vehicle to orbit: it was spent in lifting the very propellants to accelerate to orbit, in other words, to lift and accelerate itself. A 130 HP motorcar traveling at 180 km/h (110 mph) has a specific impulse about 21,500 sec, more than 40 times better: any gasoline-powered car gets better 'mileage' than any chemical rocket engine.

It is for these reasons that, until recently, interplanetary missions have inevitably utilized short bursts of thrust to accelerate space probes: short accelerations limit total propellant mass. In practice, since escape speed from Earth is 11.2 km/s, maximum probe speed is in that neighborhood. Higher speeds are feasible by means of 'gravitational assists', in trajectories purposely designed to swing by planets and extract kinetic energy from them. For instance, the Cassini-Huygens speed approaching its Saturn destination was about 40 km/s before slowing down to orbit. Planet swing-by is cheap, but takes a long time: trajectories may last even 10 years. Thus, so far, interplanetary missions are accomplished by accelerating probes for short times (a few minutes), followed by coasting at constant speed, not constant acceleration. This strategy saves mass, but stretches mission time to several years.

So, a round-trip mission's duration will be almost the professional life of a mission ground team, and if the ship is manned, most of the professional life of a crew. Besides, at constant speed and in absence of specific remedy, a crew would live under micro-gravity condition, with irreversible health consequences, among others, for their bone structure and enzymatic functions. Moving to the edge of our planetary system, to the so called Oort cloud believed to be the birthplace of comets (see Chapter 8) would mean reaching to 50,000 AU. At constant speed, trip times to the Oort cloud would be of order 17,000 years.

The conclusion is that the 'conquest of space' is meaningless without ways of shortening space travel. Hard as it is to move in the Earth's immediate vicinity, interplanetary travel is much harder, beyond anything that can be reasonably expected of chemical propulsion. No advances can be forecast in chemical propulsion because the energy it can release per unit propellant mass consumed is limited by chemistry to not much more than 10 MJ/kg. Reasonably short interplanetary missions need reasonable initial, or even constant, acceleration. This means thrust maintained for days or weeks, not minutes. This also means large power and propellant mass consumed.

So, interplanetary travel awaits a dramatic change of propulsion technology: that is, power and technology capable of raising I_{sp} by a factor 2 at the very least. Such change will automatically raise the power requirement: higher Isp means higher exhaust velocity, higher exhaust kinetic energy and its flux, i.e., higher power. In fact, power scales with velocity cubed. Doubling the I_{sp} at fixed thrust halves propellants consumption, but also raises the power needed to accelerate and exhaust the same propellants by a factor 8. So, higher I_{sp} must have power sources adequate to maintain that I_{sp} and the thrust needed.

7.2 ALTERNATIVE ENERGY SOURCES: NUCLEAR ENERGY

Making interplanetary travel time practicable for manned (and unmanned) missions means new propulsion systems and new ways of generating power must be explored. To make space-ships reasonably small, that is, to save propellant mass substantially, I_{sp} must at least double.

In any conventional (chemical) rocket I_{sp} depends the temperature (T) of burnt gases in the rocket chamber and on their mean molecular weight (MW) as given in equation (7.3).

$$I_{sp} \sim \sqrt{\frac{T}{\mathrm{MW}}} \tag{7.3}$$

The large I_{sp} of liquid H_2/O_2 rockets is the result of the low molecular weight (about 9 or 10) of combustion gas, rich not only in H_2O (MW = 18), but also in excess H_2 (MW = 2). Chamber temperatures are lowered by adding extra H_2, but the ratio T/MW turns out higher.

So, increasing I_{sp} means either raising T or lowering MW, or both. The first choice is constrained by structural material limits: the mechanical strength of almost all materials diminishes with increasing temperature. That is why liquid rocket thrust chamber walls are cooled to a temperature less than, say, 1,000 K.

If feasible, higher gas temperatures would be welcome, because they raise I_{sp}. However, the adiabatic flame temperatures of the best liquid propellants combinations do not exceed 3,500 K (and are accompanied by severe cooling problems). Some propellant combinations may exceed 3,500 K a little, but in that case at least one of the propellants is solid. When one of the propellants is solid the rocket is called a 'hybrid rocket'. Hybrid rockets have become of great interest after the sub-orbital flights of Burt Rutan's 'SpaceShipOne', but also have a thrust/volume smaller than all-liquid rockets, and the gain in I_{sp} over that of H_2/O_2 is marginal.

So, in thinking about raising I_{sp}, the obvious question one would ask is how to reach higher temperatures. Now, temperature really means internal energy. With chemical propellants the internal energy is that of chemical bonds. Chemical energy is nothing else than the potential energy of the fundamental *electro-weak force*, that is, of the Coulomb forces acting among electron shells (−) and nuclei of atoms and molecules (+). The number of fundamental forces in nature is just three, gravitational, electro-weak (including Coulomb) and nuclear, also called the 'strong' force. Thus the quest for higher temperatures producing higher I_{sp} should really become a quest for *energy* alternatives, and there is not much choice here: discarding gravity, the only option is drawing on the nuclear energy binding together nucleons (neutrons and protons) inside the atom nucleus.

This means fission, fusion (including antimatter annihilation, an extreme form of fusion), or relaxation of metastable nuclei. By analogy with combustion, the material fissioned, fused or relaxed is still called a nuclear 'fuel', or simply the fuel.

Following this approach means that the energy source, or energy conversion stage, is separate from the propulsion stage and its propellant. In chemical propulsion instead the energy source is the heat release by chemical reactions between the propellants themselves. The nuclear energy source may be a nuclear reactor, or a fusion reactor. Then the heat released from the source must be transferred to a fluid/propellant. This fluid may be exhausted as in a conventional rocket, or used in a thermodynamic cycle to produce electric power. In any event, how to transfer energy from nuclear source to propellants/fluid is a crucial item, shaping different concepts differently.

This chapter will focus on propulsion systems using fission, leaving fusion to be discussed in Chapter 8, for missions outside our Solar System. In fission the nuclei of atoms of properly chosen materials (fuels such as ^{235}U, ^{239}Pu and others) are broken apart by neutrons. The neutrons needed are produced by these materials, but their fissioning effect becomes efficient only when a 'critical' mass of material is assembled. Using the electronvolt (eV) as energy unit, fissioning ^{235}U yields 160 MeV per fission fragment, to be compared to a fraction of an electronvolt in combustion. In more common units, fission heat release per unit propellant mass, J, is vastly larger that of H_2/O_2 propellants in a rocket (about 1.35×10^7 J/kg). In fact, as any energy release process, nuclear reactions convert fuel mass into energy according to $E = mc^2$; the energy per unit mass, J, available in fission is of the order of 8.2×10^{13} using ^{235}U, almost 10^7 times larger than in combustion, as illustrated graphically in Figure 7.3. Note that in this figure energies are plotted on a *logarithmic* scale!

The theoretical foundations of nuclear reactors can be found in [Glasstone,

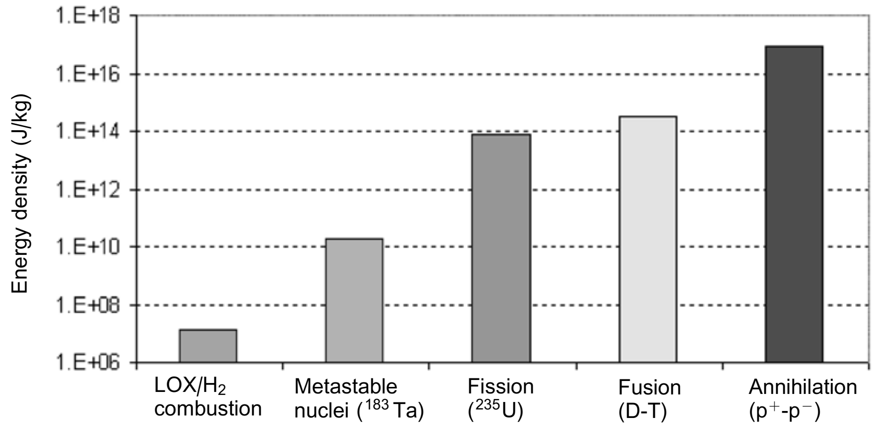

Figure 7.3. Comparison between chemical and nuclear sources.

1955]. Fission physics for propulsion applications can be found in [Hill and Peterson, 1970; Bussard and DeLauer, 1958; Lawrence et al., 1995]; recent basic fission engineering is in [Turner, 2005] and details will not be discussed here. Still, it is important to emphasize that release of nuclear energy in a reactor is unlike that by an atomic bomb. No nuclear power generator can explode like an atomic bomb, since the critical mass (a few kilograms of U in a sufficiently dense volume) is physically impossible to achieve. For instance, in solid-core reactors, the most common type, the nuclear fuel is alloyed for structural and neutronics reasons, and partitioned into individual modules, called fuel 'bars' or 'rods'. Figure 7.4 shows a classic fuel bar design from one of the NERVA reactors mentioned in section 7.5; there is literally no way the fuel can reach critical mass when distributed among bars and alloyed with a moderator material.

Because of the Chernobyl 'accident' in 1986 there persists a certain amount of confusion among the general public between a *nuclear* explosion (that of an atomic bomb), and a *thermal* explosion caused by reactor overheating and/or meltdown. What happened in Chernobyl was due to overheating following the deliberate (and foolhardy) shut-down of the cooling system to check the spin down time of the reactor turbine. Overheating caused a fire of the graphite moderator, not an atomic explosion [Del Rossi and Bruno, 2004].

So-called nuclear thermal rockets (NTR), one of the many propulsion systems based on fission, are to all practical effects miniature nuclear power stations, where solid ^{235}U-enriched fuel fissions, releasing heat to a coolant fluid playing also the role of propellant. The heat release occurs inside the structure of the rod; so, maximum temperature is limited by what the rod can tolerate without cracking, breaking or melting. Solid temperatures higher than 3,000–3,500 K cannot be realistically foreseen with this strategy; in fact, they are remarkably very close to (or lower than) those of combustion gases in chemical rockets.

The third nuclear energy source mentioned is associated with so called 'metastable' nuclei, also called nuclear isomers. These are materials in which the atomic

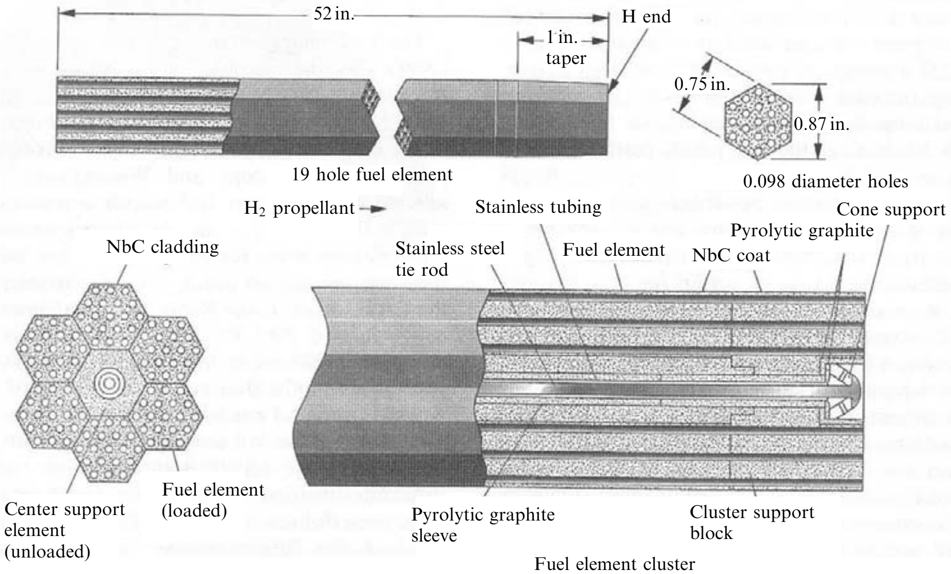

Figure 7.4. Structure and size of a NERVA-type fuel bar [Gunn, 2001].

nucleus is 'strained', that is, neutrons and protons are still bound by the nuclear force but their spatial structure, or arrangement, is not in its minimum energy state (for a general discussion of the nucleus shell structure and its consequences on nucleon energy see [Mukhin, 1987, section 2.3.2]; the theory of deformed nuclei can be found in [Myers and Swiatecki, 1966]). Such nuclei can 'snap', like a stretched rubber band, or a plastic bottle slightly crumpled, and in doing so they reach their stable configuration. During this relaxation their excess energy will be released. This is a very interesting nuclear process, since it does not fission nuclei, but simply rearranges their structure; accordingly, the energy release is intermediate between fission and chemical reactions, and neutrons are not emitted. So, radiation effects are limited to less dangerous high energy photons (mostly X- and gamma-rays). Radiation shielding is still necessary with this strategy, but is easier to deal with than in conventional fission.

Comparing energies, metastable nuclei (e.g., ^{178m}Hf, or ^{180m}Ta) have energies of order 2.4 MeV for hafnium, and about 75 keV for tantalum. Per unit mass these energies are 100–10,000 times lower than in fission, but 1,000 times larger than possible in combustion: a cubic centimeter of pure ^{180m}Ta holds 300 MJ, or 10,000 times the energy released by a cubic centimeter of gasoline when burnt with air [Walker and Dracoulis, 1999]. Of course, such nuclear isomers are rare, in the case of tantalum about 100 ppm compared to the most common isotope of tantalum, and are quite stable.

The main issues in metastable nuclei are their natural scarcity, and thus the technology and cost of separating them from their stable brothers, their geographic provenience and geopolitical issues, and especially the need for ways of releasing their energy in a controlled way. Progress about this last issue seems at hand [Collins, 2005]. All these problems notwithstanding, this nuclear energy source is the object of much interest; applications, such as high-altitude, long-endurance (HALE) airplanes, have been openly discussed [Hamilton, 2002]. However, applications are still speculative, and must wait until many fundamental issues have been sorted out and resolved in an engineering sense. Substantial theoretical and experimental work must be carried on before this source can become just as practicable as fission, so it will not be further discussed in this chapter.

7.3 LIMITS OF CHEMICAL PROPULSION AND ALTERNATIVES

All considerations made in sections 7.1 and 7.2 should convince that chemical propulsion is inadequate to explore interplanetary space and perform planetary missions within reasonable times and budgets. The main reason is low I_{sp}, at most of order 450 sec. The Tsiolkowski equation predicts most of the mass of propellants will be spent accelerating the propellants themselves, and that the payload will be a small fraction of the initial mass, of order 1–3% for ΔV of order 7–8 km/s. The Tsiolkowski relationship is:

$$\Delta V = g\, I_{sp} \ln\left(\frac{M_{\mathrm{initial}}}{M_{\mathrm{final}}}\right) \qquad \text{or:} \qquad \frac{M_{\mathrm{initial}}}{M_{\mathrm{final}}} = \exp\left(\frac{\Delta V}{g\, I_{sp}}\right) \tag{7.4}$$

where M is the initial mass of the spacecraft. The exponential dependence means dramatic reduction in mass ratio, even simply doubling the I_{sp}. Therefore, any advance in propulsion concepts to explore the Solar System must satisfy *two* separate conditions:

(1) Propellant consumption must be 'low', that is, I_{sp} must be as high as possible.
(2) Thrust must be 'high' to ensure acceleration and ΔV needed by the mission.

Meeting these two conditions poses a severe power requirement, since power $P \sim (V_e)^3 \sim (I_{sp})^3$. In fact, if $I_{sp}(V_e)$ could be doubled for the same thrust F, the propellant consumption $\dot{m}$ (in kg/s) could be halved, because

$$\dot{m} V_e = F = \text{Thrust} = \text{constant} \tag{7.5}$$

but the power demand would increase eight times. So, increasing propulsion efficiency (that is, I_{sp}) means reducing the *mass* flowrate of propellants, *not the power* required to accelerate them. The power will inexorably increase.

Remember the second limitation of chemical propulsion is 'slow' interplanetary travel. In the present context, what can be defined 'fast' is: 1–3 years at most for unmanned probes, and several months to a year for manned vehicles. This means that any advanced propulsion system must *economically* enable ΔV much larger than 10 or 12 km/s, in fact many tens of km/s. In section 7.1 we have seen that to achieve these speeds a propulsion system must be capable of sustained acceleration for days or even weeks, with a commensurate power requirement.

Now, nuclear power converts fuel mass into energy according to $E = mc^2$; the J available in fission is of order 8.2×10^{13} J/kg using ^{235}U, almost 10 million times larger than in combustion. This factor alone does justify propulsion based on nuclear reactions. However, how to exploit such J is one of the key questions. For instance, section 7.2 pointed out that typical nuclear reactors cannot operate at temperatures much higher than, say, 2,500 K. So, at a first glance, a clear advantage of replacing H_2/O_2 combustion, characterized by similar temperatures, with nuclear heating, as done in so-called nuclear thermal rockets (NTR), is not evident. However, in NTR the propellant can be pure hydrogen, and its molecular weight, 2, is much lower than the average 9 or 10 of the burnt gas produced by an H_2/O_2 rocket. At similar temperature, an NTR ejecting pure hydrogen will have I_{sp} higher by the square root of the ratio (9 to10)/2, i.e., by a factor of about 2.2. In fact, the best I_{sp} of LRE is about 450 sec; the I_{sp} of NTR tested in the past was of order 900 sec. Furthermore, above 2,500 K a certain fraction of hydrogen begins to dissociate into H atoms (MW = 1), so that I_{sp} grows a little more, perhaps near 950 sec.

I_{sp} in this range is very appealing for interplanetary travel, since the mass ratio following acceleration to a specified velocity is inversely proportional to I_{sp} according to the Tsiolkowski relationship (7.4) already seen:

$$\Delta V = g\, I_{sp} \ln\left(\frac{M_{\text{initial}}}{M_{\text{final}}}\right) \qquad \text{or:} \qquad \frac{M_{\text{initial}}}{M_{\text{final}}} = \exp\left(\frac{\Delta V}{g\, I_{sp}}\right) \tag{7.6}$$

From $I_{sp} = 450$ sec of a chemical rocket to 1,000 sec of a nuclear thermal rocket means the total mass of propellants needed to inject into LEO a given payload may be reduced by a factor of 2.5. This is as if the gross weight of the US Shuttle at lift-off (about 2,000 tons) was reduced to 800 tons.

7.3.1 I_{sp} and energy sources

The fundamental limitation of chemical propulsion is 'low' I_{sp}. One might ask, what is the explanation for this limitation. Aside from its units, for an ideal (complete, isentropic one-dimensional) expansion in a nozzle, I_{sp} coincides with the exhaust velocity, V_e. This velocity is limited because it determines the kinetic energy of the flow, and this energy cannot be higher than that molecules reach inside the thrust chamber because of chemical heat release. That is, in the chamber the heat released forms molecules of average mass m, possessing high translational, rotational and vibrational energy (call all of them internal energy E), and very little organized flow velocity. When the hot gas expands in the nozzle, molecular collisions gradually force all molecules to acquire the same *orderly* flow velocity at the expense of internal (disordered) energy. At the nozzle exit, in the ideal case this velocity is $V_e = (2\,E/m)^{1/2}$ if we neglect relativistic effects. The ratio E/m is the energy density, J, and, try as we might, even with H_2/O_2, J cannot reach above 10^7 J/kg. Ultimately, the limitation on V and I_{sp} is due to the potential of the *electro-weak force*, because it is this force that shapes chemical bonds.

The next question is then what can be expected from choosing as energy source the only alternative, that based on the *nuclear 'strong' force*.

In all three nuclear processes of section 7.2 energy is released by converting fuel mass into energy. When the ^{235}U nucleus fissions (splits) after colliding with neutrons, the total mass of its fission fragments is slightly less than its initial mass. A certain percentage, α, of the mass disappears, converted into kinetic energy and other forms of energy (call them all KE) of the fission fragments, according to $KE = mc^2$. Since c, the speed of light, is 3×10^8 m/sec, the energy released is 'large' on a human scale. Relativistically speaking, the mass lost corresponds to a decrease of the potential energy of the nuclear force binding neutrons and protons. In fact, while in Newtonian physics mass and energy are separate quantities, each separately conserved in any transformation, in relativistic physics it is the sum

$$mc^2 + \mathrm{KE} \tag{7.7}$$

that is conserved. Note that m is the *relativistic* mass, i.e., the *rest* mass, m_o, divided by $\sqrt{1-(V/c)^2}$. As usual, c is the speed of light, about 3×10^8 m/s.

Splitting the atom (fissioning) transforms potential energy of the nuclear force in KE of the fragments, their J of order 10^{13} J/kg already mentioned. The potential energy in a mass m of fuel is the fraction $\alpha\, mc^2$:

$$\text{Fuel potential energy} = \alpha\, m_{\text{fuel}}\, c^2 \tag{7.8}$$

The effect of fission is to convert the potential energy of the nuclear force (binding nucleons together) into kinetic energy of fragments (e.g., nuclides, neutrons, photons, ...). The KE of fragments, through collisions, converts into internal energy of a fluid or propellant, present as a mass M_p, and finally becomes orderly motion of particles ejected at speed V_e, or V for short. To calculate the ideal velocity V reached by a mass M_p of propellant after αm mass of fuel fissions, a relativistic energy balance must be written. Approximating (for simplicity) KE with only $0.5mV^2$, that is, neglecting neutrino and photon energies, the energy balance becomes [Bruno, 2005]

$$m_o c^2 = (1-\alpha)\, m_o c^2 + \frac{1}{2}\frac{m_o(1-\alpha)V^2}{\sqrt{1-\dfrac{V^2}{c^2}}} + \frac{1}{2}\frac{M_{po}V^2}{\sqrt{1-\dfrac{V^2}{c^2}}} \tag{7.9}$$

where m_o and M_{po} are the fuel and the propellant mass *at rest*. Rewriting this equation, a preliminary result is that

$$\frac{4\alpha^2}{(1-\alpha)\left(1+\dfrac{M_{po}}{m_o(1-\alpha)}\right)^2} = \frac{\left(\dfrac{V^4}{c}\right)}{1-\left(\dfrac{V^2}{c}\right)} \tag{7.10}$$

showing that in the limit $\alpha \to 1$ (that is, if all fuel is converted into energy, as in matter–antimatter annihilation) and if no inert mass M_p is present, the velocity V tends to the speed of light c. If inert mass M_p is added, the limit velocity is less than c, as shown by the complete solution

$$\frac{V^2}{c^2} = \frac{2}{\sqrt{1 + \dfrac{2}{A}} + 1} \qquad \text{with} \qquad A \equiv \frac{2\alpha^2}{(1-\alpha)^2 \left(+ \dfrac{M_{po}}{m_o(1-\alpha)} \right)} \tag{7.11}$$

This solution is plotted in Figure 7.5 for three different M_p/m ratios (1,000, 10,000 and 100,000) and also for the special case $M_p = 0$. For clarity, the three curves for nonzero M_p have been plotted after scaling them by 10. Note that V may become comparable to c only for α close to 1. Conventional fission processes occur with much lower mass conversion, of order 10^{-3}: a typical value of α for ^{235}U fission is 9.1×10^{-4}. Adding propellant, that is, adding M_p, the velocity (and I_{sp}) drops rapidly. However, if the reactor must work at reasonable temperature and produce significant thrust, propellant must be added, and one must accept lower I_{sp}, a necessary compromise. The M_p constraint explains why NTR tested in the past never reached $I_{sp} > 900$ sec or so. Fusion may occur at slightly higher α, of order 0.003 or 0.004 (see Chapter 8). Only complete matter–antimatter annihilation proceeds with $\alpha = 1$, and the theoretical limit speed becomes c.

The special case of $M_p = 0$ means that all the energy developed by fission ends as kinetic energy of the fragments: the work point of the engine is on the upper curve and V (or I_{sp}) is maximum for a given α. Conceptually this means fission products themselves are the propellant, ejected 'as they are', with all their kinetic energy, and perfectly collimated. Such ultimate propulsion strategy has been proposed at the Lawrence Livermore National Laboratories to maximize I_{sp}. Thrust is modest in

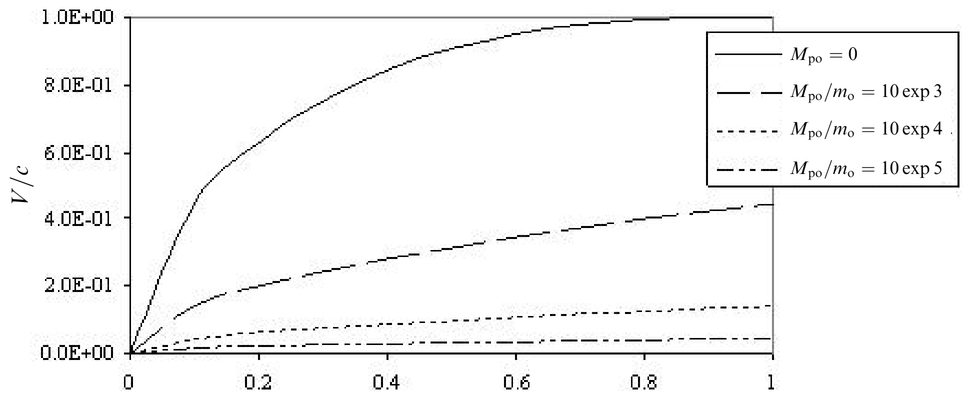

Figure 7.5. Velocity gained by leftover fuel mass in fission as a function of percentage α of mass fissioned. The three lower curves are multiplied by a factor 10 for clarity. M_{po} is the rest mass of (inert) propellant.

this strategy: the mass of fuel fissioning per unit time is naturally low, of order of (1) kg/h for large power reactors; a 1-GW rocket with $I_{sp} = 10^5$ sec would produce thrust of order 1,000 N.

Are there ways to raise I_{sp} above that of fission NTR? The answer is yes, and it comes with a price. The alternative is to convert potential energy into electricity. This strategy involves an extra step, in which fission fragments heat a working fluid (not a propellant to be accelerated). Through a conventional thermodynamic cycle, this fluid may produce mechanical power and then electricity via a electric generator; MHD generators or other solutions are also possible, each with its own efficiency [Bidault et al., 2004]. The electricity produced can feed an electric thruster like the ones of sections 7.15 to 7.19. These thrusters are capable of much higher I_{sp} than any NTR, because gas acceleration is not constrained by materials temperature, but driven by electrostatic or electromagnetic forces. The price of this strategy is the low efficiency of converting thermal into electric energy.

7.3.2 The need for nuclear (high-energy) space propulsion

The two main classes, or strategies, of nuclear propulsion systems consist of either converting fission energy into kinetic energy of a propellant, just as in any chemical rocket, or converting it into electricity powering an electric thruster. Past work in nuclear propulsion focused on the first strategy, because of the need to build large and heavy ICBMs (see the historical perspective in section 7.5), and produced engines with substantial thrust and I_{sp} close to 900 sec. Nowadays, interest in interplanetary scientific missions, such as the Jupiter icy moons and Pluto missions are focusing on high I_{sp} nuclear electric propulsion (NEP), the second strategy. One of the reasons is certainly the I_{sp} in the 3,500–4,000 sec made possible with well-tested ion electric thrusters.

At this point it is possible to draw some conclusions. Chemical propulsion is limited to I_{sp} about 450 sec. Its propellants consumption is too high for any practicable exploration of our Solar System. The only alternative, nuclear propulsion, has an energy density about 10^7 times larger: power demand may be satisfied, even though it grows with ${I_{sp}}^3$.

Exploited in the simplest way as thermal energy, nuclear propulsion can double the I_{sp} of chemical rockets, reaching Isp about 900 sec using reasonable power solid-core reactors, historically the first nuclear propulsion systems ever developed (see section 7.5). Accordingly, thrust can be significant, even in the tens or hundreds of kilonewtons. Thrust possible is closer to the thrust of chemical rockets, except that propellant consumption is exponentially lower.

Alternatively, nuclear power can be converted into electric power. This strategy does carry a penalty, but also increases I_{sp} by a factor 10: this in itself may enable interplanetary missions now unfeasible. The power demand is large at high I_{sp}. However, even the power issue becomes more manageable with a nuclear energy source. At large energy density J, power depends chiefly on how fast a fluid can absorb it. This is an engineering, not a fundamental problem, and was successfully solved in the US and in the Soviet Union for the solid-core NTR developed at that time. The real issue with high-efficiency electric propulsion is not power but thrust: thrust is power divided by I_{sp}, and tends to diminish as fast as I_{sp} is raised: an ion engine with I_{sp} of order 5,000 sec and powered by 100 MW has a thrust of only 20 N or so.

It may turn out that indeed nuclear electric propulsion for fast interplanetary missions must have power reactors in the gigawatt range: but this is not an outlandish requirement. The NTR tested at the time of the US NERVA program in the 1950s and 1960s could sustain power in the 1,000 MW range for more than 1 hour, and reached I_{sp} of order 880 sec. When NERVA was abruptly terminated in the 1970s, its technology was capable of a thrust/power ratio $= 50\,\mathrm{lb_f/MW}$, and I_{sp} close to 1,000 sec. The PHOEBUS reactor produced more than 4 GW for more than 12 minutes [Dewar, 2004]. Its thrust, if a nozzle had been fitted, would have been of order 113 tons. No other energy source can match this performance even now.

In summary, fundamental physics tells that the only non-chemical source of energy for space propulsion is nuclear. Nuclear fission has been tested since the 1950s. Fission can meet the two ideal requirements of lowering propellant consumption while still keeping thrust reasonable, that is, comparable to that of conventional rockets. It is this multiple capability, independence from propellant, large I_{sp} and large power in a compact package, that suggests nuclear propulsion as the only practicable means of reaching the planets of our Solar System; see also [Claybaugh et al., 2004]. Power is no bottleneck using nuclear propulsion. Rather, the debate is about the way of using it efficiently, that is, about specific utilization strategies. These are examined below.

7.4 NUCLEAR PROPULSION: BASIC CHOICES

Keeping in mind power is associated to high thrust at high I_{sp}, the next issue is the question of strategy. How large should I_{sp} be and still produce reasonably high thrust, so that mission time will be also reasonable? Do we really need GW-class reactors? Are there trade-offs between I_{sp} and thrust?

The answer to all these questions is, it depends on mission. At fixed power (e.g. fixed by the size of the nuclear reactor) the question can be rephrased as: What is the best way to exploit this power? In an NTR maximum temperature imposed by structural limits cannot go above 2,500 or perhaps 3,000 K, even looking far into the future. Materials capable of 2,500 K are in the testing stage. Propellant temperature must be even lower and determines I_{sp}, so that not much can be hoped for above $I_{sp} = 1{,}000$ sec. This is more than twice the I_{sp} of current chemical rockets, but it is not enough for enabling some interplanetary missions, for instance those to Neptune or Pluto. For sustained thrust of order 2 weeks, and at $I_{sp} = 1{,}000$ sec too much propellant would be necessary. The ship would be so large and massive to accommodate the propellant that acceleration would be too low. Trip time to Neptune, for instance, would increase far beyond the 4-week round trip imagined in section 7.1.

If nuclear thermal rockets are the baseline nuclear propulsion system, what are potential advances capable of raising I_{sp}? Conceptually at least, to reduce propellant consumption at fixed power, either structural temperature limitations must be bypassed, or thermodynamics must be bypassed.

The first approach leads to the so-called Rubbia engine, in which the traditional direction of the heat transfer process (fission fragments $\rightarrow$ fuel bars $\rightarrow$ propellant) is short-circuited by direct injection of fission fragments inside the propellant. Within the same approach, a different solution is to let the fuel fission in its gaseous state (that is, at much higher temperature than when solid), and heat the propellant radiatively; this is the gas-core nuclear rocket concept.

The second choice assumes the nuclear reactor must only generate electric power, leaving the job of accelerating the propellant to the Coulomb or to the Lorentz force. This means using one of the many types of already-existing electric thrusters.

In some more detail, thermal rocket solutions, whether baseline or advanced, convert the KE of fission fragments directly, or via heat exchange, into KE of propellant particles. Because the KE of fission fragments is $\sim 10^2$ to 10^3 keV ($\sim 10^6$ to 10^7 K!) and if magnetic confinement of fragments is unfeasible, temperatures may be kept reasonably low by 'diluting' the extremely high KE of fission fragments with, or in, a much larger mass of propellant M_p, as explained conceptually in section 7.3.1.

This strategy is best suited to a propulsion system where thrust must be 'high'; it also produces I_{sp} of order $(2\text{–}4) \times 10^3$ sec at most. Solid-core reactors, where temperature must be kept below, say, 2,500 K, such as the ones tested in the US and Soviet Union, can yield I_{sp} of order 800–900 sec only, are capable of thrust comparable to that of chemical rockets, and fall in this class. A conceptual scheme is shown in Figure 7.6 (note the presence of a radiation shield). Acronyms typical of this class of propulsion are nuclear thermal propulsion (i.e., NTP), or nuclear thermal rocket (NTR), since the primary mode of propulsion is based on *thermalization* of fission products, that is fragments collide with propellant molecules and divide among them their high KE until thermal equilibrium is reached. The hot propellant then expands in a conventional nozzle.

In the second choice of strategy the nuclear reactor is viewed only as a power source. This power may be converted into electricity by conventional thermodynamics cycles, such Stirling or Brayton, by direct thermionic or thermo-electric conversion, by magneto-hydro-dynamic conversion, or by more advanced processes. The electric power feeds an *electric thruster*, for instance an ion, or magneto-plasma-dynamic (MPD) thruster. Thrust is typically much lower (1–100 N) than in the first

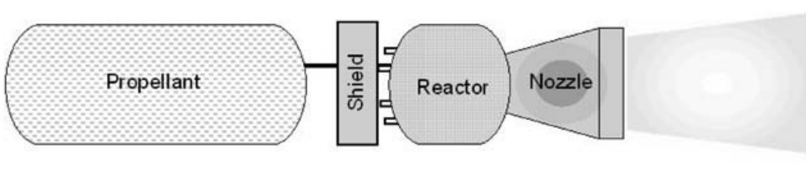

Figure 7.6. Conceptual scheme of a nuclear thermal rocket [Bond, 2002].

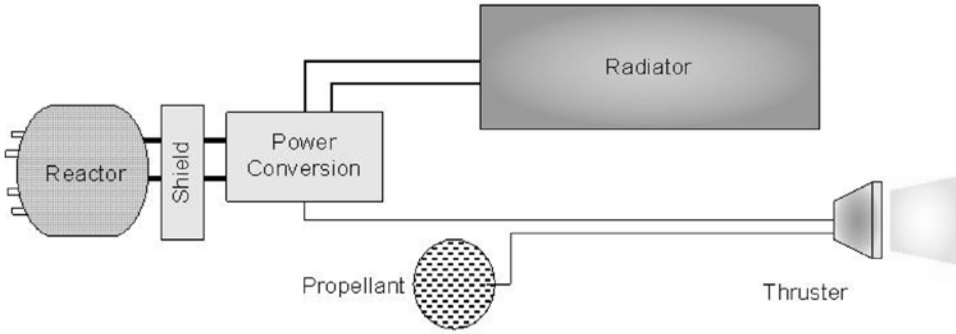

Figure 7.7. Conceptual scheme of a nuclear electric rocket. Note the mandatory radiator [Bond, 2002].

class, but I_{sp} may reach 10^6 sec. Hence, the acronym NEP (nuclear electric propulsion). The general scheme of an electric thruster is shown in Figure 7.7.

The two classes of devices represent in a way the two extreme cases of the trade-off between thrust F and I_{sp}. Because thrust power $P = FV_e$, and $V_e = I_{sp}$, at fixed power the F vs. I_{sp} curve is a hyperbola, where NTR sits on the left, NEP on the right. The specific mission will tell whether it is better to choose an engine with high F and low I_{sp}, or vice versa. In fact, quick escape from the gravitational attraction of planets requires large thrust; fast interplanetary travel, enabled by constant acceleration, needs very low propellant consumption to be feasible, and suggests high I_{sp}. Any interplanetary mission includes both these trajectory segments, so ideally one would like to have a propulsion system capable of both propulsion modes. This is the motivation for the VASIMR rocket described in section 7.22.

There is a third, radical way of exploiting nuclear energy for propulsion: repeated nuclear explosions astern of a spacecraft (pulsed nuclear propulsion is a fitting name suggested by Schmidt et al. [2002]). Hardly conceivable now, this method was proposed and investigated in the 1950s by Freeman Dyson [Dyson, 1979, 2002] and Ted Taylor, a fission bomb physicist. A concise history of this project is given in Flora [2002]; basic propulsion aspects are discussed in Schmidt et al. [2002]. This unusual propulsion technique was suggested by the results of thermo-nuclear bomb testing on Eniwetok, when teams examining the ground in the aftermath of the explosions noticed that the graphite-coated metal spheres hung some 30 ft from ground zero were left practically unscathed. Until then it was assumed that nothing could survive a close nuclear explosion. In fact, later testing and analyses showed ablation of a plate by the intense radiative environment could protect the underlying structure. Suitably sized and reinforced, a so-called 'thrust plate' could indeed receive and survive the force due to shocked matter from the bomb and its radiation. Radiation from the fireball contributes to the force, for instance by ablating the coating deposited on the thrust plate (e.g., a polymer or grease), the momentum of the ablating products working as a rocket jet exhaust. Much of the information concerning this area of ablation and its physics is still classified today, but calculations and tests done with high explosives confirmed in 1959 the concept was viable, particularly so for massive spacecraft, that must include also a shock absorber to protect the crew. In the 1950s the nuclear test ban was not in existence, so Dyson and the physicists working on this project, called Project Orion, envisaged taking off from the ground and accelerating to orbital speeds all by sequential atomic explosions. Orion was eventually designed for a spaceship large enough to do a grand tour of the planets (as far a Saturn) lasting about one year. The mass of the spaceship for such a mission was of the order 10,000 ton. Specific impulse and thrust calculations showed both could be much higher than with chemical propulsion, in particular I_{sp} of the order 10^4 to 10^6 sec were theoretically predicted. Limitation to thrust was also due to the maximum acceleration tolerable by the crew.

As there was no military application in sight, because of potential opposition by the public, and certainly that of the then Secretary of Defence McNamara, Project Orion was cancelled.

A revisited Orion ('MiniMag') had been recently resurrected by replacing atomic bombs with miniature nuclear explosions; among the motivations being that of reducing the mass of the spacecraft that must host this type of propulsion. Ground testing is carried out by substituting high intensity electro-magnetic energy pulses (theta pinch-accelerated plasma jets, described in section 8.10.2 in the context of Dense Plasma Focus devices) for nuclear mini-explosions. One of the actors in this program (not open to the public) is the Andrews Space and Technology company, based in Seattle, Washington. According to its chief scientist, Dr Dana Andrews, I_{sp} measured (in 2000) was greater than 1,000 sec. The thrust impulse should be substantial, unlike that of any NEP thruster, as the instantaneous power is much larger than any nuclear reactor can produce. Lack of information prevents saying more about this recent approach to pulsed nuclear propulsion; it looks suited for powering long interplanetary missions, as it is capable of combining the best of the two classes NP, namely, the large thrust of NTR and the high I_{sp} of NEP.

7.4.1 Shielding

A question asked by all who hear about nuclear propulsion is how crew on a nuclear-propelled spacecraft can safely live with a powerful source of radiation. The Hiroshima cloud with all its horrific effects on people still casts a shadow on anything nuclear.

Radiation from a fission reactor is a catch-all name including, in general, particles with mass and others (photons and neutrinos). Fission fragments, neutrons, electrons (beta-rays) and photons (in the X-ray and gamma bands, energy $O(0.1)$ to $O(1)$ MeV) are typical. From a distance a reactor may be assumed to be a point-source radiating isotropically, so intensity of radiation (e.g., particle fluxes, number of particles emitted per unit area and unit time) will reduce with $1/d^2$, with d being the distance from the reactor. At sufficient distance an actual shield may not be needed to protect crew and equipment of a nuclear-powered spacecraft. However, d might be impracticably large: so, a material shield is

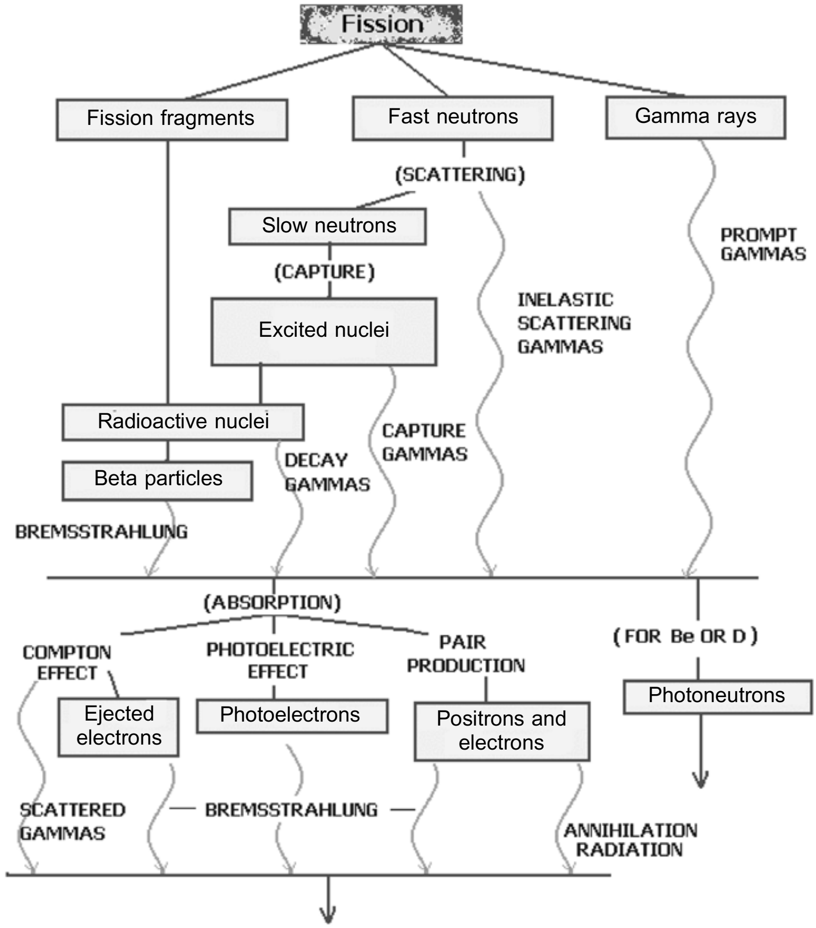

Figure 7.8. Types of radiation emitted from a fission reactor.

always included in designing a nuclear propulsion system and in drawing its mass budget.

Radiation may be roughly divided into primary and secondary. The former is the immediate result of fission, and includes also the fission fragments (FF) themselves. The latter is the effect of radioactive decay of FF, and that of primary radiation interacting with matter or with itself. The conceptual sketch of Figure 7.8 shows how complex radiation is, so this section will only outline its basic features and its effect on its shielding.

What must a well-designed shield do? In a nutshell, a shield should slow down fast neutrons enough to be captured by the shield nuclei, and absorb the energy of all *gamma* photons [Glasstone, 1955]. In fact, gamma-rays and neutrons are the most dangerous constituents of 'radiation', because they penetrate matter farthest. A shield dimensioned for these particles can stop everything else. Nevertheless, it is instructive to see how less energetic particles, such as *alpha* and *beta*, are stopped.

A shield needs not to be thought of as something necessarily separate from the engine: the shield surrounding nuclear reactors for space propulsion may include also the propellant and, in most conceptual designs, the propellant tanks, which are interposed between engine and crew.

The reader is warned about the units (cm, gram, sec) used in this section: these units are those used by nuclear physicists. They invented this field more than half a century ago, and still use them.

Absorption

The simplest model to describe absorption in a continuous medium with uniform properties assumes the change of intensity of radiation, $\mathrm{d}I$, over a distance crossed, $\mathrm{d}x$, linearly proportional to the local intensity, $I(x)$, at the distance x from the source:

$$\mathrm{d}I(x) = \mu I(x)\,\mathrm{d}x \tag{7.12}$$

where μ is the *line* absorption coefficient, its dimensions the inverse of a length. Thus $I(x) = I(0)\exp(-\mu x)$: the flux of particles from a source decreases exponentially along the direction x. At a distance $1/\mu$ from the origin the I has become 'e' times smaller.

Alpha particles ('alphas')

Alphas are He nuclei, He^{++}, a common product of radioactive decay of fission fragments. Because of their charge, alphas are readily absorbed by matter; the energy deposited during absorption ionizes materials, producing ion pairs. Penetration by alphas is quantified by their range, R, the distance from the emitting source to the point where they actually stop. Using the $I(x)$ law, the μ measured in alpha absorption is typically large. The range scales with $1/\rho$, so in STP air is $\sim$2.5–3.0 cm for isotope-emitted alphas with 5 MeV energy. In aluminum the range will decrease by the factor $\rho_{A1}/\rho_{air} \sim 1{,}600$, and in Pb this factor is $\sim$5,000. A thin aluminum sheet stops alphas effectively. Alphas emitted by ^{241}Am (an americium isotope present in most smoke detectors) do not pose any danger, precisely because they are stopped by air at a very short distance from ceiling or wall.

Beta particles ('betas')

Betas are electrons, about 3,880 times lighter than alphas. Although their momentum is lower, they are smaller than alphas and have a lower cross-section (see later). In the energy band 0.1 to 3 MeV their range in standard air varies between 11 cm and 13 m. Scaling with ρ is similar to that of alphas and is a linear function of their maximum energy, E_m. Between 0.8 and 3 MeV an experimentally determined fit for R is

$$R\rho = 0.54\,E_m - 0.15 \quad (\mathrm{g/cm^2}) \tag{7.13}$$

Gamma-rays ('gammas')

Gammas are photons of very short wavelength, 10^{-9} to 10^{-11} cm. They are typically emitted by nuclei excited by a nuclear collision or decaying. Their energies may be of

Energy (MeV)	Water	Aluminum	Iron	Lead
0.5	0.090	0.230	0.63	1.70
1.0	0.060	0.160	0.44	0.77
1.5	0.057	0.140	0.40	0.57
2.0	0.048	0.120	0.33	0.51
3.0	0.038	0.090	0.30	0.47
4.0	0.033	0.082	0.27	0.48
5.0	0.030	0.074	0.24	0.48

Figure 7.9. Gamma-rays absorption coefficient for some materials.

order several MeV. Gammas penetrate matter in depth and shields must stop them completely, as their effect on humans is highly damaging.

The line absorption of gammas follows the $I(x)$ law above, but μ turns out to be a function of $I(x)$. Gammas of 0.1 MeV energy crossing STP air have $\mu = 2 \times 10^{-4}\,\text{cm}^{-1}$ (very small, meaning longer penetration distance), decreasing exponentially to 0.4×10^{-4} at 5 MeV. The reason is again the so-called cross-section, σ, a quantity defined later, that depends on the kinetic energy of the traveling particles. For lead $\mu = 5\,\text{cm}^{-1}$ at 0.25 MeV, again exponentially decreasing to $0.5\,\text{cm}^{-1}$ at 5 MeV. So, the difference between air and lead when absorbing gammas is a factor of 10^4; see Figure 7.9.

In designing shields it was found that for almost all materials the ratio μ/ρ is about constant at a given energy, decreasing only with decreasing energy. For instance, μ/ρ at 0.5 MeV is $0.08\,\text{cm}^2/\text{g}$, while at 5 MeV is down to $0.03\,\text{cm}^2/\text{g}$, this result applying equally to H_2O, Al, Fe and Pb; see Figure 7.10. For this reason it is more convenient to rewrite $I(x)$ as

$$I(x) = I(0)\exp((\mu/\rho)\,\rho x) = I(0)\exp(\rho x/(\rho/\mu)) \tag{7.14}$$

Material	μ (cm^{-1})	ρ (g/cm^3)	μ/ρ (cm^2/g)
Uranium	0.720	18.70	0.038
Tungsten	0.680	19.30	0.035
Lead	0.480	11.30	0.042
Iron	0.270	7.80	0.034
Beryllium oxide	0.076	2.30	0.033
Boron carbide	0.072	2.50	0.029
Beryllium	0.053	1.85	0.029
Graphite	0.052	1.62	0.032
Water	0.033	1.00	0.033
Sodium	0.030	0.93	0.032

Figure 7.10. Absorption coefficient μ and μ/ρ of 4-MeV gamma-rays in some materials.

All this means that the scaling for gammas is still of the type 'density times distance'. The quantity ρ/μ (mass/unit area), can be interpreted as the mass that must 'sit' over a unit area to absorb the flux of gammas. Conversely, the greater μ/ρ, the larger the distance gammas can cross before being absorbed by matter.

Neutrons and cross-section

Neutrons are the hardest particles to stop, because they are not charged: they interact very little with matter. Similarly to alphas and betas, their interaction with nuclei is ruled by their collision 'cross-section', σ, that depends on energy and type of nucleus. The key concept of cross-section can be understood using simplified modeling: the number $\mathrm{d}C$ of neutrons *captured* by a nucleus (thus effectively stopped) per unit time when crossing a distance $\mathrm{d}x$, is assumed to be

$$\mathrm{d}C = I(N\,\mathrm{d}x)\sigma \tag{7.15}$$

with I the neutrons flux (cm^{-2}) and N the volumetric density of nuclei (cm^{-3}) so that $N\,\mathrm{d}x$ is the *area* density of nuclei; σ is a constant, that can be then interpreted as the effective rate of capture per unit flux and unit nuclei surface density. Note that *scattering is not included* in this simple model. From this model the flux $I(x)$ turns out to be

$$I(x) = I(0)\exp(N\sigma x) \tag{7.16}$$

showing the product $N\sigma$ plays the same role of the absorption coefficient of alphas and betas. The difference, as with gamma rays, is that σ is a function of energy and type of nucleus. N depends on the shield material and is easily found. The cross-section is a much more difficult quantity to measure (or predict), and, in the end, it is what controls the shielding property of a material.

Fission neutrons are classified according to their energy. *Fast* neutrons are those with energy above 0.1 MeV and up to 10 MeV, i.e., moving at velocity up to 15% of the speed of light. All neutrons promptly emitted by a fissioning nucleus are fast. Stopping fast neutrons is done only by forcing them to interact with as many nuclei as possible. This means either a shield interposing a large thickness of matter, or interposing very dense matter. In either case, quantity of matter determines neutron-stopping capability.

Slow neutrons (those below 1 MeV) are neutrons that have already collided with nuclei and have been scattered. Scattering may be elastic (momentum and KE are conserved) or inelastic (only momentum is conserved). Elastic scattering is typical of lower-energy neutrons, and is very effective when they collide with light nuclei (e.g., species such as hydrogen or lithium). In inelastic scattering, neutrons colliding with a nucleus lose part of their KE, transferring it to and exciting the nucleus. Inelastic scattering is nucleus-specific. Much work has gone into calculating or measuring σ for different materials, because this knowledge can make or break a new reactor or fuel concept. Neutrons must have sufficient energy, say, >0.1 MeV to excite nuclei (that is why they are called 'fast'). Transfering KE from a neutron to a nucleus occurs similarly to when a liquid droplet hits a larger, high surface tension drop, the surface tension being akin to the strong nuclear force. Nuclei 'vibrate' after the collision, that is the bonds among protons and neutrons stretch and relax. Eventually (in times of order 10^{-3} sec) nuclei reach their stable state by releasing energy (photons), so the ultimate effect of inelastic collisions is to heat the material. This is desirable if the ultimate purpose is to heat, for example, the propellant in NTR; it is quite undesirable if the material is the shield or structural parts of a nuclear engine.

Both types of scattering transform fast neutrons into slow neutrons and, eventually, into 'thermal neutrons', that is neutrons in thermal equilibrium with the shield material. At room temperature a thermal neutron moves at only about 2,200 m/sec.

Shielding options

From this brief discussion it is clear that the basic shield strategy is to stop neutrons and gammas. Neutrons must be captured, while gammas must be absorbed; their energies must be thermalized.

Slowing down fast neutrons is called 'moderating' in reactor physics. Slowing down neutrons is preliminary to final capture (but note that some fuels, such as ^{235}U, use slow neutrons to fission). No matter whether slow or fast, design of the shield depends crucially on σ. In many high-energy collisions the cross-section shrinks with speed, making interaction less likely. At low-energy, instead, there are interactions where the collision cross-section increases by many orders of magnitude, peaking sharply at very specific energies. These are called resonant collisions/cross-sections, and are very important in reactor safety and shielding.

To give an example of questions arising in shield design, an obvious strategy for slowing down neutrons would be to surround the reactor with LH_2, because H is a good moderator. Unfortunately, at high energy the n–H cross-section becomes small: lower energy neutrons are slowed down efficiently by H, but those with high energy are not. To stop the fast neutrons we need higher mass number elements, such as Pb, Ba and others, that slow down neutrons through inelastic collisions. These elements are poor moderators of neutrons, that is, at lower energy the deceleration via elastic collisions is insufficient. The solution to this quandary is to combine *both* families of materials in the shield.

Capture is the final step in stopping neutrons, and the final goal of the shield. Capture occurs when a slow neutron has reached such low energy through scattering that it may end up *inside* a nucleus. The new nucleus might still be stable after capturing a neutron, but more often is unstable and decays, producing a new nucleus and emitting secondary radiation This radiation may last several minutes or hours after the reactor has been shut down, i.e., after the fission neutrons have stopped for good, see later. If a fast neutron has been scattered inelastically, chances are the next few elastic collisions will result in its capture.

Capture comes with a price: excess energy is emitted as gamma-rays. For instance, Cd (cadmium) is a a good neutron capturer, but the gamma photon emitted after capture has energy of order 7.5 MeV! So, much care is needed in picking a neutron 'absorber'. Note that capturing modifies the nature and structure of the nucleus: this means that through secondary radiation new elements may form *inside* the shield. In general, all types of radiation interacting

		Relaxation length (cm)	
Material	Density (g/cm^3)	Fast neutrons	Gamma-rays
Water	1.00	$\sim$10	30
Graphite	1.62	$\sim$9	19
Beryllium	1.85	$\sim$9	18
Beryllium oxide	2.30	$\sim$9	14
Aluminum	2.70	$\sim$10	13
Iron	7.80	$\sim$6	3.7
Lead	11.30	$\sim$9	2.5

Figure 7.11. 5-MeV neutron and gamma-ray relaxation length for some materials.

with matter, whether shield, propellant or the fuel itself, may form new elements inside it; this may greatly change structural, thermal or state properties. By and large, most such changes are undesirable. For instance, in fuels this phenomenon reduces the ability of fuel to fission: in the case of ^{235}U, about 1% of new elements formed inside the fuel matrix may stop fission altogether (this is called appropriately 'fuel poisoning').

In an engineering sense, as far as the stopping ability of materials, gammas and neutrons behave similarly. In fact, it is common to replace the $I(x)$ equations by a compound expression accounting for both absorption *and* scattering:

$$I(x) = B(x)\,I(0)\exp(-x/\lambda) \tag{7.17}$$

where λ is the relaxation length, replacing $1/\mu$, and $B(x)$ is the so-called build-up factor [Glasstone, 1955, p. 595]. This expression tells that gammas and neutrons fluxes crossing a distance λ are reduced by a factor e. After much simplifying, at 'short' distances (short means $x/\lambda < 1$), B is of order 1; when the distance (or: shield thickness) is much larger than λ the factor B is of order x/λ for gammas, and somewhat smaller for fast neutrons. Figure 7.11 shows the relaxation length of several common materials, the starting step toward designing shields.

In summary, the single most important result in shielding is that mass, not type of material or thickness, is the controlling variable. This is the price of fission-based propulsion, controlling the overall thrust/mass ratio of NTR and contributing substantially to that of NEP. However, this conclusion, dating back to the work done during the Manhattan Project, does not rule out that certain fuels or material structures may reduce the weight of shields as we conceive them now. For instance, unconventional fuels with very low critical mass, of the order of grams, may fission in a reactor of size much smaller than conventional reactors, e.g., by a factor $q > 1$. Even though the overall shield *thickness* may remain unaltered, the total shield *mass* would decrease roughly by the factor $(q)^3$. Recently, work at NASA by Dr Raj Kaul and Nasser Barghouty [NASA, 2005b] on a polyethyline-based plastic called RFX-1 has raised expectations that lighter atom structures may be effective shields; references and calculations my be found in NASA [2005c].

Residual radioactivity

After a fission reactor has been switched off, it keeps emitting secondary radiation from decaying nuclei (see Figure 7.8). The intensity decreases with time t, measured typically in days, and is a function of the length of time t_0 the reactor has been operated. A simplified relationship for the residual power emitted and valid for ^{235}U fuel is [Glasstone, 1955, p. 119]

$$P_{\gamma+\beta} = 5.9 \times 10^{-3} P((t - t_0)^{-0.2} - t) \quad \text{(W)} \tag{7.18}$$

where $P_{\gamma+\beta}$ is the residual power of the combined gamma and beta particles, and P is that of the fission reactor. Equation (7.18) shows the decay is not exponential but follows a power law, therefore is somewhat slow. For instance, after 30 days of operation (representative of long interplanetary missions) it takes about 30 days of 'cooling off' to have the residual radiation down to 0.01% of the reactor power. A 1-MW reactor would still release 100 W after 30 days of shut-down.

The *activity*, measured in curies (see the Appendix at the back of the book) is directly proportional to power, so activity follows the same power law, with the constant in front of equation (7.18) replaced by 1.4 (instead of 5.9×10^{-3}).

7.5 NUCLEAR PROPULSION: A HISTORICAL PERSPECTIVE

A by-product of the need for carrying the heavy atomic and thermonuclear bombs of the 1940s, nuclear propulsion was explored in great depth in the US and Soviet Union from the late 1940s throughout the 1950s and until the early 1990s. In the US the rationale for starting its development (by the Atomic Energy Commission (AEC) in 1953, through the program ROVER) was the perceived need for a 75,000 lb_f thrust nuclear thermal rocket to power the third stage of US intercontinental ballistic missiles (ICBM). In fact, in 1956 USAF joined ROVER, but after the Atlas ICBM was flight-tested in 1958, NASA with AEC (that is, its Los Alamos Science Laboratories, LASL) were charged to replace USAF as the ROVER Program leaders. In 1961 this effort branched out (via contracts) to Westinghouse and Aerojet General; the industrial branch of ROVER was called NERVA (Nuclear Engine for Rocket Vehicle Applications).

The original organization chart of NERVA is in [Howe, 1985]. An entertaining history of ROVER/NERVA, focusing mainly on its US politics, is in [Dewar, 2004]; all technical work is in final report form [Westinghouse, 1972]; synopses can be found in [Bohl et al., 1989; Howe, 1985; Gunn, 2001]. An excellent summary of the technological path of ROVER/NERVA is in [Gunn and Ehresman, 2003].

The ultimate purpose of ROVER after 1958 was to develop reliable, safe and efficient nuclear reactors for space applications. The first phase of ROVER progressed at LASL through a series of proof-of-principle Kiwi reactors (Kiwi-A, -B), each with variants testing different fuel bars, geometry and materials. During this first phase, for instance, Kiwi-B4, an advanced design shown schematically in Figure 7.12, and on its test stand at Los Alamos in Figure 7.13, was tested at

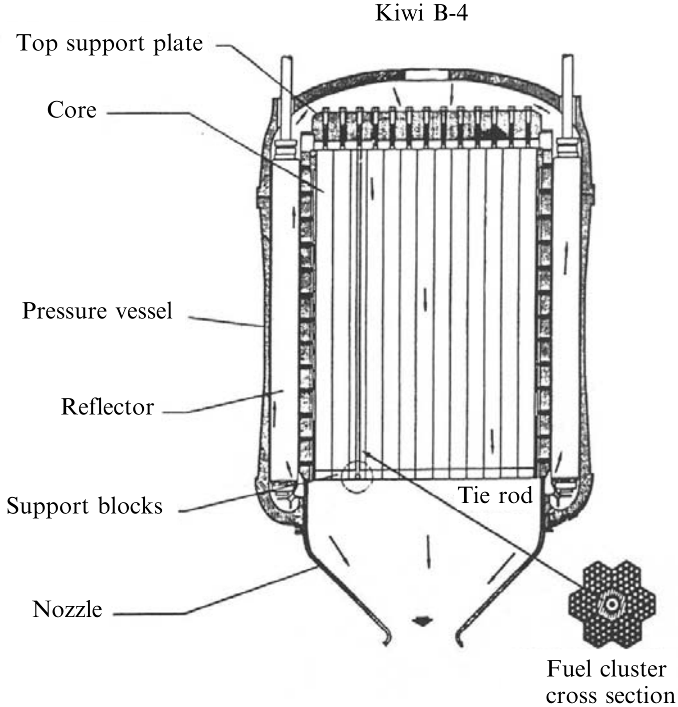

Figure 7.12. Diagram of a NERVA Kiwi nuclear reactor showing a single fuel bar cross-section; see [Gunn, 2001, Fig. 2].

1,030 MW. In 1961 program NERVA I started: its purpose was to engineer Kiwi *reactors* into *rocket* engine prototypes and to test them. NERVA spawned the NRX family of 'engines' (six in all). For instance, NRX-A3 was derived from Kiwi-B4, and tested at 1,165 MW. The general scheme of all NRX rocket engines is that of Figure 7.17.

The power of Kiwi reactors was about 1 GW, to support a projected rocket thrust of 50,000 lb_f. In 1965 Kiwi designs started evolving at LASL into PHOEBUS 1 and 2. Evolution was based on fuel rod technology and reactor diameter, that went from the 35 in of Kiwi B4E to the 55 in of PHOEBUS 2 with a commensurate power increase. On the industry side, these reactors were considered the precursor of the second phase of NERVA (NERVA II). The PHOEBUS family of reactors was the most powerful ever (see Figure 7.14, showing PHOEBUS 2 on its test stand at Los Alamos).

Meanwhile industry was concentrating on rocket engine lifetime. The NRX-A5 and 6 engines developed during the NERVA I phase were tested at more than 1 GW for up to 62 min. At the time all space missions planned assumed the engine needed to work for no more than 1 or 2 hours at most, but also to be capable of multiple restarts. A schematic drawing representative of the NRX family of engines built by

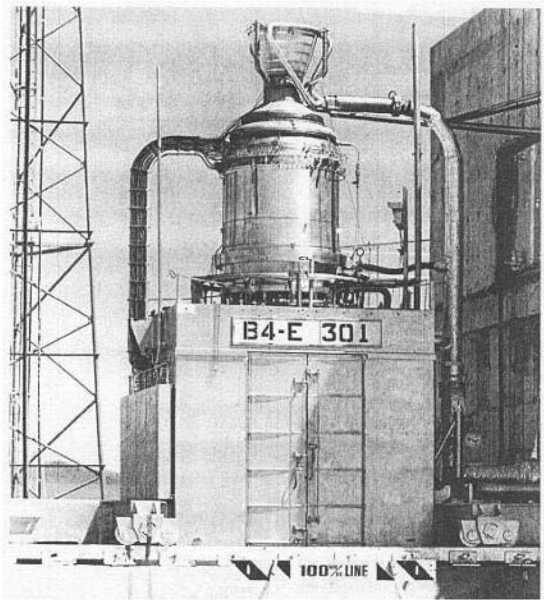

Figure 7.13. The NERVA Kiwi B4-E reactor on its test stand at Los Alamos [Dewar, 2004].

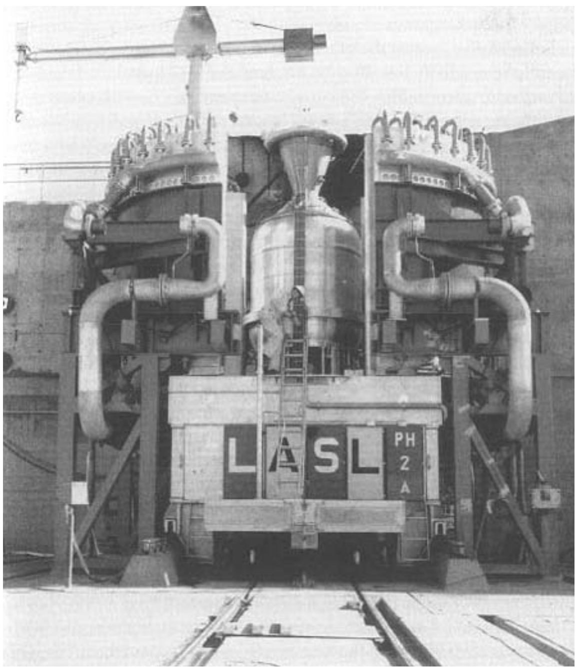

Figure 7.14. The 4-GW PHOEBUS 2 nuclear reactor on its test stand at Los Alamos [Dewar, 2004].

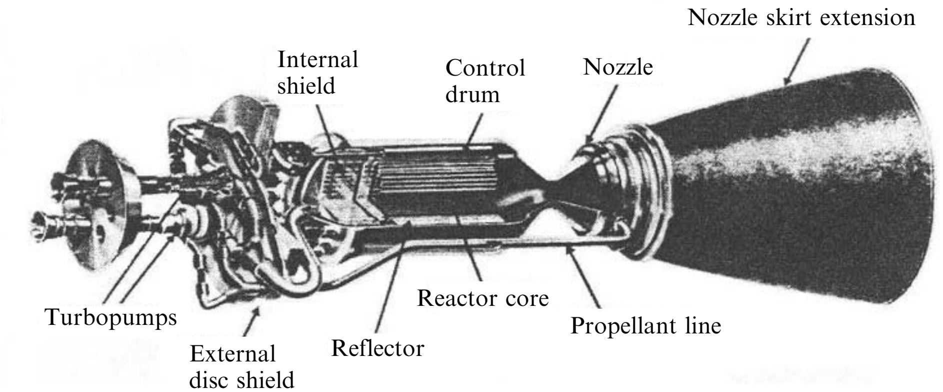

Figure 7.15. Schematic diagram of the Westinghouse NRX nuclear engine [Dewar, 2004].

Westinghouse is shown in Figure 7.15. The NRX family was based on the Kiwi B4E, that had fuel no longer in the form of uranium oxide but in the much more heat- and corrosion-resistant uranium carbide. Tests were in fact performed at a steady 2,200 K reactor temperature.

PHOEBUS progressed at LASL through versions -1A, -1B, and culminated in -2A, that reached 4,082 MW for 12.5 min. Right at that point PHOEBUS funding was suspended, mostly because the engine that could be derived did no longer have a specific mission. However, work was continued on much smaller research reactors (PEEWEE, 500 MW power) that were less time-consuming and less expensive to build, test and operate, focusing on improving fuel rods durability while raising temperature and reliability, with industry following suit in the parallel NERVA program.

At the end of the program in 1972, the NERVA NRX ETS-1, the last nuclear rocket engine developed, was tested at 1,100 MW for a total of 3 hours 48 min. ETS-1 was conceived as the direct precursor of the final NERVA I engine shown in Figure 7.18. The nominal power planned for the final NERVA I rocket was 1,500 MW, with $I_{sp} = 825$ sec. By design, this engine was *capable of 10 restarts* lasting 1 hour each. Its reliability was projected to be 0.997, that is, more than 10 times better than any current LRE. The weight was estimated at 15,000 lb, the thrust 3.34×10^5 N. Power density was ≈ 2 MW/dm^3 (200 times greater than in gasoline engines). In short-duration tests, bursts of power reached 2×10^5 MW and thrust 8.9×10^5 [Lawrence et al., 1995]. Future upgrades were planned assuming I_{sp} up to 900 sec, since progress in high-temperature materials was supposed to enable reactor operation at 2600 K.

Still in 1972, LASL did a definition study of a 16,000 lbf thrust NTR weighing 5,890 lb (including the shield) that could be carried to LEO by the US Shuttle, at that time in the planning stage. This nuclear engine was proposed to power interplanetary missions, but also to drive a ‘space tug’ from LEO to GEO and other orbits [Gunn and Ehresman, 2003]. However, because of cost, declining political support, lack of a

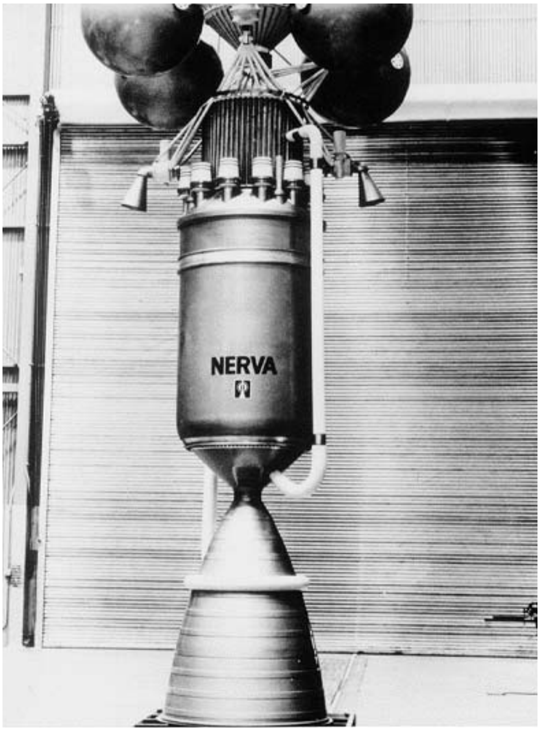

Figure 7.16. Mock-up of the NERVA 1 as it stands in Huntsville, Alabama, Space Park [Dewar, 2004].

clearly defined mission, and other reasons, this program came to an end during the Nixon presidency.

USAF kept working in nuclear propulsion under the SNTP program until 1993, with an annual budget of about $40 million. The Russians also kept working in this field at a moderate level, but the lack of interest by the US contributed to slow down their developmental work too, although they did not stop altogether, as did instead the US, choosing to concentrate on low- and medium-power NTR, below 1 MW.

Not much is left right now of NERVA. A mock-up of its final ETS engine is standing in the NASA Space Park in Huntsville, Alabama (see Figure 7.16). Conceptual work in NTR is still being carried on at NASA-Glenn Research Center by a team led by Stanley K. Borowski, who keeps in touch with the 'old-timers'. This team studies and updates continuously this technology in view of a future manned Mars mission. In its latest architecture the concept has evolved into an NTR working both as a propulsion system and as a modest power generator ($\sim$110 kW). This is the so-called 'bimodal propulsion concept'. The power generator is supposed to be used for instrumentation, support of crew activities, data transmission and refrigeration of the liquid hydrogen propellant during the trans-Mars and trans-Earth (return)

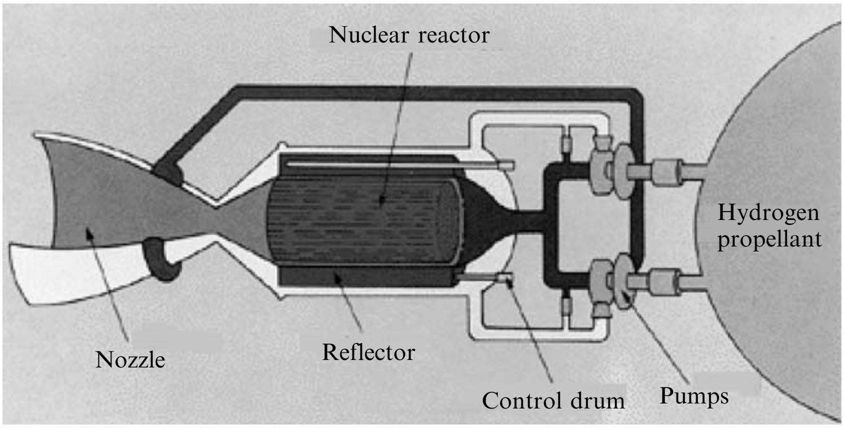

Figure 7.17. Simple scheme of a nuclear thermal rocket fed with liquid hydrogen.

mission stages [Borowski et al., 2000]. In this context, a mission to the asteroid belt has been proposed as a 'dry run' prior to any manned Mars flight. This shows a cautious, albeit perhaps too costly, approach, if Mars is selected as primary mission objective under the 2004 Space Exploration Initiative of President G.W. Bush.

The Russian work, until recently shaded in secrecy, is now better known through the work in Goldin et al. [1991], Rachuk et al. [1996], Ponomarev-Stepnoy et al. [1999], Demyanko et al. [2001], Konyukov et al. [2004], Dewar [2004]. The Russians started their NTR program in the 1950s, with Korolev, Kurchatov, and Keldysh (the three scientists collectively nicknamed 'the three Ks') playing the leading roles in their respective institutes. Their effort culminated in the fast neutron-driven RD 0410 and RD 0411 engines, that were tested both in the 'cool' and 'hot' (i.e., fissioning) mode. This program slowed down for reasons similar to those in the US, and was not resurrected, although Russian sources claim to still retain technology and especially testing capabilities. In fact, the Russian NiiCHM organization has developed very high temperature materials ($>3{,}000$ K) that would be invaluable in building a future high-performance NTR. According to Dewar [2004], nuclear reactors in the 1,000-kW range are still being investigated or tested for interplanetary missions both for thermal rockets and for power generators for NEP, and a conference on nuclear propulsion has taken place in Moscow in May 2005.

To conclude, perhaps the most significant aspect of this survey is that it shows that NP is not a new topic. Work in the 1960s and 1970s at LASL produced NTR reactors capable of 4 GW power. At a conservative $I_{sp} = 800$ sec this figure would ideally produce thrust of order 5×10^6 N (500 tons). Reactors and engines were designed and built with technology and especially design practices that many now would brand obsolete, because it used computers an order of magnitude slower than now available. Performance figures and achievements should give pause to people having second thoughts or misgivings when discussing 25- or 50-kW NEP thrusters for the JIMO missions planned by NASA and described later.

7.6 NUCLEAR PROPULSION: CURRENT SCENARIOS

Renewed attention to nuclear propulsion (NP) for interplanetary missions started in the late 1980s, motivated by interest in a manned Mars mission. It was and still is clear to the aerospace research community that NP can provide the only practical and safe propulsion system for a fast, manned Mars mission, e.g. [Asker, 1991]. Many brief (and cautious) articles have appeared in support of high-energy, short missions compared to multi-year missions relying on planetary gravitational assists such as Galileo or Cassini, e.g. [Borowski et al., 1989; Beale and Lawrence, 1989; Jones, 1992; Asker, 1991; Schmidt, 1999, 2001; Howe, 2001; Lenard, 2001; Hrbud, 2003].

Running against this trend, public acceptance of anything nuclear ebbed away in the 1980s and 1990s. Until recently the issue of nuclear propulsion could not even be discussed at the political and decision-making level: nuclear propulsion and anything nuclear, whether in space or elsewhere, remains to this day a controversial topic [Hagen and Scheffran, 2001]. This state of affairs is slowly changing; a joint JPL-NASA meeting held at JPL in the summer of 2000 [Sackheim et al., 2000] was instrumental in revealing the tide was turning, and so was also the increasing public consciousness of the greenhouse effect caused by power generation based on fossil fuel combustion.

After the joint JPL/NASA-Marshall meeting in May 2000, NASA proposed nuclear power as a technology not just for nuclear thermal rocket, but for a broad gamut of thrusters, ranging from conventional NTR proposals by NASA-Glenn [Borowski et al., 2000] to pulsed fission systems, and even eventually utilizing some form of fusion [Sackheim et al., 2000]. In this framework the original concept of 'nuclear propulsion' is replaced by 'nuclear powered thrusters', these being thermal, like in the original NERVA, electric (ion), or embodying magneto-plasma-dynamics acceleration (MPD), such as VASIMR. [Sackheim et al., 2000] provides some detail of the roadmap NASA and JPL sketched during the past few years and until January 2004.

If this roadmap is indeed going to be implemented in the US (and the publicity given to nuclear propulsion would tend to indicate it will) US investment in nuclear propulsion will grow rapidly. It should be noted that the EU has no prior expertise in this area, with the exception of the Atomic Energy Agency in the UK, and this state of affairs will be a major consideration when and if the EU starts looking at its options. For the time being, aside from some studies, ESA has decided to shelve the issue of NP in favor of investing in chemical propulsion powered Mars probes under its AURORA program [Gilles, 2004]. The US are interested instead in a number of concepts based on NP, among them a reusable nuclear 'space tug' to quickly raise satellites from LEO to GEO. The impact of such a system on the GEO satellite market, of great commercial importance to EU, does not need to be emphasized.

Recently, the Prometheus project of NASA, linked to exploration of Europa, Callisto and Ganymede by means of the Jupiter Icy Moons Orbiter (JIMO), and to the Space Exploration Initiative of President G.W. Bush has also contributed to preparing the public for nuclear power in space. Project Prometheus started in

2002, with the purpose, quoting Mr O'Keefe, NASA Administrator at that time, of battling 'the distance and time dilemma' [David, 2002]. This project was in fact called at that time the Nuclear Systems Initiative. In 2003, after a substantial budget increase to $1 billion, it became Project Prometheus [Bates, 2003].

According to published NASA plans, now on hold or being given different priorities [Berger, 2005a, b] Prometheus was to culminate in a 'New Frontier'-class mission to orbit the Jovian satellite Europa, the JIMO mission for short, in the year 2011 [*Space News*, 2003]. This mission was soon redesigned to orbit also the Callisto and Ganymede satellites, and pushed back to 2015. By now a number of NASA in-house or funded studies have been presented analyzing issues connected with space NP, see, for instance [Oleson and Katz, 2003]. The general consensus is that NEP is by far preferable to NTR at least for the JIMO, since the JIMO mission is unmanned and needs not to be especially fast. Accordingly, within Prometheus NASA established a nuclear propulsion research (NPR) program complementing and supporting the JIMO mission. NPR goals include reaching I_{sp} up to 9,000 sec and thruster lifetime of order 5–10 years. The first type of electric thruster being considered is an ion thruster, since the power required by JIMO is of order 'only' 25 kW. In fact, there are two ion thrusters concepts competing for JIMO propulsion: HiPEP and NEXIS. HiPEP, developed at NASA-Glenn in collaboration with Boeing Electron Dynamics Devices, Aerojet, University of Michigan and Colorado State University, has been tested in the laboratory at up to 40 kW with a peak I_{sp} of about 9,600 sec and 80% efficiency; it has a pirolytic graphite rectangular exit section grid. The NEXIS thruster is being developed at the Jet Propulsion Laboratory of Cal Tech with again Boeing Electron Dynamics Devices and Aerojet, and has a round C-C exit grid section [Oleson and Katz, 2003]. In the laboratory NEXIS has been operated at 27 kW with an $I_{sp} = 8{,}700$ sec and 81% efficiency [Baggett and Dankanich, 2004]. Whether power should be provided in the AC or DC mode, at what voltage, and its conditioning are all important details still under scrutiny, e.g. [Randolph and Polk, 2004; Scina et al., 2004].

If still politically supported, the mission would have a positive effect on all future NEP technology. At the time of this writing, JIMO and Prometheus are questioned no longer because of nuclear 'fears' (a good sign), but rather on financial grounds. The preliminary design of the JIMO spacecraft indicates an astonishing 50 ton mass and an estimated cost (by Dr R. Taylor, head of the Prometheus Project) just for developing the nuclear electric engine, of $4.5 billion [Reichardt, 2004]. Such figures raised and are still raising questions among analysts and review committees, and in fact has led to the decision to reduce its 2006 budget (by $100 million), just short of putting JIMO on hold (but not to shelve it) [Berger, 2005a]. In fact, Michael Griffin, the new NASA Administrator, has also criticized the JIMO mission for being overly ambitious, thus too costly, and may decide to have it performed with more conventional propulsion. Testing NEP propulsion would be reserved for a less demanding mission yet to be chosen [Berger, 2005b]. The decision at NASA has been made to concentrate resources on a manned lunar mission, where emphasis is on nuclear power, not nuclear propulsion. In fact, to ensure a safer human settlement on the Moon the consensus is that a nuclear power generator is indispensable. Building, testing and orbiting such a generator has become the first priority of the NASA nuclear program.

Much as missions to the outer planets are of interest to scientists (witness the enthusiasm after the Huygens landing on Titan), the public is far more sensitive to Mars explorations, hoping that some form of life may be found there. It is apparent that chemical propulsion for a manned mission to Mars would not be just risky, but also extremely expensive [Donahue and Cupples, 2000]. For a short period around 1999–2000 solar electric propulsion (SEP), riding high on its high performance in applications to commercial GEO satellites was, if not the favorite, at least one of the alternatives. However, solar-powered propulsion has inherently low thrust, and is hardly suited to explore the outer planets and their satellites, since solar power scales with the squared inverse of the distance from the Sun. This feature increases excessively the typical duration of interplanetary missions [Koppel et al., 2003].

A short history of manned Mars missions architectures in the US, from its Von Braun origins and including NTR but also chemical propulsion, is in [Donahue and Cupples, 2000]. This paper documents the evolution of the so-called NASA [Mars] Design Reference Mission (DRM) up to the latest version of 1999, also referred to as version 4.0. Much of the conceptual work for Mars missions has been based on NTR propulsion, but also on a rather improbable SEP solution using vast arrays of solar cells to generate the power needed by high-I_{sp} electric thrusters.

In fact, the status of propulsion for a Mars mission can be summarized as follows: technology-wise, alternatives to nuclear propulsion consist only of SEP or chemical rockets. Both were analyzed in depth, see, for instance [Donahue and Cupples, 2000]. Since energy density is low in both propulsion systems, the mass to orbit for a manned mission, composed of the empty spacecraft plus propellants or photovoltaic arrays, would require a completely new large launcher (dubbed 'Magnum'). Calculations indicated the payload of this 'Magnum' launcher should be in the 80-ton range: thus the effort required would be comparable to building a new Saturn V, but with costs reflecting the 21st century rather than the 20th. Six launches using 'Magnums' are envisaged in [Donahue and Cupples, 2000] for a single Mars mission. The latest generation of expendable rocket launchers (Atlas 5, Delta 4 Heavy or Ariane 5 Evolution) may avoid building a 'Magnum' from scratch, but this depends on the overall design and mass of the future Crew Exploration Module and Crew Launcher Vehicle cited in the Space Exploration Initiative of President G.W. Bush, and on its propulsion system, all in the preliminary planning stage at NASA. However, a preliminary heavy lift launcher powered by the liquid and solid Shuttle rocket engines has been proposed, with a first Moon trip date envisaged in 2015 or, more likely, in 2018: see *http://www.nasa.gov/home/index.html?skipIntro=1* for pictures.

The low thrust that can be obtained with SEP is recognized as its major disadvantage: the latest manned Mars DRM (1999) envisaged a SEP-powered ship slowly accelerating by spiraling for about 9 months around the Earth without a crew. Close enough to the escape speed, the crew would board the ship by means of an ad hoc 'space taxi' powered by a high-thrust chemical rocket. Adding to this complication, the 1999 Mars Design Reference Mission with the SEP option is designed around a 800-kW SEP thruster, requiring at least some 4,000 m^2 of solar cells [Larson and Wertz, 1992]. In fact, at the time of this writing, a SEP alternative for a manned Mars mission is out of the question.

The other alternative (chemical propulsion) proposed in [Donahue and Cupples, 2000] treats Mars as the equivalent of the Moon in the 1950s. Somewhat simplifying, such philosophy would consist of landing on Mars as soon as possible, to show 'it can be done', leaving it to future initiatives to gradually replace chemical propulsion with NTR and, later, with even more advanced propulsion (e.g., the VASIMR concept powered by a nuclear reactor; see section 7.22).

The obvious danger of this philosophy is likely to be the same as that of the Apollo program: after a number of very expensive Moon shots the public and the US administration lost interest and terminated it, abandoning the Moon for the next 30 years. The question is then whether the approach proposed in [Donahue and Cupples, 2000], even if financially feasible, would result in the same disappointing epilogue. Similar questions could be raised about the US Space Exploration Initiative of 2004, if an expensive new launcher or, more generally, chemical propulsion is chosen as solution.

In fact, all analyses so far carried out [e.g., Borowski et al., 1999] conclude that the mass of a conventional chemically powered propulsion system for a manned Mars mission would exceed that of NTP systems. NEP systems promise to be more efficient in terms of propellant mass, although less capable in terms of thrust. In the light of the Space Exploration Initiative these questions may become moot, resolved as they might be by non-technical arguments. At the time of this writing (2005), M. Griffin, the newly appointed NASA Administrator, has decided that the estimated mass of the 25 kW/class ion engine vehicle for a Mars mission is way too large, requiring at least two heavy-lift launches (e.g., using Delta IV Heavy, or Atlas 5). Its cost following suit, NEP for Mars has been given the lowest priority, with power generation having the first, and NTP the second. Thus the NTP solution, the dark horse in the Mars propulsion competition, has (in principle) regained the status lost since the 1970s.

In the context of manned interplanetary missions there is a critical issue that bears on arguments pro and contra nuclear propulsion, and that is the question of health-damaging effects due to extended periods in space. The space environment is rich in cosmic radiation (mostly photons and relativistic protons, the latter with energies in the 10^9 to 10^{18} eV range) harmful to humans. Solar flares may pose an even more serious danger, as they tend to be fairly unpredictable. In trips to Mars (but also to other destinations) this fact argues powerfully for shortening missions as much as possible. The experience gained by Soviet cosmonauts on MIR indicates radiation and other subtler effects (e.g., on enzymatic metabolism by micro-gravity) may affect *permanently* the human body. Nuclear propulsion, with its higher I_{sp} and reasonable thrust for longer times can shorten interplanetary missions and is the prime candidate propulsion system for manned missions.

In the following, the two classes of nuclear propulsion systems, NTR and NER, together with their many variants, will be described and briefly discussed; however, the basics of nuclear fission *reactor* technology will be first outlined. For engineering details the reader should refer to Turner [2005].

7.7 NUCLEAR REACTORS: BASIC TECHNOLOGY

Since it is the oldest technology, solid-core reactors are often taken as the baseline to gauge the performance of more advanced reactors. A nuclear propulsion system consists of a nuclear reactor (NR) coupled with a working fluid or propellant system. The fluid is heated inside a heat exchanger, the key engine component. Heat is produced by the primary fission reaction of (typically) ^{235}U, or other fissionable material (the nuclear 'fuel').

While fissioning, a reactor produces high-energy fission fragments, or FF: these are the nuclei formed by splitting of the fuel by neutrons. The FF are absorbed by the solid material encapsulating the fuel, meaning their kinetic energy is deposited as heat during their trajectory inside the core material ('thermalization'). Fission produces fission fragments at a rather low rate, of the order of kg/h; section 7.2 showed that if the material where fission fragments thermalize is cooled by a much larger flowrate of propellant/coolant, the reactor core may be kept at temperatures that will not damage it or create structural problems.

In fact, this is the strategy of most nuclear reactor concepts: the heat deposited inside the core material is removed by a coolant fluid pumped through the reactor. The fluid will heat; in a simple NTR it will be expanded and accelerated in a nozzle, producing thrust just as in any chemical rocket engine; see Figure 7.17. In a NEP system instead the hot working fluid circulates in a closed loop, drives a thermodynamic cycle, and produces, eventually, electrical power.

The energy deposition rate (thermal power) of fission fragments in a solid material may be extremely high, in fact, as high as wanted; witness the application of fission to atomic weapons. Structural material may even melt or vaporize if fission is not 'moderated' (controlled) by inserting or pulling bars (or drums, depending on design) made of neutron-absorbing material. In nuclear physics energy is conveniently measured in electronvolts (eV) rather than °F, °C or joules. For reference, FF can be released during fission with energies up to 10^2 MeV. On a per nucleon (neutron or proton) basis, average nuclear binding energy is 8 MeV/nucleon [Mukhin, 1987], and since FF may have an atomic weight of the order of 40 to 140 when using ^{235}U as fuel, their energy may reach some hundreds of megaelectronvolts, with an energy spectrum that depends on the particular fragment. Together with FF, neutrons are also emitted, with a spectrum centered around 5 MeV. To compare these energies with those in chemical rockets, note that 1 eV electron has a kinetic energy corresponding to $\sim$11,300 K. Note that to *dissociate* H_2 into two H atoms needs only $\sim$0.2 eV, and to *ionize* H, ejecting its electron and producing H^+, needs just 13.8 eV (eV, not MeV!).

What these numbers mean is that fission fragments can theoretically heat other (non-fissioning) propellant particles close to their own energy. Of course, if the mass rate of the propellant is much greater than that of FF and neutrons, the fragments' energy will redistribute and the maximum propellant temperature will be accordingly much less than that of the fragments, but still capable, if not controlled, of melting or vaporizing all engineering materials. High temperatures are desirable in propulsion based on thermodynamics, but carry also structural risks.

The main problem with NTR is thus to slow down FF by transferring their kinetic energy to a fluid in a gradual manner, that is, one that will not cause intolerable thermal stresses or temperatures. Substances called 'moderators' help in thermalizing FF. The choice of moderators is driven by the need to 'thermalize' neutrons, from their $\sim$5 MeV energy down to $\sim$0.1 eV (1,000°C or so; see section 7.4.1).

So, the maximum temperatures the heat exchanger can withstand limit the solid-core reactor performance. Thus structural materials and their reactivity with the fluid at high temperature (called also 'hot corrosion') are paramount problems, witness the effort at LASL during the 1950s and 1960s to extend the life of fuel rods.

To place NTR with solid-core reactors in perspective, with modern materials their I_{sp} can reach 1000 sec, their mass/power ratio 10^{-3} to 10^{-1} kg/kW (a typical NASA-Glenn goal for a future 75,000 lb_f thrust engine is 0.08 kg/kW), and their thrust/mass ratio 10^{-1} to 10 g. In this respect they are close relatives of chemical rockets, except their I_{sp} is higher by a factor of 2 to 3.

The working fluid par excellence is hydrogen, because it has the lowest molecular weight (MW = 2) of all species, and favorable specific heat ratio $\gamma = C_p/C_v$; helium has a strong point in its lack of reactivity and has been considered, but is much costlier and its higher γ and molecular weight (MW = 4) yields lower I_{sp} than hydrogen.

In the following sections some of the most interesting NP technologies will be presented. They have been chosen on the basis of current or recent interest, and on the amount of public domain information available. In this vein some concepts have been omitted, because their stage of development is still unknown (as in the case of propulsion by nuclear microexplosions) or because they are simply ideas waiting to be even preliminarily analyzed.

7.8 SOLID CORE NTR

A primer on this subject is [Bussard and DeLauer, 1958]; design practice and details may be found in [Turner, 2005]. A conventional solid-core NTR of the NERVA type consists of a compact nuclear reactor in which a certain number of heat exchanger channels heat flowing hydrogen propellant to the maximum temperature allowable by materials, of order 2,000 to (in the future) 3,000 K [NASA, 1990]. Hydrogen works both as propellant and as reactor coolant: below $\sim$2,500 K, at which dissociation into H atoms would start, it remains in its molecular form. This limits NTR performance to I_{sp} less than 900 sec at most, for typical chamber pressure of order 70 atm (about 1,000 psia).

Replacing hydrogen with liquid methane to increase density impulse reduces I_{sp} by a factor of nearly 2. Performance would deteriorate slightly more using water as propellant, and since water starts dissociating into oxygen and hydrogen at these temperatures, safety would become a problem, even though density impulse (the product of I_{sp} times the specific density) would be much higher using water than either hydrogen or methane. During the NERVA program water propellant was discarded precisely because of safety concerns, but probably a second look at its convenience from the viewpoint of overall mission efficiency would be advisable now.

The thrust/weight ratio of conventional NTR is lower than in chemical propulsion, of order 0.25 or even less; this because of the topology of nuclear fuel elements ('rods'), since fuel occupies a small portion of the reactor volume, and because of the radiation shield. Heat deposition inside the heat exchanger elements and friction losses were responsible in NERVA I for a substantial pressure drop (25–30%), which contributed to lower the thrust potentially attainable. While the first loss is unavoidable (it is often called the 'fundamental loss' when heating a fluid), the second could be reduced by optimizing the number and shape of rod channels.

The key elements of a solid-core NTR reactor are the fuel rods, heat exchanger (cooling) channels, control drums, moderator and the neutron reflector that prevents neutrons from escaping the reactor and slowing down nuclear reactions too much. The entire assembly must be enclosed in a pressure vessel, see Figures 7.6 and 7.17. Conceptually, a complete rocket reactor differs little from an industrial gas-cooled nuclear power reactor, see [Lawrence et al., 1995, Fig. 8.4], except temperatures are deliberately higher, to produce a compact and light power package. The NERVA I prototypes delivered about 1 GW and weighed only about 7,500 kg including the 100 : 1 area ratio nozzle. The neutron shield added 1,590 kg. Of course, the reactors were supposed to last for no longer than 1–2 hours, compared to the many thousands of hours of a commercial power utility reactor.

A significant design feature of all NTR designed and tested under the NERVA program was that fuel and heat exchangers were tightly integrated in the very design of the fuel rods. Their compactness minimized weight, but made refueling (a feature not designed nor conceived) nearly impossible in space operation. The NTR of that time were designed to be capable of multiple restarts, even up to tens of times, but they were assumed to last only until complete fuel burn-out. Once the fuel was spent, the entire NTR was to be discarded. The reason for this design philosophy was the gradual deterioration of the reactor materials caused by high temperature, pressure and neutron fluxes. Neutrons damage materials, including fuel itself, by dislocating their atoms, or creating *new* nuclei upon capture (this results in 'poisoning' the fuel).

Solid-core NTR are still the design philosophy proposed by NASA-Glenn for Mars missions (e.g., see [Borowski et al., 1999]). This philosophy runs contrary to what is ideally desirable: an engine that can be refueled on demand by reasonably simple operation. The NERVA-type design architecture may be justified on the ground of mass, safety, and operability; nevertheless, the risk is to develop throwaway nuclear launchers/space vehicles, with their associated problems of cost, environmental risks and politics. To prevent this possible outcome, structural reliability and refueling of future nuclear reactors should be a priority.

Advanced NERVA-type NTR, incorporating modern material technologies and new fuels, have been proposed and discussed, invariably for Mars missions. With advanced NTR based on past NERVA technology, mission time still exceeds 2.5 years, too long for the dose of cosmic and other sources of radiation the crew could safely stand [Flinn, 2004]. The fact is, NERVA-type engines have I_{sp} still too low to substantially reduce the total mass of an interplanetary ship. With I_{sp} of order 800 or 900 sec too much propellant is needed not only to accelerate, but also to *decelerate* a spacecraft for an interplanetary mission where it must orbit its final destination. In principle, powered deceleration can be replaced by aerobraking, if the planetary destination, like Mars, has an atmosphere (an aerobraking spacecraft loses speed by inserting in a spiral orbit that periodically 'dips' inside a planetary atmosphere, producing drag). Even with the help of aerobraking, the mass of the Mars *return* vehicle estimated by the team at NASA-Glenn is 169 tons [Tauber et al., 1990]. The Cargo Lander and Habitat Lander must be added to this mass when calculating the total mass to lift to LEO. These figures are the end result of NTR with I_{sp} of order 900 sec.

Similarly to the results of the [Donahue and Cupples, 2000] analysis, the NASA-Glenn team concluded that their NTR-powered Mars manned mission needs a 'Magnum' heavy-lift launcher capable of lofting to LEO (e.g., 407 km) some 80 tons of payload *in a single flight*. The 'Magnum' still does not exist, although the recent Space Exploration Initiative of President G.W. Bush mentions a heavy lift launcher derived from the Shuttle.

In an effort to reduce mission mass there have been recent proposals to reduce at least the engine weight of NERVA-type designs, for instance see [Mowery and Black, 1999]. The baseline design was the NRX XE Prime engine built by Westinghouse/Aerojet General and tested in the 1970s; see Figure 7.18. Its core is conceptually replaced by a beryllium 'island'. The authors' neutronics calculations show this island can replace the NERVA I reflector, reducing the weight of this conceptual engine to about one-tenth of XE Prime. The result of this exercise is a shielded rocket engine capable of 20,000 lb_f thrust and weighing about 34,000 lb, including propellant for 20 min of operation. Based on a steady 2,500 K reactor temperature, achievable using Russian structural materials, the I_{sp} predicted is about 900 sec. The calculated overall engine weight is about 7,400 lb, with a thrust/weight ratio slightly less than 3. Perhaps the most significant result of such calculations is to show that improvements are still possible on conventional NERVA-era designs by using new architectures, materials and ideas.

Even with improvements made possible by technology advances since the 1970s, conventional NTR, while more frugal with respect to chemical rockets, may still fall short of enabling truly cheaper manned interplanetary missions. This is not only due to I_{sp} below 1,000 sec, requiring still much propellant, but also to the mass of the engine and shield. If the planet has an atmosphere, aerobraking is an option; however, spacecraft in the 100-ton class have never been really designed around missions utilizing aerobraking. Presumably, reinforcing and thermally insulating their structure may add much weight. However, if I_{sp} is too low, this solution would become mandatory to avoid a powered Mars orbit capture that would consume much propellant.

It may sound disappointing, but one must conclude that NERVA-type designs, even improved with respect to the NERVA I engine, cannot be labeled 'the' practical alternative for long interplanetary missions, unless their mass can be orbited using

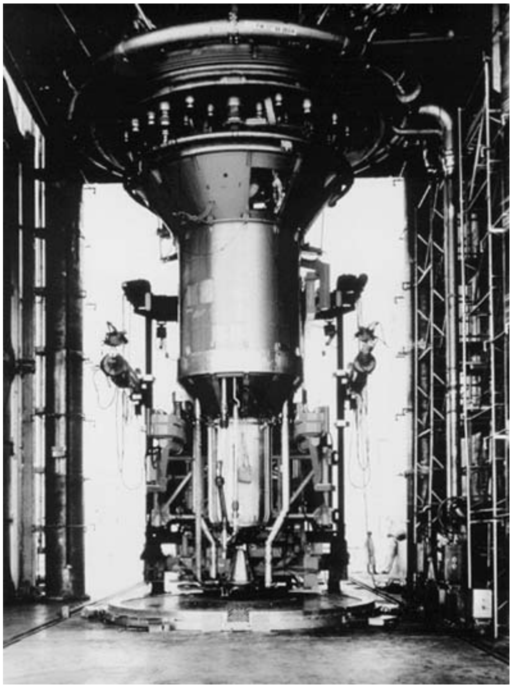

Figure 7.18. Westinghouse NRX XE experimental nuclear engine on its test stand.

low-cost launch systems, probably utilizing some form of airbreathing propulsion; see Chapters 1 and 4.

In fact, if the public accepts nuclear propulsion, NTR could, technically at least, complement and perhaps replace chemical stages in launchers: this was the initial sole motivation for the ROVER program. Assuming a $\Delta V = 8$ km/sec, typical of LEO insertion, increasing I_{sp} from the 380 sec of a LOX/LH_2 rocket engine to the 1,000 sec achievable by a NTR would reduce the propellant-to-total mass ratio from $\sim$0.9 to $\sim$0.5, reducing staging and launch costs. NTR for space launchers are being explored at the US Air Force [Vacca and Johnson, 2004].

A second class of missions where the large thrust of a NTR would be very convenient or perhaps indispensable is that of intercepting asteroids moving too close to the Earth. Even recently near-Earth objects (NEO) [NASA, 2005a] have been detected too close and too late for comfort [Jarow, 2000]. Many trajectories of known asteroids might pose a future danger to Earth, see [University of Pisa, 2005], to the point that the phrasing of the so-called Torino scale weighing the potential effects of an impacting asteroid has been recently toned down [*Nature*, 2005]. No chemical rocket can economically accelerate to the many tens of kilometers per second typical of many asteroids' orbits. In fact, if an NEO trajectory looks like posing a danger, the last desirable strategy is to intercept it head-on to destroy it, as in science fiction movies: the unpredictable fragments' orbits could be just as dangerous. A more reasonable solution is to nudge the NEO towards a different orbit, and this requires matching its velocity closely. Propulsion systems capable of large accelerations, even at the expense of efficiency, may be mandatory for such missions. Time will tell whether the ever-present NEO threat may contribute to revive NTR research.

7.9 PARTICLE BED REACTOR NTR

Following the end of the NERVA work, USAF took over research in nuclear propulsion, one of its priorities being a nuclear-powered reusable space tug (more formally, the Orbital Transfer Vehicle (OTV)). With all the safety caveats, a space tug is a striking alternative to orbit raising chemical stages for commercial satellites. USAF started in the mid-1970s by modifying the NERVA I reactor, recognizing it rightly as the critical element of the entire propulsion system. The NERVA family of reactors was still too massive (and too powerful) for the type of missions USAF had in mind, and that was what started the particle bed reactor (PBR) concept. The PBR has a configuration taking advantage of advances in fuel manufacturing. The structure of all NERVA-Kiwi family was based on long fuel bars, or rods. Cold hydrogen flowed inside multiple channels present in each rod, the entire assembly exhausting hot hydrogen inside a conventional nozzle. This geometry is essentially one-dimensional, packing relatively low energy in the unit volume.

In PBR, the fuel (^{235}U-rich uranium oxide, UO_2, or other more advanced uranium–ceramic compound) is stored inside small spheres or beads, e.g., 500 μm in diameter, in which the layering of materials encapsulating the fuel is similar to that in conventional rods. A typical bead design consists of a fuel-rich core surrounded by graphite and enclosed by an inert layer of ZrC. The particles are packed inside two coaxial cylinders, the hot inner one made of carbon–carbon composite and the outer made of aluminum alloy. These fuel elements are clustered in the engine and embedded inside the moderator, for instance beryllium, or ^{7}LiH. The hydrogen propellant flows inside the inner cylinders, where is heated, expanding in a conventional nozzle [Beale and Lawrence, 1989]. One of the many particular schemes of PBR NTR is reported in Figure 7.19.

Because of its topology, a PBR has a higher spatial fuel (and power) density than that of conventional fuel rods. The gain factor in power density could be as high as 10 [Bennett and Miller, 1993]. Power density may reach 10–75 MW/dm^3. For instance, at 10 MW/dm^3, a 1-GW reactor could be compacted inside a volume less than that of an oil drum. A Russian concept using a ternary carbide fuel claimed to have reached 40 MW/dm^3, power density of order 0.3 MW/kg, and gas exit temperature 3,100 K for 1-hour operation, or 2,000 K for 4,000 hours. USAF tested PBR sub-components for nearly 20 years, with a maximum $T \sim 3{,}000$ K maintained successfully in a single fuel element, but never designed a complete rocket engine. With hydrogen temperatures of that order it is reasonable to assume I_{sp} could be close to 1,000 sec. The power density actually measured was ~40 MW/dm^3, similar

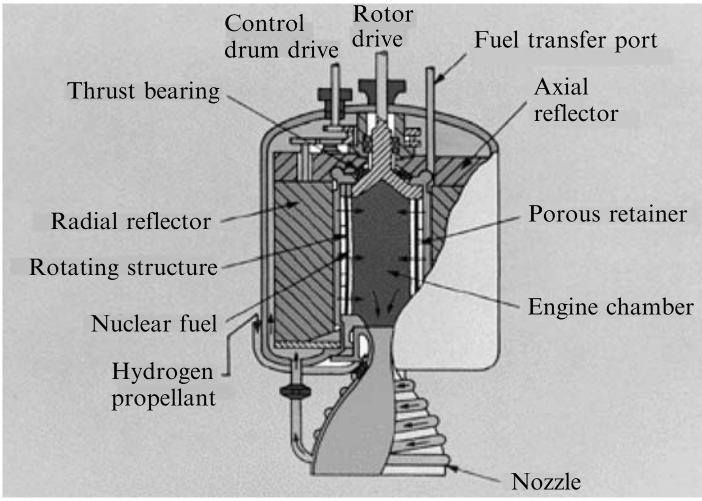

Figure 7.19. Schematic drawing of a particle bed reactor with power controlled by a rotating drum.

to that tested in Russia, confirming the advantages of PBR over conventional reactors. This work was part of the USAF SNTP program, directed mainly toward building a space tug, and was terminated in 1993.

In absolute terms, the net gain in I_{sp} foreseeable with this type of NTR propulsion, of order 100–150 sec, is significant but still barely a 13% gain over the NERVA I baseline engines. On the mass budget side, however, engine mass for the same thrust (3.3×10^5 N) was estimated at only 1,700 kg, plus some 1,500 kg for the shield, quite an improvement. Thus the thrust/weight of an actual engine should reach eventually about 20 : 1 vs. the 4 : 1 ratio achieved by NERVA I. Part of this improved performance is due to the much lower pressure drop inside the reactor compared to a NERVA-type configuration (pressure drops of order 5–6% appear feasible with PBR reactors).

Major technology problems foreseeable with a PBR engine are the durability of materials at its high design temperatures. At USAF this was the motivation for investigating CERMET (CERamics-METal) technology for fuel rods. Shield weight and volume issues are similar to those in NERVA-type engines.

All things considered, a future PBR rocket engine should be much lighter and more compact than a conventional NTR. A fast interplanetary mission to Mars would entail many hours, or even days, of operation at full power; the behavior of the engine operated during this time at 3,000 K and, say, 60 atm is probably the single most important consideration in assessing the viability of PBR as a space thruster, while there is no question that its fuel topology is a major step forward.

7.10 CERMET TECHNOLOGY FOR NTR

Evidence gathered from NERVA I and the work done on PBR indicated fuel elements survival at high temperature and pressure are among the critical issues. Driven also by the need to extend the life of fuel elements in the reactors powering the nuclear airplane planned in the 1950s and 1960s, USAF developed the CERMET reactor concept, and tested a single fuel element to check improvements in its working life.

In a CERMET NTR the fuel is stored as ^{235}U-rich UO_2 encapsulated by, or dispersed in, tungsten, molybdenum or tungsten-rhenium. No moderator (e.g., graphite) is interposed between fuel and jackets, so that the energy spectrum of fission fragments is broader, up to $O(1)$ MeV. The main task of the refractory metal is to contain fission fragments better than more conventional ceramic or metal matrices, i.e., with less damaging structural effects. CERMET fuel in this form has been tested at temperatures of order 1,900 K (in the US and Russia) with excellent results. The maximum operating T of CERMET fuel elements is 2,500 K; lifetime up to 19,000 hours at 1,900 K has been demonstrated, even after fuel elements were cycled through many restarts and shutdowns. For this reason, this type of NTR technology is considered best suited to OTV propulsion, where engines must be turned on and off very reliably for many years. The spatial density of fuel is not as high as in PBR: in fact, the estimated thrust/weight ratio is only 5–6. Pressure losses of order 30%, very high, contribute to the low absolute performance. In fact, the I_{sp} predicted in future rocket engines embodying this technology is only about 900 sec. The major advantage of this concept is therefore its very attractive and robust fuel elements technology, resulting in the ability of multiple restarts and (presumably) long maintenance-free engine life.

7.11 MITEE NTR

The Miniature Reactor Engine (MITEE) is a nuclear thermal concept developed by a group of researchers formerly or still employed at the US Brookhaven National Laboratories. This concept is associated to CERMET technology. It was proposed during the Cold War, when the US Navy formulated a requirement for a fast torpedo propulsion system. Part of the work done at that time is now being proposed for a NTR for interplanetary missions, including Mars.

Outwardly similar to conventional NTR (see Figure 7.19) , MITEE designs use fuel elements where hydrogen propellant flows radially inwards, crossing the metal matrix composite encapsulating the fissioning fuel, as shown in Figure 7.20. This flow topology produces a compact NTR. While most initial MITEE designs used only ^{235}U as fuel, recent MITEE proposals include also ^{233}U and ^{242m}Am, since these materials produce even more compact engines (^{242m}Am has a critical mass about a hundred times less than that of uranium). Published estimates of engine size and mass are surprising: total engine mass (using ^{235}U) 200 kg for a 75-MW NTR, with $I_{sp} = 1{,}000$ to 1,250 sec for the combined cycle described below (and assuming

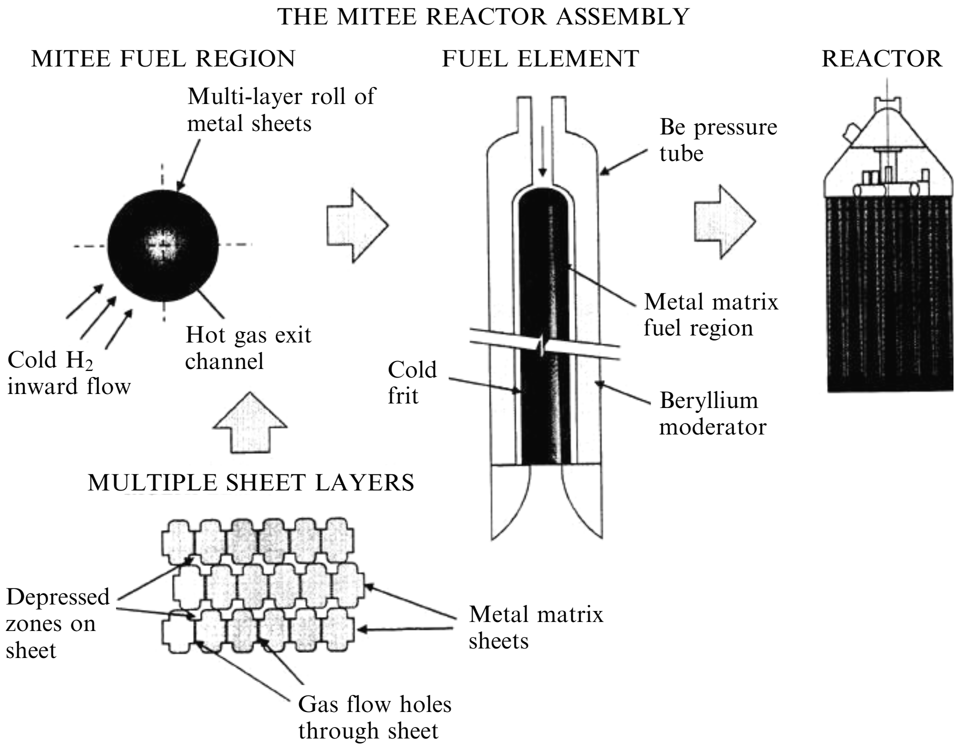

Figure 7.20. Fuel element structure and assembly inside a MITEE reactor (MITEE http://www.newworlds.com/mitee.html).

realistically that nozzle expansion is frozen) and a thrust of order 1.4×10^4 N. The engine mass is estimated to drop to 100 kg replacing ^{235}U with the much scarcer ^{242m}Am metastable isotope [Powell et al., 1998, 1999, 2004; Maise et al., 2000]. A recent MITEE NTR design is claimed to be capable of I_{sp} about 1,000 sec (based upon a hydrogen exit temperature 3,000 K), overall weight 140 kg, total one-time burn of several hours, with engine diameter 50 cm corresponding to a power density of order 10 MW/liter. Figure 7.21 shows a comparison between a hypothetical MITEE-class nuclear rocket and some typical chemical rockets for interplanetary missions already proposed or considered.

Although meant to be reasonable projections (no such engine has been built or tested so far), these are indeed extremely interesting figures, making the MITEE concept a good candidate for certain future interplanetary missions.

The MITEE concept is still in continuous evolution. For instance, it has been proposed to use part of the reactor waste heat to reheat hydrogen after expansion, re-compressing it and extracting further work from the thermodynamic cycle [Powell et al., 1999, 2004]. This cycle becomes similar to the classic turbine interstage reheating proposed some 50 years ago by Brown Boveri and recently implemented in advanced gas turbines manufactured by Alstom in Switzerland. Since excess

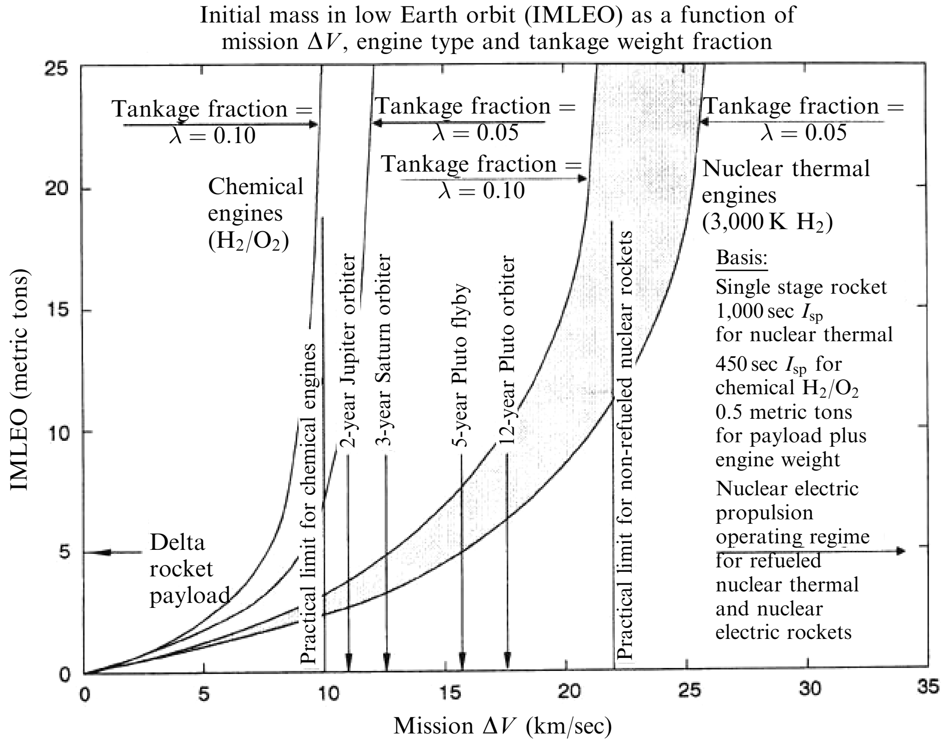

Figure 7.21. Comparison among propulsion systems, including a high-temperature MITEE rocket, for interplanetary missions (MITEE http://www.newworlds.com/mitee.html).

turbine power production is inevitable, hydrogen could also be electrically heated. According to the authors, total power transferred to hydrogen could raise its temperature to ~3,900 K using multiple cycling; correspondingly, the Isp should increase to ~1,250 sec. While interesting, this strategy is cumbersome in terms of sheer amount of machinery needed. In fact, no turbo-machine power generator has ever been tested, officially at least, in orbit. This type of NTR is actually a *hybrid* between pure NTR and NEP engines, exploiting the heat that should be wasted in space by space radiators.

The family of MITEE concepts is worth attention because of its compactness. In fact, combining some of the ideas from the MITEE designs with the basic Rubbia's engine proposal in section 7.13 should result in a beneficial synergistic effect.

7.12 GAS-CORE NTR

This is an even more advanced concept, initially proposed at the Scientific-Research Institute of Thermal Processes (now Keldysh Research Center), in Russia [Koroteev et al., 2002]. Studies started in 1954, and somewhat later also NASA-Lewis (now

NASA-Glenn Research Center) began to investigate it as well. The original suggestion for *gas-phase* fission (as opposed to fission in solid materials) actually goes back to 1949 [Bussard and DeLauer, 1958, pp. 322–327], and was motivated by the need for a fast Mars mission (200 days, with no surface stay).

For such a mission the I_{sp} and thrust requirements were estimated in the range of 1,400 sec and 10^5 N, respectively. To make such a mission viable in terms of overall mass meant raising I_{sp} without reducing the thrust needed for significant acceleration. At the time, increasing Isp was conceived possible only by raising the working fluid temperature, which is ultimately limited by the melting point of materials (electric thrusters had not been suggested yet). Hence a radical proposal, consisting of assuming that the fissioning fuel could not only be allowed to melt, but even gasify, so the heat release process could go on at much higher temperatures. Of course, to take advantage of this strategy the propellant too must be heated at higher temperature; so the real issue, and all its drawbacks, becomes how to transfer heat from the hot fissioning gas to the propellant. Gas-core temperatures planned were 20,000–50,000 K.

Two cycles ('open' and 'closed') were invented to solve the heat transfer (HT) problem. Convective HT via a heat exchanger was and is out of the question, so radiative HT was the only alternative. In both cycles it was soon found that direct radiation HT from the fissioning fuel to hydrogen was unfeasible: in fact, at temperatures up to 10,000 K and pressures of the order of a few atmospheres, hydrogen ionizes less than 1%, and thus is optically thin. For this reason, radiative HT from the uranium plasma was planned as a two-stage process, by seeding hydrogen with carbon particles. Hydrogen plays the double role of propellant and of carrier gas. Fissioning fuel would heat carbon particles directly; in turn, the hot carbon particles would then heat the hydrogen carrier, to be expanded in a conventional nozzle.

In the 'open cycle' solution, the fissioning gas is separated from the propellant by a cooler hydrogen layer (a similar solution was supposed to keep hot hydrogen from touching and destroying the vessel walls confining the reactor). A possible scheme is shown in Figure 7.22.

The open cycle gas-core reactor could (in principle) reach I_{sp} of the order of 6,000 sec using a laminar vortex to keep core plasma and hydrogen propellant separated as much as possible. To keep fuel losses sufficiently small, the hydrogen-to-core plasma mass ratio was estimated at least 200 : 1. A large amount of the power generated, as in any reactor, must be disposed of (that is, radiated away to space). Thrust available for the Mars mission engine was calculated at 5×10^5 N.

In the 'nuclear light bulb' closed cycle, shown conceptually in Figure 7.23, in addition to the cooling problems a second problem was the reprocessing of the buffer gas (with which core plasma tends inevitably to mix). Including a space radiator, the I_{sp} was estimated at 1,400–3,000 sec. Thrust was predicted between 1.5×10^5 and 1.5×10^6 N. These were encouraging figures; on the other hand, engine complexity resulted in engine mass estimated between 30 and 300 tons, depending on thrust.

A reference nuclear light bulb design by LASL had a nominal thrust 4.2×10^5 N, $I_{sp} = 1{,}870$ sec, and engine mass 32 tons. Sizing this engine predicted a 3.8 m diameter, 6.9 m long cylindrical engine. The fuel is optically thick, so that

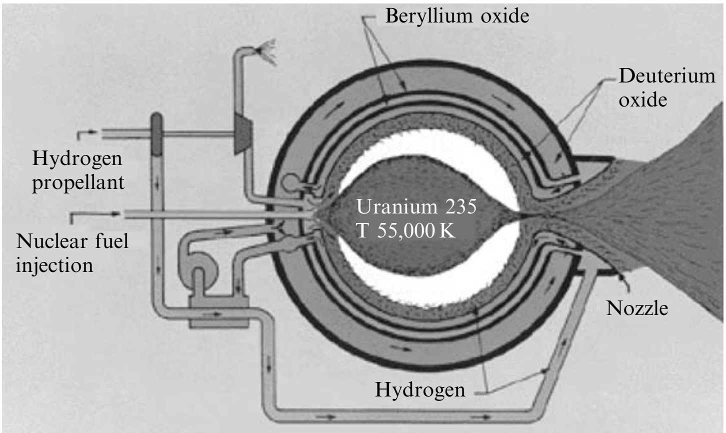

Figure 7.22. Gas-core reactor: schematic operation of an open cycle.

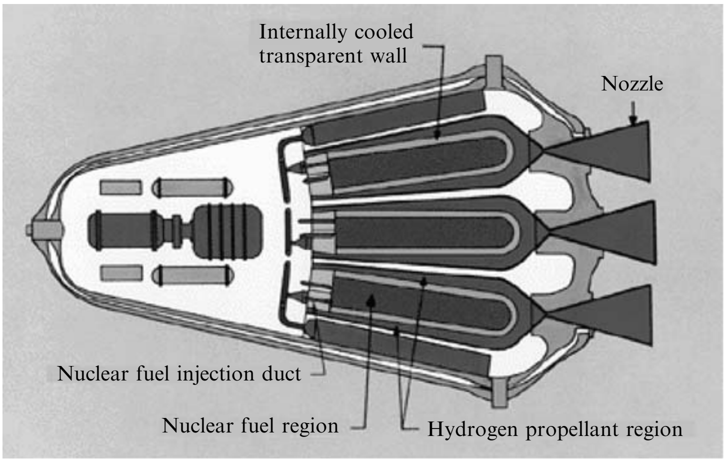

Figure 7.23. Closed cycle gas-core reactor (conceptual scheme).

only its external apparent surface would radiate with a 26 kW/cm^2 flux and at a calculated $T = 8{,}300$ K. This flux is worrisome, e.g., 10 to 100 times larger than the heat flux during re-entry from LEO. The stagnation temperature of the hydrogen propellant, seeded with 1% tungsten in this reference design, was 6,700 K. Testing of this concept actually took place using UF_6 gas (uranium hexafluoride), and replacing fission heating by radio-frequency heating. In these tests the UF_6 temperature reached 9,000 K and the heat flux measured was 7.6 kW/cm^2; the buffer gas was a fluorine–argon mixture. Deposition of uranium compounds on silica was observed to make the silica opaque, but this side-effect was not considered critical to the working of a future engine [Mensing and Latham, 1989].

Russian work on the same two cycles is similar to that in the US, but shows also some interesting differences; among them is the gas maximum temperatures below

8,000 K. Most of the work at Keldysh Research Center was done on the open cycle engine; several geometries were conceptually analyzed, see [Koroteev et al., 2002, Chapter 1]. The reference just cited contains, in fact, a detailed synthesis of the Russian work in gas-core reactors from 1954 to 1975.

More recently, work on gas-core engines for a Mars mission has been presented by LASL researchers [Howe et al., 1998]. The emphasis of this work is again on the need to ensure fast round-trip time. While a substantial amount of work is claimed to have taken place toward solving the fluid dynamics problems connected with the core gas–buffer gas interaction [Thode et al., 1997], the estimated mass budget of the spacecraft for a fast Mars mission (270 days, including 40 days on the Mars surface) remains rather substantial at 582 tons. The reason is the relatively low $I_{sp} = 3{,}000$ sec, and the large engine and shielding mass.

The present LASL state of the art of this technology is reported in [Howe, 2000]. New features proposed include the recirculating zone of hot hydrogen plasma shaped as a toroidal vortex by a central (axially directed) high-speed hydrogen jet. Part of the hydrogen jet goes directly to the nozzle, but the largest fraction is fluid dynamically forced to recirculate. The fissioning fuel is injected inside this fraction: in fact, the purpose of the vortex is to confine hydrogen long enough to absorb fission heat. Using its proprietary codes, LASL has reportedly solved most of the plasma and vortex instabilities found in the past. A combustion engineer will find an analogy between this concept and conventional flame-anchoring strategies in a rocket or gas turbine combustor: in both cases the heat release process is faster than the heat transfer to the working fluid, so that recirculation must provide enough time for the heat transfer to occur.

Some of the critical gas-core technologies appear to be: heat transfer control, flow control and (in the case of the 'nuclear light bulb'), silica transparency. In addition, most of the power generated by gas-core reactors must be radiated away, only a small fraction ending up inside the propellant. This adds the 'space radiator problem' to an already complex design. On the positive side, gas-core reactors are relatively compact (but heavy) for their thrust level. In the latest version of their design LASL researchers seem to have solved many of the closed cycle problems by doing away entirely with the silica walls, and relying on a pure fluid dynamics anchoring, as in many conventional industrial furnaces. Still, it is apparent that much work would be needed to perfect this ambitious concept.

7.13 C. RUBBIA'S ENGINE

This concept has been proposed by the 1984 Nobel prizewinner C. Rubbia, in 1998 during a CERN lecture. The very first suggestion of using fission fragments to directly heat rocket propellant was made in 1948 [Shepherd and Cleaver, 1948]. Quite independently, the same idea was also investigated in Israel by Professor Y. Ronen at Ben-Gurion University [Ronen, 2000]. In Italy this concept has been developed since 1998 by an ad hoc research team led by C. Rubbia and funded by the Italian Space Agency, ASI. A preliminary feasibility report described the main features of this engine concept as of March 1999 [Augelli et al., 1999]. The Rubbia engine differs considerably from all the NTR concepts above in that the heat transfer strategy of section 7.5 is reversed.

In Rubbia's engine, a fissioning surface layer, deposited on the inside wall of the reactor chamber, emits isotropically fission fragments. Because of the size of the reactor and of the nature of the fuel proposed (the mestable isotope ^{242m}Am) the fissioning layer may be very thin. Provided it can be kept at a reasonably low T, about half of the fragments released from the fissioning layer are injected directly into propellant pumped into the engine (hydrogen). The fragments thermalize inside the propellant, that is, redistribute their kinetic energy (up to 200 MeV) by collisions with molecules of hydrogen, raising its temperature up to 8,000–15,000 K. Because of their isotropic emission, the fission fragments not ending inside the propellant deposit energy inside the reactor walls, so cooling the walls coated with fuel while it fissions is critical.

In this concept the propellant may become *hotter than the solid walls*, overcoming the temperature limitations of wall materials. In principle, this concept should result in a simpler (and lighter) nuclear propulsion system. Provided radiative heat transfer from the hot hydrogen plasma is moderate, the I_{sp} of this concept may be much higher than for the solid-core NTR already discussed: propellant temperature is higher, and at higher temperature hydrogen is nearly completely dissociated into H atoms, lighter than H_2 molecules by a factor of 2. In fact, at chamber temperature of order 10,000 K the I_{sp} calculated is about 2500 sec.

This concept enables a Mars mission with a much smaller vehicle than at present being envisaged with either chemical propulsion or conventional (solid-core) NTR. If propellant temperature could reach 16,000 K the work already done by the ASI team indicates a Mars mission vehicle could weigh $\approx$120 tons. This would also result in a Mars round-trip time slightly more than a year, including 40 days on Mars' surface. Thus the space radiation dose to the crew would drop from the 60–120 rem estimated for the NASA Mars Reference Mission Version 3.0, lasting some 2.5 years [Drake, 1998], to a much lower 45 rem, including the radiation dose from the NTR itself [Lawrence et al., 1995, Table 8.1]. In fact, most of the radiation in a long Mars mission is due to galactic sources and solar flares, and is proportional to round-trip time (for an explanation of the radiation dose and of the rem unit see the Appendix at the back of the book).

According to the information released in the fall of 1998 at CERN, a preliminary estimate for this concept had a mass/power ratio = 1.25 kg/kW, about 10 times larger than conventional NTR. Weight and size, however, are a function of engine operating pressure, which was assumed to be 1 atm as a convenient yardstick at the time. ^{242m}Am is the fission material of choice for this engine, one of the reasons being that criticality can never be reached: its neutron cross-section vs. temperature peaks and then falls to very low values, ensuring no runaway reaction may take place. This isotope is metastable and must be manufactured, for instance, from the ^{241}Am used in all commercial smoke detectors; it is not weapon-grade material.

Because ^{242m}Am can never become critical, an external neutron source must be used to start fission. This can be accomplished using a proton (p^+) accelerator and a high atomic mass target material (e.g., tungsten) target, where the impacting p^+ beam produces a neutron shower. A non-standard way could use the compact neutron source available at atomic research laboratories in the former Soviet Union and capable of neutron fluxes $\sim 10^{19}\,\mathrm{sec}^{-1}$ [Prelas, 1998]. The so-called 'TARC' experiment of C. Rubbia at CERN showed that by enclosing the engine inside a graphite hohlraum (a cavity, behaving as a black body for neutrons), neutrons diffusion time and mean free path could be made long enough to sustain steady Am fission without an external source.

A conceptual sketch of this engine (see Figure 7.24) consists of a cavity (the 'chamber', or reactor) where ^{242m}Am is present as a layer deposited on the walls. Hydrogen is injected inside the chamber, for instance through wall holes. The Am layer fissions, saturating the chamber with high-energy fission fragments the whole chamber being surrounded by a neutron flux-enhancing material, such as graphite constituting the so-called hohlraum. The hydrogen injected inside the chamber is bombarded by fragments from the fissioning fuel, and its temperature rises. The temperature reached is determined by the hydrogen flow-rate: the higher the flow-rate, the lower the temperature. Finally, expansion through a nozzle generates thrust.

Hydrogen could be heated to extremely high temperatures in this process, because the kinetic energy of fission fragments is of order of 100 MeV; in practice, convective and radiative heat losses will eventually limit hydrogen temperature. Thrust depends on chamber pressure, size and neutron fluxes; thrust needed for a powered Mars mission depends also on the choice of trajectory. A preliminary 'fast' mission with a single ship was calculated by the ASI research team in 1999. With thrust in the 1,500 to 2,500 N range, the round-trip mission time was 369 days, including 40 days spent on Mars' surface. Since this work was funded by ASI, details of the technical solutions proposed to solve the many physics and engineering problems encountered are still ASI property. What is publicly available indicates that this novel concept is viable (no show-stoppers), and would bypass many or most of past problems associated with conventional NTR, among them the large neutron fluxes generated during their operation. The very fact that I_{sp} could be raised to a factor 2 to 4 above that of other NTR, and a factor 5 to 8 above that of LOX/LH_2 rockets, is a powerful motivation to pursue this concept further.

In the US similar ideas have produced at the Lawrence Livermore National Laboratories (LLNL) the ultimate fission fragment concept, that is, thin filament fission (as opposed to thin layer fission). As in Rubbia's engine, americium is the fuel. However, the products of the nuclear reaction themselves, i.e., the fuel fission fragments, are *the* only propellant in the LLNL proposal; that is, the fragments produced by fission are exhausted 'as produced', with all their initial kinetic energy. There is no thermalization inside a separate propellant in this concept ($M_p = 0$) and exhaust speed should ideally be of the order of 10^5 to 10^7 m/sec, that is, I_{sp} in the 10^4 to 10^6 range or higher. However, the mass flow-rate is low: in solid-core reactors the mass fissioned is of the order of a few kilograms per hour, so that is also approximately the mass flow rate of fuel ejected as fragments and working as propellant. Accordingly, the thrust is also very low. An artist's view is

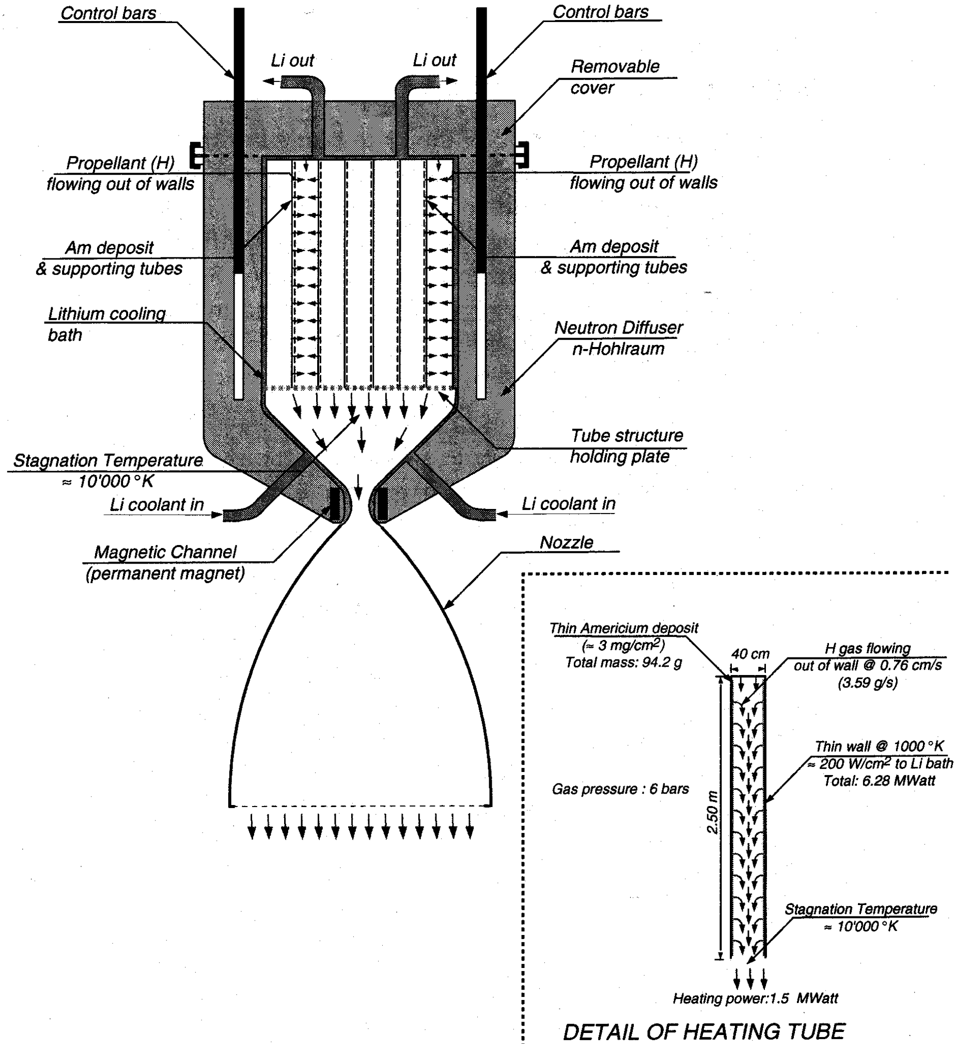

Figure 7.24. Diagram of a generic FF-heated Rubbia's engine. Details of one of the Am-coated tubes is shown in the inset. Cooling is by liquid lithium.

sketched in Figures 7.25 and 7.26. Although intriguing, there are hardly any significant details in the information from LLNL to draw conclusions or even comments.

Among the critical areas discernible at this early stage in Rubbia's engine concept are: the radiative heat loss and cooling of the reactor/chamber, the effect of chamber size (diameter) on criticality, nozzle design and operation, Americium procurement and production, fuel replacement, and certainly ground testing, a critical issue common to all the propulsion systems mentioned. Among the

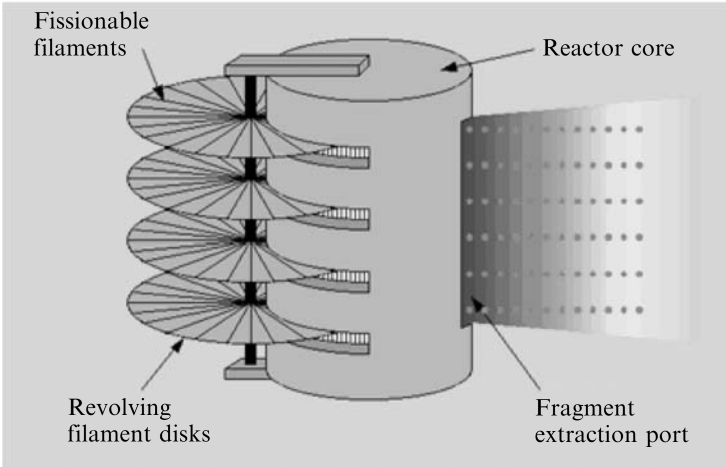

Figure 7.25. A conceptual scheme of the operation of a thin filament.

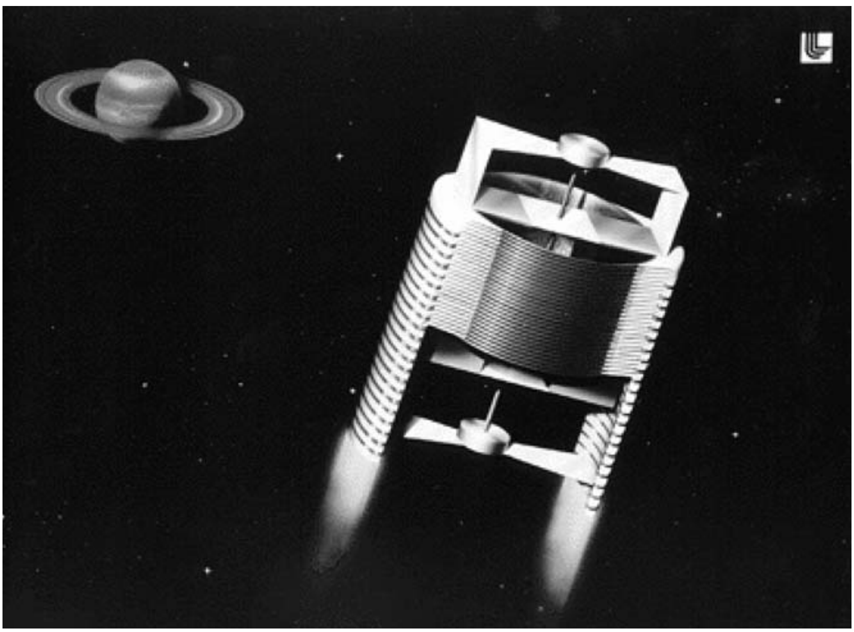

Figure 7.26. Artist's view of a filament fission-powered spacecraft.

advantages of this novel concept is the fact that Am fission can never become critical, an important factor in public acceptance. A third appealing point is the relative simplicity of the reactor design and the potentially large I_{sp} with a reasonably large thrust.

7.14 CONSIDERATIONS ABOUT NTR PROPULSION

At this stage NTR propulsion appears viable for certain fast, possibly manned, interplanetary missions; also, for some fast robotic missions in the outer Earth neighborhood (e.g., for asteroid defence). NTR is being also investigated as a replacement of commercial space launchers, although its is doubtful that it could be accepted under existing regulations (and fears) concerning the use of nuclear energy in space. Similar considerations hold for its application to OTVs (space tugs). Of interest to OTV are missions to clean up space debris from near-Earth space: nuclear-powered OTV could tow dead satellites and last stages from LEO and GEO to much more distant 'graveyard' orbits. Probably this last class of mission could become respectable only if instead of NTR the propulsion system was nuclear electric (see sections below), but the drawback would certainly be a much longer towing time. A special task NTR can accomplish faster and cheaper is changing the orbital plane of near-Earth spacecraft, a maneuver very costly in ΔV, as seen in Chapter 5.

While NTR for manned missions is probably far in the future, orbital transfer missions could have a commercial market right now, if engine and vehicle existed. The large total impulse of NTR (that is, the product of I_{sp} times the operational lifetime of the engine) makes them ideal for this class of mission. MITEE, or even Rubbia's engine, could power a space tug, the MITEE engine featuring lower I_{sp} but also lower volume. The major difference between these two concepts is probably the much prior work already done on the MITEE reactor. Rubbia's engine, projected to have much higher I_{sp}, is still a concept in the developmental stage.

Will the public accept nuclear power in space, including a space tug? The answer to the first part of this question is likely to be a qualified yes, while that to the second is very doubtful: the tug must operate too close to Earth for comfort. In any event, the policy shift toward nuclear propulsion by the current US administration, including NASA, should be complemented by an effort to educate the public about nuclear space propulsion. No effort is in progress at this time, but the public seems rather unconcerned, for instance, about the JIMO mission and its nuclear propulsion. Probably, it is preoccupied with far more pressing issues. Nevertheless this is the most important issue in nuclear propulsion and the object of much speculation among experts, see ['Aerospace America', 2004]. In fact, nuclear propulsion can be made much safer than any conventional rocket-propelled vehicle. During the NERVA program no accidents occurred [Dewar, 2004]; even a deliberate thermal explosion of a Kiwi-type reactor to check for its effects (the Kiwi-TNT experiment) found them insignificant. In this context, health and safety issues associated to nuclear propulsion are summarized in the Appendix.

The fact is, nuclear propulsion in general (not only NTR) is the only alternative to chemical propulsion for many commercial and non-commercial space missions otherwise prohibitively expensive. Under an ideal scenario in which nuclear propulsion was completely acceptable, a space strategy could consist of new NTR-powered launcher stages, featuring large thrust (i.e., greater than 10^5 N/engine) and $I_{sp} \sim 950 - 1000$ sec, and of new spacecraft powered by much smaller engines of thrust $\sim 10^3$ N and with higher $I_{sp} \sim$ 1,500–2,500 sec. Even higher I_{sp} propulsion may be possible farther in the future using nuclear-powered electric-ion or MPD thrusters such VASIMR (Variable Thrust and Specific Impulse Rocket), discussed in the next sections.

7.15 NUCLEAR ELECTRIC PROPULSION

Back in the late 1940s, at the time of the first NTR designs, suggestions were also made to utilize part of the thermal power of the nuclear reactor to generate electrical energy, not necessarily for propulsion but also for other on-board tasks (e.g., communications, radar). Several concepts were proposed; some were recently 'rediscovered' and some resurrected, many still being worth considering. Some do away completely with the 'thermal' propulsion considered in the sections on NTR; others exploit rejected heat from the reactor to generate additional electrical power, and use this power to further accelerate the propellant after nozzle expansion.

What follows is a synthetic description of these concepts; all assume the nuclear reactor is just a source of thermal power, to be coupled to an electric generator feeding electricity to a device that produces thrust, as anticipated in section 7.4. There is little conceptual difference between *conventional* satellite electric propulsion (invariably powered by solar cells) and *nuclear* electric propulsion, except in the scale of power available. Comprehensive reviews of high power NEP engines are in [Auweter-Kurtz and Kurtz, 2003, 2005; Fearn, 2004, 2005].

7.16 NUCLEAR ARCJET ROCKETS

The simplest NEP engine [Bussard and DeLauer, 1958, pp. 328–330] consists of a conventional nuclear reactor supplying heat to a thermodynamic cycle using standard machinery (for instance, a gas turbine, or a Stirling engine). The mechanical power extracted runs an electric generator. This generator feeds an electric arc, converting back electric into thermal power. The propellant is injected into the arc chamber, is heated by the arc and then expanded in a conventional nozzle. Estimated (ideal!) I_{sp} is $\approx$3,000–4,500 sec. In reality, not all propellant going through the arc is effectively heated, and in any case is not heated uniformly. Therefore the practical I_{sp} of arc heaters is typically a factor 2–3 lower than ideal [Auweter-Kurtz and Kurtz, 2003].

Experience with low-power arc heaters indicates that the total mass of the engine system for conventional arcjet thrusters is in the range 10–100 kg/kW, a major worry in space propulsion applications; if this scaling holds also for a nuclear-powered arcjet, the engine mass would be a substantial fraction of the vehicle mass. However, the thrust density (thrust/unit exit area) is higher than in most other NEP systems, with the exception of Hall ion thrusters [Auweter-Kurtz and Kurtz, 2003], and may eventually reach $\sim$3,000 N/m^2, a very interesting value for an electric thruster.

Conceptually, the arcjet mode of operation may be questioned because it is based on a double energy conversion, thermal to electric and then electric to thermal. The fortunes of this concept are tied to a certain simplicity in reaching high temperatures without worrying too much about structural material limits, since the propellant is heated by an arc (mostly by convection and diffusion) and not by a heat exchanger. A serious concern, partly explaining the low I_{sp} of the arcjet, is that much of the heat absorbed by the propellant while traversing the high-temperature arc is stored in vibrational and electronic excitation modes, i.e., in *non-equilibrium* internal modes. During the nozzle expansion this non-equilibrium energy should hopefully convert into flow translation energy, that is, the propellant flow velocity should increase, become uniform and collimated (aligned with the nozzle axis). However, this hoped-for result does not necessarily occur when the expansion is fast and starts from large non-equilibrium temperatures (arc temperatures may reach 25,000 K). What happens is that part of the thermal energy remains trapped ('frozen' is the technical term) inside the heated gas.

The difficulty of heating all propellant uniformly, and the fact that a good fraction of the energy taken from the arc has no time to convert into kinetic energy of the flow are strong reasons justifying why arcjets have been somewhat neglected as propulsion systems, either for conventional or for nuclear electric propulsion. This said, hybrid arcjets, i.e., an arcjet feeding plasma to an induction heating section, look at this time promising for a large power (>100 kW) thruster [Auweter-Kurtz, 2005]. Modules assembled together in a power pack (and suitably cooled) could produce thrust of the order 10 N/100 kW or higher, an excellent value when utilizing a nuclear reactor.

7.17 NUCLEAR ELECTRIC ROCKETS

If the nuclear reactor powers an electric thruster, the propulsion system becomes a 'pure' nuclear electric propulsion (NEP) system, or nuclear electric rocket (NER), in which acceleration is not based on expanding a fluid, but on the presence and strength of electric or magnetic fields. In juxtaposition, thermodynamic expansion has an efficiency, η, that depends on the ratio between the maximum and the minimum propellant temperature. η can be enhanced only up to a point, because of materials temperature limitations already discussed.

Both magneto-hydro-dynamic (MHD) acceleration based on the *Lorentz force*, and electrostatic acceleration based on the *Coulomb force*, as in ion thrusters for commercial TLC satellites, look very convenient thrust-producing mechanisms, because per se they do not imply thermodynamic losses. In both strategies reactor and propulsion system are separate objects, lending themselves to separate optimization of each, see Figure 7.7.

However, the electricity must be generated somehow: a nuclear reactor produces (so far) only heat. If electricity is from conventional generators, the η issue reappears: this time η is not that of the electric thruster, but that associated to the thermal to electric energy conversion process. Alternatives to conventional (thermodynamic) electricity generation have been proposed, but the step from proven physics to engineering is still a long one, e.g., see [Bidault et al., 2004; Backhaus et al., 2004]. In this area the group of Professor S. Anghaie at the University of Florida has proposed MHD power generation, by utilizing the ionized plasma from a gas-core reactor, see for instance [Smith and Anghaie, 2004] The conversion process comes also with a high price in terms of mass: for instance, stated goals at NASA-Glenn for the JIMO mission are a mass/electric power ratio less than 40 kg/kW$_e$ (the subscript indicates electric power, not the reactor-generated power). Payload and trip duration depend critically on this ratio, see [Oleson and Katz, 2003]. This ratio should be compared with NASA's same goal for NTR, that is 0.08 kg/kW! The stunning difference is the result of the naturally low efficiency of energy conversion, and of the mandatory space radiator. NTR do not need either.

Ion and MHD-based thrusters have been studied for many years; their main features can be found, for instance, in [Sutton, 1992] and will not be reported here. Almost invariably, all electric thrusters have been powered by solar cell arrays, that is, at low power. What is new in the context of NER is the scale of the power available when switching from solar arrays to nuclear reactors. Scaling thruster power from kilowatts to megawatts involves opportunities as well as engineering and technology challenges and issues. These are still far from having been satisfactorily analyzed. A recent workshop has begun to focus on some [Alta, 2003].

7.18 ELECTROSTATIC (ION) THRUSTERS

Nuclear-powered electrostatic acceleration [Bussard and DeLauer, 1958, p. 330; Sutton, 1992] is essentially that in commercial ion engines: an applied voltage creates an electrostatic field, and the Coulomb force accelerates electrically charged (ionized) propellant. With nuclear power, the only conceptual difference is in the larger voltages and power one can afford. What is known about ion engines tells that thrust is limited by space charge, breakdown voltage and size of engine exit cross-section (power density, or thrust density, W/m^2 and N/m^2, respectively). Even so, 1-MW prototypes have been built and laboratory-tested [Fearn, 2003]. Performance has been extrapolated with scaling laws at input power up to about 6 MW [Fearn, 2004]. The results indicate thrust density may reach about 300 N/m^2, a rather respectable figure, with I_{sp} of order 30,000 sec. The thrust/power ratio is about 6,900 N/MW. For comparison, a NTR has a ratio three to four times larger, but of course with an I_{sp} about 30 times lower.

Because ion engines have been installed on geostationary commercial satellites, most unmanned interplanetary missions have been studied or planned around nuclear-powered ion propulsion. This engine technology is mature and space-qualified, but has been always used, by necessity, at low power. For the JIMO mission planned by NASA the xenon propellant ion thruster is in the 16–25 kW class [Randolph and Polk, 2004; Scina et al., 2004], a veritable jump over what was possible in the past using solar cells. The robotic Venus mission being investigated at NASA-Glenn (the so-called RASC Venus mission in [McGuire et al., 2004]), also assumes a nuclear ion engine, even though near Venus photovoltaic power would be twice that available near Earth (the so-called 'solar constant', is 1,250 W/m^2 near Earth, about half of that near Venus).

Commercial ion engines use the rare gas xenon as propellant. Whether enough will be available for large (nuclear) engines and long missions must be assessed. The world production of xenon is about 59 tons/year, and its price (in 2004) about \$1,700/kg. At 1 MW power and 70% conversion efficiency, and assuming I_{sp} is 4,000 sec, the consumption of xenon per year of mission would be 13.6 tons, or more than one-fourth of the entire yearly world production. Note that operating an ion engine continuously for 1 year or more is realistic, since under these assumptions the thrust would be only 17.5 N, and the acceleration modest. In fact, a criticism leveled by current NASA Administrator M. Griffin to the JIMO mission, in its version including flybys of Callisto and Ganymede, is that it would consume twice the present world's production of xenon [Berger, 2005b].

This and other questions concerning the balance between I_{sp} and power when planning interplanetary missions can be better appreciated by looking quantitatively at their effect on propellant mass and ΔV. Note that these questions are not relevant to chemical propulsion, because thrust (applied for a very short time) is the variable controlling acceleration, not power. These are instead 'the' issues in electric propulsion, where thrust may have to last for months or years. The relevant (simplified) equations to quantify fast missions made possible by nuclear electric propulsion are:

$\dot{m} = F/I_{sp}$ — I_{sp} definition

$m_{ppl} = Ft_{acc}/I_{sp}$ — mass of propellant consumed at constant $\dot{m}$ after a time t_{acc}

$d_{acc} = 0.5a(t_{acc})^2$ — distance traveled at constant acceleration, a

$\Delta V = at_{acc}$ — ΔV acquired after time t_{acc} at acceleration a

$F = Ma$ — Newton's law; M is the total mass of the spacecraft

Then solving for time, mass m and ΔV, we have:

$$t_{acc} = \sqrt{\frac{2d_{acc}I_{sp}M}{P}}$$

$$m_{ppl} = \sqrt{\frac{2d_{acc}PM}{I_{sp}{}^3}}$$

$$\Delta V = \sqrt{\frac{2d_{acc}P}{I_{sp}M}}$$

where M, d_{acc} and power P have been assumed as input parameters. The solution set is plotted in Figures 7.27(a), 7.27(b) and 7.27(c). Note the favorable effect of I_{sp} on propellant mass and its opposite effect on acceleration time and ΔV: at fixed power, increasing thrust must come at the expense of decreasing I_{sp}, so it takes longer and longer to reach smaller and smaller ΔV.

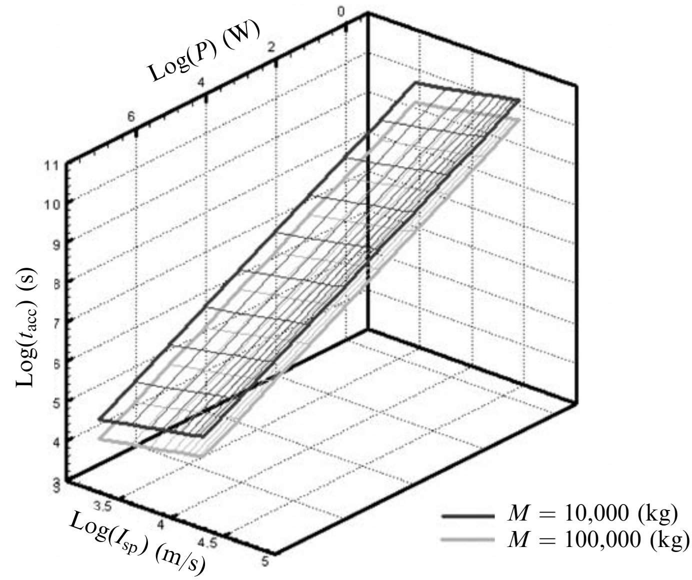

Figure 7.27(a). Acceleration time for a spacecraft of mass 10,000 and 100,000 kg as a function of power P and I_{sp}.

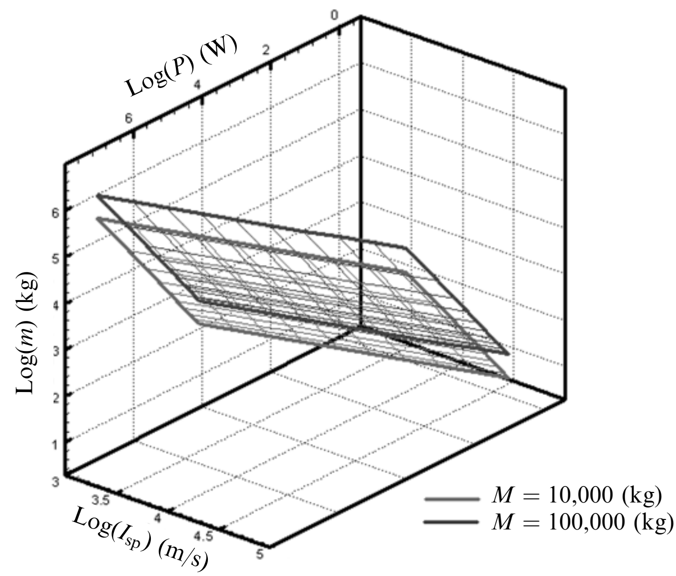

Figure 7.27(b). Propellant mass for a spacecraft of mass 10,000 and 100,000 kg as a function of power P and I_{sp}.

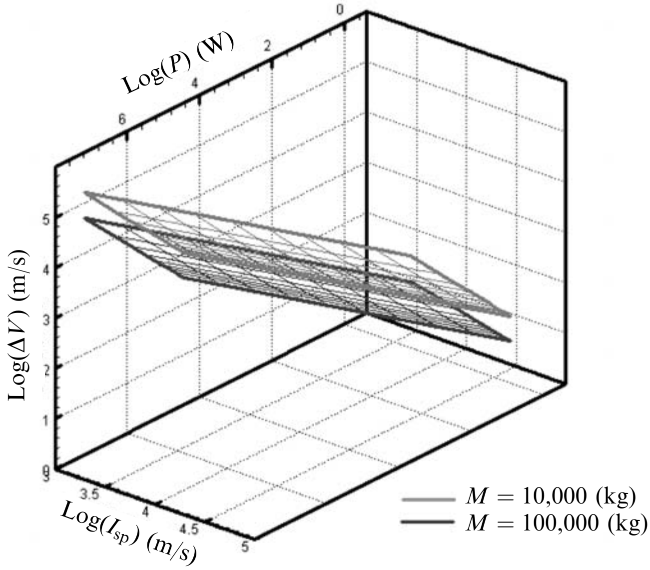

Figure 7.27(c). ΔV for a spacecraft of mass 10,000 and 100,000 kg as a function of power P and I_{sp}.

In planning an interplanetary mission where at least part, d_{acc}, of the trajectory length is flown at steady power, one may assume M and P as input. At a first glance d_{acc} should be limited to half the distance d to the final destination (past that the spacecraft should start decelerating). However, d_{acc} may turn out to be greater than d when the acceleration $a = P/(I_{sp}M)$ is very small, i.e., at very low thrust and power. In this case the spacecraft must spiral (for instance, around Earth), until reaching the right escape ΔV. At that point the ship can start accelerating along the trans-planetary trajectory.

To show problems posed by powered trajectories, consider propulsion solutions for a nominal Earth to Mars mission (minimum d about 1.5×10^8 km) using a hypothetical 0.7-MW ion engine with $I_{sp} = 4{,}000$ sec, and spacecraft mass $M = 100$ ton. Assuming $d_{acc} = 10^7$ km, equations predict $m = 5$ tons, $t_{acc} = 1{,}157$ days and $\Delta V = 2$ km/sec. This is an impracticable solution; stretching d_{acc} to 8×10^7 km (about half the Earth–Mars distance), the new solution predicts $m = 15$ tons, $t_{acc} = 3{,}450$ days and $\Delta V = 6$ km/sec, still too low. This is not only impracticable, but also costly in terms of xenon. Raising power by a factor 10 to 70 MW, the (third) solution requires $m = 135$ ton (violating the $m \ll M$ assumption), but both $t_{acc} = 33$ days and $\Delta V = 54$ km/s look good. Although calculations should be repeated, to reduce the xenon mass until satisfactory, a practicable fast mission seems within reach, but mass expended would consume a good portion of the annual worldwide production of xenon.

Note $M = 100$ tons would be an absolute minimum for an interplanetary manned spacecraft. The preliminary conclusion is that for certain (ambitious) missions current or projected ion engine technology is insufficient to produce a 'good' trajectory, meaning reasonably fast and cheap. Only much higher I_{sp}, of order 10 times those now available (that is, 40,000 sec) can provide a truly satisfactory solution: this means much more powerful nuclear reactors. Scaling electric thrusters (in this case ion engines) from the small ones working on geostationary satellites has implications beyond simply engine sizing. However, the technology developed to inject plasma beams inside fusion reactors (Tokamaks; see also Chapter 8) may supply viable solutions. To avoid quenching fusion reactions near the inner walls, plasma fed to the reactor must reach high velocity. So, the feeding device may be considered an electric ion thruster. In fact, this seems to be the case, an power levels $\sim$1 MW, with thrust of the order 20 N or more, are projected in the near future [Fearn, 2005].

7.19 MPD THRUSTERS

High-power MHD thrusters are less developed than ion engines, and to a large extent are still laboratory items. Exploiting the Lorentz force, MHD acceleration occurs when a flow of charges, e.g., electrons and ions, in all respects equivalent to a current, **J**, moves in a magnetic field **B**. The Lorentz force is $\mathbf{F} = \mathbf{J} \times \mathbf{B}$: it accelerates charged species moving in the magnetic field **B** and according to Newton's Third Principle, creates thrust. The state of a gas containing charged species, that is, an ionized gas, is called 'plasma state'. So, a plasma can be accelerated by the Lorentz force and produce thrust. Accordingly, this type of rocket engine is called a Magneto-Plasma-Dynamic thruster (MPD thruster).

The regime of an MPD thruster can be steady in the strict sense, or quasi-steady. The thrust of a quasi-steady MPD may occur in pulses or bursts; when these last long enough, or when the burst repetition rate is high enough, the averaged thrust is said to be quasi-steady. Quasi-steady MPD thrusters have been tested far more than steady MPD, one of the reasons being their lower power demand, and another their relative simplicity. For high-power applications steady MPD are better, but without a nuclear generator there is no way they can become effective space engines.

The simplest nuclear-powered MPD concept consists of a nuclear reactor generating electricity and driving an MPD accelerator. Laboratory MPD engines are of course powered by photovoltaic (solar) cells, have I_{sp} in the order of 10^3 to 10^4 sec, but their weight and size are much larger than those of ion engines. A laboratory MPD thruster may have a mass/power ratio of order 1–10^3 kg/kW, depending on scale. Most of this mass is that of the electric conductors (wiring), especially those of the magnetic coils. If superconducting wires replaced copper, coils and windings mass could be reduced by 1–2 orders of magnitude [Bruno and Giucci, 1999; Casali and Bruno, 2004].

In fact, recent advances in MPD technology have brightened the prospective of this type of electric propulsion. MPD propulsion has been dormant because the power required to reach acceptable efficiency was too large for commercial satellites and space vehicles (it takes hundreds of kilowatts to achieve efficiencies greater than

30%), and also because such power is unattainable with solar cells. Historically, MPD propellant acceleration suffers from many losses, for instance, (a) propellant composition 'frozen' during expansion, preventing conversion of internal energy, as in arcjets; (b) plasma instabilities, the bane of all plasma applications, increasing plasma resistivity, driving unstable currents and wasting power; (c) excess heating of, and near, the anode; and especially (d) cathode erosion/evaporation, reducing cathode life.

A drawback of MPD engines is also their low thrust density, by a factor 5–10 lower than other electric thrusters [Auweter-Kurtz and Kurtz, 2003]. The reason is that plasma pressure must be low enough so that collisions do not prevent charges from following the magnetic force-lines. The consequence is large internal and nozzle volumes for given thrust or power.

Together with that of power, the major issue of MPD was and still is cathode life. Because of the low thrust, missions using NEP may last 5 to 6 years [Oleson and Katz, 2003], depending on I_{sp}, and mass per unit power. Over months or years of operation even tungsten cathodes erode at the rate of approximately 0.2 μg/coulomb [Choueiri, 2000]. This figure may look insignificant, but a 20-kW MPD thruster, such as those considered for the JIMO mission, will need 20 A when operated at 1,000 V, that is 20 coulomb/sec. In a day alone about a third of a gram of tungsten will have been eroded. When Russian technology and know-how on steady plasma thrusters became available after the end of the Cold War, the pace of progress in this area quickened. Interest by USAF in a particular type of MPD propulsion (Hall thrusters) is contributing to advance this field.

In fact, the most important recent development in MPD is probably the replacement of hydrogen propellant (with high ionization energy, of order 13.8 eV) with propellants with much lower ionization potential, in particular lithium (its ionization potential is 5.37 eV). Lithium can extend cathode life by orders of magnitude [Choueiri, 1998]. Some MPD laboratories (MAI/RIAME in Moscow, CalTech Jet Propulsion Laboratory and Princeton University's Plasma and Electric Propulsion Laboratory) are now collaborating in this specific area. The Russian company NPO Energia has tested a RIAME-designed 130-kW, 43% efficiency Lorentz force MPD thruster using lithium propellant and found very low cathode erosion. Cathode lifetimes of more than 1,000 h are now within reach. Measured I_{sp} was 3,460 sec, with a thrust of order 3.2 N. Thrust of order 25 N/MW looks feasible. Future plans (in the 2010 timeframe) include a 100-kW and a 120-kW steady MPD thruster.

Before Project Prometheus was started, NASA was planning improbable 20 MW, solar-powered MPD experiments in 2012, and 100 MW in 2024, clearly for interplanetary missions such as a Mars mission. After then NASA Administrator, S. O'Keefe, put emphasis on nuclear power, the future of these plans was uncertain for some time, but still indicated that MPD propulsion was considered viable for long interplanetary missions. The major questions in this context center on the power and type of thruster, that is, below or above 100 kW and whether ion or MPD; at the moment, mission analysis by NASA is focusing on a 25-kW ion engine for future unmanned JIMO mission to Europa, Callisto and Ganymede [Bordi and Taylor, 2003].

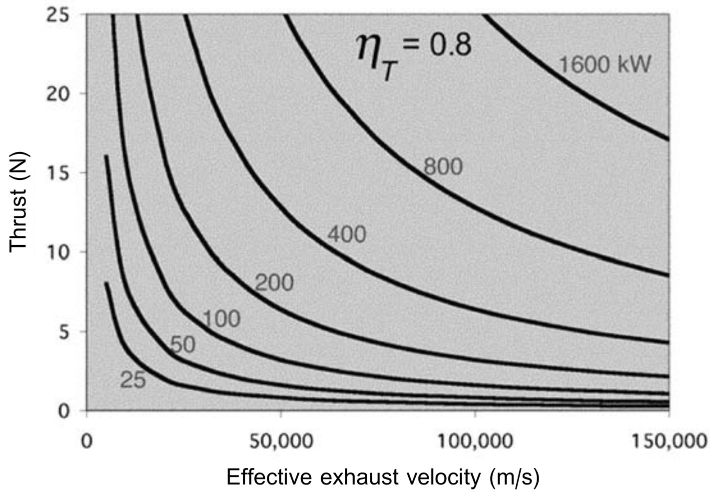

Figure 7.28. The thrust vs. I_{sp} dilemma at fixed power (thrust conversion efficiency assumed to be 0.8) [Andrenucci, 2004].

What power and which type of electric thruster to choose are issues that will benefit from a recent NASA decision to fund electric thruster research, again under Project Prometheus [Iannotta, 2004]. An Advanced Electric-Propulsion Technologies Program will compare MPD and pulsed inductive thrusters, developed at Princeton University and Northrop Grumman, respectively. The first will use lithium, while the second thruster will use liquid ammonia, a much cheaper propellant. The power will be about 10 times that for the JIMO mission, that is, of order 200 kW. Thrust conversion efficiencies are predicted to be about 70% for the Northrop thruster, vs. 60% for the lithium MPD thruster of Princeton University.

Once cathode life and propellant issues are solved, to be competitive with ion engines in fast interplanetary missions MPD thrusters must show they can handle much more than the 20 kW power of a JIMO mission: for comparison, the maximum laboratory-tested ion engine power known is 1 MW [Fearn, 2003]. Power is a key element of any NEP trajectory, because it determines the thrust and thus mission length. Figure 7.28 [Andrenucci, 2004] is indicative of the trade-off between I_{sp} and thrust typical of fixed power propulsion (a thrust conversion efficiency $= 0.8$ has been assumed in this figure). Because power $P = I_{sp} \times F$, the curves are hyperbolas, showing the main limitation of electric propulsion (in fact, of any propulsion system) is power available.

In this context it is probably useful to dispel the myth of solar power as a viable energy source for future interplanetary missions. To collect 1 MW by solar cells in LEO one would need 5,330 m^2 of cells, the area of a football field, assuming an optimistic 15% cell efficiency. Furthermore, the solar constant decreases with the square of the distance from the Sun: near Mars the solar constant is 2.2 times lower than near Earth. This means that Mars missions using solar power should be either very long, or use two or three football fields of solar cell arrays. For missions to the outer planets, such as Jupiter, the solar constant decreases so much that a practical 1-MW power source for an MPD thruster cannot be solar. A 100-MW thruster, e.g., for a manned mission, would need half a million square meters of cells. The sheer weight and cost of orbiting such array would be staggering [Koppel et al., 2003].

Although lagging behind ion engines, marrying MPD technology to nuclear power seems ideal for faster interplanetary missions, the more so because lithium is a very good coolant for advanced nuclear reactors [Buffone and Bruno, 2002]. The reactor could generate all the thermal power needed by the MPD thruster. However a 100-MW nuclear reactor is not a significant challenge as is the electric generator: there is hardly any known experience of generating 100 kW of electric power in space, let alone 100 MW. Probably this is the single most critical technology area in all NEP.

In whatever form, NEP, and in particular nuclear MPD propulsion, is a multi-technology field. For maximum performance MPD-based NEP should integrate superconductivity, electric thruster and nuclear reactor in a single electrically and thermodynamically efficient package. Assuming an MPD core mass reduction by two orders of magnitude, made perhaps possible by future superconducting wiring, the MPD accelerator could weigh 10–50 g/kW, resulting in an engine mass of order 1 ton for a 100-MW engine. An important implication is that scaling laws for MPD thrusters should be derived prior to actual engine sizing. Such laws have been derived to miniaturize much smaller self-field MPD, see [Choueiri, 1998; Casali and Bruno, 2004], but have never been tested in extrapolating to *higher* power (scaling for *ion engines* can be found in [Fearn, 2004]).

A final remark on nuclear electric propulsion is that the thermal power rejected by the thermodynamic cycle to produce electricity is of the order of 50% or more. It could be put to good use, for instance to vaporize and perhaps ionize a propellant with low ionization potential such as lithium. This would result in an additional thrust, with a lower I_{sp}, of order $O(10^3)$ sec, simultaneously reducing mass and surface of space radiators. The negative face of this proposal is a much more complex engine. Nevertheless, given their potential higher thrust, mixed ('hybrid') thermal–NEP systems warrant further study, and appear a possible interim solution for interplanetary missions. In fact, still at the conceptual stage, they are the subject of several recent investigations, and for this reason are briefly discussed below.

7.20 HYBRID/COMBINED NTR/NER ENGINES

In this class of proposed concepts the purpose is to integrate nuclear reactor, electric propulsion and superconductivity technologies in a single engine. Except solid-core NTR, all nuclear engines must necessarily reject a large fraction of the heat generated (in Rubbia' engine this is almost 50%; in other NEP concepts this fraction is even higher). NTR 'reject' most of the heat to the propellant, so a radiator is not needed at all.

In all other nuclear engines it looks convenient to recycle waste heat to generate electric power. The simplest way is through standard thermodynamics. The electric

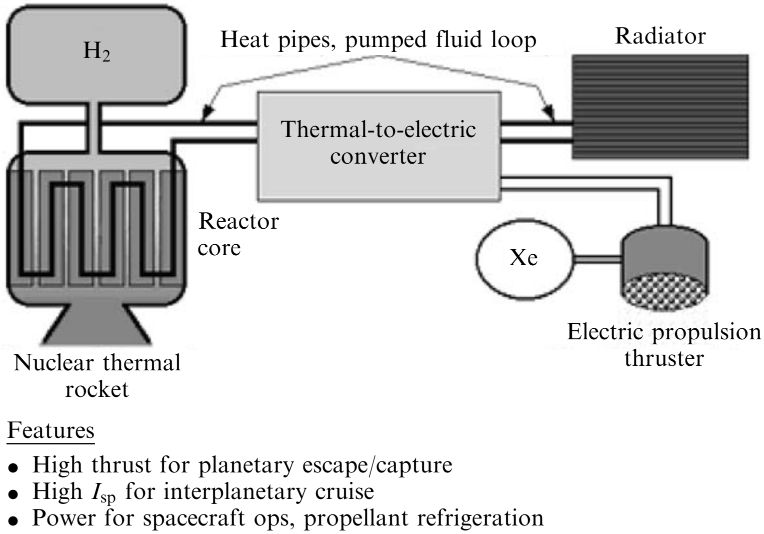

Figure 7.29. Generic hybrid nuclear thermal and nuclear electric rocket (parallel system shown).

power recovered could magneto-hydro-dynamically accelerate the exhaust from a nuclear thermal rocket (tandem hybrids, see [Augelli et al., 1999; Dujarric et al., 2000]), or feed an ion or MPD thruster (parallel hybrids). Alternatively, power recovered could fulfill special tasks. Fast telecommunication systems, synthetic aperture radars [Gafarov et al., 2004], CO_2 or iodine lasers (to melt ice) are special task candidates. In any event, even partially recovering waste heat can shrink the size of space radiators, which are massive components in nuclear propulsion.

Examples of this strategy start with the 'bimodal' NTR proposed in [Borowski et al., 1999], later expanded to 'trimodal' to include also chemical propulsion [Joyner et al., 2004]; the 'indirect' nuclear propulsion system of [Chew et al., 2004], in which a nuclear reactor heats the propellant via a heat exchanger, uncoupling the power core from the propulsion systems; and the hybrid NTR/NEP described in [Powell et al., 2004], where the waste heat of a MITEE engine (see section 7.14) is converted to electric power feeding a conventional electric thruster. The more straightforward of such proposals would be to use waste heat simply accelerate the expanded exhaust of a NTR, similarly to what done by afterburners in jet engines.

The conceptual appeal of these proposals needs to be weighed against their additional complexity. Figure 7.29 shows a parallel hybrid configuration, in which part of the waste heat from the nuclear reactor generates electricity powering an ion engine. The many subsystems suggest that complexity and mass will be much higher than a single NTR or NEP system

On the positive side, hybrids may have decisive advantages. NTR have typically large thrust and low I_{sp}, while electric thrusters feature just the opposite. In many missions the two different modes of propulsion may be present to power different segments of the trajectory. Then how to divide nuclear power between NTR and electric thruster becomes a paramount question: different missions may need different NEP to NTR power ratios. For instance, orbiting or deorbiting near planets may demand high thrust to save time: this is the case for crewed spacecrafts. For this class of missions the ideal propulsion system should be capable of large thrust at low I_{sp} to reach escape speed quickly, followed by much smaller thrust but much higher I_{sp} to keep accelerating, even at a modest rate, toward final destination. A hybrid NTR coupled with an electric thruster has such capability by design. Criteria and modes (i.e., tandem or parallel) of apportioning power between two very different propulsion systems have not been derived yet for interplanetary missions, and need to be addressed in the future. Historically, these questions were raised at the dawn of the jet engine age (early 1940s), when many airplane manufacturers were designing fighters with both jet *and* piston engines.

From the efficiency viewpoint, among the many issues of tandem hybrids is that of ionization. Ionization, needed to enable electric thrusters to work, might absorb an excessive fraction of the waste heat recovered. Performance of each engine (NTR and electric) depends on temperature in roughly opposite ways: ionization of the NTR exhaust should be as low as possible to recover most of the thermal energy; to operate a ion or MPD accelerator, ionization should be as high as possible. A tandem NTR + MPD thruster will likely require seeding the exhaust from the NTR with low ionization potential metals, for instance K, Ba or Li.

In fact, lithium could be *the* propellant for the NTR engine, alone or mixed with hydrogen. This tandem hybrid concept looks promising in the case of Rubbia-type NTR. MPD acceleration of a Li plasma, with $I_{sp} = 3{,}000$ sec, has been demonstrated even when the plasma regime was collisional. Although MHD acceleration of H or H + Li exhaust has never been tested, it is interesting to estimate its effect on the nominal performance of the Rubbia's engine reported in [Augelli et al., 1999]. The efficiency of MPD acceleration ($\sim$40–50%) should raise I_{sp} by 100–200 sec, with a simultaneous reduction of the space radiator mass. Assuming $I_{sp} = 2{,}500$ sec as baseline for the Rubbia's engine, the effect of recovering waste heat would be of order 4% to 8%.

7.21 INDUCTIVELY HEATED NTR

This concept has been called 'hybrid' by its proponents [Dujarric, 1999; Project 242 WG, 1999], in the sense that is neither a pure NTR, nor an electric thruster concept. Its thermodynamics is in fact closer to that of an arcjet as suggested by the work of Auweter-Kurtz and Kurtz, 2005] in section 7.16. In the first version of this concept, part of the nuclear power heats the propellant as in any conventional NTR; the rest heats it by means of induction coils located along the conical portion of the expansion nozzle. The induction power is generated by the waste heat rejected by the nuclear reactor. This arrangement was proposed mainly to reduce space radiator size and mass, and raised I_{sp} by an (estimated) 132 sec, to a total $I_{sp} = 1{,}041$ sec [Dujarric, 1999].

Alternatively [Augelli et al., 1999], the nuclear reactor could simply generate electricity feeding the induction loops that heat the propellant. The reactor would generate all the electric power needed by SC induction coils. This second concept is more radical, and performance will depend much on the specifics of the design. In both original and alternative concepts, success holds on the balance between energy inductively deposited in the propellant, and that lost by plasma through radiative heat transfer.

All these propulsion systems producing thrust power via conventional machinery suffer a substantial η penalty: it is inefficient to generate thermal nuclear power, convert it into electricity (with η no higher than perhaps 50%) and then convert the electricity back into heat. The only advantages conceivable at this early stage are probably the ability to manage power, and especially to control the power distribution/injection *along the engine* system: it is much easier to handle electric rather than heat power.

No estimates are available for the total mass of such systems. However, their general philosophy and layout resemble modern so-called 'clean' high enthalpy wind tunnels (for instance, the Plasmatron wind tunnel at the Von Karman Institute in Belgium [Bottin et al., 1998a, 1998b]). A mature Russian technology, Plasmatrons have shown to have good performance and little or no problem in inductively heating air to form air plasma at 7,000 to 9,000 K. By replacing air with hydrogen, for the same temperatures the I_{sp} attainable should be in the 2,000–2,500 sec range, including radiation losses. One of the problems in designing inductive heaters is predicting the effect of scaling from relatively small power and sizes up to the power required for a large engine, e.g., for a Mars mission. However, *clustering* individual thrusters of 1–2 MW power each appears feasible with an adequate cooling strategy, and 1-MW Plasmatrons are an established technology.

In conclusion, inductive NTR heating of propellant, either alone or in combination with conventional nozzle expansion is a concept worth investigating further for interplanetary missions. That is probably one of the reasons why ESA has acquired the patent rights to this technology.

7.22 VASIMR (VARIABLE SPECIFIC IMPULSE MAGNETO-PLASMA-DYNAMIC ROCKET)

VASIMR is a high power, electrothermal plasma rocket concept currently under development at its NASA Johnson Space Center in Houston by a team headed by astronaut Dr Franklin Chang Diaz [Musser and Alpert, 2000; Chang Diaz, 2000]. VASIMR technology borrows heavily from US fusion R&D, and especially from the vast experience in plasma heating by radio-frequency electromagnetic waves, or RF heating for short.

Although VASIMR can be classified as a MPD thruster, it possesses some unique features worth setting it apart from MPD propulsion. No claim is made

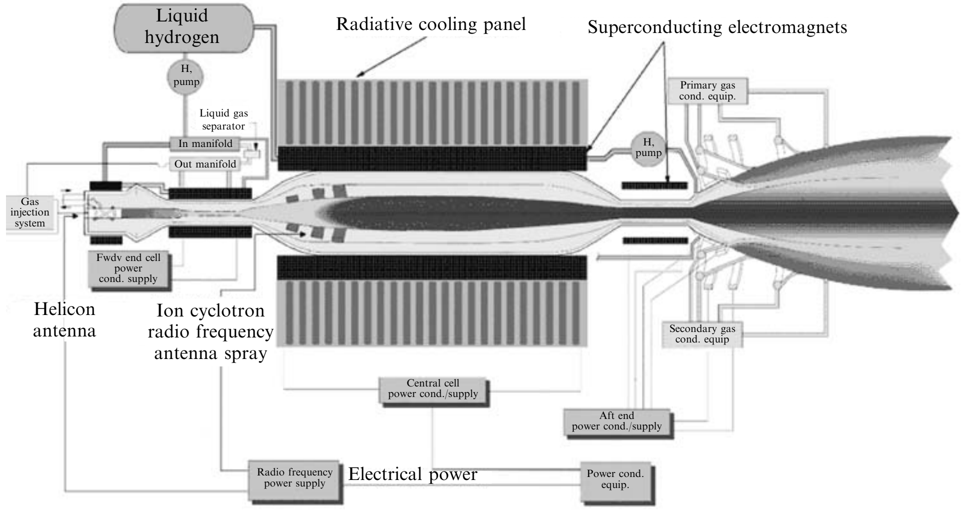

Figure 7.30. Schematic of variable specific impulse magnetoplasma rocket concept [NASA-JSC, 2000].

by NASA as to the power source of VASIMR, but I_{sp} and thrust imply power so large that a nuclear source appears to be the only practicable solution. VASIMR is of great interest because it purposely meets the requirement of an ideal interplanetary propulsion system mentioned in section 7.19, that is, higher thrust at low I_{sp} or lower thrust and high I_{sp}, so that the product of the two, the power, remains constant.

In its simplest scheme the VASIMR system consists of three major magnetic functional blocks, or cells, denoted as 'forward', 'central' and 'aft'; this configuration is called by plasma physicists an asymmetric mirror (see also Chapter 8). The forward cell handles the injection of propellant and ionizes it, turning it into plasma; the central cell acts as an amplifier to further heat the plasma using electron cyclotron resonance (ECR) to the desired energy input for the magnetic nozzle. The third, aft end-cell, is a hybrid two-stage magnetic nozzle that converts the thermal energy of the plasma into kinetic energy of axially directed flow, while ensuring plasma is kept away from the nozzle walls by a magnetic field. Without the aft end-cell, the plasma flow would tend to follow the magnetic field 'corkscrewing' (spiraling) along the magnetic field lines, and the large tangential component of the plasma velocity would be wasted (only the axial component produces the momentum change we call thrust).

With this configuration and strategy, the plasma is claimed to be controllable over a wide range of temperatures and densities. A schematic of the VASIMR system is reported in Figure 7.30.

During VASIMR operation, neutral gas (typically hydrogen, but also deuterium) is injected at the forward end-cell and ionized. The plasma is radio-frequency (RF) heated within the central cell to the desired temperature and

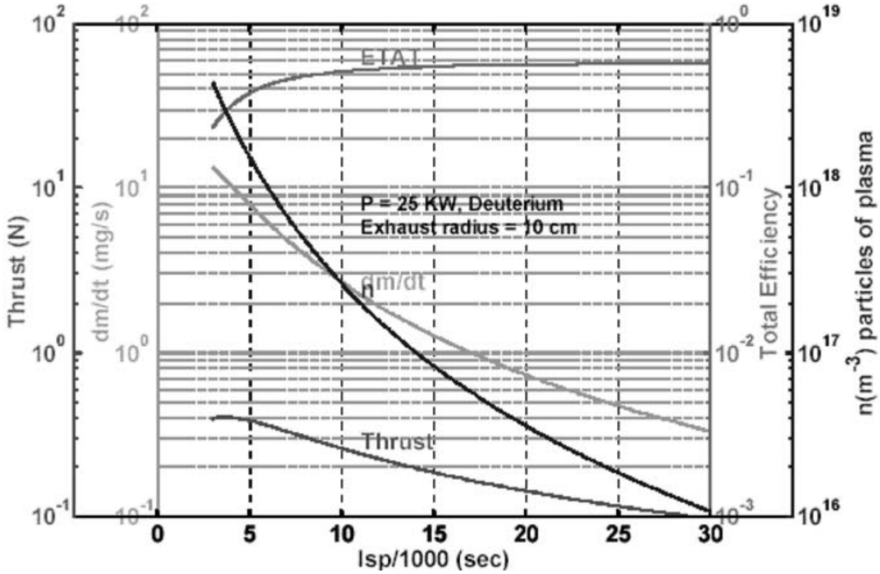

Figure 7.31. Thrust and propellant rate vs. specific impulse [ASPL, 2000].

density. RF heating exploits ECR (electron cyclotron resonance) [Ilin et al., 2000; Takao et al., 2000]: electrons readily absorb the energy of radio waves tuned to the frequency of electrons spiraling around the magnetic force lines. The heated plasma is magnetically and gas-dynamically accelerated and exhausted from the aft end-cell.

The key feature of VASIMR plasma rocket operation is its purported capability to vary, or 'modulate', the plasma exhaust while maintaining constant power. During a typical operation, two parameters are varied while keeping the power constant: thrust and exhaust velocity (i.e., I_{sp}). Therefore, during an interplanetary mission, most of the trans-planet trajectory (the portion of the trajectory from near Earth to the planet) can be traveled at a constant and moderate thrust, with a modest but useful acceleration and with high I_{sp}. When the spacecraft must slow down to reach its final destination (e.g., for planetary orbit capture), thrust may be increased, reducing capture time at the expense of a lower I_{sp}. According to the information available [Chang Diaz et al., 2000; Ilin et al., 2000], this concept is capable of an $I_{sp} = 10^4$ sec with a thrust of 1,200 N, increasing to 3×10^5 sec with a thrust of order 40 N [Chang Diaz et al., 1999; Ilin et al, 1999, 2000; ASPL, 2000]. Figure 7.31 shows how the rocket thrust and propellant flowrate depend on the specific impulse for a Mars mission spacecraft powered by a 10-MW VASIMR. Figures 7.32 and 7.33 show trajectories from Earth to Mars and vice versa.

There are several theoretical advantages in using this propulsion system for interplanetary missions. The main advantage is variable I_{sp} and thrust at constant power, so this system is adaptable to slow, high-payload robotic cargo mission as well as fast, lower-payload manned missions. The electrodeless design of the plasma generator does away with erosion. If power density will eventually be as high as

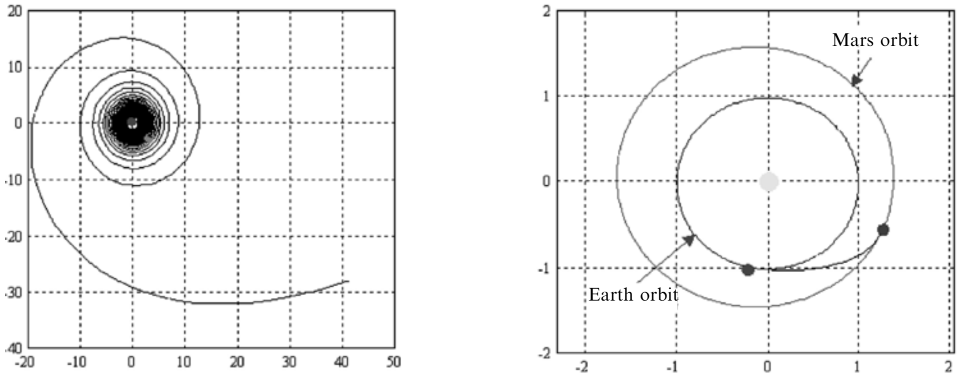

Figure 7.32. 30-day spiral trajectory from Earth and transfer to Mars [ASPL, 2000].

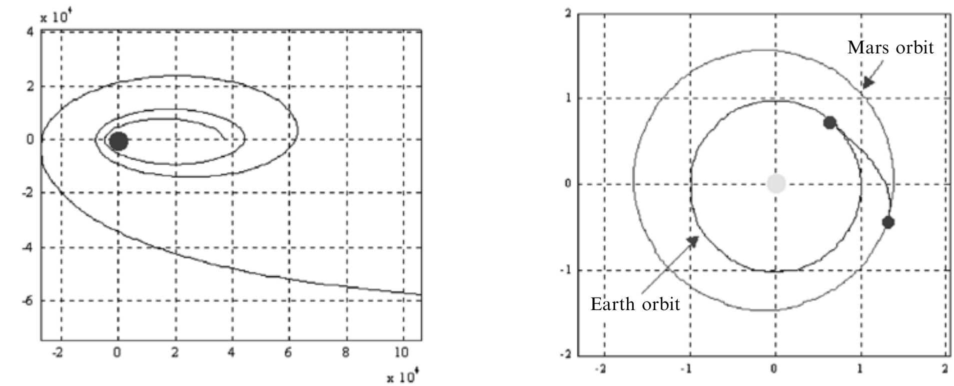

Figure 7.33. 7-day spiral trajectory from Mars and return to Earth using a VASIMR.

claimed possible, that and high I_{sp} can enable trajectories under continuous acceleration, convenient when artificial gravity is desirable. RF heating has been tested in fusion reactors for 30 years, needs high voltage but low current, and is therefore efficient. VASIMR has a powered-abort capability, an important point for manned missions.

Key technologies recognized so far are superconducting magnets (experiments at NASA-Johnson SC are in fact being currently planned); the power source; a compact and reliable RF heating system; the hybrid magnetic nozzle preventing plasma from heating the walls too much; and the cooling and shielding system (plasma radiates over a broad wavelength region).

The second key item points to nuclear power as the source of choice: an I_{sp} of order 10^4 sec coupled to a thrust of order 10^3 N means power must be of order 100 MW. With such on-board power available, storing cryogenic propellants (hydrogen or others), and operating superconducting magnets to save wiring mass do not pose problems in interplanetary missions. RF heating is still a challenge, but past US work to ignite fusion tokamaks (see Chapter 8) can help in this context.

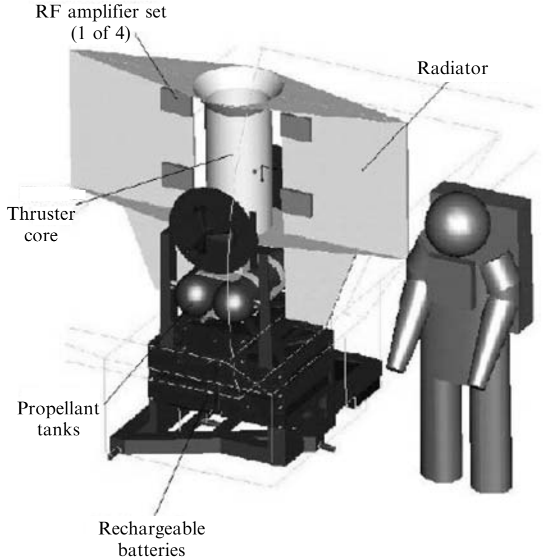

VF-24 max budget	**(kg)**
Thruster core	84
Propellant supply	30
Thermal control	95
Power	540
Structure and attachment	153
Growth margin	226
TOTAL	1128
Power	24 kW
Propellant	H,D,He

Figure 7.34. Schematic view of the system for a VASIMR flight experiment [NASA-JSC, 2000].

Among factors not initially considered by the VASIMR team is the radiation heat loss from the propellant plasma to the walls. Plasma radiation grows in importance from 9,000 K on and especially at moderate ($\sim$1 atm) pressures. Recent NASA analyses seem to indicate these losses can be contained and should not affect the theoretical performance of VASIMR. A second controversial issue is the effect of pressure on magnetic confinement of plasma. To ensure full plasma control by the magnetic fields in the second and third section of the VASIMR, plasma must be reasonably collisionless. This implies the plasma density should be low, a requirement opposite to that of keeping radiative losses under control and of achieving high power density (power/unit cross-section of the engine, or power/volume). It is practically certain that a VASIMR will be much larger compared to other types of electric thrusters, i.e., its thrust per unit exit area will be lower.

The VASIMR concept is envisioned as eventually evolving into a real space engine of power up to the 100 MW mentioned. In 2000, NASA efforts were focusing on a flight opportunity for a radiation and technology demonstration mission sponsored by JSC, GSFC, and GRC teams. The first flight experiment planned using this new technology was designed around a 10-kW solar-powered spacecraft. The spacecraft with a VASIMR engine was to be lofted to several thousands of kilometers above Earth, and perform scientific measurements of the Van Allen radiation belts. A schematic view of this system and its tentative mass budget is in Figure 7.34.

After Project Prometheus and JIMO begun to be discussed, the future of VASIMR became less clear: VASIMR suits a manned mission better than the

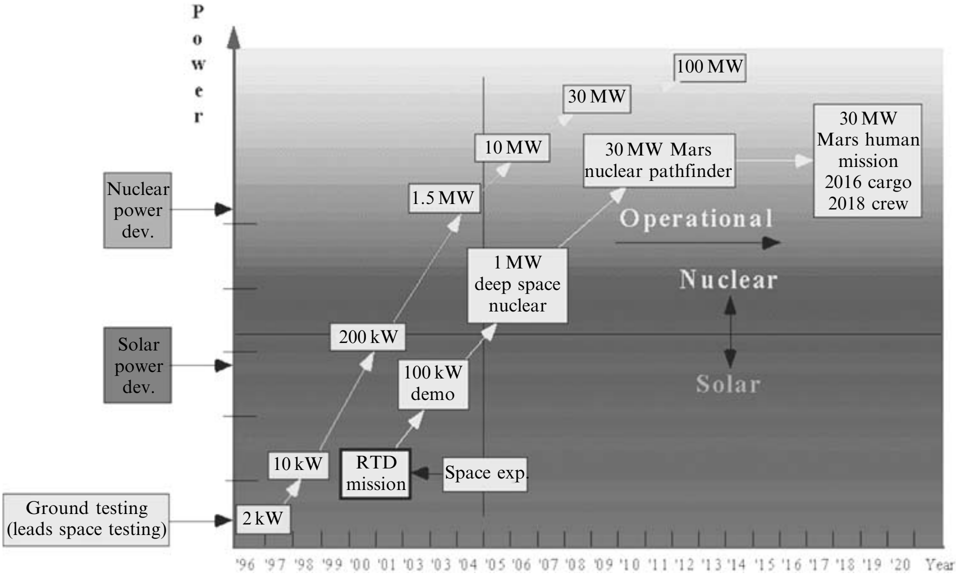

Figure 7.35. VASIMR technology development roadmap [ASPL, 2000].

slower robotic missions planned by NASA in the near or middle term. However, development by NASA at the JSC is continuing. Figure 7.35 shows an older VASIMR technology development roadmap to full implementation in 2004. Linked arrows show ground-testing always leading flight experiments and space deployment at each incremental power level.

At this stage VASIMR feasibility depends on definitive and reassuring answers to the problems of plasma radiative losses and pressure scaling. The JIMO mission is planned around an ion engine, not an MPD thruster. MPD propulsion will have to wait until a manned mission to Mars, or at least a 'dry run' precursor mission such as to an NEO, around 2015 [Claybaugh et al., 2004]. If MPD propulsion is chosen, and if all technical questions are answered, VASIMR will be the natural candidate propulsion system.

7.23 COMBINED CHEMICAL AND NUCLEAR THERMAL ROCKETS

Among the latest propulsion concepts based on nuclear power, recent proposals include injecting liquid oxygen (LOX) inside the hydrogen exhaust of an NTR. The goal is to boost thrust for a limited time [Borowski et al., 1994; Glenn and Buhlman, 1999; Dujarric, 1999; Buhlman et al., 2004; Joyner et al., 2004]. Means of raising thrust with hydrogen/oxygen combustion look convenient to reach escape speed fast, or to lift off from a planet surface. This concept could be viewed as the

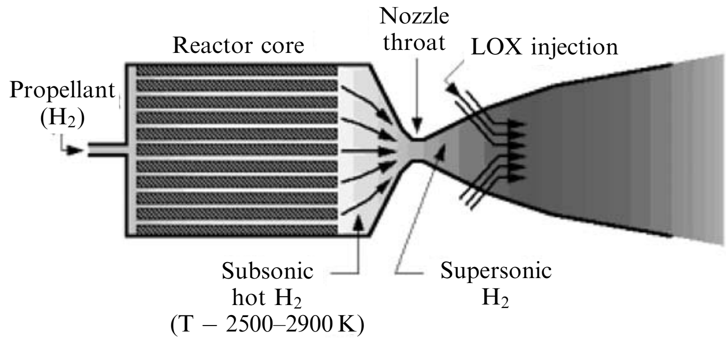

Operating mode	O/F	I_{sp} (s)	Thrust (kN)	P_{jet} (MW_j)
Pure H_2 NTR	0	940	67	308
LOX-augmented NTR	3	647	184	582

Figure 7.36. Simplified scheme of hybrid nuclear thermal and chemical (LANTR) engine.

'poor man' version of VASIMR, but its thrust would be much larger, in the 10–100-ton range, albeit with I_{sp} typical of chemical propellants or slightly larger.

As developed by Glenn and his co-workers at GenCorp Aerojet, this concept goes under the acronym of LANTR (Lox Augmented Nuclear Thermal Reactor). To increase reactivity, LOX should be injected inside the diverging part of the NTR nozzle, but not too far from the throat, because hydrogen must still be hot to ignite the LOX/H_2 mixture and burn. There is a certain gain of I_{sp} in this strategy, due to the higher hydrogen temperature with respect to conventional chemical LOX/LH_2 rockets, and to the possible presence of atomic H (this radical accelerates chemical kinetics). Accordingly, the nozzle should be designed differently from conventional expansion nozzles because hydrogen and oxygen combustion takes place precisely there, inside the expanding supersonic hydrogen stream. The oxygen is injected subsonic (as a liquid), but combustion is likely to be mostly supersonic. This is the reverse of what occurs inside the SCRJ engines described in Chapter 4 (in SCRJ it is the hydrogen fuel that is injected inside the supersonic air stream), but issues such as mixing, combustion, and turbulence are very similar. The simplest scheme of a LANTR is in Figure 7.36, showing also the I_{sp} and thrust calculated.

The LANTR concept was first tested at Aerojet [Buhlman and Neill, 2000] using gaseous O_2 and H_2. Fission heating of H_2 was simulated by using very rich H_2 combustion (mixture ratios up to 7 were possible, but only up to 1.5 were actually tested). A total of 63 tests were performed at a chamber pressures of 30 to 70 atm: the thrust increased by 40% over the standard engine. The expertise of Aerojet in supersonic combustion was critical to the successful operation of the LANTR-simulated mode.

In later tests [Buhlman et al., 2004], thrust was raised by 55%, at the expense of a larger oxygen/hydrogen ratio, 3 : 1: oxygen consumption was substantial. This aspect of LANTR must be dealt with for each specific mission. LANTR is also part of the 'trimodal' strategy being currently analyzed at NASA-Glenn by the team of Borowski, see [Joyner et al., 2004].

Because the I_{sp} calculated is not much higher than 500 sec, this concept looks promising only to boost thrust for short times. Its applications include emergencies, e.g., when aborting a mission, to speed up injection into interplanetary trajectories, to reach escape speed faster or even to take off from low-gravity asteroids or satellites, as suggested also in [Dujarric, 1999]. No mission analysis has been performed so far for a LANTR-powered vehicle. The work by Dujarric is apparently being continued, with the French aeroengine company SNECMA collaborating in a preliminary analysis of several hybrid strategies, including LOX augmentation but also plasma MHD acceleration [Dujarric et al., 2000].

7.24 CONCLUSIONS

Nearly 50 years have gone by since the Rover Project was started and the NTR engines it spawned were tested. If the vagaries of US politics, US agencies or public opposition does not get in its way, nuclear propulsion has now a chance of becoming the centerpiece of manned and unmanned planetary exploration. No other propulsion technology can—not at least within reasonable mission length and budgets.

So far, this chapter has focused on promising concepts and enabling technologies. However, there are other challenges that need to be faced and overcome before nuclear propulsion can succeed.

Paraphrasing A. Hansson [Hansson, 2001] these are: reducing the mass of the nuclear reactor and engine, including their radiation shields (much progress has been made in this area by the people working at MITEE, but not all issues have been satisfactorily resolved, and the ratio power/mass of any nuclear engine is still much lower than in chemical propulsion systems); dealing with the residual radiation emission after shutting down the nuclear reactor: a GW-class ^{235}U-powered reactor can radiate $O(10^3$ rad/sec) at 10 m many months after having been shut down, see section 7.4.1; this issue depends to a large extent on fuel fission kinetics and information is restricted); security, in the general sense: although nuclear propulsion fuels are similar to those in nuclear power utilities, and no nuclear explosion can ever be triggered, dirty bomb manufacturing by non-experts, or even fuel refining by experts to obtain fissionable material are potential security issues in the context of the present world situation. The amount of fuels processed for nuclear propulsion can be safely predicted to be negligible compared to that consumed to generate energy; however, some future fuels under discussion have very small critical masses (even 1% of that of ^{235}U), so security should not be dismissed as a minor issue.

In these authors' opinion, one of the outstanding issues is public acceptance of nuclear power in space, witness the 1997 campaign in the US, and in Florida in particular, against the radioisotope thermoelectric generator power source installed on the Cassini probe launched from Cape Canaveral.

Risks and dangers posed by using nuclear power should be neither ignored nor underestimated, and the public needs to be kept informed, and must be. The public must also be educated, in the sense that nuclear power issues should be compared and put into perspective relative to more conventional energy sources. The response given by people in the street to a recent EU survey of opinions about the so-called Chernobyl accident was indeed instructive. Most people interviewed were convinced that hundreds or thousands of people had died in Ukraine following the accident. So far, 31 among the rescue crew attempting to shut down the reactor and the firemen putting down the fire were lost [Del Rossi and Bruno, 2004].

This discrepancy between imagined and actual fatalities is telling: even among educated people nuclear power is surrounded by the fear and aura of secrecy that go back to Hiroshima, Nagasaki and to the atmospheric tests during the Cold War. Hardly any people know that the Chernobyl accident was no accident at all, but a deliberate and foolhardy experiment by a single individual to test the spinning-down time of one of the power turbines. Likewise, not many people are aware that natural background radiation here on Earth is capable of biological effects at least 10 times larger than any existing human-made source.

In this light, any positive but exclusively technical conclusion regarding use and convenience of space nuclear propulsion must be cautiously appraised. On its merit, nuclear propulsion is clearly the only practicable technology if exploring our planetary system at reasonable cost and within reasonable mission times is a requirement (regrettably, this may be a strong 'if'). This can be simply argued on the basis of energy density, 10 million times greater than that of the best chemical propellants. This factor is by itself assuring that under proper conditions, nuclear propulsion is the natural requisite of interplanetary space missions. Mass, shielding and radiation hazards, now assumed as the unavoidable penalties of nuclear propulsion, are issues in continuous evolution, and actually benefiting from other, sometimes unrelated, technology areas. Current NASA planning includes nuclear propulsion-powered robotic missions to Europa, Pluto and Venus, and eventually manned missions to Mars, signifying this mode of propulsion is no longer considered unrealistic or dangerous.

After all technical and societal issues are sorted out and solved, the key condition to transfer nuclear propulsion from technology to space-qualified engines is a steady political will and steady funding. While the US government is on record about supporting development of this technology, ESA in Europe has still to clarify its official posture. ESA is ruled by many of the EU member states, so such indecision simply mirrors reluctance from member states to take a stand. Russia has few or no qualms about nuclear power in space: informed sources have claimed some of its reconnaissance COSMOS satellites orbited in the past were in fact powered by nuclear reactors. Japan, on the contrary, has no intention of doing anything of the sort, even though it must develop new strategic surveillance satellites to reconnoiter over North Korea; because of Hiroshima and Nagasaki, Japan still prefers to rely on miniaturization and electronics powered by solar cells.

Any effort to develop this key propulsion technology, and especially if the effort should become international, must therefore enjoy a clear and lasting political will.

After deciding to go ahead with nuclear power in space, there should not be second thoughts, accepting technical hurdles are a part of life; from the start conflicting roles of different agencies, or countries should be avoided. In fact, because nuclear energy was managed by military and civilian organizations well before the space age, nuclear and space agencies find in most cases difficult to talk to each other (the Russian nuclear propulsion effort was an exception, but the key people involved, the 'three Ks', were also exceptional). An additional factor in this respect is that a typical aerospace company is smaller, or much smaller, than a company manufacturing nuclear reactors, and so are the business prospects of selling space engines. Faced with a joint nuclear/space program, the standard lawmaker committee is tempted to legislate or 'suggest' a joint team, where responsibilities are inevitable shared or diluted, rather than clearly assigned. Such politically over-cautious management was at the root of some significant disasters, notably that of the US SNAP-100 RTG satellite power source [Bennett, 1998]. The opposite example is the US Navy Nuclear Reactor program, managed very successfully for 20 years by a single and clear-headed individual, Admiral Rickover.

Finally, international treaties on nuclear power in space must be given a second look. The scope and text of the UN principles accepted by the 1992 General Assembly seem at this time to be overly restrictive and even preventing in practice the use or deployment of space nuclear propulsion. Born right after the end of the Cold War, during the rush to agree on and to approve what would have been impossible a few years before, the UN principles on nuclear power in space seem now more an obstacle than a tool for protecting humankind from the unwanted effect of nuclear energy. They should be revisited and revised, as suggested in [Lenard, 2005].

At this time humankind is searching for solutions to problems never before so severe or so dramatic: local wars, poverty, terrorism seem to focus everybody's attention, as if the oldest questions humans kept asking (Where do we come from? Where are we going? Are there other beings beside us? Or at least life? Where?) were forgotten.

In fact, these age-old questions have only been put aside, drowned by the sound and fury. In fact, humankind still wants answers to these questions. Sixty years after its birth, a war technology might provide at least one.

7.25 BIBLIOGRAPHY

'Aerospace America' (1989) 'Nuclear thermal rockets: next step into space', by S.K. Borowski, E.A. Gabris, and J. Martinell, p. 17; 'The beginnings', by R.J. Bohl, W.L. Kirk, and R.R. Holman, p. 18; 'Mars mission safety', by D. Buden, p. 22, June 1989.

'Aerospace America' (2000) Joint Propulsion Meeting Program, April 2000, pp. B64 and B70.

'Aerospace America' (2004) Roundtable discussion on NP, November 2004; see it also at: http://boss.streamos.com/wmedia/federal/aiaa/aiaa081004.wvx

Alta (2003) 'Technology and System Options towards Megawatt Level Electric Propulsion', Proceedings of the International Workshop held on 9–10 June 2003, Lerici, Italy. CD-ROM available from alta@alta-space.com

Andrenucci, M. (2004) 'Prospective Needs and Technology Options for High Power Devices', Paper presented at the International Symposium on Energy Conversion Fundamentals, 21–25 June 2004, Istanbul. Also available from alta@alta-space.com

Asker, J.R. (1991) 'Nuclear Rockets Gain Support for Propelling Mars Mission', *Aviation Week & Space Technology*, March 18, 1991, pp. 24–25.

ASPL (2000) http://spacsun.rice.edu/aspl/

Augelli, M., Bignami, G., Bruno, C., Calligarich, E., De Maria, G., Mulas, M., Musso, C., Pellizzoni, A., Piperno, W., Piva, R., Procacci, B., Rosa-Clot, M., and Rubbia, C. (1999) 'Report of the Working Group on a Preliminary Assessment of a New Fission Fragment Heated Propulsion Concept and its Applicability to Manned Missions to the Planet Mars (Project 242)', ASI Internal Report, Roma, March 15, 1999 (proprietary).

Auweter-Kurtz, M., and Kurtz, H. (2003) 'High Power and High Thrust Density Electric Propulsion for In-Space Transportation', in Proceedings of the International Workshop 'Technology and System Options towards Megawatt Level Electric Propulsion', June 9–10, 2003, Lerici, Italy. Available from alta@alta-space.com. CD-ROM only.

Auweter-Kurtz, M. and Kurtz, H. (2005) 'High Power and High Thrust Density Electric Propulsion for In-Space Transportation', Paper IAC-05-C3.5-C4.7.05, presented at the 56th International Astronautical Congress (IAC), 16–21 October 2005, Fukuoka, Japan.

Backhaus, S., Tward, E., and Petach, M. (2004) 'Traveling-wave Thermoacoustic Electric Generator', *Applied Physics Letters*, Vol. 85, No. 6, pp. 1085–1087.

Baggett, R., and Dankanich, J. (2004) 'Electric Propulsion', *Aerospace America*, December, pp. 58–59.

Bates, J. (2003) 'NASA Science Chief Lays Out Need for New Propulsion System', *Space News*, June 9, 2003, p. 8.

Beale, G.A., and Lawrence, T.J. (1989) 'Nuclear propulsion for orbital transfer', *Aerospace America*, June, pp. 27–29.

Bennett, G.L. (1998) 'Lessons of Space Nuclear Power', *Aerospace America*, July, pp. 32–40.

Bennett, G.L., and Miller, T.J. (1993) 'Progress Report on Nuclear Propulsion for Space Exploration and Science', AIAA Paper, AIAA, Renton, VA.

Berger, B. (2005a) 'NASA Sacrifices Hubble, JIMO to Focus on Moon–Mars Vision', *Space News*, February 14, 2005, pp. 8–9.

Berger, B. (2005b) 'Griffin Praised for Putting Europa Mission Back on the Table', *Space News*, May 23, 2005, p. 6. See also the Editorial in *Space News* of May 30, 2005, p. 18.

Bidault, C., Bond, R., and Sweet, D. (2004) 'Assessment of Electric Propulsion Systems for Exploration Missions: Comparison between Solar-Electric and Nuclear-Electric Propulsion Systems', AURORA Final Report to ESA-ESTEC, July 15, 2004.

Bohl, R.J., Kirk, W.L., and Holman, R.R. (1989) 'The Beginnings', *Aerospace America*, June, pp. 18–22.

Bond, R. (2002) 'Nuclear Propulsion—Options and Choices', Paper presented at the European Science Foundation Workshop on Nuclear Propulsion, Rome, Italy, May 10–11, 2002. Available from Robert.Bond@aeat.co.uk

Bordi, F., and Taylor, R. (2003) 'The Jupiter Icy Moon Orbiter Mission', in Proceedings of the International Workshop 'Technology and System Options towards Megawatt Level

Electric Propulsion', June 9–10, 2003, Lerici, Italy. Available from alta@alta-space.com. CD-ROM only.

Borowski, S.K., Gabris, E.A., and Martinell, J. (1989) 'Nuclear Thermal Rockets: Next Step to Space', *Aerospace America*, June, pp. 16–18.

Borowski, S.K., Corban, R.R., Culver, D.W., Buhlman, M.J., and McIlwain, M.C. (1994) 'A Revolutionary Lunar Space Transportation System Architecture Using Extraterrestrial LOX-Augmented NTR Propulsion', AIAA paper 94-3343, presented at the 30th AIAA/ASME/SAE/ASEE Joint Propulsion Conference, Indianapolis, IN, June 27–29, 1994.

Borowski, S.K., Dudzinski, L.A., and McGuire, M.L. (1998) 'Nuclear Thermal Rocket (NTR) Propulsion for Tomorrow's Moon/Mars Space Transportation Systems—Revolutionary Performance through Evolutionary Development', IAA Paper IAA-98-IAA.13.1.01, presented at the 49th IAF Congress, Melbourne, Sept. 28–Oct. 2, 1998. Also: NASA TM 1998-208826, December 1998.

Borowski, S.K., Dudzinski, L.A., and McGuire, M.L. (1999) 'Artificial Gravity Vehicle Design Option for NASA's Human Mars Mission Using "Bimodal" NTR Propulsion', AIAA paper AIAA-99-2545, presented at the 35th AIAA/ASME/SAE/ASEE Joint Propulsion Meeting, 20–24 June 1999, Los Angeles, CA.

Borowski, S.K., Dudzinski, L.A., and McGuire, M.L. (2000) 'Artificial Gravity Human Exploration Missions to Mars and Near Earth Asteroids Using "Bimodal" NTR Propulsion', Paper AIAA 2000-3115, presented at the 36th AIAA/ASME/SAE/ASEE Joint Propulsion Meeting, 16–19 July 2000, Huntsville, AL.

Bottin, B., Carbonaro, M., Paris, S., Van der Haegen, V., Novelli, A., and Vennemann, D. (1998a) 'The VKI 1.2 MW Plasmatron Facility for the Thermal Testing of TPS Materials', Paper presented at the 3rd European Workshop on Thermal Protection Systems, ESA-ESTEC, 25–27 March 1998, Noordwjik, The Netherlands.

Bottin, B., Carbonaro, M., Van der Haegen, Paris, S. (1998b) 'Predicted and Measured Capability of the VKI 1.2 MW Plasmatron Regarding Re-entry Simulation', in Proceedings of the Third European Symposium on Aerothermodynamics for Space Vehicles, edited by R.A. Harris, ESA Publication SP-426, Noordwijk., p. 553.

Bruno, C. (2005) 'Physics of Nuclear Propulsion – An Introduction', Paper IAC-05-C3.5-C4.7.01, presented at the 56th International Astronautical Congress (IAC), 16–21 October 2005, Fukuoka, Japan.

Bruno, C., and Giucci, S. (1999) 'Cryogenic Technology to Improve Electric Thrusters', IAF Paper IAF-99-S.4.04, presented at the 50th IAF Congress, 4–8 October 1999, Amsterdam. Also, *Acta Astronautica*, Vol. 51, No. 12 (2002), pp. 855–863.

Buffone, C., and Bruno, C. (2002) 'Cooling the Rubbia's Engine Nozzle in the Future Test Facility', Paper ISTS 2002-a-22 presented at the 23rd International Science and Technology Space Symposium, Matsue, Japan, May 26–June 2, 2002.

Buhlman, M.J., and Neill, T.M. (2000) 'Simulated LOX-Augmented Nuclear Thermal Rocket (LANTR) Testing', Paper AIAA 2000-3897 presented at the 36th AIAA/ASME/SAE/ASEE Joint Propulsion Conference, 16–19 July 2000, Huntsville AL.

Buhlman, M.J., Neill, T.M., and Borowski, S.K. (2004) 'LANTR Engine System Integration', AIAA paper 2004-3864, presented at the 40th AIAA/ASME/SAE/ASEE Joint Propulsion Conference, July 11–14, 2004, Fort Lauderdale, FL.

Bussard, R.W., and DeLauer, R.D. (1958) *Nuclear Rocket Propulsion*, McGraw-Hill, New York.

Chang Diaz, F.R. (2000) 'The Vasimr Rocket', *Scientific American*, Vol. 283, No. 5, p. 72.

Chang Diaz, F R., Squire, J.P., Ilin, A.V., McCaskill, G.E., Nguyen, T.X., Winter, D.S., Petro, A.J., Goebel, G.W., Cassady, L., Stokke, K.A., Dexter, C.E., Carter, M.D., Baity, F.W., Barber, G.C., Goulding, R.H., Sparks, D.O., Schwenterly, S.W., Bengtson, R.D., Breizman, B.N., Jacobson, V.T., Sagdeev, R.Z., Karavasilis, K., Novakovski, S.V., Chan, A.A., Glover, T.W. (1999) 'The Development of the VASIMR Engine', Proceedings of the International Conference on Electromagnetics in Advanced Application, Turin, Italy, September 1999.

Chang Diaz, F.R., Squire, J.P., Bengtson, R., Breizman, B.N., Baity, F.W., and Carter, M.D. (2000) 'The Physics and Engineering of the VASIMR Engine', AIAA paper 2000-3756, presented at the 36th AIAA/ASME/SAE/ASEE Joint Propulsion Meeting, 16–19 July 2000, Huntsville, Alabama.

Chew, G., Pelaccio, D.G., Chiroux, R., Moton, T., and White, C. (2004) 'Status and Assessment of the Indirect Nuclear Propulsion Concept', AIAA paper 2004-3868, presented at the 40th AIAA/ASME/SAE/ASEE Joint Propulsion Conference, 11–14 July 2004, Fort Lauderdale, FL.

Choueiri, E. (1998) 'The Scaling of Thrust in Self-Field MPD Thrusters', *Journal of Propulsion and Power*, Vol. 14, No. 5, pp. 744–753.

Choueiri, E. (2000) Personal communication.

Claybaugh, W., Garriott, O.W., Garvey, J., Griffin, M., Jones, T.D., Kohlhase, C., McCandless II, B., O'Neil, W., and Penzo, P.A. (2004) 'Extending the Human Presence into the Solar System', in: www.planetary.org/aimformars/initiatives.html

Collins, C. (2005) University of Texas-Dallas site, www.utdallas.edu/research/quantum/isomer/isomerPubl.htm

David, L. (2002) 'Nuclear Initiative Now Centerpiece of Planetary Effort', *Space News*, February 11, 2002, pp. 8–9.

Del Rossi, A., and Bruno, C. (2004) 'Safety Aspects in Nuclear Space Propulsion', Paper IAC-04-R.4/S.7.07, presented at the 55th International Astronautical Congress, Vancouver, 4–8 October, 2004.

Demyanko, Yu.G, Koniukov, G.V., Koroteev, A.S., Kuz'min, E.P. and Pavel'ev, [redacted]. (2001) *Nuclear Rocket Engines*, Norma Inform Publishers, Moscow [in Russian]. Chapter 1 contains a short history of the nuclear rocket engine, ARD in Russian. Reactors developed are discussed in Chapter 3.

Dewar, J.A. (2004) *To the End of the Solar System: The Story of the Nuclear Rocket*, The University Press of Kentucky, Lexington, KY.

Donahue, B., and Cupples, M. (2000) 'Comparative Analysis of Current Human Mars Mission Architectures', AIAA Paper 2000-3215, presented at the 36th AIAA/ASME/SAE/ASEE Joint Propulsion Meeting, 16–19 July 2000, Huntsville, AL.

Drake, B.G. (editor) (1998) 'Reference Mission Version 3.0 Addendum to the Human Exploration of Mars: The Reference Mission of the NASA Mars Exploration Study Team'. NASA Exploration Office Document EX-13-98-036. Also in: http://www-sn.jsc.nasa.gov/EXPLORE/addendum/LOA_For.htm and in: NASA Human Exploration of Mars: The Reference Mission of the Mars Exploration Study Team, 1997, including Addendum Version 3.0, NASA SP-607, June 1998.

Dujarric, C. (1999) 'An Innovative Hybrid Rocket Propulsion Concept for Take-Off from Planets and Interplanetary Missions', IAF Paper 99-S.6.06, presented at the 50th IAF Congress, October 4–8, 1999, Amsterdam.

Dujarric, C., Fratacci, G., and Valentian, D. (2000) 'Hybridisation of Chemical, Nucleothermal and Electric Rocket Propulsion Principles: A Possible Way to Increase Rocket Specific Impulse?', Paper IAF-00-S.6.02 presented at the 51st IAF Congress, Rio de Janeiro, October 2–6, 2000.

Dunning, J., Sankovic, J. (1999) 'NASA's Electric Propulsion Program', AIAA paper 99-2161, presented at the 35th AIAA/ASME/SAE/ASEE Joint Propulsion Conference and Exhibit, June 20–24, 1999, Los Angeles, CA.

Dyson, F. (1979) *Disturbing the Iniverse*, Harper and Row, New York [Chapter 10].

Dyson, G. (2002) *Project Orion*, Allen Lane – The Penguin Press, London.

Fearn, D. (2003) 'The Prospects of MW Power Level Gridded Ion Thrusters', in Proceedings of the International Workshop 'Technology and System Options towards Megawatt Level Electric Propulsion', June 9–10, 2003, Lerici, Italy. Available from alta@alta-space.com. CD-ROM only.

Fearn, D. (2004) 'The Application of Gridded Ion Thrusters to High Thrust, High Specific Impulse Nuclear-Electric Missions', Paper IAC-04-R.4/S.7-09, presented at the 55th International Astronautical Congress, Vancouver, Canada, October 2–9, 2004.

Fearn, D. (2005) 'The application of ion thrusters to high thrust, high specific impulse nuclear-electric missions', Paper IAC-05-C3.5-C4.7.04, presented at the 56th International Astronautical Congress (IAC), 16–21 October 2005, Fukuoka, Japan.

Flinn, E.D. (2004) 'Can People go to Mars?', *Aerospace America*, May, pp. 22–23.

Flora, M. (2005) Project Orion, www.islandone.org/Propulsion/ProjectOrion.html

Gilles, J. (2004) 'Britain Warms to European Space Exploration Plan', *Nature*, Vol. 431, p. 619.

Glasstone, S. (1955) 'Principles of Nuclear Reactor Engineering', Van Nostrand, New York, Chapter X.

Glenn, D.E., and Buhlman, M.J. (1999) 'CFD Analysis of the LOX-Augmented Nuclear Thermal Rocket (LANTR)', AIAA paper 99-2546, presented at the 35th AIAA/ASME/SAE/ASEE Joint Propulsion Meeting, June 20–24, 1999, Los Angeles, CA.

Goldin, A.Ya., Koroteev, A.S., Semyonov, V.F., Konopatov, A.D., Pavshuk, V.A. and Ponomarev-Stepnoy, N.N. (1991) 'Development of Nuclear Rocket Engines in the USSR', paper presented at the AIAA/NASA/OAI Conference on Advanced Space Exploration Initiative (SEI) Technologies, 4–6 September 1991, San Diego, CA.

Gunn, S.V. (2001) 'Nuclear Propulsion—a Historical Perspective', *Space Policy*, Vol. 17, No. 4, pp. 291–298. Reprinted with permission from Elsevier, copyright 1991.

Gunn, S.V., and Ehresman, C.M. (2003) 'The Space Propulsion Technology Base Established Four Decades Ago for the Thermal Nuclear Rocket is Ready for Current Applications', Paper AIAA 2003-4590 presented at the 39th AIAA/ASME/SAE/ASEE Joint Propulsion Conference, 20–23 July 2003, Huntsville, AL.

Hagen, R., and Scheffran, J. (2001) 'Nuclear space—an indispensable option?', *Space Policy*, Vol. 17, No. 4, pp. 261–264.

Hamilton, C.E. (2002) 'Design Study of Triggered Isomer Heat Exchanger-Combustion Hybrid Jet Engine for High Altitude Flight', US Air Force Institute of Technology PhD thesis, released as Report AIT/GAE/ENY/02-6.

Hansson, A. (2001) 'Nuclear Power and Propulsion in Space', *Space Policy*, Vol. 17, No. 4, pp. 241–242.

Hill, P.G., and Peterson, C.R. (1970) *Mechanics and Thermodynamics of Propulsion*, 1st edn, Addison-Wesley, Reading, MA, Chapter 15.

Howe, S.D. (1985) 'Assessment of the Advantages and Feasibility of a Nuclear Rocket for a Manned Mars Mission', Los Alamos National Laboratories Report LA-UR-85-2442.

Howe, S.D. (2000) 'Nuclear Rocket to Mars', *Aerospace America*, August, p. 39.

Howe, S.D. (2001) 'High Energy Density Propulsion—Reducing the Risk to Humans in Planetary Exploration', *Space Policy*, Vol. 17, No. 4, pp. 275–284.

Howe, S.D., DeVolder, B., Thode, L., and Zerkle, D. (1998) 'Reducing the Risk to Mars: the Gas Core Nuclear Rocket', in *Space Technology and Applications International Forum—1998*, edited by Mohamed S. El-Genk, Publication CP-420, The American Institute of Physics, New York, p. 1138.

Hrbud, I. (2003) 'Nuclear and Future Flight Propulsion', *Aerospace America*, December, pp. 62–63.

Iannotta, B. (2004) 'NASA Funds Research on Very High-Power Electric Thrusters', *Space News*, August 16, 2004, p. 16.

Ilin, A.V., Chang Diaz, F.R., Squire, J.P., and Carter, M.D. (1999) 'Monte Carlo Particle Dynamics in a Variable Specific Impulse Magnetoplasma Rocket', in Proceedings of the Open Systems '98 Meeting, Novosibirsk, July 1998; also in *Transactions in Fusion Technology*, Vol. 35, pp. 330–334.

Ilin, A.V., Chang Diaz, F.R., Squire J.P., Breizman, F.W., Carter, M.D. (2000) 'Particle Simulations of Plasma Heating in VASIMR', AIAA paper 2000-3753, presented at 36th AIAA/ASME/SAE/ASEE Joint Propulsion Conference, July 17–19, 2000, Huntsville, AL.

Jarow, L. (2000) 'Will a Killer Asteroid Hit the Earth?', *Time Magazine*, April 10, 2000, pp. 50–51.

Jones, L.J. (1992) 'Nuclear Thermal Propulsion', *Aerospace America*, December, p. 28.

Joyner, C. Russell, Phillips, J.E., Fowler, R.B., and Borowski, S.K. (2004) 'TRITON: a *TRI*modal, *T*hrust *O*ptimized, *N*uclear *P*ropulsion and Power System for Advanced Space Missions', AIAA paper 2004-3863, presented at the 40th AIAA/ASME/SAE/ASEE Joint Propulsion Conference, 11–14 July 2004, Fort Lauderdale, FL.

Koniukov, G.V., Petrov, A.I., Popov, S.A., Rachuk, V.S., Belogurov, Y.I., Mamontov, Yu.I., Fedik, I.I., D'yakov, Ye.K., Mogil'ny, I.A., Konovalov, V.A., et al. (2004) 'Prototype of Atomic Rocket–IRGIT Reactor', *Atomic Energy*, Vol. 97, No. 3, 173–177 [in Russian].

Koppel, C.R., Valentian, D., Latham, P.M., Fearn, D., Bruno, C., and Nicolini, D. (2003) 'Preliminary Comparison between Nuclear-Electric and Solar-Electric Propulsion Systems for Future Interplanetary Missions', AIAA paper 2003-4689, presented at the 39th AIAA/ASME/SAE/ASEE Joint Propulsion Conference, 20–23 July 2003, Huntsville, AL.

Koroteev, A.S., Prishletsov, A.B., Martishin, V.M., Pavelyev, A.A., Shcherbinin, V.P., Reshmin, A.I., and Iosilevskii, I.L. (2002) 'Rocket Engines and Powerplants Based on Gas-core Nuclear Reactor', edited by A.S. Koroteev, Mashinostroenie Publisher, Moscow (in Russian).

Larson, W.J., and Wertz, J.R. (editors) (1992) 'Space Mission Analysis and Design', Kluwer, Dordrecht, section 11.4.

Lawrence, T.J. (2005) 'Nuclear thermal rocket propulsion systems', Paper IAC-05-C3.5-C4.7.03, presented at the 56th International Astronautical Congress (IAC), 16–21 October 2005, Fukuoka, Japan.

Lawrence, T.J., Witter, J.K., and Humble, R.W. (1995) 'Nuclear Rocket Propulsion Systems', in *Space Propulsion Analysis and Design*, edited by R.W. Humble, G.N. Henry and W.J. Larson, McGraw-Hill, New York, Ch. 8, and also as otherwise cited.

Lenard, R.X. (2001) 'Societal Imperatives and the Need for Space Nuclear Power and Propulsion Systems', *Space Policy*, Vol. 17, No. 4, pp. 285–290.

Lenard, R.X. (2005) 'Nuclear safety, Legal aspects and Policy Recommendations', Paper IAC-05-C3.5-C4.7.06, presented at the 56th International Astronautical Congress (IAC), 16–21 October 2005, Fukuoka, Japan.

Maise, G., Powell, J.R., Paniagua, J., Ludewig, H., and Todosow, M. (2000) 'Compact Ultra Lightweight Nuclear Thermal Propulsion Systems for Interplanetary Space Missions', IAC paper presented at the 51st International Astronautical Congress, October 2–6, Houston, TX.

McGuire, M.L., Borowski, S.K., and Packard, T.W. (2004) 'Nuclear Electric Propulsion Application: RASC Mission Robotic Exploration of Venus', AIAA paper 2004-3891, presented at the 40th AIAA/ASME/SAE/ASEE Joint Propulsion Conference, 11–14 July 2004, Fort Lauderdale, FL.

Mensing, A.E., and Latham, T.S. (1989) 'Gas-core Technology', *Aerospace America*, June, p. 25.

Mowery, A.L., and Black, D.L. (1999) 'Space propulsion Annular Compact Engine (SPACE) A NERVA Technology Compact Nuclear Rocket', AIAA Paper 99-2548, presented at the 35th AIAA/ASME/SAE/ASEE Joint Propulsion Meeting, June 20–24, 1999, Los Angeles.

Mukhin, K.N. (1987) *Experimental Nuclear Physics*, Vol. I: *Physics of Atomic Nucleus*, Mir Publishers, Moscow, Chapter 1, p. 50; and section 2.3.2, pp. 138 et seq.

Musser, G., and Alpert, S. (2000) 'How to go to Mars', *Scientific American*, March, pp. 29–30. See also NASA-JSC (2000).

Myers, W.D., and Swiatecki, W.J. (1966) 'Nuclear Masses and Deformations', *Nuclear Physics*, Vol. 81, pp. 1–60.

NASA (1990) 'NASA/DOD/DOE Nuclear Thermal Propulsion Workshop Notebook', NASA-Lewis RC [now: -Glenn RC], Cleveland, OH.

NASA-JSC (2000) VASIMR (ASPL) http://spaceflight.nasa.gov/mars/technology/propulsion/aspl/vasimr.html

NASA (2005a) NEO site www.neo.jpl.nasa.gov/ca/

NASA (2005b) www.nasa.gov/vision/space/travelinginspace/25aug_plasticspaceships.html

NASA (2005c) www.radiationshielding.nasa.gov

Nature (2005) Vol. 434, 21 April 2005, p. 948.

Oleson, S., and Katz, I. (2003) 'Electric Propulsion for Project Prometheus', Paper AIAA 2003-5279, presented at the 39th AIAA/ASME/SAE/ASEE Joint Propulsion Conference, 20–23 July 2003, Huntsville, AL.

Ponomarev-Stepnoy, N.N., Talyzin, V.M., Pavshuk, V.A., Putko, V.Ya., Konovalov, V.A., Raskach, F.L., Ulasevich, V.K., Smetannukov, V.P., Kolganov, V.D., Fedik, I.I., et al. (1999) 'Rabotyi po Otiechiestvennogo ARD', *Atomic Energy*, Vol. 86, No. 4, 296–302 [in Russian]. In this paper there is a picture of the 'three Ks' (Korolev, Kurchatov and Keldysh) together.

Powell, J. (1999) 'Compact Nuclear Rockets', in *Scientific American*, February, p. 72.

Powell, J., Paniagua, J., Ludewig, H., Maise, G., and Todosow, M. (1998) 'MITEE: A New Nuclear Engine Concept for Ultra Fast, Lightweight Solar System Exploration Missions', in *Space Technology and Applications International Forum—1998*, edited by Mohamed S. El-Genk, Publication CP-420, The American Institute of Physics, New York, p. 1131.

Powell, J., Maise, G., Paniagua, J., Ludewig, H., and Todosow, M. (1999) 'The MITEE Family of Compact, Ultra Lightweight Nuclear Thermal Propulsion Engines for Planetary Exploration Missions', Paper IAF-99-S.6.03 presented at the 50th International Astronautical Congress, 4–8 October 1999, Amsterdam.

Powell, J.R., Maise, G., and Paniagua, J. (2004) 'MITEE and SUSEE: Compact Ultra Lightweight Nuclear Power Systems for Robotic and Human Space Exploration

Missions', Paper IAC-04-IAA-R.4/S.7-04 presented at the 55th International Astronautical Congress, October 2–8, 2004, Vancouver, Canada.

Prelas, A. (1998) Personal communication.

Project 242 WG (1999) (Proprietary) Patent Document prepared by C. Bruno, ASI-Project 242 Working Group, Italian Space Agency (ASI), Rome.

Rachuk, V.S., Belogurov, A.I., Grigorenko, L.N. and Mamontov, Yu.I. (1996) 'Russian Investigations in the Area of Nuclear Rocket Engines (NRE) Research International Programs', paper presented at the 5th International Symposium on Propulsion for Space Transportation, 22–24 May 1996, Paris.

Randolph, T.M., and Polk Jr., J.E. (2004) 'An Overview of the Nuclear Electric Xenon Ion System (NEXIS) Activity', AIAA paper 2004-3450, presented at the 40th AIAA/ASME/SAE/ASEE Joint Propulsion Conference, 11–14 July 2004, Fort Lauderdale, FL.

Reichardt, T. (2004) 'Reviewers Caution NASA over Plans for Nuclear-powered Craft', *Nature*, Vol. 431, p. 113.

Reichardt, T. (2005) 'NASA Urged to Lay Plans for Mission to Europa', *Nature*, Vol. 433, p. 342.

Ronen, Y. (2000) In *Nuclear Instrumentation and Methods in Physics Research A*, Vol. 455, pp. 442–451). See also http://rense.co./general6/earthom.htm.

Sackheim, R., Van Dyke, M., Houts, M, Poston, D., Lipinski, R., Polk, J., and Frisbee, R. (2000) 'In-Space Nuclear Power as an Enabling Technology for Deep Space Exploration', AIAA Paper 2000-3881, presented at the 36th AIAA/ASME/SAE/ASEE Joint Propulsion Meeting, 16–19 July 2000, Huntsville, AL.

Schmidt, G. (1999) 'Nuclear and Future Flight Propulsion', *Aerospace America*, December 1999, p. 66.

Schmidt, G.R., Bonometti, J.A. and Irvine, C.A. (2002) 'Project Orion and Future Prospects for Nuclear Pulsed Propulsion', *J. Propulsion and Power*, Vol. 18, No. 3, May–June 2002, 497–504.

Scina, J.E., Aulisio, M., Gerber, S.S., Hewitt, F., Miller, L., and Elbuluk, M. (2004) 'Power Processing for a Conceptual Prometheus Electric Propulsion System', AIAA paper 2004-3452, presented at the 40th AIAA/ASME/SAE/ASEE Joint Propulsion Conference, 11–14 July 2004, Fort Lauderdale, FL.

Shepherd, L.R., and Cleaver, A.V. (1948) 'The Atomic Rocket-2 and -3', *Journal of the British Interplanetary Society*, Vol. 7, No. 6, pp. 237–240; and Vol. 8, No. 1, p. 30, January 1949. Cited also in [Bussard and DeLauer, 1958, p. 319].

Smith, B. and Anghaie, S. (2004) 'Gas Core Reactor with Magnetohydrodynamic Power System and Cascading Power Cycle', *Nuclear Tchenology*, Vol. 145, No. 3, 311–318.

Space News (2003) 'NASA Nuclear Propulsion Targeted for Big Increase', January 20, 2003, p. 4.

Sutton, G.P. (1992) *Rocket Propulsion Elements*, 6th edn, Wiley Interscience, New York, Chapter 19.

Takao, Y., Noutsuka, T., Mori, Y., Uemura, K., Sou, H., and Nakashima, H. (2000) 'Electron Cyclotron Resonance (ECR) Plasma Thruster Research', Paper ISTS 2000-b-32, presented at the 22nd International Symposium on Space Technology and Science, Morioka, Japan, May 28–June 4, 2000.

Tauber, M.E., Bowles, J.V., and Yang, L. (1990) 'Use of Atmospheric Braking during Mars Missions', *Journal of Spacecraft and Rockets*, Vol. 27, No. 3, p. 514.

Thode, L.E., Cline, M.C., and Howe, S.D. (1997) 'Vortex Formation and Stability in a Scaled Gas Core Nuclear Rocket Configuration', AIAA paper 97-2955, presented at the 33rd AIAA/ASME/SAE/ASEE Joint Propulsion Conference, Seattle, 11–15 July 1997.

Turner, M.J.L. (2005) *Rocket and Space Propulsion*, Springer-Praxis, Chichester, UK, Ch. 7.

University of Pisa (2005) NEO trajectory information site, www.newton.dm.unipi.it/~neodys/astinfo/orbfit/

Vacca, K, and Johnson, A. (2004) 'Feasibility of a Nuclear Single Stage to Orbit Reusable Vehicle', Paper IAC-04-IAF-R.4/S.7-06, presented at the 55th International Astronautical Congress, Vancouver, Canada, October 4–8, 2004.

Walker, P., and Dracoulis, G. (1999) 'Energy Traps in Atomic Nuclei', *Nature*, Vol. 399, pp. 35–40.

Westinghouse (1972) 'Technical Summary Report of the NERVA Program', Vols I–VI, Westinghouse Astronuclear Laboratory Publication WANL TNR-230, Pittsburgh, PA.

8

Stellar and quasi-stellar propulsion

8.1 INTRODUCTION

Staggering as they may seem to us, interplanetary distances are puny compared to those to reach stars. Our Solar System is located about two-thirds of the way from the center of our Galaxy towards the rim—about 25,000 light-years from the galactic centre, on the inner edge of the Orion arm. Astrophysicists mapping the 21-cm hydrogen radiation found, in fact, that our Galaxy is a spiral galaxy, its five major arms, or spokes (Centaurus, Sagittarius, Orion, Perseus and Cygnus) forming its apparent 'disc'.

This disk has a diameter of some 80,000 light-years and is approximately 2,000 light-years thick Using the distance of our Earth to the Sun, the astronomical unit, AU $= 1.496 \times 10^8$ km, as yardstick, 1 light-year (9.46×10^{12} km) is approximately equal to 63,200 AU. Our Galaxy comprises some 100 million stars; their density decreases from the galactic centre towards the arms' ends, where average interstellar distances are of the order of many light years, see Chapter 1. The spiral structure of the Galaxy is such that the average distance between stars, were it a true homogeneous disc, would be about 50 light-years. In fact, stars are not uniformly distributed, their density increasing when going towards the galactic center and inside its five major arms. This explains why the Sun's nearest neighbor is only a few light-years away; see Figure 8.1.

In this picture, the basic unit of distance is no longer the size of our Solar System, or the AU, but rather 1 light-year. For comparison, our Sun's closest star (Proxima Centauri) is 4.2 light-years away, or 4,000 times the diameter of our solar system measured at Pluto's orbit. If we had means to reach Pluto in a few months, reaching Proxima Centauri at the same speed would take of the order of a millennium.

Lying behind these considerations is the question of why cross these immense distances, and which star to visit. Proxima Centauri is a star of spectral type M5e,

Name	Distance (light-years)	Spectral type	Radial velocity (km/s)	Apparent magnitude	Luminosity (Sun = 1.00)
Sun		G2V		−26.7	1.0
Proxima Centauri	4.2	M5E	−16	11.05	0.00006
α – Centauri A	4.3	G2V	−22	−0.01	1.6
α – Centauri B		K0V		1.33	0.45
Barnard Star	5.9	M5V	−108	9.54	0.00045
Wolf 359	7.6	M8E	+113	13.53	0.00002
BD + 36°2147	8.1	M2V	+84	7.50	0.0055
Luyten 726-8A	8.4	M6e	+29	12.52	0.00006
Luyten 726-8B (UV Ceti)		M6e	+32	13.02	0.00004
Sirius A	8.6	A1V	−8	−1.46	23.5
Sirius B		wd		8.3	0.003

Figure 8.1. The nearest stars. (Note: for historical reasons, between one magnitude and the next the light ratio is 2.512. The more negative the magnitude, the larger the apparent star diameter).

very different from our Sun (its type is G2 V). The symbols identifying star type were invented to classify the star's electromagnetic spectrum, which may give an idea of what sort of light one would see on a hypothetical planet orbiting a star. For instance, the Sun 'surface', or disc we see, emits light as if it was a black body radiating at the temperature 5,800 K, the yellow-green peak of its spectrum imparting that warm quality humans associate to its light. An M-type star such as Proxima Centauri would have a cooler surface temperature, about 3,600 K, its hue shifted towards the red-yellow, and having probably a large, and fascinatingly unknown, effect on life forms.

However, without planets to orbit around or to land on, it is hard to conceive the motivation of such immensely long and expensive trips. Human beings have always been driven to explore faraway places by the hope of finding new life-forms and scenery, not just light. The star to reach and the distance to cross will in the end be chosen on the basis of hints or information about the existence of planets, rather than solely by scientific curiosity about stars [Lissauer, 1999]. In fact, the number of planets found orbiting stars is steadily increasing, although the vast majority belong to the hot gaseous giants similar to Jupiter or Saturn [Schneider, 2005; Encrenaz et al., 2004]. This means that distances at which planets have actually been observed, or are suspected to be, may be even greater than those in Figure 8.1, perhaps tens or even hundreds of light-years. The thought of finding not just life, but also intelligent life might be a powerful motivation if people were actually convinced of the likelihood of its existence. However, this seems not to be the case, or at least is considered a remote possibility; see [Crawford, 2000]. These thoughts should give pause to the discussion of propulsion systems for stellar missions.

Scientifically speaking, however, there are objects and regions of space that are much farther than our known planetary system, but closer than stars, and at the same time of great interest to science. Perhaps with some exaggeration, these destinations could be dubbed quasi-interstellar (QI) destinations. Among them some of the most interesting are (in order of their known distance from Earth) the Kuiper Belt, the heliopause, the gravitational Sun lens region, and the Oort cloud. Missions to these regions are very attractive; the reasons are given briefly below.

8.1.1 Quasi-interstellar destinations

Loosely speaking, the Kuiper Belt is the region of space beyond the orbit of Neptune or Pluto conventionally extending up to 100 AU from our Sun. Until the 1950s astronomers thought Pluto was more or less the last 'planet': with the exception of comets, perhaps only one or two other objects might be lying beyond its orbit. In 1951 the Dutch astronomer Gerard Kuiper started wondering about the place of birth of *short-period* comets, since each of their passes near the Sun subtracts 0.01% of their mass; their lifetime should be also very short, some 10,000 passes, or only half a million years [Luu and Jewitt, 1996]. Since the Solar System is more than 4.5 billion years old, no comet should have survived ever since.

After discovering 'planetoids', bodies orbiting the Sun, even larger than Pluto's moon Charon and with extremely long orbital period, we know now that the space beyond Neptune and Pluto is populated. The density of objects there is much too low to form larger bodies by mutual gravitational attraction; however, the large planets (Jupiter, Saturn) can draw and pull these objects toward the Sun along highly elliptic orbits. If, as it seems, this is a realistic picture, the Kuiper Belt is a reasonably close region of space where we could find objects (KBO, or TNO, Trans Neptunian Objects, for short) dating back to the formation of the Solar System, including most short-period comets [Hahn, 2005].

In fact, during its Saturn flyby, the Cassini spacecraft took pictures of one of the Saturn satellites, Phoebe from 13,800 km. Phoebe has a retrograde orbit and an average diameter of 220 km. The pictures Cassini took were fairly good, and indicated the presence of water [Porco, 2004]. The inference is that Phoebe did not come from the rocky, 'dry' asteroid belt between Mars and Jupiter, but rather from the Kuiper Belt, the birthplace of most short-period and water-rich comets. This fact, and the peculiar retrograde orbit, tell that Phoebe is likely a KBO captured by Saturn. Similarly rich in water in the KBO Quaoar [Jewitt and Luu, 2004].

Some of the planetoids already observed have fascinating features. Table 8.1 compares two of them, Sedna and the recently discovered DW2004, to Pluto: Sedna shuttles back and forth from way beyond the Kuiper Belt (in fact, near the edge of the Oort cloud) to the Sun. Its extremely eccentric orbit may be explained by an encounter with a star [Kenyon and Bromley, 2004]. A very reasonable conjecture is that Sedna must carry traces of its immense journey on its surface. Sedna would be a very desirable mission target indeed: some comets may travel even farther, but are not as large, which poses the question of how Sedna and other planetoids came to be. An even more interesting body discovered in January 2005 is 2003 UB313, a KBO bigger than Pluto [The Planetary Report, 2005]. Its orbit passes inside that of Pluto and is tilted 45° with respect to the ecliptic plane.

Table 8.1. Comparing orbits of Pluto and of KBO.

	Diameter (km)	Distance from the Sun (10^9 km)	Orbital period (years)
Pluto	2,300	4.4 to 7.4	248
Sedna	1,280 to 1,760	11 to 113	10,500
DW2004	1,610	4.6 to 7.1	250

In the tentative budget of the 'New Frontiers' NASA program there is in fact included a 'New Horizons' 2 mission (NH 2) to explore some near KBO. One of the candidate objects is called 1999 TC36: it consists of twin bodies, some 400 to 500 km across. TC 36 is similar, albeit smaller, to the Pluto–Charon system. As planned, right now this NH 2 mission will utilize gravity assists from Jupiter and Uranus, reaching TC 36 in 2014, and is considered a 'very fast' mission.

The heliopause is a region of space interesting for altogether different reasons. The Sun and its planetary system moves relative to the Galaxy, feeling the galactic 'wind' blowing interstellar hydrogen atoms and the weak galactic magnetic field. This wind shapes the heliosphere, the region of space where the galactic wind interacts with the solar wind from the Sun's corona (mostly, protons and electrons moving outwards at 300 to 700 km/sec). The heliosphere is shaped like a drop; its pointed end is estimated to be 50 to 100 AU from the Sun. Voyager 1 and 2, and the two Pioneer spacecraft, the man-made objects farthest from Earth, are still traveling within the heliosphere. However, Voyager 1, now at some 14 billion km from Earth is sending data indicating the magnetic field is increasing. This means the solar wind (traveling at about 700 km/sec from the Sun) is beginning to interact with the interstellar gas, slowing down and getting hotter in the process, and that Voyager 1 is entering the so-called heliosheath preceding the solar bow shock [Britt, 2005].

The boundary between the inside of the heliosphere and interstellar space is the heliopause. Its scientific interests lies in the peculiar environment constituted by a very thin hydrogen plasma (that is, protons and electrons, with particle density about $1/\text{cm}^3$) immersed in a very weak magnetic field: there is literally no way such a state of matter can be reproduced in the laboratory. Short of reaching the heliopause, the behavior of this type of plasma cannot be reliably observed.

A third deep-space mission of interest is associated with relativistic effects of massive bodies on starlight propagation, and goes under the name of gravitational 'lensing' [Wambsganss, 2001]. It is known from the General Theory of Relativity that a gravitational field bends light, ever so slightly. Our Sun does that with the light of every star grazing its apparent disc. In fact, rays of parallel light from such stars are bent by an angle ε given by

$$\varepsilon = 4\frac{GM_{\text{sun}}}{rc^2} \tag{8.1}$$

where ε is the deflection of the electromagnetic wave, G is the universal gravitational

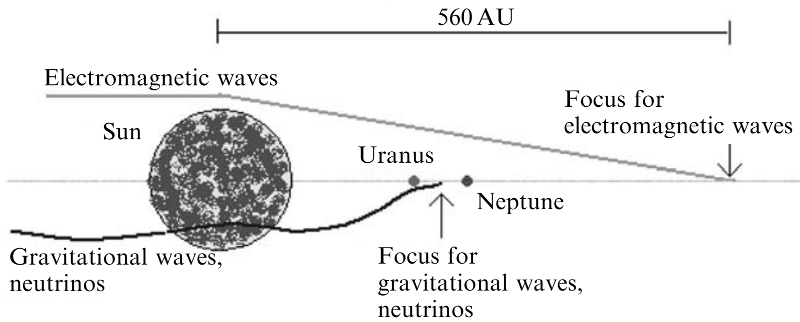

Figure 8.2. The Sun bending light acts as a lens.

constant, M is the mass of the Sun, c is the speed of light, and r is the distance of the [parallel] rays from the Sun center.

The nearer the light rays to the solar disc, the sharper the bending angle ε (see Figure 8.2). The Sun acts as a lens not just for visible starlight, but for all electromagnetic waves.

Viewed from Earth, the rays focus at a point that depends on the distance r and is 'to our back' when looking straight at the Sun. The minimum r is of course the Sun radius: when r is equal to the Sun radius, starlight rays focus at the point closest to Earth. This minimum focus is located at a distance about 542 AU (in fact, focus distance depends also on the light wavelength).

Calculations show that the angular and spatial resolution made possible by observing objects through this powerful 'lens' are worth noticing. The resolution is a function not only of the gain due to the lensing effect of the Sun, but also of the gain of the antenna on the spacecraft, proportional to its dish radius, r_{antenna}. The total gain is, in fact, the product of the two [Maccone, 2002, p. 12]:

$$\text{Total gain} = 16\pi G M_{\text{sun}} (r_{\text{antenna}})^2 \frac{\nu^3}{c^5} \tag{8.2}$$

The dependence on the cube of light frequency, ν, tells that, by choosing it well, angular resolution may become from two to four orders of magnitude better than the most accurate instrumentation ever used (e.g., that of the star-mapping Hypparcos satellite launched in 1989). Spatial resolution with a modest 12-m antenna dish positioned at the Sun lens focus could tell details of objects in the Oort cloud 145 km apart at the frequency of neutral H_2 (1,420 MHz), and 9 km apart at the higher emission frequency of water, 22 GHz. The Alpha Centauri star could be resolved at 1,250 and 80 km at the same two frequencies. Note we are talking of telling features 80 km apart on a star some 4.3 light years from Earth!

This nearly unbelievable performance has motivated conceptual planning of missions to the nearest Sun gravitational focus, that is at 542 AU from the Sun. Such is, for instance, the FOCAL mission proposed and described in [Maccone, 2002, Chapter 1).

Much farther away, about half a light year, is the so-called Oort cloud. Long ago astronomers started to suspect that long-period comets with extremely eccentric orbits spend most of their time at a distance from the Sun between 10^4 and 10^5 AU. Another Dutch astronomer, Jan Oort, conjectured that this region of space must contain millions or even billions of such comets. Similarly to that in the Kuiper Belt, interest in the Oort cloud is in the fact that it may contain farther and maybe different relics of the formation of our planetary system, and thus the oldest traces of its formation. Comets, according to C. Sagan's definition, are dirty snowballs, the dirt being the original materials ('planetesimals') our planets were made of. This is in fact the very purpose for the Rosetta mission planned by the European Space Agency: to land on a (not so distant) comet and return to Earth a sample of its 'dirt'. Analysis of this dirt would shed light on the composition of planetesimals, and perhaps on the origins of our planetary system, since we know the distribution of elements in the Solar System [Sciama, 1971]. The type and abundance of elements depends ultimately on the supernova explosion that created what astrophysicists call 'heavy matter' or 'metals' (that is, any element heavier than hydrogen and helium) in our galactic region. Material in the Kuiper Belt has undergone collisions and 'mixing' far more frequently than in the Oort cloud, where density of objects is lower and where it could be found in its pristine state. In this context, a very interesting mission could be that to Sedna, since its almost unique orbit stretches from the Sun to near the Oort cloud's edge. In other words, Sedna is one of the larger and denser quasi-interstellar objects visiting the Solar System periodically.

These examples of QI scientific missions are far from involving stellar distances (the distance traveled by FOCAL would be about 5‰ of a light year; the Oort cloud stretches no more than 0.5 light years from Earth). Nevertheless, these destinations are immensely distant compared to what travelled so far; Voyager, the farthest space object manufactured on Earth, is at 93 AU from us, and Pioneer 10 is at 87 AU [The Planetary Report, 2004]. To reach these destinations in times compatible with the lifetimes of crew and mission ground teams, we need propulsion means never developed before.

8.1.2 Times and distance

With this 'distance' caveat in mind, 1 light year will be a yardstick for stellar space trips. Moving final destination from Solar System planets to nearby stars, or even to the Oort cloud, crossing times become huge traveling at constant speed. In the hypothetical trip to Neptune at 1 'g' acceleration, used as an example in Chapter 7, the top speed reached near Neptune was 6,700 km/sec. Assume the engine turned off there: coasting to Proxima Centauri at the same speed would take 188 years. Such an engine would have to produce sufficient thrust to keep constant 1 'g' acceleration for $7\frac{3}{4}$ days, consuming a propellant mass that depends exponentially on I_{sp}. Using the Tsiolkovski's rocket equation, the propellant mass consumed, M_{ppl}, assuming an $I_{sp} = 1000$ sec typical of a nuclear thermal rocket, would be a truly astronomical number:

$$M_{ppl} = \exp\left(\frac{\Delta V}{g\,I_{sp}}\right) = \exp(683.2) = 5.131 \times 10^{296} \tag{8.3}$$

Unless the I_{sp} of the propulsion system can be drastically raised (say, from the 10^3 sec typical of nuclear thermal or current ion electric propulsion), the initial mass of the ship would be completely dominated by propellant mass, and the thrust to ensure 1 '*g*' acceleration would, accordingly, be just as immense. Thus, mass-frugal means to power such acceleration must be found. Alternatively, any such propulsion system must have a much higher I_{sp} than discussed so far. Stellar or quasi-interstellar missions using Newton's Third Law are doubly constrained: at constant speed, they take too long; at constant acceleration, they need large thrust and propellant mass. They may become feasible only for I_{sp} much larger than those seen in Chapter 7.

Bypassing the second constraint is possible, in principle, by collecting mass to utilize for propulsion while traveling, just as the airbreathing engines in Chapter 4 do in the Earth atmosphere. Interstellar space is not a mathematical void: in the disc of our Galaxy the mass density, ρ_H, of interstellar hydrogen is of order 10^{-27} kg/m^3 [Sciama, 1971, p. 25] (since a hydrogen atom weighs about 1.67×10^{-27} kg, this density corresponds to about one hydrogen atom per cubic meter). At 'sufficient speed', this density can be exploited, i.e., atoms can be captured by an appropriately designed inlet. This strategy leads to the concept of 'interstellar ramjet' [Bussard, 1960; Cassenti and Coreano, 2004]. For instance, the hydrogen collected could be fused to provide power and thrust. The power, P, collected is a function of speed, V, and inlet area, A, since $p_H\, A\, V$ is the mass of H atoms collected while flying:

$$\dot{m} = \rho_H\, A\, V \qquad \text{Mass flow}$$

$$P = \dot{m}\alpha c^2 = \rho_H\, A V \alpha c^2 \qquad \text{Power} \tag{8.4}$$

where α is the fraction of H captured actually fused, of order 3 to 4×10^{-3} (see Figure 8.3). Hence the minimum inlet area to ensure a given P, for instance 1 GW, is

$$A = \frac{P}{\rho_H\, A \alpha c^2} \tag{8.5}$$

The problem with interstellar ramjets shows when putting actual numbers in equation (8.5). Even assuming V of the order of the speed of light c, the scooping area to collect 1 GW is of order of 10^{12} m^2, or a square $10^3 \times 10^3$ km. In fact, our Sun is in a region of our Galaxy where ρ_H may be even lower than assumed in this estimate, e.g., of order 0.04 atoms/cm^3 [Cassenti and Coreano, 2004]. If relativity holds, such propulsion systems are unfeasible for the foreseeable future. In any event, the interstellar ramjet still depends on a 'booster' capable of accelerating the ramjet to that 'sufficient speed' V, and thus requires on-board propellant.

8.2 THE QUESTION OF I_{sp}, THRUST AND POWER FOR QUASI-INTERSTELLAR AND STELLAR MISSIONS

The kind of distances and times just outlined suggest key issues are somewhat similar to those examined in Chapter 7; in other words, I_{sp} (total mass of propellant to carry

Fuels (Ratios)	Reaction products	Energy density, J/kg $E/m = \alpha c^2$	Converted mass fraction $\alpha = \Delta m/m$
Chemical:			
Conventional: LO2/LH2	water, hydrogen	1.35×10^7	1.5×10^{-10}
Nuclear fission:			
U233, U235, Pu239 (~200 MeV/U235 fission)	fission fragments, neutrons, γ-rays	8.2×10^{13}	9.1×10^{-4}
Nuclear fusion:			
DT (0.4/0.6)	helium, neutrons	3.38×10^{14}	3.75×10^{-3}
CAT-DD (1.0)	hydrogen, helium neutrons	3.45×10^{14}	3.84×10^{-3}
DHe3 (0.4/0.6)	hydrogen, helium	3.52×10^{14}	3.9×10^{-3}
pB11 (0.1/0.9)	helium	7.32×10^{13}	8.1×10^{-4}
Matter plus antimatter:			
p-p- (0.5/0.5)	pions, muons, electrons, positrons, neutrons, and γ-rays	9×10^{16}	1.0

Figure 8.3. Chemical, fission and fusion energy release and their mass conversion fractions (adapted from [Kammash, 1995]).

and accelerate), thrust (and the acceleration needed to reach final destination within reasonable time spans), and the power to sustain thrust. The only difference with the discussion in Chapter 7 is the extreme influence played by these three factors in planning QI and stellar missions.

It is useful at this point to review the concept of I_{sp} already defined in Chapter 7 for nuclear propulsion. Thrust is assumed here still based on Newton's Third Law, the result of change in the momentum of propellant(s).

In reviewing that concept, in fact, it is convenient to realize that thrust is the result of an energy conversion process going through three stages. In stage one, energy is stored as potential energy, for instance chemical, or associated to rest mass as mc^2, according to relativity theory. When released, potential energy becomes the microscopic kinetic energy of particles, already existing such as unburnt fuel or inert propellant, or newly created, such as translational, rotational and vibrational energy of molecules, translational energy of neutrons, alpha and beta particles, and energy of photons, $h\nu$: this constitutes the second stage. In the first class of nuclear engines described in Chapter 7, it is the confinement effect of a nozzle, conventional or magnetic, that converts this 'microscopic' kinetic energy into the macroscopic, ordered motion of particles, that is, kinetic energy $0.5\, mV_e^2$ of the exhaust jet (stage three). It is this third and last stage that is responsible for bulk flow momentum change, and therefore for the rocket thrust.

The ideal specific impulse is nothing else than the exhaust velocity, V_e. If energy is conserved, the kinetic energy of stage two and three must be equal. So, the exhaust velocity, or I_{sp}, ideally attainable must be equal to that of the microscopic, energetic particles inside the chamber where potential energy is released and where the macroscopic (bulk) flow speed is essentially zero (stagnation). In a chemical rocket the ideal V_e will be exactly equal to the mean molecular speed at the stagnation chamber temperature. In a propulsion device based on other forms of energy conversion, equating stage two and three, and neglecting relativistic effects, shows immediately that the I_{sp} can be defined as the square root of twice the microscopic kinetic energy per unit mass, J, of the medium utilized as recipient of that energy. In fission propulsion the medium could be the very fission fragments mentioned in Chapter 7, possessing kinetic energy of order 167 MeV [Hill and Peterson, 1970, p. 475] when fissioning ^{238}U fuel. In hydrogen fusion, the energetic particles are He nuclei, possessing lower average energy, say, between 4 and 40 MeV (see Figure 8.3). However, *fused* He particles are much lighter than average *fission* fragments, so their specific energy, or energy density, J, is larger.

So, a more general definition of the ideal specific impulse becomes, neglecting relativistic effects,

$$I_{sp} = \sqrt{2J} = V(\text{m/sec}) \tag{8.6}$$

This way of writing I_{sp} shows immediately the gain in performance going from chemical ($J \sim 10^7$ J/kg) to fusion ($J \sim 10^{14}$ J/kg) propulsion (see Figure 8.3).

Fusion has a higher α, of order 3 to 4×10^{-3} (depending on fuels) than fission (the α with ^{235}U is 9.1×10^{-4}), and therefore the energy density in fusion will be higher by a factor 4–5 as shown in Figure 8.3. Thus there is a definite advantage in looking at fusion reactors as the next power source after fission. However, similarly to what was noted in Chapter 7 in the case of fission-powered rockets, if fusion energy is not utilized directly in the form of kinetic energy of fission fragments (that we have called 'stage two') but is transformed into heat, transfered to a solid and then to a propellant, it will be inevitably limited by the melting point of that solid, 2,500 to 3,000 K at most, and the I_{sp} will be no different from that of a NTR. The gas-core and the Rubbia's concepts in sections 7.14 and 7.15 circumvent somewhat the limitation imposed by the melting point of structural materials, raising I_{sp} by a factor 2 to 3 with respect to NTR; the same strategy might be possible, perhaps, also in fusion rockets, but the actual propulsion gain with respect to fission rockets of similar type will be questionable, limited only to a lower fuel consumption. Unless thrust is based on acceleration of the fusion fragments, higher I_{sp} may become feasible only with fusion-powered NEP systems, that suffer from low thermal and electric efficiencies and weight penalties.

So, generally speaking, the advantage in energy density of fusion over fission is not so extraordinary to enable a 'jump' in performance over that of fission-powered rocket systems. The ideal I_{sp} attainable by fusion may be, however, extremely high *if* fused particles are themselves the 'propellant' and are ejected with all their microscopic kinetic energy. In this case there is indeed a significant difference between fission and fusion rockets. Fission fragments from ^{235}U are 'heavy', falling into two main ranges centered roughly at about 40 and about 160 atomic mass units. Fusion fragments instead consist mainly of ^{4}He, a nucleus a factor 10 or 40 lighter. Everything else being equal, the I_{sp} potentially available with fusion rockets will be accord-

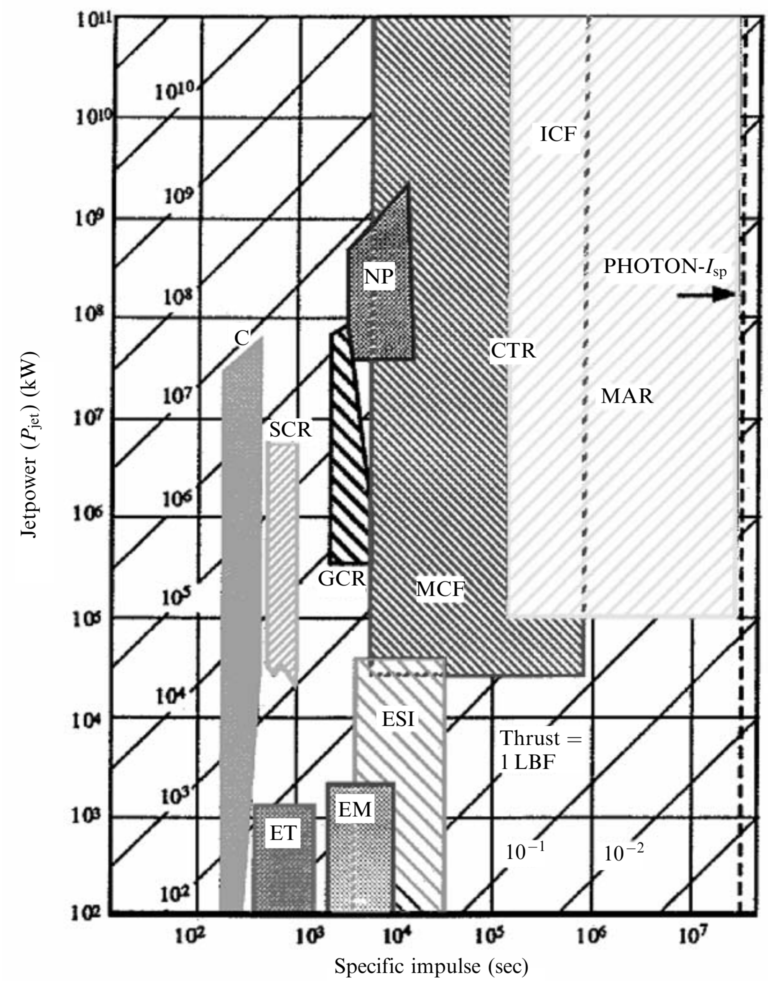

Chemical C	Gas core reactor GCR
Controlled thermonuclear reactions CTR	Inertial confinement fusion ICF
Electric propulsion EP	Magnetic confinement fusion MCF
Electromagnetic EM	Mass annihilation rocket MAR
Electrostatic ion thruster ESI	Nuclear pulsed (orion type) NP
Electrothermal ET	Solid core reactor SCR

Figure 8.4. Power and I_{sp} of chemical, fusion and fission system (adapted from [Kammash, 1995]).

ingly higher than fission by the square root of the same factor and because the specific energy of fusion products is about five times higher than in fission. Estimates of *ideal* I_{sp} with different fusion rocket concepts are given in Figure 8.4, showing the I_{sp} of a magnetic confinement (MCF) rocket may be 10^2 to 10^3 times higher than fission propulsion concepts. Similar data are in [Lawrence, 2005]. Even higher I_{sp} is predicted for a mass annihilation rocket (MAR), that may be defined, with some reason, as the extreme form of fusion in which *all* mass is converted into energy ($\alpha = 1$) [Morgan, 1982; Forward, 1985]. The last vertical line on the right of Figure 8.4 is the theoretical I_{sp} of the Saenger/Rubbia photonic rocket concept of Chapter 7. Its I_{sp} is exactly equal to c, *if* consumption of nuclear fuel is not accounted for in the mass consumption rate.

If the energy of fused particles at stage two is thermalized in a much larger mass flow of a secondary (inert) propellant, J decreases and so will temperature, a good thing for the engine structure. I_{sp} will decrease as well, depending on thermalization strategy, but less so than J, because of the square-root relationship, just as shown for fission propulsion systems in Chapter 7. For instance, the J available at stage two could heat a secondary propellant expanding in a conventional nozzle, resulting in I_{sp} of the same order of solid-core nuclear thermal rockets (about 1,000 sec). Alternatively, high J fusion products could heat a working fluid and generate electricity via conventional thermodynamic cycles, just as in nuclear electric propulsion. The electricity can then power an electric thruster, for instance a large MPD rocket: thus I_{sp} could be made very high, but efficiency of the thermodynamic cycle and of the thruster would be low, perhaps of order 30%.

Assuming no energy losses, if I_{sp} can be made higher the thrust (F) must decrease, because

$$\text{Thrust power} = FV_e = FI_{sp} \tag{8.7}$$

So, at fixed power and depending on the type of mission, a trade-off exists between the combination of high I_{sp} (low mass of propellants) and low F (low acceleration) and its reverse, that is lower I_{sp} but faster acceleration due to larger F. Figure 8.4 shows such a trade-off immediately, because thrust power is reported on the vertical axis.

Whatever the trade-off, power scales with I_{sp}^3, because $F \sim (\mathrm{d}m/\mathrm{d}t)I_{sp}$, and $\mathrm{d}m/\mathrm{d}t \sim I_{sp}$. In fact, whether the propulsion system accelerates only the mass of products of energy conversion, or adds to them inert propellant, or even scoops mass from space, tremendous power is needed to support large I_{sp}. In Chapter 7 it was seen that increasing I_{sp} by means of electric propulsion does not pose insurmountable problems. I_{sp} in the 10^5 sec range are assumed feasible in NASA studies [El-Choueiri, 2002; Mikellides, 2004]. Electromagnetic acceleration is inherently suited to produce large exhaust speeds, based as it is on applying a direct Lorentz body force to each charged particle: that is, exhaust speed is no longer tied to the rocket engine thermodynamic cycle. *Powering* such an electromagnetic system, producing large exhaust speed and I_{sp}, is instead the real challenge, since power scales as $I_{sp}^3 = V_e^3$. To illustrate this point, a propulsion system capable of 20 tons (44,100 lb) thrust with $I_{sp} = 10^5$ sec needs about 200 GW (200 *billion* watts) to function, assuming 100% efficiency. For reference, the total electric power installed in the US is of order 1,000 GW [Trumbull, 2000].

8.3 TRAVELING AT RELATIVISTIC SPEEDS

Conceptual planning of long QI or stellar missions must eventually include relativistic effects. In Chapter 7 exploration of the Solar System was proposed using constant acceleration (a) for a sizeable portion of the trip. One may think this strategy could work also for interstellar missions. Consider, for instance, a trip to Proxima Centauri at constant 1 'g' acceleration ($a = 1g = 9.807\,\mathrm{m/sec^2}$) until halfway, $S_{1/2}$, followed by deceleration with $a = -1g$ till final destination, *Newtonian* mechanics predicts a trip time

$$\text{Trip time} = 2\sqrt{\frac{2S_{1/2}}{a}} \tag{8.8}$$

Here $S_{1/2}$ is the half distance from Earth to Proxima Centauri, or about 2 light-years (a 1 'g'-trip is often proposed because this acceleration results in spacecraft living conditions equal to those due to Earth's gravity). Mid-course speed, $V_{1/2}$, is then:

$$V_{1/2} = \sqrt{2aS_{1/2}} \tag{8.9}$$

and in this example its actual value is $6.3 \times 10^8\,\mathrm{m/sec}$, or 2.1 times the speed of light! According to the Theory of Special Relativity, this is impossible, and so is the acceleration $a = 1g$ chosen for this trip. Beyond the issue of the power needed to keep accelerating for long times, this example shows there are also issues associated to the type of physics and math needed when spacecraft speed starts approaching the speed of light. Relativistic speeds need a completely different suite of physical and mathematical tools. Newtonian mechanics is insufficient to calculate or plan, even conceptually, trips over such distances when the spacecraft speed starts approaching the speed of light.

Note also that in the 1916 version of the Theory of Special Relativity [Einstein, 1916] mass 'at rest', m_o (that is, when its velocity $V = 0$) is different from the same mass, m, in motion:

$$m = \frac{m_o}{\sqrt{1 - \left(\frac{V}{c}\right)}} \tag{8.10}$$

The energy $E = mc^2$ must therefore be redefined as

$$E = \frac{m_o c^2}{\sqrt{1 - \left(\frac{V}{c}\right)}} \tag{8.11}$$

These expressions are the result of the Lorentz transformations [Einstein, 1916; Lang, 1999; Froning, 1983] introduced by Einstein because [Harwit, 1973, Chapter 5] they allow both the laws of mechanics *and* those of electromagnetism to stay the same when changing inertial frame of reference (unlike the laws of dynamics, the Maxwell equations of electromagnetism change when classical Galilean transformations are used to correlate inertial frames). In 1948 Einstein discarded the concept of relativistic mass defined by equation (8.10) in favor of relativistic energy (8.11) only, which is completely consistent with the four-dimensional momentum formulation of his original theory (see [Miller, 1981] for details).

Inspection of equation (8.11) shows that, over long trips at sustained power such that spacecraft speed starts approaching the speed of light, there appears a new problem. In Newtonian mechanics applying a thrust F to a mass M results in an acceleration F/M. The thrust power needed is FV, growing with V^3 if V is the velocity of the mass ejected. Power stays always finite. At high V/c instead, the relativistic equation (8.11) predicts that more and more energy is needed as V/c grows, tending to infinity as V approaches light speed. Because energy can be produced only by mass conversion, the implication is that to reach higher and higher speed the mass to carry would have to be larger and larger. In the end, to achieve light speed the energy required is infinite, meaning the mass to be converted into energy would also be infinitely large. Thus, following the question of power, the second question is, how much mass will be needed to accelerate a spacecraft when the energy required increases faster and faster with spacecraft speed? This question can be better posed in terms of the ratio between initial and final spacecraft mass, the mass ratio (or weight ratio) MR. This ratio must be reasonable, and the Tsiolkowski law suggests that, to keep it so, the propulsion system must be capable of I_{sp} much higher than today's, perhaps by a factor 10^2 to 10^3.

Figure 8.4 tells that only fusion rockets, or their limit case of matter–antimatter annihilation rockets, could theoretically reach such I_{sp}. For the 10-ton spacecraft previously considered in Chapter 1 the LEO weight is 1,000 tons (2,205,000 lb). That is less than some large vertical launch rocket launchers, that have lift-off mass order of 2,000 tons (4,410,000 lb). Such mass is significant to put into orbit, but an Energia class launcher with a 230-ton cargo capability could lift it in five launches. If the 300-ton configuration were used with a tandem payload section, instead of a laterally mounted cargo container, then only four launches would be necessary.

In reality, a 10-ton payload for such a mission is insufficient. For long duration at least a 100-ton spacecraft is necessary and the launch weight from LEO for a *one-way mission* is now 10,000 tons (22,050,000 lb). The results would be a massive vehicle in LEO, perhaps such as the one artistically illustrated in Figure 8.5. As propellant tanks empty, they would be discarded to reduce the empty weight of the spacecraft and therefore reduce the propellant consumed. For this duration, the ship would have to have an energy source that could sustain thrust over the duration required. At this point, the only such energy source with the I_{sp} needed is based on fusion or antimatter annihilation, and the ideal mission time, t_{mission}, would be determined by the fact that the average thrust power

$$P = FI_{sp} \tag{8.12}$$

is related to the potential energy available onboard

$$E = \alpha m_{\text{fuel}}\, c^2 \tag{8.13}$$

by the constraint that

$$P = E/t_{\text{mission}} \tag{8.14}$$

Figure 8.5. An artist's view of a future heavy-lift vehicle in LEO.

The time and distance permitted by a particular propulsion system and mass ratio are not strictly related to whether the spacecraft is manned or robotic. But the assets required to sustain conscious human beings over long durations (perhaps 10 to 20 years) result in a prohibitive weight and volume penalty. For such a mission, a future spacecraft would have to be a self-sufficient, integrated ecological support system. In this chapter only unmanned, robotic missions are considered in the determination of size and weight of spacecraft with respect to different propulsion systems.

To operate a propulsion system when speed approaches a significant fraction of the speed of light, energy and mass must be treated relativistically, and the constant acceleration strategy valid for exploring the Solar System may no longer be a template for stellar trips. The constraint $V/c < 1$ affects all aspects of spacecraft, including that of its propulsion system. For fast QI and interstellar travel the I_{sp} (or, exhaust V_e) must be much higher than ever thought possible in the past and become no longer negligible with respect to c. This means that gas-dynamics and magneto-hydro-dynamics (MHD) should be reformulated to account for relativistic effects inside the propulsion systems themselves. Although relativistic equations of motion for gases and plasmas have been developed, they are far from having been universally accepted, let alone understood, for application to realizable propulsion systems (e.g., see [Anile and Choquet-Bruhat, 1987]).

This is a strong caveat, suggesting that issues associated with relativistic propulsion systems be left aside, at least insofar as they are based on the principle of action and reaction. The analysis that follows will assume V_e/c sufficiently smaller that relativistic effects may be neglected, and will examine what propulsion systems, if any, are likely to work over interstellar or quasi-interstellar distances. Energy density and power are some of the key aspects in answering these questions.

It is also understood that theoretical considerations, for instance, about fusion and its implementation in a rocket, are solidly grounded in established physics, but that true propulsion applications do not exist yet. Therefore many if not all of the systems discussed or outlined, and all of the most innovative concepts, are speculative.

8.4 POWER SOURCES FOR QUASI-INTERSTELLAR AND STELLAR PROPULSION

The physics at our disposal is still based on that developed up to the late 1920s (special relativity and quantum mechanics, besides Newton's Third Principle). Within its formulation, energy and mass are interchangeable. Einstein's $E = mc^2$ holds the only key to potential 'new' power sources. In this light, there is no longer a question of finding 'new' power sources as much as of finding new energy technologies exploiting $E = mc^2$.

In fact, even combustion heat release (about 1.3×10^7 J/kg when burning hydrogen and oxygen), is predicted by Einstein's formula. In the rearrangement of electrons due to chemical reactions (orbitals and bonds, in chemistry parlance) what is called 'combustion' energy is actually a very slight percent mass decrease α (mass 'defect'), of order 1.5×10^{-10} [Harwit, 1973; Kammash, 1995, p. 6]. The sum of mc^2 and of the microscopic kinetic energy is of course constant, so a mass defect in any process means kinetic energy must increase. In combustion it is more practical to keep track of ('conserve') microscopic molecular kinetic energy, meaning macroscale Gibbs' energy, enthalpy or internal energy, rather than accounting also for the exceedingly small mass defect of products with respect to the reactants. This is the reason that Einstein's expression is never used in chemistry, although perfectly valid: mass would not be conserved, and the energy equation would have to contain the additional term mc^2. In fact, dynamics itself would have to be rewritten, using space-time (not space and time separately, and the 4-vector, or tensor, $\mathbf{p}$ [Harwit, 1973, Chapter 5; Miller, 1981].

Fission was the first example of deliberate searching for processes where mass could be converted into energy. The binding energy curve (Figure 8.6) [Mukhin, 1987] indicates that ^{235}U (as well as other actinides) is a good candidate nuclear 'fuel', with 200 MeV released per nucleus, yielding 8.2×10^{13} J/kg. The fraction of mass converted, α, is 9.1×10^{-4}.

8.5 FUSION AND PROPULSION

The same curve of Figure 8.6 shows He could be a good candidate 'product', if hydrogen is viewed as the 'fuel' to form it, because the binding force is larger among nucleons of ^{4}He than among four H nuclei. Indeed, this is the goal of all current nuclear fusion research: to 'fuse', or merge, four smaller H nuclei into a larger ^{4}He nucleus (actually, hydrogen isotopes deuterium, D, and tritium, T, are better than common hydrogen in this respect). This process is therefore the opposite

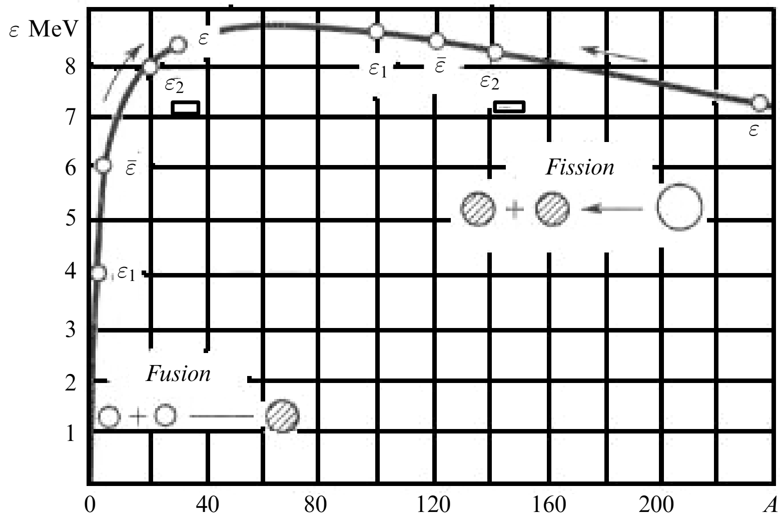

Figure 8.6. Binding energy per nucleon, as a function of mass number, A [Mukhin, 1987].

of fission, where a large nucleus, such as ^{235}U, is split and forms smaller fission fragments. A notional sketch of fusing D and T, forming a He nucleus (an alpha particle) plus a neutron is shown in Figure 8.7. Other light nuclei may be fused forming a heavier nucleus, but in practice nearly all fusion research in focused on hydrogen because its nuclear kinetics is theoretically easier to start.

For illustration only, a hydrogen fusion reaction, and its mass (kilogram) and energy (joule) budgets could be simplified as follows (see also Figure 8.3):

Reaction	4H	$\rightarrow$	He	$+$	Energy
Mass	$4(1.6725 \times 10^{-27})$	$\rightarrow$	6.645×10^{-27}	$-$	Mass
Energy	$6.693 \times 10^{-27}\,c^2$	$\rightarrow$	$6.645 \times 10^{-27}\,c^2$	$+$	$0.048 \times 10^{-27}\,c^2$

where the mass defect is 0.048×10^{-27} kg per each He atom formed, converting about 0.38% into energy with a yield $J = 3.45 \times 10^{14}$ J/kg. Note that only about 0.38% of the mass is converted into energy (the actual number depends on the specific fusion reaction, see Figure 8.3). Only in matter–antimatter annihilation does 100% of mass, for instance, that of a proton, p, and of an anti-proton, p^-, converts into energy. Accordingly, in this extreme case of fusion, the energy release is c^2 per each kg, or $J = 9 \times 10^{16}$ J/kg if the value for c is simplified as 3×10^8 m/sec. Even not going to such an extreme, on a per-mass basis, fusion yields more than 10^8 times the energy of gasoline burning with air (the reader is referred to [Chen, 1985] for a comprehensive textbook on fusion and its issues).

These striking numbers, and the relative abundance of hydrogen and deuterium on Earth (deuterium atoms constitute 2×10^{-4} of all terrestrial hydrogen atoms [Harwit, 1973, p. 257]) have motivated fusion research since the US Matterhorn Project of the 1950s. The mass defect in fusing hydrogen is still minuscule, but

Deuterium–Tritium fusion reaction

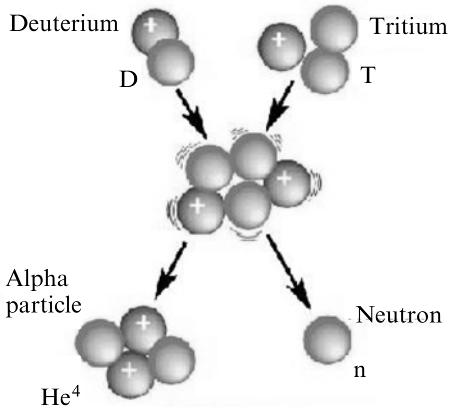

Energy multiplication about 450 : 1

Figure 8.7. Sketch of D–T fusion process (http://hif.lbl.gov/tutorial/tutorial.html).

greater by a factor of 4–5 than fissioning uranium or plutonium. The half-century funding of fusion for power generation rides on the hope to extract this energy, starting from the deuterium already present in a small but significant percentage in seawater.

The ultimate energy source is clearly total, 100%, conversion of mass via annihilation, not just a percentage of order 0.3 or 0.4 [Morgan, 1982; Forward, 1985]. Of course this energy would not be necessarily released in the most convenient form for propulsion or power. It may consist mostly of energetic particles, including gamma-rays, for instance. Direct thrust from the momenta of these particles would be very small; the alternative, thermalizing the energy of mass particles or photons in a useable device would certainly be a major technology problem; however, the experience gained in fusion physics could help.

Based on the considerations made, the large energy density of fusion suggests I_{sp} could be large as well, in particular when no inert propellant is added to the fuel injected inside the fusion reactor, and this is indeed what Figure 8.4 predicts. Assuming the numbers shown are realistic in a conceivable future, it is worth estimating their effect on length of stellar or QI missions. In doing such estimates the trade-off between I_{sp}, F and the overall power and mass demand of the propulsion system are central issues. Just as important is the impact of I_{sp} on the duration of QI and stellar missions.

8.5.1 Mission length with I_{sp} possible with fusion propulsion

An instructive exercise is to see what might be the effect on stellar trips of performance enabled by fusion energy. In [Borowski, 1987] missions at *constant thrust F* are examined to gauge these effects. A constant thrust mission is different from a mission at constant acceleration, because the mass of the ship decreases with time; its convenience as a yardstick lies in the fact that solutions are analytical. In fact, using this strategy, the round-trip time t_{ES} to go from Earth to a star, e.g., Proxima Centauri, turns out to be

$$t_{ES} = \left(\frac{4D}{g\, I_{sp}}\right) + \sqrt{\frac{DM_f}{F}} \tag{8.15}$$

where D is the straight distance to Proxima Centauri, about 4.3 light years or 4×10^{16} m, and M_f is the final mass of the ship after the trip is over. The ratio F/M_f is an acceleration, precisely that *at the trip end* (not during the trip!) and for the present purpose can be assumed to be a constant (for instance, 1 g). F is kept constant.

The inverse dependence of trip time on I_{sp} on equation (8.15) is striking, but it was also found in a different form in section 7.18, where time to accelerate, t_{acc}, was found to be proportional to I_{sp}. The dependence on F is tempered by the square root. For I_{sp} in the upper range enabled by fusion strategies (10^6 to 10^7 sec, see Figure 8.4), the first term is much smaller than the second and can be neglected.

Actual numbers using equation (8.15) indicate that reaching Proxima Centauri and back takes 508 and 51 years at $I_{sp} = 10^6$ and 10^7 sec, respectively. Average speed, V_{av}, is

$$V_{av} = \frac{D}{t_{ES}} = \frac{g\, I_{sp}}{4} \tag{8.16}$$

With the approximation made, this average velocity depends only on I_{sp}, and is of order 10^6 or 10^7 m/sec, respectively. This means Newtonian mechanics can still be used if I_{sp} is in the low range, while a small relativistic correction could be made in the high range (where V_{av}/c, about 8%, is not completely negligible). These mission times are substantial; since in relativistic physics I_{sp} has an absolute maximum, the speed of light $c = 3 \times 10^8$ m/sec), the conclusion is that a mission at constant thrust might still not be the best strategy over stellar distances.

To reduce trip time, it appears the trip should be made at a speed as close to c as practicable. Neglecting relativistic effects (therefore violating the self-imposed rule of section 8.3), at the speed of light the round trip would take of course 8.4 years for the crew. Traveling at average $V = 0.5c$ would double the trip to nearly 17 years, not accounting for the acceleration and deceleration periods. This strategy means that thrust should have a history in which acceleration ramps rapidly, followed by a period in which it stays constant until V reaches a significant fraction of c. Finally, a deceleration period should slow the spacecraft down, to enable orbit capture near the star or planet. For a given final mass, M_f, this means the power demand must be very high, since thrust power $P = FI_{sp}$, but only during the acceleration period, when F is increasing or constant. Once the ship moves at the planned fraction of c, power can be turned off and $F = 0$, the ship coasting at high speed.

A crude example may help in understanding the terms of the problem. If the time-averaged ship mass is of order 100 metric tons, and $a = 3g$ (a modest increase over 1g calculations made before, but barely tolerable by a human crew), F would be 3×10^6 N, and P, at an optimistic $I_{sp} = 10^7$ m/sec, would reach above 10^4 GW.

Fusion energy release is of order 3×10^{14} J/kg, and about 100 g/sec of D–T fuel (see section 8.6, below) would have to be fused. However, the mass conversion ratio in fusion is only about 0.3%, meaning the actual fuel flow-rate injected inside a fusion chamber would have to be 1/0.003 times higher, or 33 kg/s. During only one day, the total mass of fuel injected would be of order 2,850 tons, two orders of magnitude greater than the assumed mass of the ship. Working close to the theoretical I_{sp}, say, 10^8 m/sec, the fuel consumption would reduce to 285 tons/day, still an astonishing figure. More encouragingly, fusing a proton, and an antiproton, p^- (mass annihilation, 100% mass conversion) yields $J = c^2/\text{kg} = 9 \times 10^{16}$ J/kg; so in the same example the mass consumption would drastically reduce to 9.6 kg/day; see also [Borowski, 1995].

As of now, no nuclear process exists with yield in between that of fusion and that of annihilation. Percent mass conversion is either in the few parts per thousand (using D, T or H fuels and kinetics) or 100% (annihilation). The reason is the binding energy of Figure 8.6, that is no higher than about 8 MeV per nucleon. Until annihilation becomes a practical process, and provided relativistic effects can be dealt with, practical QI and stellar travel with technologies within our grasp and ship masses below $O(10^3)$ ton will depend essentially on distance, and will be limited by how long acceleration (thrust) can be maintained to reach a substantial fraction of the speed of light.

Before examining the details of high energy density propulsion based on fusion, an important aspect of practical QI and stellar missions is that the length of a mission, calculated in this section from the viewpoint of a spacecraft crew, may be different for the mission support team left on Earth. Effects due to missions performed at constant acceleration and reaching relativistic speeds, together with their consequence on mass ratio have already been mentioned in section 8.3, but differences in times have not, and are found in Chapter 9.

The considerations made about travel times and mass consumption in this and in the previous section should warn about presuming too much from propulsion as we know it, that is, based on Newton's Third Principle. Power and mass consumption, together with distances to cross and mission times are formidable hurdles, although mastering mass annihilation may overcome the first two. Notwithstanding all this, because of its energy density, fusion is the only power source viable for future QI, if not interstellar, space travel, and is a source that has been studied at least for half a century.

What follows deals with how fusion energy can actually be harnessed and work in a space propulsion system, with emphasis on the different technologies proposed, their drawbacks and their advantages (see [Leifer, 1999] for a brief summary).

8.6 FUSION PROPULSION: FUELS AND THEIR KINETICS

The very first proposals to utilize fusion as a power source for rocket and space propulsion were those by Maslen [Maslen, 1959] and Englert [Englert, 1962]. NASA recognized the potential of fusion at about the same time, see [Schulze and Roth,

Reaction		Yield (%)	Products (MeV)	T_{ignition}, K
1a	D + D	$\xrightarrow{50\%}$	T(1.01) + p(3.02)	300×10^6
1b		$\xrightarrow{50\%}$	He^3(0.82) + n(2.45)	
2	D + T	$\longrightarrow$	He^4(3.5) + n(14.1)	50×10^6
3	D + He^3	$\longrightarrow$	He^4(3.6) + p(14.7)	500×10^6
4	T + T	$\longrightarrow$	$He^4 + 2n + 11.3$	
5a	He^3 + T	$\xrightarrow{51\%}$	$He^4 + p + n + 12.1$	
5b		$\xrightarrow{43\%}$	He^4(4.8) + D(9.5)	
5c		$\xrightarrow{6\%}$	He^3(2.4) + p(11.9)	
6	$p + Li^6$	$\longrightarrow$	He^4(1.7) + He^3(2.3)	
7a	$p + Li^7$	$\xrightarrow{-20\%}$	$2He^4 + 17.3$	
7b		$\xrightarrow{-80\%}$	$Be^3 + n - 1.6$	
8	D + Li^6	$\longrightarrow$	$3He^4 + 22.4$	
9	$p + B^{11}$	$\longrightarrow$	$3He^4 + 8.7$	
10	$n + Li^6$	$\longrightarrow$	$T + He^4 + 4.8$	
11	$n + Li^7$	$\longrightarrow$	$T + He^4 - 2.5$	

Figure 8.8. Fusion kinetics (T = tritium; D = deuterium; p = proton; n = neutron. Energies are in megaelectronvolts (adapted from [Huba, 2002]).

1991]. A list of recent studies of generic fusion propulsion concepts is in [Santarius and Logan, 1998], where emphasis is on the power available per unit mass *of the reactor*, not per unit propellant or fuel mass. This parameter, let us call it α^* to distinguish it from the same symbol used in this book, is, in fact, *the* parameter of importance when engineering a practical reactor. The appeal of fusion propulsion stays in the fact that α^* may be in the range of a few kilowatts per kilogram.

The starting point in attempting to design conceptually a fusion propulsion system is the choice of fuel fusion cycle. The kinetics of candidate fuels are in Figure 8.8. As for to most chemical reactions, fusion reactions do not start spontaneously, but need to be 'ignited' by raising the energy of the reactants (for instance, D and T) so that their temperature is brought above a threshold. The reason is the same of combustion, that is, Coulomb repulsion among like-charged atomic particles. In fusion, the Coulomb repulsion is that among protons of the nuclei one wants to fuse together. In fact, Coulomb repulsion competes with the attraction by the 'strong' nuclear force binding nucleons. Since the nuclear force has the shortest range of all three elementary forces, its attraction is felt by nuclei only when they can be 'shoved' very close together. This means that much kinetic energy (i.e., temperature) must given or transfered to the reacting light nuclei to overcome Coulomb repulsion. Depending on reactants, threshold temperature triggering fusion among nuclei may be tens to hundreds of *million* degrees celsius. In eV units this means that reactants such as D, T or other, must be injected inside the fusion chamber at energy 10 to 100 keV. At these temperatures electrons are no longer attached to atoms, and matter is in the plasma state: the mix of positive nuclei and of negative electrons has such high kinetic energy that charge attraction is insufficient to allow them to form again the original neutral atoms.

Fusing together nuclei of D or T may occur *only* at these kinetic energies. In fact, this is the main issue in fusion: reaching sufficiently high reactants temperatures. The temperatures required to ignite fusion are difficult to achieve also because of a second condition [Lawson, 1957]: not only must the plasma reach threshold temperatures, but it must also be kept at these temperatures for a minimum 'confinement' time, τ. The Lawson condition reads, in fact,

$$n_1 n_2 \langle \sigma \nu \rangle \tau \mathrm{E_f} - \tau (P_\mathrm{B} + P_\mathrm{S}) = \frac{3}{2}(n_1 kT_1 + n_2 kT_2) \tag{8.17}$$

where $\langle \sigma \nu \rangle$ is the rate parameter, E_f is the fusion heat release and P_B, P_S are the bremsstrahlung and synchrotron radiation power losses. n_1 and n_2 are the particle number densities of the two reactants (see Figure 8.8), in general at different temperatures T_1 and T_2, respectively. k is the Boltzmann constant. Rate parameters and power losses may be found in [Huba, 2002, pp. 45 and 56–57]. Equation (8.17) is an ignition criterion based on a steady-state *ignition* power budget: it says essentially that the net rate of fusion energy generation, that is, fusion rate times energy released per fusion event (collision), minus power lost by radiation, must be equal to the kinetic energy absorbed by the reactants. In other words, the kinetic energy of reactants on the right-hand side of equation (8.17) must not only be high enough to support the fusion heat release (first term on the left-hand side), but must also compensate for the radiative heat loss (second term on the left-hand side). This condition is similar to the condition for flame anchoring, for instance, inside a gas turbine combustor; however, in a combustor the power lost is not radiative but convective, so that the confinement time τ is replaced by a fluid dynamic convection or residence time inside the combustor.

The Lawson condition (an energy 'breakeven' condition) links together temperatures, particle density and confinement time. Meeting this condition in a practical device is hard. Fusion is the power source of stars [Kaufmann, 1993, Chapter 3], and maintaining it artificially in an engine is still to be achieved. In stars it is gravitation that compresses and heats matter until temperatures become high enough to start fusing. In a reactor fuel is cold and gravitational effects are negligible, so it must be brought to ignition temperatures by other means, e.g., by radio-frequency electromagnetic waves heating. So, ignition needs an external power source, and temperatures about *10 times higher* than in our Sun. Equation (8.17) shows why: in the energy source term on the right-hand side, if n_1 or n_2 cannot be kept as large as they are in the Sun, the temperature must be higher.

By substituting in Lawson's criterion known experimental values, and simplifying the expressions for the power losses, a compact expression for the breakeven condition may be obtained:

$$n\tau^3 \sim 10^{14}\,\mathrm{sec/cm^3} \tag{8.18}$$

that is an hyperbola on the (n, τ) plane. Equation (8.18) still expresses in its extremely simplified form a balance between the source and the sink in equation (8.17): plasma at moderate density may ignite, but only if confined for a sufficient time. In practice, this is a severe constraint; for instance, for $n \sim 10^{14}\,\mathrm{cm^{-3}}$

(incidentally, a value typical of charged alpha particles near smoke detectors) the confinement time is about 1 sec, still a factor 3 or so longer than ever obtained in any fusion device tested so far. The consequence of Lawson's criterion has been to focus fusion research on fuels and kinetics characterized by a low ignition temperature, even though their energy yield might also be lower.

After ignition, hot fuel must be added to maintain steady-state fusion. This process may be steady-state or unsteady (pulsed, for instance). The fraction of energy released by fusion relative to that to heat the fuel is the 'gain', Q. This is an important number, telling the overall efficiency of the fusion energy process.

A second critical issue in picking a suitable fusion kinetics, see also [Santarius and Logan, 1998], is the type of product particles. Figure 8.8 indicates many fuel kinetics release neutrons of very high energy. Stopping neutrons is difficult, see section 7.4.1, since they are not charged. Because of this property, neutrons damage organic and inorganic matter. There is a trade-off between ignition quality and neutronics in choosing fusion kinetics. For instance, reaction 2 in Figure 8.8 is the easiest to ignite at its nominal 50 MK (million kelvins); but this number depends actually on the spatial temperature profile and on heat lost via conduction, so it can be higher. In any case, reaction 2 is also very 'dirty', in the sense that neutrons of 14.1 MeV are released. In fact, neutron energy constitutes 80% of the total energy released by this particular fusion kinetics, an extremely high percentage. Recovering neutron energy by thermalizing them is critical again because neutrons interact very little with matter. The standard recovery strategy consists of using high-energy neutrons to breed tritium fuel from the lithium blanket surrounding a fusion reactor and working as coolant.

Inspection of Figure 8.8 suggests one of the best kinetics is 1a: it needs only D (not T), a fuel that can be extracted from seawater for about \$1,000/kg. D abundance in seawater is estimated at 10^{13} ton. However, reaction 1a has a low energy yield, and its ignition at 300 MK is much harder than for reaction 2. In reality, when fusing D with D, all three reactions 1a, 1b and 2 take place simultaneously: their combined kinetics is convenient, because of the 'low' ignition temperature and because of high overall energy yield, but produces unfortunately fast neutrons.

All tritium reactions have a drawback: tritium does not exist naturally and must be 'fabricated' by nuclear processes such as reactions 10 and 11. Neutron fluxes must be of order $10^{14}/\mathrm{cm}^2$ sec [Metz, 1976] to speed reactions 10 and 11. In practice this means surrounding the fusion chamber with a lithium coolant blanket. Breeding tritium may be accomplished also by fission, as in combined fusion–fission cycles.

Likewise, reactions with ^{3}He need this rare isotope (naturally available He is ^{4}He, already scarce and expensive). ^{3}He could be mined on the lunar surface where it is produced by the solar wind. Its lunar soil abundance has been estimated [Wittenberg et al., 1986] at 10^9 kg. Were ^{3}He to become available at a reasonable price, reaction 3 would be very attractive because of its energy yield, even though its ignition temperature is high.

The most attractive 'clean' or 'aneutronic' kinetics is that of reaction 9 between a proton and a boron isotope, since it produces only high-energy helium and no other 'difficult' particles; however, its ignition temperature is theoretically infinite because of bremsstrahlung losses: its practical implementation (for instance, heating differently the two reactants) looks far into the future.

This said, given certain reactants does not necessarily mean one can impose or control a desirable kinetics, just as it happens in combustion chemistry. For instance, when injecting D and ^{3}He for reaction 3, reactions 1 and 2 would also take place, with rates and final products determined by their respective collision cross-sections (in combustion one would say, 'their respective reaction paths'). This means that neutrons would also be produced, indirectly, by reactants of 3. Only reaction 9 would be truly neutron-free (aneutronic), but until realized in practice, radioactivity, albeit milder than in fission, will remain an important fusion issue.

8.7 FUSION STRATEGIES

Assume that during the second stage of the conversion process outlined in section 8.2 fusion power is released; the next question is the same of fission power: What is the best strategy to exploit it? In Newtonian physics thrust is produced by accelerating a propellant; power is indispensable to accelerate it, but might be in forms not immediately useable, e.g., high-energy photons (gamma-rays).

During stage two of energy conversion, fusion produces high kinetic energy products such as He^{++}, H^{+}, electrons and others, see Figure 8.8. One strategy is to exploit the kinetic energy of these particles directly, letting them be free to leave the reactor with all their kinetic energy acquired, and with most of their momenta somehow aligned in the same direction of the desired thrust. For instance, this collimation may be realized by guiding particles using a magnetic field, B. In the end, this strategy is just like that in any chemical rocket or in fission fragment nuclear reactors (see section 7.15), only here the 'propellant' would be the very fusion products. One may call this propulsion strategy 'thermal fusion propulsion'. In fact, the temperature of fusion products is so high (a few MeV per He nucleus) that their ideal exhaust velocity or I_{sp} may be 10^6–10^7 m/sec. Thrust, F, will depend on the mass fused and ejected per unit time, i.e., on reactor power, see Figure 8.4. Figure 8.4 shows that to obtain a thrust $F = 100$ tons with $I_{sp} = 10^5$ sec requires a 1,000-GW reactor, with a fusing flow-rate of order 1 kg/sec. With α of order 3.5×10^{-3}, see Figure 8.1, the actual mass injected into the reactor must be $1/\alpha$ larger, or about 300 kg/sec: it is easy to see that such thrust cannot be sustained for long periods of time, and probably not even a one-way stellar mission would be feasible within a 20-year time-span. However, quasi-interstellar missions appear at least possible, if not truly practical.

As already seen in Chapter 7, the alternative strategy consists of using the fusion reactor as an electric generator, powering an electric thruster. This second strategy may be called 'electric fusion propulsion'. Of course this choice involves thermalizing fusion products inside a working fluid and using it in thermodynamic or direct-conversion cycles of some sort, just as in all ground fusion power plants concepts. Thermodynamic conversion is at most 50% efficient: the unused heat must be eliminated. In space this means space radiators, where the working fluid exchanges heat with the temperature of 'space' (the 2.72 K of the cosmic background radiation discovered by Wilson and Penzias). The weight of the best space radiators is substantial, implying a major disadvantage of this strategy when power is large.

At present most proposals being discussed to extract electric power from fusion do not go beyond standard thermodynamic cycles based on the heat extracted from the cooling jacket surrounding the reactor chamber. On the other hand, this strategy uncouples the propulsion system proper from the power generator, a better choice when thrust and I_{sp} need to be modulated. For instance, when maneuvering near gravitational fields, larger thrust (at lower I_{sp}) is better, while much smaller thrust, but with a much larger I_{sp}, is better when en route to the final destination; electric thrusters lend themselves to such trade-offs in operating mode more easily than direct thermal fusion propulsion. In fact, contrary to chemical or fission rockets, where inert matter can be added to increase thrust at the expense of I_{sp}, fusion reactors are far more intolerant of inert (that is, non-fusing) matter added. Inert matter can quench fusion kinetics immediately. At this stage of understanding of fusion it would be premature to assign a priority to the first or to the second strategy; picking one or the other will depend on factors at present beyond our knowledge, and especially on the type and scope of mission.

Although these are the two main strategies, others are still conceptually possible, and will be mentioned when needed. The next question is how to achieve fusion in practice, namely the type of fusion reactor. Work in this area began in the 1950s, and is still continuing. Fundamental information is widely available [e.g., Kammash, 1995; STAIF], so the following sections emphasize basic physics rather than engineering still farther in the future. Because no experience exists so far in fusion propulsion, the authors will feel satisfied if at least the main pluses and minuses of reactor strategies proposed are made clear.

8.8 FUSION PROPULSION REACTOR CONCEPTS

The history of fusion concepts for space propulsion goes back almost to the very beginning of the US fusion program for power generation (the Matterhorn Project). At that time plasma was imagined confined inside a 'magnetic bottle' by means of a specially shaped magnetic field, with hydrogen isotopes fusing while traveling back and forth between the two bottle ends. About half century later, we are still struggling with the many facets of confining plasma, but substantial progress has enabled plasma technology to achieve fusion, albeit for the time being by injecting inside the plasma more energy than that due to the fusion process itself: the so-called energy 'breakeven' condition must still be reached. Independently, many researchers, quite a few of them belonging to the visionary type, have proposed fusion propulsion concepts. Among them, the more promising appear to be those where plasma is not kept confined to generate electric power, but rather those where the hot plasma products are allowed to escape at their extremely high energy, sometimes after having been mixed with inert propellant. Devices of this class are called open magnetic confinement (OMC) reactors, and are discussed in section 8.10. Details of their application to propulsion is in [Romanelli and Bruno, 2005].

In the following discussion of conceptual fusion propulsion systems the level of detail is purposely kept modest, since emphasis is on the effect of fusion power on propulsion, rather than on the specifics of fusion reactors themselves.

By far, the best-known and tested fusion machine is the tokamak, to(roidal) ka (chamber) mak (machine). Fusion reactions are prevented from quenching on the cold reactor walls by magnetic confinement. This word means that the fusing plasma is guided by a magnetic field shaped in such way as to always keep it from touching reactor walls. This class of fusion reactor is called a magnetic confinement reactor, MCR. The conceptual operation of MCR is steady, but the actual mode of operation may depend on the electric transformer needed by the electromagnet supplying the magnetic field imposed. The transformer is a fusion reactor component that links the plasma, viewed as a classic secondary 'electric circuit', to the external power supply. If the electromagnet is not superconducting, the unavoidable ohmic heating forces reactor operation to be intermittent, say, stopping once per hour. In any event, the slow degradation of the plasma due to unwanted matter, e.g., detached from the walls by plasma interaction, makes periodic shutdown and cleaning inevitable on MCR conceived for ground power generation. In *space operations* such regularly scheduled maintenance may be impracticable or impossible because of safety and radiation hazards, and this is a major concern. Space-qualified MCR will probably have to meet much more stringent reliability requirements than are envisaged at the moment for ground fusion powerplants. Note that whatever experience is available for MCR comes from ground fusion *tests and experiments*: extrapolating to future space propulsion is premature and may be very risky.

Other configurations, embodying different fusion plasma confinement strategies, have been proposed, or tested, or are still at the stage of conceptual suggestions. Among alternatives the second most investigated is inertial confinement fusion reactors (ICR) in which extremely high (gigawatt) laser energy pulses are sent to a very small pellet containing the fuel(s). The energy pulse ablates, i.e., volatilizes, the external layer of the fuel pellet and raises the pellet temperature. The temperature of the volatilized gas is so high that the gas becomes a plasma, radiating very effectively. It is precisely this radiation that compresses ('implodes') the fuel, driving its density and temperature up, and (hopefully) to the point of fusion ignition. Radiative compression obtained in this way may reach 0.1 Mbar (10^5 atm).

For continuous power generation ICR need to be fed a stream of pellets; each pellet is then 'lased', fused and releases power. Thus operation of ICR is necessarily always pulsed, the repetition rate determined by the power demand. This feature may seem awkward to chemical rocket engineers, but is advantageous or convenient when releasing power at destructive energy levels. For instance, the gasoline automotive engine reaches in-cylinder temperatures above 2,500 K, far higher than the melting point of most structural materials; its pulsed operation, however, reduces heat transfer and temperatures to quite acceptable *average* values. In contrast, gas turbine engines are limited to a much lower 1,800–1,900 K precisely by their steady combustion mode of operation. The Orion concept [Dyson, 2002], in which pulsed nuclear mini-explosions were proposed to push a spaceship, is similar in many ways to an ICR, also because of its ablation physics.

It is far too soon to quantify practical merits of MCR vs. ICR, so both will be summarily described and their issues and shortcoming discussed in what follows.

8.9 MCF REACTORS

MCF reactors go back to the very beginning of fusion studies, when confining plasma was thought to be possible only by means of a steady magnetic field. In fact, since plasma must be kept hot at all times, it cannot 'touch' physical walls (they must be kept at a much lower temperature for structural reasons). Were this to happen, reactor walls would melt, plasma would cool too much and too fast (quench), and fusion would stop. Basically, plasma can be confined if the pressure exerted by the magnetic field B, proportional to B^2, is larger than the thermodynamic pressure, that microscopically is nkT, with n the number density and k the Boltzmann constant. That means that the ratio

$$\beta = 8\pi nkT/B^2 \tag{8.19}$$

must be less than unity to confine plasma at density n and temperature T (quantities in equation (8.19) must be in c.g.s. units). Since n and T are very large (remember n must meet the Lawson ignition criterion), B must be correspondingly large. Preventing plasma from contacting reactor walls looks and is a major problem. At the level of the charged particles (for instance, H^+, He^{++}, D^+, T^+, e^-) the confinement mechanism is driven by the Lorentz force. In a magnetic field of induction $\mathbf{B}$, species charged with an electric charge, q, must gyrate (that is, spiral) around the field lines at a gyration, or cyclotron, frequency Ω, proportional to B and inversely proportional to the mass of the charged particle. The gyration radius, ρ, of the helix described by the charge is proportional to the velocity component $v_\perp$ normal to B divided by Ω, that is

$$\Omega = \frac{qB}{m} \qquad \text{and:} \qquad \rho = \frac{v_\perp m}{qB} \tag{8.20}$$

The gyration frequency is important for two reasons: first, it must be higher than the plasma collision frequency: charges cannot afford to collide too frequently with other particles, otherwise their trajectories will not be guided and confined by the field lines of B, but will change randomly after each collision. Second, any reactor in which plasma is confined magnetically must host gyrating charges, so it must host field lines while particles gyrate around them with a radius ρ. This means that B intensity must be sufficiently large, both because gyration frequency is higher and because radius is smaller (the reactor becomes also smaller).

In fact, using electrons as an example of charged species, and a field of 1 tesla (intense, but manageable) the gyration radius is not larger, maybe of order 0.1 mm for electron kinetic velocities of order 10^6 m/sec. Repeating the same estimate for ions like H^+, 1,840 times heavier than electrons, the same 1-tesla field could confine H^+ within a gyration radius of a few millimetres (for reference, 1 tesla in the International System of Units is equal to 10,000 gauss in the older Gauss system. At sea level the Earth's magnetic field is 0.3 gauss. So, 1 tesla is some 33,000 times more intense than the Earth's magnetic field).

Permanent magnets can produce 1-tesla fields, but only within short distances; more rigorous treatment of this problem show fusion reactors using MCF may be made reasonably compact. Note that the size of the reactor is also dictated by the mass flow-rate of plasma eventually ejected to produce thrust: plasma density and exhaust velocity, V_e, determine the cross-section, A, of the reactor. However, small gyration radii reduce the volume of plasma taken by spiraling charges. So, the more intense the B field, the more manageable the size of the MCF reactor: confining high-energy plasma depends to a large extent on creating intense magnetic fields.

Magnetic MCF fields of order 1 to 10 tesla are quite feasible, but need large and heavy conventional electromagnets. In conventional electromagnets the field B is created by a current flowing inside copper wiring forming the magnet coil. Until so-called superconducting wires became commercially available, such B fields were prohibitively expensive if feasible. Current superconducting cables can carry currents of order 1,000 A/mm^2 (about three orders of magnitude more intense than using copper) with practically no electric resistance at all, and thus no ohmic (power) losses. These cables are at the core of the giant magnets enabling particle accelerators and fusion ignition experiments worldwide.

Much of superconducting technology is still based on so-called low-temperature superconductors (LTSC), made of materials such as Nb_3S alloys, kept at temperatures of order 20 K by liquid helium. The LTSC wires in fusion tokamak are hosted inside stainless steel jackets, thermally insulated and drenched in flowing liquid helium. As an added precaution to avoid destructive damage, a thick copper sheath surrounds the insulation, carrying the high current normally carried by the superconducting wires should the LTSC material lose suddenly its superconducting properties.

This type of construction means very expensive, very large and massive cables, all unsuitable for space applications. The realistic alternative is *high*-temperature superconducting (HTSC) materials, capable of staying superconducting at much higher temperatures (e.g., at the temperature of liquid nitrogen, 77.4 K, rather than that of liquid He, abut 4 K. These new materials are more fragile than LTSC, but are far more practical and are already moving toward commercialization. They can carry almost the same current of LTSC, but clearly with less demanding cryogenic technology [Casali and Bruno, 2004]. With HTSC technology magnetic fields are practically limited only by the maximum intensity that the superconductor can tolerate before losing its SC properties: in fact, a peculiar property of superconductors is that they lose their capability when immersed in a sufficiently intense magnetic field. In practice, up to 10 to 15 tesla look feasible.

A more recent MCF concept is the spheromak [Jarboe, 1994], see Figure 8.16, in which the magnetic field confining plasma is generated by the plasma currents themselves: no magnetic field coils link the torus, because, topologically speaking, the first wall of a spheromak is actually a 'spheroid' surface, that is, a surface very much resembling a sphere. Because of the poloidal and toroidal fields being approximately of equal strength, the spheromak plasma creates its own torus inside its spheroid volume, with the torus axis coinciding with the spheroid axis of symmetry. The mechanism of plasma generation is that of the turbulent dynamo, resembling, as far as is known, the mechanism that creates the Earth magnetic field inside the Earth's molten and electrically conducting core. The magneto-hydrodynamic regime of plasma in all MCF reactors is turbulent, so confinement efficiency and stable sustained fusion in a spheromak depends on plasma currents in a more sensitive way than in standard tokamak machines and, ultimately, is very sensitive to plasma instabilities driven by turbulence. The major interest and potential advantage of spheromaks is that they tend to be much more compact than typical MCF reactors.

8.10 MIRROR MCF ROCKETS

Historically, magnetic confinement developed at the dawn of fusion work (in the 1950s) was not based on the tokamak reactors just described: plasma was simply confined between two symmetrical, high B regions. In between these two regions, diverging B field lines shape a sort of magnetic 'sausage', pinched at the two ends by higher B. Plasma particles must therefore spiral along the B field lines, moving either way towards the two ends; under the right conditions, in their back and forth motion they periodically convert their translation into spinning (rotation) energy: ideally, they reach either end with very high gyration frequency and no translational energy at all. It is this zero-translation condition at either end that forces particles to turn back, spiraling in the direction opposite to that they came from. So, the B field acts as a 'mirror', reflecting charged particles back and forth between the two high-B end regions. By designing the B field properly, plasma can be confined long enough to absorb the ignition energy injected from outside, and to start fusing. Once ignited, feeding the reactor with fuel will keep it operating steadily.

This ideal and simplistic picture is actually far richer in important details; for instance, electrons are lighter than ions, and tend to leak at both mirror ends; the ratio between the low and the high B in the 'sausage' is critical and must be kept above a certain value; and many others, see [Kammash, 1995, Chapter 1]. A comprehensive review of mirror fusion devices and of their features and problems is that by [Post, 1987]; this review is almost 20 years old because interest in this approach for terrestrial power has not been as great as that in other concepts. Nevertheless, mirror fusion seems one of the promising technologies for rocket application. Here attention is focused only on the MCF aspects more closely related to propulsion, while an extensive discussion of its plasma confinement and reactivity issues is in [Romanelli and Bruno, 2005].

Once fuel fuses and generates energy, a mirror-configured MCF can become a fusion *rocket*: this is done by 'leaking' plasma from one of the mirror's ends and letting it escape into a magnetic nozzle. In other words, B can be made unsymme-

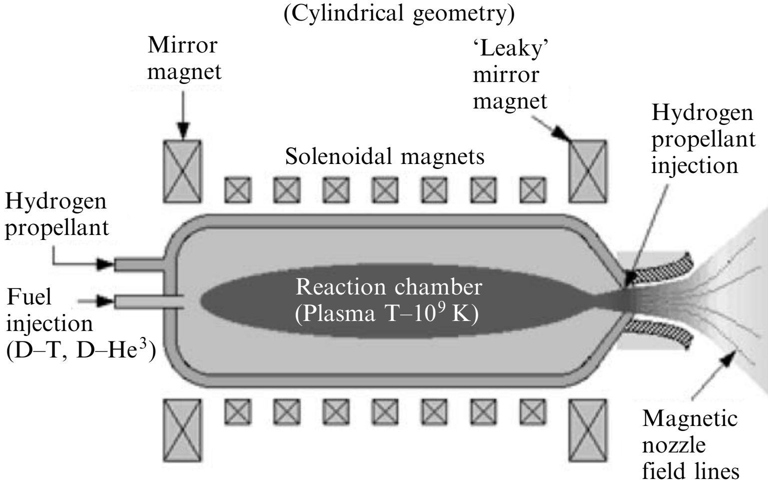

Figure 8.9. Schematic illustration of a mirror MCF rocket.

trical: then, if the plasma residence time allows the fuel enough time to fuse, adjusting B at one end lets the plasma escape, at a controlled rate, with all its high kinetic energy (speed) and momentum, creating thrust. Inert propellant may be added to increase thrust, but not inside the reactor chamber proper, on pain of quenching. Mixing between inert and fusion products must be done in the nozzle, as shown for instance in Figure 8.9.

The B field can be shaped to confine and guide the plasma just as solid walls confine the hot gas in a chemical rocket nozzle. A critical issue in designs to maximize thrust is that the rotational velocity component of the plasma particles as they go through the nozzle must be converted as much as possible into an axial component: spinning does not contribute to net momentum change (thrust). This is a goal that poses not a few problems to designers of magnetic nozzles.

This simplified conceptual scheme indicates that mirror MCF reactors can be the power core for direct thermal fusion propulsion, where plasma fusion products (ionized He, but also D, T and H not fused, and electrons) are the sole propellant; see also [Carpenter and Brennan, 1999]. Figure 8.4 shows that the exhaust velocity (i.e., the I_{sp}) can be in the 10^5–10^6 m/sec range, much larger than with nuclear thermal or nuclear electric propulsion and with a much simpler conceptual layout. In fact, a fusion mirror thruster is equivalent to a chemical rocket engine where combustion of propellants has been replaced by thermonuclear burning of D and T.

This simile should not suggest that the problems posed by interstellar or QI travel and examined in sections 8.1 to 8.5 can be quickly solved by fusion propulsion. Thrust still depends on thrust power, the product $I_{sp}F$. The much larger I_{sp} possible with fusion rockets implies that, depending on spacecraft mass, reasonable acceleration to shorten long voyages needs large F and, accordingly, very large power. For instance, a thrust of order 50 tons with I_{sp} of order 10^6 m/sec needs a 500-GW reactor. Such power is not outlandish, but the volumetric energy density in MCF reactors so far tested (tokamak and other types of fusion machines) is low, and suggests that high-I_{sp}, high-thrust MCF rockets must be voluminous and presumably also massive. Nevertheless, because of its inherent simplicity, thermal fusion propulsion is appealing to most propulsion experts, who think it is the better mode of propulsion.

8.10.1 Tokamak MCF rockets

The next stage of power fusion research took place in the 1960s and focused on curing the 'leaking' plasma problem at the two ends of the magnetic mirror. The idea was to bend the plasma sausage at the two leaking ends and join them: the result is no longer a sausage but a doughnut, in which B has two main components (one toroidal, its field aligned with the doughnut larger circumference(s), and one poloidal, the lines directed as the smaller cross-section circles). This is the tokamak reactor shown schematically in Figures 8.10 and 8.11.

The tokamak configuration is still being experimented with in most fusion research centers. A tokamak in the strict sense does not lend itself to propulsion, since its geometry is closed: a tokamak was conceived only as a power generator. Nevertheless, just as in the mirror MCF machines, a high-energy plasma jet may be allowed to escape, for instance from the region near the axis of a tokamak torus: this becomes conceptually the rocket engine called reverse field configuration (RFC) and described in section 8.12.

Alternatively, the fused plasma may be ejected through a duct *tangential* to the

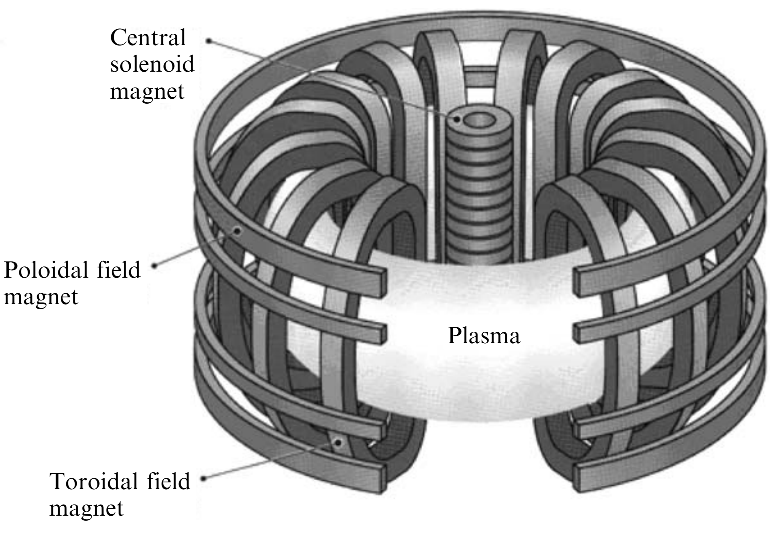

Figure 8.10. Tokamak geometry and magnets.

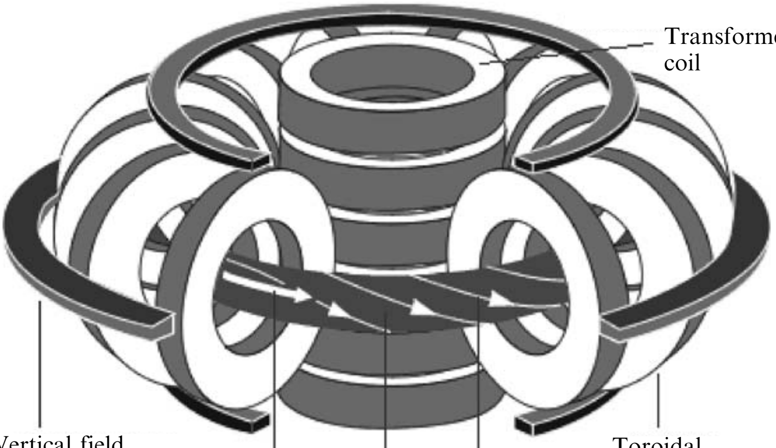

Figure 8.11. Plasma current and B field lines in a tokamak.

tokamak torus, and called a 'divertor'; see Figure 8.12. R. Bussard was the first to propose this solution; see [Bussard, 1990]. In both cases there are major problems to solve, since plasma needs to be simultaneously confined and escaping, all this at a controlled rate and while being ignited and fusing.

A cross-section of an advanced tokamak reactor doughnut, with similar poloidal and toroidal dimensions (that is, a spheromak), see Figure 8.13, shows the plasma current and its direction, with the imposed poloidal and toroidal B fields. These two fields complement each other, in the sense that a purely toroidal field would not by itself confine plasma, as drift currents would separate ions from electrons, creating ipso facto an unwelcome electric field. The poloidal field opposes this separation effect, and allows plasma to be reasonably well confined. The same figure shows also the so-called 'first wall' of the confinement structure, that is, the solid confinement structure (for instance, stainless steel) separating the plasma from the coolant blanket, the volume occupied by molten lithium that cools and at the same time absorbs the high-energy neutrons breeding tritium, followed by the radiation shield proper and the magnet. It is the thermal energy extracted mostly from the blanket that can produce electric power through conventional thermodynamics.

8.10.2 An unsteady MCF reactor: the dense plasma focus (DPF) rocket

Unlike all MCF concepts seen so far, this approach to MCF is unsteady. The basic working principle of the DPF rocket is shown on the left of Figure 8.14. The fuel, D–T or other, is injected inside the reactor chamber and is compressed by *pulsed* electromagnetic waves. Their effect on the newly formed and longitudinally

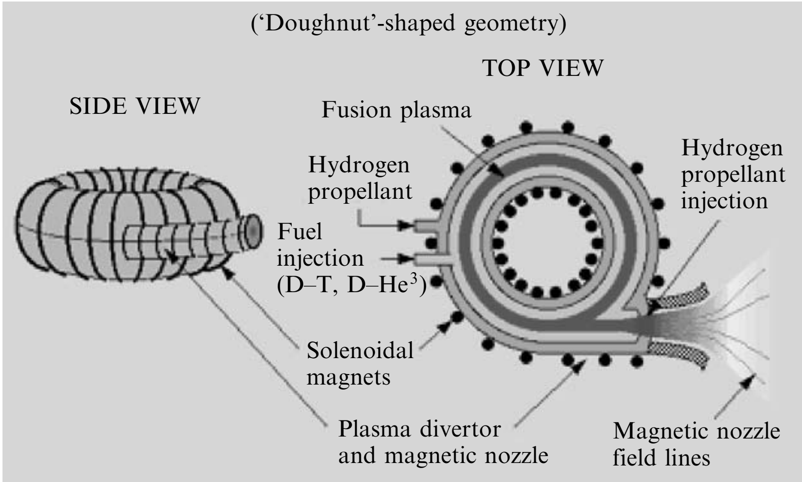

Figure 8.12. Schematic view of a tokamak MCF rocket using a divertor.

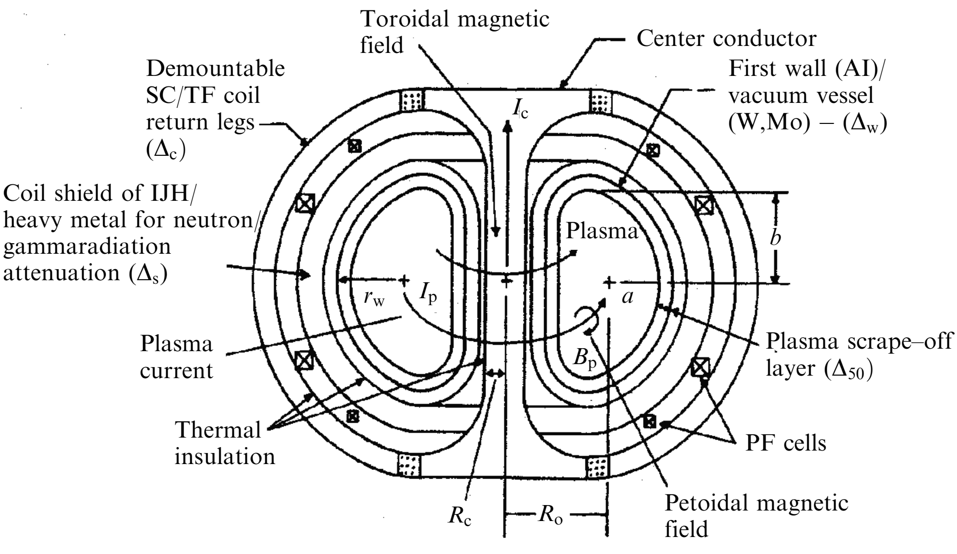

Figure 8.13. Schematic of an advanced (spherical torus) tokamak reactor (spheromak) showing first wall and thermal insulation.

accelerated plasma is to constrict the B field lines in the tangential direction (in cylindrical coordinates the tangential angle is θ). This unsteady plasma effect is called 'θ pinch': it can compress plasma to very high density, although for short times, corresponding to the duration of the electromagnetic pulse. There is some

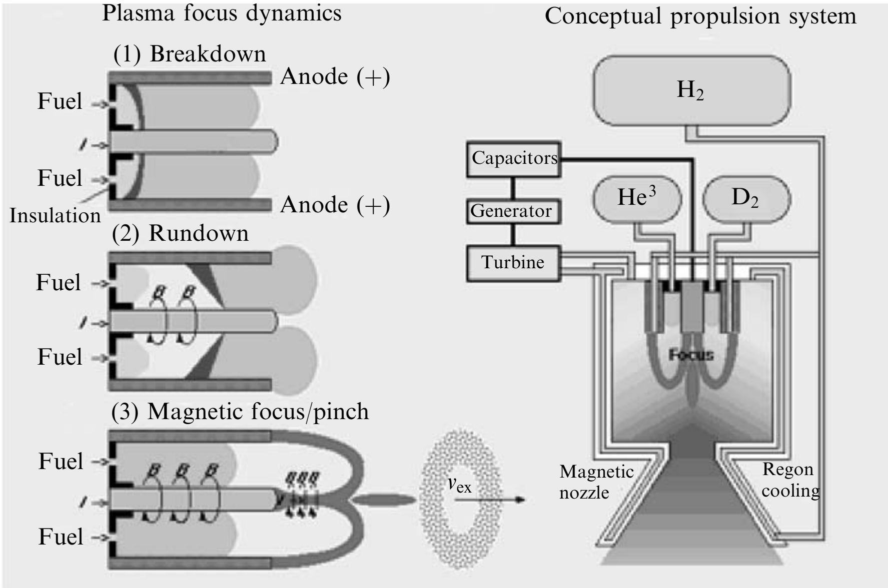

Figure 8.14. Schematics of a dense plasma focus (DPF) reactor (left) and of a rocket operating according to its principle.

experimental evidence hinting that in this unsteady mode plasma ignition may be achieved with DPF devices much smaller than steady-state MCF reactors.

Plasma periodically formed in DPF reactors may be ejected alone, as the sole propellant, or may be first thermalized in a flow of inert H_2 propellant. In this second case, temperature of inert plus plasma is lower, I_{sp} is also lower, but thrust is higher. Acceleration of the mixture formed by plasma and inert takes place in a conventional or magnetic nozzle (Figure 8.14, right). Depending on whether H_2 is added or not, the ideal I_{sp} predicted is of order 4,000 sec to 10^6 sec. In the latter case the thrust is very low.

Calculations of the potential performance of the DPF concept have showed that its gain, Q, is low: the energy it needs to ignite is probably almost equal to that obtained from fusion. However, made into a rocket engine, DPF could be a very compact propulsion system. This, and the fact that experiments with DPF are relatively inexpensive compared to those with steady MCF, explains current interest in the US, not only from researchers at universities, but also from commercial companies; see for instance [Lerner, 2004].

8.10.3 Shielding

Together with other minor factors, it is tokamak fuel kinetics that determines the fraction of fusion energy released as particle kinetic energy useable as thrust, and that in the undesirable form of radiation; see section 7.4.1.

Among the many technical issues associated to fusion and fusion propulsion, that of radiation and its shielding occupies a special place. Some of the radiation is useful, e.g., neutrons are indispensable to convert the liquid lithium coolant blanket behind the first wall into tritium needed by reactions 2, 4 or 5a of Figure 8.8; with D–T kinetics, in fact, most of the energy is deposited inside the lithium coolant by the neutron flux, of order of MW/m^2; however, most other effects damage structural materials and body tissue (see Appendix). Particles, especially high-energy neutrons, and gamma photons radiated during fusion carry enough energy to penetrate solid material and dislodge atoms from their crystal lattices. With respect to fission, fusion kinetics produces neutrons with higher average energies; see Figure 8.8. Some of these interactions with solid matter create He or H atoms directly inside lattices, embrittling the material: this was the reason for the limited life of fission nuclear thermal reactors tested in the 1960s and 1970s. The effect of high-energy neutrons on stainless steel, for instance that of the first wall, is to reduce ductility to about 1% of the original after 2 years [Kulcinski and Conn, 1974]. This is the result of forming inside the steel about 1,000 atoms of helium and hydrogen per million structural atoms. Correspondingly, steel tends to swell, about 7% to 9%, if untreated. Apparently cold working the steel tends to reduce swelling to below 1%, but these figures are revealing.

Shielding technology has come a long way since the 1970s; there are new promising and light materials, based on carbon, for instance. However, traditional shielding still must rely on quantity of matter to stop radiation, and this adds mass to fusion engines and inevitably implies radiation damage. Figure 8.15 shows, from left to right, the layers of matter going outwards from the fusing plasma at the center of a tokamak torus [Kulcinski and Conn, 1974]. Although somewhat dated, the structure shown is realistic and may be divided into three main zones: the torus inside, the blanket and the shield. The magnetic coils form the reactor outside. The magnetic field permeating the torus keeps plasma 50 cm away from the solid

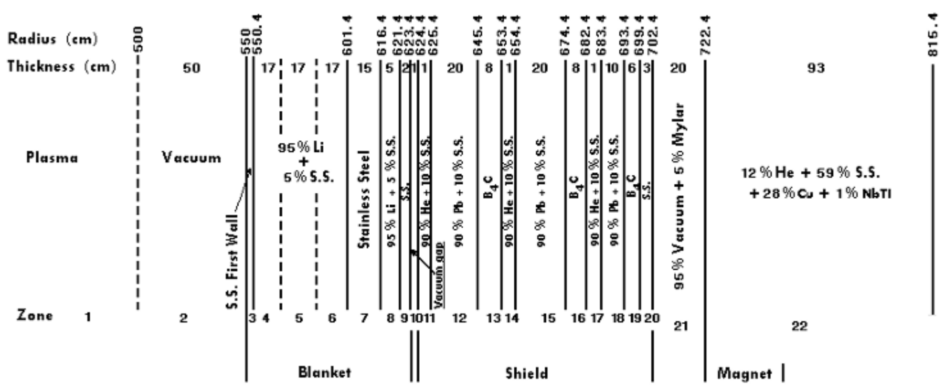

Figure 8.15. Conceptual design of a shield system for a tokamak reactor, including the lithium cooling system breeding tritium (adapted from [Kulcinski and Conn, 1974]).

first wall, in this example made of 0.4 cm thick stainless steel (S.S.). Ideally, nothing should exist between the edge of plasma and the first wall. Beyond the wall is the lithium blanket and its recirculating system, extracting most of the 14 MeV neutrons thermalizing inside lithium, and providing most of the thermal power. Note that lithium contains a certain percentage of steel, since it is corrosive with most metals. Tritium is bred by neutrons deposited inside the lithium blanket and is extracted (in this particular scheme) by two independent circuits, so that one may be closed while the second is in service. A thermal insulation vacuum gap separates the blanket from the shield proper, made of boron carbide and lead. The carbide slows down and thermalizes neutrons that have not been stopped by the blanket, while lead absorbs gamma-rays. In this design helium is used to cool the shield assembly. A final vacuum gap insulates the reactor from the low-temperature superconducting magnet, made of NbTi and comprising a copper 'lifesaver', in case the superconducting mode of operation ceased for any reason. The shield shown is designed for a 5-GW (thermal) fusion tokamak, and the blanket + shield structure is about 172 cm thick.

A conceptual way around the radiation problem is to look for a fusion kinetics that does not release neutrons, the particles more difficult to stop. Protons carry in the average the same momentum as neutrons, but their charge means they can interact with, and be stopped by, matter (or by an external electro-magnetic field) far more easily, requiring less shielding mass. The problem with this approach is that the energy yield of 'aneutronic' kinetics is lower than for D–T; see Figure 8.11, and their ignition temperature even 10 times higher. Just as outlined in section 7.4.1, the first task of a shielding design is to slow down and stop *unwanted* neutrons, not all of them if one wants to breed tritium.

The cooling system integral to a tokamak for industrial power generation constitutes also the heat exchanger extracting the fusion energy deposited in the coolant by high-energy particles, and thermalized as heat. In a fusion propulsion system utilizing electricity (to power electric thrusters, but also for other on-board tasks) it seems clear that such an extraction system must be more efficient and hopefully more compact than the conventional machinery of Rankine, Brayton or Stirling cycles of terrestrial power plants. For instance, direct conversion into electricity via thermionics, although a low (<10–12%) efficiency process, is feasible, as may be other more speculative ways based on modern advances in electronics. A tokamak MCF configuration is thus naturally suited for the second type of propulsion strategy that is called electric fusion propulsion.

8.10.4 Direct thermal MCF vs. electric MCF rockets

Although far from having been discussed to the extent deserved, the description of MCF mirror thrusters above suggests the MCF propulsion system is the better when choosing between thermal and electric. A tokamak MCF reactor coupled to an electrical generator, followed by an electric thruster would probably be a more controversial (albeit feasible) configuration. Just as commented in Chapter 7 when fission NEP was being discussed, a propulsion system configuration constituted by two separate energy and thrust generators does have its merits, the main one being that each component may be optimized to some extent independently. The drawback of fusion electric propulsion is that it must include machinery for energy conversion. Thermal energy must be converted into electricity, and at the current state of technology this may be done in the simplest and most reliable way only via a thermodynamic cycle. All thermodynamic energy conversion carries an efficiency penalty. Although combining two different cycles (Brayton and Rankine, for instance) may increase conversion efficiency by a few percentage points, combined power generation further complicates an already complex conversion scheme. In the end, the efficiency of conventional cycles reaches at most 50%. The remaining thermal energy can be used for other important tasks (radar, laser telecommunications, cryogenics are the ones that come to mind) but the greatest fraction would have to be rejected somehow to a lower temperature sink. Typical terrestrial sinks are rivers, or colder air. In space, that means space radiators, because no conduction or convection may take place. Space radiators add to total mass, having a weight/power ratio of order 0.01 to 0.15 kg/kW. At a conservative 0.1 kg/kW figure, radiator mass is 100 tons per each gigawatt of thermal power.

The electric power extracted at such high price can power an electric magneto-plasma-dynamic (or perhaps even ion) thruster capable of I_{sp} in the 10^4 to 10^5 m/sec in the near- or mid-term (say, 10 to 20 years from now). MPD rockets are capable of higher I_{sp}, but have lower thrust density compared to ion engines [Auweter-Kurtz and Kurtz, 2003]. The combined fusion power source and MPD rocket will be predictably a large assembly, as shown later by estimates of mass budgets. Besides, electric power switching and conditioning for GW-class thrusters operated at high currents or high voltage or both, would certainly be extraordinary technology challenges.

This said, fusion electric propulsion based on *direct conversion* (i.e., entirely bypassing thermodynamics) is a future development potentially impacting in a positive way on these considerations. Direct conversion has a relatively short history, and is limited to low power (<1 kW) applications such as the RTG (Radio-isotope Thermionic Generators) built for the Galileo and Cassini missions. RTG exploit the emission of charged particles from high-temperature solid materials to produce electrical power. Their efficiency is even less than thermodynamic conversion, being in the 10–15% range at best. Their major appeal is that they are static devices (no moving parts).

The most investigated type of direct conversion is that based on magneto-hydro-dynamics, a technology developed and tested for more than twenty years in the EU, the Soviet Union and the US [Messerle, 1995]. It consists of passing a ionized hot gas in a duct between a magnetic field B. If the $\mathbf{B}$ vector is normal to the gas velocity $\mathbf{u}$, an electric field normal to both is generated by the motion of ions, and energy can be extracted. This class of generators is therefore the exact reverse of MPD electric thrusters described in Chapter 7. In MPD thrusters applying external $\mathbf{E}$ and $\mathbf{B}$ creates an accelerating Lorentz force $\mathbf{F}$; in MHD generation, slowing down $\mathbf{u}$ in a field $\mathbf{B}$ creates an electric field $\mathbf{E}$ and thus a voltage.

MHD generation is inherently suited to extract energy from fusion, in that fusion products are a plasma. Any fusion kinetics producing few or no neutrons, e.g., reactions 6, 8 or 9 in Figure 8.8) would be ideal in this context. Handling such energetic particles in an MHD generator would be difficult, but the extraction process would be much more efficient than others based on any thermodynamic cycles or thermionics. MHD generation was abandoned in the mid-1980s mainly because of the difficult engineering problems posed by working with high-temperature ionized gas. This gas was at the time the hot exhaust products of coal burners, at temperatures of order 1,800 K. Since spontaneous ionization at this temperature was negligible (ionizing air nitrogen needs about 15 eV), the coal combustion products exhaust was seeded with alkaline metals (K, Ba, Na, ...) that ionize much more easily, at energies of order 3–4 eV. These metals are extremely corrosive, and ruined MHD extraction duct sections very rapidly. Revisiting this technology is mandatory for direct conversion of heat into electricity; in fusion propulsion the question of ionization would no longer constitute a problem (rather, the high plasma energy would).

Are there new ideas in direct energy conversion? The answer is a qualified yes. Some are actually at the stage of just ideas. For instance, interesting work has been carried on since the 1980s in converting energy from radioactive decay of radionuclides producing alpha and beta particles into electricity, see [Brown, 1989]. This may seem identical to the RTG process, in which energy of alphas and betas is thermalized and the heat released produces electrons; in fact, this is not so. This novel concept is based on the fact that the energy of particles emitted by radionuclides also includes that of the electromagnetic field they generate because of their charge and motion. The fraction of energy in the form of electromagnetic field is much greater than that present as kinetic energy and captured by RTG. Time will tell whether these new concepts are indeed practicable in an engineering sense. Success in this area hinges on the chances of fusion propulsion to be investigated with significant resources. At the moment these are slight, but continuing interest by Japan in the GAMMA-10 mirror machine (at the Tsukuba research center), by Russia in the GOL-3 gas-dynamic mirror reactor at Novosibirsk and recent (2004) interest by ESA in fusion propulsion, e.g., see [Romanelli and Bruno, 2005], may be positive signs.

To conclude this section, at the stage of our knowledge far more work is needed to reach firm conclusions concerning the best solution to convert MCF thermal into electrical energy. By all reasoning made, an educated guess is that electric fusion propulsion is probably much more complicated than direct thermal fusion propulsion, although conceptually more flexible in terms of thrust and I_{sp} modulation. This is also the preliminary conclusion of the report in [Romanelli and Bruno, 2005].

8.11 FUSION PROPULSION—INERTIAL CONFINEMENT

Historically, this strategy for confining fusion fuel was proposed about 10 years after the Matterhorn fusion project, of the 1950s in [Basov and Krokhin, 1964] and [Dawson, 1964]. Two factors contributed to start work in inertial confinement: the first was the realization that MCF presented more difficult problems than initially thought; the second was the availability of pulsed lasers in the GW class. The second factor especially suggested the possibility of bypassing the MCF need of large continuous heating power to ignite. The Lawson condition for ignition, equation (8.17), is a steady-state energy balance linking particle density n to confinement time τ. Density in MCF reactors cannot be very high, because otherwise the plasma becomes collisional and the magnetic field ineffective; inevitably, the only way to compensate for low n is to heat the plasma for a long time τ. During this time plasma instabilities, radiation losses and other factors tend to reduce substantially the amount of heating that the plasma should theoretically absorb. On the n, τ plane the MCF strategy occupies the rightmost end of the hyperbola.

In inertial confinement fusion these problems may be bypassed by striking a solid fuel pellet (not a fuel plasma) with a very high power laser. The pellet could be made, for instance, of frozen D–T fuel encapsulated by a metal case. In fact, inertial confinement fusion (ICF) envisaged a whole group of lasers (e.g., the Los Alamos 'SHIVA' laser assembly, or that at the National Ignition Facility at the Lawrence Livermore National Laboratory, LLNL), each simultaneously beaming a power pulse to a single fuel pellet. At the National Ignition Facility energy up to 1.8 MJ may be deposited within 4×10^{-9} sec, corresponding to an instantaneous power of 450 TW (1 TW $= 10^3$ GW $= 10^6$ MW). At such energy deposition the outside surface of the pellet ablates, creating a spherically symmetric high-speed jet that compresses the pellet: the pellet implodes [Daiber et al., 1966], and reaches the density required for fusion ignition on a timescale of order 10^{-9} sec, or about 10^9 shorter than the 1-sec confinement time typical of current tokamak. Accordingly, there is hardly any time for plasma instabilities and other unwanted effects to develop before ignition. So, unlike MCF, ICF heating is totally unsteady, but if one still wanted to have a mental picture of this strategy, the $n\tau$ scaling of equation (8.18) would indicate it occupies the *leftmost end* of the hyperbola. A notional scheme of ICF is shown in Figure 8.16. Some typical features of pulsed lasers are reported in [Huba, 2002, p. 50].

In the simplest scheme of an hypothetical ICF rocket, pellet after pellet of fuel is injected inside the fusion reactor chamber and fused by the laser(s). The hot plasma is expanded in a nozzle and produces thrust. How much thrust is produced will depend on mass fused, that is, on pellet injection repetition rate. The nozzle will probably be a magnetic nozzle, where an external field B not only guides the collisional plasma, but also limits the heat transfered from the plasma to the nozzle walls. Figure 8.17 shows schematically how to realize ICF using multiple laser beams.

To predict ignition conditions in ICF reactors the Lawson's criterion (a *steady-state* power budget) cannot be applied, since the ICF process is deliberately made *unsteady*. The correct criterion, as in all unsteady processes, must be based on characteristic times. In fact [Kammash, 1995, p. 17], the ignition constraints of ICF can be reduced to their simplest terms by introducing just two characteristic times, $t_d = R/c_s$, the destruction time of a pellet of radius R by pressure waves generated by the laser pulse in the fuel plasma, traveling at plasma sound speed, c_s; and the time, t_b, for fuel 'burning' (that is, fusing). The burning time, t_b, may be estimated by imposing that the burning rate of plasma scales (as in all collision

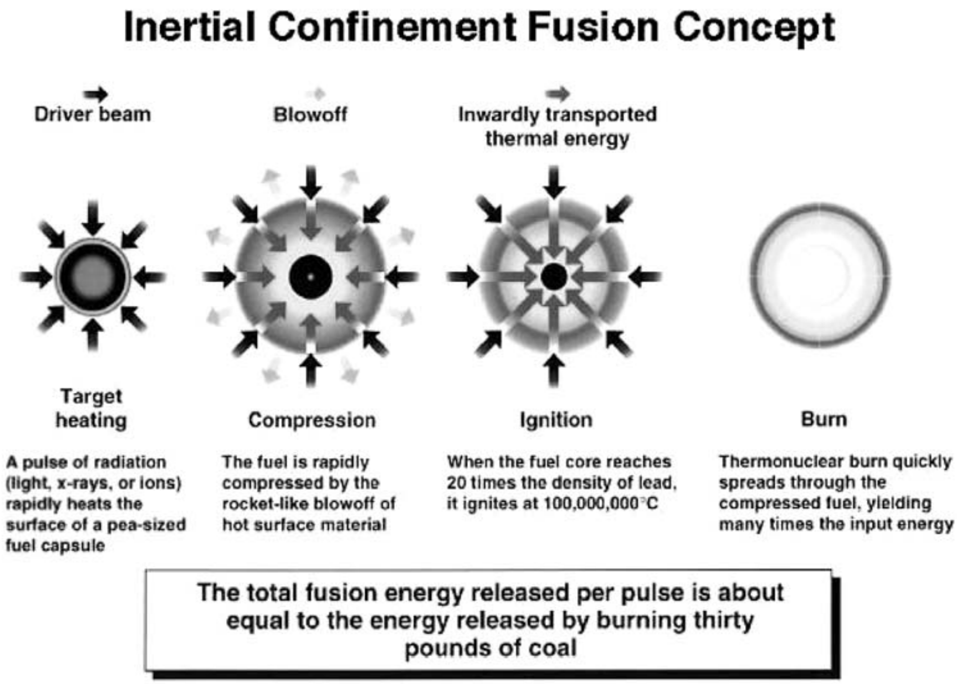

Figure 8.16. Schematic operation of inertial confinement fusion (http://hif.lbl.gov/tutorial/tutorial.html).

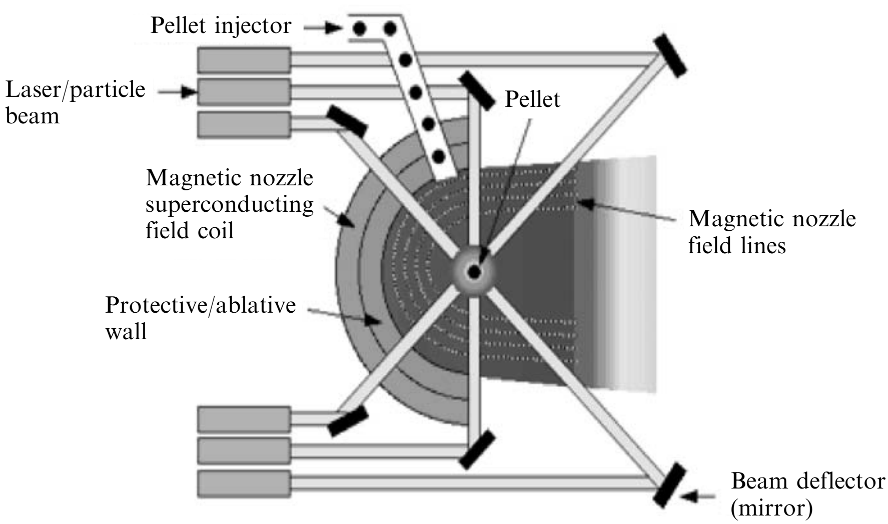

Figure 8.17. Conceptual operation of an inertial confinement fusion reactor rocket with its magnetic nozzle.

kinetics processes) as $(\rho/m_i)/t_b$, that is as concentration (density divided by particles mass) per unit time. This rate of burn must be proportional to the collisonal cross-section among plasma particles, σ. Here ρ is the plasma density and m_i is the mass of the plasma ion, He^{++}, T^+, D^+ or H^+). In essence, t_d is a residence or travel time, and t_b is a kinetic time.

The ratio f_b between these two times, $f_b = t_d/t_b$ is a measure of the fuel burn fraction: if f_b is less than one, during the pellet implosion the pressure wave travels too fast, and destroys the pellet *before* fuel is burnt. For fusion to occur, burn time should be much faster than destruction time, that is, f_b should be much greater than 1. By expressing sound speed and collision cross-section as a function of temperature, it can be shown that the burn fraction is essentially proportional to the product ρR:

$$f_b \sim \rho R \tag{8.21}$$

As a rough order of magnitude, the first and simplest condition for fusion ignition that ensures high efficiency, can be written (in the c.g.s. units still beloved of physicists) as

$$\rho R \gg 1 \text{ (g/cm}^2\text{, a surface density)} \tag{8.22}$$

Note that this criterion depends on the system of units one uses: it is not cast in terms of numbers such as Mach or Reynolds. The physical meaning of this criterion is the following: for fusion to occur the energy deposited on the fuel pellet must be 'high' enough. High energy will compress the pellet and make it denser. However, to fuse it, the density that counts is that of the thinner surface layer where energy is deposited, not the volumetric density. So, the smaller the pellet, the higher the density ρ to achieve.

One may think then that using large enough pellets fusion will start without any problem. In fact, raising R does not automatically ensure the right density! Raising R means, in fact, that *more energy* must be deposited to achieve the same energy per unit area. So, the ICF ignition condition hints obliquely to a key issue, that of the ICF energy budget. The net energy available from ICF will be that released by fusion *minus* that used up by the laser beam(s) to compress the pellet. Their ratio, Q, is the 'gain' of ICF, and a major subject of investigation in fusion physics.

By further manipulating the expression for ρR it is possible to recast it in terms of the n and τ appearing in the Lawson's criterion for magnetic confinement, obtaining for ICF ignition the condition

$$n\tau^3 \sim \frac{\rho R}{m_i c_s} \quad (\text{sec/cm}^3) \tag{8.23}$$

With $\rho R = 3\,\text{g/cm}^2$, a numerical value considered typical by the ICF community, equation (8.23) becomes numerically

$$n\tau^3 \sim 10^{15} \quad (\text{sec/cm}^3) \tag{8.24}$$

Comparing the two different breakeven/ignition criteria, that is, for MCF and for imploding ICF, the second appears ten times 'harder' to meet. This is not completely true, however, since MCF systems barely meeting the Lawson criterion burn less fuel

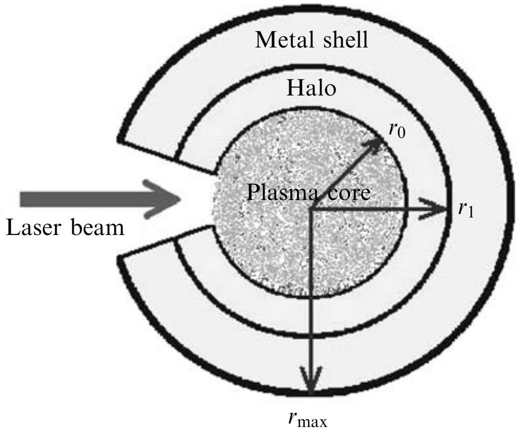

Figure 8.18. Sketch of MICF pellet.

than ICF systems under these same critical conditions. The real advantage of ICF over MCF is actually that ICF does not need externally applied magnetic confinement. This makes it very attractive for propulsion, because it does away with large-B magnets, superconducting or not, and their associated mass and complexity issues. On the other hand, ICF propulsion needs powerful lasers or particle beams. Although these components tend to be massive, ICF should be considered as an alternative to MCF-based propulsion systems.

More recently the ICF concept based on laser energy deposition 'from the outside in' has moved to one in which energy is injected through a hole reaching to the hollow center of the (spherical) fuel pellet. Compression still occurs via ablation, this time taking place on the inside surface. In addition, the plasma generated by the laser pulse forms its own magnetic field B. The B field is generated in a time of the order of nanoseconds: accordingly, the Maxwell equations predict B will be so intense as to confine plasma. Besides this timescale, the other key difference with MCF is that the spatial confinement scale is much smaller, since it is of the order of the pellet size (a few millimeters). Impulsive confinement prevents the plasma just forming from bursting immediately through the pellet case. This fusion strategy has been dubbed MICF (see Figure 8.18).

8.11.1 Inertial electrostatic confinement fusion

Among conceptual fusion schemes, this is one of the simplest and most aesthetically appealing, but has been only partially explored, mainly because it is by far one of the most recent. R. Bussard described this concept, that he called 'charged-particle-electric-discharge-engine', or QED for short, in a 1990 paper [Bussard, 1990]. The fuel (positively charged after having been stripped of its electrons) is injected in a radially symmetric mode into the reactor, made of a spherical wire mesh. The wire mesh (the anode) is kept at a potential of order $-100\,\mathrm{kV}$, and attracts the fuel

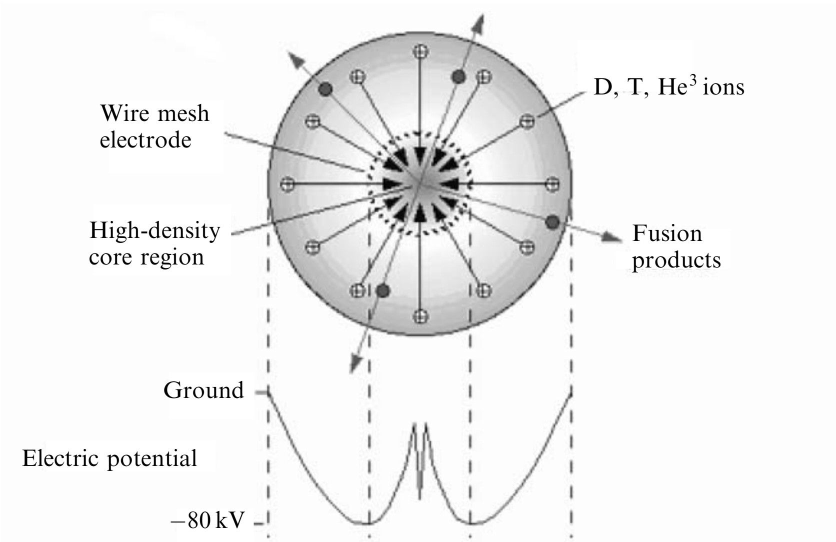

Figure 8.19. Conceptual scheme of an inertial electrostatic confinement reactor and of the radial distribution of its electric acceleration potential.

electrostatically. While attracted and traveling toward the anode the fuel is accelerated and compressed, because density increases as $1/r^3$, with r the distance from the center of the sphere (see Figure 8.19). For sufficiently negative mesh potential, at some distance r from the center the fuel should satisfy the Lawson criterion and ignite. Fusion products tends to escape isotropically, and should be collimated in a beam in some way, otherwise net thrust would be zero. This concept is being investigated in the US at the University of Illinois; see also [Miley et al., 1995].

8.12 MCF AND ICF FUSION: A COMPARISON

The plasma responsible for thrust in rockets based on mirror MCF is controlled by B fields, as mentioned in section 8.9. At a B of the order of a few tesla, gyration radius may be of the order 1 cm, and overall plasma cross-section ('bottle' cross-sectional area) is determined by the mass flow-rate to obtain a certain thrust. In sizing an MCF fusion chamber the next question is, what is the length of the mirror 'bottle'. An accurate estimate involves much calculating and assuming, but a quick answer for estimating purposes only may be obtained by noticing that the length, L, of the bottle, or of the torus radius in the case of a tokamak, is, once more, ruled by the need to contain plasma for a time sufficiently long for fusion to start and self-sustain.

A simple kinematic criterion can therefore be derived to estimate L (for a much more detailed analysis of this problem see [Romanelli and Bruno, 2005]). This criterion states that the average distance traveled by the average ion while fusing must be contained within the magnetic bottle size L (it must be shorter than L). Ion distance traveled is proportional to ion velocity, that scales with $\sqrt{E}$, or $\sqrt{T}$ from Boltzmann, times the residence time in the bottle, τ. To account for the shape of the ion trajectory (not rectilinear!) and that depends on the shape of the magnetic bottle, L is weighted with the ratio $\beta_{\max} > 1$ between peak and mean B field inside the bottle. In essence, if τ is the residence time of the fusing plasma,

$$\sqrt{E} \sim \frac{V}{m} \sim \frac{3}{2}\sqrt{T}$$

is the average ion energy, or temperature, or velocity per unit mass of the ion,

$$\beta_{\max} = \frac{B_{\max}}{B_0} \frac{\text{Peak magnetic field within the bottle}}{\text{Mean magnetic field within the bottle}} \tag{8.25}$$

and L is the length of the magnetic bottle, then the condition for fusion becomes:

$$\tau\sqrt{E} \sim \beta_{\max} L$$

This criterion tells that the effective length of the reactor to accommodate fusing particles (accounting also for the effect of the particular shape of the B field) must be equal to the length traveled by ions. Since the product $n\tau$ must satisfy the Lawson criterion for ignition, coupling together equations (8.17) and (8.25) in fact constrains the actual length of the fusion chamber in MCF rockets.

Not surprisingly, the major factor in scaling L is the extremely high ion energy, E, due to fusion. Since ion speed is high, even short ignition/residence times τ mean very long distances traveled while confined. After some calculating, the result is that a mirror MCF propulsion system must have a length, L, many orders of magnitude greater than the bottle cross-section, in practice of the order of many tens, or even hundred, meters. The physics of *mirror fusion* propulsion seems to result in very thin and very long engine shapes. Whatever their shape, imposing B fields over distances of orders of tens of meters means unfortunately large mass. This implies that superconducting magnets may become critical components/technology in designing practical mirror fusion rockets.

One could compact MCF rocket engines by switching from a mirror to a tokamak topology: the length, L, of the bottle is 'turned end-on-end', and the overall size of the reactor decreases by a factor roughly π. Although it is hard at our stage of fusion knowledge to conceive practical ways of producing direct (thermal) thrust from a standard tokamak, reverse field configuration (RFC) reactors have been proposed (see Figure 8.20) that can embed a tokamak geometry within a mirror propulsion configuration. Combining the best of two worlds, the goal of RFC reactors is to fuse plasma while letting it escape at one end, for instance to the right, in Figure 8.20, to produce thrust. The advantage of RFC reactors is their compactness, similar to that of spheromaks from which they differ because of the poloidal magnetic field, more intense than the toroidal field (in spheromaks they are comparable). The RFC operating mode is relatively new, so not much work has been done to predict its performance, and especially to estimate its overall size and mass, e.g., see [Romanelli and Bruno, 2005].

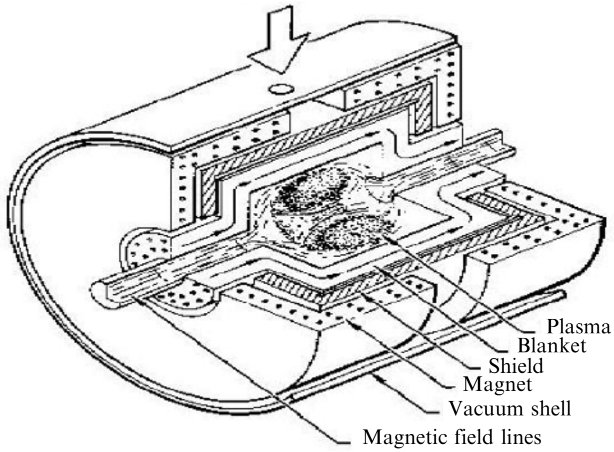

Figure 8.20. Sketch of an RFC reactor with neutral beam port.

If RCF reactors cannot be made to work as practical thermal rockets, tokamak MCF may be restricted only as electric power sources of relatively low overall efficiency. On-board power generation is necessary in any case for spacecraft, but from the viewpoint of space propulsion, direct propulsion via a mirror bottle looks conceptually a better solution than using a tokamak to generate electrical power.

Comparing MCF rockets to ICF, the first obvious remark is that size of the ICF power-releasing chamber upstream of the nozzle is roughly that of the single pellet, i.e., of order of millimeters, much smaller than any mirror rocket. Pellets will be hit one by one by lasers as they are injected inside the ICF reactor chamber. The ICF reactor may be visualized, for instance, as a simple channel, where fuel pellets are injected and ignite.

However, the energy released during a single fusion episode (pulse) is so large that the micro-explosion of a fusing pellet must be prevented from damaging the ICF reactor walls. Damage can occur caused by a combination of radiation and conduction heat transfer, plus the effect of momentum deposited on walls by the hot expanding plasma. Unlike steady-state fusion, however, the time over which energy release may damage the chamber will be short: the situation is similar to that in an automotive combustion engine, where instantaneous combustion temperatures may exceed 2,500 K, but the confinement time is so short that cylinder walls may be made of aluminum and may be cooled by water. That situation is paralleled by ICF when compared to MCF.

To prevent a fusing pellet from damaging the chamber walls the standard remedy is to use a magnetic field. The volume of space where B must compress the hot plasma created by the fusing and exploding pellet will be two orders of magnitude or more smaller than in MCF. Calculations of the magnetic field B_0 to impose near reactor channel wall to stop pellet debris at a safe distance, d, from the wall itself is tedious. To first order, B_0 is given by:

$$(B_0)^2 = \frac{8\mathrm{KE}d}{(R_c)^3}\left(R_c - d\ln\left(\frac{R_c}{d}\right)\right)^{-1} \tag{8.26}$$

where R_c is the radius of the channel where the pellet fuses and KE is the initial kinetic energy of the exploding pellet. The spatial distribution of B may be found by noting that the flux of B must be conserved, so that in a constant area channel the field B must scale with R^2 (the lateral surface of a cylinder):

$$\frac{B}{B_0} = 1 - \left(\frac{R}{R_c}\right) \tag{8.27}$$

Since d is presumably much greater than R_c then B_0 depends mostly on the channel size R_c and on the initial velocity, or kinetic energy, KE, of the exploding pellet plasma. Assuming typical masses and energies of pellets (e.g., for a D–T pellet the mass is of order 0.25 gram), the B field that can prevent damage to the ICF channel turns out to be of order 0.33 tesla, not very intense. This result might be considered counterintuitive: one may think it impossible to have a miniature thermonuclear explosion harnessed inside a channel of a few centimeters diameter. In fact, the mass of pellets considered for controlled ICF is a minute fraction of that in a thermonuclear warhead, and scaling of confinement effects is non-linear. Fundamental physics therefore indicates ICF rockets may work without recourse to exotic technology. On a much grander scale, that was also the conclusion of the Orion Project in the 1950s. The goal of Orion was to drive a spaceship by repeated nuclear explosions a certain distance away from a pusher plate attached to its stern [Dyson, 2002]; this project is apparently being resurrected, although using micronuclear explosions. The DPF reactor of Figure 8.14 could, in fact, partially simulate its operation.

To summarize this comparison, ICF propulsion needs smaller fusion chambers; its power and thrust will depend on pellet injection repetition rate. Total mass depends most significantly on the power laser assembly, probably the single most critical component. MCF rockets may need much longer reactors in mirror configuration, or more compact ones (perhaps by a factor of 3–4) in an RCF configuration. If electric thrusters are preferred, then energy conversion machinery must be added, and thermal fusion power may be two or three times that needed to produce thrust.

Whatever the MCF mode, based on what is known MCF will probably be an order of magnitude larger, and presumably heavier than an ICF propulsion system. Figure 8.21 shows size, mass, performance and other critical parameters of two mirror MCF rocket conceptual designs using D–T or D–He^3 fuels; similar tables are in [Williams, 2004], together with design criteria for a reference mission to Mars or Europa (well within our Solar System!). Even for these relatively short missions, the total mass of the fusion power system is estimated above 7,000 tons, an astonishing figure (the reader is in fact cautioned about some of the parameters used in [Kammash, 1995], e.g., neutron fluxes, as they are even two orders of magnitude

Parameter	D–T Rocket	D–He^3 Rocket
Gain factor Q	1	1
Plasma β	0.95	0.95
Vacuum magnetic field B_{p0}	15.846	184.81
Plasma length L, m	50	50
Plasma radius r_p, cm	7.071	7.071
Injection energy E_{in}, keV	20	200.0
Ratio of D and He^3 densities D : He^3		6 : 4
Equilibrium fuel ion density n_i, cm^{-3}	4.728×10^{16}	4.359×10^{17}
Equilibrium fuel ion temperature T_i, keV	6.555	84.629
Fuel ion confinement time τ_i, s	2.862×10^{-3}	7.859×10^{-4}
Fusion power P_f, MW	4.171×10^4	1.429×10^7
Neutron power P_n, MW	3.336×10^4	2.061×10^4
Bremsstrahlung radiation power P_b, MW	2.281×10^3	1.757×10^6
Synchrotron radiation power P_s, MW	3.465×10^2	7.478×10^6
Neutron wall loading W_n, MW/m^2	622.039	384.2
Surface heat flux W_s, MW/m^2	42.526	32758.3
Thrust F, N	4.970×10^4	6.760×10^6
Thrust power P_F, MW	5.503×10^4	2.773×10^7
Magnet mass M_m, Mg	37.4	2265.5
Radiator mass M_{rad}, Mg	7128.2	3.555×10^5
Refrigerator mass M_{ref}, Mg	12.5	755.2
Shield mass M_s, Mg	50.2	15.9
Total mass M_{tot}, Mg	7228.3	3.585×10^5
Specific power, kW/kg	7.613	77.343
Specific impulse I_{sp}, s	1.129×10^5	4.183×10^5

Figure 8.21. Mass budgets for two MCF propulsion systems (adapted from [Kammash, 1995]).

higher than in experimental fusion reactors, see [Romanelli and Bruno, 2005]). ICF propulsion systems have received less attention, so that similar detailed analyses have not yet been performed; the example in Figure 8.22 is far less informative. The conclusion is that such estimates need to be taken with many grains of salt; see also [AIAA, 2004]. For instance, the mass budget in Figure 8.21 is inconsistent; the total length of the mirror engine (of order 50 m) is reasonable if the plasma number density is indeed as high as $10^{22}\,cm^{-3}$: in fact, in the most advanced tokamak in operation (the ITER fusion reactor) plasma density is an order of magnitude lower because of instabilities. Since the mirror engine length scales linearly with density, using a more reasonable value such as $10^{21}\,cm^{-3}$ predicts a length of order 500 m. Notice also that the D–^{3}He engine has $Q = 1$, meaning a neutral energy budget (power obtained equal to auxiliary power to create plasma), leaving no net power generation. The neutron flux (of order 600 MW/m^2) is more than 10 times that ever obtained in any tokamak reactor, therefore it sounds wildly optimistic besides posing enormous structural problems due to radiation damage.

Driver:	Mass, metric ton
Lasers	110
Radiators	92
Optics, Structure	18
Energy handling	42
	262
Thrust chamber	
Shield coil	126
heat rejection	40
	166
Overhead:	
Payload shield	17
Fuel tank	16
Reactors	5
Truss	20
	58
Total	486

Figure 8.22. ICF propulsion system—mass budget (adapted from [Kammash, 1995]).

Even with the prospective of future improvements these remarks suggest one should be very cautious in assessing fusion technology.

Inspection of the data in Figure 8.21 shows that MCF mass budgets are totally dominated, as many expect, by the space radiator. In the D–T-powered rocket the radiator mass is about 98% of the total mass. This effect is due to the figure of merit assumed in conventional radiator technology, of order 1 kg/KW to be dissipated into space, assuming a maximum radiator temperature of order 600 K. In fact, NASA estimates that space radiators may be capable of between 0.015 and 0.2 kg/KW in its future nuclear electric propulsion systems. Remember also that in fission NTR no radiator is necessary: all the heat released by fission ends inside the propellant. In thermal fusion rockets instead a large percentage of the power released is in the form of kinetic energy of neutrons and radiation, both not directly useable for thrust. This power eventually thermalizes within the reactor structure, and must be disposed of by a space radiator.

The cooling issue is thus the major issue in current designs of MCF mirror rockets. From this viewpoint, ways to recover the radiation thermal load, for instance to produce electric power for an additional MPD rocket, may turn out to be indispensable to reduce space radiator mass and reach a reasonable mass budget. The resulting propulsion system would be hybrid, the thrust being partly direct thermal and partly fusion-electric.

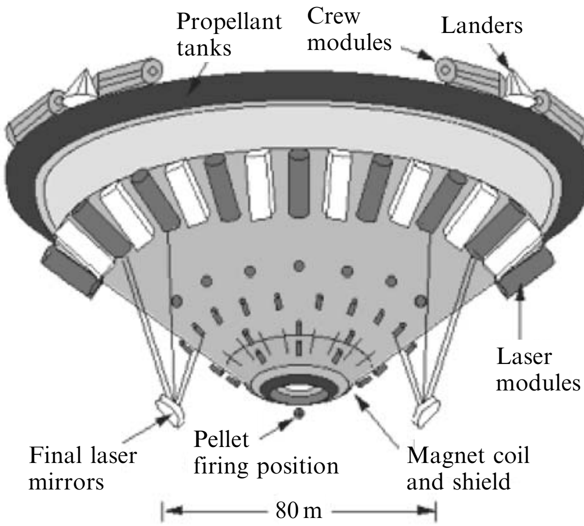

Figure 8.23. Schematic view of the VISTA ICF rocket-powered vehicle.

For ICF (see Figure 8.22) the story is different, because the contribution of bremsstrahlung radiation to the energy budget is relatively small, mostly because of pulsed mode operation. Accordingly, the estimated radiator mass is less than 10% of the total engine mass, compared with more than 98% for the two MCF concepts in Figure 8.20.

Note that the electromagnet coil to protect the ICF rocket chamber, when added to the laser(s), makes up for 50% of the total mass. In Figure 8.22 the magnet coils are assumed to have been made of conventional electric conductors. Superconducting coils should reduce mass by at least one or two orders of magnitude. Therefore, the critical component of ICF rockets is the laser assembly needed to trigger fusion inside the pellets. In addition to their mass penalty, lasers absorb a good fraction of the fusion power, a second important penalty. ICF propulsion appears (in principle) to lead towards much more compact but less performing rocket propulsion systems compared to MCF rockets. The mass budget of ICF and its technical challenges are indeed formidable [Cassenti, 2004].

Figure 8.23 shows an artist's view of a ICF rocket-powered spacecraft called VISTA (Vehicle for Interplanetary Space Transport Applications), using multiple laser beams focusing simultaneously on single fuel pellets. Most of the lower (conical) part of VISTA constitutes the 'spike' magnetic nozzle guiding the plasma. Spike nozzles are obtained by conventional nozzles by turning their shape inside out: thrust is applied on the *external* surface of the spike. In this figure this feature is supposed to minimize heat transfer problems. Dark and light rectangular boxes are the lasers and the power sub-components. Noting the size of VISTA it is no surprise its estimated mass is 5,800 tons, including a 100-ton payload for a 60-day Mars round-trip (no mention of using VISTA for QI missions). In VISTA the ICF rocket is fed extra inert hydrogen propellant to raise thrust. Most of the mass (4,100 tons) is in fact hydrogen propellant (D–T mass is only about 10% of hydrogen, or 40 tons). Total thrust power is 30 GW at a pellet repetition rate of 30 Hz. Estimated I_{sp} is 17,000 sec, rather low because of the inert hydrogen mass addition; see Figure 7.5. The VISTA concept has recently been revisited taking advantage of the so-called 'fast ignition' pellet heating [Nakashima et al., 2005]. By reducing ignition energy the VISTA spacecraft may weigh only 1/7 of the original. Work on 'fast ignition' heating is in progress in Japan and Russia.

In fact, after looking at the main critical areas of fusion propulsion, what sort of performance may be generally expected? The answer is matter of (informed) speculation, because self-sustaining fusion per se has not yet been demonstrated experimentally. Based on the calculated energies of fusion products, practical I_{sp} of order 10^5 to, perhaps, 10^6 sec can be predicted with both D–T and D–He^3 MCF rockets. An ICF rocket may be ideally capable of similar I_{sp} during a single pulse, but a significant fraction of the pellet (its metal jacket) has higher molecular weight (e.g., Ti, 48, or W, 163) than He. Besides, an ICF rocket works in the pulsed mode (average I_{sp} is lower than instantaneous). In fact, the ICF mass budget shown in Figure 8.21 was estimated by calculating an He exhaust speed 3.75×10^5 m/sec, and a tungsten (from the pellet jacket) exhaust velocity only 4.4×10^4 m/sec, consistent with its much higher molecular weight. The effective I_{sp} is weighted toward the heavy tungsten ions speed, rather than towards that of the He nuclei.

Comparison between *thrust* available with the two strategies depends on power assumed for a specific mission. Perhaps a better comparison is a comparison done per unit mass of engine. MCF reactors using D–He^3 fuel yield about 2×10^{-2} N/kg, vs. about 0.7×10^{-2} for the more practical D–T combination, a factor two and a half higher. In both cases the thrust/mass ratio seems not too low, but the mass of the engine alone is astounding. Superconducting coils may help somewhat, but not decisively, in designing MCF propulsion systems. Current MCF rocket concepts should be revisited by including ways of exploiting the large neutron and photon energy fluxes that thermalize and must be rejected by massive space radiators. Information in [Brown, 1989] may be a possible starting point to this goal. Alternative, more compact concepts have been summarily proposed that may lower mass and size of MCF, see [Kammash, 1995, pp. 161 and 179]. These innovative concepts have been insufficiently analyzed to reach conclusion regarding performance, thrust and weight.

As a final note, work in fusion propulsion continues in the US (mainly at LASL), and in Russia but its low funding level and the many technical problems still to solve suggest no major breakthroughs are forthcoming anytime soon.

8.13 CONCLUSIONS: CAN WE REACH STARS?

The focus of this chapter has been on giving a technology answer to a question going back to the first men gazing at the stars: What is there? Are there beings like us? Can we go there? To answer the last question, we enrolled the ultimate known power source, fusion. The calculations and analyses presented, however, leave the question still without a clear answer: within the constraints posed by the physics we know, even fusion propulsion is rather limited if stars are our destination. Stripping fusion rocket concepts of their exotic mystique leads to a rather disappointing future scenario: thrust may even be in the 10^5 N range and I_{sp} in the 10^5 sec, but at the price of strikingly large engine mass (hundreds or thousands of tons). These I_{sp} are infinitely better than those of chemical propulsion, but still way lower than needed to carry on interstellar travel and exploration within reasonable human timescales. The first fundamental limitation in traveling over quasi-interstellar and stellar distances is that mass conversion into energy by fusion is about a factor 5 larger than in fission, but still limited to fractions of a percent. Fusion propulsion will make traveling beyond our Solar System practicable, but only to destinations much closer than the nearest star: even the Oort cloud is too far away to be explored by a manned vehicle. The mass of a ship bound for Proxima Centauri and still meeting the constraints posed by our physics would be so large, and the time to cross the gulf between our Solar System would be so long, as to effectively make manned trips in practice unfeasible, although not physically impossible.

Only matter annihilation can lower mass consumption significantly, and enable practical travel of robotic spacecraft and (perhaps) some crewed ships. Matter–antimatter 'fusion' is still at the conceptual level, and was not analyzed in this chapter (its energy is released essentially in the form of radiation not easily made into thrust). Harnessing antimatter is the last hope for practical interstellar travel: the scientific and engineering challenges are formidable, but the performance could also be so outstanding to enable travel speed close to light speed.

At these speeds there is a second fundamental limitation. Physics itself rules out, for the time being, any process in which matter could be accelerated beyond the speed of light. It is very difficult, except in science fiction novels, to envisage a ship where the crew lives and works without external support for many years or even a decade, knowing that any form of communication would take years to send and receive, and that (if everything turns out well, and if the 'twin paradox' holds) when they go back they would find a different Earth and all their friends, family and colleagues already dead.

Robotic interstellar trips are easier to conceive: by building matter–antimatter propelled robotic spacecraft, radiation and shielding would be less critical problems, and acceleration could be much higher than the 1g human beings can sustain. If the time paradoxes due to relativity still apply, their impact on the will and resources to invest in such trips would be critical. Short of breakthroughs in physics that enable the control of inertia, interstellar missions, whether manned or unmanned, will be realized only when trip times of the order of many decades become not only feasible, but also accepted by the public.

In the same skeptical spirit, it is doubtful that efficient unmanned exploration can be carried on as done so far for Mars: telecommunication times will be too long to respond to specific situations. Any robotic 'crew' that can be designed to carry on stellar or quasi-stellar exploration will have to be endowed with such sophisticated artificial intelligence the likes of which we cannot even imagine at present.

However, these rather sobering or pessimistic conclusions may be the ultimate key to stellar travel. Perhaps, if no breakthroughs in physics ever occur, at a certain point in its history humankind will accept that stars cannot be 'visited' but only reached, that is, once in a lifetime. That means that, as happened on Earth in the past, some humans will choose to leave Earth for good. When this happens, fusion will then be the means of propulsion.

8.14 BIBLIOGRAPHY

AIAA (2004) 'Special Project Report – Recommended Design Practices for Conceptual Nuclear Fusion Space Propulsion Systems, AIAA SP-108-2004, Reston, VA.

Anile, A., and Choquet-Bruhat, Y. (eds) (1987) *Relativistic Fluid Dynamics*, Springer-Verlag, Berlin.

Auweter-Kurtz, M., and Kurtz, H. (2003) 'High Power and High Thrust Density Electric Propulsion for In-Space Transportation', in Proceedings of the International Workshop 'Technology and System Options Towards Megawatt Level Electric Propulsion', June 9–10, 2003, Lerici, Italy. Available from alta@alta-space.com. CD-ROM only.

Basov, N.G. and Krokhin, O.N. (1964) 'Laser-initiated Thermonuclear Fusion' (in Russian), *Sov. Phys. JETP.*, Vol. 19, 123. Also in English in IEEE (1968), *J. Quantum Elect.*, Vol. 4, 864.

Borowski, S.K. (1987) 'A Comparison of Fusion/Antiproton Propulsion Systems for Interplanetary Travel', AIAA Paper 87-1814.

Borowski, S.K. (1995) 'Comparison of Fusion/Antiproton Propulsion Systems for Interplanetary Travel', in *Fusion Energy for Space Propulsion*, edited by T. Kammash, Progress in Astronautics and Aeronautics Series, Vol. 167, AIAA, Washington, DC.

Britt, R.R. (2005) 'NASA Voyager 1 Team Says Spacecraft Has Reached Solar System's Outer Layer', *Space News*, May 30, 2005, p. 17.

Brown, P. (1989) 'Apparatus for Direct Conversion of Radioactive Decay Energy to Electrical Energy', US Patent No. 4,835,433.

Bussard, R.W. (1960) 'Galactic Matter and Interstellar Flight', *Acta Astronautica*, Vol. VI, pp. 179–195.

Bussard, R.W. (1990) 'Fusion as Electric Propulsion', *Journal of Propulsion*, Vol. 6, No. 5, pp. 567–574.

Carpenter, S.A., and Brennan, K.M. (1999) 'Overview and Status of a Mirror Fusion Propulsion System Design Study', *Acta Astronautica*, Vol. 44, No. 7–12, 471–506.

Casali, D., and Bruno, C. (2004) 'Superconducting Materials Applied to Electric Propulsion', *AIAA Journal of Spacecrafts and Rockets*, Vol. 41, No. 4, July–August 2004, pp. 671–676.

Cassenti, B.N. (2004) 'Engineering Challenges in Inertial Confinement Fusion Propulsion', AIAA Paper 2004-3533, presented at the 40th AIAA/ASME/SAE/ASEE Joint Propulsion Conference, July 11–14, 2004, Fort Lauderdale, FL.

Cassenti, B.N., and Coreano, L. (2004) 'The Interstellar Ramjet', AIAA Paper 2004-3568, presented at the 40th AIAA/ASME/SAE/ASEE Joint Propulsion Conference, July 11–14, 2004, Fort Lauderdale, FL.

Chen, F.F. (1985) *Introduction to Plasma Physics and Controlled Fusion* (Vol. I and II), Plenum Press, New York.

Crawford, I. (2000) 'Where are They?', *Scientific American*, Vol. 283, No. 7, pp. 28–33.

Dawson, J.M. (1964) *Physics of Fluids*, Vol. 7, p. 981.

Daiber, J.W., Hertzberg, A., and Wittliff, C.E. (1966) 'Laser-Generated Implosions', *Physics of Fluids*, Vol. 9, No. 3, pp. 617–619.

Dyson, G. (2002) 'Project Orion', Allen Lane – The Penguin Press, London.

Choueiri, E. (2002) Personal communication.

Einstein, A. (1916) *Uber die spezielle und allgemeine Relativitaetstheorie (gemeinvestaendlich)* (Sections 11–16), Newton-Compton Publisher, Rome.

Encrenaz, T., Bribing, J.P., Blanc, M., Barucci, M.-A., Roques, F. and Zoucka, P.H. (2004) *The Solar System* (Chapter 14, Table 14.1), Springer, Berlin.

Englert, G.W. (1962) 'Toward Thermonuclear Rocket Propulsion', *New Scientist*, Vol. 16, No. 307, pp. 16–18.

Forward, R.L. (1985) 'Antiproton Annihilation Propulsion', *J. Propulsion*, Vol. 1, No. 5, 570–374.

Hahn, J. (2005) 'When Giants Roamed', *Nature*, Vol. 435, pp. 432–433. Complete articles on early Solar System formation and the role of the Kuiper belt can be found in the three papers by Tsiganis et al., Morbidelli et al. and Gomes et al. in the same issue, pp. 459–469.

Harwit, M. (1973) *Astrophysical Concepts*, Wiley, New York.

Hill, P.G., and Peterson, C.R. (1970) *Mechanics and Thermodynamics of Propulsion*, 1st edn, Addison-Wesley, Reading, MA, Ch. 15, p. 471.

Huba, J.D. (2002) 'NRL Plasma Formulary', NRL/PU/6790-02-450, The Office of Naval Research, Washington, DC, p. 44.

Jarboe, T.R. (1994) 'Review of Spheromak Research', *Plasma Physics Controlled Fusion*, Vol. 36, pp. 945–990.

Jewitt, D.C. and Luu, J. (2004) 'Crystalline water ice on the Kuiper belt object (50000) Quaoar', *Nature*, Vol. 432, 9 December 2004, 731–733.

Kammash, T. (1995) 'Principles of Fusion Energy Utilization in Space Propulsion', in *Fusion Energy for Space Propulsion*, edited by T. Kammash, Progress in Astronautics and Aeronautics Series, Vol. 167, AIAA, Washington, DC.

Kaufmann, III, W.J. (1993) *Discovering the Universe*, 3rd edn, W.H. Freeman, New York, Ch. 17 and Appendix 4.

Kenyon, S.J. and Bromley, B.C. (2004) 'Stellar encounters as the origin of distant Solar System objects in highly eccentric orbits', *Nature*, Vol. 432, 2 December 2004, 598–602.

Kulcinski, G.L., and Conn, R.W. (1974) 'The Conceptual Design of a Tokamak Fusion Power Reactor, UWMAK-1', *The Campaigner*, Vol. 7, No. 9–10, pp. 50–62.

Lang, K.R. (1999) *Astrophysical Formulae*, 3rd edn, Springer-Verlag, Berlin, p. 145 et seq.

Lawrence, T.J. (2005) 'Nuclear thermal rocket propulsion systems', Paper IAC-05-C3.5-C4.7.03, presented at the 56th International Astronautical Congress (IAC), 16–21 October 2005, Fukuoka, Japan.

Lawson, J.D. (1957) 'Some criteria for power producing thermonuclear reactions' in the *Proceedings of the Royal Society of London, Section B, Vol. 70, pp. 1–6*.

Leifer, S.D. (1999) 'Reaching for the Stars', *Scientific American*, Vol. 232, No. 2, pp. 74–75.

Lerner, E.J. (2004) see www.lawrencevilleplasmaphysics.com.

Lissauer, J. (1999) How Common are Habitable Planets?', *Nature*, Vol. 402 Supplement, No. 6761, pp. C11–C14.

Luu, J.X., and Jewitt, D.C. (1996) 'The Kuiper Belt', in *Scientific American*, Vol. 274, No. 5, pp. 32–39.

Maccone, C. (2002) '*The Sun as a Gravitational Lens: Proposed Space Missions*, IPI Press, Aurora, CO, p. 1.

Maslen, S.H. (1959) 'Fusion for Space Propulsion', Institute of Radio Engineers Transactions on Military Electronics, Vol. MIL-3, No. 2, pp. 52–57.

Messerle, H.K. (1995) *Magneto-Hydro-Dynamic Electrical Power Generation*, Wiley, Chichester, UK.

Metz, W.D. (1976) 'Fusion Research (II): Detailed Reactor Studies Identify More Problems', *Science*, Vol. 193, p. 38–40 and p. 76.

Mikellides, P.G. (2004) 'Modeling and Analysis of a Megawatt-Class Magnetoplasmadynamic Thruster', *Journal of Propulsion and Power*, Vol. 20, No. 21, pp. 204–210. See also the Proceedings of the 'Technology and System Options towards Megawatt Level Electric Propulsion' Workshop, June 9–10, 2003, Lerici, Italy, alta@alta-space.com

Miley, G.H., Satsangi, A.J., DeMora, J., Javedani, J.B., Gu, Y., Burton, R.L., and Nakashima, H. (1995) 'Innovative Technology for an Inertial Electrostatic Confinement Fusion Propulsion Unit', in *Fusion Energy for Space Propulsion*, edited by T. Kammash, Progress in Astronautics and Aeronautics Series, Vol. 167, AIAA, Washington, DC, pp. 161–178.

Miller, A.L. (1981) *Albert Einstein Special Theory of Relativity*, Addison-Wesley, Reading, MA.

Morgan, D.L. (1982) 'Concepts for the Design of an Antimatter Annihilation Rocket', *J. British Interplanetary Soc.*, Vol. 135, 405–408.

Mukhin, K.N. (1987) *Experimental Nuclear Physics*, Vol. 1: *Physics of Atomic Nucleus*, Mir Publishers, Moscow, p. 50.

Nakashima, H. Kajimura, Y., Kozaki, Y. and Zacharov, Yu.P. (2005) 'A Laser Fusion Rocket Based on Fast Ignition Concept', Paper IAC-05-C3.5-C4.7.07, preented at the 56th International Astronautical Congress (IAC), 16–21 October 2005, Fukuoka, Japan.

Porco, C. (2004) 'Cassini Captain's Log: 2004.184', *The Planetary Report*, Vol. XXIV, No. 5, pp. 12–18.

Post, R.F. (1987) 'The Magnetic Mirror Approach to Fusion', *Nuclear Fusion*, Vol. 27, pp. 1579–1739.

Romanelli, F., and Bruno, C. (2005) 'Assessment of Open Magnetic Fusion for Space Propulsion', ESA-ESTEC Final Report, ESA-ARIADNA Contract 18853/05/NL/MV, Noordwijk.

Saenger, E. (1956) 'Die Erreichbarkeit der Fixsterne', in Rendiconti del VII Congresso Internazionale Astronautico, Associazione Italiana Razzi (Proceedings of the VII International Astronautical Congress), Rome, pp. 97–113. Also in: Mitteilungen der Landesgruppe Nordbayern der DGRR vom 13.05.1958.

Santarius, J.F. and Logan, B.G. (1998) 'Generic magnetic fusion rocket', *J. Propulsion and Power*, Vol. 14, No. 4, 519–524.

Schneider, J. (2005) 'The Extrasolar Planets Encyclopedia', www.obspm.fr/encycl/encycl.html

Schulze, N.R., and Roth, J.R. (1991) 'The NASA-Lewis Program on Fusion Energy for Space Power and Propulsion, 1958–1978', *Fusion Technology*, Vol. 19, No. 1, pp. 11–28.

Sciama, D.W. (1971) *Modern Cosmology*, Cambridge University Press, London, p. 71.

STAIF: the Institute for Space and Nuclear Power Studies, MSC01-1120, University of New Mexico, Albuquerque, NM 87131-0001, holds a Space Technology and Applications International Forum (STAIF) every year. The American Institute of Physics prints its proceedings (see the AIP website). Many papers deal with nuclear propulsion, including advanced fission and fusion.

The Planetary Report (2004) Vol. XXIV, No. 6, p. 5.

Trumbull, C.P. (ed.) (2000) *2000 Britannica Book of the Year*, Encyclopedia Britannica, Chicago, p. 824.

Wambsganns, J. (2001) 'Gravity's Kaleidoscope', *Scientific American*, Vol. 284, No. 11, pp. 52–59.

Williams, C.H. (2004) 'Application of Recommended Design Practices for Conceptual Nuclear Fusion Space Propulsion Systems', Paper AIAA 2004-3534, presented at the 40th AIAA/ASME/SAE/ASEE Joint Propulsion Conference, July 11–14, 2004, Fort Lauderdale, FL. Also published as: 'Special Project Report – Recommended Designed Practices for Conceptual Nuclear Fusion Space Propulsion Systems', Special Publication SP-108-2004, AIAA, Reston, VA.

Wittenberg, L.J., Santarius, J.F., and Kulcinski, G.L. (1986) 'Lunar Source of He^3 for Commercial Fusion Power', *Fusion Technology*, Vol. 10, p. 167.

9

View to the future and exploration of our Galaxy

Figure 9.1 is a picture of the Andromeda Galaxy (M-31), a galaxy within the neighborhood of the galactic cluster that includes the Milky Way, our Galaxy. The Milky Way is some 100,000 light-years in diameter with its central bulge about 20,000 light-years in depth. That central bulge contains the very massive black hole that drives the kinetics of the Galaxy [*Science News*, 2005] In Chapter 8 we have seen that our Solar System is on one of the spiral arms some 32,000 light-years from the center, and there is a group of stars (about seven) that are within 10 light-years of our sun. Beyond that local group, our galactic stars are much more distant. So even if we travel at the speed of light, our nearby star neighbors are up to a 20-year round-trip away. Can we overcome such distances, or are we bound to our Solar System, or at most our nearby stars? That is the question that dominates our view to the future.

Researchers can now theorize quantum physics approaches to traveling at fractional light speed, and even at greater than light (superluminal) speed. The validity of some of these theories is now being established by NASA Glenn Research Center. Earth's Galaxy contains up to 100,000 million stars. The Earth is about 32,000 light-years from the center. Without super light speed, the Galaxy is isolated from our ability to explore it in any realistic time frame. Except for our very nearby galactic neighbors the Galaxy is off-limits without superluminal speed. The distances are almost not comprehensible. At 1,000 times the speed of light, it would take 32 years for us to reach the Galactic center. Yet some researchers think that to consider superluminal speed is no more daunting than the past century's researchers considering supersonic travel: although they need to be sifted, there are indeed concepts that appear to be based on solid physics. Many of these are presented at the annual International Astronautics Federation Congress. Some will be discussed in terms of what might be possible. As already pointed out in Chapter 8, and shown in Figure 9.2, we are nowhere near having the capability to

Figure 9.1. Andromeda Galaxy from the GALEX/JPL website.

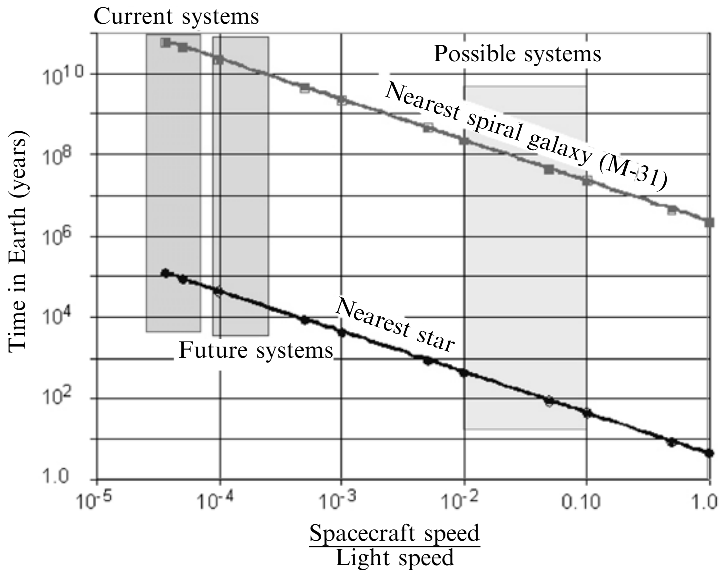

Figure 9.2. Journey time as a function of spacecraft speed.

reach the nearest star in our current projection of future systems for this century. However, are there possibilities, or potentials?

We can indeed marshal and calculate the numbers, but the possibility of achieving the conditions computed remains questionable. Again our foe is inertia and mass. Froning states [Froning, 2004]:

> It is well known that enormous amounts of rocket propellant are required to overcome gravitational and inertial resistance to Earth-to-orbit flight. Here, overcoming gravitational and inertial resistance to upward and forward flight requires impartation of about 7.5 km/s velocity to Earth-to-orbit rocket ships, and this requires that about 90 percent of single-stage-to-orbit (SSTO) rocket ship weight be propellant. Thus, if field actions and reactions of field propulsion could significantly reduce gravitational and inertial resistance, rocket thrust and propellant needs would be significantly reduced. But a major obstacle to reducing such resistance by field propulsion is current lack of understanding as to the origins of gravitation and inertia—of why and how they instantly arise to resist vehicle acceleration (or deceleration) and the vehicle's upward flight. Although the relation of gravity and inertia to parameters such as motions, distances, and ponderosities of material bodies are well known, there is no consensus whatsoever as to the origins of gravity and inertia.

Froning [Froning, 2004] discusses three possible origins of mass and three possible origins of inertia; however, none of the six possibilities have been confirmed, as we began this chapter. So, until quantum physics can change the situation, we are confined, optimistically, to about 10 light-years from our Sun, but the speed at which we can reach destinations within this sphere is wholly dependent on the specific impulse of the propulsion systems we can create. Today we are limited to the leading edge of the Oort cloud. If practical fusion rockets are a reality we could probably get a little farther, but to reach the trailing edge of the Oort cloud we need a factor of 10 increase in specific impulse. To reach 10 light-years requires a 10,000-fold increase in specific impulse. Thus what we need to do now is concentrate on getting from the surface of the Earth to orbit and to maneuver efficiently while in orbit, so when these far-in-the-future propulsion advances are made, we will have the Earth-orbit–moon infrastructure to take advantage of these developments.

9.1 ISSUES IN DEVELOPING NEAR AND FAR GALACTIC SPACE EXPLORATION

Reaching speeds close to that of light (relativistic speeds) in traveling through space is predicted to have major effects. In Chapter 8 some of these effects have been mentioned. They are the result of the Theory of Special Relativity created by Einstein. According to the Theory of Special Relativity, there are no privileged frames of reference such as the famed 'absolute inertial frame' of classical physics. The fact is that the laws of dynamics appear the same in all frames of reference moving at constant velocity relative to each other (inertial but not absolute frames). This statement can be rephrased by saying that the laws of dynamics are 'invariant' with respect to Galilean transformations, i.e., they remain the same in two frames of references in uniform motion (constant velocity) relative to each other. Experiments by Michelson and Morley also showed the speed of light is invariant with the frames of reference, i.e., does *not* increase or decrease due to the relative velocity between two inertial frames, a disconcerting and counterintuitive result that troubled many physicists. These two facts ultimately resulted in Einstein's intuition that simultaneous events cannot exist. The second motivation for abandoning absolute frames of references and Galilean transformations was the need to make not only the laws of dynamics, but also the laws of electromagnetism invariant when changing frames of reference: in fact, contrary to the laws of dynamics, they change in a Galilean transformation. This mathematical result was unacceptable, amounting to the existence of different electromagnetism 'physics' in different inertial frames. The work done by Larmor, Lorentz and Einstein himself convinced him that the Galilean transformations had to be replaced by the Lorentz transformations, in which the characteristic ratio between frame speed and the speed of light appear (see below). It is because of these new relationships between two inertial frames of reference that a clock on a spacecraft moving at constant velocity with respect to an Earth's observer would appear to him/her to run at a different speed than a clock on Earth. In other words Earth time is *not* spaceship time. The revolutionary character of Special Relativity stays in the fact that there cannot be a 'third', or 'impartial' observer capable of judging the 'right' time between the two. The two frames in relative inertial motion are equally 'right', each in its own frame, a consequence that alone can 'explain' the twins paradox so often cited in connection to relativity. So, Earth time and ship time are different, but it is Earth time we must be concerned with, because that is the time in which the project team is living. H. David Froning has spent a career investigating deep space travel possibilities, and the authors wish to acknowledge his contribution to this section [Froning, 1980, 1981, 1985, 1986, 1989; Froning et al., 1998; Froning and Roach, 2002].

To recall, the Lorentz transformation of Special Relativity [Einstein, 1916; Lang, 1999] results in a time relationship for the Earth observer and for the spacecraft traveler as follows:

$$t_{\text{earth}} = \frac{t_{\text{spacecraft}}}{\sqrt{1-(V/c)^2}} \qquad t_{\text{spacecraft}} = t_{\text{earth}}\sqrt{1-(V/c)^2} \tag{9.1}$$

Note that in the Galilean transformations of classical physics the two times are assumed identical, that is

$$t_{\text{earth}} = t_{\text{spacecraft}} \tag{9.1a}$$

because the speed of light seemed at that time to be infinite. This classical result is in fact predicted by the Lorentz transformations when imposing $c \to \infty$.

So as, the spacecraft approaches the speed of light, the crew's apparent time is shorter than the observer's apparent time on Earth. Both perceive that the event or journey has occurred over an equal duration. It is not until the spacecraft crew returns to Earth that the discrepancy in perceived times becomes apparent. Researchers have derived the relativistically correct equations for a spacecraft journey's duration (t_e) in an Earth-bound observer frame of reference, and for the journey duration (t_{sc}) of that same spacecraft in its own moving reference [Froning, 1980]. For the simple case of one-dimensional *rectilinear* motion, Krause has derived the expressions for (t_e) and (t_{sc}) for a spacecraft acceleration (a_{sc}) in its own moving frame during the initial half of the total journey distance (S) followed by a constant spacecraft deceleration ($-a_{sc}$) during the final half of the total journey [Krause, 1960]. The reader is warned that the relationships below can be easily derived and are valid only when the motion is rectilinear, i.e., when the space-time continuum is only two-dimensional, not a very realistic assumption but one that simplifies solution of this problem. In the fully four-dimensional space-time, or Minkowski's space, the effect of changing velocity (acceleration) is much more complex. There is in fact an important consequence with respect to changing velocity, because velocity is a vector. Even simply inverting direction invalidates the consequences of the Lorentz transformations, that are strictly valid between *inertial* frames, that is, with constant relative velocity. That is because velocity is defined by a magnitude (speed) and a direction. If either changes, then it had to be the result of acceleration. The most common concept of acceleration is a change in the magnitude of the speed. However, a constant speed turn is in fact an acceleration from a continuously varying direction. The direction of the acceleration is perpendicular to the flight path, and pointed at the center of (instantaneous) rotation. This acceleration is called centrifugal acceleration. Centrifugal acceleration is the result of any rotation of the velocity vector. Thus a spacecraft crew in orbit is under a constant acceleration, balanced of course by their gravitational weight. In space the thrust from a propulsion system is necessary to initiate any acceleration, whether positive or negative. Because there are no aerodynamic forces in space, any motion initiated will continue until it is negated by a counter propulsion force of equal magnitude and opposite direction. In the two-dimensional continuum assumed in the example by Krause the two times, crew's and Earth's, are given by the following equations:

$$t_{\mathrm{e}} = 2\sqrt{\frac{S}{a_{\mathrm{sc}}}\left(1 + \frac{a_{\mathrm{sc}}S}{4c^2}\right)}$$

$$t_{\mathrm{sc}} = \frac{2c}{a_{\mathrm{sc}}}\left[\cosh^{-1}\left(1 + \frac{a_{\mathrm{sc}}S}{2c^2}\right)\right] \tag{9.2}$$

These equations can be solved for a number of different destinations as a function of spacecraft acceleration, and their times compared. The life of a deep-space management team is probably about 20 Earth years. If we wish to travel farther into space, that is, faster relative to the Earth time frame of reference, then we must travel faster. But before discussing travel times, we need to establish the *absolute limit*, or boundary, posed by Special Relativity, that is, when spacecraft speed equals light speed. For such a flight profile, the maximum spacecraft velocity will be assumed to be reached at the journey midpoint only, see Figure 9.3. From the starting point to the midpoint the spacecraft has a continuous and constant positive acceleration. From the midpoint to the end point the spacecraft has a continuous and constant negative acceleration. Saenger derived the ratio of the spacecraft velocity (V) to light speed (c) at the journey midpoint, as given in equation (9.3) [Saenger, 1956].

$$\frac{V}{c} = \tanh\left[\cosh^{-1}\left(1 + \frac{a_{\mathrm{sc}}S}{2c^2}\right)\right] \tag{9.3}$$

The value of the hyperbolic tangent approaches 1 as the value of the hyperbolic arc cosine approaches infinity. So in this solution objects *never reach light speed* unless

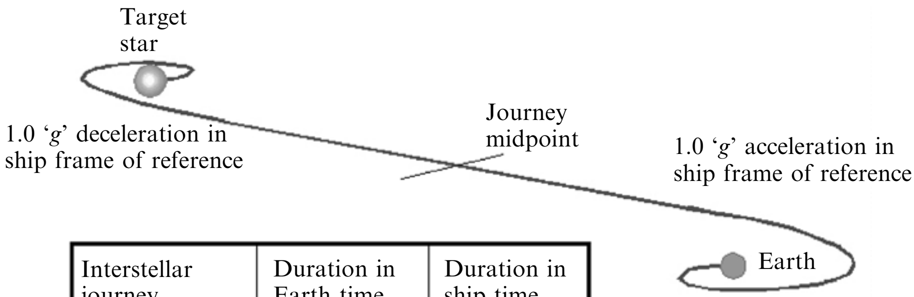

Interstellar journey	Duration in Earth time	Duration in ship time
Earth to nearest star	4.53 years	2.86 years
Earth to Galaxy center	33,000 years	24.7 years
Earth to nearest spiral galaxy	2.2 million years	28.3 years

Figure 9.3. Specific examples of Earth versus ship times.

their acceleration is also infinite. Said otherwise, reaching light speed requires reaching also infinitely large kinetic energy, because V/c tends to 1 and the Lorentz transformation factor (the square root at the denominator) tends to infinity. In section 8.3 we have seen this is the result of the fact that *potential* energy grows with the Lorentz transformation factor $(1 - V^2/c^2)^{-1/2}$. However, the hyperbolic tangent has a value of 0.9999, or V is only 0.01% less (30 km/sec less) than light speed when the value of the hyperbolic arc cosine function is 70.7. So the ‘$V/c \approx 1$’ curve on Figure 9.4 represents actually 0.9999 of light speed.

The two equations (9.2) for Earth time and spacecraft crew time can be solved, for instance, for three sample destinations: one of the nearest stars, Alpha Centauri, 4.32 light-years distant; the Galactic Center, 33,000 light-years away; and the nearest spiral galaxy, Andromeda, 2,200,000 light-years away. Figure 9.4 shows that with the flight profile just assumed, to a hypothetical Earth observer time on the spacecraft seem to flow more slowly than Earth time. In terms of Earth time, the mission time appears to be approaching a constant value. In the spacecraft the clock onboard would appear to run slower and slower as the acceleration is increased, so that *to the crew* the transit time to final destination continuously decreases as the acceleration increases, just as expected. Remember these are one-way missions: if the spacecraft were to return to Earth, both the Earth observer's time and spacecraft's crew time would double. These results are shown in Figure 9.4, where solid lines are Earth time and broken lines are crew or spaceship time. Each of the Earth observer time curves (solid lines) approach asymptotically the time corresponding to the distance from Earth, *measured in light-years*, as the spacecraft velocity approaches light speed. The spacecraft crew time (broken line) breaks away from the Earth observer line above some acceleration threshold. The greater the distance, the lower the value where the

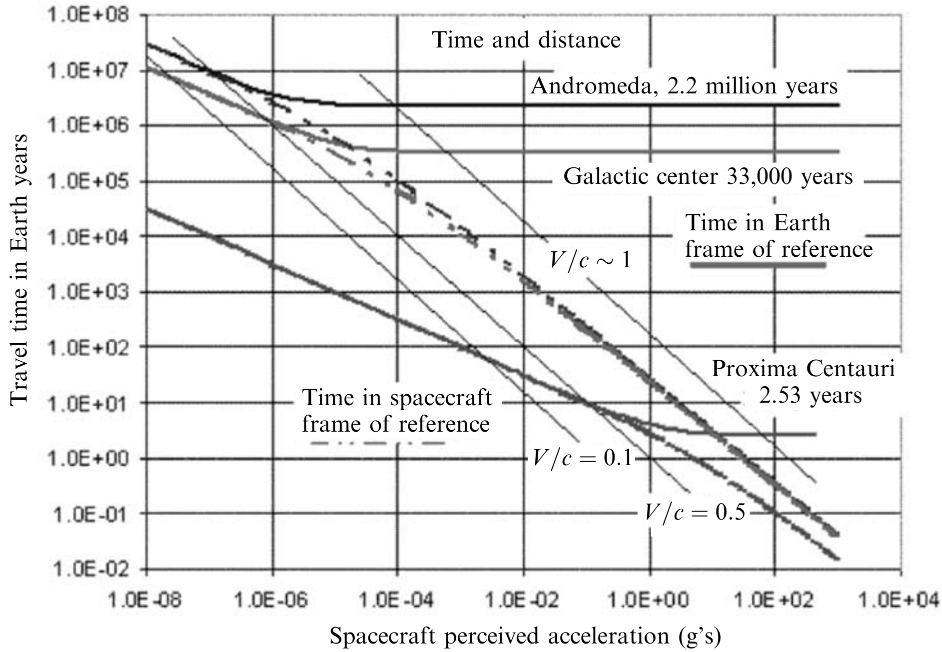

Figure 9.4. Flight profile and differences between crew and Earth times.

spacecraft/crew perceived acceleration curve breaks away from the Earth observer line. For the nearby Alpha Centauri star the observer and the spacecraft crew time curves are relatively close until almost 1 '*g*' acceleration (9.8067 m/sec^2). For the two more distant destinations, and for practical accelerations, there are orders-of-magnitude differences between Earth and crew times. One of the many problems with interstellar travel is the different times predicted between non-inertial frames by Special Relativity. Note again that in these calculations the effect on times due to the non-inertial frames of reference when the ship accelerates and even inverts its velocity, see [Boniolo, 1997], have been neglected.

The ship time to the nearest star (4.3 light-years) is about 58% of Earth time. The difference is not sufficient to terribly disconcert the arriving crew: the Earth team perceives the trip as 1.86 years longer than the crew. However, as the distance and acceleration increases to reach the center of the Milky Way (about 33,000 light-years) the discrepancy in clocks is startling. The ship clock has only registered 24.7 years, while on Earth 30,000 years have gone by. That is more distant to the future than the past Ice Age is to the present! The crew would have no concept of what to expect when returning, and there would be probably no chance of any communication with anything or anyone on Earth. Moving to the nearest spiral galaxy (2.2 million light-years) the clock on the spacecraft would have only registered 28.3 years, while the Earth clock would have registered 2.2 million years. That is about the time in the past the first human-like beings appeared on Earth. So how we address the different clock rates, so that deep-space exploration can be managed by Earth-based mission teams within their 20 years or so of professional life, is a very good question for long interstellar travel. Whether the spacecraft is manned or robotic, for distant space destinations there would be no one on Earth that knew *what* was returning to Earth, or *why*.

Putting aside the effects of the Theory of Special Relativity on clocks, it is worth mentioning the root of the problem, that is, the definition of time or, more correctly, of passing time. Humans perceive the present moment as having special significance. As the clock ticks, one moment passes and another comes into existence, and we call the process the flow of time. Researchers, however, argue that there is no special moment, not even the 'present', that is any more special than any other moment. Objectively, past, present, and future must be equally real (physicists talk about 'absolute past' and 'absolute future' in Minkowski's space-time, see [Miller, 1981; Boniolo, 1997]. That is, all of eternity is laid out in a four-dimensional domain composed of time and three spatial dimensions. What is observed as the passage of time is actually that earlier states of the world are different from earlier states of the world we remember. 'The fact that we remember the past, rather than the future, is an observation not of the passage of time but of the asymmetry of time—a clock measures duration between events much as a measuring tape measures distances between places; it does not measure the "speed" with which one moment succeeds another. Therefore, it appears that the flow of time is subjective, not objective' [Davies, 2002]. In a special issue of *Scientific American* [*Scientific American*, 2002] the main topic is 'A Matter of Time'. Davies [Davies, 2002] provides an example of that in 'What time is right now?' An Earthling in Houston and a person on a spacecraft crossing our Solar System at 80% of the speed of light attempt to answer the question: 'What is happening on Mars right now?' A resident of Mars has agreed to eat lunch when the clock on Mars reads 12:00 p.m. and transmit a signal at the same time.

The puzzling comparison among times of the events between the Earthling, Martian and Spaceman is in Figure 9.5. The real difficulty is that we really do not have a real definition of time! Quoting again from the *Scientific American* article, 'Neither scientists nor philosophers know what time is or why it exists. The best thing they can say it that time is an extra dimension akin, but not identical, to space.' The physicist Bryce DeWitt has obtained a theory of quantum mechanical gravitation (the Holy Grail of physics at this time) by eliminating time from the theory itself, as if time were not a physical variable of interest. This is also the opinion of the physicist Julian Barbour [Lemonick, 2001], who is convinced that time is an illusion created by our brain, an idea put forward by Fred Hoyle in one of his fiction books (*The Black Cloud*) in the 1960s and also mentioned by Gribbin [Gribbin, 1992, Ch. 7]. As we shall see, the way out of this quandary is to travel in another non-time dimension, if such a postulated dimension exists. *If* the space-time continuum is more than four-dimensional, that is made of three space coordinates and time, there is a way to reach the most distant star and galaxies in less than human lifetimes.

As we approach the speed of light there is another problem, the problem of mass

Time	Observer	Event
before noon	Earth	Earthling and Martian exchange light signals and determine the distance between them is 20 light-minutes and synchronize clocks.
before noon	Spacecraft	Spaceman and Martian exchange light signals and determine the distance between them is 12 light-minutes and synchronize clocks.
12:00 p.m.	Earth	Earthling assumes Martian has begun to eat lunch, and prepares to wait 20 minutes for verification.
12:00 p.m.	Spacecraft	Spaceman hypothesizes Martian has begun to eat lunch, and prepares to wait 12 minutes for verification.
12:07 p.m.	Spacecraft	Signal arrives disproving hypothesis; spaceman infers Martian began eating lunch before noon.
12:11 p.m.	Earth	Knowing spacecraft's speed Earthling deduces spaceman has encountered the light signal on its way to Mars.
12:15 p.m.	Spacecraft	Spaceship arrives at Mars and spaceman and Martian notice that their two clocks are out of sync, but disagree as whose is correct.
12:20 p.m.	Earth	Signal arrives at Earth. The Earthling has confirmed the hypothesis that noon on Mars is noon on Earth.
12:25 p.m.	Earth	Ship arrives at Mars.
12:33 p.m.	Spacecraft	Signal arrives at Earth. The clock discrepancies demonstrate that there is no universal present moment.

Figure 9.5. What time is on Mars? (Adapted from [Davies, 2002]).

anticipated in Chapter 8. As spacecraft speed increases toward the speed of light, its kinetic energy increases; this is predicted by the Einstein relationships (see equation (8.11)), and for all practical purposes it is as if at the speed of light the vehicle mass is infinite. One wonders what is a reasonable mass ratio, MR, for a long mission carried on at speed close to that of light. By including relativistic physics, a *minimum* mass ratio needed by a very efficient propulsion system (that is, with the highest specific impulse, I_{sp}) can be estimated. The most efficient interstellar rocket ever considered was conceived by Saenger [Saenger, 1956]. It was called a 'photon rocket', because it converts all of its onboard propellant into a perfectly collimated radiation (photon) beam. The ideal photon rocket has the highest ideal $I_{sp} = c$, although its thrust (the effect of photon recoil on the spacecraft) is tiny. Saenger derived the expression for the mass ratio MR of this ideal spacecraft performance assuming a flight profile in which the spacecraft moves at constant acceleration, a_{sc}, till *reaching the speed of light* at the mid-distance $S_{1/2}$, and then decelerates at the same rate to its final destination:

$$\mathrm{MR} = \exp\left(2\cosh^{-1}\left(1 + \frac{a_{sc}S}{2c^2}\right)\right) \tag{9.4}$$

This equation incorporates Einstein's relativistic effects, so the mass ratio approaches infinity as the spacecraft speed approaches light speed. In this trajectory the mathematical expression calculated by Saenger for the mid-point velocity is, as seen in equation (9.3):

$$\frac{V}{c} = \tanh\left(\cosh^{-1}\left(1 + \frac{a_{sc}S}{2c^2}\right)\right) \tag{9.5}$$

These equations have a kind of counterpart in the transonic drag equations of aerodynamics predicting infinite drag at Mach number 1; this result worried physicists after World War II, but in fact was due to linearization of the equations themselves. Some might doubt then whether relativistic effects are the result of a discontinuity due to a similar mathematical treatment, or are a true physical discontinuity when $V = c$. Calculation of the mass ratio needed to accelerate near the speed of light yields inordinately high values, just as evaluating drag with linearized aerodynamics near Mach number 1 yields unrealistically high drag. To most physicists there is no question: because of the Michelson–Morley experiment and accurate measurements of time differences between satellite and Earth clocks, Special Relativity 'works'. However, some keep doubting, because the discontinuity when $V = c$ seems a pure mathematical artefact, that is, the effect of the Lorentz transformations based on the invariance of c. Still almost all physicist are convinced of the validity of Special Relativity.

Combining the rocket (Tsiolkovski's) and the MR equations one can estimate the average I_{sp} needed for a specific mission, as given below. In the simple flight profile chosen by Saenger, for example, when the mass ratio approaches infinity the specific impulse (I_{sp}) approaches zero. For speed less than 91% of the speed of light, the limit I_{sp} (here in seconds) is

$$\begin{aligned} \mathrm{MR} &= \exp\left(\frac{\Delta V}{g_o I_{sp}}\right) = \exp\left(2\cosh^{-1}\left(1 + \frac{a_{sc}S}{2c^2}\right)\right) \\ I_{sp} &= \frac{\Delta V/g_o}{2\cosh^{-1}\left(1 + \frac{a_{sc}S}{2c^2}\right)} \quad \text{(sec)} \end{aligned} \tag{9.6}$$

When the spacecraft speed is in the vicinity of light speed, as measured by the difference $\Delta c = c - V_{sc}$, an approximation for the weight ratio and I_{sp} is:

$$\begin{aligned} \Delta c &= 299{,}796\text{-}V_{sc} \quad \text{(km/sec)} \\ \mathrm{MR} &= \frac{599{,}475}{\Delta c} \\ I_{sp} &= 1{,}373{,}120\,(\Delta c)^{0.076744} \quad \text{(sec)} \end{aligned} \tag{9.7}$$

For instance, an incremental spacecraft speed of 5,994.75 km/sec makes the absolute speed 97.85% of light speed, and the resulting mass ratio of 100 may be tractable. The corresponding I_{sp} is 2,676,900 seconds. That is about three orders of magnitude (1,000 times) greater than the best space engines can provide today. Traveling close to light speed with reasonable MR requires either dramatic improvements in propulsion or radically new ways of conceiving propulsion and space travel. Some are discussed below.

9.2 BLACK HOLES AND GALACTIC TRAVEL

The time, energy and logistic limits posed by travelling to our closest stars (let alone to Galactic destinations) motivate the search for propulsion means alternative to what is based on current physics. This is a common goal among science fiction writers and scientists alike. The measurements taken from scientific satellites indicate the space-time continuum of the Theory of General Relativity is nearly flat; if space-time could be 'warped', that is, curved, the force and energy available from gravitation would be much larger than predicted by the simple Newton's Law. Then a new propulsion system would, in principle, be possible. Such system has been proposed by Mills [Mills, 1997] and was examined in [Ford and Roman, 2000]. The conclusions regarding feasibility are for the moment rather speculative, but at least open a new door that does not violate Relativity or any other basic physical principle. In fact, contrary to popular belief, General Relativity allows for a number of effects that are positively unexpected or 'strange', some far stranger than fiction. As it is often said, the basic equations of physics, including the field equations of General Relativity, tell immediately what cannot be achieved or done, that is, all that is forbidden; they do not tell all that is possible to do. They behave like the English Laws of the old joke about what is lawful and what is not in England, Germany, Russia and Italy.* In particular, General Relativity equations are rather difficult to solve, and progress in solving them and extracting results has come step by step, sometime each correcting or modifying the previous one.

Among the most interesting of these results are those concerning black holes. By now the work of Stephen Hawking and Roger Penrose, publicized by the popular press has made this term known, even widespread to the point of becoming a metaphor. However, its strange and disconcerting properties are still being investigated by theoreticians and are far from having been completely explored; their importance to propulsion is that they carry important implications for space (and time) travel. That is to say that the physics of black holes may conceivably result in some far future in replacing the very idea of space travel with the more physically consistent idea of space-time travel [Gribbin, 1992].

A black hole is a true discontinuity in the space-time continuum. A black hole is not 'made' out of matter, although it attracts and collects matter, so it is not another type of exotic star such as the neutron star or the pulsar. It may be defined simply in terms of the geometry of the four-dimensional space-time as a purely geometric concept, characterized by a center and a surface [Kaufmann, 1993]. It is now

* 'In England all is permitted, except what is explicitly forbidden. In Germany all is forbidden, except what is explicitly permitted. In Russia all is forbidden, even what is explicitly permitted. In Italy all is permitted, even what is explicitly forbidden.'

recognized that black holes are the final products of massive stars at the end of their life-cycle. If their mass is too big to end as a white dwarf or neutron star, the gravitational force compressing a spent star's matter is no longer compensated by the pressure developed by thermonuclear reactions: mass keeps compressing and shrinking, density increases and so does gravitation, until not even light may escape. The radius of the collapsing star at this point is called the Schwartzschild radius (M. Schwartzschild was the first to discover this effect when solving Einstein field equations of General Relativity in 1916), and defines the so-called 'event horizon': an external observer cannot see any longer, past this distance, inside the collapsing star. Observationally speaking, the star disappears. Meanwhile, inside the collapsing star gravitation curves space-time more and more, till a 'hole' is punched in its fabric: the star matter is swallowed by this singularity, as (for a *static* hole at least), density and gravitational force become infinitely large. The curvature of space increases sharply going towards the hole and is perfectly equivalent to that created by mass: for this reason a black hole is also characterized by a mass, that is, the *equivalent* mass that would have the same gravitational effect. So, inside the event horizon the pull of the black hole singularity cannot be overcome by any force or thrust, as gravitation bends even photons' trajectories, let alone propellant accelerated by a propulsion system. Outside this horizon space tends to become gradually flatter, and the pull decreases, tending to that of an equivalent ordinary mass. For instance, a black hole with mass equal to that of 10 times our Sun would start behaving like a star of that mass from a distance of order three or four AU [Kaufmann, 1993].

In 1939 Oppenheimer and Volkoff [Oppenheimer and Volkoff, 1939] calculated the limit mass of a star beyond which the star would collapse into a singularity. In 1971 the Uhuru satellite designed to monitor space X-ray emissions and launched from the San Marco platform off the Kenyan coast observed a strong source of X-rays from a supergiant blue star in the Cygnus constellation, later found in fact to be a binary system. The other star, named Cygnus X-1, had a mass estimated at more than 10 times that of our Sun, but compressed within a 300 km diameter, and was (and still is) invisible. In the Harvard College Observatory the giant star took the catalog name HDE 226868; we know now its companion, Cygnus X-1, is very likely a black hole. Much progress in this field has been made since the 1970s: at present black holes are considered the natural final evolution of massive stars, and their estimated average distribution density is therefore significant: e.g., statistically there should be a black hole within 15 light-years from our Sun, although it cannot be observed directly [DeWitt and DeWitt, 1973].

Meanwhile Kerr, in 1963, had already calculated some properties of a *rotating* black hole, and the work by Newman in 1965 had explored the properties of *charged* black holes. Their joint solutions of the theory of General Relativity is called now the Kerr–Newman solution, to which theoretician Paul Davies added later quantum mechanics effects. So far, all these results were obtained by solving Einstein's field equations: no rotating black hole has been deduced from observational astrophysics yet. However, this fact has not deterred theoreticians from investigating more and more features of these objects. In fact, when Carl Sagan decided to write his novel

Contact [Sagan, 1983] he asked Kip Thorne, the leading gravitation physicist at CalTech, to help him in checking mathematically whether black holes could be exploited for space-time travel [Gribbin, 1992]. The answer was positive [Thorne, 1995]. In fact, General Relativity solutions for static black holes had already shown the existence of channels ('wormholes' is their popular name) punched by black holes between different regions of space-time. This means that black holes may be seen as the entrance into these channels leading to places in our universe, or even to a *different* universe. These General Relativity solutions are the so-called 'Rosen–Einstein bridge' solutions. This class of solutions, however, indicate that a *neutral* and *static* black hole evolves and lasts only for an instant and that the space-time inside shrinks to a mathematical point. The difference with *rotating* or *charged* Kerr–Newman black holes is that the latter class allows for finite size and duration of the wormholes. The singularity at the center of Kerr–Newman black holes is not a point but rather a ring, and if the black hole is sufficiently large and massive, objects of finite size may enter and travel without being torn apart from the gravitational tidal forces typically associated to smaller black holes, inherently possessing sharper space-time curvature [Gribbin, 1992]. In principle at least, these General Relativity solutions imply a spaceship may go through a massive black hole and emerge in a different part of our universe in a local time (ship time) much shorter than if the spaceship had to travel along the ordinary (nearly flat) space-time continuum, and without exceeding light speed. In other words, the transfer from one part of the universe to another does not violate the 'speed limit'. The ship would simply take a shortcut created by the intense curvature of space-time near a singularity.

However, there are important catches: the trip through a rotating or a charged black hole is one-way, unless the charge (or angular velocity) of the black hole is so large that the singularity at its center, still annular, becomes in the language of gravitation, 'naked'. Naked simgularities are those, as predicted by General Relativity, where the event horizon does not exist. By using this class of black holes traveling both ways becomes possible spacewise but not timewise: the spaceship would be able to return to its point of departure, but the time would precede that of departure! This disconcerting fact can be shown using the so-called Penrose diagrams, and is due to the extreme effects typical of singularities in space-time. Space and time can no longer be kept separate as in our ordinary, nearly flat space-time [Kaufmann, 1993; Thorne, 1995].

Are there such rotating or charged black holes? As said, none has been 'observed'. An inference shared by many astrophysicists, however, is that quasars *may* be such objects: they are indeed massive, a fact that can be deduced by their enormous rate of electromagnetic energy release, and they rotate. If this is indeed so, quasars are natural connections to other regions of space-time.

A second important catch about using black holes as shortcuts between regions of space-time is due to the fact that any object moving in space must have a speed less than that of light. When the spaceship enters a black hole it is preceded by the gravitational waves its mass is radiating isotropically, and that travel at light speed. This gravitational radiation may be amplified by the black hole to the point of altering the space-time curvature in front of the ship itself and preventing its very entrance. Phrasing this problem differently, the question is, how sensitive, or stable, a black hole is to perturbations? Indeed, the exact Kerr solution does show the solution is sensitive. However, precisely this 'weakness' of the solution when facing any practical application shows that there is an opportunity (if something is unstable, its equilibrium may be in some way altered in *either* direction, not just that undesired). This viewpoint may open a new way of looking at black holes, that is, as the next step in space travel.

In fact, work on the ship mass effect on the Kerr–Newman black hole spurred by C. Sagan's questions to Kip Thorne showed that black holes may be born naturally (and are therefore common), so that, in some way, perturbations must either dissipate or be insufficient to 'close' a black hole. The researchers [Morris et al., 1985] working with K. Thorne at finding solutions to C. Sagan's questions decided literally to engineer black holes to meet the objectives of the plot in *Contact* (an instance of a fiction book motivating a theory). The team at CalTech did what is called 'reverse engineering' of a black hole. In other words, they assumed the features such a wormhole should have in order to be a practical means of transportation, and then set out to find what was necessary to make it, based on what is known from General Relativity. Perhaps the most important result they obtained is that the matter inside the black hole must be capable of exotic properties, i.e., either anti-gravity or negative pressure, to keep the wormhole steady and to prevent its contraction during the spaceship transit. Such exotic matter may for instance consist of cosmic strings. All these properties, hard to find or even conceive in ordinary matter, are, however, nothing radically new. The Casimir effect indicates such exotic properties are not only theoretically possible, but can also be theoretically observed, and strings theories been investigated since the 1980s.

The last step in this quest was taken by M. Visser [Visser, 1989] and may very well be what will enable unbound space-time travel in a future still to be imagined by our generation. Visser's proposal consists of a space-gate unlike the ones discussed so far. The major problem with conventional black holes is the distortion of space time, subjecting travelers and their ships to intense gravitational tidal forces. These forces become moderate only for very large (massive) black holes, where gravitation is distributed over a vast enough portion of space, and consequently space-time curvature is mild. Relaxing the assumption of rotating or charged holes, where exotic matter would prevent the ring inside from closing due to the gravitational disturbance generated by the ship transit, Visser proposes a star-gate in the shape of a flat-faced cube. The key point (and problem) is that space-time would be held flat by exotic matter delimiting its edges. A spaceship can cross such gate without feeling any force induced by space-time, and without touching the exotic matter holding the gate together. All the associated complex physics is still the outcome of solutions of the field equations developed by Einstein in his General Relativity theory; so they are reliable to the extent that his theory is reliable, but we have in fact nothing better in the sense of a consistent model tested mathematically and at least in part experimentally.

In juxtaposition, there are efforts under way to find *new* physics, physics that would enable us to bypass limitations, such as the ones posed by the speed of light limit. It is this limit that is assumed to be the main issue blocking our path towards the exploration of stars and of our Galaxy. In this context, it must be said that certainly we have not explored all there is to know in our understanding of the physical laws. After all, what we know has been found by looking at a very small portion of our universe. Are the laws we know the same elsewhere? Do they change with time? Even looking only at the progress in black hole theory, the fact remains that we have barely scratched the potential of the General Relativity equations. Probably the single most severe shortcoming in our efforts to exploit their potential is our limited conception of space and time, this last appearing more and more frequently questioned or questionable. Probably we should abandon our concept of space travel in favor of space-time travel. All these questions and attitudes motivate the search for laws still undiscovered, constituting what has been given in recent years the catchy nickname of 'breakthrough' physics. This nickname was chosen by scientists and engineers frustrated by the constraints posed by 'known' physics. This 'breakthrough' physics sometimes adopts General Relativity equations, and sometimes modifies them to suit a particular goal, or replaces them with something else, that invariably has not stood the test of time and peer reviews. It is hard to judge the merits of ideas or models based on completely 'new' physics that should, in the best intentions of the authors, provide new means of propulsion.

Other current attempts to provide solutions to the problem of space travel consist in simplifying, or modeling in a simpler way, some of the results that have been extracted from General Relativity. Although the language may not be rigorous, or the description not completely consistent with the formalism of General Relativity, they may provide an easier picture of what is actually predicted. For instance, the complexity of describing the Kerr–Newman solution may be simulated (abridged in one dimension) by introducing a 'hyperspace', that will replace the four-dimensional metric of the field equations. This is the attempt D. Froning made in using his k-tau hyperspace in section 9.3.

9.3 SUPERLUMINAL SPEED: IS IT REQUIRED?

At subluminal speed we have shown that round-trip conventional (i.e., exploiting Newton's Third Principle) spacecraft journeys to distant galactic destinations cannot be accomplished within the lifespan of the Earth-bound project team. But what if the spacecraft can exceed the speed of light? Some investigators have been so bold to postulate the possible existence of faster-than-light entities [Tanka, 1960; Bilaniuk, 1962]. There is a mathematical approach to the Lorentz transformations that avoids violating Einstein's Special Relativity that involves introducing the so-called imaginary square root of minus one ('i' is its mathematical symbol). The consequence is that all results become real numbers (and not imaginary, in the mathematical sense!) only if the speed of the spacecraft is *greater* than the speed of light. If the spacecraft speed could be much greater than the speed of light, then the distance divided by speed becomes vanishingly small, even over enormous distances. Thus destinations that are millions of light years distant from Earth could be reached in short intervals of time if the ship acceleration could be quite large and the speed or the spacecraft many times the speed of light. But even if the ship speed is many multiples of the speed of light, the duration in spacecraft time is the distance divided by the speed of light, and that determines the spacecraft time elapsed during the mission and the physical aging of the crew [Jones, 1982]. Thus, even with an 80-year lifespan of the spacecraft crew, the crew could only reach, and return from, stars that are less than 40 light years distant from Earth. So for *less-than-light speed* (subluminal) travel, it was the lifespan of the Earth-bound observers that was the limitation; for *greater-than-light speed* (superluminal) travel, it is the lifespan of the spacecraft crew that is the limitation. In both cases limitations are equally severe: without a radically different approach to propulsion we are confined to the region around our Solar System.

The passage of time within a spacecraft will appear to slow down to zero for an hypothetical 'inertial' observer if the speed of the spacecraft reaches the speed of light. Thus in effect, all sense of time will seem to vanish for beings that reach the speed of light. But let us imagine that this vanished sense of something is replaced with something that has nothing to do with either time or distance [Froning, 1983]. Although the essence of this something is as yet a postulate unknown, it has been given the designation tau (τ). Tau has no correspondence with time or distance; its essence cannot be measured in terms of spatial or temporal separations: it is a dimensionless quantity devoid of any units involving distance or time. Just as it is possible to multiply a time by a constant (such as ct) that gives it the units of distance, it is also possible to multiply tau (τ) by a constant that results in a term ($k\tau$) that is also in distance units. Although the metric of $k\tau$ can be made the same as ct, it must be measured along an axis that is perpendicular to the x–ct-plane, as tau represents something that is neither time nor distance, as shown in Figure 9.6. In a sense, devising such τ is akin to simplifying the field equations of General Relativity

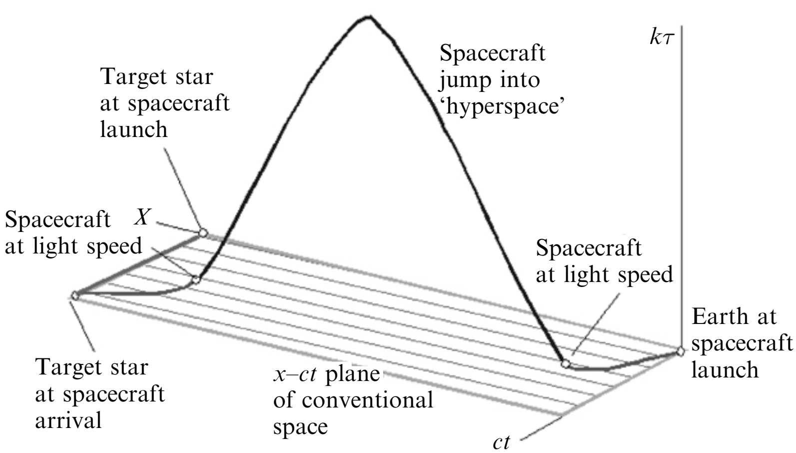

Figure 9.6. The ship jumps out of conventional space into Einstein space-time.

for illustration purposes, as they cannot yet predict what really happens when a spacecraft enters and passes through wormholes such as those of section 9.2. Since when traveling at the speed of light no apparent time elapses, the spacecraft would arrive instantly and simultaneously at all locations along the path of flight. Thus to the crew on the spacecraft, all spatial separations would collapse to zero along this path-of-flight. There is no relativistic dilatation, as all spatial separations are transverse to a light-speed spacecraft's flight. The spacecraft in effect 'jumps' into a dimension 'perpendicular' to the normal three spatial dimensions and time. In order to accomplish the 'jump' the spacecraft must achieve light speed and fly a specific flight path. There is a specific trajectory that can be determined to accomplish the jump [Froning, 2003]. So the first criterion to meet is that the spacecraft must achieve light speed and fly a specific trajectory. In a sense the spacecraft 'soars' over space and time of the x–ct plane. The flight segment in this hyperspace can be represented as a parabolic-like trajectory over the x–ct plane and in the x–$k\tau$ plane, Figure 9.6. The spacecraft then returns to light speed and an inverse trajectory returns the spacecraft to the physical x–ct plane. There is no material motion associated with the spacecraft travel in the x–$k\tau$ plane, because the plane contains no time. The spacecraft travel along the x–$k\tau$ plane would be imperceptible to the slower-than-light-speed observers as the travel occurs within a plane of event/existence that is at a right angle to the x–ct plane. Thus the spacecraft would disappear after reaching light speed, followed immediately by its reappearance trillions of miles away in the proximity of the target star, when the spacecraft returns to sub-light speed, Figure 9.6. As the spaceship travels upon the x–$k\tau$ plane the 'unfolding of tau' is not the same as the 'passage of time' upon the x–ct plane. Here, our classical concept of time is perceived as an inexorable movement toward the 'future' from the 'past'. As referenced from the *Scientific American* article cited, this perception has no mathematical or physically based reality. By contrast, the essence of tau must be such that $k\tau$ both increases and decreases during the spacecraft's travel in the x–$k\tau$ plane. Of course, spacecraft navigation in the x–$k\tau$ plane is impossible unless position and direction can be determined for each increment of tau as tau unfolds with the spacecraft. There is a detailed mathematical derivation of this strange journey in [Froning, 1983].

Going back to more conventional propulsion, the solution to the aging of the crew problem is to accelerate at very high rates. Of course that would crush occupants and equipment. So the underlying discovery that could enable far space exploration for both humans and machines is an anti-mass/inertia device counteracting the inertial forces produced by the acceleration. And the accelerations required are significant: Figure 9.7 shows the effect of increasing the acceleration of the spacecraft with respect to the Earth frame of reference. A nominal 2-year trip at conventional 1 'g' acceleration shrinks to a 1.7-hour trip at 10,000 'g', i.e., a reduction to one ten-millionth of the 2-year mission. With that shrinkage, the 30-year mission to the Galaxy center would take just 2.9 years! So the key to rapid travel to distant destination is not super-light speed, but super-fast accelerations. That requires the discovery of an anti-inertia/mass system to permit the human body and physical structures to withstand such accelerations and loads. At this time no

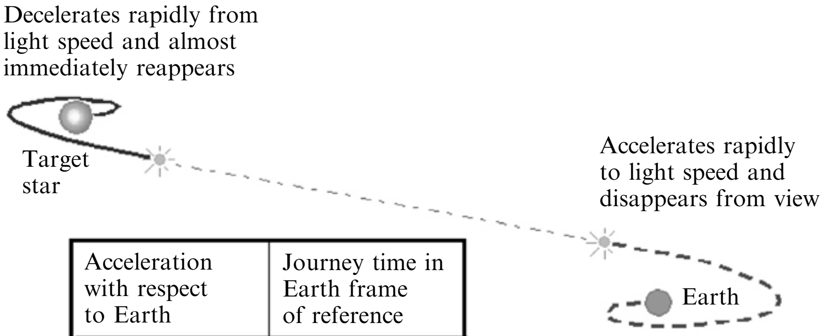

Acceleration with respect to Earth	Journey time in Earth frame of reference
1 '*g*'	2 years
100 '*g*'	1 week
10,000 '*g*'	1.7 hours

Figure 9.7. High acceleration results in shorter Earth trip times.

one appears to have the energy source, anti-inertia or anti-gravity approach that would permit such accelerations or the flight speeds that approach light-speed. In fact, no one has a reasonable beginning of a theory about inertia.

In summary, rapid transit to distant stars and galaxies would involve the spacecraft accelerating to light speed at very large values of acceleration, meaning quite beyond human or material limitations unless mass/inertia was controlled and drastically reduced or eliminated. When so, the spacecraft would be disappearing from human sight. Almost 'immediately', in terms of spacecraft clock, the spacecraft would reappear billions of kilometers away close to the target star or galaxy. During those moments when the spacecraft disappeared the spacecraft would have 'jumped' over the so-called space-time continuum in an arching flight path. If the theories and postulates are correct, the maximum speed necessary to achieve is, at most, light-speed, and *superluminal speeds are of no time benefit*.

If our Cosmos possess a greater spatial dimensionality than three-dimensional space (length, height and width) and one-dimensional time then a spacecraft will be able to 'soar' above the time and space realm of existence and travel great distances in only the time required to accelerate to light speed and then decelerate from light speed to the target destination. The key requirement is to be able to achieve light speed and no greater. So there is hope that in some future time and place a spacefaring civilization might learn to journey through space on round-trip journeys to further stars. If this greater dimensionality does not exist, the stupendous gulf of cosmic space appears to be an insurmountable barrier that can never be overcome.

9.4 CONCLUSIONS

A legitimate question is whether the ideas for travelling to destinations in our Galaxy discussed in this chapter may be considered even remotely practicable. In fact, the main result shows that wormholes travel between galactic or even intergalactic travel does not violate any current physics, including the speed of light limit, and is completely predictable from General Relativity. Furthermore, subject to progress in the physics we already have at our disposal, wormholes may be designed, again using General Relativity. As they depend on the existence of black holes, they look at the moment impracticable to build in an engineering sense of course, but the relative abundance of them in our Sun immediate neighbourhood gives hope appropriate ones may be found. Skepticism concerning these galactic travel concepts is justified, but this was also the case with the learned people that in the 1400s and 1500s were exposed to the sketches and drawings of parachutes and flying machines invented by Leonardo da Vinci. In this age we 'know better' and admire his farsightedness, perhaps criticizing his naiveté and lack of boldness. In this light, probably, some of the ideas about using gravitation and space-time curvature will become eventually a practical device. Certainly, they are from the only proven physics we can use now and for some time in the future, and allow (with some provisos) solving or neatly bypassing questions connected with the time paradoxes: so the usual criticism of time machines, such as that by H.G. Wells, is that they violate the principle of causality. As a consequence, all the precautions time travellers must take to avoid accidentally or deliberately killing one's ancestors become unnecessary using General Relativity as mentioned. Rather than travelling in space, and then putting up with redressing the many problems caused by time, the approach developed by Einstein and its consequences (black holes and intense gravitational effects) provides new opportunities and ways of reaching stars in our Galaxy and beyond. So the answer to the initial question in this section is, literally, 'Time will tell'.

9.5 BIBLIOGRAPHY

Bilaniuk, (1962) Personal communication.

Boniolo, G. (ed.) (1997) *Filosofia della Fisica* (Philosophy of Physics), Mondadori, Milan, Chapter 1 (in Italian). This textbook covers from relativity to logical quantum mechanics. Chapter 1 (pp. 1–167) deals with the Principle of Special Relativity and its 'paradoxes' in detail. In N. Falletta's *Paradoxicon*, Chapter 20 explains the 'twins paradox' for the general public.

Davies, P. (2002) 'That Mysterious Flow', *Scientific American*, Vol. 287, No. 3, pp. 24–29.

DeWitt, C., and DeWitt, B.C. (eds) (1973) *Black Holes*, Gordon & Breach, London, 1973. This is a collection of chapters by Hawking, Carter, Bardeen, Gursky, Novikov, Thorne and Ruffini on black holes theory and data. It is a good snapshot of the initial stage of research on this topic.

Ford, L.H., and Roman, T.A. (2000) 'Negative Energy, Wormholes and Warp Drive', *Scientific American*, Vol. 282, No. 1, pp. 30–37.

Froning, H.D. (2004) 'Field Propulsion for Future Flight', AIAA-2004-3761, 40th Joint Propulsion Conference, July 2004, Fort Lauderdale, FL.

Froning, H.D., Jr. (1980) 'Propulsion Requirements for a Quantum Interstellar Ramjet', *Journal of the British Interplanetary Society*, Vol. 33, No. 7, pp. 265–270.

Froning, H.D., Jr. (1983) 'Requirements for Rapid Transport to the Further Stars', *Journal of the British Interplanetary Society*, Vol. 36, pp. 227–230.

Froning, H.D., Jr. (1985) 'Use of Vacuum Energies for Interstellar Flight', MDC paper H1496, 36th Congress of the International Astronautical Federation, October 1985, Stockholm, Sweden.

Froning, H.D., Jr. (1986) 'Investigation of Very High Energy Rockets for Future SSTO Vehicles', MDC paper H1496, 37th Congress of the International Astronautical Federation, October 1986, Innsbruck, Austria.

Froning, H.D., Jr. (1987) 'Investigation of Antimatter Airbreathing Propulsion for Single-Stage-To-Orbit Ships', MDC paper H2618, 38th Congress of the International Astronautical Federation, October 1987, Brighton, United Kingdom.

Froning, H.D., Jr. (1989) 'Interstellar Studies—Their Role in Astronautical Progress and the Future of Flight', MDC paper H5276, 40th Congress of the International Astronautical Federation, October 1987, Malaga, Spain.

Froning, H.D., Jr. (2003) 'Investigation of a "Quantum Ramjet for Interstellar Flight"' MDAC paper G7887, AIAA/SAE/ASME 17th Joint Propulsion Conference, Colorado Springs, July 1981, CO.

Froning, H.D., Jr. and Roach, R.L. (2002) 'Preliminary Simulations of Vehicle Interactions with the Quantum Vacuum by Fluid Dynamic Approximations', AIAA-2002-3925.

Froning, H.D., Jr., Barrett, Terence W., and Hathaway, George (1998) 'Experiments Involving Specially Conditioned EM Radiation, Gravitation, and Matter', AIAA-98-3138.

Goff, A., and Siegel, J. (2004) 'Can Conventional Warp Drive Avoid Temporal Paradox', AIAA 2004-3699, 40th Joint Propulsion Conference, July 2004, Fort Lauderdale, FL.

Goldin, G. and Svetlichny, G. (1994) 'Nonlinear Schrödinger equations and the separation property', *Journal of Mathematical Physics B*, 3322–3332.

Gribbin, J. (1992) *In Search for the Edge of Time*, Bantam Press, Transworld Editions Ltd, London.

Jones (1982) Personal communication.

Kaufmann, W.J., III (1993) *Discovering the Universe*, W.H. Freeman, New York, Chapter 15.

Krause, H.G.L. (1960) 'Relativistic Rocket Mechanics', NASA Report TFF-36, Washington, DC.

Miller, A.L. (1981) *Albert Einstein's Special Theory of Relativity*, Addison-Wesley, Reading, MA.

Mills, Marc, G. (1997) 'Challenge to Create the Space Drive', *AIAA Journal of Propulsion and Power*, Vol. 13, No. 5, pp. 577–582.

Morris, M., Yurtsever, U., and Thorne, K. (1985) http://www.zamandayolculuk.com/cetinbal/EinsteinRosenBridges.htm

Oppenheimer, J.R. and Volkoff, G.M. (1939) 'On massive neutron cores', *Physical Review*, Vol. 55, p. 374.

Saenger, E. (1956) 'Die Erreichbarkeit der Fixsterne', in Rendiconti del VII Congresso Internazionale Astronautico, Associazione Italiana Razzi (Proceedings of the VII International Astronautical Congress), Rome, pp. 97–113. Also in: Mitteilungen der Landesgruppe Nordbayern der DGRR vom 13.05.1958.

Sagan, C. (1985) *Contact*, Pocket Books, New York.

Science News (2005) GALEX Team, JPL/NASA, M. Seibert/Caltech, *Science News*, Vol. 167, No. 8. http://www.sciencenews.org/articles/20050219/toc.asp

Scientific American (2002) Vol. 287, No. 3, pp. 20–54. This is a special issue dedicated to the concept of time.

Tanka, S. (1960) Personal communication.

Thorne, K.S. (1995) Black Holes and Time Warp: Einstein's Outrageous Legacy, W.W. Norton, New York.

Visser, M. (1989) 'Traversable wormholes: Some simple examples', *Physical Review D*, Vol. 39, pp. 3182–3184.

Appendix

Nuclear propulsion—risks and dose assessment

A.1 INTRODUCTION

'Radiation' and 'nuclear' are words that tend to spread fear among people. Even in highly technologically developed countries, the public has little or no knowledge of radiation, and when they do it usually associates it with weapons, accidents, fallout and cancer. Only specialists know about natural background exposure or about medical use of radiation. In this context the use of nuclear energy for rockets may encounter strong resistance.

The purpose of this appendix is to inform the non-specialist about what radiation and dose are, about effects of radiation on humans and about sources of radiation, including estimates of the dose from nuclear propulsion systems.

A.2 RADIOACTIVITY

Radioactivity is the process undergone by unstable nuclei (radionuclides), as well as nuclei in excited states, causing spontaneous changes, or transformations, in composition and/or internal energy of the nucleus. This means that radioactivity may change a chemical element into another, releasing or absorbing energy in the process. The most common transformations are three: alpha decay, beta decay and gamma decay.

A.2.1 Alpha decay

In alpha decay the nucleus of an element with mass number A_1 and atomic number Z_1 emits an alpha particle. Alpha particles are made of two protons and two neutrons, that is, a helium nucleus. The original nucleus is replaced by a new nucleus whose mass number A_2 is equal to $A_1 - 4$ and atomic number Z_2 is $Z_1 - 2$, and an alpha particle.

For instance, ^{222}Rn ($A_{\mathrm{Rn}} = 222$, $Z_{Rn} = 86$) decays into ^{218}Po, meaning that the nucleus of ^{222}Rn emits an alpha particle ($A_\alpha = 4$, $Z_\alpha = 2$), leaving as remainder a nucleus whose mass number is 218 (222 – 4) and atomic number (86 – 2) = 84, that is, ^{218}Po.

The mass (energy) of the parent nucleus must exceed the sum of the masses (energies) of the daughter nucleus and alpha particle emitted. The condition for a-decay to occur can be expressed as follows [Mukhin, 1987]:

$$M(A, Z) > M(A - 4, Z - 2) + M(\mathrm{H}_{\mathrm{e}}^4) \tag{A.1}$$

A.2.2 Beta decay

Beta decay is the spontaneous transformation of an unstable nucleus into a new nucleus with charge differing by $\Delta Z = \pm 1$, because of the emission of an electron (β^- decay) or a positron (β^+ decay) or the capture of an electron (*e*-capture).

In the first case (β^- decay) one of the neutrons of the nucleus becomes a proton, after emitting an electron. The mass number A does not change, while the new nucleus has an atomic number higher by 1.

Tritium (^{3}H, often symbolized by a T), $A_{\mathrm{T}} = 3$ $Z_{\mathrm{T}} = 1$, β^- decays into ^{3}He, $A_{\mathrm{He}} = 3$ $Z_{\mathrm{He}} = 2$, meaning that one of the two neutrons of the tritium nucleus emits an electron and becomes a proton; the mass number does not change, i.e., $A_{\mathrm{T}} = A_{\mathrm{He}}$, while the positive charge of the new nucleus increases by 1,

$$Z_{\mathrm{He}} = Z_{\mathrm{T}} + 1 \tag{A.2}$$

The energy condition is that the mass (energy) of the parent nucleus is higher than the sum of the masses (energies) of the daughter nucleus and the electron, and is expressed by [Mukhin, 1987]:

$$M(A, Z) > M(A, Z + 1) + m_{\mathrm{e}} \tag{A.3}$$

In the β^+ decay the unstable nucleus emits a positron (i.e., a positive electron). The β^+ decay can be treated as the transformation of a proton into a neutron, because also in this case the parent nucleus and the daughter nucleus have the same mass number A, while the atomic number of the daughter Z is lower by 1. The proton mass is lower than the neutron mass (energy). The transformation of the proton into a neutron is possible since the proton is bonded to a nucleus and the excess energy to become a neutron is supplied by the nucleus itself. The energy condition can be expressed in analogy with the β^- case [Mukhin, 1987].

$$M(A, Z) > M(A, Z - 1) + m_{\mathrm{e}} \tag{A.4}$$

C^{11}, $A_{\mathrm{C}} = 11$ $Z_{\mathrm{C}} = 6$, decays β^+ into B^{11}, $A_{\mathrm{B}} = 11$ $Z_{\mathrm{B}} = 5$, and the missing charge of boron-11 is that of the positron emitted.

The third type of beta decay is the electron capture: it consists in the capture of an electron by a nucleus from its own electron shell. For heavy nuclei with the K shell close to the nucleus, this phenomenon (also defined K-capture) is quite common; captures from L shell (L-capture), M shell (M-capture), etc. have also been observed. After the capture, the nucleus has the same mass number A, but its atomic number Z decreases by 1: the electron captured and one of the protons of the nucleus become a neutron in the daughter nucleus.

For instance, Be^7, $A_{Be} = 7$, $Z_{Be} = 4$, after capturing an electron from its K shell, becomes Li^7, $A_{Li} = 7$ $Z_{Li} = 3$, the mass number does not change $A_{Be} = A_{Li} = 7$, while the atomic number Z of the lithium is lower by 1. The mass (energy) condition is that the sum of the masses (energies) of the captured electron and the parent nucleus is higher than the mass (energy) of the daughter nucleus [Mukhin, 1987].

$$M(A, Z) > M(A, Z+1) + m_e \tag{A.5}$$

Because of the vacancy created in the electron shell, there is the transition of one of the shell electrons to that vacancy, accompanied by the emission of X-rays.

A.2.3 Gamma rays

Unstable nuclei going from an excited energy state down to a less energetic, and eventually stable, state can emit energy quanta in the γ-ray wavelength ($10^{-8} \geq \lambda \geq 2 \times 10^{-11}$ cm). There can be single transitions, where the nucleus goes directly from an excited state to the ground (stable) state following the emission of a single γ quantum, or there can be multiple transitions, i.e., a cascade of transitions bringing the nucleus to the ground state and involving multiple emissions of γ quanta. The energy of the γ quantum emitted is determined by the difference in energy of the two energy levels between which the transition has occurred.

There are different mechanisms responsible for exciting nuclei and leading to gamma radiation. Quite commonly, alpha and beta decays can leave the nucleus in an excited state. An alpha decay is usually followed by the emission of low-energy γ quanta (<0.5 MeV), while after a beta decay higher γ quanta are emitted (energy up to 2–2.5 MeV) [Mukhin, 1987].

A.3 RADIATION AND DOSE QUANTITIES AND UNITS

An ad hoc set of quantities and related units required to describe radiation decay and its effects has been developed since the effects of nuclear radiation were discovered and gradually understood [Klein, 1988]. A list of them follows.

A.3.1 Activity (Bq)

Given any radiation decay (α, β, γ, etc.), the **activity** of an element is the rate at which any and all transitions (i.e., emissions of α, β, γ rays) occur. A radionuclide has an activity of 1 **becquerel** (Bq), when it undergoes one transition per second. An older unit is the curie (Ci), equivalent to 3.7×10^{10} transitions per second. This is 'the quantity of emanation in equilibrium of 1 gram of radium' (Mme Curie said: 'la quantité d'émanation en équilibre avec un gramme de radium'), that is that quantity of radon-222 in equilibrium with one gram of its parent radium-226 [http://physics.nist.gov/GenInt/Curie/1913.html]. It is worth noting here that not only for activity but also for all other quantities both SI units and old ones, partly deriving from the c.g.s. system, are currently used.

$$1\,\mathrm{Bq} = 1 \text{ transition/second}$$

$$1\,\mathrm{Ci} = 3.7 \times 10^{10}\,\mathrm{Bq} \tag{A.6}$$

Activity is *not* a synonym of power or energy and has *nothing to do with* the effects of radiation on matter, living or not.

A.3.2 Half-life (sec)

The **half-life** is the time period over which half the nuclei of a given radionuclide decay. The half-life, depending on the radionuclide considered, varies from billions of years (i.e. U^{238} has a half-life of 4.468×10^9 years) down to small fractions of seconds (i.e. Po^{214} has 164 microseconds). An example may help: Pb^{214} has a half life of 26.8 min, and this means that if there are N nuclei of Pb^{214} at time zero, after 26.8 minutes there will be $N/2$ nuclei (the other $N/2$ have become Bi^{214} because of beta decay), after 53.6 minutes there will be $N/4$ nuclei of Pb^{214} ($3/4N$ have become Bi^{214}) and so on.

A.3.3 Absorbed dose, *D* (Gy)

When radiation passes through matter it releases energy. The **absorbed dose** is the energy deposited by radiation inside matter per mass unit. Its SI unit is the **gray** (Gy), equivalent to 1 joule deposited per kilogram of absorbing target material (1 J/kg). The older unit is the rad (radiation absorbed dose), defined as the deposition of 100 ergs per **gram** [IRCP, 1990].

$$G_y = 100\,\mathrm{rad} \tag{A.7}$$

A.3.4 Equivalent dose, *H* (Sv)

Biological effects caused by radiation are dependent not only upon the dose absorbed (Gy) but also, and above all, upon the *kind* of radiation. 'Sparsely' ionizing radiations such as gamma-rays, X-rays or beta-rays are less effective in damaging then 'densely' ionizing radiation such as alpha particles or fission fragments. In order to take into account this difference, a corrective weighting factor dependent on the kind of radiation and energy has been introduced. Weighting factors range from 1 (for photons or electrons) up to 20 (for alpha particles), and is dimensionless (see Figure A.1). Those specific for neutrons are given in Figure A.2. [IRCP, 1990].

Radiation and energy	Weighting factor, w_r
Photons, all energy	1
Electrons, all energy	1
Neutrons, <10 keV	5
10–100 keV	10
100 keV–2 MeV	20
2 MeV–20MeV	10
>20 MeV	5
Protons, all	1
Protons, (not recoil) >2 MeV	5
Alpha particles, all energy	20
Fission fragment, all energy	20
Heavy nuclei, all energy	20

Figure A.1. Weighting factors for different types of radiation.

The sum of the total radiation doses, D, combined with the proper weighting factor w_r gives the **equivalent dose, H** [IRCP, 1990]:

$$H = \sum w_r D \tag{A.8}$$

Since w_r is dimensionless, the equivalent dose, H, has the same dimensions as the absorbed dose, D, i.e., joules per kilogram. Its SI unit is the **sievert** (Sv). The older unit is the **rem** (roentgen equivalent man), whereby

$$\text{Sv} = 100\,\text{rem} \tag{A.9}$$

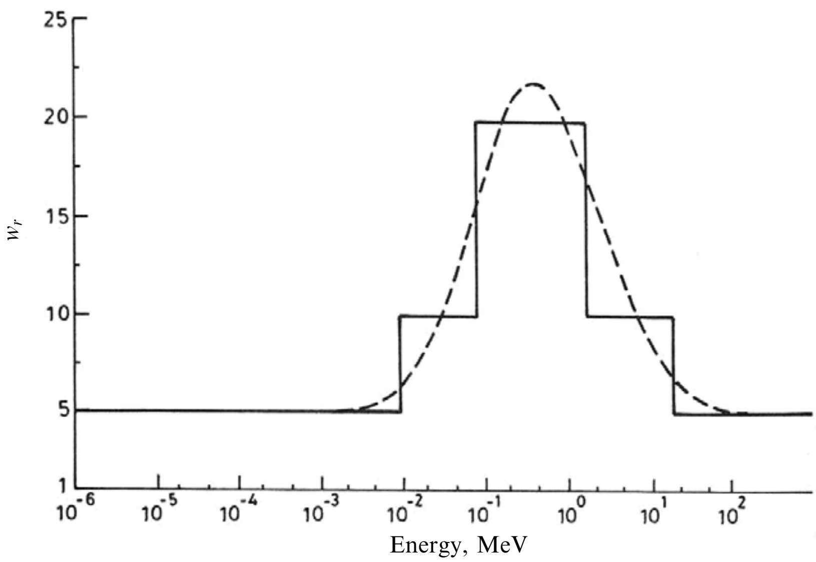

Figure A.2. Weighting factors for neutrons.

Organ or tissue	Weighting factor, w_T
Gonads	0.20
Red bone marrow	0.12
Colon	0.12
Lung	0.12
Stomach	0.12
Bladder	0.05
Breast	0.05
Liver	0.05
Oesophagus	0.05
Thyroid	0.05
Skin	0.01
Bone surfaces	0.01
Remainder	0.05

Figure A.3. Weighting factors for tissues/organs.

A.3.5 Effective dose, *E* (Sv)

Consequences of radiation on the human body depend on the particular organ or tissue hit by radiation, as different organs have different responses to radiation exposure. This is the reason why another weighting factor (w_T) must be introduced (see Figure A.3 [ICRP, 1990].

The sum of the equivalent dose, D, with the tissue weighting factor gives the **effective dose**, **E** [ICRP, 1990]. The dimensions of the effective dose are *the same as* absorbed dose and equivalent dose, joules per kilogram. Its SI unit is the same as that of the equivalent dose: **sievert**.

$$E = \sum w_T H \tag{A.10}$$

A.3.6 Collective dose (man Sv)

Absorbed, equivalent and effective dose apply to **individuals** or average individuals. In order to assess the dose received by a **group** or **population**, it is useful to introduce the **collective dose**. It is obtained by summing up the individual doses of each person of the group considered. Its SI unit is **man Sv**. A collective dose of 1,000 man Sv corresponds to 1,000 people receiving each 1 mSv or 10 people 100 mSv. This quantity is defined for a specific source of radiation or for a specific practice causing exposure, and is a convenient measure when considering nuclear accidents [UNSCEAR, 1993].

A.3.7 Dose commitment (Sv)

Some events, such as weapon tests, release radioactivity directly into the environment and cause a continuous exposure over a long time period, including several generations. In order to take into account the dose committed to a typical, though hypothetical, individual at the moment and in the future, the so-called 'dose commitment' is used. This is the integral over a specified time period (typically 250 or 10,000 years) of the average dose rate, per person, to a specified group (even the whole world population) after the event considered. Its SI unit is the sievert (Sv) [UNSCEAR, 1993]. If an event delivers a dose commitment of 1.4 mSv for 250 years, a hypothetical individual, born at the moment of the event and died 250 years old, would receive a dose of 1.4 mSv during his entire life.

A.4 EFFECTS OF IONIZING RADIATION

Ionizing radiation interacts with matter changing the state of atoms and molecules. In cells there are two types of consequences after radiation interaction: the cell may die or it may be modified. These two different consequences give rise to different implications for the whole body: there can be deterministic and stochastic effects.

A.4.1 Deterministic effects

Radiation may kill cells of a tissue/organ. If the numbers of cells killed is low, the tissue keeps on functioning without any serious consequence. If the number of cells killed increases, the tissue is harmed and loses its function, and eventually the tissue or even the organ itself may die. It is clear that an increasing number of dead cells causes more and more serious damage to the tissue. This depends on the fact that cell depletion is a dynamic process in competition with proliferation of unaffected cells. If the loss of cell is low it can be quickly compensated by repopulation (no damage or short time effects); if the loss is large there is a drastic non-compensated reduction of tissue cells (serious damage and/or death). The proportion of cells killed depend on dose, therefore the severity of effects depends on dose as well. These effects are defined as deterministic and have dose thresholds.

Some deterministic effects are: temporary or permanent sterility, depression of the blood-forming system, skin reddening, desquamation, skin loss, lens inflammation, cataract. A peculiar case of deterministic effect is the radiation syndrome from acute and whole body irradiation. If the dose is high enough, the strong cell depletion in vital organs (blood-forming organs, gastro-intestinal tract etc.) causes death. An acute whole body exposure dose **between 3 and 5 Gy**, without any specific medical treatment, causes the death of 50% of the population exposed.

Figure A.4 gives some thresholds for deterministic effects are shown. The thresholds, like all thresholds for deterministic effects, apply to people in normal health [UNSCEAR, 1993].

A.4.2 Stochastic effects

If a cell is not directly killed by radiation but somehow modified, the outcome will be different from those included among deterministic effects. *In vitro* cellular researches

Deterministic effect	Threshold, Gy
Male temporary sterility	
acute exposure	0.15
chronic exposure (per year)	0.4
Male permanent sterility	
acute exposure	3.5–6
chronic exposure (per year)	2
Female permanent sterility	
single exposure	2.5–6
chronic exposure (per year)	0.2
Depression of blood formation	
acute bone marrow exposure	0.5
long-term exposure (per year)	0.4
Lens opacities (sparsely ionizing radiation)	2–10
Lens opacities (densely ionizing radiation)	1–2
Lens opacities (chronic exposure to sparsely ioniz. rad. per year)	0.15
Dry skin desquamation (3 weeks after exposure)	3–5
Moist desquamation (blistering after 1 month)	20
Tissue necrosis	50

Figure A.4. Threshold for deterministic effects.

show that damage from radiation to deoxyribonucleic acid (DNA) gives rise to most of the detrimental effects. There are two mechanisms by which radiation may damage DNA: direct or indirect interaction. In the first case ionizing radiation directly damages a gene, in the second case radiation produces active chemical radicals near the DNA. The diffusing radicals may interact with DNA and induce chemical changes. Very efficient mechanisms exist (enzyme actions) to repair DNA, whatever the cause of harm. If only one of the two symmetric strands forming the DNA is damaged, the use of information on the other strand makes the repair process highly probable and successful, though it is *not always error-free*. If both strands are damaged at the same location, information is lost forever: the repair process is more difficult and genetic changes are likely. Such changes are defined as genetic mutations. The very nature of this process of damage/repair gives rise to effects that are random and statistical, and therefore are defined as stochastic. Stochastic effects can be somatic (i.e., cancer induction), that is they occur on the exposed individual, or hereditary: damaged cells are those whose function is to transmit genetic information to offspring. As there is no evidence that below a certain dose the repair process is totally effective, differently from deterministic effects, there is no threshold in this case [UNSCEAR, 1993].

A.4.2.1 Radiation-induced cancer

There is substantive evidence that almost all cancers originate from a single cell. However, single changes in the cell genetic code are usually insufficient to initiate a cancer. Several cell mutations (two to seven) are required in the carcinogenesis process from pre-neoplasia to cancer. Radiation may act at several stages of the process, but it seems to have a major role in the initial conversion of the cell to a pre-neoplastic state. A pre-neoplastic cell is immersed in an environment of normal cells, which tend to suppress and constrain pre-neoplastic properties. Overcoming these constraints results in a cancer.

Cancer may be triggered by many factors such as smoke, chemical agents etc., and it is therefore impossible to determine whether radiation is the cause of a particular type of cancer or not. The only way to ascertain a correlation between radiation and cancer induction is statistical. Epidemiology is the study of the distribution of diseases among people, and it is still an observational rather then experimental science: therefore bias or confounding factors are highly probable. In the present context, the so-called Life Span Study (LSS) is an ad hoc study on survivors of Hiroshima and Nagasaki which has produced a significant amount of data on effects of exposure to radiation on humans. Studies of people partially exposed to radiation due to medical investigations or treatments are another source of data, together with information available from studies of occupational exposures, i.e., in the Mayak facility in Russia, and the Chernobyl accident [UNSCEAR, 2000].

From a general point of view, linear (or linear-quadratic) no-threshold dose response is to be expected, even though for certain cancers and at low doses correlations are less precise about it. Some interesting results are those for solid cancers obtained by the Life Span Study (LSS) where EER (excess relative risk) (Figure A.5) and EAR (excess absolute risk) (Figure A.6) are estimated. EER and EAR represent

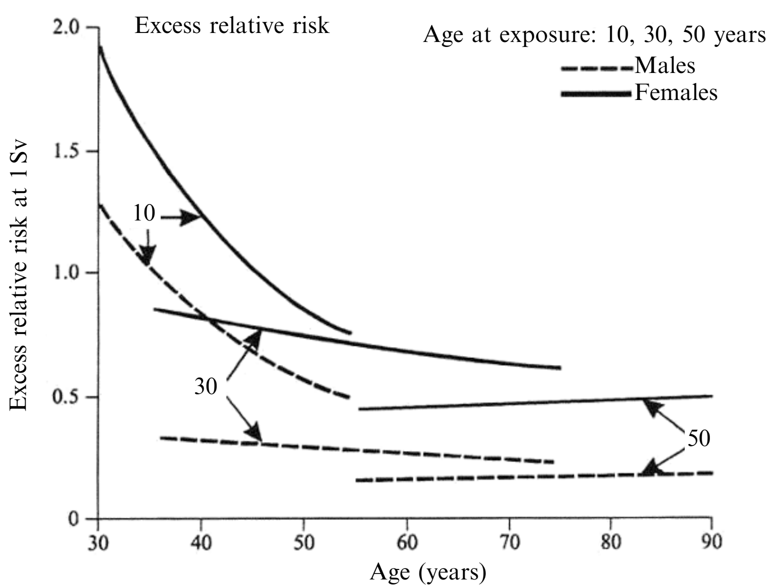

Figure A.5. Excessive relative risk at 1 Sv.

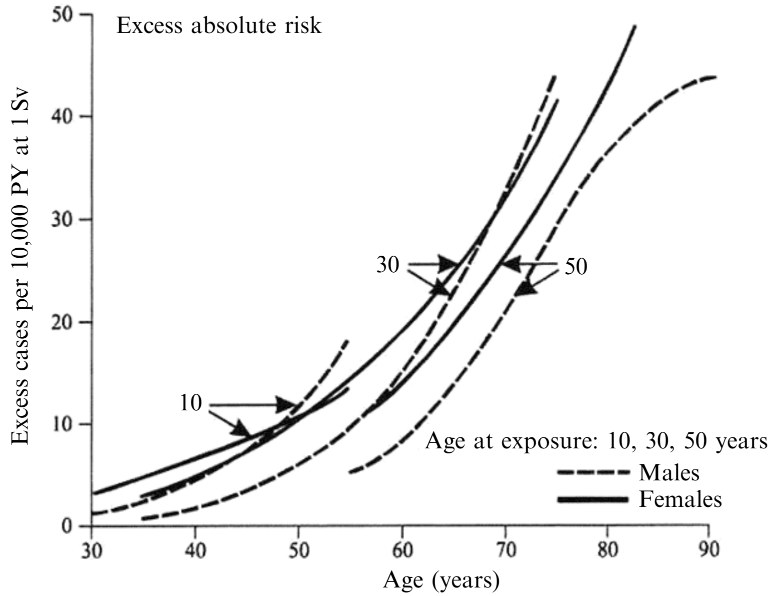

Figure A.6. Excessive absolute risk at 1 Sv.

the increased cancer rate in an exposed group relative to an unexposed group, measured on relative and absolute scales. An EER of 1 corresponds to a doubling of the cancer rate. EAR may be expressed as the number of excess cases of cancers per, for example, 10,000 persons. They can be expressed per unit dose or per a specific dose (i.e., 1 Sv) [UNSCEAR, 2000].

A.4.2.2 Hereditary effects

No radiation-induced hereditary disease has been demonstrated in humans so far. However ionizing radiation is recognized as mutagenic and experiments on plants and animals have clearly shown that radiation may cause genetic effects, and there is no reason to believe that humans are an exception.

It has been estimated that for a population exposed to radiation in one generation, the risk, expressed as number of cases per million persons per gray, in the progeny of the first post-radiation generation is: 750–1,500 autosomal dominant and X-linked diseases; 250–1,200 chronic multifactorial diseases; and 2,000 congenital abnormalities. The total radiation-induced cases are 3,000–4,700 per gray per million and represent 0.41–0.67% of the total 738,000 cases per million [UNSCEAR, 2001]

A.5 SOURCES OF RADIATION EXPOSURE

The radiation to which humans are exposed originates from various sources. It can be natural radiation or can be produced by human activities.

A.5.1 Natural radiation exposure

Natural radiation, also defined **background radiation**, has always existed in nature, and life has developed, and keeps on proliferating, in a naturally radioactive environment. There are different sources of background radiation and they can be responsible for either internal or external exposure. Doses from natural sources are summarized in Figure A.10. The **worldwide annual effective dose is 2.4 mSv** and, considered a world population of 5.3 billion people, the collective dose is 13×10^6 man Sv [UNSCEAR, 2000].

A.5.1.1 Cosmic rays

Cosmic rays are a source of external exposure. They can be divided into primary and secondary radiation. Primary radiation can be further divided, depending on its origin, into galactic and solar, the second being less significant. Outside the Earth atmosphere the main component of cosmic radiation is positively charged particles, mostly protons, of energy between 10^2 and 10^5 MeV; they constitute the so-called primary radiation (galactic and solar). When these particles approach Earth they are deflected by the terrestrial magnetic field according to their momentum. In their travel toward the ground, primary radiation particles interact with the atmosphere, producing many particles such as electrons, photons, mesons, protons and neutrons: these are called the secondary radiation.

Secondary radiation particles themselves can interact with the atmosphere or decay, producing so-called avalanche ionization: from a single starting event up to 10^8 particles can be generated. At about 20 km from sea level cosmic radiation is constituted almost exclusively of its secondary component [Galli and Mancini, 1996]. The typical range of effective dose per person per year is 0.3–1.0 mSv, with average effective dose $\sim$ 0.4 mSv [UNSCEAR, 2000]. For locations high above the sea level very large doses are received, i.e., in La Paz, Bolivia (3,600 m), the average dose due to cosmic rays is 2.02 mSv per year. A flight at an altitude of 8 km causes a dose rate of 2.8 μSv h^{-1} [Galli and Mancini, 1996].

A.5.1.2 Terrestrial radiation

Inside the Earth there are radionuclides whose half life ($T_{1/2}$) is comparable with the Earth's age. **In fact the Earth's core is still hot thanks to the energy released by radionuclides in their decay processes**. The most significant for dose computation are K^{40} ($T_{1/2} = 1.28 \times 10^9$ yr), Th^{232} ($T_{1/2} = 1.41 \times 10^{10}$ yr), U^{238} ($T_{1/2} = 4.47 \times 10^9$ yr); of secondary importance are Rb^{87} ($T_{1/2} = 4.7 \times 10^{10}$ yr) and U^{235} ($T_{1/2} = 7.04 \times 10^8$ yr). Most radionuclides belong to one of the three families of uranium, thorium and actinium (see Figures A.7, A.8 and A.9) [Galli and Mancini, 1996]. In all three families radon (Rn) appears. Radon appearance is the clearest evidence that the Earth's crust is radioactive. Terrestrial radiation can be responsible for internal or external exposure.

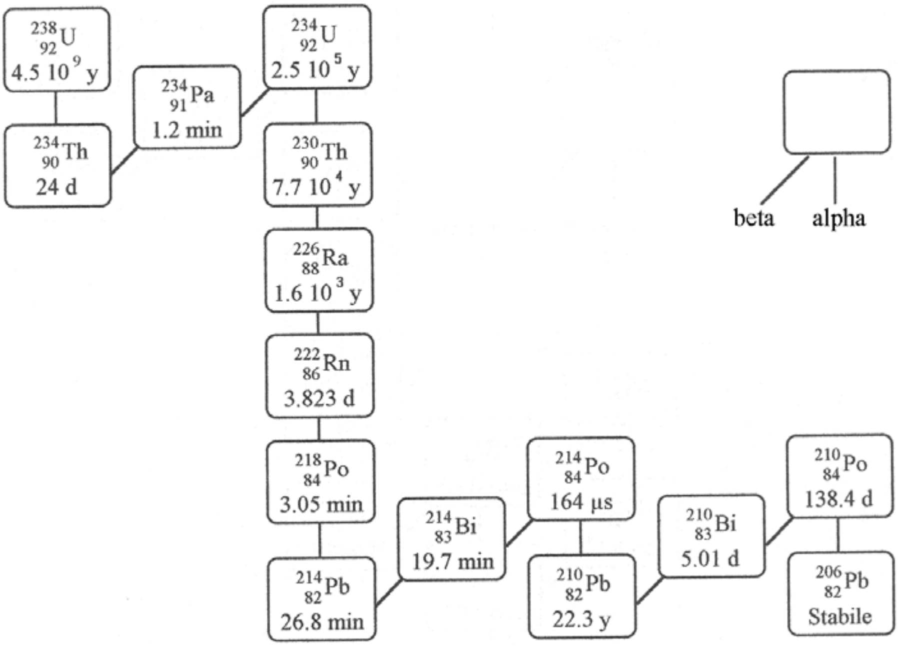

Figure A.7. Uranium-238 decay chain.

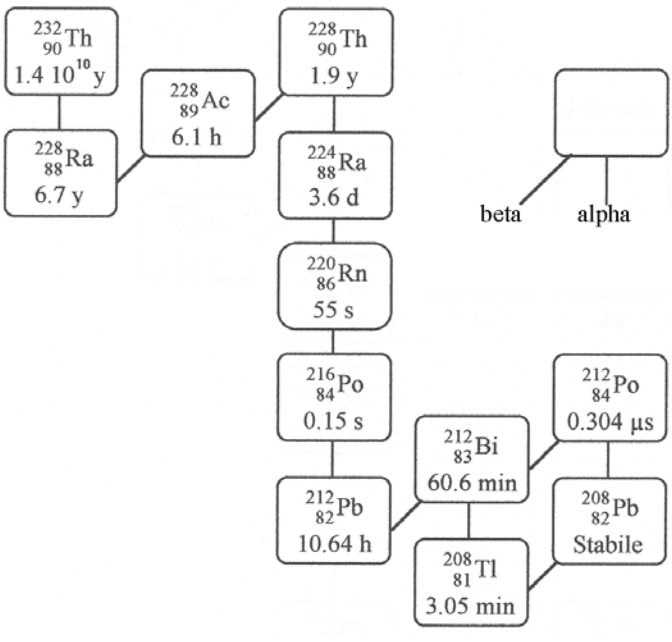

Figure A.8. Thorium-232 decay chain.

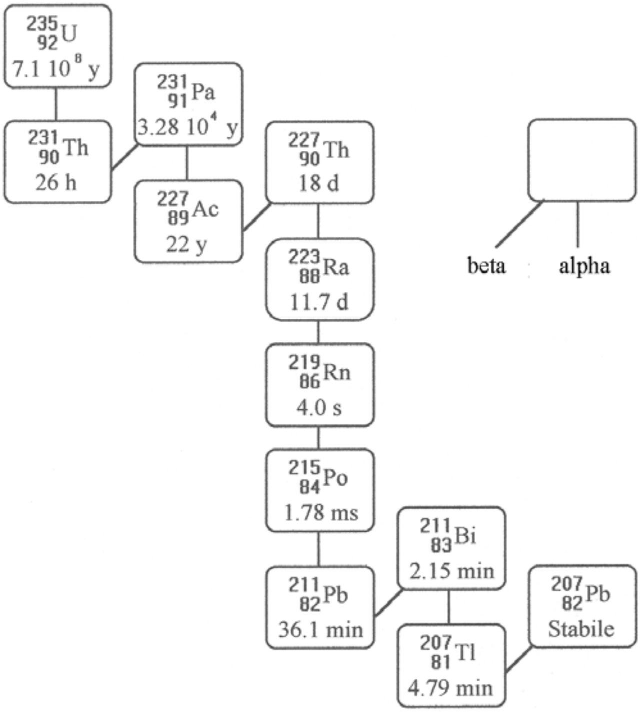

Figure A.9. Uranium-235 decay chain.

A.5.1.2.1 External exposure from terrestrial radiation

External exposure to gamma-rays from natural radionuclides can occur both outdoors, since radionuclides are present in the Earth's crust, and indoor, as they may be present in construction material. Combining outdoor and indoor exposure, for a person spending 80% of time indoors, a range of **0.3–0.6 mSv per person per year is typical**. Worldwide-averaged annual effective exposure is estimated at ~0.5 mSv [UNCEAR, 2000].

A.5.1.2.2 Internal exposure from terrestrial radiation

Potassium isotopes are present in the human body with a weight percentage 0.18%; the isotope K^{40} has an isotopic abundance 1.18×10^{-4}, and its main decay mechanism is beta. The annual dose from K^{40} is estimated to be 0.165 mSv. Some isotopes (the most significant being Pb^{210} and Po^{210}) can be ingested through food and water. The typical range of the annual effective dose is **0.2–0.8 mSv**, but higher values are detected in South America (due to the large quantity of Po^{210} present in 'yerba mate', an herb used in drinks) and arctic and sub-arctic areas (where Po^{210} and Pb210 tend to accumulate in moose meat). Worldwide-averaged annual effective dose is 0.3 mSv.

Some radioisotopes may be inhaled, the most significant radioisotope in this case being Rn^{222} and, much less importantly, Po^{210} (smoking 10 cigarettes a day doubles

Source	Worldwide average annual effective dose (mSV)	Typical range (mSV)
External exposure		
Cosmic rays	0.4	0.3–1.0
Terrestrial gamma rays	0.5	0.3–0.6
Internal exposure		
Inhalation (mainly radon)	1.2	0.2–10
Ingestion	0.3	0.2–0.8
Total	2.4	1–10

Figure A.10. Mean dose value for natural background radiation.

Po^{210} introduction). Typical range of inhaled dose is **0.2–10 mSv**. The range is so wide because the contribution is mainly given by radon and its contribution depends on its indoor accumulation. The worldwide-averaged annual effective dose due to inhalation is **1.2 mSv**. A summary of background radiation sources is given in Figure A.10 [UNSCEAR, 2000].

A.5.2 Medical radiation exposure

Ionizing radiation for medical purposes, both in diagnosis and in treatment, is widely used. It must be noted that most of these procedures are carried out in countries where only one-quarter of the world population lives. World health care has been divided into four qualitative levels, depending on the number of physicians available.

Diagnostic exposures are characterized by low doses to individuals, while therapeutic exposure is usually much larger. High doses are used to treat diseases, especially cancer. The number of diagnostic procedures is much larger than treatment procedures (the ratio is about 450 to 1): this is due to the widespread use of X-rays (they contribute to 78% of collective dose).

The worldwide-averaged annual effective dose is **0.4 mSv**, the total collective dose estimated is $2{,}500 \times 10^6$ man Sv. Figure A.11 shows effective doses reported for each health care level [UNSCEAR, 2000]. Figure A.12 [Galli and Mancini, 1996] shows the effective dose for some diagnostic examinations.

A.5.3 Exposure from atmospheric nuclear testing

Until the Treaty Banning Nuclear Weapon Tests in the Atmosphere, in Outer Space, and Under Water, signed in Moscow on August 5th 1963, almost all nuclear explosions (fissions and fusions) to test weapons were carried out in the atmosphere, mostly in the northern atmosphere, e.g., in the former Soviet Union at Semipalatinsk in Kazakhstan 456 tests were carried out between 1949 and 1989 [http://www.nato.int/science/e/grants]; after the treaty almost all explosions have been conducted underground. The two time periods of most intense atmosphere tests

Health care level	Population per physician	Annual number of examinations per 1000 persons	Average annual effective dose to population (mSv)
I	<1,000	920	1.2
II	1,000–3,000	150	0.14
III	3,000–10,000	20	0.02
IV	>10,000	<20	<0.02
Worldwide average		330	0.4

Figure A.11. Average dose from medical use.

Examination	Effective dose per examination (mSv)
Chest radiography	0.14
Mammography	0.5
Angiography	12
Urography	3.7
Dental	0.03

Figure A.12. Doses from some examinations.

were 1952–1958 and 1961–1962 (see Figure A.13). The total number of atmospheric tests was 543 and the total yield estimated is 440 megatons (189 megatons from fission) [UNSCEAR, 2000].

The total collective effective dose resulting from weapon tests to date is 3×10^7 man Sv; 7×10^6 man Sv will be delivered within the first 250 years (until 2200); the remainder, due to the long life of the C^{14} radionuclide produced, in the next 10,000 years. The annual average effective dose varies both with time (decreasing thanks to the ban treaty) and with location: in the northern hemisphere the dose is higher than in the southern. The average effective dose estimated for the year 1999 is 5.87 μSv in the northern hemisphere, 2.68 μSv in the southern and 5.51 globally (see Figure A.14).

A.5.4 Exposure from nuclear power production

Today about 17% of electricity produced worldwide, i.e. about 250 gigawatt, is nuclear. Assuming that this practice continues over the next 100 years, the maximum collective dose can be estimated from the cumulative dose over the period of practice. The normalized 100-year collective dose is 6 man Sv per gigawatt and per year. The annual dose is 1,500 man Sv (6×250), resulting in a maximum annual dose per person of 0.2 μSv [UNSCEAR, 2000].

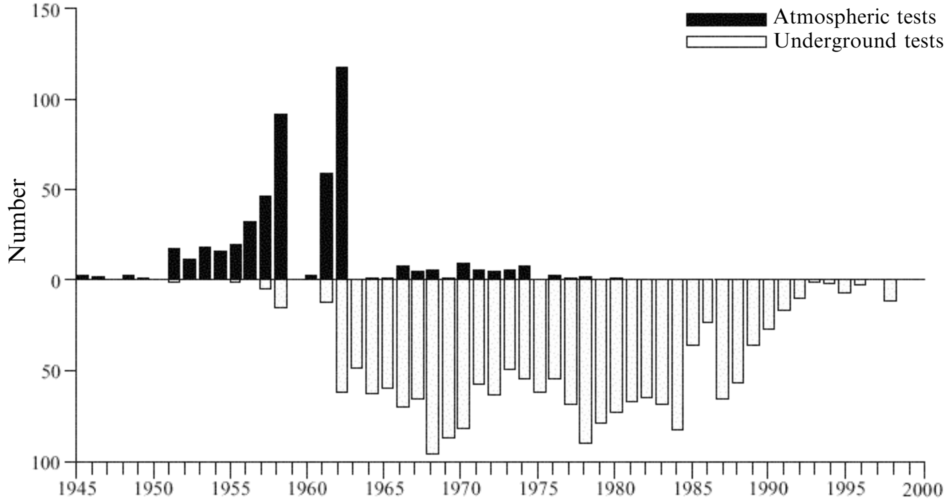

Figure A.13. Number of weapons tests per year.

	Average annual effective dose (μSv)		
Year	Northern Hemisphere	Southern Hemisphere	World
1945	0.64		0.57
1955	16.8	3.34	15.4
1965	48.7	11.7	44.6
1975	14.8	5.01	13.7
1985	8.98	2.78	8.30
1995	6.61	2.55	6.20
1996	6.42	2.57	5.97
1997	6.23	2.59	5.85
1998	6.05	2.63	5.63
1999	5.87	2.68	5.51
1945–1999	1076	328	994
1999–2099	264	157	253
2099–2199	63	53	62
2200–	2181	2180	2181
1945–	3580	2720	3490

Figure A.14. Doses from weapons tests.

A.5.5 Exposure from major accidents

There have been accidents in using nuclear energy or radioactive elements. In medical and diagnostic practice accidents may occur (a few hundreds of all types each year), and usually have serious consequence. The probability that any member of the public be involved is, however, very small, and, by and large, the consequences do not affect the public.

Weapons production and transportation have resulted in several accidents, but the collective dose committed is small. The two most serious accidents in nuclear weapons production were at Kyshtym, in the former USSR, and at the Windscale plant at Sellafield (UK), both in 1957. The first accident caused a collective dose of 2,500 man Sv over the next 30 years. The Sellafield accident caused a total collective dose in Europe (including England) of about 2,000 man Sv.

The two most important accidents in power plants were those at Three Mile Island and Chernobyl [UNSCEAR, 2000; World Nuclear Association website], although the Chernobyl installation produced energy only as a byproduct, the plant being chiefly a plutonium-producing facility, and although what happened can hardly be defined as an accident. At Three Mile Island the containment system, missing at Chernobyl, prevented a large amount of fission fragments from spreading in the environment: the total collective effective dose was $\leq$40 man Sv, with the maximum dose to nearby individuals $\leq$1 mSv. The Chernobyl accident had much more serious consequences. It caused the death of 30 people among the rescue workers within a few weeks, and 1,800 cases of thyroid cancer in the children exposed; no other health impact has been detected up to the year 2000. The worldwide average annual effective dose per person due to the Chernobyl accident, estimated for the year 2000, is 0.002 mSv, down from its peak 0.04 mSv in 1986 [UNSCEAR, 2000]. Note that cancer rates went up by 3% in the affected area, but the childrren who contracted thyroid cancer had a 99% survival rate rather than 80–85% previously estimated [*Nature*, 2005]. In fact, according to a report by the Chernobyl Forum to be released, poverty and mental-health problems pose a much greater threat to the local community than radiation.

A different type of accident occurred about 20 years ago in Taiwan. Recycled steel, accidentally contaminated with radioactive ^{60}Co was formed into construction steel for more than 180 buildings, occupied by about 10,000 persons from periods ranging from 9 to 20 years. The radiation dose received averaged about 0.4 Sv, for a total collective dose of 4,000 person Sv. The observed cancer rate of these people was 3.5 per 10^5 person-years; congenital heart malformations among children, during the same period were 1.5×10^{-3}. These figures were recently compared with the averages over Taiwan's general population, which are 116 cancers per 10^5 person-years and 23 malformations $\times 10^{-3}$. The conclusions, see [Chen et al., 2004] seem to indicate that a 'moderate' dose of radiation is beneficial. This finding should be, and probably will be, compared again with tests on animals, in order to corroborate or disprove it; in any event, it seems to agree with a similar finding for laboratory mice (for a comprehansive description of this effect, technically called 'hormesis', see [Mortazavi, 2005]). A possible explanation is based on the so-called theory of radiative hormesis: according to hormesis, a 'low' level of stress prepares biological organisms to face and overcome larger disruptions, either internal or external. The Taiwan study hints this level could be of the order of 50 mSv per year in the case of cancers.

Source	Worldwide annual per caput dose (mSv)	Range or trend
Natural background	2.4	Typical range 1–10 mSv. Sizeable population also 10–20 mSv
Diagnostic medical use	0.4	Typical range 0.04–1.0 mSv at lowest and highest level of health care.
Atmospheric nuclear testing	0.005	Has decreased from a maximum of 0.15 mSv in 1963. Higher in northern hemisphere and lower in southern hemisphere.
Chernobyl accident	0.002	Has decreased from a maximum of 0.04 mSv in 1986. Higher in locations near the accident area.
Nuclear power production	0.0002	Has increased with expansion of plants but decreased thanks to improved practice.

Figure A.15. Annual per caput doses in the year 2000.

A.5.6 Occupational exposure

There are jobs in which workers are routinely exposed to radiation, both because of man-made sources (i.e., medical practice, people employed in nuclear fuel cycle facilities etc.) and because of enhanced levels of natural radiation (i.e., airplane crews flying at a height of 8 km receive a dose of 2.8 μSv per hour). This kind of exposure does not affect other members of the public, but it is interesting to see the dose (Figure A.15) that these workers receive in order to have a better understanding of the issue [UNSCEAR, 2000].

A.5.7 Exposure from nuclear propulsion systems

A new source of dose could in principle result from future nuclear propulsion systems. Rubbia's engine (section 7.13) and MITEE (section 7.11) [Rubbia, 2000; Powell et al., 1998, 1999; G. Maise, personal communication] are two of the most promising systems: an assessment of the dose committed to the public arising from their use is necessary in order to show the impact they could have.

To set to rest a very old misconception, there is literally no way a nuclear reactor, whether for power generation or propulsion, could trigger a nuclear explosion: the reason is the impossibility of reaching the proper conditions of confinement time and critical mass.

However, what could happen is that, because of coolant loss, or other reasons, 'runaway' fission in a reactor can heat too much the reactor core, eventually melting it down This is called a loss of coolant accident, or LOCA. When this happens (it did in the case of Chernobyl), high-temperature chemical reactions can occur, especially if water or graphite moderators are present. Water could be dissociated by the high temperatures, producing hydrogen and oxygen and possibly burning or exploding, and graphite could burn in an oxygen or hydrogen atmosphere. Besides, excessive heat release rates may also cause explosions simply due to rapid thermal expansion of the nuclear 'fuel' or other reactor material. LOCAs are most serious in nuclear reactors. In the absence of a containment structure, radionuclides from the core can be ejected by the chemical or thermal explosion and contaminate the nearby environment.

This said, it should be clear that this type of accident is in fact due to chemistry, not fission (the use by the popular press of the term 'nuclear explosion' in this context is due to ignorance and is misleading).

To test the effects of an actual meltdown due to runaway fission, during the NERVA program a test was performed at Los Alamos in which a Kiwi nuclear reactor was deliberately allowed to explode by excluding the cooling system (this was the so-called Kiwi-TNT test). The results are reported in [Dewar, 2002, 2004]. The reactor was totally destroyed, but contamination was limited to a relatively small area, of order 100 m. After clearing appropriately the site of debris, activities were resumed. This test did much to allay fears that a NERVA-type core meltdown and explosion could in any way produce a large-scale catastrophe. A nuclear rocket reactor must be inherently far smaller than that in power plants, so the outcome of the Kiwi-TNT test is not surprising.

There is a specific and more serious concern in propulsion applications, where a nuclear reactor must be orbited, i.e., lifted through the Earth atmosphere, perform its interplanetary mission starting from LEO or MEO, and (possibly) be parked again in Earth orbit at the end of its mission. The question is: What could happen during each of these three legs?

Any reactor will contain fissile fuel, of order $O(1)$ to $O(10)$ kg depending on fuel type. Of course no reactor will be operated while being lifted off, but the danger exists of an accident, such as that of the 'Challenger', in which the conventional launcher could explode, damaging the reactor to be orbited and spreading fissile material from the damaged reactor stored in the payload bay either in the atmosphere or on the ground.

During the interplanetary trajectory, however, any accident would not affect Earth.

The most dangerous occurrence would be if the reactor, containing all the (new) radionuclides produced during operation in space, were for some reason to *re-enter* Earth's atmosphere accidentally: in fact, no space agency is considering deliberate re-entering of nuclear reactors, so that such event would have to be unplanned, unwanted and therefore accidental. The consequences would be the spreading of many families of radionuclides in the atmosphere, at a height that can be estimated at roughly between 40 and 10 km, at the peak of aerodynamic heating. The total mass of radionuclides spread would be approximately the same as of the original fuel, i.e., $O(1)$ to $O(10)$ kg. Additional contamination would come from secondary radioactivity, that is, induced in the reactor structural materials.

As for the actual consequences, this event is similar to what happens during an atomic explosion in the atmosphere, where fissionable material and bomb structure are vaporized and released. Data from atmospheric atomic tests exist that can be effectively used to estimate these effects. In any event, the quantity of radionuclides in an atomic explosion is many times larger than in any nuclear reactor at this time envisaged for space missions; accordingly, radioactive contamination is expected to be smaller.

A.5.7.1 Nuclear accidents in the Rubbia engine

Like all nuclear propulsion concepts, the Rubbia engine is not planned to fission whilst in the atmosphere. The dose to the public would be the highest in a hypothetical accidental re-entry, for instance at the end of a Mars mission. For each kilogram of americium loaded, the total collective dose committed for the following 250 years is estimated at 9.5 man Sv. The individual dose commitment over the following 250 years would be 1.8×10^{-6} mSv. In the case of an americium stockpile of 15 kg, typical of a manned Mars mission using the Rubbia engine, the total collective dose committed for the first 250 years would be 140 man Sv, while the individual value would be 3×10^{-5} mSv [Rubbia, 2000].

In addition, the fuel considered in the Rubbia engine (Am-242m) was purposely chosen because of its neutron cross-section sharply decreasing with temperature. This feature means that any runaway fission in Am-242m would automatically stop above a certain temperature, and the reactor regime would be brought back to a stable state.

A.5.7.2 Nuclear accidents in a MITEE engine

Also in the case of MITEE the most catastrophic accident would be the total destruction of the vehicle accidentally re-entering the atmosphere after a mission. Like Rubbia's engine, MITEE is planned not to fission while in the Earth atmosphere, so that in this case too, a prompt criticality accident (explosion caused by overheating) would have less considerable consequences than the total destruction of a chemical explosion or unwanted re-entry in the atmosphere after returning from a Mars mission. The average dose commitment over the following 250 years would be about 1.6×10^{-8} mSv for each kilogram of uranium loaded, and for a typical MITEE configuration the average dose commitment for 250 years would therefore be about 4×10^{-7} mSv [UNSCEAR, 1993; Powell et al., 1998, 1999; G. Maise, personal communication].

A.5.7.3 Safety in ground testing of future nuclear rockets

A key worry in planning nuclear propulsion revolves around the issue of ground testing. In the past, Kiwi and PHOEBUS were all tested at Los Alamos in the open air. The book by Dewar recounts details of those tests and the safety measures employed; it suffices to say here that no accidents involving loss of life or damage to people took place during the entire US program [Dewar, 2002, 2004]. The paper in [Dewar, 2002], for instance, documents how the effluents from the nuclear furnace test reactor were treated at LASL during the last stages of the ROVER program.

Nevertheless, planning future ground tests is a definite concern. However, at least in the case of the type of reactor envisaged by C. Rubbia and investigated by the Italian Space Agency, ASI, under the Project P 242, the following considerations apply.

The Rubbia engine is modular, each module being a self-standing generator of hot hydrogen gas. About 30 to 40 modules compose the engine. For a manned Mars mission the thrust, F, required is of order 10^3 N, while the specific impulse I_{sp} is of order 2,500 sec. Comparison with the NERVA thermal engine tested at Los Alamos ($F = 334{,}000$ N, $I_{sp} = 825$ sec, mass flow rate = 40 kg/sec) shows that the single module of the Rubbia engine to be tested in an appropriate test facility will process a mass flow rate of hydrogen of order 2.5 g/sec. So, the scale factor between a module of the Rubbia engine and NERVA is about 16,000. The amount of hydrogen, and therefore of fission fragments deposited inside the hydrogen used as propellant, will be exceedingly small.

As a consequence, testing a single module of the Rubbia engine may be performed in a closed loop, and this appears also feasible for all nuclear rockets that are of comparable thrust, and that are built following a modular philosophy, therefore also MITEE, or NEP thrusters. In fact ways of efficiently separating fission fragments from hydrogen have already been described in the Final Report of ASI on the Rubbia Engine [Augelli et al., 1999]. Closed-loop tests can be performed in any reasonably self-contained facility and building, thus ensuring that no radiation escapes.

A.5.8 Comparison of exposures

The doses received by an individual from the main different sources in year 2000 are summarized in Figure A.16. Their values are given in annual per caput effective dose (mSv). The values are averaged, meaning that there are significant variations in exposure to individuals, depending on location, diet, personal habits and so forth.

Source	Effective dose/Dose commitment (mSv)	Comment
Rubbia's Engine Accident → Catastrophic LEO Re-entry	1.8×10^{-6}	Dose committed for 250 years (per kg fuel)
MITEE Accident → Catastrophic LEO Re-entry	1.6×10^{-8}	Dose committed for 250 years (per kg fuel)
Natural Background	2.4	Average effective dose in 1 year
Dental x-ray examination	0.03	Average effective dose from a single examination
Flying at 8 km for 10 hours	2.8×10^{-8}	1 hour gives $2.8 \times 10\,\mu$Sv

Figure A.16. Comparison of doses from different sources.

The largest contribution to total dose is from the natural background: 2.4 mSv, but typical values may range from 1 up to 10 mSv, with large groups of population receiving a dose of 10–20 mSv. The second most important source, 0.4 mSv, is from the medical use of radiation. It has an increasing trend, thanks to increasingly available medical radiation facilities. The third cause is the fallout from past weapons tests; i.e., 0.005 mSv. The value has been decreasing thanks to the Treaty Banning Nuclear Weapon Tests, the maximum value being reached in 1963, when it was 7% of the natural background. Other man-made sources, like the Chernobyl accident and nuclear power production, are much smaller, 0.002 mSv and 0.0002 mSv, respectively.

A.6 CONCLUSIONS

The individual dose commitments for 250 years arising from a rather improbable total 'crash' of Rubbia's engine, 1.8×10^{-6} mSv, and MITEE, 1.6×10^{-8} mSv, are insignificant compared to other sources of exposure. Should the Rubbia engine 'crash', a hypothetical individual born in the year of crash and dying at age 250, would have received all along his life a 3×10^{-5} mSv dose, much lower than the dose imparted by a dental examination (0.03 mSv); the same would be true for a MITEE accident of the same type. The average dose from natural background to each individual is 2.4 mSv in one single year. Figure A.16 shows contributions to dose compared to other sources.

The contribution to individual average dose from the crash of Rubbia's engine or MITEE seems therefore not a reason of concern to public health.

A.7 BIBLIOGRAPHY

Augelli, M., Bignami, G., Bruno, C., Calligarich, E., De Maria, G., Mulas, M., Musso, C., Pellizzoni, A., Piperno, W., Piva, R., et al. (1999) 'Report of the Working Group on a Preliminary Assessment of a New Fission Fragments Heated Propulsion Concept and its Applicability to Manned Missions to the Planet Mars (Project 242)', ASI Internal Report, Roma, 15 March 1999.

Chen, W.L., et al. (2004) 'Is Chronic Radiation an Effective Prophylaxis against Cancer?', *Journal of American Physicians and Surgeons*, Vol. 9, No. 1, pp. 6–10.

Dewar, J.A. (2002) 'The Story of the Nuclear Rocket: Lessons for the future', IAC paper IAC-02-IAA.2.4.06, presented at the 53rd International Astronautical Congress—The World Space Congress, Oct. 10–19, 2002, Houston, TX, USA.

Dewar, J.A. (2004) *To the End of the Solar System: The Story of the Nuclear Rocket*, University Press of Kentucky, Lexington, KY.

Galli, G., and Mancini, C. (1996) 'Esposizione alla Radioattività Ambientale', *Ingegneria Nucleare e Tecnologie Energetiche*, Vol. 38, No. 1–4.

ICRP (1990) Publication 60, 'Recommendations of the International Commission on Radiological Protection'. *Annals of the ICRP*, Vol. 21, No. 1–3.

Klein, H.A. (1988) *The Science of Measurement: A Historical Survey*, Dover, New York, Ch. 49.

Mortazavi, S.M.J. (2005) 'An Introduction to Radiation Hormesis', www.angelfire.com/mo/radioadaptive/inthorm/html

Mukhin, K.N. (1987) *Physics of Atomic Nucleus*, Vol. I, Mir Publishers, Moscow.

Nature (2005) 'Chernobly: Poverty and stress pose "bigger threat" than radiation', *Nature*, Vo. 437, 8 September 2005, 181.

Powell, J., Maise, G., and Paniagua, J. (1998) 'MITEE: An Ultra Lightweight Nuclear Engine for New and Unique Planetary Science and Exploration Mission', IAF paper IAF-98-R.1.01, presented at the 49th International Astronautical Congress, Sept. 28–Oct. 2, 1998, Melbourne, Australia.

Powell, J., Maise, G., and Paniagua, J. (1999) 'The MITEE Family of Compact, Ultra Lightweight Nuclear Thermal Propulsion Engines for Planetary Space Exploration', IAF paper IAF-99-5.6.03, presented at the 50th International Astronautical Congress, Oct. 4–8, 1999, Amsterdam, The Netherlands.

Rubbia, C. (2000) *Fission Fragments Heating for Space Propulsion*. European Organization for Nuclear Research (CERN), Geneva.

UNSCEAR (1993) United Nations Scientific Committee on the Effects of Atomic Radiation, 'Sources and Effects of Ionizing Radiation', Report to the General Assembly, with Scientific Annexes, United Nations, New York.

UNSCEAR (2000) United Nations Scientific Committee on the Effects of Atomic Radiation, 'Sources and Effects of Ionizing Radiation',Report to the General Assembly, with Scientific Annexes, United Nations, New York.

UNSCEAR (2001) United Nations Scientific Committee on the Effects of Atomic Radiation, 'Hereditary Effects of Radiation', Report to the General Assembly, with Scientific Annexes. United Nations, New York.

World Nuclear Association site, http://www.world-nuclear.org

Index

Colour section

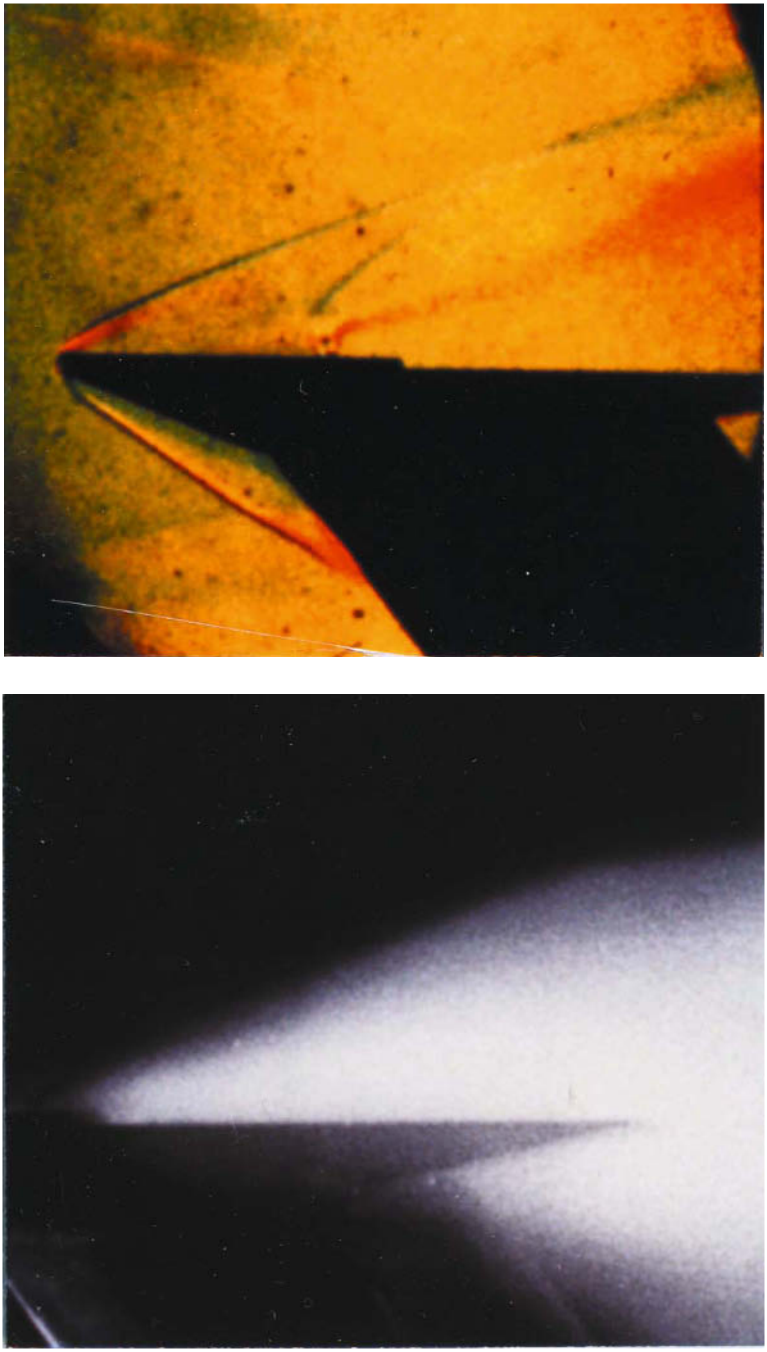

Figure 4.21. 300°C hydrogen injected into supersonic air stream at flight conditions corresponding to a scramjet combustor for an aircraft flying at Mach 8. Tests circa 1962.

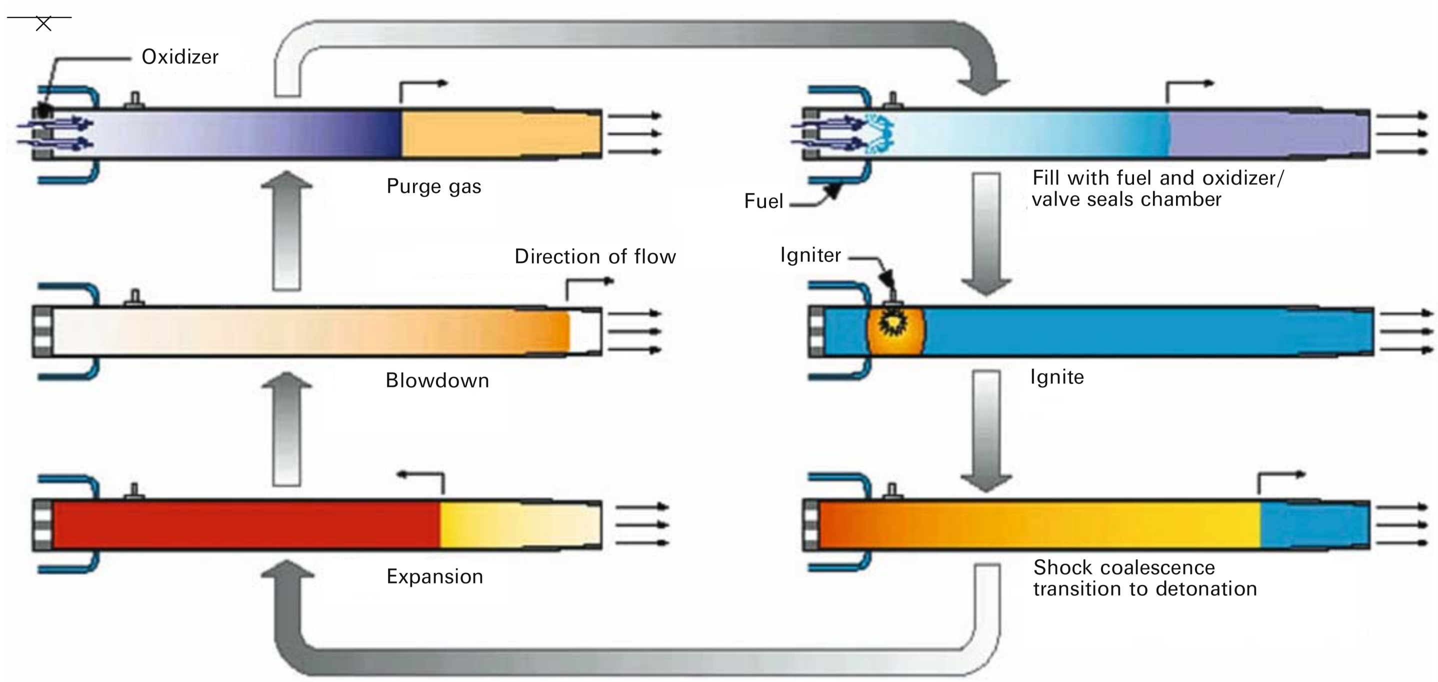

Figure 4.24. The pulse detonation rocket engine (PDRE) operational cycle.

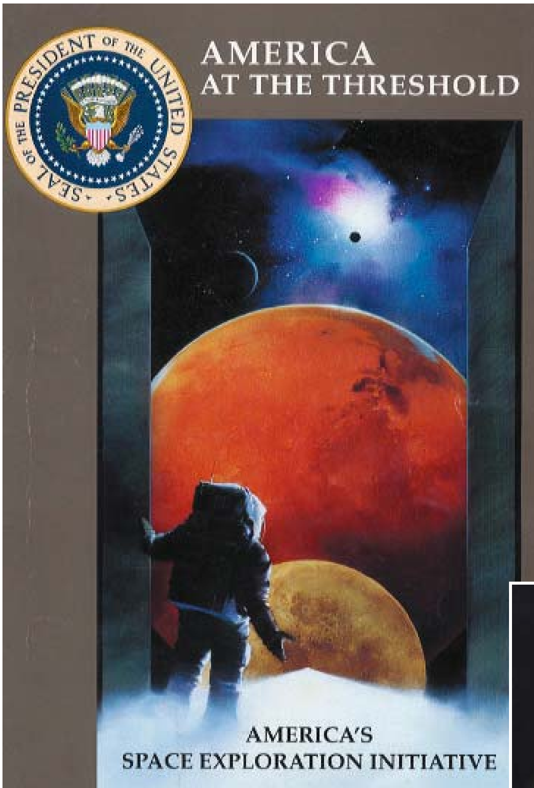

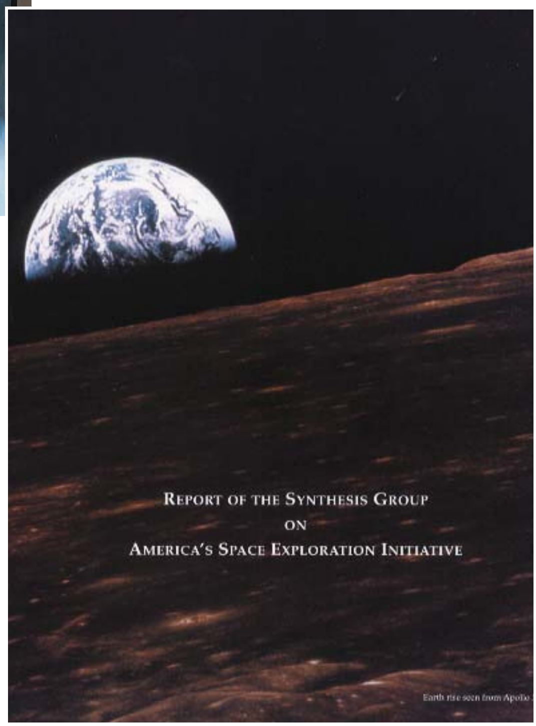

Figure 6.1. A Presidential Study to continue the exploration in the future by General Thomas Stafford (retired) an Apollo and Apollo–Soyuz astronaut. The key to expanding human exploration of the Solar System is the exploration of the Moon and the establishment of a Moon-base that is the prototype for Mars and other human-compatible planets.

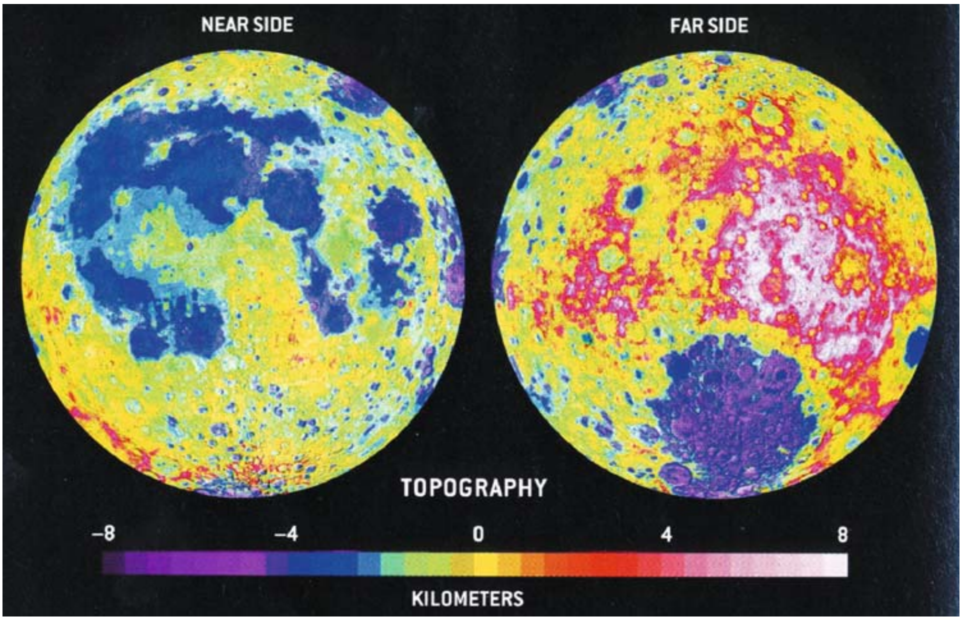

Figure 6.15. Moon topography from the laser ranger measurements by *Clementine* and *Lunar Prospector* spacecraft. (From *Scientific American* [Spudis, 2003].)

Figure 6.16. Photo of Earth-rise from Apollo 10 command module in lunar orbit [Stafford, 1991].

Printing: Mercedes-Druck, Berlin
Binding: Stein+Lehmann, Berlin